



MICROBIAL DEGRADATION OF PLASTICS

EDITED BY: Ren Wei, Jun Yang and Nick Wierckx
PUBLISHED IN: Frontiers in Microbiology



frontiers

Frontiers eBook Copyright Statement

The copyright in the text of individual articles in this eBook is the property of their respective authors or their respective institutions or funders. The copyright in graphics and images within each article may be subject to copyright of other parties. In both cases this is subject to a license granted to Frontiers.

The compilation of articles constituting this eBook is the property of Frontiers.

Each article within this eBook, and the eBook itself, are published under the most recent version of the Creative Commons CC-BY licence.

The version current at the date of publication of this eBook is CC-BY 4.0. If the CC-BY licence is updated, the licence granted by Frontiers is automatically updated to the new version.

When exercising any right under the CC-BY licence, Frontiers must be attributed as the original publisher of the article or eBook, as applicable.

Authors have the responsibility of ensuring that any graphics or other materials which are the property of others may be included in the CC-BY licence, but this should be checked before relying on the CC-BY licence to reproduce those materials. Any copyright notices relating to those materials must be complied with.

Copyright and source acknowledgement notices may not be removed and must be displayed in any copy, derivative work or partial copy which includes the elements in question.

All copyright, and all rights therein, are protected by national and international copyright laws. The above represents a summary only. For further information please read Frontiers' Conditions for Website Use and Copyright Statement, and the applicable CC-BY licence.

ISSN 1664-8714

ISBN 978-2-88966-605-8

DOI 10.3389/978-2-88966-605-8

About Frontiers

Frontiers is more than just an open-access publisher of scholarly articles: it is a pioneering approach to the world of academia, radically improving the way scholarly research is managed. The grand vision of Frontiers is a world where all people have an equal opportunity to seek, share and generate knowledge. Frontiers provides immediate and permanent online open access to all its publications, but this alone is not enough to realize our grand goals.

Frontiers Journal Series

The Frontiers Journal Series is a multi-tier and interdisciplinary set of open-access, online journals, promising a paradigm shift from the current review, selection and dissemination processes in academic publishing. All Frontiers journals are driven by researchers for researchers; therefore, they constitute a service to the scholarly community. At the same time, the Frontiers Journal Series operates on a revolutionary invention, the tiered publishing system, initially addressing specific communities of scholars, and gradually climbing up to broader public understanding, thus serving the interests of the lay society, too.

Dedication to Quality

Each Frontiers article is a landmark of the highest quality, thanks to genuinely collaborative interactions between authors and review editors, who include some of the world's best academicians. Research must be certified by peers before entering a stream of knowledge that may eventually reach the public - and shape society; therefore, Frontiers only applies the most rigorous and unbiased reviews.

Frontiers revolutionizes research publishing by freely delivering the most outstanding research, evaluated with no bias from both the academic and social point of view. By applying the most advanced information technologies, Frontiers is catapulting scholarly publishing into a new generation.

What are Frontiers Research Topics?

Frontiers Research Topics are very popular trademarks of the Frontiers Journals Series: they are collections of at least ten articles, all centered on a particular subject. With their unique mix of varied contributions from Original Research to Review Articles, Frontiers Research Topics unify the most influential researchers, the latest key findings and historical advances in a hot research area! Find out more on how to host your own Frontiers Research Topic or contribute to one as an author by contacting the Frontiers Editorial Office: frontiersin.org/about/contact

MICROBIAL DEGRADATION OF PLASTICS

Topic Editors:

Ren Wei, University of Greifswald, Germany

Jun Yang, Beihang University, China

Nick Wierckx, Forschungszentrum Jülich, Germany

Citation: Wei, R., Yang, J., Wierckx, N., eds. (2021). Microbial Degradation of Plastics. Lausanne: Frontiers Media SA. doi: 10.3389/978-2-88966-605-8

Table of Contents

- 04 Editorial: Microbial Degradation of Plastics**
Ren Wei and Nick Wierckx
- 07 A Quantum Mechanism Study of the C-C Bond Cleavage to Predict the Bio-Catalytic Polyethylene Degradation**
Junyu Xu, Ziheng Cui, Kaili Nie, Hao Cao, Min Jiang, Haijun Xu, Tianwei Tan and Luo Liu
- 14 Shotgun Metagenomics Reveals the Benthic Microbial Community Response to Plastic and Bioplastic in a Coastal Marine Environment**
Lee J. Pinnell and Jeffrey W. Turner
- 27 Actinobacteria as Promising Candidate for Polylactic Acid Type Bioplastic Degradation**
Natthicha Butbunchu and Wasu Pathom-Aree
- 37 Degradation of Recalcitrant Polyurethane and Xenobiotic Additives by a Selected Landfill Microbial Community and Its Biodegradative Potential Revealed by Proximity Ligation-Based Metagenomic Analysis**
Itzel Gaytán, Ayixon Sánchez-Reyes, Manuel Burelo, Martín Vargas-Suárez, Ivan Liachko, Maximilian Press, Shawn Sullivan, M. Javier Cruz-Gómez and Herminia Loza-Tavera
- 56 A Novel Polyester Hydrolase From the Marine Bacterium *Pseudomonas aestusnigri* – Structural and Functional Insights**
Alexander Bollinger, Stephan Thies, Esther Knieps-Grünhagen, Christoph Gertzen, Stefanie Kobus, Astrid Höppner, Manuel Ferrer, Holger Gohlke, Sander H. J. Smits and Karl-Erich Jaeger
- 72 Biotransformation of Phthalate Plasticizers and Bisphenol A by Marine-Derived, Freshwater, and Terrestrial Fungi**
Lena Carstens, Andrew R. Cowan, Bettina Seiwert and Dietmar Schlosser
- 93 Unraveling 1,4-Butanediol Metabolism in *Pseudomonas putida* KT2440**
Wing-Jin Li, Tanja Narancic, Shane T. Kenny, Paul-Joachim Niehoff, Kevin O'Connor, Lars M. Blank and Nick Wierckx
- 108 Toward Biorecycling: Isolation of a Soil Bacterium That Grows on a Polyurethane Oligomer and Monomer**
María José Cárdenas Espinosa, Andrea Colina Blanco, Tabea Schmidgall, Anna Katharina Atanasoff-Kardjalieff, Uwe Kappelmeyer, Dirk Tischler, Dietmar H. Pieper, Hermann J. Heipieper and Christian Eberlein
- 117 Microbial Degradation and Valorization of Plastic Wastes**
Jiakang Ru, Yixin Huo and Yu Yang
- 137 High Throughput Screening for New Fungal Polyester Hydrolyzing Enzymes**
Simone Weinberger, Reinhard Beyer, Christoph Schüller, Joseph Strauss, Alessandro Pellis, Doris Ribitsch and Georg M. Guebitz
- 145 UV Pretreatment Impairs the Enzymatic Degradation of Polyethylene Terephthalate**
Patricia Falkenstein, Daniel Gräsing, Pavlo Bielytskyi, Wolfgang Zimmermann, Jörg Matysik, Ren Wei and Chen Song



Editorial: Microbial Degradation of Plastics

Ren Wei^{1*} and Nick Wierckx²

¹ Junior Research Group Plastic Biodegradation, Institute of Biochemistry, University of Greifswald, Greifswald, Germany,

² Institute of Bio- and Geosciences IBG-1: Biotechnology, Forschungszentrum Jülich GmbH, Jülich, Germany

Keywords: plastic pollution, plastic degradation, microorganisms, recycling, upcycling

Editorial on the Research Topic

Microbial Degradation of Plastics

The accumulation of mismanaged plastic waste in natural environments poses a serious threat to our oceans, wildlife, and human health. As the global demand on plastics is growing continuously, the trend of plastic emission into open environments is unlikely to reduce until 2030 unless key policies, consumption behaviors and waste management measures regarding plastic products will be radically transformed immediately (Borrelle et al., 2020).

While abiotic environmental degradation contributes considerably to the fragmentation of large plastic debris resulting in micro- and nanoplastic pollution (Min et al., 2020), the role of microorganisms in the plastic degradation under natural conditions is still poorly understood. In recent years, various microbes have been reported capable of depolymerizing synthetic polymers at laboratory conditions (Wierckx et al., 2018). Nonetheless, the microbial degradation extents and rates of conventional petroleum-based plastics such as polyethylene (PE) and polystyrene (PS) can differ remarkably to those of biodegradable polyesters such as polylactic acids (PLA). Microbial biotechnology has been repeatedly proposed as an option of sustainable disposal approach of plastic waste although the reality and promise of biotechnological recycling methods is not yet unambiguously clarified among scientific communities, plastic end-users and policy makers (Wei et al., 2020).

As a response to this research field of rapidly increasing interest, we proposed this Research Topic and could finally collect 11 high-quality contributions based on both original research and literature survey by scientists from all over the world.

Ru et al. provided a comprehensive review on the microorganisms and enzymes able to degrade mass-produced recalcitrant petrochemical plastics reported since the 1970s. While PE and PS have been shown to be degraded by several microorganisms, albeit very slowly, the key depolymerases involved in the breakdown of carbon-carbon backbones remain still unknown. For a better understanding of the enzymatic degradation of vinyl polymers, Xu et al. carried out quantum mechanism calculations to model the cleavage of the carbon-carbon bond at the C_β position under both acidic and alkaline conditions.

Microbial communities are a valuable source of enzymes with degrading activities on synthetic polymers. Pinnell and Turner reported the shotgun metagenomic sequencing of biofilms fouling polyethylene terephthalate (PET), polyhydroxyalkanoate (PHA) and ceramic placed at the sediment-water interface of a coastal lagoon. While PET plastic biofilms were indistinguishable compared to the ceramic biofilm control, PHA bioplastic biofilms were distinct as indicated by the dominant presence of sulfate-reducing microorganisms (SRM) and a significant enrichment of phylogenetically diverse polyhydroxybutyrate (PHB) depolymerases. Their findings indicate that the plastisphere SRM play an important role in PHA biodegradation. Gaytán et al. studied the polyurethane (PUR) degrading activity of a landfill microbial mixed culture which can grow

OPEN ACCESS

Edited by:

Kian Mau Goh,
University of Technology
Malaysia, Malaysia

Reviewed by:

Rajesh K. Sani,
South Dakota School of Mines and
Technology, United States

*Correspondence:

Ren Wei
ren.wei@uni-greifswald.de

Specialty section:

This article was submitted to
Microbiotechnology,
a section of the journal
Frontiers in Microbiology

Received: 30 November 2020

Accepted: 25 January 2021

Published: 11 February 2021

Citation:

Wei R and Wierckx N (2021) Editorial:
Microbial Degradation of Plastics.
Front. Microbiol. 12:635621.
doi: 10.3389/fmicb.2021.635621

on aqueous PUR dispersion as a sole carbon source. Physicochemical analyses suggested the cleavage of various functional groups in the polymers. Along with the metagenomic analysis, tentative microbial PUR degradation pathways were proposed. Weinberger et al. cultivated a fungal library with aliphatic and aromatic polyesters, leading to the identification of new strains that produce polyester hydrolyzing enzymes. This method will enable exploring the available fungal diversity and thus broadening the spectrum of candidate enzymes for plastic recycling. The increasing commercial demand on bio-based and biodegradable plastics such as PLA requires also environment-friendly disposal methods using microorganisms (Butbunchu and Pathom-Aree). By summarizing the findings about PLA degradation by Actinobacteria since 1997, *Pseudonocardia* are identified as the most important family. Moreover, esterases and proteases found in various Actinobacteria capable of degrading PLA will hold the promise for future application in the bioplastic waste management.

Many studies have focused on the enzymatic degradation of PET during the last decade (Wei and Zimmermann, 2017). Bollinger et al. reported the high-resolution structural elucidation and functional characterization of a novel PET hydrolyzing enzyme (PE-H) identified in the genome of the marine bacterium *Pseudomonas aestusnigri*. PE-H was shown to degrade amorphous PET at 30°C. By structural modeling and mutagenesis study, a Y250S variant was constructed to exhibit increased PET hydrolytic activity as a result of the rearrangement of the active site conformation, thereby providing new knowledge on the structural features required for efficient polyester degradation. Based on previous reports regarding the PET polymer chain mobility associated with enzymatic degradation (Wei et al., 2019a,b), Falkenstein et al. could evaluate the feasibility of UV radiation as a potential pretreatment method to stimulate the subsequent biocatalytic depolymerization of PET. Although UV treatment has caused significant chain scissions at the surface layer of amorphous PET films, the resulting increased surface crystallinity drastically impaired the efficiency of enzymatic degradation.

As engineered whole-cell catalysts have been recently considered with great potential for plastic degradation (Yan et al., 2020), the microbial metabolism of plastic monomers and additives will become a research focus both in the contexts of environmental degradation of plastic pollution and of biotechnological plastic upcycling, i.e., utilization of plastic

hydrolysates as feedstocks for microbial production of chemicals with high value (Wierckx et al., 2015; Salvador et al., 2019; Ru et al.). Carstens et al. characterized the biotransformation of phthalate esters, ubiquitously used as plasticizers, by marine, freshwater, and terrestrial fungi. This study indicated an important role of fungi in the environmental biodegradation of complex plastic-derived molecules. Cárdenas Espinosa et al. isolated *Pseudomonas* sp. TDA1 which was able to grow on an oligomeric PUR diol solution, as well as on the PUR-derived 2,4-diaminotoluene. Li et al. took a laboratory evolution and reverse engineering approach to enable efficient metabolism of 1,4-butanediol by *P. putida* KT2440, and to characterize the underlying pathways and their regulation. This work builds upon the previous engineering (Franden et al., 2018) and evolution (Li et al., 2019) of *P. putida* KT2440 on ethylene glycol. One third of the original research papers are focused on *Pseudomonas*, including two on monomer metabolism (Cárdenas Espinosa et al.; Li et al.) and one as a source of plastic-degrading enzymes (Bollinger et al.). This is not surprising given the conspicuous potential of this organism in this field of research (Wierckx et al., 2015; Wilkes and Aristilde, 2017; Schwanemann et al., 2020; Ru et al.), especially concerning plastics upcycling (Tiso et al., 2020).

In summary, this Research Topic collects 11 scientific contributions which consolidate and expand our knowledge on the recent advances in this very active research field. We sincerely hope that more scientists will be inspired and encouraged by our Research Topic to make their own contributions to tackle the global challenge caused by plastic pollution.

AUTHOR CONTRIBUTIONS

All authors contributed to writing and approval of this editorial.

ACKNOWLEDGMENTS

The authors acknowledge the financial support provided by the MIX-UP project which has received funding from the European Union's Horizon 2020 research and innovation programme under Grant Agreement No. 870294. NW further acknowledges funding from the Bio Based Industries Joint Undertaking under the European Union's Horizon 2020 research and innovation programme under Grant Agreement No. 887711 for the project Glaukos.

REFERENCES

- Borrelle, S. B., Ringma, J., Law, K. L., Monnahan, C. C., Lebreton, L., Mcgivern, A., et al. (2020). Predicted growth in plastic waste exceeds efforts to mitigate plastic pollution. *Science* 369, 1515–1518. doi: 10.1126/science.aba3656
- Franden, M. A., Jayakody, L. N., Li, W.-J., Wagner, N. J., Cleveland, N. S., Michener, W. E., et al. (2018). Engineering *Pseudomonas putida* KT2440 for efficient ethylene glycol utilization. *Metab. Eng.* 48, 197–207. doi: 10.1016/j.ymben.2018.06.003
- Li, W.-J., Jayakody, L. N., Franden, M. A., Wehrmann, M., Daun, T., Hauer, B., et al. (2019). Laboratory evolution reveals the metabolic and regulatory basis of ethylene glycol metabolism by *Pseudomonas putida* KT2440. *Environ. Microbiol.* 21, 3669–3682. doi: 10.1111/1462-2920.14703
- Min, K., Cui, F., and Mathers, R. T. (2020). Ranking environmental degradation trends of plastic marine debris based on physical properties and molecular structure. *Nat. Commun.* 11:727. doi: 10.1038/s41467-020-14538-z
- Salvador, M., Abdulmutalib, U., Gonzalez, J., Kim, J., Smith, A. A., Faulon, J.-L., et al. (2019). Microbial genes for a circular and sustainable bio-PET economy. *Genes* 10:373. doi: 10.3390/genes10050373
- Schwanemann, T., Otto, M., Wierckx, N., and Wynands, B. (2020). *Pseudomonas* as versatile aromatics cell factory. *Biotechnol. J.* 15:1900569. doi: 10.1002/biot.201900569

- Tiso, T., Narancic, T., Wei, R., Pollet, E., Beagan, N., Schröder, K., et al. (2020). Bio-upcycling of polyethylene terephthalate. *bioRxiv [Preprint]*. doi: 10.1101/2020.03.16.993592
- Wei, R., Breite, D., Song, C., Gräning, D., Ploss, T., Hille, P., et al. (2019a). Biocatalytic degradation efficiency of postconsumer polyethylene terephthalate packaging determined by their polymer microstructures. *Adv. Sci.* 6:1900491. doi: 10.1002/advs.201900491
- Wei, R., Song, C., Gräning, D., Schneider, T., Bielytskyi, P., Böttcher, D., et al. (2019b). Conformational fitting of a flexible oligomeric substrate does not explain the enzymatic PET degradation. *Nat. Commun.* 10:5581. doi: 10.1038/s41467-019-13492-9
- Wei, R., Tiso, T., Bertling, J., O'Connor, K., Blank, L. M., and Bornscheuer, U. T. (2020). Possibilities and limitations of biotechnological plastic degradation and recycling. *Nat. Catal.* 3, 867–871. doi: 10.1038/s41929-020-00521-w
- Wei, R., and Zimmermann, W. (2017). Biocatalysis as a green route for recycling the recalcitrant plastic polyethylene terephthalate. *Microb. Biotechnol.* 10, 1302–1307. doi: 10.1111/1751-7915.12714
- Wierckx, N., Narancic, T., Eberlein, C., Wei, R., Drzyzga, O., Magnin, A., et al. (2018). “Plastic biodegradation: Challenges and opportunities,” in *Consequences of Microbial Interactions With Hydrocarbons, Oils, and Lipids: Biodegradation and Bioremediation*, ed R. Steffan (Cham: Springer International Publishing), 1–29.
- Wierckx, N., Prieto, M. A., Pomposiello, P., De Lorenzo, V., O'Connor, K., and Blank, L. M. (2015). Plastic waste as a novel substrate for industrial biotechnology. *Microb. Biotechnol.* 8, 900–903. doi: 10.1111/1751-7915.12312
- Wilkes, R. A., and Aristilde, L. (2017). Degradation and metabolism of synthetic plastics and associated products by *Pseudomonas* sp.: capabilities and challenges. *J. Appl. Microbiol.* 123, 582–593. doi: 10.1111/jam.13472
- Yan, F., Wei, R., Cui, Q., Bornscheuer, U. T., and Liu, Y.-J. (2020). Thermophilic whole-cell degradation of polyethylene terephthalate using engineered *Clostridium thermocellum*. *Microb. Biotechnol.* doi: 10.1111/1751-7915.13580. [Epub ahead of print].

Conflict of Interest: The authors declare that the research was conducted in the absence of any commercial or financial relationships that could be construed as a potential conflict of interest.

Copyright © 2021 Wei and Wierckx. This is an open-access article distributed under the terms of the Creative Commons Attribution License (CC BY). The use, distribution or reproduction in other forums is permitted, provided the original author(s) and the copyright owner(s) are credited and that the original publication in this journal is cited, in accordance with accepted academic practice. No use, distribution or reproduction is permitted which does not comply with these terms.



A Quantum Mechanism Study of the C-C Bond Cleavage to Predict the Bio-Catalytic Polyethylene Degradation

Junyu Xu¹, Ziheng Cui¹, Kaili Nie¹, Hao Cao², Min Jiang³, Haijun Xu¹, Tianwei Tan¹ and Luo Liu^{1*}

¹ Beijing Key Laboratory of Bioprocess, Beijing University of Chemical Technology, Beijing, China, ² Laboratory of Biomufacturing and Food Engineering, Institute of Food Science and Technology, Chinese Academy of Agricultural Sciences, Beijing, China, ³ State Key Laboratory of Materials-Oriented Chemical Engineering, College of Biotechnology and Pharmaceutical Engineering, Nanjing University of Technology, Nanjing, China

OPEN ACCESS

Edited by:

Ren Wei,
Leipzig University, Germany

Reviewed by:

Bo Yu,
Institute of Microbiology (CAS), China
Jan Baeyens,
University of Warwick,
United Kingdom

*Correspondence:

Luo Liu
liuluo@mail.buct.edu.cn

Specialty section:

This article was submitted to
Microbiotechnology, Ecotoxicology
and Bioremediation,
a section of the journal
Frontiers in Microbiology

Received: 07 February 2019

Accepted: 26 February 2019

Published: 12 March 2019

Citation:

Xu J, Cui Z, Nie K, Cao H,
Jiang M, Xu H, Tan T and Liu L (2019)
A Quantum Mechanism Study of the
C-C Bond Cleavage to Predict
the Bio-Catalytic Polyethylene
Degradation.
Front. Microbiol. 10:489.
doi: 10.3389/fmicb.2019.00489

The growing amount of plastic solid waste (PSW) is a global concern. Despite increasing efforts to reduce the residual amounts of PSW to be disposed off through segregated collection and recycling, a considerable amount of PSW is still landfilled and the extent of PSW ocean pollution has become a worldwide issue. Particularly, polyethylene (PE) and polystyrene (PS) are considered as notably recalcitrant to biodegradation due to the carbon-carbon backbone that is highly resistant to enzymatic degradation via oxidative reactions. The present research investigated the catalytic mechanism of P450 monooxygenases by quantum mechanics to determine the bio-catalytic degradation of PE or PS. The findings indicated that the oxygenase-induced free radical transition caused the carbon-carbon backbone cleavage of aliphatic compounds. This work provides a fundamental knowledge of the biodegradation process of PE or PS at the atomic level and facilitates predicting the pathway of plastics' biodegradation by microbial enzymes.

Keywords: polyethylene, oxidation, carbon-carbon bond cleavage, quantum mechanism, bond dissociation energy (BDE)

INTRODUCTION

Plastics are widely used in industrial and household applications because of their low weight, durability and low production cost (Andrady, 2015). However, the growing amount of plastic solid waste (PSW) is a global concern. The widespread use of plastics, the lack of waste management and casual social behavior, however, pose a major threat to the environment (Leja and Lewandowicz, 2010). Despite increasing efforts to reduce the residual amounts of PSW to be disposed off through segregated collection and recycling, a considerable amount of PSW is still landfilled and the extent of PSW ocean pollution has become a worldwide issue (Baeyens et al., 2010; Brems et al., 2012).

Considering their abundance of plastics in the environment, biodegradation of plastics could be the most effective way. Decades ago, several biodegradable aliphatic polyesters such as PLA and

PHB, were produced to replace petrochemical plastics (Tokiwa et al., 2009). However, the most commonly used plastics are still synthetic polymers obtained from petrochemical hydrocarbons and derivatives (Geyer et al., 2017). Polyethylene (PE) and polystyrene (PS) are amongst the most important mass-produced plastics and largely manufactured into short-life products including packaging materials for food and disposable dishware (Plastics Europe, 2018). PE and PS are highly stable polymers and notably resistant to biodegradation (Ho et al., 2017). The carbon-carbon backbone in PE and PS is highly resistant to enzymatic cleavage by oxidation-reduction (Goldman, 2010). Additionally, the high molecular weight and strong hydrophobic character hamper their biodegradation (Albertsson and Karlsson, 1993).

Recently, several microbes and microbial enzymes have been shown able to catalyze the degradation of various petrochemical plastics including PE and PS (Wei and Zimmermann, 2017). Shimpi et al. (2012) reported the biodegradation of modified PS by using a pure strain of *Pseudomonas aeruginosa*. Motta et al. (2009) used the *Curvularia* species to investigate the degradation of atactic PS. These results suggested that the biodegradation of PS material through using selected microbial strains might become a feasible solution for reducing the huge amount of waste and disposed plastics.

Sivan et al. isolated the actinomycete *Rhodococcus ruber* (C208) to degrade PE and PS (Mor and Sivan, 2008; Santo et al., 2013), and demonstrated that laccase, a copper-binding enzyme, played a crucial role in the oxidation and degradation of PE by *R. ruber* (Santo et al., 2013). In addition to laccase, several oxidoreductases were shown to be involved in the biodegradation of PE and PS, such as the AlkB family hydroxylases and hydroquinone peroxidase (Nakamiya et al., 1997; Jeon and Kim, 2015).

The catalytic mechanism of oxidoreductases with respect to the cleavage of PE and PS still remains unexplained. The present work applied quantum mechanism calculations to unveil the bio-catalytic mechanism of PE and PS degradation by oxidoreductase, with the P450 monooxygenase catalyzed reaction being treated as a typical saturated carbon-carbon bond cleavage reaction (Matthews et al., 2017). This work attempts to provide fundamental insights into the possible biodegradation of plastics with a C-C backbone.

MATERIALS AND METHODS

Computation Methods

In this work, geometry optimizations, relaxed scan and natural population analysis (NPA) charges were calculated by the Gaussian 09 software package (Frisch et al., 2013) at the B3LYP/6-31+G(d,p) theoretical level. The frequency of structures was also calculated at same level to ensure that the stable structures have no imaginary frequency, and only one imaginary frequency for the transition state. Fuzzy bond orders, spin density and spin population analysis were calculated by Multiwfn (Lu and Chen, 2012). Relaxed force constants were calculated by Compliance (Brandhorst and Grunenberg, 2008; Brandhorst and Grunenberg, 2010).

Analysis of Three Bond Strength Descriptors

The bond dissociation energy (BDE), widely used in the literature as a kind of bond strength descriptor can be defined as the standard enthalpy (H) change when a bond is cleaved by homolysis to produce two fragments. In some cases, it is however better to calculate the standard enthalpy change when a bond is cleaved by heterolysis. These calculations of Bond Dissociation Energy (BDE, at 298K) are shown in the following equation:

$$BDE(298K) = H(RH_2\bullet) + H(\bullet COOH) - H(RCH_2 - COOH)$$

However, the numerical value of BDE, as an intrinsic strength of a particular bond, depends on the stable molecule and the stability of the fragments, such as electronic ground state, minimum conformation, etc. (Grunenberg, 2017). The bond order is a quantitative description of chemical bonds and has been widely used by chemists to understand the nature of molecular electronic structure and predict the molecular reactivity, aromaticity, and stability (Lu and Chen, 2013). The fuzzy bond order exhibits very little basis set sensitivity and will not be deteriorated by using diffuse basis functions (Mayer and Salvador, 2004). For the same type of bonds, the fuzzy bond order positively correlates to bond strength.

Force constants are widely used as an intuitive bond strength descriptor. However, the numerical values of rigid force constants depend on the choice of coordinate systems. In order to overcome this disadvantage and achieve a higher precision, the compliance matrix, which is a second-order tensor containing non-zero coupling elements (Grunenberg, 2017), was adopted in this work to describe the bond strength.

RESULTS AND DISCUSSION

Model Structures and Charge Distribution Analysis

In this work, the structures of **Figure 1** were investigated to determine the cleavage of the C-C bond close to the carboxyl group under both acidic or alkaline conditions. Since the four molecules are very similar, spin density and NPA charges were calculated to ensure that these structures are reliable. The bond length of the C2-C3 bonds (C3 is the alpha carbon, C2 is the carboxylic carbon atom) in the molecules and the NPA charges of certain atoms are given in **Table 1**. It is specifically mentioned here that for the structure shown in **Figures 1A,E**, a stable configuration is not obtained after a plenty of structural optimizations. The C2-C3 bond cleavage occurred in every optimization attempt with molecule **Figure 1E** as the initial structure. Therefore, structures with optimization are adopted as the basis for this part of the study.

The results of the spin density in **Figure 1** show that there are no unpaired electrons in the ionic structures, while some unpaired electrons exist in the free radical structures mainly in O1, O4, and C5. As shown in **Table 1**, NPA charges of the C5s in ionic structures for both an alkaline and an acidic environment are positive, while the NPA charges are negative for the two other

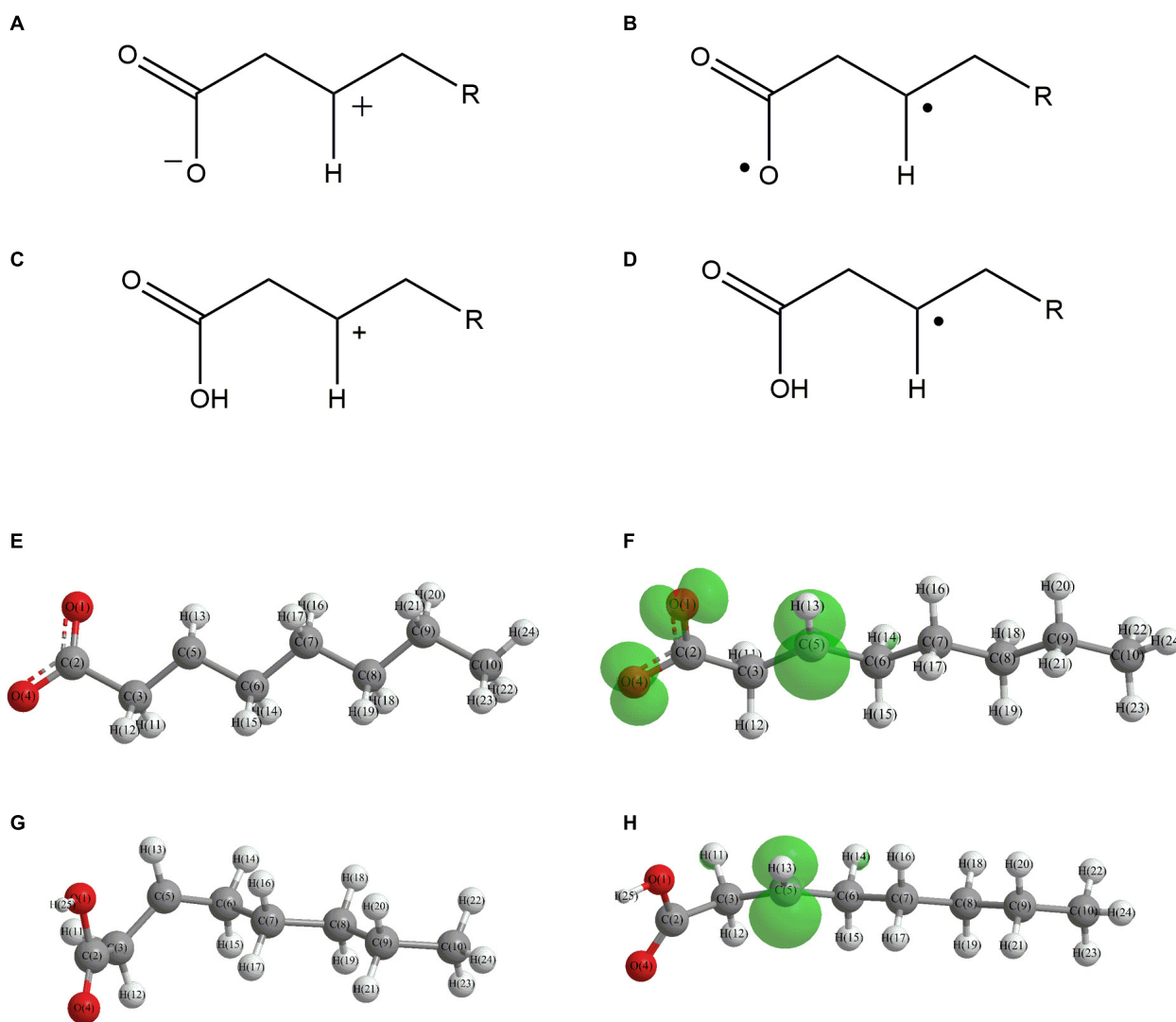


FIGURE 1 | Molecular structure: **(A)** Ionic structure in alkaline condition; **(B)** Free radical structure in alkaline condition; **(C)** Ionic structure in acidic condition; **(D)** Free radical structure in acidic condition. **(E–H)** are corresponding spin density for molecules **(A–D)**, which was marked with green. The value of the iso-surface is 0.01. The carbon atoms, C2 is the carboxylic carbon atom, C3 is the alpha carbon.

TABLE 1 | Bond lengths of C2–C3 bonds and certain atomic NPA charges.

molecule	bond lengths of C2–C3 bonds/ Å	NPA charges of C5/a.u.	NPA charges of O1/a.u.	NPA charges of O4/a.u.
	1.569	0.173	−0.625	−0.579
	1.502	−0.128	−0.473	0.388
	1.551	0.230	−0.506	−0.723
	1.515	−0.124	−0.735	−0.604

structures. Compared to the NPA charges of oxygen atoms of the ionic structure, there are more negative charges in the oxygen atom O1 in ionic structure in alkaline environment. Therefore, these structures are appropriate for further calculations.

Effect of the Structure on C–C Bond Cleavage

The Ionic Structure Under Alkaline Condition

For structure **(A)** of **Figure 1**, no stable corresponding structure was obtained after several rounds of optimization. Therefore, an optimized free fatty acid was used as template, a hydride ion at C_β was removed to obtain the approximate structure for further calculation. The approximate structure is shown in **Figure 1E**.

Firstly, a geometry optimization was performed for this structure, and the result is shown in **Figure 2A**. It is obvious

that the molecule is cleaved into a linear olefin and CO₂ which are obtained from the cleavage of the fatty acid carboxylate. Then, a potential energy surface relaxed scan was performed along the distance of the C2-C3 bond in the molecule as shown in **Figure 1E**, to describe the energy of this system. The result of the scan is shown in **Figure 2B**, demonstrating that the energy decreases quickly as the distance increases initially, which indicates that the C2-C3 bond in the molecule as shown in **Figure 1A** is very unstable.

For a more thorough study, the transition state which is shown in **Figure 3A**, was also calculated based upon the unstable structure as shown in **Figure 1E**. The vibration direction of the imaginary frequency is mainly along the direction of the C2-C3 bond stretching. A stable structure with a minimum in potential energy surface and connecting the transition state structure was calculated as shown in **Figure 3B**. The stable structure consists of a linear olefin and CO₂ as the products derived from the cleavage of fatty acids. The energy of the molecule, as shown in **Figure 1E** is 110.7 kJ/mol higher than the energy of the transition state, which confirms the high instability of the molecule as shown in **Figure 1E**. Through the above calculations, it is clear that the ionic structure in an alkaline environment is close to the transition state structure

in its potential energy surface, which indicates the instability of the C2-C3 bond.

The Free Radical Structure Under Alkaline Condition

Based upon the free radical structure in an alkaline environment as shown in **Figure 1F**, a transition state optimization was carried out. The change of spin multiplicity caused by the cleavages of C2 and C3 did not consider here. The distance of C2-C3 in this transition structure is 2.23 Å, which means that this molecule is divided into two parts. **Table 2** and **Figure 4** show the result of the spin population analysis which was carried out to determine the distribution of single electrons in the transition structure. This analysis shows that more than 80% (about two electrons) of single electrons are on the part of the free carboxyl group, indicating that a linear olefin was produced. Assessing the normal mode corresponding to the imaginary frequency, it was found that the composing displacements tend to lead in the directions of the structure derived from the cleavage of the fatty acid carboxylate. Therefore, the transition state structure connects the product consisting of a linear olefin and CO₂. The energy of the transition state includes zero-point correction and is 109.8 kJ/mol relative to the molecule as shown in **Figure 1F**. Due to the high energy of the transition state, it is not easy to cleave the bond in this structure.

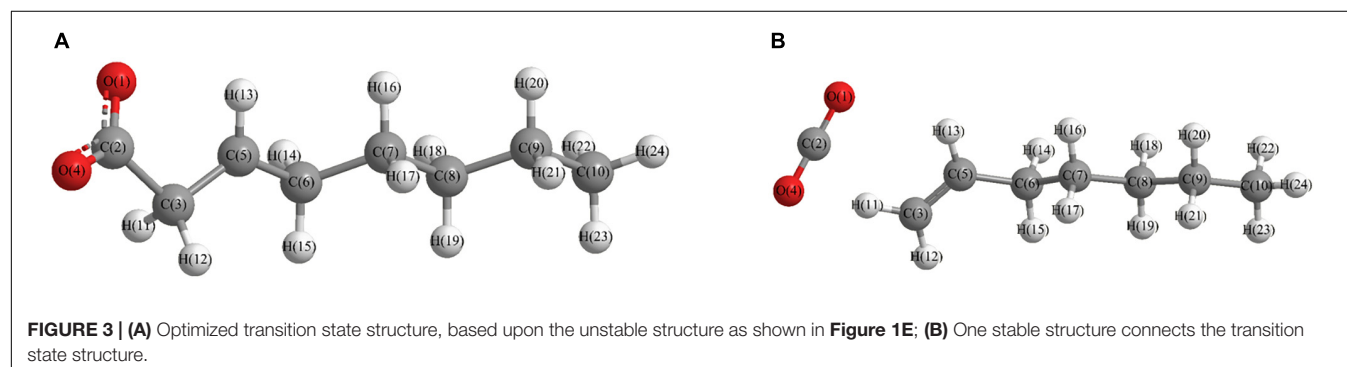
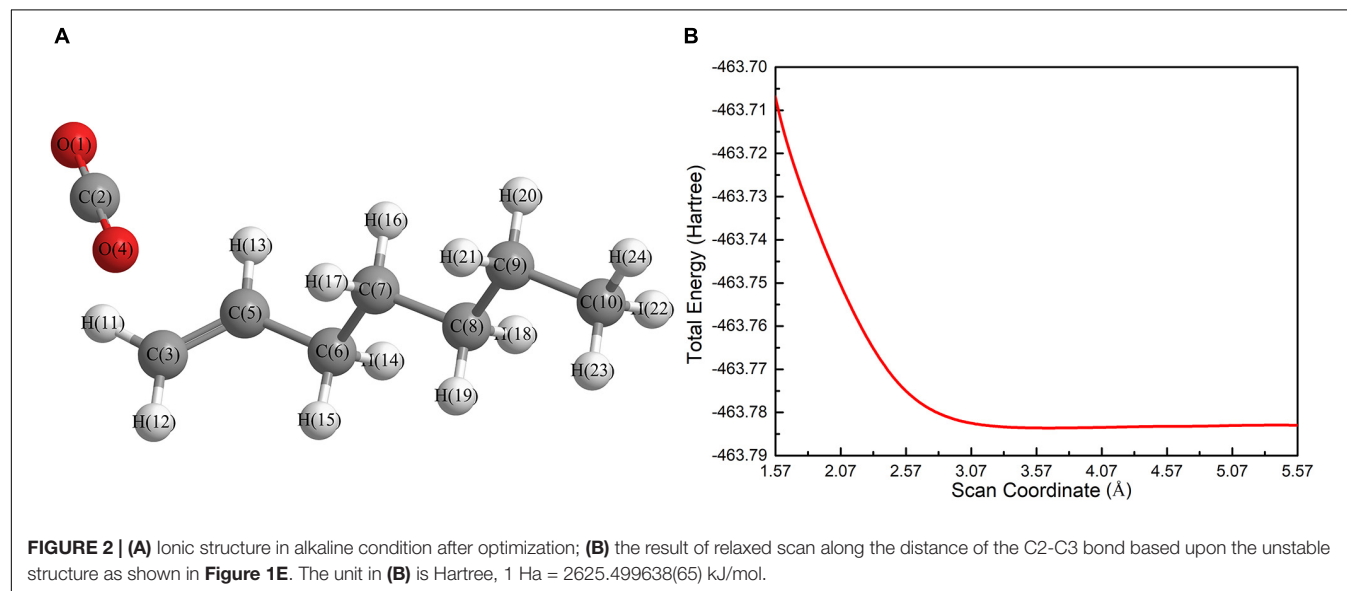
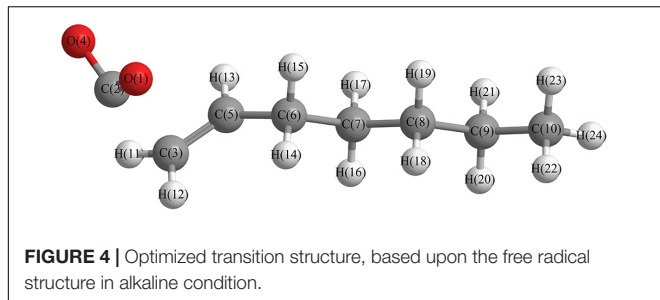


TABLE 2 | Result of spin population analysis based on the transition structure shown in **Figure 4**.

Atomic space	Value	% of sum	% of sum abs
O1	0.64107952	32.054013	30.046278
C2	0.42337472	21.168761	19.842834
C3	-0.06553244	-3.276626	-3.071391
O4	0.64994558	32.497317	30.461815
C5	0.30392666	15.196351	14.244512

**TABLE 3** | Bond orders, relaxed force constants and BDEs of the C2-C3 bonds in the selected molecules.

Selected molecules			
bond orders of C2-C3 bond	1.073	1.065	0.98
relaxed force constants of C2-C3 bond (mdyn/Å)	4.237	4.184	2.941
BDE (kJ/mol)	351.86	350.07	279.84

As can be seen from **Table 3**, when a hydrogen atom has been removed from C_β, the changes of BDEs, relaxed force constants and the bond orders are very small. So the C2-C3 bond strengths in both structures are very similar and the lack of a hydrogen atom at the location of C_β has little influence on the C2-C3 bond strength.

By comparing the third column with the fourth column in **Table 3**, it is obvious that the bond order, relaxed force and BDE of the C2-C3 bond in the free radical structure in an alkaline environment are much higher than the C2-C3 bond in a carboxylate anion, which indicates that the C2-C3 bond strength of the free radical structure in an alkaline environment is stronger. Because decarboxylation is less favorable at low temperatures and highly sensitive to conditions for carboxylic acids, decarboxylation of the molecule in **Figure 1F** is more difficult.

Ionic Structure Under Acidic Condition

If there is a linear olefin produced, the C2-C3 bond in this structure should be cleaved by heterolysis, and hence **Table 4** gives the heterolytic bond dissociation energies of the C2-C3 bonds. By comparing the second and the fourth columns in **Table 4**, it can be seen that the values of the bond order, relaxed force constant, BDE and heterolytic bond dissociation energy of

the C2-C3 bond become much smaller when a hydrogen anion is removed from C_β in a carboxylic acid, which indicates that the bond strength becomes much weaker. Comparing the fourth column in **Table 4** to the fourth column in **Table 3**, it can be seen that the values of the bond orders, the relaxed force constants and the BDEs of the C2-C3 bonds are very close, so the C2-C3 bond strengths in the two structures are basically the same.

As the absence of a hydrogen anion in a carboxylic acid may cause the O-H bond to become weaker, it was decided to investigate the O-H bond strength of the ionic structure in an acidic environment and determine whether it has an impact on the decarboxylation. As can be seen from **Table 4**, when a hydrogen anion is removed from C_β in a carboxylic acid, the values of the bond order and the relaxed force constant of the O-H bond decrease slightly and the heterolytic bond dissociation energies of the O-H bond become much smaller. The reason why the heterolytic bond dissociation energy varies significantly may be due to the major configuration changes from the segmentation optimization calculation (C-C bond cleavage), which affects the calculation of the heterolytic bond dissociation energy. In summary, the absence of a hydride ion does not significantly affect the strength of the O-H bond and therefore does not affect C-C bond cleavage.

TABLE 4 | Bond orders, relaxed force constants, BDEs and heterolytic bond dissociation energies of the C2-C3/O-H bonds in the structures of selected molecules.

Selected molecules				
Bonds	C2-C3	O-H	C2-C3	O-H
bond order of C2-C3/O-H bond	1.039	0.833	0.965	0.807
relaxed force constant of C2-C3/O-H bond (mdyn/Å)	4.115	7.813	2.915	7.692
BDE (kJ/mol)	363.32	–	269.58	–
heterolytic bond dissociation energy (kJ/mol)	1173.24	1437.5	216.08	748.33

TABLE 5 | Bond orders, relaxed force constants, BDEs and heterolytic bond dissociation energies of the C2-C3/O-H bonds in the structures of selected molecules.

Selected molecules				
Bonds	C2-C3	O-H	C2-C3	O-H
bond order of C2-C3/O-H bond	1.039	0.833	1.033	0.831
relaxed force constant of C2-C3/O-H bond (mdyn/Å)	4.115	7.813	3.968	7.813
BDE (kJ/mol)	363.32	–	361.13	–
heterolytic bond dissociation energy (kJ/mol)	–	1437.50	–	1422.34

Free Radical Structure Under Acidic Condition

Table 5 shows that the bond order, relaxed force constant, and BDE of C2-C3 bond are not significantly changed in the absence of a hydride atom at C_β position. Moreover, the bond order, relaxed force constant, and BDE of this structure are much larger than the corresponding value of molecule in the fourth column of **Table 3**. Therefore, the bond strength of C2-C3 bond in this structure is very high. **Table 5** also shows that the bond order, relaxed force constant, heterolytic bond dissociation energy of O-H bond do not change significantly, in the absence of a hydride atom at C_β position, indicating that the bond strength of the O-H bond does not change significantly, and hence does not affect C-C bond cleavage.

In summary, in the ionic structure, the absence of a hydrogen anion at the C_β position significantly reduces the bond strength of C2-C3. Therefore, whether in an acidic environment or an alkaline environment, C-C bond cleavage is more likely to occur in the ionic structures. On the other hand, in an alkaline environment, the C2-C3 bond is more unstable because of the presence of a carboxylate anion that promotes the tendency of push electrons. Therefore, the ionic structure under alkaline conditions is most advantageous for the removal of carboxyl groups.

CONCLUSION

The enzymatic cleavage of C-C bond in aliphatic compounds by quantum mechanism calculation was investigated. Under

certain conditions, the enzyme could abstract a hydrogen anion from the aliphatic compounds, causing the absence of a hydride anion at the C_β position, which significantly reduces the bond strength of C2-C3 bond and finally results in the C-C bond cleavage. The results reveal that oxidase or oxygenase could be involved in the C-C bond cleavage in PE/PS, thus facilitating their biodegradation.

DATA AVAILABILITY

All datasets generated for this study are included in the manuscript and/or the supplementary files.

AUTHOR CONTRIBUTIONS

TT, MJ, HX, and LL conceived and designed the experiments. JX and ZC carried out the experiments. JX, ZC, KN, and HC analyzed the data. All authors wrote the manuscript.

FUNDING

This study was funded by the National Natural Science Foundation of China (Grant Number 21676016, 21861132017, 21676015, and 21838001), and the Fundamental Research Funds for the Central Universities (XK1802-8).

REFERENCES

- Albertsson, A. C., and Karlsson, S. (1993). Aspects of biodeterioration of inert and degradable polymers. *Int. Biodeterior. Biodegradation* 31, 161–170. doi: 10.1016/0964-8305(93)90002-J
- Andrady, A. L. (2015). *Plastic Products: Plastics and Environmental Sustainability*. Hoboken, NJ: John Wiley & Sons, 83–119. doi: 10.1002/9781119009405.ch4
- Baeyens, J., Brems, A., and Dewil, R. (2010). Recovery and recycling of post-consumer waste materials. Part 2. Target wastes (glass beverage bottles, plastics, scrap metal and steel cans, end-of-life tyres, batteries and household hazardous waste). *Int. J. Sustain. Eng* 3, 232–245. doi: 10.1080/19397038.2010.507885
- Brandhorst, K., and Grunenberg, J. (2008). How strong is it? The interpretation of force and compliance constants as bond strength descriptors. *Chem. Soc. Rev.* 37, 1558–1567. doi: 10.1039/b717781j
- Brandhorst, K., and Grunenberg, J. (2010). Efficient computation of compliance matrices in redundant internal coordinates from Cartesian Hessians for nonstationary points. *J. Chem. Phys.* 132:184101. doi: 10.1063/1.3413528
- Brems, A., Baeyens, J., and Dewil, R. (2012). Recycling and recovery of post-consumer plastic solid waste in a European context. *Thermal Sci.* 16, 1027–1035. doi: 10.2298/TSCI120111121B
- Frisch, M. J., Trucks, G. W., Schlegel, H. B., Scuseria, G. E., Robb, M. A., Cheeseman, J. R., et al. (2013). *Gaussian 09, Revision D.01*. Wallingford, CT: Gaussian, Inc.
- Geyer, R., Jambeck, J. R., and Law, K. L. (2017). Production, use, and fate of all plastics ever made. *Sci. Adv.* 3:e1700782. doi: 10.1126/sciadv.1700782
- Goldman, A. S. (2010). ChemInform Abstract: organometallic chemistry: carbon—carbon bonds get a break. *Nature* 463, 435–436. doi: 10.1038/463435a
- Grunenberg, J. (2017). Ill-defined chemical concepts: the problem of quantification. *Int. J. Quantum. Chem.* 117:e25359. doi: 10.1002/qua.25359
- Ho, B. T., Roberts, T. K., and Lucas, S. (2017). An overview on biodegradation of polystyrene and modified polystyrene: the microbial approach. *Crit. Rev. Biotechnol.* 38, 1–13. doi: 10.1080/07388551.2017.1355293
- Jeon, H. J., and Kim, M. N. (2015). Functional analysis of alkane hydroxylase system derived from *Pseudomonas aeruginosa* E7 for low molecular weight polyethylene biodegradation. *Int. Biodeterior. Biodegradation* 103, 141–146. doi: 10.1016/j.ibiod.2015.04.024
- Leja, K., and Lewandowicz, G. (2010). Polymer biodegradation and biodegradable polymers - a review. *Pol. J. Environ. Stud.* 19, 255–266.
- Lu, T., and Chen, F. (2012). Multiwfn: a multifunctional wavefunction analyzer. *J. Comput. Chem.* 33, 580–592. doi: 10.1002/jcc.22885
- Lu, T., and Chen, F. (2013). Bond order analysis based on laplacian of electron density in fuzzy overlap space. *J. Phys. Chem. A* 117, 3100–3108. doi: 10.1021/jp4010345
- Matthews, S., Belcher, J. D., Tee, K. L., Girvan, H. M., Mclean, K. J., Rigby, S. E., et al. (2017). Catalytic Determinants of Alkene Production by the Cytochrome P450 Peroxygenase OleTJE. *J. Biol. Chem.* 292, 5128–5143. doi: 10.1074/jbc.M116.762336
- Mayer, I., and Salvador, P. (2004). Overlap populations, bond orders and valences for ‘fuzzy’ atoms. *Chem. Phys. Lett.* 383, 368–375. doi: 10.1016/j.cplett.2003.11.048
- Mor, R., and Sivan, A. (2008). Biofilm formation and partial biodegradation of polystyrene by the actinomycete *Rhodococcus ruber*. *Biodegradation* 19, 851–858. doi: 10.1007/s10532-008-9188-0
- Motta, O., Proto, A., De, C. F., De, C. F., Santoro, E., Brunetti, L., et al. (2009). Utilization of chemically oxidized polystyrene as co-substrate by filamentous fungi. *Int. J. Hyg. Environ. Health* 212, 61–66. doi: 10.1016/j.ijheh.2007.09.014
- Nakamiya, K., Sakasita, G., Ooi, T., and Kinoshita, S. (1997). Enzymatic degradation of polystyrene by hydroquinone peroxidase of *Azotobacter beijerinckii* HM121. *J. Biosci. Bioeng.* 84, 480–482. doi: 10.1016/S0922-338X(97)82013-2
- Plastics Europe (2018). *Plastics – the Facts 2018*. Available at: www.plasticseurope.org retrieved in 2018.
- Santo, M., Weitsman, R., and Sivan, A. (2013). The role of the copper-binding enzyme - laccase - in the biodegradation of polyethylene by the actinomycete

- Rhodococcus ruber. *Int. Biodeterior. Biodegradation* 84, 204–210. doi: 10.1016/j.ibiod.2012.03.001
- Shimpi, N., Mishra, S., and Kadam, M. (2012). Biodegradation of polystyrene (PS)-poly(lactic acid) (PLA) nanocomposites using *Pseudomonas aeruginosa*. *Macromol. Res.* 20, 181–187. doi: 10.1007/s13233-012-0026-1
- Tokiwa, Y., Calabia, B. P., Ugwu, C. U., and Aiba, S. (2009). Biodegradability of Plastics. *Int. J. Mol. Sci.* 10, 3722–3742. doi: 10.3390/ijms10093722
- Wei, R., and Zimmermann, W. (2017). Microbial enzymes for the recycling of recalcitrant petroleum-based plastics: How far are we? *Microb. Biotechnol.* 10, 1308–1322. doi: 10.1111/1751-7915.12710

Conflict of Interest Statement: The authors declare that the research was conducted in the absence of any commercial or financial relationships that could be construed as a potential conflict of interest.

Copyright © 2019 Xu, Cui, Nie, Cao, Jiang, Xu, Tan and Liu. This is an open-access article distributed under the terms of the Creative Commons Attribution License (CC BY). The use, distribution or reproduction in other forums is permitted, provided the original author(s) and the copyright owner(s) are credited and that the original publication in this journal is cited, in accordance with accepted academic practice. No use, distribution or reproduction is permitted which does not comply with these terms.



Shotgun Metagenomics Reveals the Benthic Microbial Community Response to Plastic and Bioplastic in a Coastal Marine Environment

Lee J. Pinnell and Jeffrey W. Turner*

Department of Life Sciences, Texas A&M University – Corpus Christi, Corpus Christi, TX, United States

OPEN ACCESS

Edited by:

Ren Wei,
Leipzig University, Germany

Reviewed by:

Michael Pester,
German Collection of
Microorganisms and Cell Cultures
GmbH (DSMZ), Germany
Dirk Tischler,
Ruhr University Bochum, Germany

*Correspondence:

Jeffrey W. Turner
jeffrey.turner@tamucc.edu

Specialty section:

This article was submitted to
Microbiotechnology, Ecotoxicology
and Bioremediation,
a section of the journal
Frontiers in Microbiology

Received: 14 February 2019

Accepted: 20 May 2019

Published: 07 June 2019

Citation:

Pinnell LJ and Turner JW (2019)
Shotgun Metagenomics Reveals the
Benthic Microbial Community
Response to Plastic and Bioplastic in
a Coastal Marine Environment.
Front. Microbiol. 10:1252.
doi: 10.3389/fmicb.2019.01252

Plastic is incredibly abundant in marine environments but little is known about its effects on benthic microbiota and biogeochemical cycling. This study reports the shotgun metagenomic sequencing of biofilms fouling plastic and bioplastic microcosms staged at the sediment–water interface of a coastal lagoon. Community composition analysis revealed that plastic biofilms were indistinguishable in comparison to a ceramic biofilm control. By contrast, bioplastic biofilms were distinct and dominated by sulfate-reducing microorganisms (SRM). Analysis of bioplastic gene pools revealed the enrichment of esterases, depolymerases, adenylyl sulfate reductases (*aprBA*), and dissimilatory sulfite reductases (*dsrAB*). The nearly 20-fold enrichment of a phylogenetically diverse polyhydroxybutyrate (PHB) depolymerase suggests this gene was distributed across a mixed microbial assemblage. The metagenomic reconstruction of genomes identified novel species of *Desulfovibrio*, *Desulfobacteraceae*, and *Desulfobulbaceae* among the abundant SRM, and these genomes contained genes integral to both bioplastic degradation and sulfate reduction. Findings indicate that bioplastic promoted a rapid and significant shift in benthic microbial diversity and gene pools, selecting for microbes that participate in bioplastic degradation and sulfate reduction. If plastic pollution is traded for bioplastic pollution and sedimentary inputs are large, the microbial response could unintentionally affect benthic biogeochemical activities through the stimulation of sulfate reducers.

Keywords: plastic, bioplastic, biodegradation, sulfur cycling, coastal sediments, metagenomics

INTRODUCTION

Microorganisms rapidly colonize and form biofilms on biotic and abiotic surfaces in marine environments (Dang and Lovell, 2016). As such, marine microbial communities are commonly distinguished as free-living or particle-associated (DeLong et al., 1993; Crump et al., 1999; Hollibaugh et al., 2000). A particle-associated lifestyle is thought to provide microorganisms with increased nutritional resources and environmental stability (Azam et al., 1994). Detrital aggregates, in particular, are hot spots of microbial diversity that are fundamentally distinct in comparison to free-living communities (DeLong et al., 1993; Crump et al., 1999). Particles are also habitats of enhanced enzyme activity (Karner and Herndl, 1992; Kellogg and Deming, 2014) that contribute to the rapid turnover of particulate organic

matter (Biddanda and Pomeroy, 1988; Azam and Long, 2001) and it is clear that particle-associated microorganisms play an important role in biogeochemical processes (Ploug et al., 1999; Seymour et al., 2017).

Plastic pollution has introduced a new surface for microbial colonization and biofilm formation (Zettler et al., 2013; Oberbeckmann et al., 2014). A recent global assessment of all mass-produced plastics estimated that 4.9 billion tons of plastic waste was discarded in landfills or natural environments (Geyer et al., 2017). Oceans serve as a sink for said waste with an estimated 4.8–12.7 million metric tons entering the oceans annually (Jambeck et al., 2015; Geyer et al., 2017). It is clear that marine microorganisms colonize and form biofilms on floating plastic debris and it is also clear that plastic-associated microbial communities are distinct compared to free-living communities (Bryant et al., 2016; Oberbeckmann et al., 2016).

Several studies have characterized pelagic microbe-plastic interactions (Carson et al., 2013; Zettler et al., 2013; Bryant et al., 2016) but relatively few studies have characterized microbe-plastic interactions in benthic systems (Harrison et al., 2014; De Tender et al., 2015; Nauendorf et al., 2016). In the North Pacific Gyre, a previous study reported that microplastics were colonized by diatoms (Carson et al., 2013) and a separate study reported an increased concentration of Chl *a* and an increased abundance of nitrogenase genes in microplastic biofilms (Bryant et al., 2016). By contrast, understanding of benthic microbe-plastic interactions is limited. The transport of plastic debris to benthic systems is facilitated by sinking; debris with a density higher than seawater (1.02 g cm^{-3}) sinks immediately while floating debris loses buoyancy with biofouling (Barnes et al., 2009; Andrady, 2011). Sinking is therefore an important process and benthic systems are sinks for plastic debris accumulation (Thompson et al., 2004; Van Cauwenberghe et al., 2015).

In coastal regions, benthic microorganisms support primary producers in the overlying water column by the remineralization of organic-rich debris (Klump and Martens, 1981). The remineralization of carbon in anoxic coastal sediments is predominantly carried out *via* sulfate reduction (Jørgensen, 1977). The microbial pathway for dissimilatory sulfate reduction involves the reduction of sulfate to sulfite by sulfate adenylyltransferases (Sat) and adenylyl-sulfate reductases (AprBA), followed by the reduction of sulfite by sulfite reductases (DsrAB) (Anantharaman et al., 2018). Climate warming and eutrophication are expanding the distribution of anoxic sediments worldwide (Vigneron et al., 2018) and recent studies have clearly shown that sulfate and sulfite reducers are more abundant, diverse, and widespread than previously believed (Müller et al., 2014; Anantharaman et al., 2018; Hausmann et al., 2018; Vigneron et al., 2018; Zecchin et al., 2018). Yet, the effect plastic pollution may have on sulfate-reducing microorganisms (SRM) is an open question.

In 2018, the United Nations Environmental Program reported that more than 60 countries approved bans or levies on single-use plastics (UNEP, 2018). In the same year, the European Parliament approved a ban on the top 10 single-use plastics and called

for a reduction in single-use plastics (European Commission, 2018). The proposal states “this systemic change and material substitution will also promote bio-based alternatives and an innovative bioeconomy.” In the wake of legislative actions and increased public awareness, the production of bioplastics such as polyhydroxyalkanoate (PHA) is predicted to increase tenfold (Aeschelmann and Carus, 2015). If bioplastic is similarly discarded, the subsequent increase in bioplastic waste entering the oceans will introduce yet another surface for microbial colonization; and, while some research has investigated the response of marine organisms to bioplastic (Eich et al., 2015; Pauli et al., 2017), little is known about how microorganisms respond to bioplastic versus petroleum-based plastic.

The aim of this study was to characterize the microbial communities and individuals that form biofilms on plastic (polyethylene terephthalate; PET) and bioplastic (PHA) in a coastal benthic habitat. For comparative purposes, ceramic pellets were included as a biofilm control. This study was primarily designed to address two questions. Does the introduction of either plastic or bioplastic select for a distinct microbial community compared to a biofilm control, and does this introduction promote a significant shift in taxa or enzyme pools with implications for polymer degradation or biogeochemical cycling? We hypothesized that the PET biofilms would be indistinguishable from the ceramic biofilms whereas the introduction of PHA would select for the growth of a distinct microbial assemblage involved in polymer degradation and biogeochemical cycling.

MATERIALS AND METHODS

Site Description

The Laguna Madre (Texas, USA) is a large coastal lagoon in the northern Gulf of Mexico (NGOM). The lagoon is divided into two sections: Upper Laguna Madre (ULM) and Lower Laguna Madre (LLM). The microcosms described in this study were deployed adjacent to a dredge material island at $27^{\circ}32'39.0''\text{N}$ and $97^{\circ}17'07.7''\text{W}$ in the ULM (**Supplementary Figure S1**). The ULM is 76 km in length, 6 km in width, has an average depth of 0.8 m, and is separated from the NGOM by the Padre Island National Seashore (Tunnell, 2002). The dredge material island itself is remote to the nearest population center (Corpus Christi, TX) and is therefore relatively free of plastic pollution.

Sample Deployment and Collection

A microcosm was designed to circumvent the challenges of isolating preexisting plastic debris from heterogeneous sediment samples. A microcosm also permitted the inclusion of a ceramic biofilm control. Briefly, 6.0 g of ceramic pellets (Lyman Products, Middletown, CT, USA), 3.0 g of PET pellets (M&G Chemicals, Ettelbruck, Luxembourg), and 3.0 g of PHA pellets (Doctors Foster and Smith, Rhinelander, WI, USA) were deployed in triplicate inside custom-made microbial capsules (MicroCaps; **Supplementary Figure S2**) at the sediment–water interface for 28 days (May 24, 2016 to June 21, 2016).

All pellets were approximately 3–4 mm in diameter and, therefore, the PET and PHA pellets were considered microplastics (Andrady, 2011). MicroCaps utilized 315- μ m Nitex mesh to contain the pellets and permit the exchange of water, nutrients, bacteria, and some grazers but limit the entry of larger organisms. The microcosms and triplicate 1-L seawater samples (also from the sediment–water interface) were collected at the end of the exposure. All samples were stored on ice and processed immediately upon return to the laboratory, with the extraction procedure starting within 2 h of sample collection. Substrates were washed three times with 25 ml of 0.22- μ m filter-sterilized, site-specific seawater to remove any organisms not part of the biofilm. Seawater (100 ml) was pre-filtered through 315- μ m Nitex mesh and the microbial community was collected by membrane filtration on a 0.22- μ m polycarbonate filter (Millipore Sigma, Burlington, MA, USA) in triplicate. Environmental parameters from the start and end of the exposure period were collected using a 6,920 V2–2 Multi-Parameter Water Quality Sonde (YSI, Yellow Springs, OH, USA) and varied minimally as follows: water temperature (28.56–29.28°C), salinity (37.78–40.28), pH (8.35–8.47), and DO (8.30–5.68 mg L⁻¹).

DNA Isolation

Genomic DNA was isolated in triplicate for each sample type (seawater, ceramic, PET, and PHA) using a modified version of a high-salt and sodium dodecyl sulfate-based method (Zhou et al., 1996). The only modification from the original procedure was that instead of 5.0 g of soil, DNA was isolated from a quartered 0.22- μ m polycarbonate filter (seawater), 6.0 g of ceramic pellets, 3.0 g of PET, or 3.0 g PHA pellets. Due to their higher density, 6.0 g of ceramic was approximately equal in volume to 3.0 g of either plastic type. Following isolation, DNA was quantified (ng μ l⁻¹) and assayed for quality (A_{260}/A_{280} and A_{260}/A_{230}) using a BioPhotometer D30 (Eppendorf, Hamburg, Germany) and the “ds_DNA” methods group with default settings. Final DNA concentrations were verified using a Qubit Fluorometer (Thermo Fisher Scientific, Waltham, MA, USA). The DNA was stored in the dark at –20°C prior to sequencing.

Metagenome Sequencing

Metagenomic library preparation and sequencing were carried out by Molecular Research LP (Shallowater, TX, USA). A total of 12 metagenomes were sequenced: three seawater, three ceramic, three PET, and three PHA. Libraries were prepared using the Nextera XT DNA Library Preparation Kit (Illumina Inc., San Diego, CA, USA) and diluted to 10.0 pM. The average library size was determined using an Agilent 2,100 Bioanalyzer (Agilent Technologies, Santa Clara, CA, USA). Sequencing was performed on the Illumina HiSeq 2,500 platform using 2×150 bp paired-end read chemistry. The DNA concentration (ng μ l⁻¹) and average size (bp) of the sequencing libraries and the number of sequence reads produced are reported in **Supplementary Table S1**. Raw sequence reads were submitted to the European Nucleotide Archive and the European Bioinformatics Institute's

(EBI) Metagenomics Pipeline (Mitchell et al., 2016) version 3.0, which includes an automated workflow for read processing. Briefly, overlapping reads were merged with SeqPrep (John, 2011), low-quality reads and adapter sequences were trimmed using trimmomatic (Bolger et al., 2014), and reads less than 100 bp were removed using BioPython (Cock et al., 2009). Identification of the 16S rRNA reads was performed using rRNASelector (Lee et al., 2011) and FragGeneScan (Rho et al., 2010) was used to find reads containing predicted coding sequences (pCDS) greater than 60 nucleotides in length. The number of sequenced reads ranged from 26,860,030 to 36,522,626, with an average of 30,888,258 reads per sample. Following quality control and merging, the number of remaining reads ranged from 11,273,807 to 22,918,149, with an average of 16,270,447 processed reads per sample.

Microbial Community Composition

Operational taxonomic units (OTUs) were assigned using the QIIME (Caporaso et al., 2010) version 1.9 closed-reference OTU picking protocol and the SILVA 128 SSU 97% database (Quast et al., 2013) with reverse strand matching enabled. Beta-diversity was analyzed using weighted UniFrac (Lozupone et al., 2011) values calculated in QIIME. Permutational Multivariate Analysis of Variance (PERMANOVA) was used to test for significant differences between communities using Primer 7 with the PERMANOVA+ package (Clarke and Gorley, 2015) (PRIMER-E Ltd., Plymouth, UK). PERMANOVA was performed using 999 permutations based on the weighted UniFrac from the beta-diversity analysis in QIIME. Due to the low number of unique permutations possible for pairwise tests, Monte Carlo simulations were used to generate *p*'s for all pairwise comparisons.

Enrichment of Alpha/Beta Hydrolases

Predicted coding sequences (pCDS) from each of the 12 metagenomes were aligned against a modified database¹ of protein sequences from the ESTHER database of alpha/beta hydrolases (Hotelier et al., 2004). Proteins included in the modified database were restricted to depolymerases, esterases, lipases, and cutinases as these were previously implicated in plastic-microbe interactions (Yoshida et al., 2016). To reduce redundancy within the database, CD-HIT (Clarke and Gorley, 2015) version 4.7 was used to cluster protein sequences with default settings. The modified database used here included 10 protein families containing a total of 1,079 protein sequences. Alignments were performed using the command-line version of blastp, as implemented in BLAST+ (Camacho et al., 2009) version 2.6.0, with an expect value (*e*) cutoff of 10⁻⁵, a minimum alignment length of 30 amino acids, and a minimum percent identity of 50%. To visualize the effect of sample type on hydrolase profiles, proportions of positive alignments were normalized to the total number of positive alignments per sample, and a hierarchical cluster analysis based on a Bray-Curtis resemblance matrix was performed. To test for significant

¹turnerlab.tamucc.edu/research/databases

differences among profiles, a similarity profile analysis (SIMPROF) (Clarke et al., 2008) using 999 permutations and a significance level of 0.05 was performed in Primer 7. Additionally, the abundance of protein sequences was normalized to the total pCDS and compared between all samples ($n = 12$).

Relatedness of Polyhydroxybutyrate Depolymerases

Processed reads for each of the PHA samples ($n = 3$) were co-assembled using MEGAHIT (Li et al., 2015) version 1.1.1. Co-assembly was performed using the “meta-large” preset for large and complex communities, and MEGAHIT was called as follows:

```
megahit -presets meta-large -r input --min-contig-len 1,000 -o output -t 40.
```

To recover the coding sequences of a significantly enriched polyhydroxybutyrate (PHB) depolymerase (identified using the hydrolase database above), the representative PHB depolymerase gene sequence was aligned to the 118,520 co-assembled contigs using tblastn with an e cutoff of 10^{-5} , a minimum alignment length of 100 bp, and a minimum percent identity of 50%. An alignment to NCBI's RefSeq genomic database was carried out with the same parameters in an effort to include gene sequences from previously described organisms. The relatedness of the 46 PHB depolymerase gene sequences from this study and gene sequences from the top 10 most similar genera from RefSeq was inferred by constructing a maximum-likelihood (ML) tree with IQ-TREE (Nguyen et al., 2015) version 1.6.1. Sequences were aligned using the M-Coffee mode of T-Coffee (Notredame et al., 2000) that combines results from eight different aligners and the tree was generated with 1,000 ultrafast bootstraps (Minh et al., 2013) using the best-fit model (TPM3u + F + R3) as determined by ModelFinder (Kalyaanamoorthy et al., 2017). The phylogenetic tree was annotated with FigTree version 1.4.3². Sequence similarity between the 46 PHB depolymerase gene sequences was determined using trimAl (Capella-Gutiérrez et al., 2009) version 1.4.15.

Recovery and Analysis of Genomes of Sulfate-Reducing Microorganisms

To characterize individual SRM within the PHA biofilm community, metagenome-assembled genomes (MAGs) were recovered using a previously described method (Parks et al., 2017). Briefly, the processed reads were mapped to the co-assembled PHA metagenomic contigs (produced using MEGAHIT above) with BWA (Li and Durbin, 2010) version 0.7.15-r1142 using the BWA-MEM algorithm with default parameters. Genomes were recovered with MetaBAT (Kang et al., 2015) version 2.12.1 using default MetaBat2 settings and a minimum contig size of 2000 bp. The resulting bins were merged, filtered, and refined using CheckM (Parks et al., 2015) version 1.0.11 and RefineM version 0.0.23, as described previously (Parks et al., 2017). Of the 46 bins produced, six MAGs were retained for further exploration based on criteria

adopted by Parks et al. (Parks et al., 2017): an estimated quality of ≥ 50 (completeness – $5\times$ contamination), scaffolds resulting in an $N50 \geq 10$ kb, containing <100 kb ambiguous bases, and consisting of $<1,000$ contigs and < 500 scaffolds. Of those six MAGs, the three belonging to SRM as inferred with the “tree_qa” function in CheckM were explored further.

The three SRM MAGs were analyzed with the Pathosystems Resource Integration Center's (PATRIC) (Wattam et al., 2017) comprehensive genome analysis service. The PATRIC database contains over 190,000 bacterial genomes and has been increasingly used in environmental studies (Harke et al., 2015; Skennerton et al., 2016; Ortiz-Álvarez et al., 2018). The automated PATRIC service includes annotation with RASTtk (Brettin et al., 2015), prediction of nearest neighbors with Mash/MinHash (Ondov et al., 2016), clustering of homologous proteins with OrthoMCL (Enright et al., 2002), alignment of conserved clusters with MUSCLE (Edgar, 2004), trimming with Gblocks (Talavera and Castresana, 2007), and concatenation followed by inference of a ML tree with RAxML (Stamatakis, 2014). All complete *Desulfovibrionaceae*, *Desulfobacteraceae*, and *Desulfobulbaceae* genomes in the PATRIC database ($n = 43$, 21, and 11, respectively) were included in the analysis. The resulting tree was annotated using FigTree version 1.4.3. Subsequently, these three MAGs were compared to all publicly available *Desulfovibrionaceae*, *Desulfobacteraceae*, and *Desulfobulbaceae* genomes in GenBank ($n = 122$, 107, and 65, respectively) by average nucleotide identity (ANI) using fastANI (Jain et al., 2018), using $>95\%$ ANI as the intraspecies threshold and $<83\%$ as an interspecies threshold. Additionally, PATRIC's “Protein Family Sorter” tool was used to identify sulfate-reducing proteins within the three SRM MAGs. To identify any polymer degradation protein sequences within the MAGs, pCDS were generated using Prodigal (Hyatt et al., 2010) version 2.6.3 and were aligned against the custom hydrolase database (described above) using the same search parameters.

Dissimilatory Sulfur Reduction Potential

Predicted coding sequences (pCDS) from each of the 12 metagenomes were aligned against three databases representing the three steps of the dissimilatory sulfate reduction pathway. The database for the first step of the pathway (reduction of sulfate to adenylyl sulfate [APS]) included all sulfate adenylyltransferase (SAT/MET3) protein sequences in the UniProtKB protein database. The database for the second step of the pathway (reduction of APS to sulfite) included all APS reductase (AprBA) protein sequences in the UniProtKB protein database. To address redundancy within both databases, CD-HIT (Clarke and Gorley, 2015) version 4.7 was used to cluster protein sequences with default settings. This resulted in 612 and 239 protein sequences for the SAT/MET3 and AprBA databases, respectively. These two custom-made databases are also publicly available (see text footnote 1). For the third step of the pathway (reduction of sulfite to sulfide), metagenomes were aligned against a published database of DsrAB (Müller et al., 2014) protein sequences. Alignments were performed using BLAST+ (Camacho et al., 2009) version 2.6.0 (blastp)

²<http://tree.bio.ed.ac.uk/software/figtree/>

with an e cutoff of 10^{-5} , a minimum alignment length of 30 amino acids, and a minimum percent identity of 50%. Positive alignments were normalized to the total pCDS, and the abundance of SAT/MET3, AprBA, and DsrAB sequences was compared between all samples ($n = 11$; PET2 failed normality testing).

Statistical Analyses

Unless stated otherwise, R (R Core Team, 2017) version 3.4.0 was used for statistical analysis of data. The combination of Shapiro–Wilk tests and quantile–quantile plots were used to test data for normality. One-way ANOVAs were generated using the R package multcomp, using a Tukey's *post hoc* test with Westfall values.

Data Availability

All sequence reads were made available through the project accession ERP017130 at the European Nucleotide Archive. The six MAGs were deposited as Madre1, 2, 3, 4, 5, and 6 at GenBank under the accession numbers QZKZ00000000, QZLA00000000, QZLB00000000, QZLC00000000, QZLD00000000, and QZLE00000000, respectively.

RESULTS

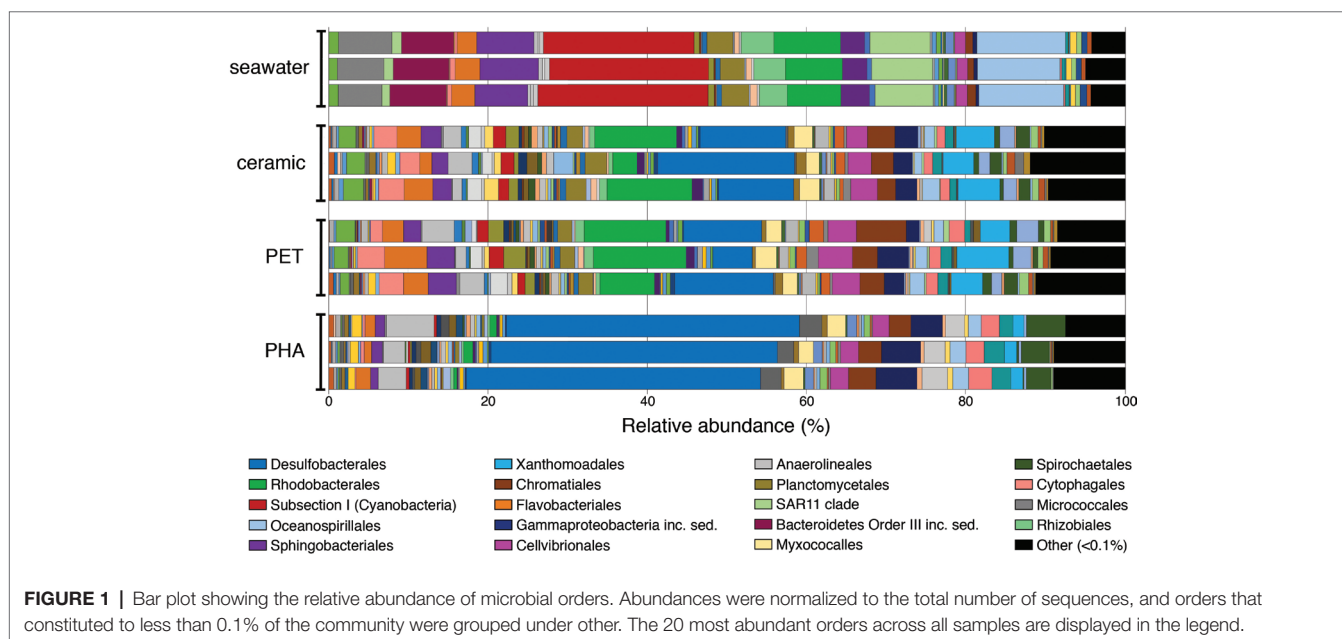
Microbial Community Composition

Overall trends in the seawater-, ceramic-, PET-, and PHA-associated community compositions were visualized using the taxonomic rank of order based on the normalized proportion of OTUs assigned to each of the 12 samples (three seawater, three ceramic, three PET, and three PHA samples; **Figure 1**). The comparison of weighted UniFrac values revealed a significant difference between all three biofilm communities (ceramic, PET, and PHA) and the seawater community

(PERMANOVA; $p < 0.05$). Additionally, a significant difference was found between the PHA biofilm communities and both the ceramic and PET biofilm communities (PERMANOVA; $p < 0.05$). By contrast, there was no significant difference between the PET and ceramic biofilm communities. Hierarchical clustering based on a Bray–Curtis resemblance matrix of OTU taxonomic assignments determined that the PET and ceramic biofilm communities were more closely related to the PHA biofilm community than to the seawater community (PERMANOVA; $p < 0.05$).

At the phylum level, OTUs belonging to Proteobacteria were the most abundant among all four community types, representing 42, 55, 59, and 72% of all OTUs in seawater, ceramic, PET, and PHA samples, respectively (**Supplementary Table S2**). Cyanobacteria was the second most abundant phylum in the seawater community (22%), making up a larger proportion of the community compared to the PET and ceramic biofilm communities (~6% for each), and even more so compared to the PHA biofilm community (0.7%). The presence of Chloroflexi (4%), Spirochaetes (4%), and Firmicutes (2%) among the most abundant phyla was unique to the PHA biofilm communities. A detailed report of taxonomic rank based on normalized proportion is provided in **Supplementary Table S2**.

The OTUs assigned to orders Subsection I of Cyanobacteria, Oceanospirillales, SAR11, and Sphingobacteriales were among the top five most abundant in the seawater community only, making up 20, 11, 8, and 7% of the total OTUs in seawater, respectively. The orders Desulfobacterales, Rhodobacterales, Xanthomonadales, and Cellvibrionales were all among the top five most abundant orders in both the PET and ceramic biofilm communities. The abundance of Proteobacteria (72% of all OTUs) within the PHA biofilm community reflected the dominance of the order Desulfobacterales, an order of SRM that represented 37% of all OTUs and more than half of all Proteobacteria.



Similar to the trends with phyla, the abundant orders within the PHA biofilm community were unique, with the orders of Gammaproteobacteria *incertae sedis*, Anaerolineales, and Spirochaetales being in the top five most abundantly assigned OTUs in the PHA biofilm communities.

Two genera of Cyanobacteria (*Synechococcus* and *Prochlorococcus*) represented almost 20% of all OTUs within the seawater community but made up a very small proportion (<1%) of all three biofilm communities. Members of uncultured genera from *Desulfobacteraceae*, *Rhodobacteraceae*, and *Flammeovirgaceae* were among the five most abundant genera in the PET and ceramic biofilm communities, representing almost 20% of all OTUs. Three genera within *Desulfobacteraceae* and an uncultured genus of *Desulfobulbaceae* combined to represent 20% of all OTUs within the PHA biofilm, reinforcing the dominance of SRM in that community (Supplementary Table S2).

Enrichment of Alpha/Beta Hydrolases

The comparison of normalized sequence abundance data revealed a significant enrichment of depolymerase and esterase gene sequences within the PHA biofilm communities versus the seawater, ceramic, and PET biofilm communities (ANOVA; $p < 0.05$; Figure 2). The increase in depolymerases was nearly 20-fold, while the increase in esterases was approximately 2.5-fold. The significant increase in depolymerases was largely attributed to a polyhydroxybutyrate (PHB) depolymerase that constituted 60% of all hydrolases in the PHA biofilm communities but less than 0.4% of all hydrolases in other community types (Figure 3). Conversely, no hydrolases were enriched in the PET biofilm community versus either the

ceramic biofilm or seawater communities. Hierarchical clustering based on a Bray-Curtis resemblance matrix of hydrolase relative abundance confirmed that PHA biofilm enzyme pools were significantly different from all other community types (SIMPROF; $p < 0.05$). Seawater enzyme pools were also unique, while the PET and ceramic biofilms were indistinguishable (Figure 3).

Relatedness of Polyhydroxybutyrate Depolymerases

To characterize the enriched PHB depolymerases within the PHA biofilm communities, the three PHA metagenomes were co-assembled, resulting in 118,520 contigs totaling 245 Mbp. The N50 of the co-assembly was 2,119 bp, and the lengths of the smallest and longest contigs were 1,000 and 107,130 bp, respectively. The average contig length was 2,251 bp. The PHB depolymerase gene sequence was detected in 46 contigs. The average sequence identity between the 46 PHB depolymerase gene sequences was 54.0% with a range of 7.8–98.9%, and the ML tree illustrated the diversity of those 46 genes along with PHB depolymerase gene sequences from 10 known PHB degraders (Supplementary Figure S3).

Recovery and Analysis of SRM Genomes

Six high-quality MAGs were recovered from the co-assembled PHA biofilm metagenomes. Initial MAG identification was inferred with CheckM: Madre1 was placed in the genus *Desulfovibrio*, Madre2 in the *Desulfobacteraceae* family, Madre3 in the *Desulfobulbaceae* family, Madre4 in the *Spirochaetaceae* family, and Madre5 and Madre6 within the Gammaproteobacteria

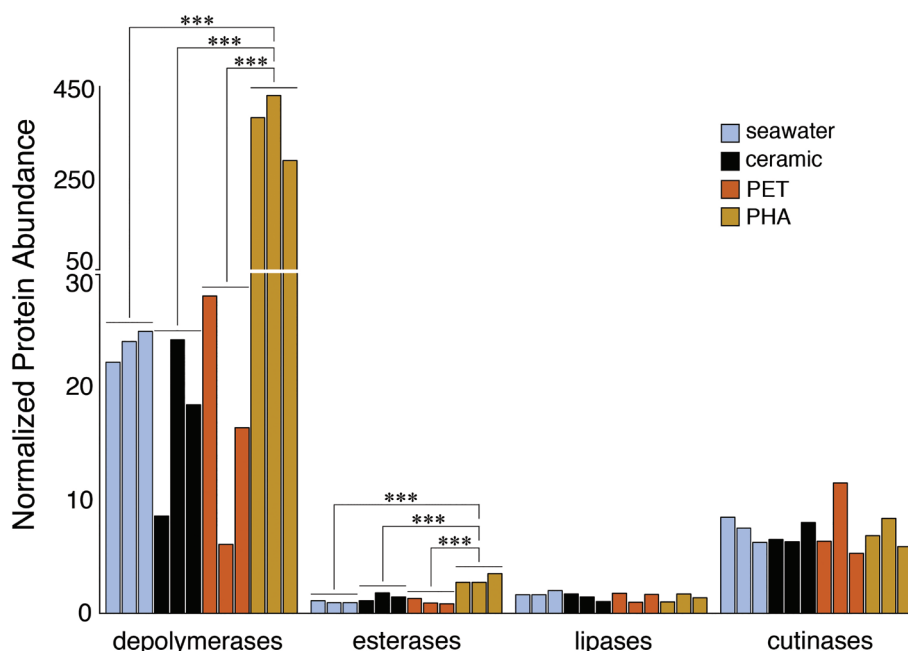


FIGURE 2 | Bar plot showing the relative abundance of depolymerases, esterases, lipases, and cutinases. Gene sequences were normalized to the total number of pCDS in each sample, with individual samples plotted and grouped together based on community association (seawater, ceramic, PET, and PHA). Significance was determined using ANOVA (** $p < 0.001$, $n = 3$).

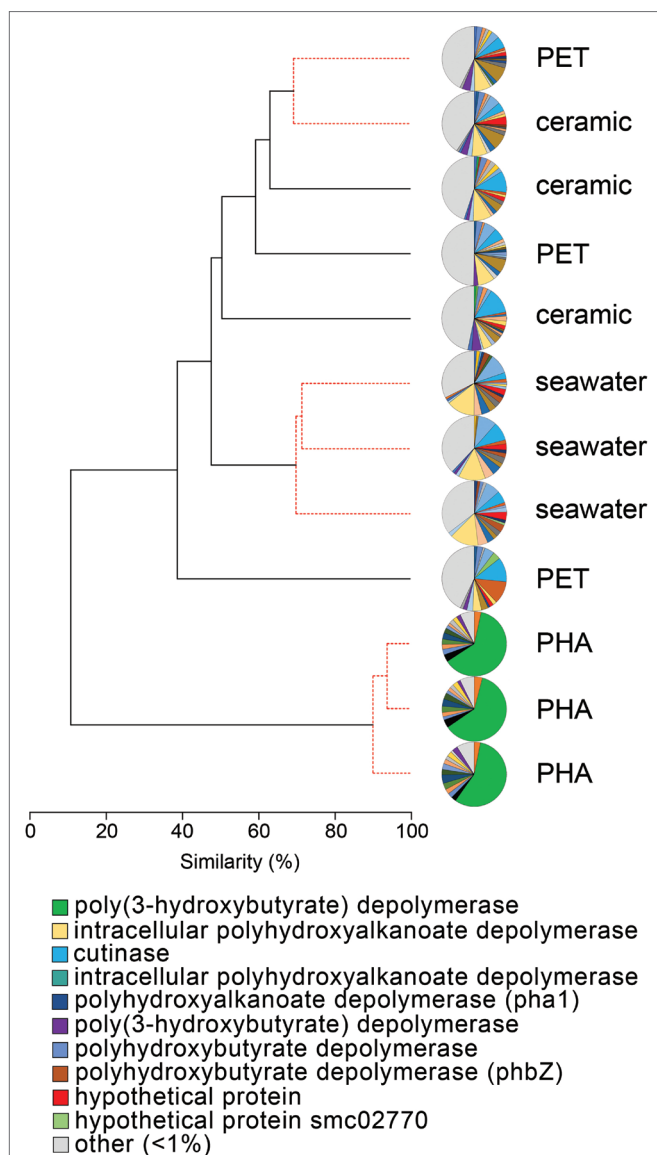


FIGURE 3 | The relatedness of biofilm communities based on a normalized comparison of hydrolase gene pools. The PHB depolymerase, abundant in the PHA communities, is shown in green. Hierarchical clustering was performed based on a Bray-Curtis resemblance matrix. Solid black lines indicate hydrolase gene pools significantly different from one another, while dotted red lines indicate enzyme pools that are not significantly different (SIMPROF analysis; $p < 0.05$). The 10 most abundant enzymes across all samples are displayed in the legend.

order (Table 1). The three SRM MAGs (Madre1, 2, and 3) averaged 391 contigs, a N50 value of 18,335 bp, and a maximum contig length of 76,914 bp. The genome sizes ranged from 3,852,664 to 5,613,049 bp (Madre1 and Madre2, respectively), while the number of genes ranged from 3,829 to 5,179 (Madre1 and Madre2, respectively), and the GC content ranged from 46.9 to 59.8% (Madre3 and Madre1, respectively).

The identities of the three PHA-associated SRM genomes were further explored by building a genome-scale phylogenetic tree that included 43 *Desulfovibrionaceae*, 21 *Desulfobacteraceae*, and 11 *Desulfobulbaceae* reference genomes (Figure 4). The phylogeny confirmed the initial CheckM-based placement of the three MAGs and further refined their closest relatives. Madre1 was related to the type strain *Desulfovibrio gigas* DSM 1382 (ATCC 19364) (Le Gall, 1963; Morais-Silva et al., 2014). Madre2 was related to the uncultured *Desulfobacula toluolica* Tol2, an aromatic carbon-degrading SRM isolated from a seawater pond in Massachusetts (Wöhlbrand et al., 2013). Madre3 was related to the uncultured *Desulfofustis* sp. PB-SRB1 that was recovered from the “pink berry” consortia of the Sippewissett salt marsh (Wilbanks et al., 2014). However, a species could not be assigned to Madre 1, 2, or 3 given that each showed less than 83% ANI with the 122 *Desulfovibrionaceae*, 107 *Desulfobacteraceae*, and 65 *Desulfobulbaceae* reference genomes available in Genbank. The full tree, without collapsed branches, is included in the supplemental material (Supplementary Figure S4).

Analysis of the three SRM MAGs revealed the presence of SAT/MET3 (Madre1, 2, and 3), AprBA (Madre2, and 3), and DsrAB (Madre1, 2, and 3) protein sequences. Additionally, the alignment of their pCDS to the custom hydrolase database revealed the presence of two distinct PHA depolymerase sequences in both Madre1 and Madre3.

Dissimilatory Sulfur Reduction Potential

The enrichment of dissimilatory sulfur reduction protein sequences within the PHA biofilm communities was assessed through the alignment of metagenomic pCDS against databases of sulfate adenylyltransferases (SAT/MET3), adenylyl sulfate (APS) reductases (AprBA), and sulfite reductases (DsrAB). The comparison of normalized sequence abundance revealed no significant differences in SAT/MET3 protein abundances. A significant enrichment in AprBA and DsrAB was detected in the PHA biofilm communities (ANOVA; $p < 0.05$; Figure 5).

TABLE 1 | Six high quality MAGs were recovered from the three PHA co-assembled metagenomes.

MAG	Completeness (%)	Contamination (%)	Quality	Genome size (Mbp)	Contigs	GC%	Taxonomy
Madre1	92.60	1.80	83.60	3.85	434	59.8	<i>Desulfovibrio</i>
Madre2	97.40	2.26	86.10	5.61	410	50.5	<i>Desulfobacteraceae</i>
Madre3	98.13	2.20	87.13	4.40	330	46.9	<i>Desulfobulbaceae</i>
Madre4	54.63	0.00	54.63	1.50	389	50.0	<i>Spirochaetaceae</i>
Madre5	76.65	2.26	65.35	2.77	339	39.7	<i>Gammaproteobacteria</i>
Madre6	72.41	1.72	63.81	2.77	201	41.1	<i>Gammaproteobacteria</i>

MAGs with a quality score (% completeness – 5 × % contamination) greater than 50 were considered high quality.

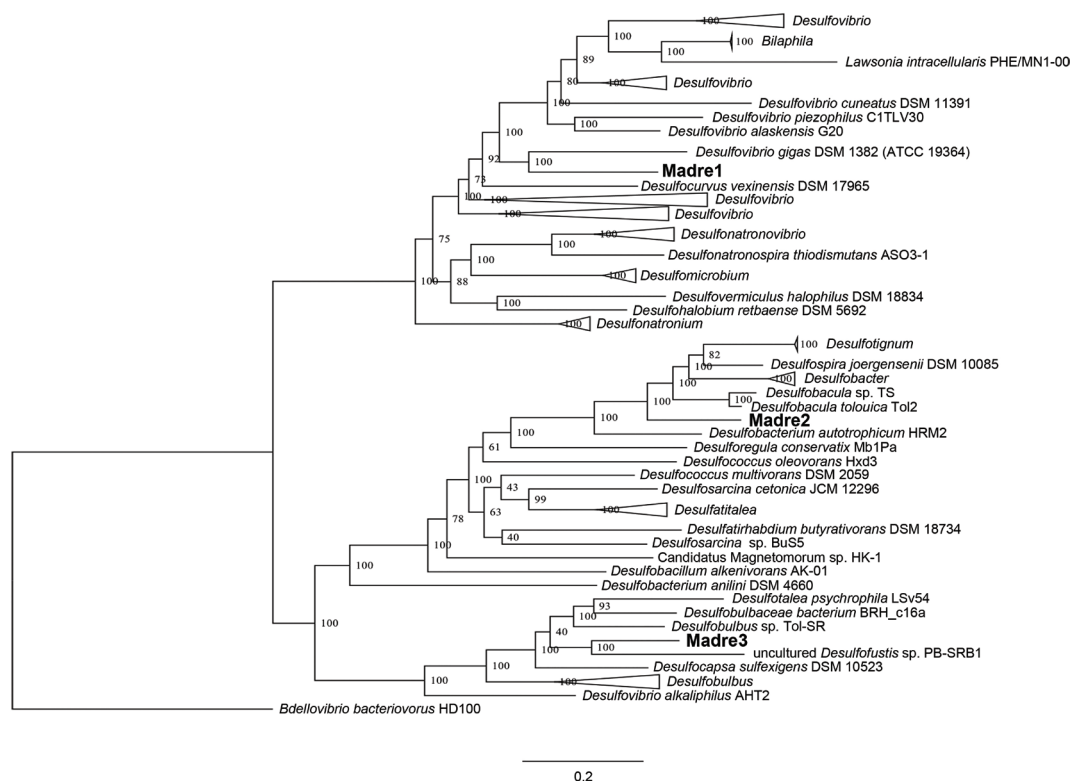


FIGURE 4 | Genome-scale maximum-likelihood tree showing the relatedness of the three PHA biofilm SRM (Madre1, Madre2, and Madre3) to members of the *Desulfovibrionaceae*, *Desulfobacteraceae*, and *Desulfobulbaceae*. The Madre SRM were highlighted in bold font. Node labels show the bootstrap support values. Branch lengths represent the average number of substitutions per site. The tree was rooted to a more distantly related Deltaproteobacteria that is not a known SRM (*Bdellovibrio bacteriovorus* HD1000).

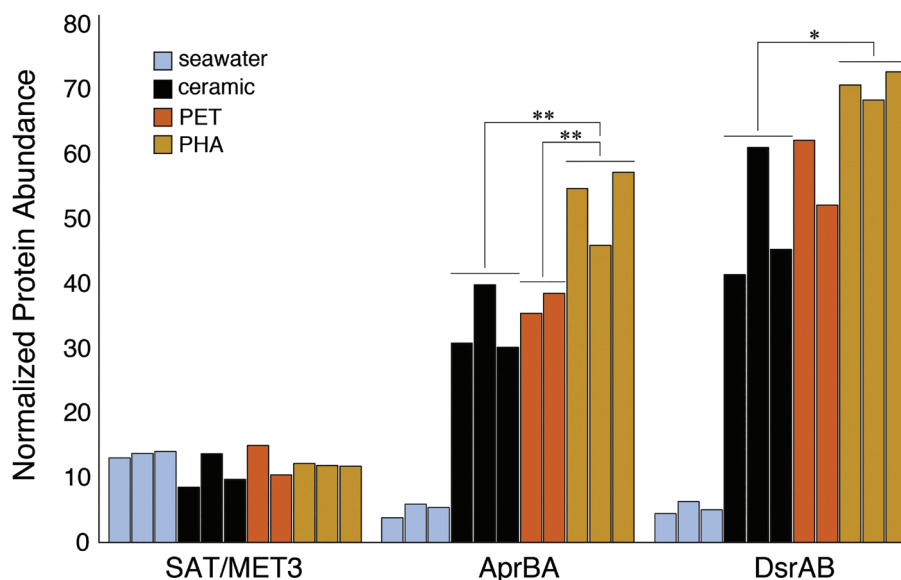


FIGURE 5 | Bar plot showing the relative abundance of sulfate adenylyltransferase (SAT/MET3), APS reductase (AprAB), and dissimilatory sulfite reductase (DsrAB) protein sequences. Protein sequences were normalized to the total number of pCDS in each sample, with individual samples plotted and grouped together based on community association (seawater, ceramic, PET, and PHA). Significance was determined using ANOVA (** $p < 0.01$, * $p < 0.05$, $n = 2-3$).

DISCUSSION

Plastic is a prominent marine pollutant. Numerous studies have characterized microbe-plastic interactions in pelagic systems, yet the effects of plastic pollution on benthic microbiota and biogeochemical cycling remain unclear. To address this knowledge gap, we conducted an *in situ* microcosm designed to ask how the benthic microbial community responds to plastic and bioplastic in coastal marine sediments. Coastal sediments are especially vulnerable to plastic loading due to their proximity to population centers and urban environments (Barnes et al., 2009), and the majority of plastic debris entering the oceans accumulates in coastal zones (Barnes et al., 2009; Thompson et al., 2009).

The comparison between surface-associated and free-living lifestyles has been a long-studied question in microbial ecology and, thereby, considerable literature is available to inform the study of surface-associated bacterial communities (Biddanda and Pomeroy, 1988; Karner and Herndl, 1992; DeLong et al., 1993; Crump et al., 1999; Hollibaugh et al., 2000; Kellogg and Deming, 2014). Based on this literature, it was hypothesized that all surface-associated communities (i.e., ceramic, plastic, and bioplastic) would be distinct in comparison to free-living communities, and the results of this study supported that hypothesis. The more salient question was the distinction between different surfaces, and this study revealed that PET was not colonized by a distinct community in comparison to the ceramic biofilm control. This finding is supported by a recent study demonstrating that pelagic microbial communities associated with PET were indistinguishable from those associated with a glass biofilm control (Oberbeckmann et al., 2016). Similarly, it was previously demonstrated that inert surfaces such as glass, ceramic, and coral skeleton have little influence on marine microbial community composition (Witt et al., 2011). The lack of distinction between PET and ceramic could also be due to the remote location of the study site seeing that previous reports of plastic degradation have occurred in highly polluted habitats that would select for and enrich plastic degraders (Nanda et al., 2010; Singh and Gupta, 2014; Yoshida et al., 2016).

Whereas PET was not colonized by a distinct microbial community, the introduction of PHA promoted a significant and distinct response. In particular, SRM were the dominant members of the PHA-associated assemblage (see Figure 3). Typically, the three most common SRM families (*Desulfobacteraceae*, *Desulfobulbaceae*, and *Desulfovibrionaceae*) account for between 5 and 20% of the total bacterial community in estuarine sediments (Bowen et al., 2012; Cheung et al., 2018). In this study, these three families made up a similar fraction of the plastic- and ceramic-associated benthic communities (9 and 12%, respectively) but they accounted for over 39% of the PHA-associated benthic community.

Naturally occurring PHAs are carbon and energy storage polymers that are accumulated as intracellular granules that aid survival during periods of nutrient limitation and environmental stress (Dawes and Senior, 1973; Obruca et al., 2018). The ability to produce and degrade PHA is thought to

be widespread (Reddy et al., 2003) but its prevalence among SRM and its importance in carbon and sulfur cycling has not been thoroughly characterized. A previous study has reported PHA accumulation in *Desulfococcus multivorans*, *Desulfobotulus sapovorans*, *Desulfonema magnum*, and *Desulfobacterium autotrophicum* (Hai et al., 2004). Importantly, two culture-dependent studies have shown that addition of PHA to incubation bottles was correlated with sulfide production in anoxic lake sediments (Mas-Castellà et al., 1995; Urmeneta et al., 1995). Taken together, the accumulation of PHA in SRM, the PHA stimulation of sulfide production, and the PHA-selection of SRM (in this study) indicate that PHA is an important carbon source for sulfate reduction. However, it remains unknown if the sulfate reducers in our study can directly degrade PHA or if they rely on primary fermenters to first degrade the polymer into simple organic substrates.

A key reaction in PHA degradation is its depolymerization. In this study, a nearly 20-fold increase in the abundance of depolymerases indicated that PHA stimulated the growth of PHA-degrading bacteria. Further, the large diversity of the 46 depolymerases, recovered from the metagenome-assembled genomes, suggested these enzymes were distributed across a mixed microbial consortium. Although we did not measure enzyme activity, the increased abundance and diversity of these depolymerases support the hypothesis that PHA biofilms were sites of enhanced enzyme activity. Additional support for this hypothesis will be made available in a parallel and forthcoming 15-month study wherein weight loss and scanning electron microscopy were used to quantify PHA degradation at the same study site (Figure 6).

Previous studies have shown, using adenylate sulfite reductases (*aprBA*) and dissimilatory sulfite reductases (*dsrAB*) as functional markers, that sulfate reduction is more diverse and widespread than previously thought (Müller et al., 2014; Anantharaman et al., 2018; Hausmann et al., 2018). Further, the detection of *apr* and *dsr* genes in new phyla, made possible through the construction of genomes from metagenomes, has expanded the known diversity of sulfate-reducing microorganisms (Anantharaman et al., 2018; Hausmann et al., 2018). Here, we demonstrated that bioplastic communities were significantly enriched with both sulfate and sulfite reductases. We also reconstructed genomes from metagenomes to discover new *Desulfovibrio*, *Desulfobacula*, and *Desulfofustis* species (Madre 1, 2, and 3, respectively). While it remains unknown if SRM possessing depolymerases (i.e., Madre1 and Madre 3) can directly degrade PHA, an ongoing study will shed light on their growth requirements. Despite this open question, the increased abundance of sulfate-reducing enzymes and the discovery of three uncultured sulfate-reducing species lend additional support to the hypothesis that sulfate reduction in marine sediments is stimulated by the addition of PHA.

In a scenario where bioplastic use and pollution are more common, what remains unclear is the larger effect of the PHA-selection for SRM. Sulfate-reducing bacteria play a critical role in biogeochemical cycling as sulfate reduction is responsible for ~50% of organic carbon mineralization in marine sediments (Jørgensen, 1982), and the stimulation of SRM has been shown

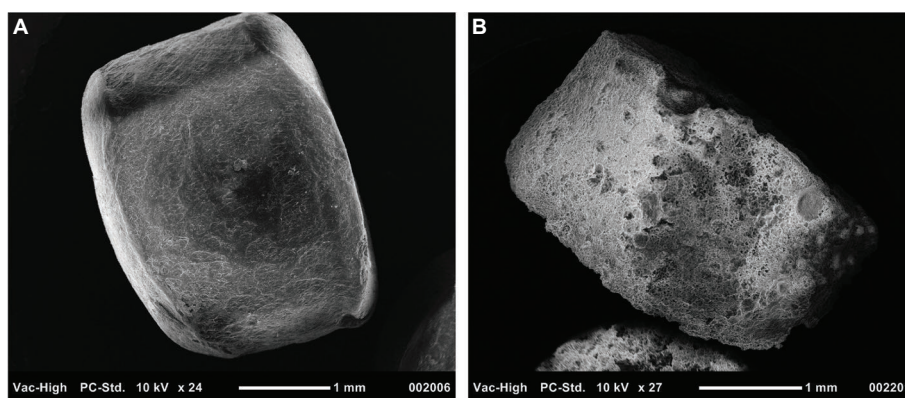


FIGURE 6 | Scanning electron microscopy image of PHA pellets used to visualize signs of biodegradation. Panel (A) displays a pellet that was not exposed to benthic microbial communities, while Panel (B) shows a pellet exposed for 230 days.

to suppress the growth of methanogenic archaea through the diversion of carbon flow from methane to carbon dioxide (Gauci et al., 2004). For example, the stimulation of SRM in coastal rice fields, through the application of sulfate-containing amendments, was shown to inhibit methane production (Lindau et al., 1994; Denier van der Gon et al., 2001). It is thus possible that bioplastic pollution and its stimulation of SRM could have unintended consequences that affect the balance between sulfate reduction and methanogenesis. More generally, it is also possible that bioplastic loading could alter the natural syntrophic cycling of PHA in marine sediments.

In conclusion, this study demonstrated that the introduction of plastic had no measurable effect on the benthic microbial community. By contrast, the introduction of bioplastic selected for a distinct microbial community that was enriched for hydrolases and dominated by SRM. Recovered genomes, representing the three most common families of SRM, contained depolymerases as well as *aprBA* and *dsrAB* reductases. Findings indicate that SRM play an important role in PHA degradation in coastal marine sediments. Given that sulfate reduction is a key process in the oceanic sulfur cycle, we recommend that future scientific investigation, government legislation, and best-management practices related to plastic pollution consider the effects of plastic as well as bio-based alternatives on benthic biogeochemical activities.

DATA AVAILABILITY

The datasets generated for this study can be found in ENA/EBI Metagenomics & NCBI, ERP017130 & QZKZ00000000, QZLA00000000, QZLB00000000, QZLC00000000, QZLD00000000, QZLE00000000.

AUTHOR CONTRIBUTIONS

All authors contributed to this study's design, implementation, analyses, and writing.

FUNDING

This study was funded by the Texas General Land Office Coastal Management Program (GLO-CMP), the Texas Research and Development Fund (TRDF), Texas Sea Grant (TSG), and the National Sciences and Engineering Research Council of Canada (NSERC). The majority of computational data analysis was performed on TAMU-CC's high-performance computing cluster, which is funded in part by the National Science Foundation's CNS MRI Grant (No. 1429518).

ACKNOWLEDGMENTS

This study would not have been possible without the support of our friends and colleagues. Specifically, we thank Thomas Merrick for his assistance with data analysis, Robert "Bobby" Duke and the entire Center for Coastal Studies staff for assistance in the field, and Nicole C. Elledge for her assistance with large-scale ANI comparisons.

SUPPLEMENTARY MATERIAL

The Supplementary Material for this article can be found online at: <https://www.frontiersin.org/articles/10.3389/fmicb.2019.01252/full#supplementary-material>

TABLE S1 | Library preparation and sequencing information.

TABLE S2 | The top five members from each taxonomic rank based on normalized proportion per sample. Means ($n = 3$) plus or minus the standard error of mean are reported for each of the taxonomic assignments.

FIGURE S1 | Map of sampling location showing the Upper Laguna Madre (ULM) along the northwestern Gulf of Mexico (Texas, USA) with the sampling site labeled.

FIGURE S2 | Example of the sampling device designed for this experiment. Each sampling device (D) consisted of a PVC frame containing four MicroCaps: (A) polyethylene terephthalate (PET), (B) polyhydroxyalkanoate (PHA), or (C) ceramic pellets. A total of twelve MicroCaps ($n = 4$ of each sample type) were

deployed at the water-sediment interface using a randomized experimental design as shown in panel (D).

FIGURE S3 | Maximum-likelihood tree showing the diversity of the 46 enriched PHB depolymerase gene sequences. Node labels show the bootstrap support values. Branch lengths represent the average number of substitutions per site. The tree was rooted to the original PHB depolymerase sequence.

REFERENCES

- Aeschelmann, F., and Carus, M. (2015). Biobased building blocks and polymers in the world: capacities, production, and applications – status quo and trends towards 2020. *Ind. Biotechnol.* 11, 154–159. doi: 10.1089/ind.2015.28999.fae
- Anantharaman, K., Hausmann, B., Jungbluth, S. P., Kantor, R. S., Lavy, A., Warren, L. A., et al. (2018). Expanded diversity of microbial groups that shape the dissimilatory sulfur cycle. *ISME J.* 12, 1715–1728. doi: 10.1038/s41396-018-0078-0
- Andrady, A. L. (2011). Microplastics in the marine environment. *Mar. Pollut. Bull.* 62, 1596–1605. doi: 10.1016/j.marpolbul.2011.05.030
- Azam, F., and Long, R. A. (2001). Oceanography: sea snow microcosms. *Nature* 414, 495–498. doi: 10.1038/35107174
- Azam, F., Smith, D. C., Steward, G. F., and Hagström, Å. (1994). Bacteria-organic matter coupling and its significance for oceanic carbon cycling. *Microb. Ecol.* 28, 167–179. doi: 10.1007/BF00166806
- Barnes, D. K., Galfani, F., Thompson, R. C., and Barlaz, M. (2009). Accumulation and fragmentation of plastic debris in global environments. *Philos. Trans. R. Soc. Lond. Ser. B Biol. Sci.* 364, 1985–1998. doi: 10.1098/rstb.2008.0205
- Biddanda, B. A., and Pomeroy, L. R. (1988). Microbial aggregation and degradation of phytoplankton-derived detritus in seawater. I. Microbial succession. *Mar. Ecol. Prog. Ser.* 42, 79–88. doi: 10.3354/meps042079
- Bolger, A. M., Lohse, M., and Usadel, B. (2014). Trimmomatic: a flexible trimmer for Illumina sequence data. *Bioinformatics* 30, 2114–2120. doi: 10.1093/bioinformatics/btu170
- Bowen, J. L., Morrison, H. G., Hobbie, J. E., and Sogin, M. L. (2012). Salt marsh sediment diversity: a test of the variability of the rare biosphere among environmental replicates. *ISME J.* 6, 2014–2023. doi: 10.1038/ismej.2012.47
- Brettin, T., Davis, J. J., Disz, T., Edwards, R. A., Gerdes, S., Olsen, G. J., et al. (2015). RASTtk: a modular and extensible implementation of the RAST algorithm for building custom annotation pipelines and annotating batches of genomes. *Sci. Rep.* 5, 8365. doi: 10.1038/srep08365
- Bryant, J. A., Clemente, T. M., Viviani, D. A., Fong, A. A., Thomas, K. A., Kemp, P., et al. (2016). Diversity and activity of communities inhabiting plastic debris in the North Pacific Gyre. *mSystems* 1, e00024–e00016. doi: 10.1128/mSystems.00024-16
- Camacho, C., Coulouris, G., Avagyan, V., Ma, N., Papadopoulos, J., Bealer, K., et al. (2009). BLAST+: architecture and applications. *BMC Bioinformatics* 10, 421. doi: 10.1186/1471-2105-10-421
- Capella-Gutiérrez, S., Silla-Martínez, J. M., and Gabaldón, T. (2009). trimAl: a tool for automated alignment trimming in large-scale phylogenetic analyses. *Bioinformatics* 25, 1972–1973. doi: 10.1093/bioinformatics/btp348
- Caporaso, J. G., Kuczynski, J., Stombaugh, J., Bittinger, K., Bushman, F. D., Costello, E. K., et al. (2010). QIIME allows analysis of high-throughput community sequencing data. *Nat. Methods* 7, 335–336. doi: 10.1038/nmeth.f.303
- Carson, H. S., Nerheim, M. S., Carroll, K. A., and Eriksen, M. (2013). The plastic-associated microorganisms of the North Pacific Gyre. *Mar. Pollut. Bull.* 75, 126–132. doi: 10.1016/j.marpolbul.2013.07.054
- Cheung, M. K., Wong, C. K., Chu, K. H., and Kwan, H. S. (2018). Community structure, dynamics and interactions of bacteria, Archaea and fungi in subtropical coastal wetland sediments. *Sci. Rep.* 8, 14397. doi: 10.1038/s41598-018-32529-5
- Clarke, K., and Gorley, R. (2015). *PRIMER v7: User manual/tutorial*. (Plymouth, UK: PRIMER-E Ltd).
- Clarke, K. R., Somerfield, P. J., and Gorley, R. N. (2008). Testing of null hypotheses in exploratory community analyses: similarity profiles and biota-environment linkage. *J. Exp. Mar. Biol. Ecol.* 366, 56–69. doi: 10.1016/j.jembe.2008.07.009
- Cock, P. J. A., Antao, T., Chang, J. T., Chapman, B. A., Cox, C. J., Dalke, A., et al. (2009). Biopython: freely available python tools for computational molecular biology and bioinformatics. *Bioinformatics* 25, 1422–1423. doi: 10.1093/bioinformatics/btp163
- Crump, B. C., Armbrust, E. V., and Baross, J. A. (1999). Phylogenetic analysis of particle-attached and free-living bacterial communities in the Columbia River, its estuary, and the adjacent coastal ocean. *Appl. Environ. Microbiol.* 65, 3192–3204.
- Dang, H., and Lovell, C. R. (2016). Microbial surface colonization and biofilm development in marine environments. *Microbiol. Mol. Biol. Rev.* 80, 91–138. doi: 10.1128/MMBR.00037-15
- Dawes, E. A., and Senior, P. J. (1973). “The role and regulation of energy reserve polymers in micro-organisms” in *Advances in Microbial Physiology*. eds. A. H. Rose and D. W. Tempest (London, UK: Academic Press), 135–266.
- De Tender, C. A., Devriese, L. I., Haegeman, A., Maes, S., Ruttink, T., and Dawyndt, P. (2015). Bacterial community profiling of plastic litter in the Belgian part of the North Sea. *Environ. Sci. Technol.* 49, 9629–9638. doi: 10.1021/acs.est.5b01093
- DeLong, E. F., Franks, D. G., and Alldredge, A. L. (1993). Phylogenetic diversity of aggregate-attached vs. free-living marine bacterial assemblages. *Limnol. Oceanogr.* 38, 924–934. doi: 10.4319/lo.1993.38.5.0924
- Denier van der Gon, H. A., van Bodegom, P. M., Wassmann, R., Lantin, R. S., and Metra-Corton, T. M. (2001). Sulfate-containing amendments to reduce methane emissions from rice fields: mechanisms, effectiveness and costs. *Mitig. Adapt. Strat. Gl.* 6, 71–89. doi: 10.1023/A:1011380916490
- Edgar, R. C. (2004). MUSCLE: multiple sequence alignment with high accuracy and high throughput. *Nucleic Acids Res.* 32, 1792–1797. doi: 10.1093/nar/gkh340
- Eich, A., Mildenerberger, T., Laforsch, C., and Weber, M. (2015). Biofilm and diatom succession on polyethylene (PE) and biodegradable plastic bags in two marine habitats: early signs of degradation in the pelagic and benthic zone? *PLoS One* 10:e0137201. doi: 10.1371/journal.pone.0137201
- Enright, A. J., Van Dongen, S., and Ouzounis, C. A. (2002). An efficient algorithm for large-scale detection of protein families. *Nucleic Acids Res.* 30, 1575–1584. doi: 10.1093/nar/30.7.1575
- European Commission (2018). *Directive of the European parliament and of the council on the reduction of the impact of certain plastic products on the environment*. (Brussels, Belgium: European Commission).
- Gauci, V., Matthews, E., Dise, N., Walter, B., Koch, D., Granberg, G., et al. (2004). Sulfur pollution suppression of the wetland methane source in the 20th and 21st centuries. *Proc. Natl. Acad. Sci. USA* 101, 12583–12587. doi: 10.1073/pnas.0404412101
- Geyer, R., Jambeck, J. R., and Law, K. L. (2017). Production, use, and fate of all plastics ever made. *Sci. Adv.* 3:e1700782. doi: 10.1126/sciadv.1700782
- Hai, T., Lange, D., Rabus, R., and Steinbüchel, A. (2004). Polyhydroxyalkanoate (PHA) accumulation in sulfate-reducing bacteria and identification of a class III PHA synthase (PhaEC) in *Desulfococcus multivorans*. *Appl. Environ. Microbiol.* 70, 4440–4448. doi: 10.1128/AEM.70.8.4440-4448.2004
- Harke, M. J., Davis, T. W., Watson, S. B., and Gobler, C. J. (2015). Nutrient-controlled niche differentiation of western Lake Erie cyanobacterial populations revealed via metatranscriptomic surveys. *Environ. Sci. Technol.* 50, 604–615. doi: 10.1021/acs.est.5b03931
- Harrison, J. P., Schratzberger, M., Sapp, M., and Osborn, A. M. (2014). Rapid bacterial colonization of low-density polyethylene microplastics in coastal sediment microcosms. *BMC Microbiol.* 14, 1–15. doi: 10.1186/s12866-014-0232-4
- Hausmann, B., Pelikan, C., Herbold, C. W., Köstlbacher, S., Albertsen, M., Eichorst, S. A., et al. (2018). Peatland Acidobacteria with a dissimilatory sulfur metabolism. *ISME J.* 12, 1729–1742. doi: 10.1038/s41396-018-0077-1

FIGURE S4 | The complete phylogenetic tree containing the three PHA biofilm SRBs recovered in this study (highlighted in yellow). The coloration of labels corresponds to different taxa contained within the tree. Branch labels show the bootstrap support values. Unlabeled nodes have support values of 100. Branch lengths represent the average number of substitutions per site. The tree is rooted to a distantly related Deltaproteobacteria (*Bdellovibrio bacteriovorus*).

- Hollibaugh, J. T., Wong, P. S., and Murrell, M. C. (2000). Similarity of particle-associated and free-living bacterial communities in northern San Francisco Bay, California. *Aquat. Microb. Ecol.* 21, 103–114. doi: 10.3354/ame021103
- Hotelier, T., Renault, L., Cousin, X., Negre, V., Marchot, P., and Chatonnet, A. (2004). ESTHER, the database of the α/β -hydrolase fold superfamily of proteins. *Nucleic Acids Res.* 32, D145–D147. doi: 10.1093/nar/gkh141
- Hyatt, D., Chen, G.-L., Locascio, P. F., Land, M. L., Larimer, F. W., and Hauser, L. J. (2010). Prodigal: prokaryotic gene recognition and translation initiation site identification. *BMC Bioinformatics* 11:119. doi: 10.1186/1471-2105-11-119
- Jain, C., Rodriguez-R, L. M., Phillippy, A. M., Konstantinidis, K. T., and Aluru, S. (2018). High-throughput ANI analysis of 90K prokaryotic genomes reveals clear species boundaries. *Nat. Commun.* 9:5114. doi: 10.1038/s41467-018-07641-9
- Jambeck, J. R., Geyer, R., Wilcox, C., Siegler, T. R., Perryman, M., Andrady, A., et al. (2015). Plastic waste inputs from land into the ocean. *Science* 347, 768–771. doi: 10.1126/science.1260352
- John, J. S. (2011). SeqPrep. Available at: <https://github.com/jstjohn/SeqPrep> (Accessed September 14, 2016).
- Jørgensen, B. B. (1977). The sulfur cycle of a coastal marine sediment (Limfjorden, Denmark). *Limnol. Oceanogr.* 22, 814–832. doi: 10.4319/lo.1977.22.5.0814
- Jørgensen, B. B. (1982). Mineralization of organic matter in the sea bed—the role of sulphate reduction. *Nature* 296, 643–645. doi: 10.1038/296643a0
- Kalyaanamoorthy, S., Minh, B. Q., Wong, T. K. F., von Haeseler, A., and Jermin, L. S. (2017). ModelFinder: fast model selection for accurate phylogenetic estimates. *Nat. Methods* 14, 587–589. doi: 10.1038/nmeth.4285
- Kang, D. D., Froula, J., Egan, R., and Wang, Z. (2015). MetaBAT, an efficient tool for accurately reconstructing single genomes from complex microbial communities. *PeerJ* 3:e1165. doi: 10.7717/peerj.1165
- Karner, M., and Herndl, G. J. (1992). Extracellular enzymatic activity and secondary production in free-living and marine-snow-associated bacteria. *Mar. Biol.* 113, 341–347.
- Kellogg, C. T. E., and Deming, J. W. (2014). Particle-associated extracellular enzyme activity and bacterial community composition across the Canadian Arctic Ocean. *FEMS Microbiol. Ecol.* 89, 360–375. doi: 10.1111/1574-6941.12330
- Klump, J. V., and Martens, C. S. (1981). Biogeochemical cycling in an organic rich coastal marine basin—II. Nutrient sediment-water exchange processes. *Geochim. Cosmochim. Acta* 45, 101–121. doi: 10.1016/0016-7037(81)90267-2
- Le Gall, J. (1963). A new species of *Desulfovibrio*. *J. Bacteriol.* 86, 1120–1120.
- Lee, J., Yi, H., and Chun, J. (2011). rRNASelector: a computer program for selecting ribosomal RNA encoding sequences from metagenomic and metatranscriptomic shotgun libraries. *J. Microbiol.* 49, 689–691. doi: 10.1007/s12275-011-1213-z
- Li, H., and Durbin, R. (2010). Fast and accurate long-read alignment with burrows-wheeler transform. *Bioinformatics* 26, 589–595. doi: 10.1093/bioinformatics/btp698
- Li, D., Liu, C.-M., Luo, R., Sadakane, K., and Lam, T.-W. (2015). MEGAHIT: an ultra-fast single-node solution for large and complex metagenomics assembly via succinct de Bruijn graph. *Bioinformatics* 31, 1674–1676. doi: 10.1093/bioinformatics/btv033
- Lindau, C. W., Alford, D. P., Bollich, P. K., and Linscombe, S. D. (1994). Inhibition of methane evolution by calcium sulfate addition to flooded rice. *Plant Soil* 158, 299–301. doi: 10.1007/BF00009503
- Lozupone, C., Lladser, M. E., Knights, D., Stombaugh, J., and Knight, R. (2011). UniFrac: an effective distance metric for microbial community comparison. *ISME J.* 5, 169–172. doi: 10.1038/ismej.2010.133
- Mas-Castellà, J., Urmeneta, J., Lafuente, R., Navarrete, A., and Guerrero, R. (1995). Biodegradation of poly- β -hydroxyalkanoates in anaerobic sediments. *Int. Biodeterior. Biodegrad.* 35, 155–174. doi: 10.1016/0964-8305(95)00066-E
- Minh, B. Q., Nguyen, M. A. T., and von Haeseler, A. (2013). Ultrafast approximation for phylogenetic bootstrap. *Mol. Biol. Evol.* 30, 1188–1195. doi: 10.1093/molbev/mst024
- Mitchell, A., Bucchini, F., Cochrane, G., Denise, H., Hoopen, P., Fraser, M., et al. (2016). EBI metagenomics in 2016 - an expanding and evolving resource for the analysis and archiving of metagenomic data. *Nucleic Acids Res.* 44, D595–D603. doi: 10.1093/nar/gkv1195
- Morais-Silva, F. O., Rezende, A. M., Pimentel, C., Santos, C. I., Clemente, C., Varela-Raposo, A., et al. (2014). Genome sequence of the model sulfate reducer *Desulfovibrio gigas*: a comparative analysis within the *Desulfovibrio* genus. *Microbiology* 3, 513–530. doi: 10.1002/mbo3.184
- Müller, A. L., Kjeldsen, K. U., Rattei, T., Pester, M., and Loy, A. (2014). Phylogenetic and environmental diversity of DsrAB-type dissimilatory (bi) sulfite reductases. *ISME J.* 9, 1152–1165. doi: 10.1038/ismej.2014.208
- Nanda, S., Sahu, S., and Abraham, J. (2010). Studies on the biodegradation of natural and synthetic polyethylene by *Pseudomonas* spp. *J. Appl. Sci. Environ. Manag.* 14, 57–60. doi: 10.4314/jasem.v14i2.57839
- Nauendorf, A., Krause, S., Bigalke, N. K., Gorb, E. V., Gorb, S. N., Haeckel, M., et al. (2016). Microbial colonization and degradation of polyethylene and biodegradable plastic bags in temperate fine-grained organic-rich marine sediments. *Mar. Pollut. Bull.* 103, 168–178. doi: 10.1016/j.marpolbul.2015.12.024
- Nguyen, L.-T., Schmidt, H. A., von Haeseler, A., and Minh, B. Q. (2015). IQ-TREE: a fast and effective stochastic algorithm for estimating maximum-likelihood phylogenies. *Mol. Biol. Evol.* 32, 268–274. doi: 10.1093/molbev/msu300
- Notredame, C., Higgins, D. G., and Heringa, J. (2000). T-coffee: a novel method for fast and accurate multiple sequence alignment. *J. Mol. Biol.* 302, 205–217. doi: 10.1006/jmbi.2000.4042
- Oberbeckmann, S., Loeder, M. G., Gerdt, G., and Osborn, A. M. (2014). Spatial and seasonal variation in diversity and structure of microbial biofilms on marine plastics in northern European waters. *FEMS Microbiol. Ecol.* 90, 478–492. doi: 10.1111/1574-6941.12409
- Oberbeckmann, S., Osborn, A. M., and Duhaime, M. B. (2016). Microbes on a bottle: substrate, season and geography influence community composition of microbes colonizing marine plastic debris. *PLoS One* 11:e0159289. doi: 10.1371/journal.pone.0159289
- Obruca, S., Sedlacek, P., Koller, M., Kucera, D., and Pernicova, I. (2018). Involvement of polyhydroxyalkanoates in stress resistance of microbial cells: biotechnological consequences and applications. *Biotechnol. Adv.* 36, 856–870. doi: 10.1016/j.biotechadv.2017.12.006
- Ondov, B. D., Treangen, T. J., Melsted, P., Mallonee, A. B., Bergman, N. H., Koren, S., et al. (2016). Mash: fast genome and metagenome distance estimation using MinHash. *Genome Biol.* 17:132. doi: 10.1186/s13059-016-0997-x
- Ortiz-Álvarez, R., Fierer, N., de los Ríos, A., Casamayor, E. O., and Barberán, A. (2018). Consistent changes in the taxonomic structure and functional attributes of bacterial communities during primary succession. *ISME J.* 12, 1658–1667. doi: 10.1038/s41396-018-0076-2
- Parks, D. H., Imelfort, M., Skennerton, C. T., Hugenholtz, P., and Tyson, G. W. (2015). CheckM: assessing the quality of microbial genomes recovered from isolates, single cells, and metagenomes. *Genome Res.* 25, 1043–1055. doi: 10.1101/gr.186072.114
- Parks, D. H., Rinke, C., Chuvochina, M., Chaumeil, P.-A., Woodcroft, B. J., Evans, P. N., et al. (2017). Recovery of nearly 8,000 metagenome-assembled genomes substantially expands the tree of life. *Nat. Microbiol.* 2, 1533–1542. doi: 10.1038/s41564-017-0012-7
- Pauli, N.-C., Petermann, J. S., Lott, C., and Weber, M. (2017). Macrofouling communities and the degradation of plastic bags in the sea: an *in situ* experiment. *R. Soc. Open Sci.* 4:e170549. doi: 10.1098/rsos.170549
- Ploug, H., Grossart, H.-P., Azam, F., and Jørgensen, B. B. (1999). Photosynthesis, respiration, and carbon turnover in sinking marine snow from surface waters of Southern California bight: implications for the carbon cycle in the ocean. *Mar. Ecol. Prog. Ser.* 179, 1–11. doi: 10.3354/meps179001
- Quast, C., Pruesse, E., Yilmaz, P., Gerken, J., Schweer, T., Yarza, P., et al. (2013). The SILVA ribosomal RNA gene database project: improved data processing and web-based tools. *Nucleic Acids Res.* 41, D590–D596. doi: 10.1093/nar/gks1219
- R Core Team (2017). *R: A language and environment for statistical computing*. (Vienna, Austria: R Foundation for Statistical Computing). Available at: <https://www.R-project.org/>
- Reddy, C. S. K., Ghai, R., Rashmi, and Kalia, V. C. (2003). Polyhydroxyalkanoates: an overview. *Bioresour. Technol.* 87, 137–146. doi: 10.1016/S0960-8524(02)00212-2
- Rho, M., Tang, H., and Ye, Y. (2010). FragGeneScan: predicting genes in short and error-prone reads. *Nucleic Acids Res.* 38:e191. doi: 10.1093/nar/gkq747
- Seymour, J. R., Amin, S. A., Raina, J.-B., and Stocker, R. (2017). Zooming in on the phycosphere: the ecological interface for phytoplankton-bacteria relationships. *Nat. Microbiol.* 2:17065. doi: 10.1038/nmicrobiol.2017.65

- Singh, J., and Gupta, K. (2014). Screening and identification of low density polyethylene (LDPE) degrading soil fungi isolated from polythene polluted sites around Gwalior City (MP). *Int. J. Curr. Microbiol. App. Sci.* 3, 443–448.
- Skenneron, C. T., Haroon, M. F., Briegel, A., Shi, J., Jensen, G. J., Tyson, G. W., et al. (2016). Phylogenomic analysis of *Candidatus 'Izimaplasma'* species: free-living representatives from a *Tenericutes* clade found in methane seeps. *ISME J.* 10, 2679–2692. doi: 10.1038/ismej.2016.55
- Stamatakis, A. (2014). RAxML version 8: a tool for phylogenetic analysis and post-analysis of large phylogenies. *Bioinformatics* 30, 1312–1313. doi: 10.1093/bioinformatics/btu033
- Talavera, G., and Castresana, J. (2007). Improvement of phylogenies after removing divergent and ambiguously aligned blocks from protein sequence alignments. *Syst. Biol.* 56, 564–577. doi: 10.1080/10635150701472164
- Thompson, R. C., Moore, C. J., vom Saal, F. S., and Swan, S. H. (2009). Plastics, the environment and human health: current consensus and future trends. *Philos. Trans. R. Soc. Lond. Ser. B Biol. Sci.* 364, 2153–2166. doi: 10.1098/rstb.2009.0053
- Thompson, R. C., Olsen, Y., Mitchell, R. P., Davis, A., Rowland, S. J., John, A. W. G., et al. (2004). Lost at sea: where is all the plastic? *Science* 304:838. doi: 10.1126/science.1094559
- Tunnell, J. W. (2002). "Geography, climate, and hydrography" in *The Laguna Madre of Texas and Tamaulipas*. eds. J. W. Tunnell and F. W. Judd (College Station, Texas: Texas A&M University Press), 7–27.
- UNEP (2018). *Single-use plastics: A roadmap for sustainability*. (Nairobi, Kenya: United Nations Environment Programme).
- Urmeneta, J., Mas-Castella, J., and Guerrero, R. (1995). Biodegradation of poly-(beta)-hydroxyalkanoates in a lake sediment sample increases bacterial sulfate reduction. *Appl. Environ. Microbiol.* 61, 2046–2048.
- Van Cauwenberghe, L., Devriese, L., Galgani, F., Robbins, J., and Janssen, C. R. (2015). Microplastics in sediments: a review of techniques, occurrence and effects. *Mar. Environ. Res.* 111, 5–17. doi: 10.1016/j.marenvres.2015.06.007
- Vigneron, A., Cruaud, P., Alsop, E., de Rezende, J. R., Head, I. M., and Tsismetzis, N. (2018). Beyond the tip of the iceberg: a new view of the diversity of sulfite- and sulfate-reducing microorganisms. *ISME J.* 12, 2096–2099. doi: 10.1038/s41396-018-0155-4
- Wattam, A. R., Davis, J. J., Assaf, R., Boisvert, S., Brettin, T., Bun, C., et al. (2017). Improvements to PATRIC, the all-bacterial bioinformatics database and analysis resource center. *Nucleic Acids Res.* 45, D535–D542. doi: 10.1093/nar/gkw1017
- Wilbanks, E. G., Jaekel, U., Salman, V., Humphrey, P. T., Eisen, J. A., Facciotti, M. T., et al. (2014). Microscale sulfur cycling in the phototrophic pink berry consortia of the Sippewissett salt marsh. *Environ. Microbiol.* 16, 3398–3415. doi: 10.1111/1462-2920.12388
- Witt, V., Wild, C., and Uthicke, S. (2011). Effect of substrate type on bacterial community composition in biofilms from the great barrier reef. *FEMS Microbiol. Lett.* 323, 188–195. doi: 10.1111/j.1574-6968.2011.02374.x
- Wöhlbrand, L., Jacob, J. H., Kube, M., Musmann, M., Jarling, R., Beck, A., et al. (2013). Complete genome, catabolic sub-proteomes and key-metabolites of *Desulfobacula toluolica* Tol2, a marine, aromatic compound-degrading, sulfate-reducing bacterium. *Environ. Microbiol.* 15, 1334–1355. doi: 10.1111/j.1462-2920.2012.02885.x
- Yoshida, S., Hiraga, K., Takehana, T., Taniguchi, I., Yamaji, H., Maeda, Y., et al. (2016). A bacterium that degrades and assimilates poly(ethylene terephthalate). *Science* 351, 1196–1199. doi: 10.1126/science.aad6359
- Zecchin, S., Mueller, R. C., Seifert, J., Stingl, U., Anantharaman, K., von Bergen, M., et al. (2018). Rice Paddy *Nitrospirae* carry and express genes related to Sulfate respiration: proposal of the new genus "*Candidatus* Sulfobium". *Appl. Environ. Microbiol.* 84, e02224–e02217. doi: 10.1128/AEM.02224-17
- Zettler, E. R., Mincer, T. J., and Amaral-Zettler, L. A. (2013). Life in the "plastisphere": microbial communities on plastic marine debris. *Environ. Sci. Technol.* 47, 7137–7146. doi: 10.1021/es401288x
- Zhou, J., Bruns, M. A., and Tiedje, J. M. (1996). DNA recovery from soils of diverse composition. *Appl. Environ. Microbiol.* 62, 316–322.

Conflict of Interest Statement: The authors declare that the research was conducted in the absence of any commercial or financial relationships that could be construed as a potential conflict of interest.

Copyright © 2019 Pinnell and Turner. This is an open-access article distributed under the terms of the Creative Commons Attribution License (CC BY). The use, distribution or reproduction in other forums is permitted, provided the original author(s) and the copyright owner(s) are credited and that the original publication in this journal is cited, in accordance with accepted academic practice. No use, distribution or reproduction is permitted which does not comply with these terms.



Actinobacteria as Promising Candidate for Polylactic Acid Type Bioplastic Degradation

Natthicha Butbunchu^{1,2} and Wasu Pathom-Aree^{3,4*}

¹ Master of Science Program in Applied Microbiology (International Program), Faculty of Science, Chiang Mai University, Chiang Mai, Thailand, ² Graduate School, Chiang Mai University, Chiang Mai, Thailand, ³ Department of Biology, Faculty of Science, Chiang Mai University, Chiang Mai, Thailand, ⁴ Center of Excellence in Microbial Diversity and Sustainable Utilization, Faculty of Science, Chiang Mai University, Chiang Mai, Thailand

OPEN ACCESS

Edited by:

Ren Wei,
University of Greifswald, Germany

Reviewed by:

Georg M. Guebitz,
University of Natural Resources
and Life Sciences, Vienna, Austria
Wenming Zhang,
Nanjing Tech University, China

*Correspondence:

Wasu Pathom-Aree
wasu.p@cmu.ac.th;
wasu215793@gmail.com

Specialty section:

This article was submitted to
Microbiotechnology, Ecotoxicology
and Bioremediation,
a section of the journal
Frontiers in Microbiology

Received: 30 September 2019

Accepted: 22 November 2019

Published: 19 December 2019

Citation:

Butbunchu N and
Pathom-Aree W (2019) Actinobacteria
as Promising Candidate for Polylactic
Acid Type Bioplastic Degradation.
Front. Microbiol. 10:2834.
doi: 10.3389/fmicb.2019.02834

Poly(lactic acid) (PLA) is one of the most commercially available and exploited bioplastics worldwide. It is an important renewable polymer for the replacement of petroleum-based plastic materials. They are both biodegradable and bio-based plastic. Microbial degrading activity is a desirable method for environmental safety and economic value for bioplastic waste managements. Members of the phylum actinobacteria are found to play an important role in PLA degradation. Most of the PLA degrading actinobacteria belong to the family *Pseudonocardiaceae*. Other taxa include members of the family *Micromonosporaceae*, *Streptomyetaceae*, *Streptosporangiaceae*, and *Thermomonosporaceae*. This mini-review aims to provide an overview on PLA degrading actinobacteria including their diversity and taxonomy, isolation and screening procedures and PLA degrading enzyme production from 1997 to 2019. Consideration is also given to where to sampling and how we might use these beneficial actinobacteria for PLA waste management.

Keywords: actinobacteria, polylactic acid, biodegradation, PLA-degrading enzyme, serine protease, bioplastic

INTRODUCTION

Plastics are polymeric materials widely used globally with an important role in everyday life. Increasing demand promotes global plastic market to grow continuously (Mekonnen et al., 2013; Geyer et al., 2017). Conventional petroleum-derived plastics such as polyethylene terephthalate, PET are commonly used as single-use packaging which caused environmental problems from their resistant to degradation. Over the past few decades, awareness on our dependence on limited oil supply has been increased. These have inspired researchers all over the world to search for alternative renewable plastics. Eventually, bioplastics have been successfully developed (Vink et al., 2003, 2004). Bioplastics are large family of different materials. The word “bio-plastics” refers to either biodegradable plastics, bio-based plastics or features both properties (Tokiwa et al., 2009; Alshehrei, 2017). Bio-based is the term for material partly derived from renewable resources, while bio-degradable is a chemical process during which available microorganisms in the environments convert materials into natural substances (de Wilde, 2009; Song et al., 2009, 2011). Recently, there are bioplastic alternatives for almost all conventional plastics. Among currently available bioplastics, poly(lactic acid) (PLA) is one of the bio-based and biodegradable plastic of great commercial value (Karan et al., 2019). It is an aliphatic polyester manufactured by ring-opening polymerization of lactide or by polycondensation of lactic acid monomers derived from the fermentation of starch as a feedstock (Garlotta, 2001; Calabria et al., 2010; Karamanlioglu et al., 2017). PLA exhibited many excellent properties such as thermoplastics, gas barrier, UV resistant, elastic, rigid, hydrophobic, and biocompatible tissue (Farrington et al., 2005; Carosio et al., 2014;

Scarfato et al., 2015; Farah et al., 2016). Therefore, it can be used for various applications such as food packaging and fiber suitable for technical textile application. Moreover, PLA has been used extensively in the medical field due to their ability to be incorporated into human and animal bodies as medical implants, drug delivery materials, and surgical sutures (Jalil, 1990; Ikada and Tsuji, 2000; Ahmed et al., 2018). Biodegradability of PLA is a critical consideration for the development of suitable biological treatments for waste management. A number of microorganisms and their enzymes are involved in biodegradation process especially, bacteria and filamentous fungi (Williams, 1981; Torres et al., 1996; Jarerat and Tokiwa, 2001; Kim et al., 2008; Szumigaj et al., 2008; Bubpachet et al., 2018). Actinobacteria are the first bacteria that found to degrade PLA (Pranamuda et al., 1997). This discovery opened up a view on actinobacteria as potential PLA degrading microorganisms.

DIVERSITY OF PLA-DEGRADING ACTINOBACTERIA: HOW TO FIND AND WHERE TO LOOK?

Polylactic acid-degrading ability in microorganisms are not widely distributed as PLA degraders are less discovered than other types of plastic degrading microorganisms (Nishida and Tokiwa, 1993; Pranamuda et al., 1997; Suyama et al., 1998; Tokiwa et al., 2009). Actinobacteria are among the few microorganisms with potential for PLA degradation (Jarerat et al., 2002, 2003; Sukkhum et al., 2009a,b, 2011, 2012; Chomchoei et al., 2011; Konkitt et al., 2012; Penkhrue et al., 2015, 2018; Panyachanakul et al., 2017, 2019). PLA-degrading actinobacteria are affiliated with 26 species in 11 genera namely *Actinomadura*, *Amycolatopsis*, *Kibdelosporangium*, *Micromonospora*, *Nonomuraea*, *Pseudonocardia*, *Saccharothrix*, *Streptoalloteichus*, *Streptomyces*, *Thermomonospora*, and *Thermopolyspora* (Table 1).

The most dominant PLA degrading actinobacteria are members of the genus *Amycolatopsis* namely *Amycolatopsis* sp. HT-32 (Pranamuda et al., 1997), *Amycolatopsis* sp. 3118 (Ikura and Kudo, 1999), *Amycolatopsis* sp. KT-s-9 (Tokiwa et al., 1999), *Amycolatopsis mediterranei* ATCC 27649 (Pranamuda and Tokiwa, 1999), *Amycolatopsis* sp. 41 (Pranamuda et al., 2001), *Amycolatopsis* sp. K104-1 (Nakamura et al., 2001), *Amycolatopsis orientalis* ssp. *orientalis* (Li et al., 2008), *Amycolatopsis thailandensis* CMU-PLA07^T (Chomchoei et al., 2011), and *Amycolatopsis* sp. SCM_MK2-4 (Penkhrue et al., 2015). Members of the genus *Amycolatopsis* are well known producers of secondary metabolites which can be exploited for biotechnological applications (Tan and Goodfellow, 2015; Sangal et al., 2018). *Amycolatopsis* species are commonly found in arid or hyper-arid soils (Tan and Goodfellow, 2015) as exemplified by the description of recent novel *Amycolatopsis* from desert soils (Busarakam et al., 2016; Idris et al., 2018). However, these sources have been explored only for bioactive compounds producing *Amycolatopsis*. We opine that arid and hyper-arid environments might harbor diverse *Amycolatopsis* strains with potential PLA degrading properties.

Recently, research on PLA-degrading actinobacteria is focus on the mechanisms of degradation and their enzymatic role. The success of such studies relies on the ability to obtain these PLA-degraders in pure culture under laboratory conditions. In general, there are three approaches for the selective isolation of PLA degrading actinobacteria from environmental samples. The first approach is a simple direct isolation from the samples. Environmental samples are taken, prepared for an appropriate serial dilution and spread directly on emulsified PLA agar. After incubation at suitable temperature, plates were observed for the clear zone around colonies as an indicator for PLA degradation. For instance, the first PLA degrading actinobacterium in the family *Pseudonocardiaceae*, *Amycolatopsis* sp. HT-32 was isolated from soil samples and reported to form clear zone around colonies on emulsified PLA plate within 14 days (Pranamuda et al., 1997). Many PLA degrading actinobacteria were isolated from various environmental samples by dilution spread plate on emulsified PLA agar using this approach including a novel species, *Amycolatopsis oliviviridis* (Table 1). This direct isolation plate assay using emulsified PLA provides a convenient and easy way for screening large numbers of isolates for PLA degraders.

The second approach involves repeated adaptation and selection procedures. In this approach, basal agar plates were seeded with samples then, overlaid with PLA film. Colonies growing and appearing on the PLA films were selected and cultured in 10 mL basal medium containing 0.2% (w/v) PLA film at 30°C for 8 weeks to observe PLA degradation (Ikura and Kudo, 1999). The strains that decreased the film weight by more than 5.5% were transferred to a new liquid medium and incubated at 30°C and 37°C for 4 weeks, and strains that efficiently decreased the film weight were isolated. This method allows adaptation of actinobacteria to PLA degradation as PLA is a synthetic polymer generally not available in nature. Highly efficient PLA-degrading strains could be obtained by this adaptation approach as exemplified in the recent report on the degradation of PLA packaging by *Streptomyces* sp. KCU215 (Yottakot and Leelavatcharamas, 2019).

The third approach involved an enrichment step. Enrichment method is a very useful microbiological tool which is used to support the growth of interested microbes and to increase their small number in environmental samples to detectable levels (Pham and Kim, 2012). Briefly, a soil sample is cultured in a basal medium containing 0.1% (w/v) PLA film before the sample-enriched culture broth was spread onto the emulsified PLA agar. Novel actinobacteria, *Amycolatopsis thailandensis* CMU-PLA07^T has been successfully isolated from natural park soil sample in northern Thailand using this approach (Chomchoei et al., 2011).

Over the past two decades, researchers have relied on conventional isolation methods to search for PLA degrading microorganisms in particular actinobacteria. However, it is well accepted that only a small fraction (approximately 1%) of bacteria exists in nature can be grown in the laboratory (Pham and Kim, 2012; Stewart, 2012). Modern molecular biological techniques provide a powerful tool to explore diversity of PLA degrading microorganisms in the environments. Most available techniques involve the analysis of nucleic acids extracted directly from the environments to study microbial diversity, thus avoid limitations

TABLE 1 | List of PLA-degrading actinobacteria, their degrading enzymes and degradation detection methods from 1997 to 2019.

Family	Genus	Species/strain	Sample sources	Isolation medium	Isolation method	Degradation detection method	Enzyme type	References
<i>Micromonosporaceae</i>	<i>Micromonospora</i>	<i>Micromonospora echinospora</i> B12-1	Soil	Emulsified PLA agar	Plate count and clear zone	Turbidity method	–	Sukkhum et al., 2009b
		<i>Micromonospora viridifaciens</i> B7-3	Soil	Emulsified PLA agar	Plate count and clear zone	Turbidity method	–	Sukkhum et al., 2009b
<i>Pseudonocardiaceae</i>	<i>Amycolatopsis</i>	<i>Amycolatopsis</i> sp. HT-32	Soil from paddy fields, weed fields, roadsides, and dumping grounds	0.1% (w/v) emulsified PLA	Plate count and clear zone	Film-weight loss; monomer production	Protease	Pranamuda et al., 1997
		<i>Amycolatopsis</i> 3118	Not specified	Basal medium	Plate count and clear zone	Film-weight loss; monomer production	Protease	Ikura and Kudo, 1999
		<i>Amycolatopsis</i> sp. KT-s-9	Not specified	PLLA emulsified and silk plates	Plate count and clear zone	–	Protease	Tokiwa et al., 1999
		<i>Amycolatopsis mediterranei</i> ATCC 27649	Not specified	–	–	Clear zone method	–	Pranamuda and Tokiwa, 1999
		<i>Amycolatopsis</i> sp. 41	Not specified	Emulsified PLA agar	Plate count and clear zone	Film-weight loss; monomer production	Protease	Pranamuda et al., 2001
		<i>Amycolatopsis</i> sp. K104-1	Soil	0.1% emulsified PLLA	Plate count and clear zone	Turbidity method	Serine protease	Nakamura et al., 2001
		<i>Amycolatopsis orientalis</i> ssp. <i>orientalis</i>	**IFO 12362	–	–	Film-weight loss	Serine protease	Li et al., 2008
		<i>Amycolatopsis thailandensis</i> CMU-PLA07 ^T	Natural park soil	Basal medium with PLA film	Plate count and clear zone	–	–	Chomchoei et al., 2011
		<i>Amycolatopsis oliviviridis</i> SCM_MK2-4	Agricultural soils	Emulsified PLA agar	Plate count and clear zone	Turbidity method	Protease, esterase and lipase	Penkhrue et al., 2015, 2018
		<i>Saccharothrix</i>	*JCM 9114	–	–	Film-weight loss; monomer production	Protease	Jarerat and Tokiwa, 2003; Nair et al., 2012
		<i>Kibdelosporangium</i>	*JCM 7912	–	–	Film-weight loss; monomer production	Protease	Jarerat et al., 2003
	<i>Pseudonocardia</i>	<i>Pseudonocardia alni</i> AS4.1531 ^T	Chinese culture collection	Basal medium with 0.1% (w/v) gelatin and 50 mg PLA films	–	Film-weight loss; monomer production	–	Konkit et al., 2012

(Continued)

TABLE 1 | Continued

Family	Genus	Species/strain	Sample sources	Isolation medium	Isolation method	Degradation detection method	Enzyme type	References
Streptomycetaceae	Streptoalloteichus	Pseudonocardia sp. RM423	Kasetsart University, Thailand	Emulsified-PLA	Clear zone	Film-weight loss; CO ₂ content	–	Apinya et al., 2015
		Streptoalloteichus sp.	*JCM and **IFO	Emulsified-PLA and silk fibroin agar	Plate count and clear zone	Total organic carbon (TOC); residual films in the culture broth	–	Jarerat et al., 2002
	Streptomyces	Streptomyces sp. APL3	Compost soils	Emulsified PLA agar	Plate count and clear zone	–	Serine hydrolase	Sriyapai et al., 2018
		Streptomyces sp. KJU215	Botanical garden soil	Emulsified PLA agar	Plate count and clear zone	PLA-packaging weight loss and surface change	–	Yottakot and Leelavatcharamas, 2019
Streptosporangiaceae	Thermopolyspora	Thermopolyspora	Compost	–	Molecular technique	–	–	Sangwan and Wu, 2008
		Thermopolyspora flexuosa FTPLA	Compost	Mineral agar media with PLA suspension	Plate count and TGGE method	–	–	Husárová et al., 2014
Thermomonosporaceae	Nonomuraea	Nonomuraea terrinata L44-1	Soil	Emulsified PLA agar	Plate count and clear zone	Turbidity method	–	Sukkhum et al., 2009b
		Nonomuraea fastidiosa T9-1	Soil	Emulsified PLA agar	Plate count and clear zone	Turbidity method	–	Sukkhum et al., 2009b
	Thermomonospora	Thermomonospora	Compost	–	Molecular technique	–	–	Sangwan and Wu, 2008
		Thermobifida alba AHK119	Compost	–	–	–	Cutinase	Hu et al., 2010; Kitadokoro et al., 2019
	Actinomadura	Actinomadura keratinilytica T16-1	Soil	Emulsified PLA agar	Plate count and clear zone	Turbidity method	Serine protease	Sukkhum et al., 2009b
		Actinomadura sp. TF1	Compost soils	Emulsified PLA agar	Plate count and clear zone	–	Serine hydrolase	Sriyapai et al., 2018

*Obtained from JCM (Japan Collection of Microorganisms); **Obtained from IFO (Institute for Fermentation, Osaka).

of the culture dependent approach. This culture independent approach offers a useful tool for the detection of new group of PLA degrading actinobacteria.

Additional genera of PLA-degrading actinobacteria were found from compost samples using culture independent approach (Sangwan and Wu, 2008; Sangwan et al., 2009; Husárová et al., 2014). Total genomic DNA were extracted from the prepared mixtures sample and amplified by polymerase chain reaction (PCR) of small-subunit rRNA gene sequences to compare microbial community in compost before (day 0) and after PLA degradation (days-60) (Sangwan and Wu, 2008). Members of uncultured bacterial phyla at day 0 are mixture of Actinobacteria, Bacteroidetes, Chloroflexi, Firmicutes, Gemmatimonadetes, Planctomycetes, Proteobacteria, and TM7 while Actinobacteria are dominant in day-60 sample. The majority of cloned gene sequences identified belonged to members of the phyla Actinobacteria in the genera *Actinomadura*, *Amycolatopsis*, *Pseudonocardia*, *Salinispora*, *Thermomonospora*, and *Thermopolyspora*. Actinobacteria especially those belonging to the genera *Thermopolyspora* and *Thermomonospora*, are suggested to have important roles in biodegradation of PLA under composting conditions as these two genera were subsequently isolated from the compost sample at the end of the experiment. The PLA degradation under aerobic composting was observed as a change in PLA molecular weight and polydispersity index (PDI, \bar{M}_w/\bar{M}_n). After 60 days of composting, the \bar{M}_n of PLA was reduced from 1.3×10^5 to approximately 5564 Da. The PDI comparison of PLA sample before and after 60 days of composting was slightly decreased (before composting, $\bar{M}_w/\bar{M}_n=1.5$; after 60 days composting, $\bar{M}_w/\bar{M}_n=1.1$) (Sangwan and Wu, 2008).

Cultivation experiment on the same day-60 compost found that most bacterial isolates selected for identification were belonged to the genera *Rhizobium*, *Bacillus*, and *Tuberibacillus*, with only two actinobacterial isolates belonged to the genera *Thermomonospora* and *Thermopolyspora*. The discrepancy between cultivation and molecular studies strongly suggested that culture dependent and independent approaches should be used in combination to search for new PLA degrading microorganisms from environmental samples. Similar result was reported by Husárová et al. (2014), PLA degrading bacteria identified as *Thermopolyspora flexuosa* FTPLA was isolated from compost and also detected by temperature gradient gel electrophoresis (TGGE) analysis. From these studies, it is evident that compost is also an interesting source for PLA degrading actinobacteria. These works highlight the importance of using novel molecular ecological techniques for *in situ* identification of novel microorganisms involved in biodegradation of polymeric materials in particular PLA and guided the isolation of such organisms in pure culture.

ACTINOBACTERIA AS POTENTIAL PLA DEGRADER – ENZYMATIC DEGRADATION AND INDUCERS

Polymeric materials like a poly(lactic acid) can be degraded by several microorganisms using their secreted enzymes by

hydrolysis reaction (Banerjee et al., 2014). Many studies have been conducted on purification of depolymerase enzymes from PLA degrading microorganisms. Key enzymes which play an important role in depolymerization of PLA are carboxylesterase, cutinases, lipases, and serine proteases (Hajighasemi et al., 2016). Interestingly, only serine protease is identified as an important enzyme in PLA-degrading activities of actinobacteria in the genus *Amycolatopsis* (Tokiwa and Jarerat, 2004; Lim et al., 2005; Tokiwa and Calabria, 2006; Kawai, 2010). Serine protease usually follows a two-step reaction of hydrolysis. In the first step, PLA substrate binds to the surface of serine protease at the active site. Second step involves the cleavage of peptide-like bonds in PLA through reaction of catalytic amino acids (Ser, Asp, and His) collaborates with water (Hedstrom, 2002). However, little information on the purification and characterization of PLA degrading enzymes are available.

Purified PLA degrading enzymes have been reported from three PLA degrading *Amycolatopsis*. The first report dealing with the purification of a poly(L-lactic acid) degrading enzyme was purified from mesophilic actinobacteria, *Amycolatopsis* sp. strain 41 with a molecular weight of 40 kDa (Pranamuda et al., 2001). This enzyme is able to degrade PLLA powder, casein, silk fibroin, succinyl-(L-alanyl-L-alanyl-L-alanine)-p-nitroanilide (Suc-(Ala)₃-pNA), but not polycaprolactone (PCL) nor polyhydroxybutyrate (PHB) with optimum pH and temperature of 6.0 and 37–45°C, respectively. The enzyme production could be induced by silk powder from silkworm cocoons. These authors suggested that this purified enzyme is a protease with higher PLLA degrading activity than proteinase K.

Extracellular PLA depolymerase from *Amycolatopsis* sp. strain K104-1 was purified and characterized (Nakamura et al., 2001). The purified enzyme can degrade high-molecular-weight PLA in emulsion and solid film to lactic acid. This enzyme also degraded casein and fibrin but did not hydrolyze collagen type I, triolein, tributyrin, PHB, or PCL. It has a molecular weight of 24 kDa with an optimum pH and temperature of 9.5 and 55–60°C, respectively. The PLA degrading activity was inhibited by di-isopropyl fluorophosphates (DFP) and phenylmethanesulphonylfluoride (PMSF) which indicated that this purified enzyme was a serine type protease.

Three novel PLA-degrading enzymes namely PLAase I (24.0 kDa), II (19.5 kDa), and III (18.0 kDa) were purified from *A. orientalis* ssp. *orientalis* (Li et al., 2008). The optimum pH was between 9.5–10.5 and temperature of 50–60°C. These purified enzymes could degrade high molecular weight PLA film as well as casein. The PLA degrading activity of all three enzymes are higher than proteinase K. They were identified as serine-like protease as their PLA degrading activities were strongly inhibited by serine protease inhibitors such as phenylmethylsulfonylfluoride and aprotinin. In addition, N-terminal amino acid sequence of the protein was determined for the initial 17 residues (IIGGSNATSGPYAARLF). Seven N-terminal amino acid residues were 100% identical to fibrinolytic proteases from the earthworm while ten N-terminal amino acid residues also revealed 80% identical to collagenolytic serine proteases from the hepatopancreas of the Kamchatka crab (Nakamura et al., 2001).

From these results, purified depolymerase enzymes from PLA degrading *Amycolatopsis* strains are classified as serine protease which is specific to poly(L-lactic acid) (Matsuda et al., 2005; Tokiwa and Calabia, 2006; Kawai, 2010; Kawai et al., 2011; Wierckx et al., 2018).

Poly(lactic acid)-degrading enzyme was also purified from *Actinomadura keratinilytica* T16-1 with molecular weight of 30 kDa is able to degrade Suc-(Ala)₃-pNA, gelatin, PLA and casein but not PCL (Sukkhum et al., 2009b). The optimum pH and temperature were 10.0 and 70°C, respectively. N-terminal amino acid sequence of the purified enzyme was determined for the initial 15 residues (GYQNNPPSAGLDRAA). The hydrolyzing activity of the purified enzyme was inhibited by DFP, EDTA, and PMSF. This observation indicated that PLA-degrading enzyme produced from *A. keratinilytica* T16-1 is serine protease.

It has been reported that several actinobacteria exhibited a high level of PLLA-degrading activity when liquid culture medium were supplemented with poly(amino acids) inducers such as silk fibroin, elastin, gelatin, some peptides, and amino acids (Jarerat et al., 2004; Tokiwa and Calabia, 2006). For example, the PLLA-degrading enzyme activity of *A. orientalis* was increased from 0 U/mL to 450 U/mL in the medium supplemented with silk fibroin (0.1% w/v). Similarly, the supplement of 0.1% (w/v) elastin was able to increase the PLA-degrading enzyme activity of *Lentzea waywayandensis* (formerly *Saccharothrix waywayandensis*) to 96 U/mL compared to culture control without inducer (0 U/mL) (Jarerat et al., 2004). Most inducers contain L-alanine which is similar to L-lactic acid subunits of PLA in the stereochemical position of chiral carbon (Qi et al., 2017). For example, the PLLA-degrading activity of *Amycolatopsis* sp. 41 was increased with the addition of silk powder into the culture medium from 8 mg TOC/h/mL to 258 mg TOC/h/mL within 5 days (Pranamuda et al., 2001). PLLA-degrading enzymes of *L. waywayandensis* and *Kibdelosporangium aridum* were capable of degrading high molecular weight PLA film (\bar{M}_n : 3.4×10^5) in a liquid medium containing 0.1% (w/v) gelatin (Jarerat and Tokiwa, 2003; Jarerat et al., 2003).

The induction of PLA-degrading enzyme activities of two actinobacteria *L. waywayandensis* and *A. orientalis* was investigated using various poly(L-amino acids) (silk fibroin, gelatin, elastin, and keratin), peptides [(Ala)₂, Ala-Gly, (Gly)₂, (Gly)₃, Gly-Ala, and (Gly)₂-Ala] and amino acids (alanine, glycine, serine leucine, lysine, methionine, and valine) (Jarerat et al., 2004). The enzyme activities were varied between different strains and inducers. Silk fibroin was the best inducer for *A. orientalis* and elastin for *L. waywayandensis*. A clean biological recycling of PLA under mild condition (40°C) using enzyme from *A. orientalis* IFO12362^T without organic solvent was also proposed (Jarerat et al., 2006). However, repolymerization of the degradation products was not carried out. *Pseudonocardia alni* AS4.1531^T was also reported to respond to 0.1% (w/v) gelatin inducer (Konkit et al., 2012). Similar result was observed in *Pseudonocardia* sp. RM423 in liquid medium with 0.3% (w/v) gelatin as an inducer (Apinya et al., 2015). Strain RM423 was augmented into soil to assist the indigenous

microorganisms with PLA degradation under both mesophilic and thermophilic conditions.

DEVELOPMENT AND APPLICATION OF PLA DEGRADATION BY ACTINOBACTERIA

Development of microbial-degradation process and formulation of PLA-degrading enzyme production media are needed as a sustainable technology for PLA waste management. Single culture, co-culture and microbial consortium were tried out to find the most effective biodegradable conditions. A comprehensive study on development of actinobacteria for PLA-degradation was reported in *A. keratinilytica* T16-1. Strain T16-1 is a novel actinobacteria isolated from Thai forest soil that showed the highest PLA-degrading activity at high temperature (50°C) in liquid medium supplemented with PLA film as a carbon source (Sukkhum et al., 2009b, 2011). The fermentation processes for PLA degrading enzyme production by strain T16-1 has been well-studied. Biodegradation efficiency of strain T16-1 was investigated in shake flask culture. Factors affecting the enzyme production by *A. keratinilytica* T16-1 and medium optimization were investigated using response surface methodology (Sukkhum et al., 2009a). Poly(L-lactide)-degrading enzyme production by this strain was carried out in a 3L airlift fermenter under the obtained optimum conditions. The optimal conditions of crude enzyme production were demonstrated as 0.43 vvm aeration rate, pH 6.85 and temperature of 46°C. The obtained enzyme showed potential for PLA polymer recycle as L-lactic acid was found as the major degrading product. A yield of 800 mg/L L-lactic acid was obtained from the degradation of 4,000 mg/L L-PLA powder at 60°C for 8 h (Sukkhum et al., 2012).

In addition, re-polymerization of PDLLA recycling process was evaluated by statistical methods based on central composite design (CCD) to develop new technologies for reducing plastic waste in the near future. Approximately 6,700 mg/L PLA powder was degraded by the crude enzyme under optimized conditions (Youngpreda et al., 2017). The degradation products were re-polymerized to form a PLA oligomer (\bar{M}_w 378 Da). PLA-degrading enzyme activity of *A. keratinilytica* T16-1 was improved and reached 150 U/mL within 72 h in an up-scale 3L airlift fermenter (Panyachanakul et al., 2017). Furthermore, a suitable immobilization material and optimum medium for PDLLA-degrading enzyme production by *A. keratinilytica* T16-1 was investigated. A scrub pad gave the best performance, giving a crude enzyme activity of 30.03 U/mL in shake flask culture. PDLLA-degrading enzyme production of 766.33 U/mL with 15.97 U/mL·h of enzyme productivity were achieved with the optimum fermentation conditions of 0.25 vvm aeration, 170 rpm agitation and 45°C incubation temperature for 48 h in batch fermentation using 5L stirrer fermenter. Recently, a scale-up for PLA degrading enzyme production by *A. keratinilytica* T16-1 in a 5L stirred tank bioreactor was carried out under batch condition (Panyachanakul et al., 2019). The best condition for PLA degradation was an agitation speed of 50 rpm at 60°C under a controlled pH of 8.0. A potential method for

TABLE 2 | General features of the genome of representative *Amycolatopsis* species.

Species/Strains	Accession number	Genome size (bp)	Contigs	No. of coding sequences	tRNAs	G + C content (%)
<i>Amycolatopsis alba</i> DSM 44262 ^T	KB913032	9,811,274	1	9228	62	68.7
<i>Amycolatopsis balhimycina</i> DSM 44591 ^T	AJ508239	10,858,503	1	10190	65	70.8
<i>Amycolatopsis japonica</i> MG417-CF17	CP008953	8,961,318	1	8532	67	68.9
<i>Amycolatopsis mediterranei</i> U32	CP002000	10,236,715	1	9946	63	71.3
<i>Amycolatopsis orientalis</i> B-37	CPCC200066	9,490,992	1	8647	62	68.8
<i>Amycolatopsis thailandensis</i> JCM 16380 ^T	NZ_NMQT00000000.1	9,348,263	421	8990	67	68.8
<i>Amycolatopsis tolypomycina</i> DSM 44544 ^T	NZ_FNSO00000000	10,363,431	4	9780	64	71.7

commercial PLA material degradation by this crude enzyme was also reported. However, lactic acid as degradation products showed inhibitory effect on PLA degradation process. PLA degradation efficiency could be enhanced using simultaneous PLA degradation and dialysis method. The maximum conversion efficiency (percentage of PLA that had been degraded to liberated lactic acid) of 89% was achieved after incubation for 72 h under optimum condition.

Poly(lactic acid) recycling methods such as chemical hydrolysis and pyrolysis have been previously reported (Tsuji and Nakahara, 2002; Fan et al., 2003). However, biological recycling process is considered to be a more environmentally friendly and sustainable approach for PLA waste management. PLA degrading enzymes from actinobacteria such as *A. orientalis* (mesophilic condition) and *A. keratinolytica* T16-1 (thermophilic condition) are proved to be a potential candidate for biological recycling of PLA. Large scale fermentation of PLA degrading enzyme as exemplified in *A. keratinolytica* T16-1 is opened up the opportunity for a sustainable PLA waste management.

GENOMIC INSIGHTS INTO PLA-DEGRADING ACTINOBACTERIA OF THE GENUS *Amycolatopsis*

The genome sequences of six representatives *Amycolatopsis* strains, namely *A. alba* DSM 44262 (accession number: KB913032), *A. balhimycina* DSM 44591^T (accession number: AJ508239), *A. japonica* MG417-CF17 (accession numbers: CP008953), *A. orientalis* B-37 (accession numbers: CPCC200066), *A. mediterranei* U32 (accession numbers: CP002000), and *A. thailandensis* JCM 16380^T (accession numbers: NZ_NMQT00000000.1) were obtained from GenBank. These six phylogenetically closely related strains were selected based on whole genome comparison (data not shown) to test whether comparative genomics could provide useful information for the selection of PLA degrading strains. *A. tolypomycina* DSM 44544^T (accession numbers: NZ_FNSO00000000) was also included in an analysis as a distantly related strain with the six *Amycolatopsis* strains. *A. alba*, *A. orientalis*, *A. mediterranei*, and *A. thailandensis* have been previously reported to have PLA degrading ability (Pranamuda and Tokiwa, 1999; Li et al., 2008; Chomchoei et al., 2011). All sequences were annotated using the Rapid

Annotation Subsystem Technology (RAST) server (Aziz et al., 2008). The distribution of PLA-degrading genes in the genomes was determined using the SEED server (Overbeek et al., 2014) with focus on genes encoding for protein degradation, serine endopeptidase and those regulating the effect of PLA-degrading activities. Genomic features of these six *Amycolatopsis* strains were listed in **Table 2**.

Serine proteases/serine endopeptidases (EC 3.4.21.-) are enzymes responsible for PLA degradation. It was purified and characterized from PLA-degrading actinobacteria, *Amycolatopsis* sp. (Pranamuda et al., 2001; Li et al., 2008). Comparative genomics reveal that serine endopeptidase related genes such as *sspA* and *blaSE* are present in protein degradation subsystem category of all representatives *Amycolatopsis* species (**Supplementary Table 1**). However, there is no report on PLA degrading activities of either *A. balhimycina* DSM 44591^T or *A. japonica* MG417-CF17. It is reasonable to believe that these two species will have PLA degrading property similar to their phylogenetically related neighbors. Interestingly, these genes encoding for PLA degrading enzymes are also present in genomes of *A. tolypomycina* DSM 44544^T which is distantly related to the six representative strains. From this small set of comparison, it seems that these genes related to PLA degradation are conserved within the members of the genus *Amycolatopsis*. We believe that this genomic analysis will provides a powerful tool for exploiting genetics potential of actinobacteria for PLA degradation.

CONCLUSION AND FUTURE PERSPECTIVES

This mini-review provides evidence to support the view that actinobacteria are potential PLA degrading microorganisms. Several members of actinobacteria are able to degrade poly(lactic acid) bioplastics either under laboratory conditions or under field trials (**Table 1**). Selective isolation and cultivation of PLA degrading actinobacteria under laboratory conditions is proving to be a challenge. There is still a room for improvement in selective isolation procedures and strategies to target specific actinobacterial taxa of interest. A sound taxonomic data will provide a ground for an improved isolation and cultivation for PLA degrading actinobacteria. Comparative genomics offer a

tool for screening of potential PLA degrading actinobacteria as exemplified in this study. The accumulation of high-quality whole genome data provides a useful information to support the search for novel actinobacterial strains with PLA degrading ability. Actinobacteria are well known for their ability to produce bioactive compounds. However, their potential as PLA degraders is just becoming apparent. PLA degrading actinobacteria such as *Amycolatopsis* and *Actinomadura* have shown promise which deserves research attention as market demand for PLA plastics are continuously on the rise.

AUTHOR CONTRIBUTIONS

NB contributed to the data for diversity of PLA degrading actinobacteria, their enzyme production and inducers, whole genome analysis and **Tables 1, 2**. WP-A conceived the idea, wrote and revised the manuscript.

REFERENCES

- Ahmed, T., Shahid, M., Azeem, F., Rasul, I., Shah, A. A., Noman, M., et al. (2018). Biodegradation of plastics: current scenario and future prospects for environmental safety. *Environ. Sci. Pollut. Res.* 25, 7287–7298. doi: 10.1007/s11356-018-1234-9
- Alshehri, F. (2017). Biodegradation of synthetic and natural plastic by microorganisms. *J. Appl. Environ. Microbiol.* 5, 8–19. doi: 10.12691/jaem-5-1-2
- Apinya, T., Sombatsompop, N., and Prapagdee, B. (2015). Selection of a *Pseudonocardia* sp. RM423 that accelerates the biodegradation of poly(lactic) acid in submerged cultures and in soil microcosms. *Int. Biodeterior. Biodegrad.* 99, 23–30. doi: 10.1016/j.ibiod.2015.01.001
- Aziz, R. K., Bartels, D., Best, A. A., DeJongh, M., Disz, T., Edwards, R. A., et al. (2008). The RAST server: rapid annotations using subsystems technology. *BMC Genom.* 9:75. doi: 10.1186/1471-2164-9-75
- Banerjee, A., Chatterjee, K., and Madras, G. (2014). Enzymatic degradation of polymers: a brief review. *Mater. Sci. Technol.* 30, 567–573. doi: 10.1179/1743284713Y.0000000503
- Bubpachat, T., Sombatsompop, N., and Prapagdee, B. (2018). Isolation and role of polylactic acid-degrading bacteria on degrading enzymes productions and PLA biodegradability at mesophilic conditions. *Polym. Degrad. Stab.* 152, 75–85. doi: 10.1016/j.polymdegradstab.2018.03.023
- Busarakam, K., Brown, R., Bull, A. T., Tan, G. Y., Zucchi, T. D., da Silva, L. J., et al. (2016). Classification of thermophilic actinobacteria isolated from arid desert soils, including the description of *Amycolatopsis deserti* sp. nov. *Antonie van Leeuwenhoek* 109, 319–334. doi: 10.1007/s10482-015-0635-8
- Calabia, B. P., Tokiwa, Y., Ugwu, C. U., and Aiba, S. (2010). “Chapter 25 biodegradation,” in *Poly(lactic acid): Synthesis, Structures, Properties, Processing, and Applications*, eds R. Auras, L. T. Lim, S. E. M. Selke, and H. Tsuji, (New Jersey: Wiley Publishing), 423–430.
- Carosio, F., Colonna, S., Fina, A., Rydzek, G., Hemmerlé, J., Jierry, L., et al. (2014). Efficient gas and water vapor barrier properties of thin poly (lactic acid) packaging films: functionalization with moisture resistant Nafion and clay multilayers. *Chem. Mater.* 26, 5459–5466. doi: 10.1021/cm501359e
- Chomchoei, A., Pathom-aree, W., Yogota, T., Kanonguch, C., and Lumyong, S. (2011). *Amycolatopsis thailandensis* sp. nov., a poly(L-lactic acid)-degrading actinomycete, isolated from soil. *Int. J. Syst. Evol. Microbiol.* 61, 839–843. doi: 10.1099/ijs.0.023564-0
- de Wilde, B. (2009). *Anaerobic Digestion*, Vol 4. Mönchengladbach: Bioplastics Magazine.
- Fan, Y., Nishida, H., Hoshihara, S., Shirai, Y., Tokiwa, Y., and Endo, T. (2003). Pyrolysis kinetics of poly(L-lactide) with carboxyl and calcium salt end structures. *Polym. Degrad. Stab.* 79, 547–562. doi: 10.1016/S0141-3910(02)00374-9
- Farah, S., Anderson, D. G., and Langer, R. (2016). Physical and mechanical properties of PLA, and their functions in widespread applications—a comprehensive review. *Adv. Drug Deliv. Rev.* 107, 367–392. doi: 10.1016/j.addr.2016.06.012
- Farrington, D. W., Davies, J. L. S., and Blackburn, R. S. (2005). “Chapter 6: poly(lactic acid) fibers,” in *Biodegradable and Sustainable Fibres*, ed. R. S. Blackburn, (Amsterdam: Elsevier), 191–220.
- Garlotta, D. (2001). A literature review of poly(lactic acid). *J. Polym. Environ.* 9, 63–84. doi: 10.1023/A:1020200822435
- Geyer, R., Jambeck, J. R., and Law, K. L. (2017). Production, use, and fate of all plastics ever made. *Sci. Adv.* 3, e1700782. doi: 10.1126/sciadv.1700782
- Hajighasemi, M., Nocek, B. P., Tchigvintsev, A., Brown, G., Flick, R., Xu, X., et al. (2016). Biochemical and structural insights into enzymatic depolymerization of polylactic acid and other polyesters by microbial carboxylesterases. *Biomacromolecules* 17, 2027–2039. doi: 10.1021/acs.biomac.6b00223
- Hedstrom, L. (2002). Serine protease mechanism and specificity. *Chem. Rev.* 102, 4501–4524. doi: 10.1021/cr000033x
- Hu, X., Thumarat, U., Zhang, X., Tang, M., and Kawai, F. (2010). Diversity of polyester-degrading bacteria in compost and molecular analysis of a thermoactive esterase from *Thermobifida alba* AHK119. *Appl. Microbiol. Biotechnol.* 87, 771–779. doi: 10.1007/s00253-010-2555-x
- Husárová, L., Pekařová, S., Stloukal, P., Kucharzcyk, P., Verney, V., Commereuc, S., et al. (2014). Identification of important abiotic and biotic factors in the biodegradation of poly (L-lactic acid). *Int. J. Biol. Macromol.* 71, 155–162. doi: 10.1016/j.ijbiomac.2014.04.050
- Idris, H., Nouioui, I., Pathom-aree, W., Asenjo, J. A., and Goodfellow, M. (2018). *Amycolatopsis vastitatis* sp. nov., an isolate from a high altitude subsurface soil on Cerro Chajnantor, northern Chile. *Antonie van Leeuwenhoek* 111, 1523–1533. doi: 10.1007/s10482-018-1039-3
- Ikada, Y., and Tsuji, H. (2000). Biodegradable polyesters for medical and ecological applications. *Macromol. Rapid Commun.* 21, 117–132. doi: 10.1002/(SICI)1521-3927(20000201)21:3<117::AID-MARC117>3.0.CO;2-X
- Ikura, Y., and Kudo, T. (1999). Isolation of a microorganism capable of degrading poly-(L-lactide). *J. Gen. Appl. Microbiol.* 45, 247–251. doi: 10.2323/jgam.45.247
- Jalil, R. (1990). Biodegradable poly(lactic acid) and poly(lactide-co-glycolide) polymers in sustained drug delivery. *Drug Dev. Ind. Pharm.* 16, 2353–2367. doi: 10.3109/03639049009058555
- Jararat, A., Pranamuda, H., and Tokiwa, Y. (2002). Poly(L-lactide)-degrading activity in various actinomycetes. *Macromol. Biosci.* 2, 420–428. doi: 10.1002/mabi.200290001

FUNDING

A scholarship from the Thailand Graduate Institute of Science and Technology (TGIST), National Science and Technology Development Agency (NSTDA) (Grant No. SCA-CO-2562-9844-TH) is gratefully acknowledged.

ACKNOWLEDGMENTS

NB is grateful to the Graduate School, Chiang Mai University for TA/RA scholarship for the academic year 2018–2019.

SUPPLEMENTARY MATERIAL

The Supplementary Material for this article can be found online at: <https://www.frontiersin.org/articles/10.3389/fmicb.2019.02834/full#supplementary-material>

- Jararat, A., and Tokiwa, Y. (2001). Degradation of poly (L-lactide) by a fungus. *Macromol. Biosci.* 1, 136–140. doi: 10.1002/1616-5195(20010601)1:4<136::aid-mabi136>3.0.co;2-3
- Jararat, A., and Tokiwa, Y. (2003). Poly(L-lactide) degradation by *Saccharothrix waywayandensis*. *Biotechnol. Lett.* 25, 401–404. doi: 10.1023/A:1022450431193
- Jararat, A., Tokiwa, Y., and Tanaka, H. (2003). Poly (L-lactide) degradation by *Kibdelosporangium aridum*. *Biotechnol. Lett.* 25, 2035–2038. doi: 10.1023/B:BILE.0000004398.38799.29
- Jararat, A., Tokiwa, Y., and Tanaka, H. (2004). Microbial poly(L-lactide)-degrading enzyme induced by amino acids, peptides, and poly(L-amino acids). *J. Polym. Environ.* 12, 139–146. doi: 10.1023/B:JOEE.0000038545.69235.f2
- Jararat, A., Tokiwa, Y., and Tanaka, H. (2006). Production of poly(L-lactide)-degrading enzyme by *Amycolatopsis orientalis* for biological recycling of poly(L-lactide). *Appl. Microbiol. Biotechnol.* 72, 726–731. doi: 10.1007/s00253-006-0343-4
- Karamanlioglu, M., Preziosi, R., and Robson, G. D. (2017). Abiotic and biotic environmental degradation of the bioplastic polymer poly(lactic acid): a review. *Polym. Degrad. Stab.* 137, 122–130. doi: 10.1016/j.polymdegradstab.2017.01.009
- Karan, H., Funk, C., Grabert, M., Oey, M., and Hankamer, B. (2019). Green bioplastics as part of a circular bioeconomy. *Trends Plant Sci.* 24, 237–249. doi: 10.1016/j.tplants.2018.11.010
- Kawai, F. (2010). “Poly(lactic acid) (PLA)-degrading microorganisms and PLA depolymerases,” in *Green Polymer Chemistry: Biocatalysis and Biomaterials*, eds H. N. Cheng and R. A. Gross (Washington, DC: American Chemical Society), 405–414. doi: 10.1021/bk-2010-1043.ch027
- Kawai, F., Nakadai, K., Nishioka, E., Nakajima, H., Ohara, H., Masaki, K., et al. (2011). Different enantioselectivity of two types of poly (lactic acid) depolymerases toward poly (L-lactic acid) and poly (D-lactic acid). *Polym. Degrad. Stab.* 96, 1342–1348. doi: 10.1016/j.polymdegradstab.2011.03.022
- Kim, M. N., Kim, W. G., Weon, H. Y., and Lee, S. H. (2008). Poly(L-lactide)-degrading activity of a newly isolated bacterium. *J. Appl. Polym. Sci.* 109, 234–239. doi: 10.1002/app.26658
- Kitadokoro, K., Kakara, M., Matsui, S., Osokoshi, R., Thumarat, U., Kawai, F., et al. (2019). Structural insights into the unique polylactate-degrading mechanism of *Thermobifida alba* cutinase. *FEBS J.* 286, 2087–2098. doi: 10.1111/febs.14781
- Konkit, M., Jararat, A., Kanonguch, C., Lumyong, S., and Pathom-aree, W. (2012). Poly (lactide) degradation by *Pseudonocardia alni* AS4.1531^T. *Chiang Mai J. Sci.* 39, 128–132.
- Li, F., Wang, S., Liu, W., and Chen, G. (2008). Purification and characterization of poly(L-lactic acid)-degrading enzymes from *Amycolatopsis orientalis* ssp. *orientalis*. *FEMS Microbiol. Lett.* 282, 52–58. doi: 10.1111/j.1574-6968.2008.01109.x
- Lim, H.-A., Raku, T., and Tokiwa, Y. (2005). Hydrolysis of polyesters by serine proteases. *Biotechnol. Lett.* 27, 459–464. doi: 10.1007/s10529-005-2217-8
- Matsuda, E., Abe, N., Tamakawa, H., Kaneko, J., and Kamio, Y. (2005). Gene cloning and molecular characterization of an extracellular poly (L-lactic acid) depolymerase from *Amycolatopsis* sp. strain K104-1. *J. Biotechnol.* 187, 7333–7340. doi: 10.1128/JB.187.21.7333-7340.2005
- Mekonnen, T., Mussone, P., Khalil, H., and Bressler, D. (2013). Progress in bio-based plastics and plasticizing modifications. *J. Mater. Chem. A*, 1, 13379–13398. doi: 10.1039/C3TA12555F
- Nair, N. R., Nampoothiri, K. M., and Pandey, A. (2012). Preparation of poly(L-lactide) blends and biodegradation by *Lentzea waywayandensis*. *Biotechnol. Lett.* 34, 2031–2035. doi: 10.1007/s10529-012-1005-5
- Nakamura, K., Tomita, T., Abe, N., and Kamio, Y. (2001). Purification and characterization of an extracellular poly(L-lactic acid) depolymerase from a soil isolate, *Amycolatopsis* sp. strain K104-1. *Appl. Environ. Microbiol.* 67, 345–353. doi: 10.1128/AEM.67.1.345-353.2001
- Nishida, H., and Tokiwa, Y. (1993). Distribution of poly (β-hydroxybutyrate) and poly (ε-caprolactone) aerobic degrading microorganisms in different environments. *J. Environ. Polym. Degrad.* 1, 227–233. doi: 10.1007/BF01458031
- Overbeek, R., Olson, R., Pusch, G. D., Olsen, G. J., Davis, J. J., Disz, T., et al. (2014). The SEED and the rapid annotation of microbial genomes using subsystems technology (RAST). *Nucleic Acids Res.* 42, D206–D214.
- Panyachanakul, T., Kitpreechavanich, V., Tokuyama, S., and Krajangsang, S. (2017). Poly(DL-lactide)-degrading enzyme production by immobilized *Actinomadura keratinilytica* strain T16-1 in a 5-L fermenter under various fermentation processes. *Electron. J. Biotechnol.* 30, 71–76. doi: 10.1016/j.ejbt.2017.09.001
- Panyachanakul, T., Sorachart, B., Lumyong, S., Lorliam, W., Kitpreechavanich, V., and Krajangsang, S. (2019). Development of biodegradation process for poly(DL-lactic acid) degradation by crude enzyme produced by *Actinomadura keratinilytica* strain T16-1. *Electron. J. Biotechnol.* 40, 52–57. doi: 10.1016/j.ejbt.2019.04.005
- Penkhru, W., Khanongnuch, C., Masaki, K., Pathom-aree, W., Punyodom, W., and Lumyong, S. (2015). Isolation and screening of biopolymer-degrading microorganisms from northern Thailand. *World J. Microbiol. Biotechnol.* 31, 1431–1442. doi: 10.1007/s11274-015-1895-1
- Penkhru, W., Sujarit, K., Kudo, T., Ohkuma, M., Masaki, K., Aizawa, T., et al. (2018). *Amycolatopsis oliviviridis* sp. nov., a novel polylactic acid (PLA)-bioplastic degrading actinomycete isolated from paddy soil. *Int. J. Syst. Evol. Microbiol.* 68, 1448–1454. doi: 10.1099/ijsem.0.002682
- Pham, V. H. T., and Kim, J. (2012). Cultivation of unculturable soil bacteria. *Trend Biotechnol.* 30, 475–484. doi: 10.1016/j.tibtech.2012.05.007
- Pranamuda, H., and Tokiwa, Y. (1999). Degradation of poly (L-lactide) by strains belonging to genus *Amycolatopsis*. *Biotechnol. Lett.* 21, 901–905. doi: 10.1023/A:1005547326434
- Pranamuda, H., Tokiwa, Y., and Tanaka, H. (1997). Polylactide degradation by an *Amycolatopsis* sp. *Appl. Environ. Microbiol.* 63, 1637–1640.
- Pranamuda, H., Tsuchii, A., and Tokiwa, Y. (2001). Poly (L-lactide)-degrading enzyme produced by *Amycolatopsis* sp. *Macromol. Biosci.* 1, 25–29. doi: 10.1002/1616-5195(200101)
- Qi, X., Ren, Y., and Wang, X. (2017). New advances in the biodegradation of poly(lactic) acid. *Int. Biodeter. Biodegr.* 117, 215–223. doi: 10.1016/j.ibiod.2017.01.010
- Sangal, V., Goodfellow, M., Blom, J., Tan, G. Y. A., Klenk, H.-P., and Sutcliffe, I. C. (2018). Revisiting the taxonomic status of the biomedically and industrially important genus *Amycolatopsis*, using a phylogenomic approach. *Front. Microbiol.* 9:2281. doi: 10.3389/fmicb.2018.02281
- Sangwan, P., Way, C., and Wu, D.-Y. (2009). New insight into biodegradation of polylactide (PLA)/clay nanocomposites using molecular ecological techniques. *Macromol. Biosci.* 9, 677–686. doi: 10.1002/mabi.2008.00276
- Sangwan, P., and Wu, D. Y. (2008). New insight into polylactide biodegradation from molecular ecological techniques. *Macromol. Biosci.* 8, 304–315. doi: 10.1002/mabi.200700317
- Scarfato, P., Maio, L. D., and Incarnato, L. (2015). Recent advances and migration issues in biodegradable polymers from renewable sources for food packaging. *J. Appl. Polym. Sci.* 132, 42597. doi: 10.1002/app.42597
- Song, J., Kay, M., and Coles, R. (2011). “Chapter 11: bioplastics,” in *Food and Beverage Packaging Technology*, eds R. Coles, and M. Kirwan, (Chichester: Blackwell Publishing), 295–319.
- Song, J. H., Murphy, R. J., Narayan, R., and Davies, G. (2009). Biodegradable and compostable alternatives to conventional plastics. *Philos. Trans. R. Soc. Lond. B. Biol. Sci.* 364, 2127–2139. doi: 10.1098/rstb.2008.0289
- Sriyapai, P., Chansiri, K., and Sriyapai, T. (2018). Isolation and characterization of polyester-based plastics-degrading bacteria from compost soils. *Microbiology* 87, 290–300. doi: 10.1134/S0026261718020157
- Stewart, E. J. (2012). Growing unculturable bacteria. *J. Bacteriol.* 194, 4151–4160. doi: 10.1128/JB.00345-12
- Sukkhum, S., Shinji, T., and Kitpreechavanich, V. (2012). Poly(L-lactide)-degrading enzyme production by *Actinomadura keratinilytica* T16-1 in 3 L airlift bioreactor and its degradation ability for biological recycle. *J. Microbiol. Biotechnol.* 22, 92–99. doi: 10.4014/jmb.1105.05016
- Sukkhum, S., Tokuyama, S., and Kitpreechavanich, V. (2009a). Development of fermentation process for PLA-degrading enzyme production by a new thermophilic *Actinomadura* sp. T16-1. *Biotechnol. Bioproc. Eng.* 14, 302–306. doi: 10.1007/s12257-008-0207-0
- Sukkhum, S., Tokuyama, S., Tarmura, T., and Kitpreechavanich, V. (2009b). A novel poly (L-lactide) degrading actinomycetes isolated from Thai forest soil, phylogenic relationship and the enzyme characterization. *J. Gen. Appl. Microbiol.* 55, 459–467. doi: 10.2323/jgma.55.459
- Sukkhum, S., Tokuyama, S., Kongsaeer, P., Tamura, T., Ishida, Y., and Kitpreechavanich, V. (2011). A novel poly (L-lactide) degrading thermophilic

- actinomycetes, *Actinomadura keratinilytica* strain T16-1 and *pla* sequencing. *Afr. J. Microbiol. Res.* 5, 2575–2582. doi: 10.5897/AJMR10.722
- Suyama, T., Tokiwa, Y., Ouichanpagdee, P., Kanagawa, T., and Kamagata, Y. (1998). Phylogenetic affiliation of soil bacteria that degrade aliphatic polyesters available commercially as biodegradable plastics. *Appl. Environ. Microbiol.* 64, 5008–5011.
- Szumigaj, J., Żakowska, Z., Klimek, L., Rosicka-Kaczmarek, J., and Bartkowiak, A. (2008). Assessment of polylactide foil degradation as a result of filamentous fungi activity. *Polish J. Environ. Stud.* 17, 335–341.
- Tan, G. Y. A., and Goodfellow, M. (2015). “Amycolatopsis,” in *Bergey’s Manual of Systematic Bacteriology*, ed. W. B. Whitman, (Hoboken, NJ: John Wiley & Sons), 1–40.
- Tokiwa, Y., and Calabia, B. P. (2006). Biodegradability and biodegradation of poly(lactide). *Appl. Microbiol. Biotechnol.* 72, 244–251. doi: 10.1007/s00253-006-0488-481
- Tokiwa, Y., Calabia, B. P., Ugwu, C. U., and Aiba, S. (2009). Biodegradability of plastics. *Int. J. Mol. Sci.* 10, 3722–3742. doi: 10.3390/ijms10093722
- Tokiwa, Y., and Jarerat, A. (2004). Biodegradation of poly(L-lactide). *Biotechnol. Lett.* 26, 771–777. doi: 10.1023/B:BILE.0000025927.31028.e3
- Tokiwa, Y., Konno, M., and Nishida, H. (1999). Isolation of silk degrading microorganisms and its poly(L-lactide) degradability. *Chem. Lett.* 28, 355–356. doi: 10.1246/cl.1999
- Torres, A., Li, S. M., Roussos, S., and Vert, M. (1996). Screening of microorganisms for biodegradation of poly(lactic acid) and lactic acid-containing polymers. *Appl. Environ. Microbiol.* 62, 2393–2397.
- Tsuji, H., and Nakahara, K. (2002). Poly(L-lactide). IX. Hydrolysis in acid media. *J. Appl. Polym. Sci.* 86, 186–194. doi: 10.1002/app.10813
- Vink, E. T. H., Rábago, K., Glassner, D. A., Springs, B., O’Connor, R. P., Kolstad, J., et al. (2004). The sustainability of NatureWorks™ polylactide polymers and Ingeo™ polylactide fibers: an update of the future. *Macromol. Biosci.* 4, 551–564. doi: 10.1002/mabi.200400023
- Vink, E. T. H., Rábago, K. R., Glassner, D. A., and Gruber, P. R. (2003). Applications of life cycle assessment to NatureWorks™ polylactide (PLA) production. *Polym. Degrad. Stab.* 80, 403–419. doi: 10.1016/S0141-3910(02)00372-5
- Wierckx, N., Narancic, T., Eberlein, C., Wei, R., Drzyzga, O., Magnin, A., et al. (2018). “Plastic biodegradation: challenges and opportunities,” in *Consequences of Microbial Interactions with Hydrocarbons, Oils, and Lipids: Biodegradation and Bioremediation*, ed. R. Steffan, (Berlin: Springer International Publishing), 1–29. doi: 10.1007/978-3-319-44535-9_23-1
- Williams, D. F. (1981). Enzymic hydrolysis of polylactic acid. *Eng. Med.* 10, 5–7. doi: 10.1243/EMED-JOUR-1981-010-004-02
- Yottakot, S., and Leelavatcharamas, V. (2019). Isolation and optimization of polylactic acid (PLA)-packaging-degrading actinomycete for PLA-packaging degradation. *Pertanika J. Trop. Agric. Sci.* 42, 1111–1129.
- Youngpreda, A., Panyachanakul, T., Kitpreechavanich, V., Sirisansaneeyakul, S., Suksamrarn, S., Tokuyama, S., et al. (2017). Optimization of poly(DL-lactic acid) degradation and evaluation of biological re-polymerization. *J. Polym. Environ.* 25, 1131–1139. doi: 10.1007/s10924-016-0885-1

Conflict of Interest: The authors declare that the research was conducted in the absence of any commercial or financial relationships that could be construed as a potential conflict of interest.

Copyright © 2019 Butbunchu and Pathom-Aree. This is an open-access article distributed under the terms of the Creative Commons Attribution License (CC BY). The use, distribution or reproduction in other forums is permitted, provided the original author(s) and the copyright owner(s) are credited and that the original publication in this journal is cited, in accordance with accepted academic practice. No use, distribution or reproduction is permitted which does not comply with these terms.



Degradation of Recalcitrant Polyurethane and Xenobiotic Additives by a Selected Landfill Microbial Community and Its Biodegradative Potential Revealed by Proximity Ligation-Based Metagenomic Analysis

OPEN ACCESS

Edited by:

Ren Wei,

University of Greifswald, Germany

Reviewed by:

Wei-Min Wu,

Stanford University, United States

Gabriela Vázquez-Rodríguez,

Autonomous University of the State

of Hidalgo, Mexico

*Correspondence:

Herminia Loza-Tavera

hlozat@unam.mx

[†] These authors have contributed
equally to this work

Specialty section:

This article was submitted to
Microbiotechnology, Ecotoxicology
and Bioremediation,
a section of the journal
Frontiers in Microbiology

Received: 25 September 2019

Accepted: 10 December 2019

Published: 22 January 2020

Citation:

Gaytán I, Sánchez-Reyes A,
Burelo M, Vargas-Suárez M,
Liachko I, Press M, Sullivan S,
Cruz-Gómez MJ and Loza-Tavera H
(2020) Degradation of Recalcitrant
Polyurethane and Xenobiotic
Additives by a Selected Landfill
Microbial Community and Its
Biodegradative Potential Revealed by
Proximity Ligation-Based
Metagenomic Analysis.
Front. Microbiol. 10:2986.
doi: 10.3389/fmicb.2019.02986

Itzel Gaytán^{1†}, Ayixon Sánchez-Reyes^{1†}, Manuel Burelo², Martín Vargas-Suárez¹,
Ivan Liachko³, Maximilian Press³, Shawn Sullivan³, M. Javier Cruz-Gómez⁴ and
Herminia Loza-Tavera^{1*}

¹ Departamento de Bioquímica, Facultad de Química, Universidad Nacional Autónoma de México, Mexico City, Mexico,

² Departamento de Química Analítica, Facultad de Química, Universidad Nacional Autónoma de México, Mexico City,
Mexico, ³ Phase Genomics Inc., Seattle, WA, United States, ⁴ Departamento de Ingeniería Química, Facultad de Química,
Universidad Nacional Autónoma de México, Mexico City, Mexico

Polyurethanes (PU) are the sixth most produced plastics with around 18-million tons in 2016, but since they are not recyclable, they are burned or landfilled, generating damage to human health and ecosystems. To elucidate the mechanisms that landfill microbial communities perform to attack recalcitrant PU plastics, we studied the degradative activity of a mixed microbial culture, selected from a municipal landfill by its capability to grow in a water PU dispersion (WPUD) as the only carbon source, as a model for the BP8 landfill microbial community. The WPUD contains a polyether-polyurethane-acrylate (PE-PU-A) copolymer and xenobiotic additives (*N*-methylpyrrolidone, isopropanol and glycol ethers). To identify the changes that the BP8 microbial community culture generates to the WPUD additives and copolymer, we performed chemical and physical analyses of the biodegradation process during 25 days of cultivation. These analyses included Nuclear magnetic resonance, Fourier transform infrared spectroscopy, Thermogravimetry, Differential scanning calorimetry, Gel permeation chromatography, and Gas chromatography coupled to mass spectrometry techniques. Moreover, for revealing the BP8 community structure and its genetically encoded potential biodegradative capability we also performed a proximity ligation-based metagenomic analysis. The additives present in the WPUD were consumed early whereas the copolymer was cleaved throughout the 25-days of incubation. The analysis of the biodegradation process and the identified biodegradation products showed that BP8 cleaves esters, C-C, and the recalcitrant aromatic urethanes and ether groups by hydrolytic and oxidative mechanisms, both in the soft and the hard segments of the copolymer. The proximity ligation-based metagenomic analysis allowed the reconstruction of five genomes, three of them from novel species. In the metagenome,

genes encoding known enzymes, and putative enzymes and metabolic pathways accounting for the biodegradative activity of the BP8 community over the additives and PE-PU-A copolymer were identified. This is the first study revealing the genetically encoded potential biodegradative capability of a microbial community selected from a landfill, that thrives within a WPUD system and shows potential for bioremediation of polyurethane- and xenobiotic additives-contaminated sites.

Keywords: biodegradation, microbial community, polyether-polyurethane-acrylate, xenobiotic additives, metagenomics, Hi-C proximity-ligation, community structure, biodegradative potential

INTRODUCTION

Plastic pollution represents a pervasive anthropogenic threat for the survival of natural ecosystems. Worldwide, plastics have become so abundant that they have been proposed as geological markers for the Anthropocene era (Zalasiewicz et al., 2016). In 2017, a total of 348 million tons of plastics were manufactured (Plastics Europe, 2018) and their production keeps increasing. Polyurethanes (PU) are versatile plastics produced as thermoplastics, thermosets, coatings, adhesives, sealants and elastomers that are incorporated into our daily life in building insulation, refrigerators and freezers, furniture and bedding, footwear, automotive, clothing, coatings, adhesives, and others. PU was ranked as the sixth most used polymer worldwide with a production of 18 million tons in 2016 (Cornille et al., 2017). The extensive utilization of PU generates wastes that are mainly disposed in municipal landfills where, because of its structural complexity will remain as polymeric structures for decades, or are burned generating toxic substances that negatively impact human health and ecosystems (Cornille et al., 2017). Furthermore, some PU such as polyether (PE)-PU are more recalcitrant than others, and additionally, some PU-based liquid formulations contain additives that include secondary alcohols and glycol ethers that function as solvents or coalescent agents. Glycol ethers enter the environment in substantial quantities, are toxic for many microbial species (Kawai, 2010; Varsha et al., 2011; Malla et al., 2018) and represent a potential hazard for human health (Organization for Economic Co-operation and Development, 2003).

Over the last three decades, several research groups have isolated microorganisms capable of attacking PU (Oceguera-Cervantes et al., 2007; Cregut et al., 2013; Álvarez-Barragán et al., 2016; Gamerith et al., 2016; Osman et al., 2018; Magnin et al., 2019) and degrading xenobiotic additives (Ojo, 2007; Varsha et al., 2011). Also, the degradation capabilities of several fungal and bacterial communities over PU in compost, soil or liquid cultures (Zafar et al., 2014; Shah et al., 2016; Vargas-Suárez et al., 2019), and over some xenobiotics in different activated sludges (Ferrero et al., 2018) have been assessed. However, PU biodegradation is still a challenge for environmental and biological disciplines and little is known about structure or potential degradative enzymatic pathways of microbial communities capable of PU biodegradation. Metagenomics provides access to the structure and genetic potential of microbial communities, helping to understand the ecophysiological relationships governing the dynamics of their

populations in the environment. Recently, a new approach has been developed that allows the reconstruction of individual genomes of microbial species using physical interactions between sequences within cells (Burton et al., 2014). This approach involves Hi-C proximity ligation and yields direct evidence of sequences co-occurrence within a genome. It is used for *de novo* assembly, identification of complete and novel genomes (Press et al., 2017) and for testing functional and phylogenetic hypotheses, surpassing other methods for clustering contigs by taxonomic origins (Wu et al., 2014; Breitwieser et al., 2019; Shaiber and Eren, 2019).

To characterize the biodegradation process of the recalcitrant plastic PE-PU by microbial communities, we adopted the commercial water PU dispersion PolyLack® (Sayer Lack, México) that contains a proprietary aromatic polyether-polyurethane-acrylate (PE-PU-A) copolymer and the xenobiotic additives *N*-methylpyrrolidone (NMP), isopropanol (IP) 2-butoxyethanol (2-BE), dipropylene glycol butyl ether (DPGB), and dipropylene glycol methyl ether (DPGM). In this work, we provide comprehensive chemical and physical evidences of the capacity of a selected landfill microbial community to degrade an aromatic PE-PU-A copolymer and the aforementioned xenobiotic additives. In addition, we analyzed the structure and phenotypic potential of this community by applying the Hi-C proximity ligation technology. Based on these analyses, we identified a novel microbial landscape that can deal with PE-PU-A and xenobiotics additives degradation and proposed putative metabolic pathways and genes that can account for these capabilities. This is one of the few studies that combine physical and chemical analyses with metagenomics to elucidate possible metabolic pathways involved in xenobiotics biodegradation. Furthermore, this is the first metagenomic analysis of a polyurethane-degrading enriched landfill community. Understanding these pathways will help to design environmental biotechnological strategies that contribute to mitigate plastics and xenobiotics pollution and to achieve a better environmental quality.

MATERIALS AND METHODS

Site Location and Sampling Procedure

Deteriorated PU foam samples were collected at El Bordo Poniente (BP) landfill, located at Nezahualcóyotl Estado de México, México (19°27'10"N; 99°0'58"W). The samples were visually identified in piles of waste and in lixivate waters,

gathered by hand with sterile latex gloves and placed in sterile plastic bags for transportation to the laboratory. Then, they were immediately used to start the enrichment cultures.

Microbiological Techniques

For obtaining the enriched microbial community from the BP8 sample, approximately 1 cm³ was cut over a sterile Petri dish using a sterile scalpel. This PU foam piece was inoculated in 125 mL Erlenmeyer flask with 25 mL of minimal medium (MM) (Nakajima-Kambe et al., 1995) containing PolyLack® (0.3% v/v), as the sole carbon source (MM-PolyLack). PolyLack® Aqua Brillante (Sayer Lack, Prod. Num. UB-0800, México), mainly used for coating of wood floors with moderate transit, contains a proprietary aromatic PE-PU-A copolymer ($\leq 30\%$ w/v), and the additives NMP ($\leq 6\%$ v/v), 2-BE ($\leq 5\%$ v/v), IP ($\leq 3\%$ v/v), DPGB ($\leq 2\%$ v/v), DPGM ($\leq 1\%$ v/v), and silica ($\leq 3\%$ w/v) (Sayer Lack. Hoja de Datos de Seguridad de Materiales. PolyLack® Aqua Brillante, UB-0800. 09.18.2014. Version 4/0. México). The flask was incubated at 30°C and 220 rpm for 7 days. Two ml of this culture were transferred to 25 ml of fresh MM-PolyLack and cultured for 7 days, repeating two more times, for a total of 28 days, before being conserved in MM-PolyLack glycerol 30% at -70°C . The microbial mixed culture obtained from the landfill community, named as BP8, was propagated and conserved by inoculating 25 ml of fresh MM-PolyLack with a 500 μl glycerol from the original enriched community, incubated for 7 days and used to prepare new glycerols. BP8 growth was quantified by dry weight. For that, flasks with MM-PolyLack (25 ml) were inoculated with fresh cells (3 mg/ml) harvested from pre-cultures grown in MM-PolyLack for 48 h at 37°C, 220 rpm. At different incubation times, cells of one flask were harvested, washed three times with phosphate buffer (50 mM, pH 7) and dried to constant weight.

Cell-Substrate Interactions Techniques

For Cell surface hydrophobicity (CSH) measurements, cells were washed twice and suspended in phosphate buffer (0.05 M, pH 7) to an optical density (OD) of 0.6 (600 nm). The mixture of cell suspension (2 ml) and *n*-hexadecane was vortexed for 3 min and after that, the organic and aqueous phases were allowed to separate for 30 min. OD was measured in the cell suspension (aqueous phase). CSH is expressed as the percentage of adherence to hexadecane and it was calculated as follows: $100 \times [1 - (\text{OD}_{600} \text{ of the cell suspension after 30 min}) / (\text{OD}_{600} \text{ of the initial cell suspension})]$ (Rosenberg et al., 1980). Emulsification capacity of the culture medium was determined by mixing 2 ml of cell-free supernatant (CFS) and 3 ml of *n*-hexadecane in glass test tubes. The tubes were vigorously vortexed for 2 min and afterward let to stand at room temperature. The emulsification index (EI₂₄) was calculated after 24 h as follows: $100 \times [\text{emulsified layer height} / \text{total liquid column height}]$ (Cooper and Goldenberg, 1987). To observe cell-copolymer interactions, cells were fixed with 3% (v/v) glutaraldehyde in phosphate buffer (100 mM, pH 7.4), at 4°C overnight, washed three times, dehydrated with serial dilutions of ethanol, coated with gold and analyzed in a JEOL JSM-5900-LV electron microscope.

Analytical Techniques

Nuclear magnetic resonance (NMR) spectra from dried PolyLack® dissolved in C₅D₅N (30 mg/ml) were recorded at 298 K in a Bruker Avance 400 NMR (Billerica, MA, United States) at 400 MHz (¹H). For most of the analytical techniques, CFS were obtained by centrifugation at $17,211 \times g$ for 10 min, filtered through Whatman grade 41 paper, and dried at 37°C for 5 days. Carbon content was determined in a Perkin Elmer Elemental Analyzer (2400 CHN/O, Series II, Shelton, CT, United States). For gas chromatography coupled to mass spectrometry (GC-MS) analysis, 25 ml CFS were extracted in 6 ml LC-18 cartridges (Supelco) at a flow rate of 2 ml/min, eluted with 2 ml chloroform:methanol (1:1, v/v) and concentrated to 0.5 ml. Samples were injected in an Agilent GC system (7890B, Santa Clara, CA, United States) using two 5% phenyl-methylpolysiloxane columns (15 m \times 250 μm \times 0.25 μm). Oven was heated from 50 to 300°C at 20°C/min, Helium was used as carrier gas at a flow rate of 1 ml/min. The injector temperature was 300°C. For the quantification of additives, pure compounds (Sigma-Aldrich Chemicals $\geq 98\%$ purity) were used for standard curves. Identification of biodegradation products was performed in an Agilent Quadrupole Mass Analyzer (5977A MSD, Santa Clara, CA, United States) with electronic ionization energy of 1459 EMV and the mass range scanned at 30–550 amu. Scan rate was 2.8 spec/s. Data acquisition was performed with the Enhanced MassHunter software system. Compounds were identified based on mass spectra compared to the NIST database (2002 Library). Fourier transform infrared spectroscopy (FTIR) analyses were performed in dried CFS, by using a Perkin Elmer spectrometer (Spectrum 400, Waltham, MA, United States) in attenuated total reflection mode; 64 scans with a resolution of 4 cm⁻¹ were averaged in the range of 500–4000 cm⁻¹, processed and analyzed (Spectrum v6.3.5.0176 software). Derivative thermogravimetric analyses (DTG) were performed in a Perkin Elmer Thermogravimetric Analyzer (TGA 4000, Waltham, MA, United States) on 2.5 mg of dried CFS samples heated 30–500°C at a rate of 20°C/min, under a N₂ atmosphere. Differential scanning calorimetry (DSC) was performed analyzing 10 mg of dry CFS in a Q2000 (TA Instrument, New Castle, DE, United States) at a rate of 10°C/min, under a nitrogen flow of 50 ml/min, at a 20–600°C range. For Gel permeation chromatography (GPC) of PE-PU-A copolymers, liquid CFS were extracted in a similar way that described above for GC-MS analysis, but the 2 ml chloroform:methanol (1:1, v/v) elution was evaporated to dryness at 25–30°C. The dried sample was resuspended in tetrahydrofuran (THF) at 15 mg/ml of solids, then filtrated through 0.45 μm Whatman filters and injected in a Waters 2695 Alliance Separation Module GPC (Milford, MA, United States) at 30°C in THF, using a universal column and a flow rate of 0.3 ml/min. All the analyses were performed at least in three replicates.

Hi-C Proximity Ligation-Based Metagenomic Analysis

BP8 community cells cultured for 5 days in 50 ml of MM-PolyLack were harvested and washed three times with phosphate

buffer. Cells were resuspended in 20 ml TBS buffer with 1% (v/v) formaldehyde (J. T. Baker) (crosslinker) and incubated 30 min with periodic mixing. The crosslinker was quenched with glycine (0.2 g) (Bio-Rad) for 20 min, thereafter cells were centrifuged, lyophilized and frozen at -20°C . For DNA extraction, cell pellets (100 μl of solid cellular material, equivalent to $10^9 - 10^{10}$ cells) were resuspended in 500 μl of TBS buffer containing 1% (v/v) Triton X-100 and protease inhibitors (Press et al., 2017). DNA was digested with *Sau3AI* and *MluCI* and biotinylated with DNA Polymerase I Klenow fragment (New England Biolabs) followed by ligation reactions incubated for 4 h and then overnight at 70°C to reverse crosslinking. The Hi-C DNA library was constructed by using the HyperPrep Kit (KAPA Biosystems, Wilmington, MA, United States). A shotgun library was also prepared from DNA extracted from non-crosslinked cells using Nextera DNA Sample Preparation Kit (Illumina). The two libraries were paired-end sequenced using NextSeq 500 Illumina platform (Illumina, San Diego, CA, United States). *De novo* metagenome draft assemblies from the raw reads were made using the metaSPAdes assembler (Nurk et al., 2017). Hi-C reads were then aligned to the contigs obtained from the shotgun library using the Burrows-Wheeler Alignment tool (Li and Durbin, 2010) requiring exact read matching. The ProxiMeta algorithm was used to cluster the contigs of the draft metagenome assembly into individual genomes (Press et al., 2017). Additionally, we performed a community taxonomic profiling from shotgun reads using MetaPhlAn tool (Segata et al., 2012). Genome completeness, contamination, and other genomic characteristics were evaluated using CheckM pipeline (Parks et al., 2015). Phylogenetic analysis was performed using the single copy molecular markers, DNA gyrase subunit A and ribosomal proteins L3 and S5, selected from each deconvoluted genome and compared to homologous sequences from GenBank. Alignments were cured with Gblocks tool¹ and WAG plus G evolutionary models were selected using Smart Model Selection tool (Lefort et al., 2017). Finally, phylogeny was inferred with the graphical interface of SeaView (Gouy et al., 2010) using the Maximum Likelihood method. To compare genetic relatedness, Average Nucleotide Identity (ANI) between the genomes and the closest phylogenetic neighbors was calculated (Yoon et al., 2017). Open reading frames were identified using MetaGeneMark (Zhu et al., 2010). KO assignments (KEGG Orthology) and KEGG pathways reconstruction were performed with GhostKOALA server and KEGG Mapper tool, respectively (Kanehisa et al., 2016). All the xenobiotic degradation pathways were manually curated to only report those pathways in which most of the enzymes were encoded in the BP8 metagenome.

RESULTS

Growth and Interactions of BP8 Cells With PolyLack®

The BP8 community cultivated in MM-PolyLack for 25 days exhibited a biphasic growth with a first phase, from 0 to 13 days,

presenting a growth rate (2–4 days) of 0.008 h^{-1} and a second phase, from 13 to 25 days, with a growth rate (13–20 days) of 0.005 h^{-1} . Biomass increased from 0.32 to 2.9 mg/ml and consumed 50.3% of the carbon from the medium at 25 days (Figure 1A). EI_{24} initial value was 70%, it decreased to 24% at 20 days and increased again to 70%. CSH started at 62% and decreased to 25% at the first growth phase; thereafter it increased to 42% and remained constant until 20 days to increase to 67% at the end of the second phase (Figure 1B). SEM analysis at 10 days of cultivation revealed multiple-sized (0.5–1.5 μm) rod-shaped cells aggregated and attached to copolymer particles (Figure 1C).

Chemical and Physical Changes in PolyLack® Components Generated by the BP8 Community

To characterize the biodegradative activity of the BP8 community on the PolyLack® components, we performed different analytical techniques. GC-MS analysis of the CFS revealed that BP8 metabolized the xenobiotic additives, NMP and IP at the first day of cultivation and 2-BE at the fourth day. DPGM and DPGB were metabolized 84 and 73%, respectively, at the first day and remained constant until the end of the experiment (Figure 2A and Supplementary Table S1). Since the PE-PU-A copolymer structure is unknown, we proposed a hypothetical structure (Figure 3), based on $^1\text{H-NMR}$, the manufacturer's technical sheet and in the most frequently used chemicals for the synthesis of this copolymer (Pardini and Amalvy, 2008; Gite et al., 2010; Maurya et al., 2018). Since the first day of cultivation, complex and diverse chemical compounds such as aromatics, nitrogen-containing, ethers, esters, aliphatics, alcohols and organic acids, derived from the copolymer breakdown were observed. During the first 3 days (log phase) the degradation products were low abundant, at 10 days (intermediate lag phase) accumulation occurred, and during the second log phase their abundance decreased. Notably, isocyanates [2,4-toluene diisocyanate (TDI) and methylene diphenyl diisocyanate (MDI)] derivatives were aromatic amines observed maximal at the beginning and diminished throughout the cultivation period (Figure 2B, Supplementary Figure S1, and Supplementary Table S2), suggesting that metabolization of the urethane groups is being achieved. FTIR of dried CFS revealed changes in PE-PU-A functional groups. The signal intensity of the C=O stretch from urethane and acrylate carbonyl groups (1730 cm^{-1}) increased at 5 days and lately decreased, suggesting hydrolysis and subsequent catabolism of urethanes and acrylates. The signal for aromatic groups C=C stretch (1600 cm^{-1}) considerably decreased at 20 days, while the signal for aromatic C-C stretch (1380 cm^{-1}) showed variable intensities at different days, and a new C-C signal for aromatics (1415 cm^{-1}) appeared at 20 days, indicating the cleavage of the aromatic rings. The urethane N-H bending plus C-N stretch signal (1550 cm^{-1}) slightly decreased at 15 days and increased at the end of the cultivation time, whereas urethane C-N stretching band (1231 cm^{-1}) significantly increased, indicating urethane attack. Signals associated with urethane C-O-C stretch (1086 cm^{-1} , 1049 cm^{-1}) and C-O-C symmetric stretch (977 cm^{-1}) decreased during the cultivation period, indicating microbial activity on the

¹http://phylogeny.lirmm.fr/phylo.cgi/one_task.cgi?task_type=gblocks

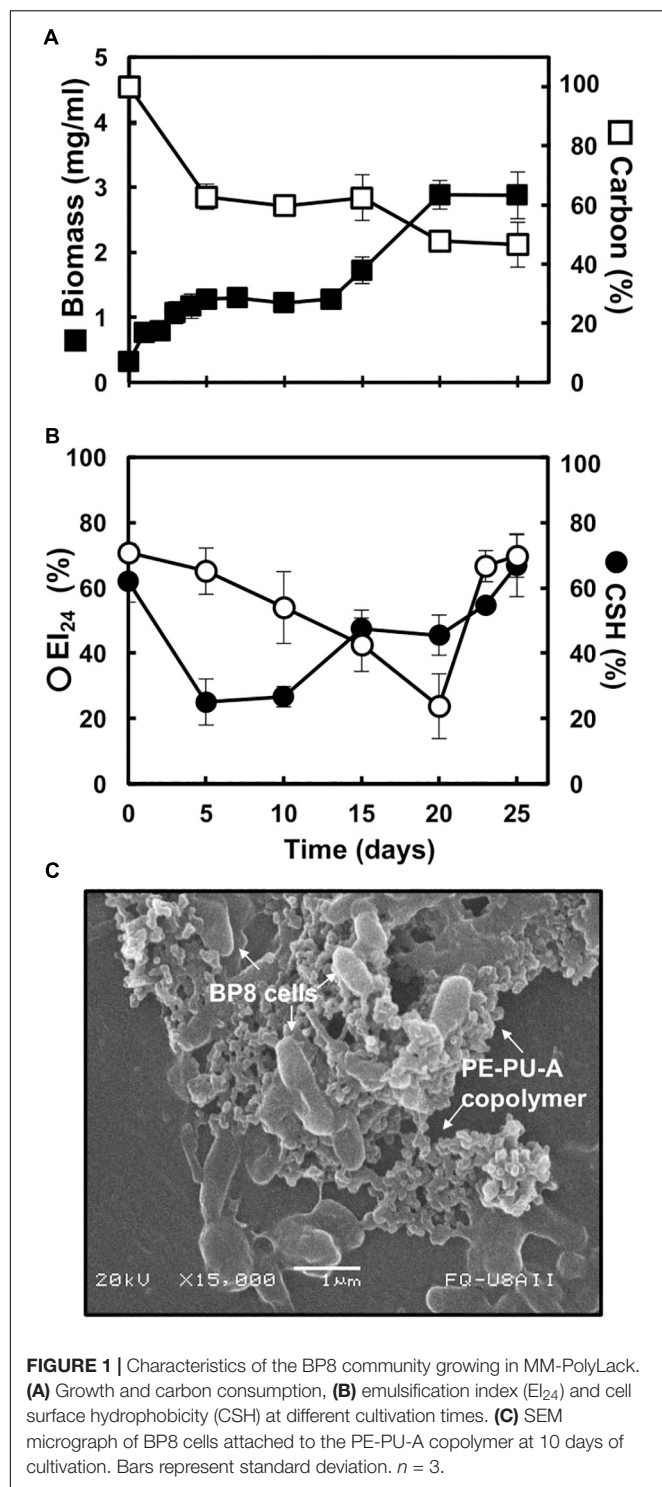


FIGURE 1 | Characteristics of the BP8 community growing in MM-PolyLack. **(A)** Growth and carbon consumption, **(B)** emulsification index (EI_{24}) and cell surface hydrophobicity (CSH) at different cultivation times. **(C)** SEM micrograph of BP8 cells attached to the PE-PU-A copolymer at 10 days of cultivation. Bars represent standard deviation. $n = 3$.

ether groups. The signal for the acrylate's vinyl group $C=CH_2$ out of plane (850 cm^{-1}) decreased at 20 days, indicating the cleavage of the acrylate component. Also, the aliphatic chain signals (704 and 520 cm^{-1}) decreased during the cultivation period (Figure 4A). DTG thermograms exhibited four stages of thermal decomposition corresponding to the functional groups

of the copolymer. Stages II and IV, for urethane and ether groups respectively, reduced their masses at early cultivation times, while stage III, for esters, steadily kept reducing its mass during the whole experimental period. Interestingly, stage I, which accounts for low molecular weight compounds, in this case biodegradation products, showed a fluctuating behavior that increased at 10 days, and decreased afterward (Figure 4B). DSC analysis of the copolymer showed multiple thermal transitions revealing complex microstructures: the glass transition temperature (T_g : 50.2°C) reflects the proportion of soft and hard segments; the three melting temperatures (T_m -I: 70°C , T_m -II: 210.6°C , T_m -III: 398.1°C) are associated with the hard segments of the polymer and the crystallization temperature (T_c : 459.6°C) is attributed to heat-directed crystallization of copolymer chains (Cipriani et al., 2013; Sultan et al., 2014) (Figure 4C). BP8 biodegradative activity caused T_g decrease (46.2°C), changes in T_m s, and strong decrease in T_c area, indicating that BP8 disrupts both, the soft and the hard segments (associated with urethane groups) (Figure 4C and Supplementary Table S3). GPC analysis showed that the number-average molecular weight (M_n) of the copolymer steadily decreased 35.6% up to the end of the culture time, meanwhile the weight-average molecular weight (M_w) increased about 10% , from 0 to 15 days of cultivation, and then decreased 26% from 15 to 25 days. The Polydispersity index (PDI) increased over 2, at 25 days of cultivation with BP8. Analysis of Molecular weight distribution (MWD) of the degraded samples showed shifts toward higher molecular weights than control up to 20 days of analysis. However, at 25 days, a strong shift to lower molecular weights was observed (Table 1 and Supplementary Figure S2). Abiotic controls of different cultivation times were evaluated and no changes were observed (Table 1). All these results indicate that the degradative activity of the BP8 community generated changes in the soft and hard segments of the copolymer microstructure resulting from the attack to the different functional groups, including the more recalcitrant ether and urethane groups.

Community Structure and Metagenomic Deconvolution of the BP8 Community

Analysis of the BP8 community taxonomic profile with MetaPhlAn, by using 17,282,414 reads, detected five bacterial orders (abundance), *Rhodobacterales* (83%), *Rhizobiales* (8.9%), *Burkholderiales* (6.8%), *Actinomycetales* (0.83%), *Sphingobacteriales* (0.08%), and one viral order *Caudovirales* (0.33%). Bacteria included 16 genera, being the most abundant *Paracoccus* (83%) and *Ochrobactrum* (8.7%) (Figure 5). The shotgun Illumina library was used to create a draft *de novo* metagenome assembly. After parsing contigs lesser to 1000 bp, this assembly had 5339 contigs with 21,228,807 bp in size. Subsequently, we mapped the Hi-C reads to the draft shotgun assembly generating 3,072 contigs with a total length of 17,618,521 bp. The alignment of Hi-C reads to this assembly allowed the deconvolution of five genome clusters, three near complete drafts (completeness $>95\%$), and two substantially complete drafts (completeness 89 and 71%) (Parks et al., 2015) (Table 2). The phylogenetic analysis showed well-supported

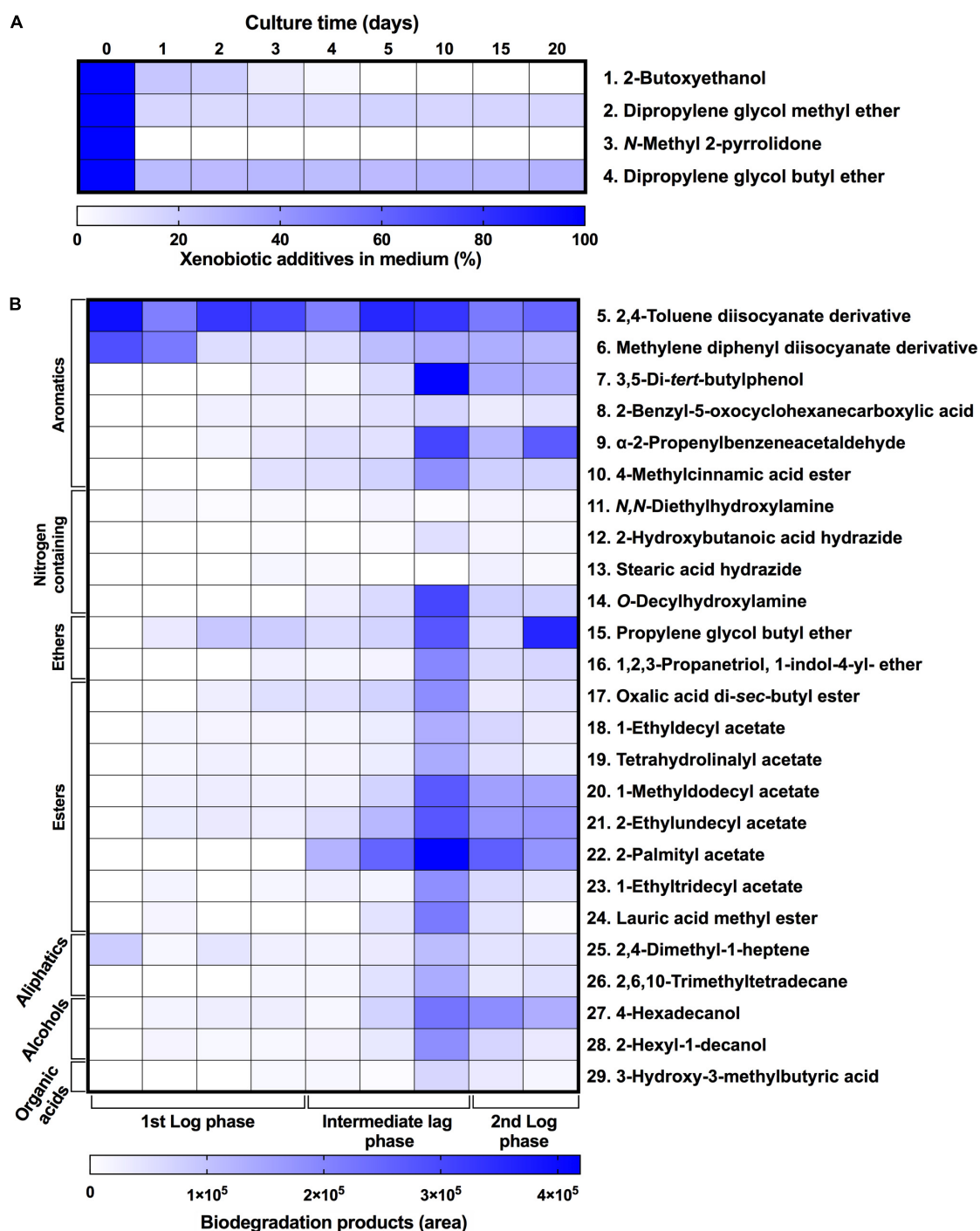


FIGURE 2 | Xenobiotic additives consumed **(A)** and PE-PU-A biodegradation products generated **(B)** by the BP8 community. Cell-free supernatants were extracted at different cultivation times with chloroform:methanol and analyzed by GC-MS. **(A)** Additives were quantified using standard curves for each compound and **(B)** biodegradation products by analyzing their areas in independent chromatograms. $n = 3$. Compounds with mass spectra similarity values over 700 were considered the same compounds of the Library hits. The numbers in the compounds correspond to signals in the chromatograms of **Supplementary Figure S1**.

clades within *Paracoccus*, *Chryseobacterium*, *Parapedobacter*, a member of the *Microbacteriaceae* family, and *Ochrobactrum intermedium* (Figure 6). The deconvoluted genomes of

Paracoccus sp. BP8 and *O. intermedium* BP8.5 showed low novelty scores and high ANI values compared to their closest phylogenetic relatives. In contrast, *Chryseobacterium* sp. BP8.2,

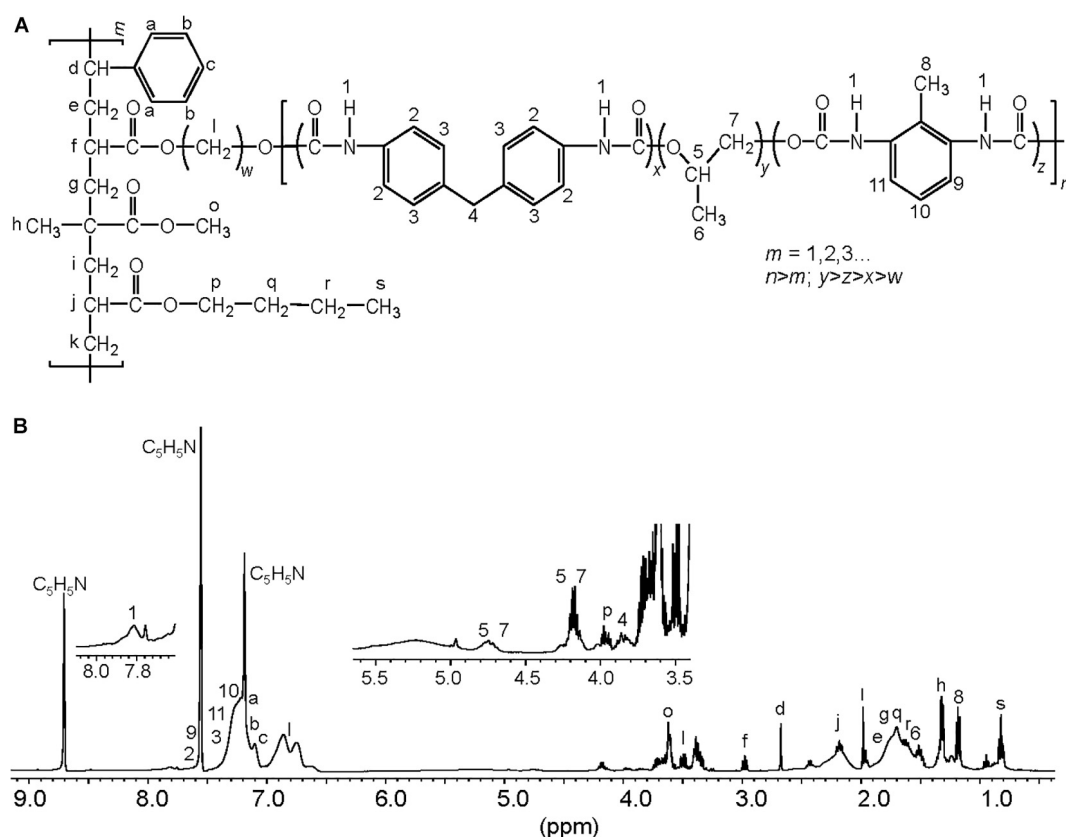


FIGURE 3 | Proposed chemical structure for the PE-PU-A copolymer present in PolyLack®. **(A)** This structure was proposed based on the **(B)** ¹H-NMR analysis of dried PolyLack®, the information included in the manufacturer technical manual (SayerLack. Poly Lack Aqua Brillante UB-0800), the GC-MS analysis (**Figure 2**), and the most frequent acrylates used in the synthesis of these types of copolymers (Pardini and Amalvy, 2008; Maurya et al., 2018). Synthesis of PE-PU-A copolymers starts by the polycondensation of polyols [polypropylene glycol (PPG)] (y moiety) and diisocyanates (TDI and MDI) (x and z moieties) followed by end capping with acrylates' mixture (m moiety). From the most frequently used acrylates we selected methyl methacrylate, butyl acrylate, hydroxy acrylate and styrene as representatives in this structure. In the ¹H-NMR spectrum, chemical shifts are provided in parts per million from SiMe₄ as internal reference. Signal 1 is assigned to carbamate groups (NH-COO); signals a, b, c, 2, 3, 9-11 are assigned to the aromatic protons; signals 4 and 8 correspond to the protons of methylene (CH₂) and methyl (CH₃) groups in MDI and TDI, respectively; signals 5-7 correspond to PPG; signals l correspond to the hydroxyl proton (CH₂-O) and methylene groups (CH₂) in the chain of hydroxy-acrylate; signals f, j, o and p correspond to the acrylic groups (CH-COO, CH₂-COO or CH₃-COO); signals d (CH), e, g, i, k, q, r (CH₂), h and s (CH₃) are assigned to methylene and methyl groups in the acrylate mixtures.

Parapedobacter sp. BP8.3 and the *Microbacteriaceae* bacterium BP8.4 showed high novelty scores and low ANI values (<95%) indicating they are new species. GC content and genomes' sizes were similar to the closest relatives except for the *O. intermedium* BP8.5 genome size, probably because of the low genome completeness (**Table 2** and **Supplementary Table S4**).

Analysis of the Xenobiotic Metabolism Encoded in the BP8 Metagenome

In all the genomes, except in *O. intermedium* BP8.5, the genes and proteins assigned were in the range reported for the phylogenetically related members (**Table 2** and **Supplementary Table S4**). Reconstruction of the metabolic pathways encoded in the BP8 metagenome was performed with 18,386 ORFs from which 8,637 were annotated into KEGG Orthology groups and the rest was not assigned to any orthologous functional category. Analysis of the BP8

xenobiotic metabolism identified 215 sequences encoding 59 unique proteins participating in pathways for benzoate (ko00362), fluorobenzoate (ko00364), aminobenzoate (ko00627), chlorocyclohexane and chlorobenzene (ko00361), and *n*-alkanes (ko00071) degradation. The most relevant enzymes are listed in **Table 3**. The genes for benzoate metabolism include all the enzymes for benzoate and 4-methoxybenzoate activation as well as 4-methoxybenzoate monooxygenase, an O-demethylating enzyme that transforms methoxybenzoate to hydroxybenzoate, and for their subsequent transformation to β-ketoadipate (first 18 EC numbers in **Table 3**). Two genes encoding carboxymethylene butanolidase that cleaves the ring of cyclic ester dienelactone to produce maleylacetate, acting on the fluorobenzoate and chlorocyclohexane and chlorobenzene metabolisms, were identified. Genes encoding enzymes for the aminobenzoate pathway, such as 4-hydroxybenzoate decarboxylase that participates in the transformation of phenol into hydroxybenzoate, amidase that transforms benzamide

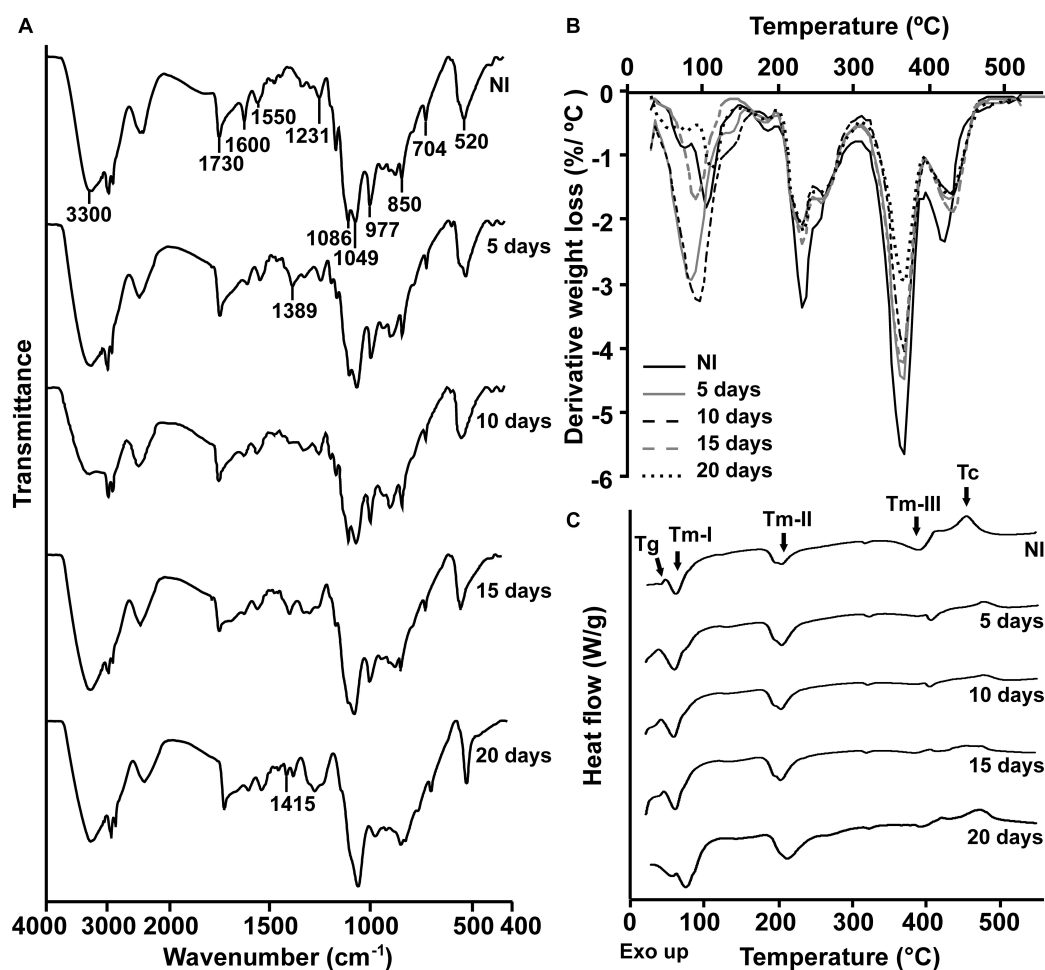


FIGURE 4 | Physical and chemical analyses of the aromatic PE-PU-A copolymer after incubation with the BP8 community. **(A)** FTIR spectra. **(B)** DTG analysis. Thermal degradation stages correspond to the following functional groups: (I) Low molecular weight compounds, (II) Urethane, (III) Ester, (IV) Ether. **(C)** DSC analysis. Glass transition temperature (Tg) represents the relative amount of soft and hard segments; melting temperatures, Tm-I, Tm-II, and Tm-III are associated with hard domains, and crystallization temperature (Tc) represents heat-directed crystallization of copolymer chains. NI, non-inoculated.

into benzoate, and benzoyl phosphate phosphohydrolase that converts benzoyl phosphate into benzoate, were identified. All the genes encoding enzymes needed for chlorocyclohexane and

chlorobenzene degradation, the specific 2,4-dichlorophenol 6-monooxygenase, the enzymes that transform 4-chlorophenol to *cis*-acetylacrylate (EC 1.13.11.1, EC 5.5.1.1, and EC 3.1.1.45), and the 2-haloacid dehalogenase, which eliminates halogens from alkanes, were found. Likewise, genes encoding enzymes for *n*-alkanes degradation (Table 3 Alkanes metabolism), as well as all the enzymes for beta-oxidation were also detected.

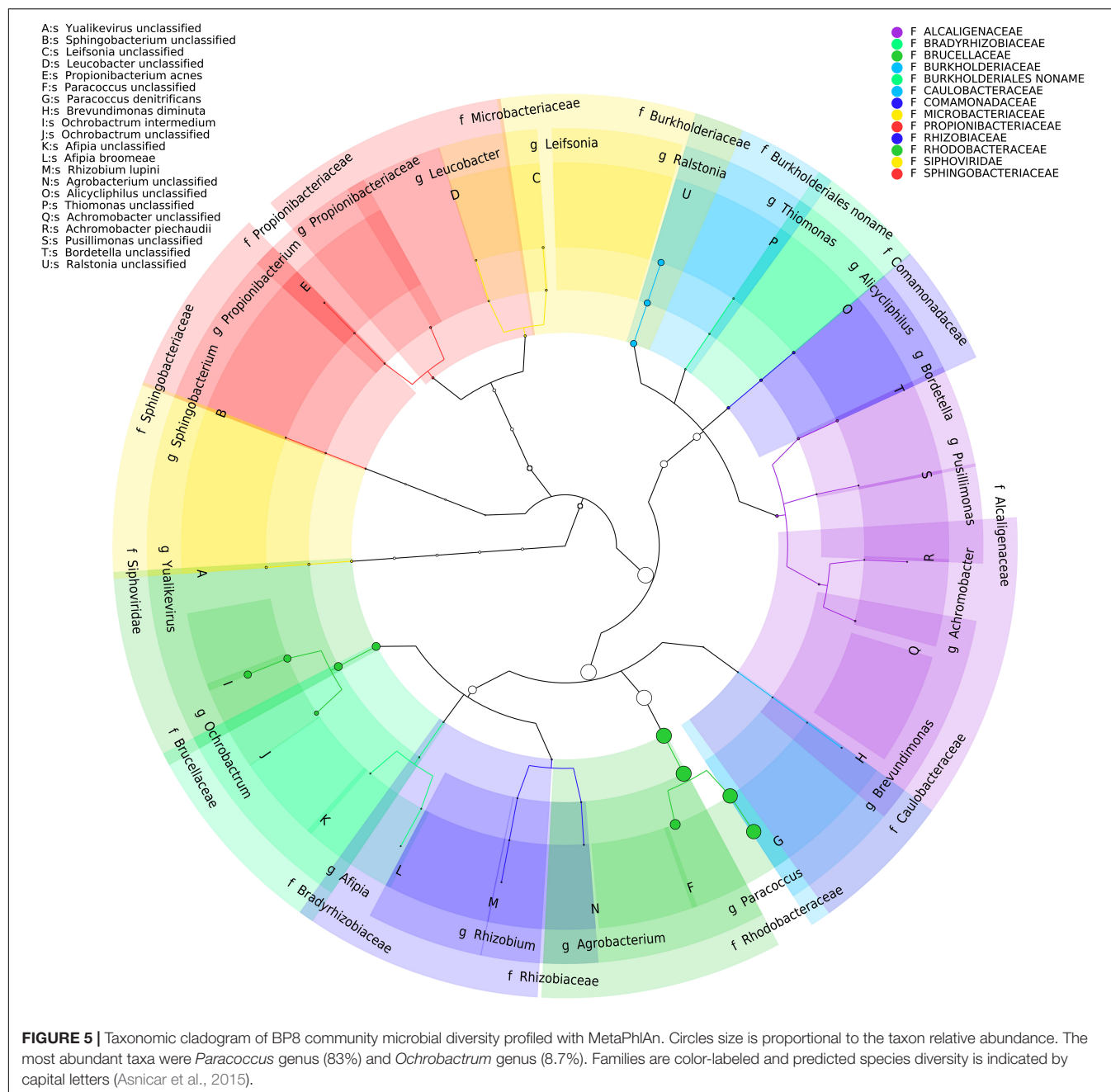
TABLE 1 | Molecular weight and polydispersity index of the PE-PU-A copolymer during cultivation with the BP8 community.

Culture time (days)	Mn (g/mol)	Mw (g/mol)	PDI
Non-inoculated	101,896 ± 8,098	208,490 ± 7,600	2.0 ± 0.3
5	96,798 ± 712	210,837 ± 26,098	2.2 ± 0.1
10	89,258 ± 5,825	223,581 ± 18,736	2.5 ± 0.3
15	82,577 ± 1,168	229,372 ± 26,416	2.7 ± 0.3
20	73,406 ± 9,225	187,925 ± 50,737	2.4 ± 0.3
25	65,609 ± 990	169,925 ± 5,080	2.6 ± 0.2

Number-average molecular weight (Mn), weight-average molecular weight (Mw) and polydispersity index (PDI) were calculated by Gel permeation chromatography with monodisperse polystyrene calibration standards and using THF as eluent. *n* = 3.

BP8 Community Phenotypic Potential to Biodegrade the Xenobiotic Additives of PolyLack® NMP Degradation

Genes encoding putative proteins for NMP degradation, with significant similarity (>40%) to the enzymes of *Alicyclophilus denitrificans* BQ1 (Solís-González et al., 2018) were identified in several BP8 genomes (Table 3). However, only in *Paracoccus* sp. BP8 a gene cluster (RQP05666.1–RQP05671.1) comparable to the BQ1 *nmp* cluster was identified.



Isopropanol Degradation

Genes encoding proteins with significant similarity to NAD⁺-dependent secondary alcohol dehydrogenase (ADH) with capability to oxidize IP to acetone were identified in the BP8 metagenome (Kotani et al., 2003), but not the genes encoding the enzymes for the oxidative transformation of acetone. However, the three genes encoding acetone carboxylase that transforms acetone into acetoacetate were identified. Similarly, the genes encoding 3-oxoacid-CoA transferase, in *Paracoccus* sp. BP8, and acetoacetate-CoA ligase, in *O. intermedium* BP8.5, that convert, both of them, acetoacetate into acetoacetyl-CoA, were observed. Besides, genes for acetyl-CoA C-acetyltransferase,

which transforms acetoacetyl CoA to acetyl CoA that enters the TCA pathway, were also found in the BP8 metagenome (**Figure 7A** and **Table 3**).

Glycol Ethers Degradation

In the BP8 metagenome, homologous genes to polyethylene glycol (PEG)-degrading ADHs and aldehyde dehydrogenases (ALDHs) (Ohta et al., 2006; Tani et al., 2007), and diverse enzymes that could attack the ether bonds, such as glycolate oxidase (RQP04511.1, RQP04512.1, RQP04513.1, RQP11464.1, RQP19624.1, RQP19625.1, RQP16322.1, RQP16256.1), dye decoloring peroxidase (RQP04907.1, RQP09154.1) and

TABLE 2 | General features of the deconvoluted genomes from the BP8 metagenome.

Cluster ID	Genome Size (bp)	Num Contigs	Contig N50	^a Completeness (%)	^b Relative Abundance (%)	Novelty Score (%)	GC (%)	Identification	Genes assigned	Proteins assigned
1	4,275,656	282	51,004	89.4	57.7	1.6	67.8	<i>Paracoccus</i> sp. BP8	4,225	4,073
2	2,157,639	388	7,081	95.6	3.7	98.7	47.3	<i>Chryseobacterium</i> sp. BP8.2	2,253	2,185
3	5,478,545	1098	6,493	95.5	12.5	99.2	48.1	<i>Parapedobacter</i> sp. BP8.3	5,310	5,173
4	2,790,120	158	39,967	97.7	3.6	94.0	71.3	^c <i>Microbacteriaceae</i> bacterium BP8.4	2,850	2,705
5	2,916,513	1146	2,823	71.0	22.5	2.5	58.4	<i>Ochrobactrum</i> <i>intermedium</i> BP8.5	3,472	3,162

^aCompleteness was calculated based on 40 single copy gene markers (Parks et al., 2015). All the genomes' drafts have at least 18 tRNAs and, except for cluster 5, at least one rDNA gene copy. ^bRelative abundance was normalized according to the reads distribution along the deconvoluted taxon. ^cFor *Microbacteriaceae* bacterium BP8.4 no further classification was possible even that nine single-copy markers were analyzed.

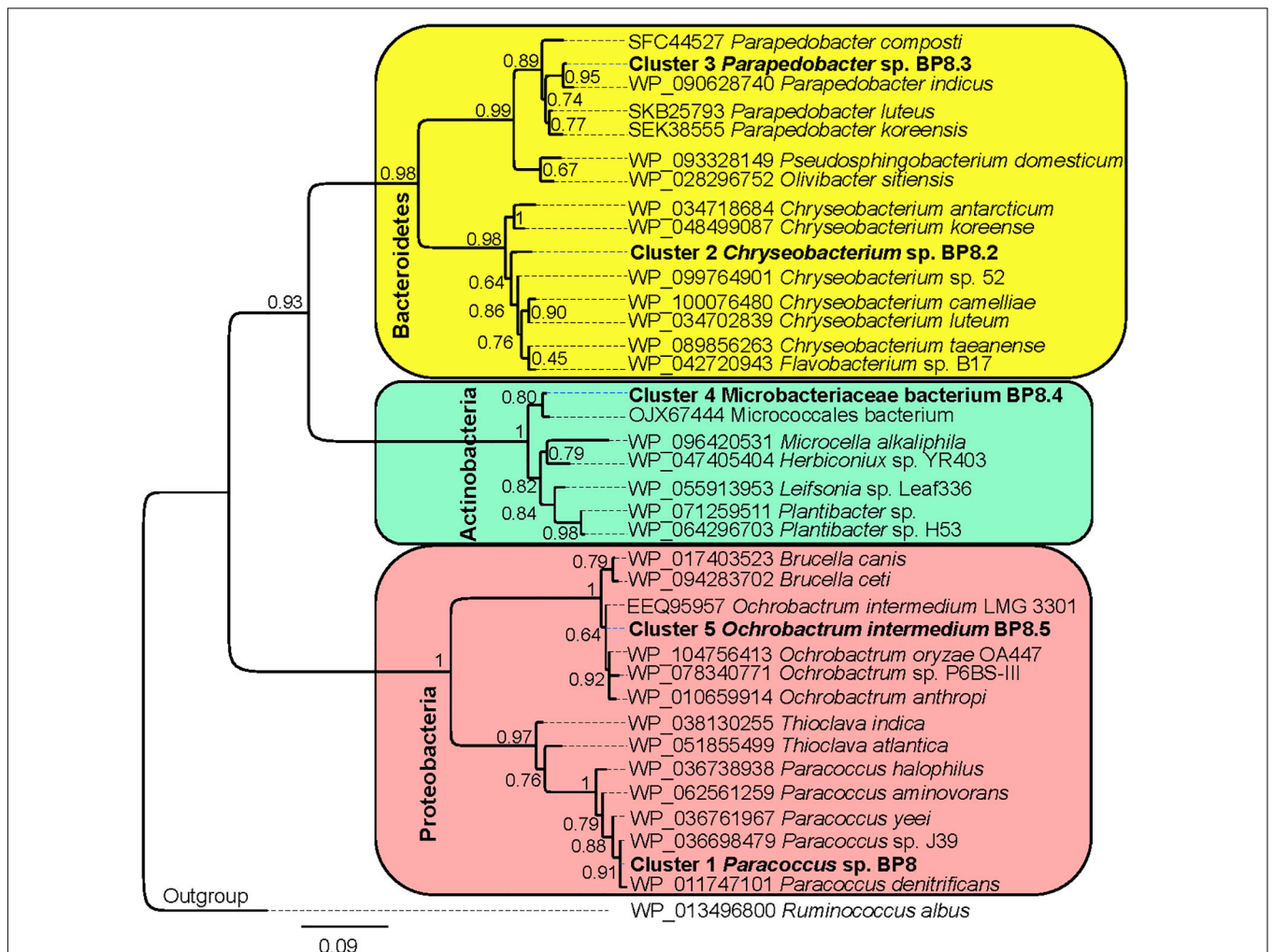


FIGURE 6 | Maximum likelihood phylogeny for taxonomic delimitation of the deconvoluted genomes from the BP8 metagenome. The analysis was performed with three phylogenetic markers: ribosomal protein L3, ribosomal protein S5 and DNA gyrase A subunit, which generated similar results. The analysis for ribosomal protein L3 is presented. Branch support values are indicated in the corresponding nodes. Bar indicates the number of expected substitutions per site under the WAG + G model. A sequence of *Ruminococcus albus* (Firmicutes) was used as outgroup. Key genome clusters are highlighted in bold and different Phyla are indicated at the left. Sequences for L3 ribosomal proteins of the deconvoluted genomes are accessible in the NCBI GenBank under accession numbers RQP07704.1, RQP15098.1, RQP16503.1, RQP08603.1, and RQP16393.1 for clusters 1–5, respectively.

TABLE 3 | Distribution of genes encoding relevant proteins involved in xenobiotics degradation in the BP8 metagenome.

Activity	K Number	EC	Name	<i>Paracoccus</i> sp. BP8	<i>Chryseobacterium</i> sp. BP8.2	<i>Parapedobacter</i> sp. BP8.3	<i>Microbacteriaceae</i> bacterium BP8.4	<i>O. intermedium</i> BP8.5
Benzoate and related compounds metabolism								
Benzoate/toluate 1,2- dioxygenase	K05549	1.14.12.10	<i>benA-xylX</i>	1	–	–	–	–
	K05550		<i>benB-xylY</i>	1	–	–	–	–
	K05784	1.18.1.-	<i>benC-xylZ</i>	1	–	–	–	–
Dihydroxycyclohexadiene carboxylate dehydrogenase	K05783	1.3.1.25	<i>benD-xylL</i>	1	–	–	–	–
<i>p</i> -Hydroxybenzoate 3-monooxygenase	K00481	1.14.13.2	<i>pobA</i>	1	–	–	–	1
Catechol 1,2-dioxygenase	K03381	1.13.11.1	<i>catA</i>	1	–	–	–	–
Catechol 2,3-dioxygenase	K07104	1.13.11.2	<i>catE</i>	1	–	–	1	1
Protocatechuate 3,4-dioxygenase	K00448	1.13.11.3	<i>pcaG-pcaH</i>	1	–	–	–	1
	K00449			1	–	–	–	1
Muconate cycloisomerase	K01856	5.5.1.1	<i>catB</i>	1	–	–	1	–
3-Carboxy- <i>cis,cis</i> -muconate cycloisomerase	K01857	5.5.1.2	<i>pcaB</i>	1	–	–	–	1
Muconolactone isomerase	K01856	5.3.3.4	<i>catC</i>	1	–	–	–	–
4-Carboxymuconolactone decarboxylase	K01607	4.1.1.44	<i>pcaC</i>	2	–	–	–	1
Enol-lactone hydrolase	K01055	3.1.1.24	<i>pcaD</i>	3	–	–	–	1
β -ketoadipate:succinyl- CoA transferase,	K01031	2.8.3.6	<i>pcaI-pcaJ</i>	1	–	–	–	2
	K01032			1	–	–	–	1
β -ketoadipyl-CoA thiolase	K00632	2.3.1.16	<i>pcaF</i>	–	1	1	1	1
2-Oxopent-4-enoate hydratase (benzoate)	K02554	4.2.1.80	<i>mhpD</i>	–	–	–	1	–
4-Hydroxy 2-oxovalerate aldolase	K01666	4.1.3.39	<i>mhpE</i>	–	–	–	2	–
Acetaldehyde dehydrogenase	K04073	1.2.1.10	<i>mhpF</i>	–	–	–	2	–
4-Methoxybenzoate monooxygenase (O-demethylating)	K22553	1.14.99.15	CYP199A2	1	–	–	–	–
Carboxymethylene butanolidase	K01061	3.1.1.45	<i>clcD</i>	–	–	–	1	1
4-Hydroxybenzoate decarboxylase	K03186	4.1.1.61	<i>ubiX</i>	2	–	1	–	1
Amidase	K01426	3.5.1.4	<i>amiE</i>	1	–	–	1	1
Benzoyl phosphate phosphohydrolase	K01512	3.6.1.7	<i>acyP</i>	–	–	1	1	–
2,4-Dichlorophenol 6-monooxygenase	K10676	1.14.13.20	<i>tfdB</i>	1	–	–	–	–
2-Haloacid dehalogenase	K01560	3.8.1.2		2	–	–	–	1
Alkanes metabolism								
Alkane 1-monooxygenase	K00496	1.14.15.3	<i>alkB1_B2</i>	2	–	–	–	–
			<i>alkM</i>					
Ferredoxin NAD ⁺ reductase component	K00529	1.18.1.3	<i>hcaD</i>	2	–	–	–	1
Unspecific monooxygenase	K00493	1.14.14.1		2	–	–	–	1
Long-chain-alkane monooxygenase	K20938	1.14.14.28	<i>LadA</i>	–	–	–	1	–
Alcohol dehydrogenase propanol preferring	K13953	1.1.1.1	<i>adhP</i>	2	–	1	–	1
Aldehyde dehydrogenase (NAD ⁺ dependent)	K00128	1.2.1.3	ALDH	6	2	–	–	3
Aldehyde dehydrogenase (NADP dependent)	K14519	1.2.1.4	<i>aldH</i>	–	1	–	–	–
Lipocalin family protein	K03098	–	<i>Blc</i>	–	1	1	–	1
Long chain fatty acid transport protein	K06076	–	<i>fadL</i>	1	–	–	–	–

(Continued)

TABLE 3 | Continued

Activity	K Number	EC	Name	<i>Paracoccus</i> sp. BP8	<i>Chryseobacterium</i> sp. BP8.2	<i>Parapedobacter</i> sp. BP8.3	<i>Microbacteriaceae</i> bacterium BP8.4	<i>O. intermedium</i> BP8.5
N-methylpyrrolidone metabolism								
<i>N</i> -methylhydantoin amidohydrolase	K01473	3.5.2.14	<i>nmpA</i>	5	–	–	–	1
	K01474		<i>nmpB</i>	5	–	–	1	–
Aminoacid oxidase	–	–	<i>nmpC</i>	3	–	–	2	1
Succinate-semialdehyde dehydrogenase	K00135	1.2.1.16	<i>nmpF</i>	7	–	1	2	1
Isopropanol metabolism								
^a Alcohol dehydrogenase propanol preferring	K13953	1.1.1.-	<i>adh1</i>	1	–	–	–	–
Alcohol dehydrogenase	K18369	1.1.1.-	<i>adh2</i>	2	–	–	–	–
^b Aldehyde dehydrogenase	K00138	1.2.1.-	<i>adh3</i>	1	–	–	1	–
	K10854		<i>acxB</i>	1	–	–	–	–
Acetone carboxylase	K10855	6.4.1.6	<i>acxA</i>	1	–	–	–	1
	K10856		<i>acxC</i>	1	–	–	–	–
3-Oxoacid-CoA transferase	K01028	2.8.3.5		1	1	1	1	–
	K01029			1	1	1	1	–
Acetoacetate-CoA ligase	K01907	6.2.1.16	<i>acsA</i>	–	–	–	–	1
Acetyl-CoA C-acetyltransferase	K00626	2.3.1.9	<i>atoB</i>	10	1	1	3	5
Glycol ethers and polypropylene glycols metabolism								
^c Alcohol dehydrogenase,	–	1.1.1.-	<i>pegdh</i>	3	–	–	–	3
^d Aldehyde dehydrogenase	–	1.2.1.3	<i>pegC</i>	3	–	–	1	–
Glycolate oxidase	K00104	1.1.3.15	<i>glcD</i>	1	–	–	–	2
	K11472		<i>glcE</i>	1	–	–	–	1
	K11473		<i>glcF</i>	1	–	–	1	1
Superoxide dismutase	K04564	1.15.1.1	SOD2	–	1	3	1	1
	K04565		SOD1	1	1	–	–	–
Dye decoloring peroxidase	K15733	1.11.1.19	<i>DyP</i>	1	–	–	1	–
Glutathione S-transferase	K00799	2.5.1.18	<i>gst</i>	11	–	–	–	8
Acyl Co-A synthetase	K01897	6.2.1.3	ACSL	2	3	2	2	1
S-(hydroxymethyl) glutathione dehydrogenase	K00121	1.1.1.284	<i>frmA</i>	3	–	–	–	2
S-formylglutathione hydrolase	K01070	3.1.2.12	<i>fghA</i>	1	–	–	–	1

^a*Adh1* was identified by BLAST analysis using the *adh1* sequence (Acc. num. BAD03962.1) reported for *Gordonia* sp. TY-5 (Kotani et al., 2003) as query (Query cover >99%; E-value =4E-42; Identity 34%). The gene accession number in the BP8 metagenome is RQP06405.1. ^b*Adh3* genes were identified by BLAST analysis using the *adh3* sequence (Acc. num. BAD03965.1) reported for *Gordonia* sp. TY-5 (Kotani et al., 2003) as query (Query cover = 97%; E-value = 1E-97; Identity = 38.8%). The gene accession numbers in the BP8 metagenome are RQP06404.1 and RQP13157.1. These genes were classified as aldehyde dehydrogenases by KEGG, similarly as described in Kotani et al. (2003). ^c*Pegdh* genes were identified by BLAST analysis using the polyethylene glycol dehydrogenase sequence (*pegdh*) from *Sphingopyxis terrae* (Acc. num. BAB61732) (Ohta et al., 2006) as query (Query cover = 97%; E-value = 2.0E-122; Identity = 38.5%). The gene accession numbers in the BP8 metagenome are RQP05609.1, RQP06903.1, RQP07092.1, RQP19606.1, RQP18819.1, RQP20974.1. ^d*Pegc* genes were identified by BLAST using polyethylene glycol aldehyde dehydrogenase sequence from *Sphingopyxis macrogoltabida* (Acc. num. BAF98449.1) (Tani et al., 2007) as query (Query cover = 98%; E-value = 1.0E-80; Identity = 38%; Similarity = 56%). The gene accession numbers in the BP8 metagenome are RQP06197.1, RQP04172.1, RQP06015.1, RQP13157.1. Only RQP06197.1 was identified as K00128 by KEGG.

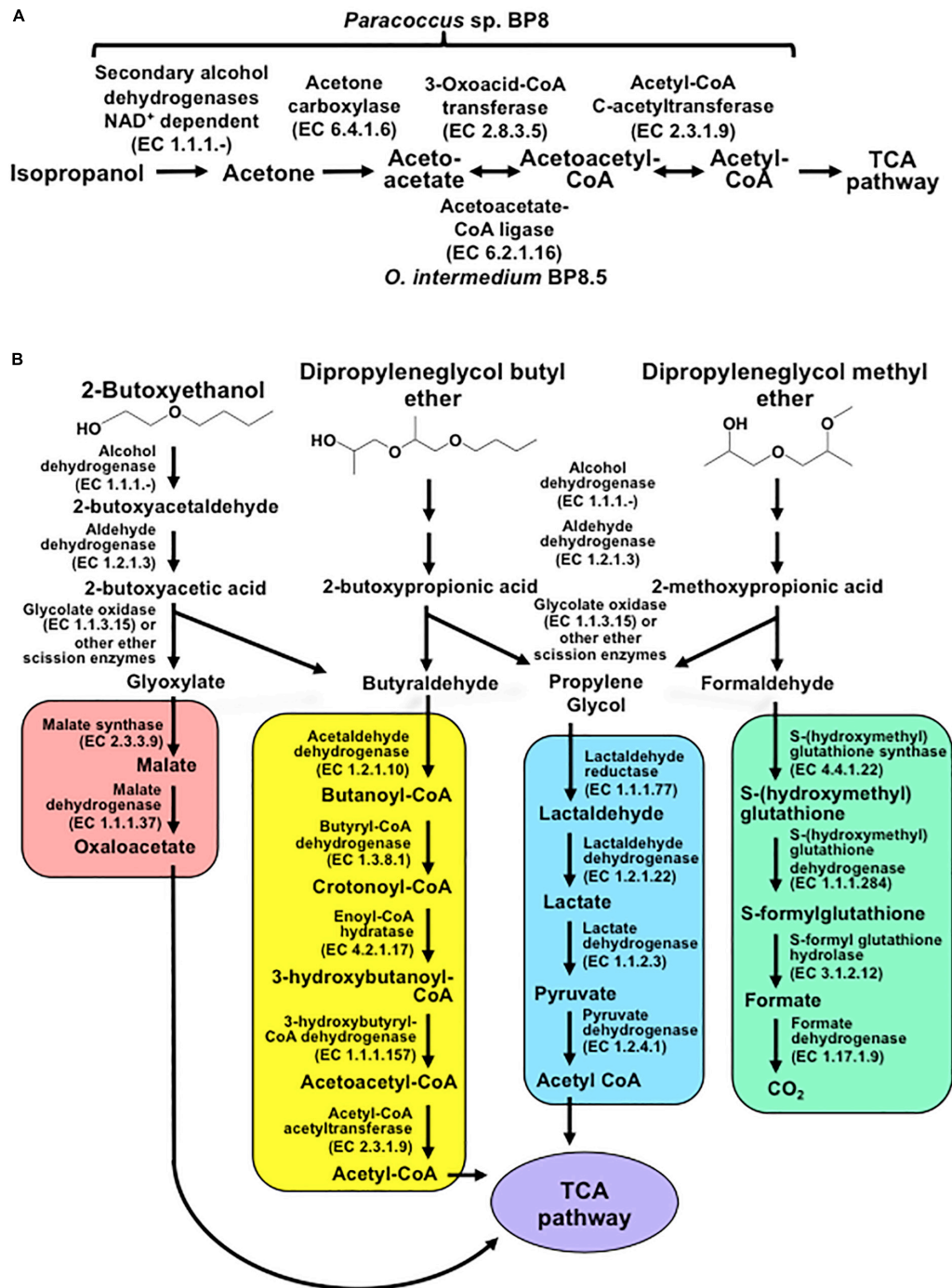


FIGURE 7 | Potential degradation pathways for isopropanol **(A)** and glycol ethers **(B)** encoded in the BP8 metagenome. **(A)** *Paracoccus* sp. BP8 genome encodes ADH enzymes that can oxidize IP to acetone, but genes encoding enzymes for the oxidative metabolism of acetone were not found. Instead, genes encoding the reductive transformation of acetone to acetyl CoA, acetone carboxylase, 3-oxoacid-CoA transferase and acetyl-CoA C-acetyltransferase, were identified. In *O. intermedium* BP8.5 genome, acetoacetate-CoA ligase, which performs the same reaction that 3-oxoacid-CoA transferase, is encoded. All the enzymes for the TCA pathway are encoded in the BP8 metagenome (see **Table 3**). **(B)** Subsequent oxidations of glycol ethers' hydroxy terminal groups by PEG-DH and PEG-ALDH will produce 2-butoxyacetic acid from 2-BE, 2-butoxypropionic acid from DPGB and 2-methoxypropionic acid from DPGM. Subsequent cleavage of carboxylates' ether bonds by ether scission enzymes such as glycolate oxidase, dye decoloring peroxidase, 4-methoxybenzoate monooxygenase and/or unspecific monooxygenase, would generate the metabolizable intermediaries glyoxylate, butyraldehyde, propylene glycol and formaldehyde. Glyoxylate would be funneled to the glyoxylate metabolism (red rectangle), butyraldehyde to the butanoate metabolism (yellow rectangle), propylene glycol to the pyruvate metabolism (blue rectangle), and formaldehyde to the formate metabolism (green rectangle). Pathways for glyoxylate, butanoate, pyruvate and formate metabolisms as well as the TCA pathway (purple ellipse) were fully reconstructed from the BP8 metagenome based on KEGG annotated genes, using KEGG Mapper.

superoxide dismutase (RQP04715.1, RQP13424.1, RQP09887.1, RQP11889.1, RQP18047.1, RQP18034.1, RQP09190.1, RQP20377.1), as well as genes encoding enzymes involved in glutathione metabolism, which have been proposed to participate in PEG metabolism (Somyoonsap et al., 2008) were identified (Figure 7B and Table 3).

BP8 Community Phenotypic Potential to Biodegrade Polyurethane

Genes encoding PU-esterases verified for PU degradation (Nomura et al., 1998; Stern and Howard, 2000; Ufarté et al., 2017) and confirmed carbamate-hydrolyzing enzymes, i.e., arylamidase A (Zhang et al., 2012), amidase (Yun et al., 2016), urethanase (Liu et al., 2016), and carbaryl hydrolase (Hashimoto et al., 2006), were searched by standalone BLASTP analyses. Six and five sequences with similarity to PU-esterases and carbamate hydrolases were retrieved from the BP8 metagenome, respectively (Table 4). We also identified genes encoding ureases (EC 3.5.1.5), suggested to act on PU degradation (Yang et al., 2015), in *Parapedobacter* sp. BP8 (RQP19536.1, RQP19537.1, RQP19538.1) and *O. intermedium* BP8.5 (RQP17756.1, RQP17448.1, RQP17449.1, RQP17450.1) genomes.

DISCUSSION

The BP8 Microbial Community Displays a Diauxic Growth Phase That Seems Not to Be Based on the Utilization of Different Carbon Sources

To elucidate the mechanisms that landfill microbial communities perform to degrade the recalcitrant PE-PU plastic, we studied the degradative activity of the selected BP8 microbial community because of its capability to grow in PolyLack®. PolyLack® is a WPUD that contains a proprietary PE-PU-A copolymer and several xenobiotic additives (NMP, IP, 2-BE, DPGB and DPGM). Chemical and physical analyses demonstrated that BP8 consumes the additives and breaks the copolymer. Hi-C based metagenomic analysis allowed us to unveil the phenotypic potential to degrade PU and xenobiotics of five deconvoluted genomes from the community. The diauxic growth of BP8 observed during 25 days of cultivation in MM-PolyLack suggested that two different metabolic processes were involved in degrading the components of the WPUD. We hypothesized that the additives were consumed during the first phase whereas the copolymer was broken during the second one. However, the biomass increment and the carbon decrease observed in the first growth phase (Figure 1A) resulted not only from additive consumption, but also from the copolymer breakdown (Figures 2, 4, Table 1, Supplementary Figure S1, and Supplementary Tables S1, S2). The simultaneous degradation of additives and copolymer observed in this analysis do not account for the diauxic behavior of the community. Interestingly, based on the slight *Mw* increase and the continuous *Mn* decrease of the copolymer observed during the first 15 days of cultivation, clearly observed in the MWD analysis, we suggest that BP8 community might

preferentially attack low molecular weight fractions. Thus, the larger molecules would remain in the culture media and would be cleaved after 15 days of cultivation as evidenced by the continuous decrease in *Mn* and the steep decrease on *Mw* observed from 15 to 25 days (Table 1 and Supplementary Figure S2). Changes in these parameters resulting from polymer biodegradation have been reported for polyethylene (Albertsson et al., 1998) and polystyrene (Yang et al., 2018). Therefore, it seems that an enhanced PU-degrading community, able to attack more complex polymers could be selected after 15 days of cultivation, coincidental with the second exponential growth phase. Further studies to test this possibility are needed.

The BP8 Microbial Community Exhibits Variable Cell-Surface Interactions That Could Be Involved in the Biodegradation Process

PolyLack® additives and copolymer, as well as the degradation products generated by BP8 activity, have effects on the emulsifying capacity of the culture medium, consequently in cell-substrate interactions that have impact on the biodegradation process. PolyLack® has intrinsic emulsifying properties provided by the additives and PE-PU-A copolymers (Honarkar, 2018), which determine the initial EI₂₄ of the culture medium (70%) (Figure 1B). The initial and almost complete additives degradation during the first 5 days of cultivation accounts for a 5% decrement in the EI₂₄ (Figure 2A and Supplementary Table S1). The larger loss of the emulsifier capacity observed from 5 to 20 days must be the result of hydrophilic moieties cleavage from the copolymer. The further increase observed in this parameter might be generated by BP8 biosurfactant production. Surfactants enhance substrate bioaccessibility and modify cell hydrophobicity improving biodegradation (Tzintzun-Camacho et al., 2012). CSH reflects the capability of BP8 cells to attach the PE-PU-A hydrophobic moieties and other hydrophobic components of the culture medium, favoring cell-substrate interactions that enhance biodegradation. The variability in CSH behavior during the cultivation period is consequence of modifications on cell envelopes composition and properties induced by changes in the culture medium. The changes in CSH and EI₂₄ observed in this experiments reveal the complex cell-substrate interactions involved in promoting BP8 accessibility to PolyLack®, hence its biodegradation.

The BP8 Metagenomic Analysis Allowed to Identify Known Additive- and PU-Degrading Enzymes and to Propose New Activities and Metabolic Pathways Involved in Biodegradation

Exploring the BP8 metagenome, genes encoding enzymes presumably involved in the degradation of the PolyLack® additives were identified in several of the deconvoluted genomes. Genes for NMP degradation, similar to the ones reported for *A. denitrificans* BQ1 (Solís-González et al., 2018) were identified in the *Paracoccus* sp. BP8 genome. *Paracoccus* strains, able

TABLE 4 | Esterases and carbamate hydrolyzing enzymes encoded in the BP8 metagenome.

Enzyme Query Organism (Accession number)	E.C. num.	Amino acids in the query	Hit in the BP8 metagenome	E value/ ^a Identity/ Similarity	Amino acids in the hit	References
Polyurethane esterase <i>Delftia acidovorans</i> (BAA76305)	3.1.1.6	548	<i>Parapedobacter</i> sp. BP8.3 (RQP17780.1)	1.0E–07/ 32%/48%	640	Nomura et al., 1998
Polyurethanase esterase A <i>Pseudomonas chlororaphis</i> (AAD22743)	3.1.1.-	617	<i>Paracoccus</i> sp. BP8 (RQP07762.1)	4.0E–16/ 34%/50%	783	Stern and Howard, 2000
			<i>Paracoccus</i> sp. BP8 (RQP06646.1)	2.0E–14/ 33%/46%	980	
			<i>Paracoccus</i> sp. BP8 (RQP04598.1)	7.0E–12/ 30%/43%	854	
			<i>Paracoccus</i> sp. BP8 (RQP06839.1)	5.0E–12/ 32%/43%	612	
Esterase CE_Ubrb uncultured bacterium (SIP63154)	3.1.1.-	295	<i>Microbacteriaceae</i> bacterium BP8.4 (RQP12977.1)	8.0E–05/ 35%/48%	309	Ufarté et al., 2017
Arylamidase A <i>Paracoccus huijuniae</i> (AEX92978)	3.4.11.2	465	<i>Paracoccus</i> sp. BP8 (RQP04489.1)	6.0E–25/ 41%/52%	471	Zhang et al., 2012
Amidase <i>Ochrobactrum</i> sp. TCC-2 (ANB41810)	3.5.1.4	474	<i>Microbacteriaceae</i> bacterium BP8.4 (RQP11486.1)	2.0E–47/ 35%/49%	475	Yun et al., 2016
			<i>O. intermedium</i> BP8.5 (RQP19215.1)	6.0E–24/ 39%/50%	326	
Urethanase <i>Lysinibacillus fusiformis</i> (KU353448)	3.5.1.4	472	<i>Microbacteriaceae</i> bacterium BP8.4 (RQP12064.1)	1.0E–60/ 32%/48%	499	Liu et al., 2016
Carbaryl hydrolase <i>cahA</i> <i>Arthrobacter</i> sp. RC100 (BAC15598)	3.6.3.5	506	<i>Paracoccus</i> sp. BP8 (RQP06118.1)	1.0E–15/ 35%/48%	326	Hashimoto et al., 2006

to utilize NMP as carbon source, have been reported (Cai et al., 2014), but the genes sustaining this capability have not been described. IP biodegradation occurs by oxidative pathways in *P. denitrificans* GH3 and *Gordonia* sp. TY-5. In these strains, IP is transformed by NAD⁺-dependent secondary ADH into acetone that is oxidized by a specific monooxygenase to produce methyl acetate, which is transformed to acetic acid and methanol (Kotani et al., 2003; Geng et al., 2015). However, the enzymes for metabolizing acetone by these reactions are not encoded in the BP8 metagenome. Instead, genes encoding the enzymes acetone carboxylase, 3-oxoacid-CoA transferase, and acetyl-CoA C-acetyltransferase were identified. These enzymes would produce acetoacetate, acetoacetyl-CoA and acetyl-CoA, respectively (Schühle and Heider, 2012) (**Figure 7A** and **Table 3**). The possibility that IP degradation occurs by transformation to acetyl-CoA, via acetone in BP8 is supported by the observation that in the *Paracoccus* sp. BP8 genome, a gene encoding an ADH (RQP05888.1), homologous to the *Gordonia* sp. TY-5 adh2, and genes encoding the acetone carboxylase subunits (RQP05866.1, RQP05867.1, RQP05889.1) are contiguously located. Adjacent to these genes, a sequence encoding a sigma-54-dependent transcriptional regulator (RQP05868.1) was observed, suggesting an operon-like organization. This presumptive IP degradative operon has not been described in any other bacteria. Degradation of 2-BE, DPGM and DPGB, the glycol ethers present in PolyLack®,

has not been reported in bacteria. Degradation pathways for PEG and polypropylene glycol (PPG) reported in *Sphingomonads* species and *Microbacterium* (formerly *Corynebacterium*) sp. No. 7 (Kawai, 2010; Ohtsubo et al., 2015) show similar reactions where the glycols' hydroxyl terminal groups are sequentially oxidized by specific ADHs and ALDHs to produce aldehydes, and thereafter carboxylic acids (Ohta et al., 2006; Tani et al., 2007), suggesting a widespread strategy for glycol ethers metabolism in prokaryotes. Nevertheless, few enzymes involved in scission of ether bonds, present in these compounds, have been identified in bacteria. A glycolic acid oxidase (Yamanaka and Kawai, 1991) and a glycolic acid dehydrogenase (Enokibara and Kawai, 1997) have been reported acting on PEG, although several other enzymes such as superoxide dismutase, monooxygenase, ether hydrolase, carbon-oxygen lyase, peroxidase and laccase have been suggested (Kawai, 2010). Homolog genes for specific ADHs and ALDHs were identified in the *Paracoccus* sp. BP8 genome (**Table 3**). Therefore, we hypothesize that degradation of 2-BE could be carried out by subsequent oxidations of the hydroxy terminal groups by PEG-DH and PEG-ALDH to produce 2-butoxyacetic acid, followed by scission of the ether bonds by glycolate oxidase or other ether scission enzymes to produce, glyoxylate and butyraldehyde (Tachibana et al., 2002; Kawai, 2010). Glyoxylate would be funneled to the glyoxylate metabolism and butyraldehyde to the butanoate metabolism (**Figure 7B**, left). DPGB and DPGM can be respectively

degraded, by initial oxidation of the hydroxy terminal groups, to 2-butoxypropionic acid and to 2-methoxypropionic acid that has been reported as a metabolite in the degradation of DPGM by rats (Miller et al., 1986). These carboxylates can be ether-cleaved by ether scission enzymes to produce butyraldehyde and propylene glycol from DPGM and propylene glycol and formaldehyde from DPGM. Propylene glycol can be funneled to the pyruvate metabolism by lactaldehyde and lactate dehydrogenases, as suggested in *P. yeii* TT13 (Lim et al., 2018) and formaldehyde can enter to the formate metabolism where glutathione-dependent enzymes would oxidize it to formate and, subsequently, to CO₂ (Figure 7B and Table 3). Genes encoding homologs for PEG-DH and PEG-ALDH (*pegdh* and *pegc*) from *Sphingopyxis terrae* and *S. macroglabrida*, and for possible ether scission enzymes that could act over the aforementioned carboxylic acids, glycolate oxidase (*glcD*, *glcE*, *glcF*), dye decoloring peroxidase, 4-methoxybenzoate monooxygenase and unspecific monooxygenase were identified in *Paracoccus* sp. BP8 (see Table 3). Besides, the pathways for glyoxylate, butanoate, pyruvate and formate metabolisms as well as the TCA pathway were fully reconstructed from the BP8 metagenome (Figure 7B). Additionally, in PEG metabolism, long chains of PEG-carboxylate can be processed by acyl-CoA synthetase and glutathione-S transferase forming glutathione-conjugates (Somyoonsap et al., 2008). Although these reactions would not be needed for glycol ethers catabolism, they could be required for the degradation of long PPG moieties that are part of the PE-PU-A copolymer (Figure 3A).

By using different analytical techniques, we demonstrate that the BP8 community attacks the main functional groups of the PE-PU-A copolymer; from the more enzymatically susceptible ester bonds, present in acrylate and carbamate, to the more recalcitrant C-C from aliphatics and aromatics, C-N from urethane, and C-O-C from ether bonds of PPG (Figures 2–4). The changes in the chemical and physical properties of the polymer when incubated with BP8, and the generation of diverse degradation products, some of them potential metabolic intermediates in the degradation process, are evidences of the BP8's degradative capability, which is sustained by the diverse xenobiotic degrading enzymes encoded in its metagenome (Table 3). Some of the biodegradation products (Figure 2B and Supplementary Table S2) seem to be the result of oxidative reactions on C-C bonds flanking TDI, MDI or the acrylates' styrene ring (Figures 3A, 4), generating aromatic compounds containing hydroxyl, aldehydes or organic acids. Additionally, the copolymer aromatic compounds could be destabilized by monooxygenases, which introduces hydroxyl groups to the aromatic rings, and by dioxygenases that catalyzes reductive dihydroxylation, generating central intermediates that can be cleaved by dearomatizing dioxygenases producing carboxylic acids (Ladino-Orzuela et al., 2016). The enzymes for the complete benzoate metabolism are encoded in the BP8 metagenome and could account for PE-PU-A aromatic rings catabolism (Table 3). Aliphatic chains from acrylates and PPG can be metabolized by alkane 1-monooxygenases, that activate aliphatic chains by terminal or subterminal oxidations and by the activities of ADHs and ALDHs, generating compounds that can be channeled by beta-oxidation into the fatty acids metabolism (Table 3).

If terminal oxidations are introduced, primary alcohols are generated and transformed into aldehydes, carboxylic acids and acyl-CoA. If subterminal oxidations of aliphatic chains occur, secondary alcohols are formed, which upon breakdown, will produce ketones and thereafter esters, which are hydrolyzed to alcohol and organic acids (Rojo, 2009). Many different esters compounds were identified in the BP8's degradation products, suggesting that sub-terminal oxidation of alkanes could be an important route in PU metabolism (Figures 2–4). The cleavage of ester bonds by PU-esterases would produce alcohols and organic acids and the cleavage of urethane groups by carbamate-hydrolases would produce nitrogen-containing compounds and aromatic isocyanate derivatives. As we detected these degradation products by GC-MS analysis (Figure 2B, Supplementary Figure S1 and Supplementary Table S2), hydrolysis of ester and urethane bonds are accomplished during PE-PU-A degradation by BP8. The identification of several PU-esterases and carbamate hydrolases encoded in most of the BP8 genomes support this conclusion (Table 4).

The Biodegradative Activity in BP8 Community Seems to Be Dominated by the Most Abundant Species, but Specialized Reactions Seem to Occur in Poorly Represented Species

The metabolic reactions proposed for the degradation of the additives and the PE-PU-A copolymer present in PolyLack® by the BP8 community are based on the phenotypic potential encoded in its metagenome. The use of Hi-C proximity ligation-based technology allowed to define, with high confidence, what genes belong to each of the different species of BP8 (Table 3). In this community, xenobiotic degradation is a niche dominated by *Paracoccus* sp. BP8 and *Ochrobactrum intermedium* BP8.5. In their genomes, key enzymes for different steps of biodegradation are widely represented (Table 3), which must be the reason for their preponderance in the BP8 community. In addition, *Microbacteriaceae* bacterium BP8.4 genome encodes enzymes for the metabolism of aromatic compounds suggesting that metacleaveage ring excision and muconate lactone formation might be functional. On the other hand, *Chryseobacterium* sp. BP8.2 and *Parapedobacter* sp. BP8.3 genomes, harbor genes encoding complementary metabolic activities for alkanes oxidation, such as hydrolysis and oxidation of linear intermediates. The finding of such a diverse genetic repertoire in the BP8 metagenome suggests a remarkable metabolic versatility, with strong hydrolytic and oxidative capabilities that can play significant roles in the degradation of diverse environmental contaminants. The abundance and distribution of these catabolic enzymes among the different members of the BP8 community, suggest syntrophic mechanisms driving community behavior. However, incomplete genome reconstruction in the deconvolution analysis, resulting in potential pathway gaps in certain genomes, cannot be ruled out, nor can the collapsing of multiple strains into a single cluster. On the other hand, although *Paracoccus* and *Ochrobactrum* are predominant in the BP8 community by far, we cannot discard that specific enzymatic activities encoded in genomes

of little abundant species can be crucial for the successful performance of BP8.

The BP8 Microbial Community as a Promising Source for Environmental Biotechnology Strategies

The present work provides deep understanding of the biodegradative activity of a landfill microbial community capable of PU and xenobiotics degradation. Results reveal the taxonomic composition of the BP8 community and its outstanding phenotypic potential, reflected in the catalytic capabilities displayed by its members to cleave different recalcitrant functional groups. This is one of the few studies integrating analytical chemistry with metagenomics for proposing metabolic pathways involved in xenobiotics biodegradation, and the first metagenomic analysis of a PU-degrading selected landfill community. Moreover, the knowledge generated about the members of the BP8 community, the potential metabolic pathways involved in PU and additives degradation, and in which species specific enzymatic reactions are carried out, could be exploited for our benefit. Some possibilities include the assembling of specific consortia for increased PU-degrading ability, the overexpression of additives- or PU-degrading proteins to be used in environmental biotechnology strategies for waste treatment, or the development of new biocatalyzers for novel industrial applications. Altogether, these features place BP8 community as a quite promising source for developing environmental biotechnology strategies contributing to mitigate anthropogenic plastics and xenobiotics pollution, for achieving better environmental quality.

DATA AVAILABILITY STATEMENT

The datasets generated for this study can be accessed from GenBank under BioProject Accession number: PRJNA488119. The microbial shotgun “*de novo*” assembly and the log file for the assembly run done with metaSPAdes software were deposited at Mendeley: <https://data.mendeley.com/datasets/bkwf2xhytj/1>.

AUTHOR CONTRIBUTIONS

IG, AS-R, MB, MV-S, IL, and HL-T contributed to conception and design of the study. IG and MB conducted the analytical techniques and interpreted the results along with MC-G and HL-T. IL, MP, and SS performed metagenomics experiments.

REFERENCES

- Albertsson, A. C., Erlandsson, B., Hakkarainen, M., and Karlsson, S. (1998). Molecular weight changes and polymeric matrix changes correlated with the formation of degradation products in biodegraded polyethylene. *J. Environ. Pol. Degrad.* 6, 187–195. doi: 10.1023/A:1021873631162
- Álvarez-Barragán, J., González-Hernández, R., Domínguez-Malfavón, L., Vargas-Suárez, M., Aguilar-Osorio, G., and Loza-Tavera, H. (2016). Biodegradative activity of selected environmental fungi on a polyester polyurethane varnish

AS-R and HL-T analyzed the metagenomic data. IG, AS-R, MB, MV-S, IL, MC-G, and HL-T wrote the manuscript. All authors contributed to manuscript revision, read and approved the submitted version.

FUNDING

This work was funded by Programa de Apoyo a Proyectos de Investigación e Innovación Tecnológica, Dirección General de Asuntos del Personal Académico, Universidad Nacional Autónoma de México grants IN217114, IN223317, and IN227620, and Programa de Apoyo a la Investigación y el Posgrado, Facultad de Química, Universidad Nacional Autónoma de México, grant 5000-9117. IL, MP, and SS were supported in part by NIAID grant 2R44AI122654-02A1.

ACKNOWLEDGMENTS

IG and MB acknowledge Consejo Nacional de Ciencia y Tecnología for their Ph.D. scholarships and to Posgrado en Ciencias Bioquímicas, UNAM and Posgrado en Ciencias Químicas, UNAM for the supports granted during their Ph.D. studies. AS-R acknowledges Dirección General de Asuntos del Personal Académico, UNAM, for his scholarship for a postdoctoral position at Facultad de Química, UNAM. We thank Unidad de Servicios de Apoyo a la Investigación y a la Industria, Facultad de Química, UNAM for the analytical support provided by Ch. Marisela Gutiérrez Franco, Ch. Rafael Iván Puente Lee, Ch. Víctor Hugo Lemus, and Ch. Elvira del Socorro Reynosa in the FTIR, SEM, carbon quantification, and DTG, respectively. The technical support of MSc. Fernando de Jesús Rosas Ramírez in the use of the GC-MS equipment is appreciated. Also, we are grateful to Gerardo Cedillo, Salvador López and Karla E. Reyes from Instituto de Investigaciones en Materiales (IIM-UNAM) for their assistance in NMR, GPC, and DSC analyses, respectively, and to Taylor Reiter and C. Titus Brown for help with metagenomic analysis. This manuscript has been released as a preprint at bioRxiv, first posted online September 8, 2019; <http://dx.doi.org/10.1101/760637> (Gaytán et al., 2019).

SUPPLEMENTARY MATERIAL

The Supplementary Material for this article can be found online at: <https://www.frontiersin.org/articles/10.3389/fmicb.2019.02986/full#supplementary-material>

- and polyether polyurethane foams. *Appl. Environ. Microbiol.* 82, 5225–5235. doi: 10.1128/AEM.01344-1316
- Asnicar, F., Weingart, G., Tickle, T. L., Huttenhower, C., and Segata, N. (2015). Compact graphical representation of phylogenetic data and metadata with GraPhlAn. *PeerJ* 3:e1029. doi: 10.7717/peerj.1029
- Breitwieser, F. P., Perte, M., Zimin, A. V., and Salzberg, S. L. (2019). Human contamination in bacterial genomes has created thousands of spurious proteins. *Genome Res.* 29, 954–960. doi: 10.1101/gr.24537.3.118

- Burton, J. N., Liachko, I., Dunham, M. J., and Shendure, J. (2014). Species-level deconvolution of metagenome assemblies with Hi-C-based contact probability maps. *G3* 4, 1339–1346. doi: 10.1534/g3.114.011825
- Cai, S., Cai, T., Liu, S., Yang, Q., He, J., Chen, L., et al. (2014). Biodegradation of N-methylpyrrolidone by *Paracoccus* sp. NMD-4 and its degradation pathway. *Int. Biodeterior. Biodeg.* 93, 70–77. doi: 10.1016/j.ibiod.2014.04.022
- Cipriani, E., Bracco, P., Kurtz, S. M., Costa, L., and Zanetti, M. (2013). In-vivo degradation of poly(carbonate-urethane) based spine implants. *Pol. Degrad. Stabil.* 98, 1225–1235. doi: 10.1016/j.polymdegradstab.2013.03.005
- Cooper, D. G., and Goldenberg, B. G. (1987). Surface active agents from *Bacillus* species. *Appl. Environ. Microbiol.* 53, 224–229.
- Cornille, A., Auvergne, R., Figovsky, O., Boutevin, B., and Caillol, S. (2017). A perspective approach to sustainable routes for non-isocyanate polyurethanes. *Eur. Pol. J.* 87, 535–552. doi: 10.1016/j.eurpolymj.2016.11.027
- Cregut, M., Bedas, M., Durand, M. J., and Thouand, G. (2013). New insights into polyurethane biodegradation and realistic prospects for the development of a sustainable waste recycling process. *Biotechnol. Adv.* 31, 1634–1647. doi: 10.1016/j.biotechadv.2013.08.011
- Enokibara, S., and Kawai, F. (1997). Purification and characterization of an ether bond-cleaving enzyme involved in the metabolism of polyethylene glycol. *J. Ferment. Bioeng.* 83, 549–554. doi: 10.1016/S0922-338X(97)81135-X
- Ferrero, P., San-Valero, P., Gabaldón, C., Martínez-Soria, V., and Peña-Roja, J. M. (2018). Anaerobic degradation of glycol ether-ethanol mixtures using EGSB and hybrid reactors: performance comparison and ether cleavage pathway. *J. Environ. Manag.* 213, 159–167. doi: 10.1016/j.jenvman.2018.02.070
- Gamerith, C., Herrero, A. E., Pellis, A., Ortner, A., Vielnascher, R., Luschig, D., et al. (2016). Improving enzymatic polyurethane hydrolysis by tuning enzyme sorption. *Pol. Degrad. Stabil.* 132, 69–77. doi: 10.1016/j.polymdegradstab.2016.02.025
- Gaytán, I., Sánchez-Reyes, A., Burelo, M., Vargas-Suárez, M., Liachko, I., Press, M., et al. (2019). Degradation of recalcitrant polyurethane and xenobiotic additives by a selected landfill microbial community and its biodegradative potential revealed by proximity ligation-based metagenomic analysis. *BioRxiv* [Preprint]. doi: 10.1101/760637
- Geng, Y., Deng, Y., Chen, F., Jin, H., Tao, K., and Hou, T. (2015). Biodegradation of isopropanol by a solvent-tolerant *Paracoccus denitrificans* strain. *Prep. Biochem. Biotechnol.* 45:4919. doi: 10.1080/10826068.2014.923452
- Gite, V. V., Mahulikar, P. P., and Hundiwal, D. G. (2010). Preparation and properties of polyurethane coatings based on acrylic polyols and trimer of isophorone diisocyanate. *Prog. Org. Coat.* 68, 307–312. doi: 10.1016/j.porgcoat.2010.03.008
- Gouy, M., Guindon, S., and Gascuel, O. (2010). SeaView version 4: a multiplatform graphical user interface for sequence alignment and phylogenetic tree building. *Mol. Biol. Evol.* 27, 221–224. doi: 10.1093/molbev/msp259
- Hashimoto, M., Mizutani, A., Tago, K., Ohnishi-Kameyama, M., Shimojo, T., and Hayatsu, M. (2006). Cloning and nucleotide sequence of carbaryl hydrolase gene (*cahA*) from *Arthrobacter* sp. RC100. *J. Biosci. Bioeng.* 101, 410–414. doi: 10.1263/jbb.101.410
- Honarkar, H. (2018). Waterborne polyurethanes: a review. *J. Disper. Sci. Technol.* 39, 507–516. doi: 10.1080/01932691.2017.1327818
- Kanehisa, M., Sato, Y., and Morishima, K. (2016). BlastKOALA and GhostKOALA: KEGG Tools for functional characterization of genome and metagenome sequences. *J. Mol. Biol.* 428, 726–731. doi: 10.1016/j.jmb.2015.11.006
- Kawai, F. (2010). The biochemistry and molecular biology of xenobiotic polymer degradation by microorganisms. *Biosci. Biotechnol. Biochem.* 74, 1743–1759. doi: 10.1271/bbb.100394
- Kotani, T., Yamamoto, T., Yurimoto, H., Sakai, Y., and Kato, N. (2003). Propane monooxygenase and NAD⁺-dependent secondary alcohol dehydrogenase in propane metabolism by *Gordonia* sp. strain TY-5. *J. Bacteriol.* 185, 7120–7128. doi: 10.1128/JB.185.24.7120-7128.2003
- Ladino-Orzuela, G., Gomes, E., da Silva, R., Salt, C., and Parsons, J. R. (2016). Metabolic pathways for degradation of aromatic hydrocarbons by bacteria. *Rev. Environ. Contamination Toxicol.* 237, 105–121. doi: 10.1007/978-3-319-23573-8-5
- Lefort, V., Longueville, J. E., and Gascuel, O. (2017). SMS: smart Model Selection in PhyML. *Mol. Biol. Evol.* 34, 2422–2424. doi: 10.1093/molbev/msx149
- Li, H., and Durbin, R. (2010). Fast and accurate long-read alignment with burrows-wheeler transform. *Bioinformatics* 26, 589–595. doi: 10.1093/bioinformatics/btp698
- Lim, J. Y., Hwang, I., Ganzorig, M., Pokhriyal, S., Singh, R., and Lee, K. (2018). Complete genome sequence of *Paracoccus yeei* TT13, isolated from human skin. *Genome Announc.* 6:e1514-17. doi: 10.1128/genomeA.01514-17
- Liu, X., Fang, F., Xia, X., Du, G., and Chen, J. (2016). Stability enhancement of urethanase from *Lysinibacillus fusiformis* by site-directed mutagenesis. *Sheng Wu Gong Cheng Xue Bao* 32, 1233–1242. doi: 10.13345/j.cjb.150527
- Magnin, A., Hoornaert, L., Pollet, E., Laurichesse, S., Phalip, V., and Averous, L. (2019). Isolation and characterization of different promising fungi for biological waste management of polyurethanes. *Microbial. Biotechnol.* 12, 544–555. doi: 10.1111/1751-7915.13346
- Malla, M. A., Dubey, A., Yadav, S., Kumar, A., Hashem, A., and Abd Allah, E. F. (2018). Understanding and designing the strategies for the microbe-mediated remediation of environmental contaminants using omics approaches. *Front. Microbiol.* 9:1132. doi: 10.3389/fmicb.2018.01132
- Maurya, S. D., Kurmvanshi, S. K., Mohanty, S., and Nayak, S. K. (2018). A review on acrylate-terminated urethane oligomers and polymers: synthesis and applications. *Pol. Plast Technol. Eng.* 57, 625–656. doi: 10.1080/03602559.2017.1332764
- Miller, R. R., Langvardt, P. W., Calhoun, L. L., and Yahrmak, M. A. (1986). Metabolism and disposition of propylene glycol monomethyl ether (PGME) beta isomer in male rats. *Toxicol. Appl. Pharmacol.* 83, 170–177. doi: 10.1016/0041-008x(86)90334-90330
- Nakajima-Kambe, T., Onuma, F., Kimpara, N., and Nakahara, T. (1995). Isolation and characterization of a bacterium which utilizes polyester polyurethane as a sole carbon and nitrogen source. *FEMS Microbiol. Lett.* 129, 39–42. doi: 10.1016/0378-1097(95)00131-N
- Nomura, N., Shigeno-Akutsu, Y., Nakajima-Kambe, T., and Nakahara, T. (1998). Cloning and sequence analysis of a polyurethane esterase of *Comamonas acidovorans* TB-35. *J. Ferment. Bioeng.* 86, 339–345. doi: 10.1016/S0922-338X(99)89001-1
- Nurk, S., Meleshko, D., Korobeynikov, A., and Pevzner, P. A. (2017). metaSPAdes: a new versatile metagenomic assembler. *Genome Res.* 27, 824–834. doi: 10.1101/gr.213959.116
- Oceguera-Cervantes, A., Carrillo-García, A., López, N., Bolaños-Núñez, S., Cruz-Gómez, M. J., Wachter, C., et al. (2007). Characterization of the polyurethanolytic activity of two *Alicyciphilus* sp. strains able to degrade polyurethane and N-methylpyrrolidone. *Appl. Environ. Microbiol.* 73, 6214–6223. doi: 10.1128/AEM.01230-07
- Ohta, T., Kawabata, T., Nishikawa, K., Tani, A., Kimbara, K., and Kawai, F. (2006). Analysis of amino acid residues involved in catalysis of polyethylene glycol dehydrogenase from *Shingopyxis terrae*, using three-dimensional molecular modeling-based kinetic characterization of mutants. *Appl. Environ. Microbiol.* 72, 4388–4396. doi: 10.1128/AEM.02174-05
- Ohtsubo, Y., Nagata, Y., Numata, M., Tsuchikane, K., Hosoyama, A., Yamazoe, A., et al. (2015). Complete genome sequence of a polypropylene glycol-degrading strain, *Microbacterium* sp. No. 7. *Genome Announc.* 3:e1400-15. doi: 10.1128/genomeA.01400-15
- Ojo, O. A. (2007). Molecular strategies of microbial adaptation to xenobiotics in natural environment. *Biotechnol. Mol. Biol. Rev.* 2, 1–3.
- Organization for Economic Co-operation and Development (2003). *SIDS Initial Assessment Report For SIAM 17. Propylene Glycol Ethers*. Paris: Organization for Economic Co-operation, and Development.
- Osman, M., Satti, S. M., Luqman, A., Hasan, F., Shah, Z., and Shah, A. (2018). Degradation of polyester polyurethane by *Aspergillus* sp. strain S45 isolated from soil. *J. Polym. Environ.* 26, 301–310. doi: 10.1007/s10924-017-0954-950
- Pardini, O. R., and Amalvy, J. I. (2008). FTIR, ¹H-NMR spectra, and thermal characterization of water-based polyurethane/acrylic hybrids. *J. Appl. Pol. Sci.* 107, 1207–1214. doi: 10.1002/app.27188
- Parks, D. H., Imelfort, M., Skennerton, C. T., Hugenholtz, P., and Tyson, G. W. (2015). CheckM: assessing the quality of microbial genomes recovered from isolates, single cells, and metagenomes. *Genome Res.* 25, 1043–1055. doi: 10.1101/gr.186072.114
- Plastics Europe (2018). *Plastics – the Facts 2018. an Analysis of European Plastics Production, Demand and Waste Data*. Association of Plastics Manufacturers. Available at: <http://www.plasticseurope.org> (accessed August 19, 2019).

- Press, M. O., Wiser, A. H., Kronenberg, Z. N., Langford, K. W., Shakya, M., Lo, C.-C., et al. (2017). Hi-C deconvolution of a human gut microbiome yields high-quality draft genomes and reveals plasmid-genome interactions. *BioRxiv* [Preprint]. doi: 10.1101/198713
- Rojo, F. (2009). Degradation of alkanes by bacteria. *Environ. Microbiol.* 11, 2477–2490. doi: 10.1111/j.1462-2920.2009.01948.x
- Rosenberg, M., Gutnick, D., and Rosenberg, E. (1980). Adherence of bacteria to hydrocarbons: a simple method for measuring cell-surface hydrophobicity. *FEMS Microbiol. Lett.* 9, 29–33. doi: 10.1016/0378-1097(80)90106-8
- Schühle, K., and Heider, J. (2012). Acetone and butanone metabolism of the denitrifying bacterium *Aromatoleum aromaticum* demonstrates novel biochemical properties of an ATP-dependent aliphatic ketone carboxylase. *J. Bact.* 194, 131–141. doi: 10.1128/JB.05895-11
- Segata, N., Waldron, L., Ballarín, A., Narasimhan, V., Jousson, O., and Huttenhower, C. (2012). Metagenomic microbial community profiling using unique clade-specific marker genes. *Nat. Methods* 9, 811–814. doi: 10.1038/nmeth.2066
- Shah, Z., Gulzar, M., Hasan, F., and Shah, A. A. (2016). Degradation of polyester polyurethane by an indigenously developed consortium of *Pseudomonas* and *Bacillus* species isolated from soil. *Pol. Degrad. Stabil.* 134, 349–356. doi: 10.1016/j.polymdegradstab.2016.11.003
- Shaiber, A., and Eren, A. M. (2019). Composite metagenome-assembled genomes reduce the quality of public genome repositories. *mBio* 10:e725-19. doi: 10.1128/mBio.00725-19
- Solis-González, C. J., Domínguez-Malfavón, L., Vargas-Suárez, M., Gaytán, I., Cevallos, M. A., Lozano, L., et al. (2018). Novel metabolic pathway for N-methylpyrrolidone degradation in *Alicyclophilus* sp. BQ1. *Appl. Environ. Microbiol.* 84:e2136-17. doi: 10.1128/AEM.02136-2117
- Somyoosap, P., Tani, A., Charoenpanich, J., Minami, T., Kimbara, K., and Kawai, F. (2008). Involvement of PEG-carboxylate dehydrogenase and glutathione S-transferase in PEG metabolism by *Sphingopyxis macrogoltabida* strain 103. *Appl. Microbiol. Biotechnol.* 81, 473–484. doi: 10.1007/s00253-008-1635-7
- Stern, R. V., and Howard, G. T. (2000). The polyester polyurethanase gene (*pueA*) from *Pseudomonas chlororaphis* encodes a lipase. *FEMS Microbiol. Lett.* 185, 163–168. doi: 10.1111/j.1574-6968.2000.tb09056.x
- Sultan, M., Islam, A., Gull, N., Bhatti, H., and Safa, Y. (2014). Structural variation in soft segment of waterborne polyurethane acrylate nanoemulsions. *J. Appl. Pol. Sci.* 132:41706. doi: 10.1002/app.41706
- Tachibana, S., Kawai, F., and Yasuda, M. (2002). Heterogeneity of dehydrogenases of *Stenotrophomonas maltophilia* showing dye-linked activity with polypropylene glycols. *Biosci. Biotech. Biochem.* 66, 737–742. doi: 10.1271/bbb.66.737
- Tani, A., Charoenpanich, J., Mori, T., Takeichi, M., Kimbara, K., and Kawai, F. (2007). Structure and conservation of a polyethylene glycol-degradative operon in sphingomonads. *Microbiology* 153, 338–346. doi: 10.1099/mic.0.2006/000992-990
- Tzintzun-Camacho, O., Loera, O., Ramírez-Saad, H. C., and Gutiérrez-Rojas, M. (2012). Comparison of mechanisms of hexadecane uptake among pure and mixed cultures derived from a bacterial consortium. *Int. Biodeterior. Biodeg.* 70, 1–7. doi: 10.1016/j.ibiod.2012.01.009
- Ufarté, L., Laville, E., Duquesne, S., Morgavi, D., Robe, P., Klopp, C., et al. (2017). Discovery of carbamate degrading enzymes by functional metagenomics. *PLoS One* 12, 1–21. doi: 10.1371/journal.pone.0189201
- Vargas-Suárez, M., Fernández-Cruz, V., and Loza-Tavera, H. (2019). Biodegradation of polyacrylic and polyester polyurethane coatings by enriched microbial communities. *Appl. Microbiol. Biotechnol.* 103, 3225–3236. doi: 10.1007/s00253-019-09660-y
- Varsha, Y. M., Naga Deepthi, C. H., and Chenna, S. (2011). An emphasis on xenobiotic degradation in environmental clean-up. *J. Bioremed. Biodegrad.* S11, 001. doi: 10.4172/2155-6199.S11-001
- Wu, Y.-W., Tang, Y.-H., Tringe, S. G., Simmons, B. A., and Singer, S. W. (2014). MaxBin: an automated binning method to recover individual genomes from metagenomes using an expectation-maximization algorithm. *Microbiome* 2:26. doi: 10.1186/2049-2618-2-26
- Yamanaka, H., and Kawai, F. (1991). Purification and characterization of a glycolic acid (GA) oxidase active toward diglycolic acid (DGA) produced by DGA-utilizing *Rhodococcus* sp. No. 432. *J. Ferment. Bioeng.* 7, 83–88. doi: 10.1016/0922-338X(91)90228-90229
- Yang, S.-S., Malawi Brandon, A., Andrew Flanagan, J. C., Yang, J., Ning, D., Cai, S.-Y., et al. (2018). Biodegradation of polystyrene wastes in yellow mealworms (larvae of *Tenebrio molitor* Linnaeus): factors affecting biodegradation rates and the ability of polystyrene-fed larvae to complete their life cycle. *Chemosphere* 191, 979–989. doi: 10.1016/j.chemosphere.2017.10.117
- Yang, Y., Kang, Z., Zhou, J., Chen, J., and Du, G. (2015). High-level expression and characterization of recombinant acid urease for enzymatic degradation of urea in rice wine. *Appl. Microbiol. Biotechnol.* 99, 301–308. doi: 10.1007/s00253-014-5916-z
- Yoon, S.-H., Ha, S. M., Lim, J., Kwon, S., and Chun, J. (2017). A large-scale evaluation of algorithms to calculate average nucleotide identity. *Antonie Van Leeuwenhoek* 110, 1281–1286. doi: 10.1007/s10482-017-0844-844
- Yun, H., Liang, B., Qiu, J., Zhang, L., Zhao, Y., Jiang, J., et al. (2016). Functional characterization of a novel amidase involved in biotransformation of trichloroan and its dehalogenated congeners in *Ochrobactrum* sp. TCC-2. *Environ. Sci. Technol.* 51, 291–300. doi: 10.1021/acs.est.6b04885
- Zafar, U., Nzerem, P., Langarica-Fuentes, A., Houlden, A., Heyworth, A., Saiani, A., et al. (2014). Biodegradation of polyester polyurethane during commercial composting and analysis of associated fungal communities. *Bioresour. Technol.* 158, 374–377. doi: 10.1016/j.biortech.2014.02.077
- Zalasiewicz, J., Waters, C. N., Ivar do Sul, J. A., Corcoran, P. L., Barnosky, A. D., Cearreta, A., et al. (2016). The geological cycle of plastics and their use as a stratigraphic indicator of the Anthropocene. *Anthropocene* 13, 4–17. doi: 10.1016/j.ancene.2016.01.002
- Zhang, J., Yin, J.-G., Hang, B.-J., Cai, S., He, J., Zhou, S.-G., et al. (2012). Cloning of a novel arylamidase gene from *Paracoccus* sp. strain FLN-7 that hydrolyzes amide pesticides. *Appl. Environ. Microbiol.* 78, 4848–4855. doi: 10.1128/AEM.00320-12
- Zhu, W., Lomsadze, A., and Borodovsky, M. (2010). *Ab initio* gene identification in metagenomic sequences. *Nucleic Acids Res.* 38:e132. doi: 10.1093/nar/gkq275

Conflict of Interest: IL, MP, and SS are employees and shareholders of Phase Genomics Inc., a company commercializing proximity ligation technology.

The remaining authors declare that the research was conducted in the absence of any commercial or financial relationships that could be construed as a potential conflict of interest.

Copyright © 2020 Gaytán, Sánchez-Reyes, Burelo, Vargas-Suárez, Liachko, Press, Sullivan, Cruz-Gómez and Loza-Tavera. This is an open-access article distributed under the terms of the Creative Commons Attribution License (CC BY). The use, distribution or reproduction in other forums is permitted, provided the original author(s) and the copyright owner(s) are credited and that the original publication in this journal is cited, in accordance with accepted academic practice. No use, distribution or reproduction is permitted which does not comply with these terms.



A Novel Polyester Hydrolase From the Marine Bacterium *Pseudomonas aestusnigri* – Structural and Functional Insights

Alexander Bollinger¹, Stephan Thies¹, Esther Knieps-Grünhagen¹, Christoph Gertzen^{2,3}, Stefanie Kobus², Astrid Höppner², Manuel Ferrer⁴, Holger Gohlke^{3,5}, Sander H. J. Smits^{2,6} and Karl-Erich Jaeger^{1,7*}

¹ Institute of Molecular Enzyme Technology, Heinrich Heine University Düsseldorf, Jülich, Germany, ² Center for Structural Studies, Heinrich Heine University Düsseldorf, Düsseldorf, Germany, ³ Institute for Pharmaceutical and Medicinal Chemistry, Heinrich Heine University Düsseldorf, Düsseldorf, Germany, ⁴ Institute of Catalysis, Consejo Superior de Investigaciones Científicas, Madrid, Spain, ⁵ Institute of Biological Information Processing (IBI-7: Structural Biochemistry), John von Neumann Institute for Computing and Jülich Supercomputing Centre, Forschungszentrum Jülich GmbH, Jülich, Germany, ⁶ Institute of Biochemistry, Heinrich Heine University Düsseldorf, Düsseldorf, Germany, ⁷ Institute of Bio- and Geosciences IBG-1: Biotechnology, Forschungszentrum Jülich GmbH, Jülich, Germany

OPEN ACCESS

Edited by:

Ren Wei,
University of Greifswald, Germany

Reviewed by:

Gert Weber,
Helmholtz-Gemeinschaft Deutscher
Forschungszentren (HZ), Germany
Weidong Liu,
Tianjin Institute of Industrial
Biotechnology (CAS), China

*Correspondence:

Karl-Erich Jaeger
karl-erich.jaeger@fz-juelich.de

Specialty section:

This article was submitted to
Microbiotechnology, Ecotoxicology
and Bioremediation,
a section of the journal
Frontiers in Microbiology

Received: 07 November 2019

Accepted: 17 January 2020

Published: 13 February 2020

Citation:

Bollinger A, Thies S,
Knieps-Grünhagen E, Gertzen C,
Kobus S, Höppner A, Ferrer M,
Gohlke H, Smits SHJ and Jaeger K-E
(2020) A Novel Polyester Hydrolase
From the Marine Bacterium
Pseudomonas aestusnigri – Structural
and Functional Insights.
Front. Microbiol. 11:114.
doi: 10.3389/fmicb.2020.00114

Biodegradation of synthetic polymers, in particular polyethylene terephthalate (PET), is of great importance, since environmental pollution with PET and other plastics has become a severe global problem. Here, we report on the polyester degrading ability of a novel carboxylic ester hydrolase identified in the genome of the marine hydrocarbonoclastic bacterium *Pseudomonas aestusnigri* VGXO14^T. The enzyme, designated PE-H, belongs to the type IIa family of PET hydrolytic enzymes as indicated by amino acid sequence homology. It was produced in *Escherichia coli*, purified and its crystal structure was solved at 1.09 Å resolution representing the first structure of a type IIa PET hydrolytic enzyme. The structure shows a typical α/β -hydrolase fold and high structural homology to known polyester hydrolases. PET hydrolysis was detected at 30°C with amorphous PET film (PETa), but not with PET film from a commercial PET bottle (PETb). A rational mutagenesis study to improve the PET degrading potential of PE-H yielded variant PE-H (Y250S) which showed improved activity, ultimately also allowing the hydrolysis of PETb. The crystal structure of this variant solved at 1.35 Å resolution allowed to rationalize the improvement of enzymatic activity. A PET oligomer binding model was proposed by molecular docking computations. Our results indicate a significant potential of the marine bacterium *P. aestusnigri* for PET degradation.

Keywords: *Pseudomonas aestusnigri*, marine bacteria, polyester degradation, polyethylene terephthalate, PET, crystal structure

INTRODUCTION

The modern society depends on the production and use of synthetic polymers which are uniformly present in both, basic and high-tech applications. The low production costs for plastic made from fossil feedstock and the high durability of the material are major advantages but have become a burden for the global ecosystem. Plastic waste is produced at a much faster rate than it is recycled (Moharir and Kumar, 2019); hence, it is disposed in landfills at a large extend where it can take

centuries to degrade completely. Moreover, small plastic particles, so-called microplastics, usually evade municipal waste collection, being directly released into waste water and spread easily around the globe (Rochman, 2018). Hence, plastic waste accumulates in the environment to a large extent with very slow biodegradation to occur (Lebreton et al., 2018).

Where most plastics are inert polyolefins, consisting of carbon-carbon bonds, heteroatomic plastics like polyamides, polyurethanes and polyesters provide chemical groups of higher reactivity and thus are more easily degraded biologically (Wei and Zimmermann, 2017). The most abundant polyester plastic, present for example in packaging waste, is polyethylene terephthalate (PET) (Adrados et al., 2012). In the European Union, five million metric tons of this polyester were used for the production of plastics in 2017 (PlasticsEurope, 2018).

Enzymes catalyzing the degradation of polyesters such as polycaprolactone (PCL), polylactic acid (PLA), or PET are found within the class of carboxylic ester hydrolases (E.C. 3.1.1), most of them are classified as cutinases (E.C. 3.1.1.74), enzymes naturally adapted to act on polymeric ester substrates, e.g., the wax cuticle of plants (Nikolaivits et al., 2018). Studies on the identification of polyester degrading enzymes have shown that only a small fraction of carboxylic ester hydrolases is able to degrade synthetic polyester substrates. In a comprehensive metagenomics screening study, a subset of 23 carboxylesterases were tested for PLA hydrolysis, yielding seven positive hits (Popovic et al., 2017). More recently, by screening of over 200 different purified hydrolases for activity on synthetic polyesters, 36 positive enzymes were identified of which 10 enzymes showed high activity on multiple polyester substrates (Hajighasemi et al., 2018). For PET degradation, comprehensive activity-based screening studies are missing. However, a bioinformatics study using a hidden Markov model succeeded to identify PET hydrolase genes using the UniProtKB database and more than 100 metagenome datasets, many of which originated from marine sources (Danso et al., 2018). The reported frequency of PET hydrolases was, dependent on the origin of the metagenomic sample, between 0.0001 and 1.5 hits per megabases of sequence, with the highest hit rate in a metagenome obtained from an oil polluted environment (Danso et al., 2018). In contrast to the marine origin of many predicted PET hydrolases, most of the PET degrading enzymes studied so far originate from terrestrial sources, with Cut190 from *Saccharomonospora viridis* (Kawai et al., 2014), Tha_Cut1 from *Thermobifida alba* (Ribitsch et al., 2012), Thc_Cut1 and Thc_Cut2 from *T. cellulolytica* (Ribitsch et al., 2012), Tfu_0883, Tfu_0882 and TfCut2 from *T. fusca* (Chen et al., 2010; Roth et al., 2014) and LCC identified from a leaf-branch compost metagenome (Sulaiman et al., 2012) for example. All these enzymes share a characteristic thermostability which is in line with the lifestyle of their thermophilic host organism or the respective environment. This feature is beneficial for the degradation of solid PET, since the glass transition temperature of PET, i.e., the temperature where the polymer becomes flexible and thus more accessible to enzymatic degradation, is about 75°C (Wei et al., 2019a). However, biodegradation of PET can also occur at lower temperatures, as demonstrated with PETase from *Ideonella sakaiensis*, the first such enzyme originating from

a mesophilic organism (Yoshida et al., 2016). This enzyme outcompetes other cutinases for the hydrolysis of crystalline PET at 30°C as demonstrated in a comparative study with the leaf-branch compost cutinase (LCC) and a cutinase from the *Thermobifida* group (Yoshida et al., 2016). The elucidation of PETase three-dimensional structures by different groups (Han et al., 2017; Austin et al., 2018; Chen et al., 2018; Joo et al., 2018; Liu B. et al., 2018; Liu C. et al., 2018; Palm et al., 2019), lead to a proposal for the degradation mechanism and structural hallmarks responsible for superior activity as reviewed by Taniguchi et al. (2019). Structural features compared to other cutinase structures include an additional disulfide bond for improved stability at the position of the active site histidine, allowing for increased flexibility of the adjacent extended loop region (Fecker et al., 2018), thus facilitating the interaction with the polymer (Joo et al., 2018). Based on sequence and structural information, Joo et al. defined different types of PET degrading enzymes: Most known cutinases were assigned to type I, and enzymes possessing an additional disulfide bond and an extended loop region were assigned to type II, which was subdivided into types IIa and IIb based on the amino acid composition of respective regions (Joo et al., 2018). Crystal structures are published for several representatives of type I (Roth et al., 2014; Sulaiman et al., 2014; Miyakawa et al., 2015; Ribitsch et al., 2017), for type IIb just one enzyme with solved crystal structures exists (Han et al., 2017; Austin et al., 2018; Fecker et al., 2018; Joo et al., 2018; Liu B. et al., 2018; Liu C. et al., 2018; Palm et al., 2019), and, to the best of our knowledge, no crystal structure is known for a type IIa enzyme.

Recently, we observed that the marine bacterium *Pseudomonas aestusnigri* showed polyester degrading activity (Molitor et al., 2020). In this study, we identified the polyester hydrolase named PE-H which belongs to type IIa of PET hydrolases and demonstrated its activity toward PET as a substrate. We also report on the first crystal structure of a type IIa PET hydrolase. By a site-directed mutagenesis approach, inspired by known PETase structural features, we obtained a PE-H variant with significantly improved activity. The crystal structure of this variant was solved as well allowing us to rationalize our biochemical findings.

MATERIALS AND METHODS

Enzyme Production and Purification

Construction of the Expression Plasmid

The gene coding for the enzyme PE-H (locus tag B7O88_RS11490 of NCBI Reference Sequence NZ_NBYK01000007.1) was cloned into expression vector pET-22b(+) (Novagen) in frame with the vector-encoded hexa histidine tag utilizing *Xba*I and *Xho*I endonuclease restriction sites (Green and Sambrook, 2012). The gene was amplified by polymerase chain reaction (PCR) with Phusion High-Fidelity DNA Polymerase (Thermo Scientific) following the manufacturer's recommendations. Genomic DNA from *Pseudomonas aestusnigri* was isolated with the DNeasy, Blood and Tissue Kit (Qiagen GmbH) according to the manufacturer's

protocol and used as template with oligonucleotides PE-H_fw (AGGTCTAGATGGAGGCTACACCTCATG) and PE-H_rv (GTGCTCGAGGTACGGGCAGTTGCCGCGATAATC). The resulting recombinant plasmid pET22b_PE-H_{c6H} was used to transform chemical competent *E. coli* DH5 α cells (Woodcock et al., 1989) for replication and *E. coli* BL21(DE3) cells (Hanahan, 1983) for T7 DNA polymerase driven expression (Studier and Moffatt, 1986).

Recombinant Protein Production

Protein production was carried out in Erlenmeyer flasks filled to 1/10 of the maximal volume with auto induction media (20 g/l tryptone from casein, 5 g/l NaCl, 5 g/l yeast extract, 6 g/l Na₂HPO₄, 3 g/l KH₂PO₄, 0.6% glycerol, 0.2% lactose, 0.05% glucose) (Studier, 2005) modified as described in¹ supplemented with 100 μ g/ml ampicillin, for 24 h at 30°C with shaking (160 rpm). The culture was inoculated to an optical density of 0.05 (λ = 580 nm) from a culture grown overnight in LB media (Luria/Miller, Carl Roth GmbH & Co. KG) supplemented with 0.5% glucose and 100 μ g/ml ampicillin. After the designated production time cells were collected by centrifugation for 30 min at 6,000 \times g, 4°C, the supernatant was discarded, and cell pellets were stored at -20°C or used subsequently.

Protein Purification

Purification of PE-H was performed by immobilized metal ion affinity chromatography (IMAC) and size exclusion chromatography (SEC). Cell pellets were resuspended in lysis buffer (20 mM Na₂HPO₄ pH 7.4, 500 mM NaCl, 10 mM imidazole) at 10% (w/v) and disrupted using a high-pressure homogenizer (EmulsiFlex-C5, AVESTIN Europe, GmbH) with three passages at about 8,000 psi. Cell debris and insoluble aggregates were removed by centrifugation (30 min, 4°C, 36,000 \times g), soluble proteins were mixed with about 5 ml Ni-NTA matrix (Ni-NTA Superflow, Qiagen GmbH) per liter of culture, the matrix was washed and equilibrated with lysis buffer prior to this, and incubated for 30 min at 4°C. The matrix was filled into a gravity flow column and washed with at least 10 column volumes (CV) of washing buffer (20 mM Na₂HPO₄ pH 7.4, 500 mM NaCl, 30 mM imidazole) before elution with 3 CV of elution buffer (20 mM Na₂HPO₄ pH 7.4, 500 mM NaCl, 500 mM imidazole). Eluted proteins were concentrated by centrifugal ultrafiltration (Vivaspin 20, 10,000 MWCO, Satorius AG) and desalted using 100 mM potassium phosphate buffer pH 7.4 with PD-10 desalting columns (GE Healthcare) according to the manufacturer's recommendation. Prior to protein crystallization studies, SEC was applied to further improve protein purity. An ÄKTA Explorer system (GE Healthcare) equipped with a HiLoad 16/60 Superdex 200 prep grade column (GE Healthcare) was used and proteins were eluted with 1.5 CV of 10 mM potassium phosphate buffer pH 7.4 as the mobile phase at a flow rate of 1 ml/min. Fractions of 5 ml volume were collected and tested individually for esterase activity with 4-nitrophenyl butyrate as the substrate. Protein containing fractions, as determined by absorption at λ = 280 nm, with esterase activity were pooled,

concentrated by centrifugal ultrafiltration, and analyzed or stored at 4°C.

Determination of Protein Concentration

Protein concentrations were determined using a micro-volume spectrophotometer (NanoDrop, Thermo Fisher Scientific) using protein specific molecular weight (32,308 Da) and extinction coefficient (48,610 M⁻¹cm⁻¹) as calculated using the ProtParam web service (Gasteiger et al., 2005).

Sodium Dodecyl Sulfate Polyacrylamide Gel Electrophoresis (SDS-PAGE)

SDS-PAGE analysis was carried out according to Laemmli (1970). Protein containing samples were mixed with sample buffer [50 mM Tris-HCl pH 6.8, 0.03% (w/v) bromophenol blue, 10% (v/v) glycerol, 4% (w/v) SDS, 2% (v/v) 2-mercaptoethanol], boiled for 5–10 min at 98°C, and applied to a 12% polyacrylamide gel using the Mini-PROTEAN system (Biorad GmbH) with Laemmli buffer [25 mM Tris-HCl pH 8.8, 192 mM glycine, 0.1% (w/v) SDS]. After separation for 15 min at 100 V and 40 min at 200 V, staining of the gel with Coomassie solution [10% (w/v) ammonium sulfate; 1.2% (v/v) phosphoric acid (85% aqueous solution), 0.1% Coomassie Brilliant Blue R250, 20% methanol] was applied (Blakesley and Boezi, 1977). Visual documentation was done using an Advanced Imager system (INTAS Science Imaging Instruments GmbH).

Biochemical Characterization

Qualitative Determination of Polyester Hydrolase Activity

Rapid qualitative determination of polyester hydrolase activity was carried out on agar plates containing Impranil DLN-SD (Covestro AG) as the substrate as described earlier (Molitor et al., 2020). 1.5% (w/v) agar-agar (Carl Roth GmbH & Co. KG) was added to either LB media (Luria/Miller, Carl Roth GmbH & Co. KG) for assessment of polyester hydrolase activity of bacteria, or to 100 mM potassium phosphate buffer pH 7.4, for assessment of polyester hydrolase activity of purified enzymes, and sterilized by autoclaving (20 min at 121°C). The molten agar media were allowed to cool down (about 60°C) before addition of heat labile compounds (e.g., antibiotics) and 1% (v/v) Impranil DLN-SD. The media was mixed with a magnetic stirrer, poured into Petri dishes, and dried for 15–30 min under a sterile laminar flow hood (Herasafe KS, Thermo Fisher Scientific). To assess activity, bacterial cells were transferred with a sterile toothpick to the plates and incubated at the respective optimal growth temperature for 1–3 days, or purified enzymes were dissolved in 100 mM potassium phosphate buffer pH 7.4 and directly applied to the plates.

Quantitative Determination of Esterase Activity

Esterase activity of purified enzymes was quantified using the substrates 4-nitrophenyl butyrate (pNPB) or hexanoate (pNPH) as described earlier (Nolasco-Soria et al., 2018). Briefly, 10 μ l of enzyme solution was combined with 190 μ l substrate solution (1 mM 4-nitrophenyl ester, 5% acetonitrile, 100 mM potassium

¹https://openwetware.org/wiki/Lidstrom:Autoinduction_Media

phosphate buffer pH 7.4) in a flat bottom 96-well microtiter plate and the reaction was followed at 30°C in a microplate reader (SpectraMax i3x, Molecular Devices, LLC) at $\lambda = 410$ nm. Initial reaction velocity corrected by a control reaction without enzyme was used to calculate the release of 4-nitrophenol per minute using formula [1].

$$\frac{V[\text{min}^{-1}] * v_{\text{mtp}} * F}{d[\text{cm}] * \epsilon [\text{mM}^{-1} * \text{cm}^{-1}] * v_{\text{enz}} * c [\text{mg} * \text{ml}^{-1}]} = A [U * \text{mg}^{-1}] \quad (1)$$

V is the initial reaction velocity, v_{mtp} the volume in the well of the microtiter plate, F the dilution factor, d the path length, ϵ the extinction coefficient of 4-nitrophenol at pH 7.4, v_{enz} the volume of the enzyme sample, c the enzyme concentration and A the specific enzyme activity. One unit (U) was defined as the amount of enzyme needed to release 1 μmol of 4-nitrophenol per minute.

Determination of Protein Thermal Melting Point

Protein melting curves were measured by nano differential scanning fluorimetry (nanoDSF) using a Prometheus device (NanoTemper Technologies, Inc.), according to the manufacturer's recommendation. Briefly, purified enzyme (protein concentration 4–8 mg/ml) in 20 mM Tris pH 8 buffer was loaded into NanoTemper capillary tubes and applied to the Prometheus device for a melting scan at 10% excitation power, from 20 to 95°C at a heating rate of 1°C per minute.

Enzymatic Hydrolysis of BHET and PET and Quantification of Reaction Products

For hydrolysis of BHET and PET films, the enzymatic reaction was set up as described earlier (Yoshida et al., 2016) with minor modifications. The reaction mixture in a total volume of 300 μl was composed of 500 nM purified enzyme in 20 mM potassium phosphate buffer pH 7.4 with 20% (v/v) dimethyl sulfoxide (DMSO) and either 0.75 μl 400 mM BHET (95% purity, Sigma Aldrich) dissolved in DMSO or a circular piece of PET film (6 mm diameter). The PET pieces were produced from either amorphous PET film (0.25 mm thickness, Goodfellow Cambridge, Ltd.) or PET film derived from a commercial single use PET water bottle (trademark “Gut und Günstig” EDEKA) using a puncher, were washed with ethanol p.A., and were dried under a sterile laminar flow hood prior to use. The reaction mixtures were incubated for 24 h for BHET or 48 h for PET film at 30°C. BHET hydrolysis was stopped by removing the enzymes using ultrafiltration with centrifugal filters with a molecular weight cutoff (MWCO) of 10,000 Da (VWR International GmbH). PET film hydrolysis was stopped by heat inactivation of the enzymes for 20 min at 85°C and subsequent filtration with polyamide syringe filters of 0.2 μm pore size. The reaction filtrates were analyzed with an UPLC System (Acquity UPLC, Waters GmbH) equipped with an Acquity UPLC BEH C18 column (1.7 μm particle size) adapted from a published method (Yoshida et al., 2016). The mobile phase consisted of (A) 20 mM Na_2HPO_4 pH 2.5 (pH adjusted with H_2SO_4) and (B) methanol, the effluent was monitored at $\lambda = 240$ nm. The column was kept at constant temperature of 35°C and a flow rate of 0.208 ml/min.

The program was 75% (A) and 25% (B) for 1.28 min, followed by a linear gradient to 100% (B) in 2 min, hold 100% (B) for 3 min, linear gradient from 100 to 25% (B) in 1 min and hold 25% (B) until minute 8.28 was reached. For terephthalic acid (TA) and BHET, commercially available standards were used to calculate amounts from calibration curves. For MHET no commercial standard was available. Therefore, a series of enzymatic reactions with BHET as substrate and MHET as major product was performed as described above and the percental distribution of the BHET and the MHET peak areas in combination with the known amount of the substrate BHET was used to calculate a calibration curve for enzymatic hydrolysis of MHET.

Site Directed Mutagenesis

To introduce single and multiple amino acid substitutions to PE-H, site directed mutagenesis was carried out. Therefore, QuikChange PCR was applied as described earlier (Edelheit et al., 2009) with mutagenic primer pairs (Table 1) and the recombinant plasmid pET22b-PE-H_{C6H} as a template. *E. coli* DH5 α (Woodcock et al., 1989) cells were transformed with the recombinant plasmids by heat-shock (Hanahan, 1983) for vector replication, plasmid DNA was isolated with innuPREP Plasmid Mini Kit 2.0 (Analytic Jena AG), and mutations were verified by Sanger sequencing (eurofins genomics GmbH and LGC genomics GmbH). Cloning was simulated and sequence analysis was carried out using Clone Manager software (Sci-Ed Software).

TABLE 1 | Oligonucleotide sequences of primers used for site directed mutagenesis of PE-H.

Name	Sequence (5'→3')
S171A	GGCGTCATTGGCTGGGCGATGGGCGGTGGCGGC GCCGCCACCGCCCATCGCCAGCCAAATGACGCC
D217A	CTTTGCCGTGTGAGTCGGCGGTGATCGCGCCGGTC GACCGGCGCGATCACCGCCGACTCACAGGCCAAAG
H249A	CAATGGTGGCAGCGCTACTGCGGTAAATGGC GCCATTACCGCAGTACGCGCTGCCACCATTTG
G254S	CACACTGCGGTAATAGCGGCAGCATCTACAAC GTTGTAGATGCTGCCGCTATTACCGCAGTAGTG
S256N	GCGGTAATGGCGCAACATCTACAACGATGTG CACATCGTTGTAGATGTTGCCGCAATTACCGC
I257S	GGTAATGGCGGCAGCAGTACACGATGTGCTG CAGCACATCGTTGTAGCTGTGCGGCCATTACC
Y258N	GTAATGGCGGCAGCATCAACAACGATGTGCTGAGC GCTCAGCACATCGTTGTTGATGCTGCCGCCATTAC
N259Q	GGCGGCAGCATCTACCAGGATGTGCTGAGCCGG CCGGCTCAGCACATCCTGGTAGATGCTGCCGCC
ext.loop	GCAGCCACTACTGCGGTAATCGGGCAACTCGAATCAGGATG CCGAACCGGCTCAGCACATCCTGATTCGAGTTGCCGAATTAC
Y250S	AATGGTGGCAGCCACTCCTGCGGTAATGGCGGC GCCGCCATTACCGCAGGAGTGGCTGCCACCAT
Q294A	CACACTTCGACTCTGCCATCTCCGATTATCGC GCGATAATCGGAGATGGCAGAGTCGGAAGTGTG
I219Y	GTGAGTCGGATGTGTACGCGCCGGTCTCCAG CTGGAGGACCGGCGGTACACATCCGACTCACA

Crystallization

Wild Type Enzyme PE-H

Several crystals were observed by using commercial kits from NeXtal (Qiagen, Hilden, Germany) and Molecular Dimensions (Suffolk, England) for initial screening. 0.1 μ L homogenous protein PE-H (11 mg/ml, in 10 mM potassium phosphate buffer pH 7.4) was mixed with 0.1 μ L reservoir solution and equilibrated against 40 μ L reservoir solution in sitting drop MRC3 plates (Swissci) at 12°C. Crystals or needles appeared with this vapor diffusion method after a few days.

Variation of one of these conditions [0.1 M sodium acetate pH 4.5, 16% (w/v) PEG 3000] via grid screen (sitting drop, 1 μ L + 1 μ L over 300 μ L reservoir at 12°C) resulted in well diffracting crystals with a maximum size of 120 \times 30 \times 20 μ m after 1 week in an optimized condition composed of 0.1 M sodium acetate pH 4.5, 16% (w/v) PEG 3000, 0.036 mM LysoFos Choline14.

Enzyme Variant PE-H Y250S

Initial screening was performed as for the wild type (WT) PE-H (14 mg/ml of PE-H Y250S). Within 3 weeks, rod shaped crystals appeared and reached their maximum size of 75 \times 35 \times 20 μ m in 0.2 M lithium sulfate, 0.1 M sodium citrate pH 3.5 and 28% (v/v) PEG 400.

To cryoprotect the crystals, all drops were overlaid with 2 μ L mineral oil before the crystals were harvested and flash frozen in liquid nitrogen.

Data Collection and Structure Determination

Data sets of a single crystals of the wild type enzyme PE-H were collected at the ID29 at ESRF (Grenoble, France) at 100K equipped with a Dectris Pilatus 6M detector. Data sets for enzyme variant PE-H Y250S were collected at P13 at DESY (Hamburg, Germany) at 100K equipped with a Dectris Pilatus 6M detector.

Data sets were processed with XDS (Kabsch, 2010). For PE-H, the XDS_ASCII.HKL-file together with the protein sequence was used as input in autotrickshaw webservice² to obtain initial phases via molecular replacement. These output files were directly used in ARP/wARP webservice³ for further model building and phase improvement. Subsequently, the model was further built and refined manually using COOT (Emsley et al., 2010) software followed by REFMAC5 from the ccp4 suite (Collaborative Computational Project, 1994). For PE-H Y250S, the refined wild type structure served as search model in molecular replacement. Further model building and refinement was performed as already described. Structures were deposited in the protein data bank⁴ under the accession codes 6SBN (WT PE-H) and 6SCD (PE-H Y250S). All structure related figures were prepared with PyMOL (Schrödinger, LLC, United States)⁵, for the structure based alignments we used the PDBeFold webserver⁶.

²<http://www.embl-hamburg.de/Auto-Rickshaw/>

³<https://arpwarp.embl-hamburg.de>

⁴<https://www.rcsb.org>

⁵<https://pymol.org/2/>

⁶<http://www.ebi.ac.uk/msd-srv/ssm/cgi-bin/ssmserver>

Molecular Docking Computations

For the molecular docking, ligands BHET, MHET, and 2-HE(MHET)₄ were drawn and converted into a 3D structure with Maestro (Schrödinger, LLC, New York). The ligands and proteins were protonated according to pH 7.4 using the Epik routine in Maestro. The ligands were subsequently docked into the binding pocket of the respective enzymes using a combination of AutoDock as a docking engine and the DrugScore²⁰¹⁸ distance-dependent pair-potentials as an objective function (Goodsell et al., 1996; Sottriffer et al., 2002; Dittrich et al., 2019). In the docking, default parameters were used, with the exception of the clustering RMSD cutoff, which was set to 2.0 Å. Binding modes were considered valid, if they were part of a cluster that comprised at least 20% of all docking poses.

Bioinformatic Tools and Software

Multiple sequence alignment was carried out with Clustal Omega using default settings (Sievers et al., 2011), basic local alignment searches (BLAST) were done using the web service of the National Center for Biotechnology Information (NCBI) (Altschul et al., 1990; Wheeler et al., 2003), for data visualization, GraphPad Prism (GraphPad Software, Inc., United States) and OriginLab (OriginLab Corporation, United States) were used. For the identification and description of molecular cavities, the MOLE 2.5 software (Sehnal et al., 2013) was used employing default options with an 8.0 probe radius.

RESULTS

PE-H From *Pseudomonas aestusnigri* Is a Polyester Hydrolase

Pseudomonas aestusnigri, a bacterium belonging to the *P. pertucinogena* phylogenetic lineage, shows hydrolytic activity on different polyester substrates (Molitor et al., 2020). Additionally, we observed hydrolytic activity indicated by formation of clear halos upon growth of *P. aestusnigri* on agar plates containing Impranil DLN, an anionic aliphatic polyester-polyurethane used for surface coating of textiles (Figure 1A). Bioinformatic analysis of the *P. aestusnigri* genome sequence (Gomila et al., 2017) led us to predict the existence of a polyester hydrolase coding gene (Bollinger et al., 2020). The respective gene was cloned into a pET-22b(+) expression vector and produced by expression in *E. coli* BL21(DE3). The recombinant bacteria showed significant hydrolytic activity when grown on Impranil DLN containing solid media (Figure 1B). Hence, the predicted polyester hydrolase gene indeed codes for a functional polyester hydrolase which we named PE-H. The respective gene (locus tag: B7O88_RS11490) codes for a protein of 304 amino acids (protein id: WP_088276085.1) comprising a signal peptide of 25 amino acids for Sec-dependent translocation as predicted by SignalP (Almagro Armenteros et al., 2019). For further characterization, the protein was produced in soluble form along with its native signal peptide and fused to the vector-encoded hexa-histidine tag, which allowed a one-step purification by immobilized metal ion chromatography (IMAC) (Figure 1D). The purified protein has a

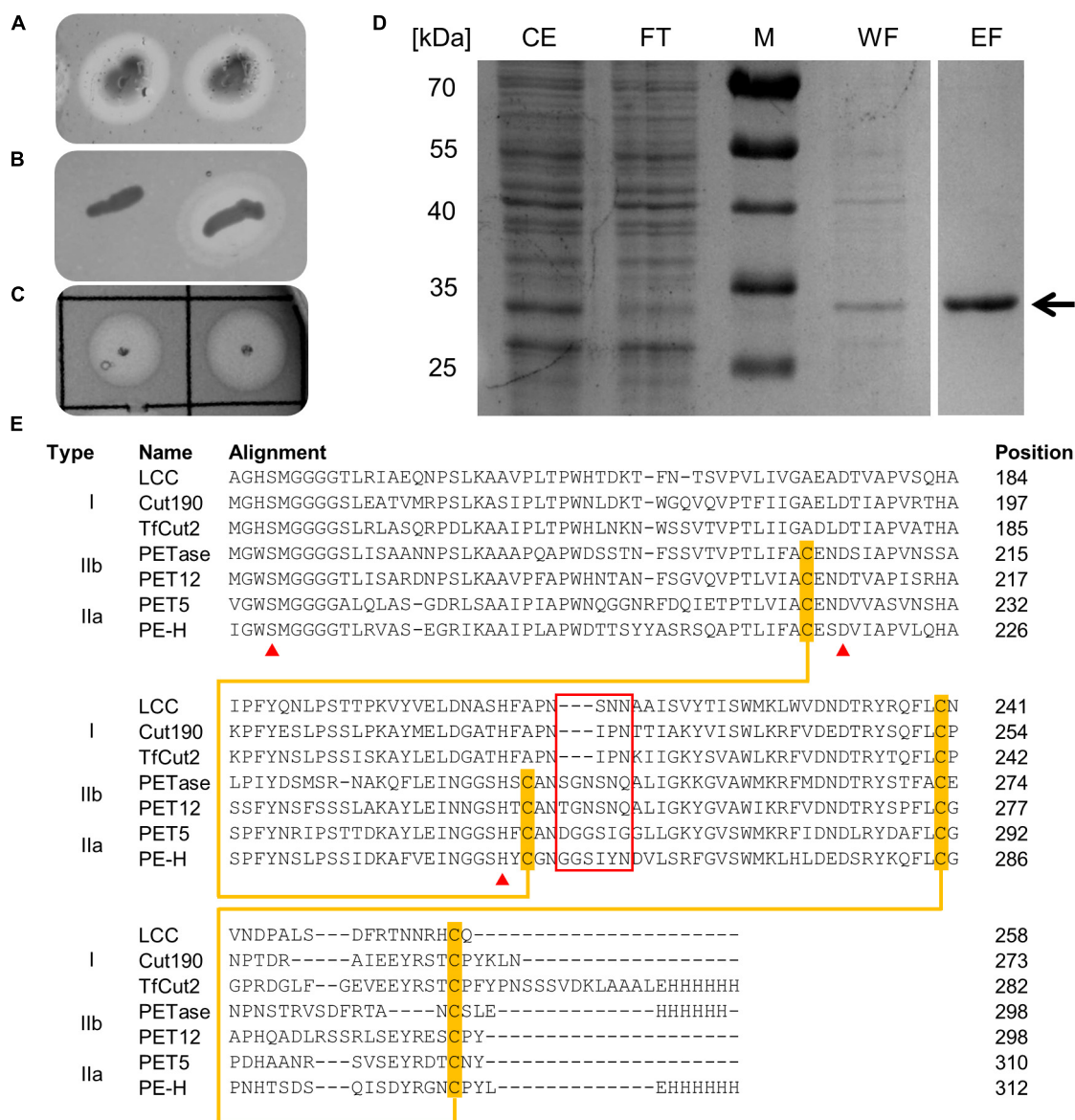


FIGURE 1 | (A) Colonies of *P. aestusnigri* grown on an Impranil DLN containing agar plate show clearing halos, indicating polyester hydrolase activity. **(B)** Hydrolytic activity of *E. coli* BL21(DE3) empty vector control (left) and PE-H production strain (right) on Impranil DLN containing agar plate. **(C)** Hydrolytic activity of purified PE-H on Impranil DLN containing agar plate. **(D)** Coomassie brilliant blue stained gel after SDS-PAGE of cell extracts of *E. coli* BL21(DE3) containing plasmid pET22b_PE-H_{c6H} before and after purification by IMAC; the position of PE-H is indicated by an arrow. Lanes contained cell extract (CE), flow through (FT), washing step (WF), and eluted protein (EF); the size of the molecular weight standards (M) are indicated on the left. **(E)** Part of a multiple sequence alignment of PE-H with amino acid sequences of different PET hydrolytic enzymes using the program Clustal Omega. The full length alignment can be found in the **Supplementary Figure S1**. The enzymes were assigned to different types of polyester hydrolases (Joo et al., 2018). Amino acid residues of the catalytic triad are marked by a red triangle, disulfide forming cysteine residues are highlighted in orange and connected by an orange line. Amino acids forming the extended loop region which is specific for type II PET hydrolytic enzymes are framed in red. Abbreviations are: leaf-branch compost metagenome cutinase (LCC); *Saccharomonospora viridis* cutinase (Cut190); *Thermobifida fusca* cutinase (TfCut2); *Ideonella sakaiensis* PET hydrolase (PETase); *Polyangium brachysporum* PET hydrolase (PET12); *Oleispira antarctica* PET hydrolase (PET5).

molecular weight of about 32 kDa and prominent activity toward the polymer substrate Impranil DLN (**Figure 1C**). Furthermore, a basic local alignment search using BLAST (Altschul et al., 1990; Wheeler et al., 2003) with the protein sequences in the protein database (PDB) as search set revealed similar sequences of cutinases and PET hydrolytic enzymes originating from *S. viridis*,

Thermobifida sp. and *I. sakaiensis* with 48–51% identity at more than 80% query coverage.

The relation of PE-H to cutinases and other PET hydrolytic enzymes was analyzed by multiple sequence alignments of the amino acid sequence of PE-H with representative examples of each type of proven PET hydrolytic enzymes as proposed by

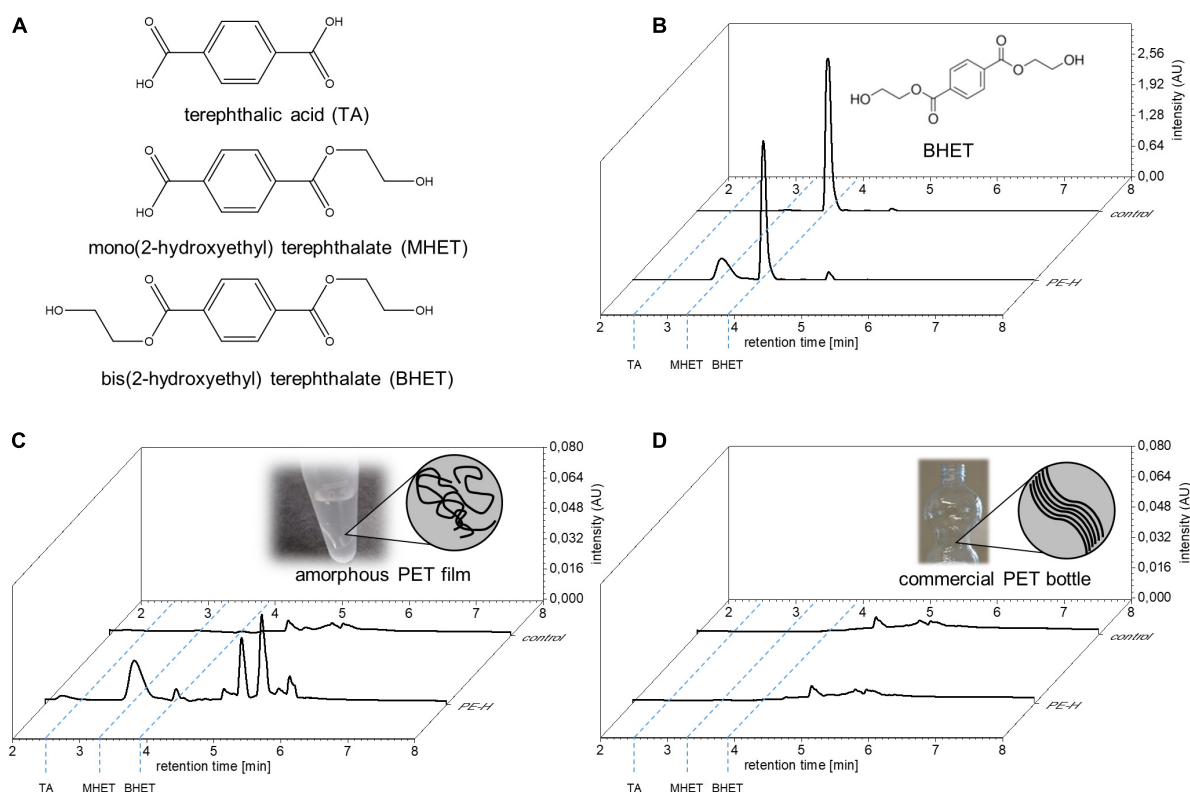


FIGURE 2 | Hydrolysis of PET by PE-H. **(A)** Structural formula of aromatic reaction products obtained by hydrolysis of PET or BHET. **(B)** UPLC analysis of reaction products obtained with PE-H and the substrates bis(2-hydroxyethyl) terephthalate (BHET), **(C)** amorphous PET film (PETa) and **(D)** PET film derived from a commercial single use PET bottle (PETb). The UPLC trace at 240 nm wavelength is shown for the control reaction without addition of the enzyme (trace in the back, labeled as control), and the enzyme reaction (trace in front, labeled PE-H). The retention times of the standard compounds terephthalic acid (TA), and bis(2-hydroxyethyl) terephthalate (BHET) as well as of the reaction product mono(2-hydroxyethyl) terephthalate (MHET) are indicated by blue dashed lines. The respective substrate of the reaction is depicted in the back of each diagram. For BHET, the structural formula is given; for PET films, a cartoon representation is shown to illustrate the different arrangement of PET fibers in amorphous and crystalline films.

Joo et al. (2018) was done using Clustal Omega. For type I, sequences, the leaf-branch compost metagenome cutinase LCC (Sulaiman et al., 2012), the cutinase Cut190 from *S. viridis* (Kawai et al., 2014), and the cutinase TfCut2 from *T. fusca* (Roth et al., 2014) were used. PETase from *I. sakaiensis* (Yoshida et al., 2016) and PET12 from *Polyangium brachysporum* (Danso et al., 2018) served as examples for type IIb and PET5 from *Oleispira antarctica* (Danso et al., 2018) for type IIa, as demonstrated before (Taniguchi et al., 2019). The alignment revealed a clear discrimination of PE-H from cutinases of type I, owing to an additional disulfide bond and additional amino acids close to the catalytically active histidine (Figure 1E and Supplementary Figure S1). Both characteristics are typical for PET hydrolytic enzymes of type II (Joo et al., 2018). Furthermore, due to the amino acid composition of the region constituting additional amino acids, known as extended loop in case of PETase (Joo et al., 2018), PE-H can be classified as a type IIa PET hydrolytic enzyme together with PET5 from *Oleispira antarctica* (Danso et al., 2018). In fact, PE-H is a close homolog of the enzymes encoded by *Pseudomonas sabulinigri*, *P. pachastrellae*, and *P. litoralis* [all belong to the phylogenetic lineage of *P. pertucinogena* (Peix et al., 2018)], which were proposed as

PET-degrading enzymes of type IIa by *in silico* sequence comparison (Joo et al., 2018).

PE-H Degrades PET

The classification of PE-H as a type IIa PET degrading enzyme suggested PET degrading activity. Therefore, we tested the enzymatic activity of PE-H with the substrates monomeric bis(2-hydroxyethyl) terephthalate (BHET), amorphous PET film (PETa) and PET film derived from a commercial single use PET bottle (PETb). The PET polymer consists of esterified terephthalic acid (TA) and ethylene glycol (EG), allowing for TA, EB, and esters of both compounds with different degree of polymerization as degradation products, for example BHET or mono(2-hydroxyethyl) terephthalate (MHET) (Figure 2A). The enzyme hydrolyzed both BHET (Figure 2B) and PETa (Figure 2C), releasing mono(2-hydroxyethyl) terephthalate (MHET), but no terephthalic acid (TA). When PETb was used as a substrate, no hydrolysis product was detected (Figure 2D).

The determination of the crystal structure of PETase from *I. sakaiensis* (Yoshida et al., 2016) by different groups in 2017/2018 (Han et al., 2017; Austin et al., 2018; Chen et al., 2018; Fecker et al., 2018; Joo et al., 2018; Liu B. et al., 2018;

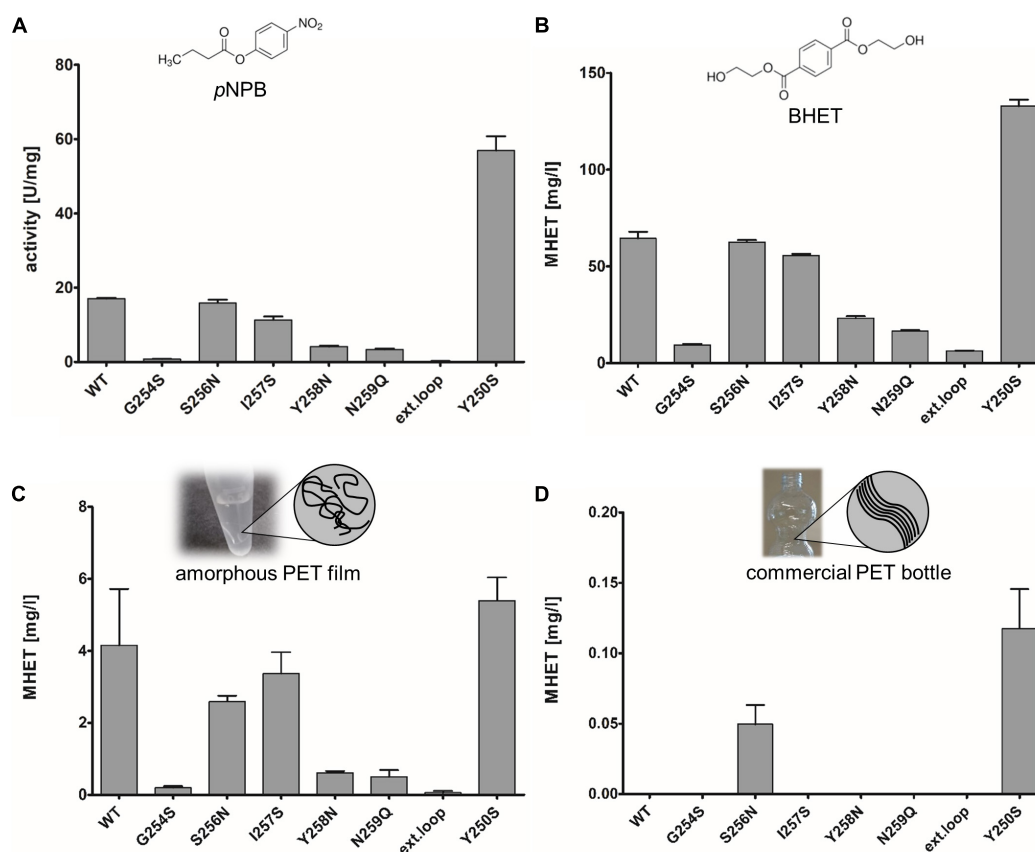


FIGURE 3 | Enzymatic activity of PE-H and different variants constructed by site directed mutagenesis. Substrates were **(A)** 4-nitrophenyl butyrate (pNPB), **(B)** bis(2-hydroxyethyl) terephthalate (BHET), **(C)** amorphous PET film, and **(D)** PET from a commercial single use bottle. Standard deviations of three individual reactions are shown as error bars. The respective substrate is depicted above each diagram. For pNPB and BHET, structural formulas are shown; for amorphous and commercial PET a cartoon representation is shown to illustrate the different arrangement of PET fibers.

Liu C. et al., 2018; Palm et al., 2019) allowed for detailed insights into the structure-function relationship of PETase with regard to PET degradation. By structural comparison to cutinases, the active site cleft of PETase was shown to be wider and shallower which seemed to be important for the PET hydrolytic activity of PETase (Austin et al., 2018; Liu B. et al., 2018). Moreover, a number of regions on the protein surface were proposed to be important for the efficient PET hydrolysis, among them (i) serine residue S238 which showed an important contribution to the enzyme activity (Joo et al., 2018), (ii) tryptophan residue W159 with proposed contribution in π -stacking interaction with terephthalic acid moiety of PET (Han et al., 2017; Chen et al., 2018), and (iii) a conserved extended loop region consisting of six amino acids connecting $\beta 8$ - $\alpha 6$ (Joo et al., 2018), which was proposed to mediate substrate binding. The amino acid composition of PE-H differs at the corresponding positions (**Supplementary Table S1**) prompting us to introduce a series of single amino acid substitutions into PE-H by site directed mutagenesis and subsequently evaluate the activity of the respective enzyme variants with different substrates.

The substitution of active site amino acids by alanine led to inactive variants as expected (data not shown). The extended

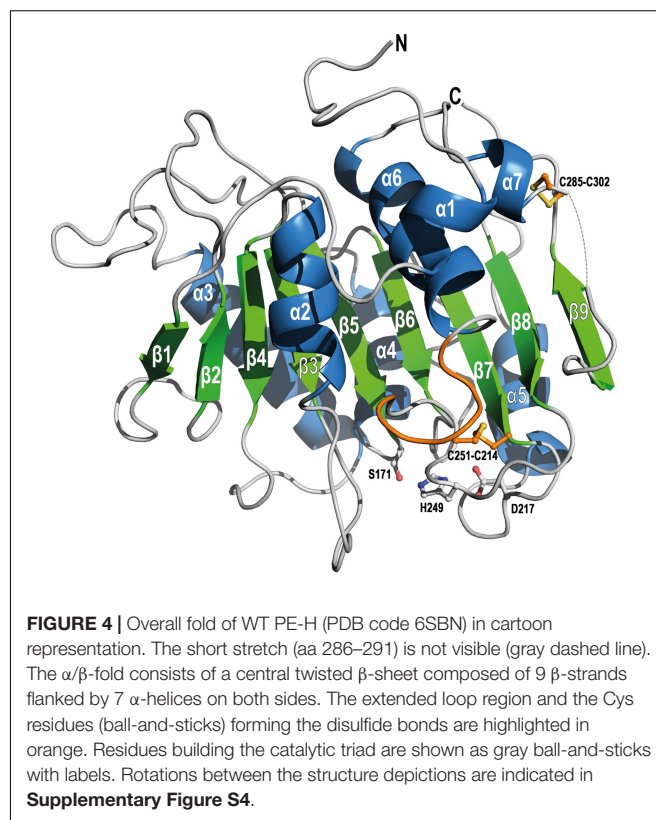
loop region can be found for PE-H as well, with an amino acid composition representative for polyester hydrolases of type IIa (Joo et al., 2018). Both, single substitutions at each position of the extended loop to those present in PETase, and the exchange of the entire extended loop region to that of PETase were constructed and the resulting variants were produced, purified, and tested for activity against the substrates 4-nitrophenyl butyrate (pNPB), BHET, and PET film. In comparison to the wild type enzyme PE-H, neither the single substitution variants nor the loop exchange variant, designed to match the amino acid residues at the corresponding positions of PETase (**Supplementary Table S1**), showed a higher specific activity toward BHET or PET film. Of these variants, G254S, Y258N, N259Q, and the variant with the combined mutations also showed a significantly decreased esterase activity determined with pNPB as the substrate (**Figure 3A**). The reduced activity of the variants was accompanied by a decrease in melting temperature of about 5–10°C (**Supplementary Table S2**) in comparison to the wild type enzyme (T_m at about 51°C), indicating a destabilizing effect of the mutations. Variant PE-H S256N, I257S, and Y250S showed a less drastic decrease in melting temperature of about 1–3°C.

Interestingly, the variant Y250S of PE-H showed a more than threefold increase in specific activity for *p*NPB, assuming a general importance of this amino acid position for enzymatic activity. The same trend was observed with BHET as the substrate (**Figure 3B**), showing decreased activity of all variants compared to the wild type except for variant Y250S. Similar results were obtained with PETa as the substrate with variant Y250S producing more MHET than the wild type enzyme or any other variant tested (**Figure 3C**). Nevertheless, the effect was less clear compared to the soluble substrates BHET and *p*NPB. The activity of the enzyme on PET derived from a commercial single use bottle as determined by MHET release appeared to be in general low. Only two variants, Y250S and S256N, led to detectable formation of MHET from PETb, but only at low amounts (**Figure 3D**).

PE-H Crystal Structure Confirms Similarity to PET Degrading Enzymes

In order to gain insight into the molecular basis of the polyester hydrolytic activity of PE-H and its variant Y250S, we solved the crystal structures of both enzymes. The PE-H structure was solved at 1.09 Å resolution, containing one monomer in the asymmetric unit, with 10.7% for R_{work} and 13.7% for R_{free} . Although the electron density was of extremely good quality, the N-terminal part (aa 1–37) and one short stretch (aa 286–291) were not visible. The structure of variant PE-H Y250S was solved at 1.35 Å resolution; here, only the N-terminus (aa 1–39) is missing. Electron densities around the active site of PE-H and variant Y250S are shown in **Supplementary Figure S2**. The crystal structure of PE-H Y250S contained a PEG molecule bound to the protein surface (**Supplementary Figure S3**). Data collection and structure refinement statistics are given in the **Supplementary Material (Supplementary Table S3)**. The PE-H protein shows a canonical α/β -fold consisting of a central twisted β -sheet composed of 9 β -strands flanked by 7 α -helices on both sides (**Figure 4**), as already reported for homologous structures, i.e., cutinases and PETases (Han et al., 2017; Numoto et al., 2018). Two disulfide bonds are present in PE-H connecting C214–C251 and C285–C302 as is common for type II PET degrading enzymes.

Both structures reported here display a nearly identical overall fold (WT PE-H to PE-H Y250S: rmsd 0.188 Å over 217 C α atoms) with main differences in two loop regions: the loop connecting β_3 – α_2 (aa 98–104) adopts a “close” conformation in WT PE-H with regard to the active site cleft, with a loop connecting β_4 – α_3 (aa 123–128) positioned parallel to it, while both are shifted against each other in the Y250S mutant (**Figure 5A**), thereby creating more space in the catalytic site. The highly conserved residues S171, D217 and H249 build the catalytic triad which is located closely below the surface with the S171 position known as the “nucleophilic elbow”. The oxyanion hole is constituted by the backbone NH groups of M172 and F98. The loop arrangement narrowing the active site cleft in the wild type enzyme is stabilized by a polar contact between the hydroxyl group of Y250 and the backbone amine of E102 (**Figure 5B**). This structural rearrangement further leads to an increased active site cavity volume from 153 Å³ for WT PE-H to 362 Å³ for variant



Y250S as determined with the program MOLE2.5. A comparison of the active site cleft molecular surface of WT PE-H and variant Y250S shows the altered topology affecting the observed increase in active site cavity volume. In WT PE-H, residues of the loop connecting β_3 – α_2 (F98, V99, S100) together with D129 and I219 are arranged in a way that access to the active site is limited, whereas PE-H variant Y250S shows a much deeper cleft (**Figure 5C**).

To identify structural homologs of PE-H, we performed structural alignments of both PE-H structures independently against the PDB. At maximum, we found 60 similar protein chains with rmsd values in the range of 1.1 to 2.7 Å for C α atoms and 53% sequence identity at maximum (data not shown). For PE-H, the Cut190 triple mutant (TM) S176A/S226P/R228S (PDB 5ZRR) from *S. viridis* is the most similar (rmsd 1.18 Å); for variant Y250S, it is the PETase double mutant (DM) R103G/S131A (PDB 5XH3) from *I. sakaiensis* (rmsd 1.17 Å). The 10 protein chains most similar to both PE-H structures described here are listed in **Supplementary Table S4**. To further analyze the different architecture of both PE-H variants reported here, we compared their surfaces with those of their structurally most similar homolog (**Supplementary Figure S5**). All four molecules share a similar pattern of surface charge which is dominated by larger patches of either positive or negative charge or hydrophobic areas, respectively. With regard to the active site cleft, Cut190 TM shows a similar narrowed active site as does WT PE-H, whereas PETase DM has a larger and deeper cleft as is the case for variant Y250S.

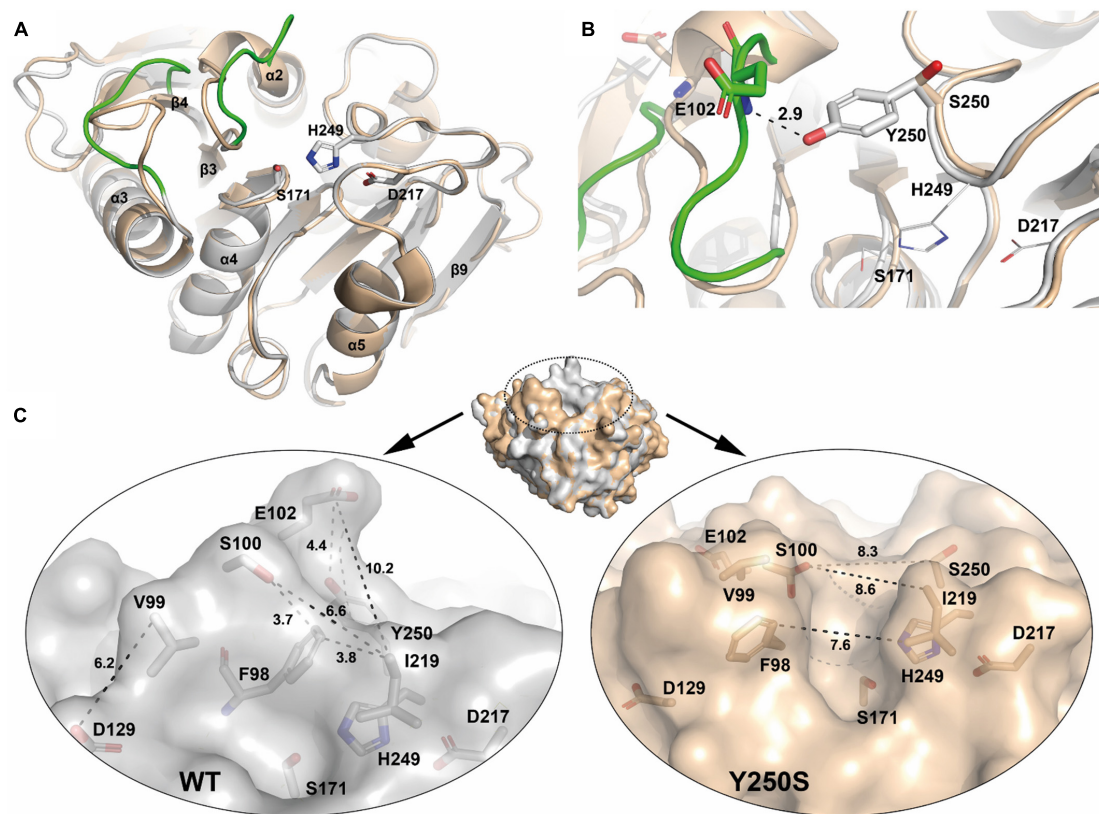


FIGURE 5 | Superposition of PE-H (PDB code 6SBN, silver) and its variant Y250S (PDB code 6SCD, wheat). **(A)** The top view on the active site and the different orientation of the two loops is shown. Residues of the catalytic triad are depicted as sticks with labels, loops of PE-H are colored in green to highlight the structural differences. **(B)** A zoom in the active site cleft with the catalytic residues depicted as lines. Remarkably, Y250 (gray sticks) makes a polar contact with E102 (green sticks) in the wild type protein, the distance is shown as a dashed line and given in Å, whereas in variant Y250S, residue E102 (wheat sticks) is far apart [color code as in **(A)**]. **(C)** Surface representation of WT PE-H (silver) and variant Y250S (wheat), on top, both structures are superposed with the catalytic cleft indicated by a dashed circle. In the panels, the differences in both structures are displayed in detail; with WT PE-H in the left panel and variant Y250S in the right panel. Residues confining the active site cleft are depicted as sticks, labeled, and connected by dotted lines, with the corresponding distances given in Å. Rotations between the different structure depictions are indicated in **Supplementary Figure S4**.

Superimposition of the PE-H structure and the structures of Cut190 (**Figure 6A**) and PETase (**Figure 6B**) revealed a high structural identity. PE-H possesses a disulfide bond linking residues C285 and C302 which is also present in Cut190, and a second disulfide bond located close to the active site (**Figure 6A**, C251–C214); both these disulfide bonds are also present in PETase (**Figure 6B**). These three structures which represent PET hydrolytic enzymes of types I, IIa, and IIb differ mainly within five loop regions (**Figures 6C,D**) comprising PE-H amino acid positions 68–71, 84–87, 97–102, 124–130, and 254–259. Three of these regions at positions 97–102, 124–130, and 254–259 are located in the vicinity of the active site indicating a putative contribution to substrate binding.

Molecular Docking Computations Suggest PE-H Substrate Binding Mode

Substrate binding was analyzed by docking the PET tetramer 2-HE(MHET)₄, BHET, and MHET to wild type PE-H and variant Y205S using predicted protonation states at pH 7.4 for both the

ligands and proteins. Lowest-energy configurations of the ligands in the proteins from the largest cluster were taken as binding poses as done previously (Diedrich et al., 2016; Krieger et al., 2017). Binding modes were considered valid, if at least 20% of all poses are contained in this cluster. During the docking, ligands were allowed to explore the whole protein to ensure an unbiased sampling of potential binding poses.

The predicted binding poses provide mechanistic insights into the function of PE-H and highlight the differences between wild type PE-H and variant Y250S. In PE-H, MHET and BHET are predicted to bind adjacent to the catalytic site (**Figure 7A**). In the *apo* crystal structure, the catalytic site of PE-H is apparently too narrow to allow favorable substrate binding (**Figure 5C**). This suggests that in PE-H a conformational change is necessary to accommodate a substrate. BHET and MHET bind with the phenyl rings to a hydrophobic groove and are additionally stabilized via hydrogen-bonding interactions to S103, D106, S248, and S256 (**Figure 7B**). Although no valid binding mode was identified for 2-HE(MHET)₄, as no cluster contained more than 4% of all binding poses, the lowest-energy pose found in

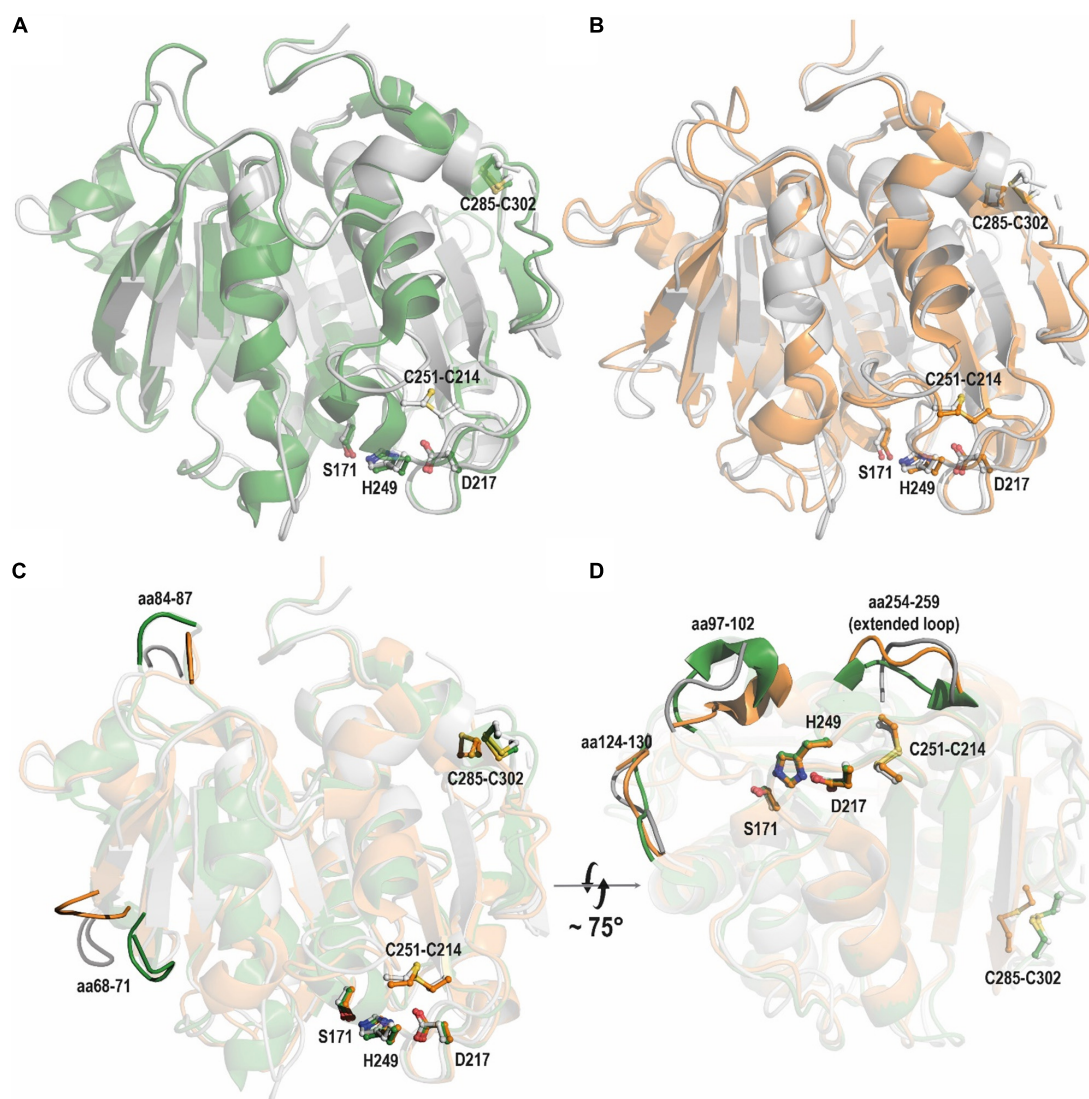


FIGURE 6 | Overlay of PE-H WT (PDB code 6SBN, gray) with **(A)** Cut190 (PDB code 4WFI, green) and **(B)** PETase (PDB code 6ANE, orange). Residues of the active site and disulfide bonds are represented as sticks with labels (according to PE-H numbering). **(C)** Superimposition of PE-H (PDB code 6SBN, gray), PETase (PDB code 6ANE, orange), and Cut190 (PDB code 4WFI, green). Five regions of the superimposition are represented in full tone on fade-out color to highlight the differences of the structures. In **(D)** the structures are turned from bottom to top.

this docking is located in the adjacent groove like BHET and MHET (**Figure 7B**), which hints at the groove's importance for the function of PE-H.

In the variant Y250S, the catalytic site has twice the volume than in wild type PE-H. As a result, the predicted binding pose of MHET is located in the catalytic site, whereas BHET still binds to the same groove as in PE-H (**Figure 7C**). MHET is stabilized by hydrophobic interactions to F98, V99, M172, and I219, and the ester carbonyl carbon is placed at an optimal distance to be attacked by S171 (**Figure 7D**). A second binding pose of BHET, which is $0.43 \text{ kcal}\cdot\text{mol}^{-1}$ less favorable than the lowest-energy one, is found in the catalytic site similar to MHET (**Figure 7E**) and is thereby in an optimal position to be hydrolyzed by S171. Again, no valid binding modes were

identified for 2-HE(MHET)₄, likely owing to the size of the ligand. The presence of binding poses for BHET adjacent to the active site suggests a possible polymer binding mode, where one polymer unit binds to the groove adjacent to the catalytic site, a second unit bridges the distance to the catalytic site, and a third unit is cleaved from the polymer chain (**Figure 7F**).

DISCUSSION

Enzymes acting on PET are almost exclusively homologs of cutinases with many of them originating from thermophilic actinobacteria (Nikolaivits et al., 2018). PETase from *I. sakaiensis* was the first enzyme isolated from a mesophilic host and

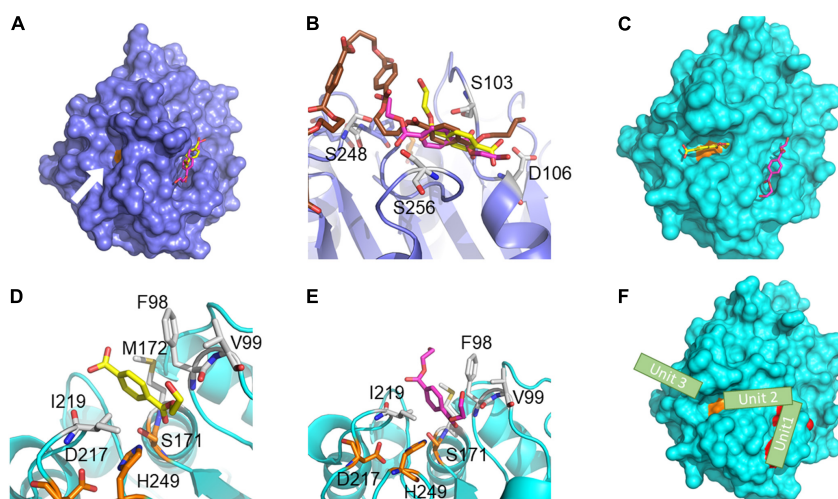


FIGURE 7 | Predicted ligand binding modes in wild type PE-H and variant Y250S. The predicted binding poses of BHET (magenta), MHET (yellow), and 2-HE(MHET)₄ (brown) in WT PE-H (navy) and the variant Y250S (cyan). In **(A,C,F)** S171 is shown in orange, and in **(B,D,E)** the catalytic triad (S171, D217, and H249) is shown in orange and interacting residues are shown in white. **(A)** In wild type PE-H, BHET and MHET bind to a groove adjacent to the catalytic site (white arrow). **(B)** BHET and MHET bind to the hydrophobic groove and are stabilized by hydrogen bonding interactions with S103, D106, S248, and S256. 2-HE(MHET)₄ binds similarly to BHET and MHET in the groove adjacent to the catalytic site. **(C)** In the variant Y250S, MHET binds to the catalytic site, while BHET occupies the hydrophobic groove. **(D)** MHET binds to the catalytic site and is stabilized by hydrophobic interactions to F98, V99, M172, and I219 such that S171 can attack the carbonyl carbon for ester hydrolysis. **(E)** A second binding pose of BHET binds similar to MHET. **(F)** Proposed mechanism of PET polymer interaction. Residues G254, Y258, and N259, which when substituted decrease esterase activity, are shown in red. One polymer unit (stylized green rectangle) binds to the groove adjacent to the catalytic site, a second unit bridges the distance to the catalytic site, and a third unit is cleaved from the polymer chain at the catalytic unit.

catalyzing the biodegradation of PET at mild temperature of 30°C (Yoshida et al., 2016). Structural studies showed characteristic features discriminating PETase from cutinases with PET hydrolytic activity (Joo et al., 2018) and lead to the proposal of three subclasses of PET hydrolyzing enzymes. With this information, novel PET hydrolytic enzymes were identified, among them enzymes from marine origin (Danso et al., 2018). This finding is of considerable interest because the oceans are known to be a sink for the worldwide plastic waste (Lebreton et al., 2018).

A Novel PET Degrading Enzyme From the Marine Bacterium *P. aestusnigri*

In this study, we have identified the protein PE-H, a novel polyester hydrolase from the marine bacterium *P. aestusnigri* which hydrolyses different polyethylene terephthalate substrates with mono(2-hydroxyethyl) terephthalate (MHET) as the major hydrolysis product. The formation of MHET, but not TA as hydrolysis product was previously described for other PET degrading enzymes, for example TfCut2 from *T. fusca* (Barth et al., 2015; Wei et al., 2016), Thc_Cut2 from *T. cellulossilytica* (Herrero Acero et al., 2011), and PETase from *I. sakaiensis* (Yoshida et al., 2016). However, in case of TfCut2, MHET was almost completely hydrolyzed to TA after 24 h of reaction (Barth et al., 2015), and the cutinases Thc_Cut1 from *T. cellulossilytica* and Thf42_Cut1 from *T. fusca* were reported to release more TA than MHET from PET film after a reaction time of 120 h (Herrero Acero et al., 2011). Hence, PE-H accumulating MHET from PET film appears to be common feature among PET hydrolyzing

enzymes, but the almost complete absence of TA after 48 h of reaction was not observed before.

Hydrolysis of PET by PE-H yielded 4.2 (± 1.6) mg/L MHET after a reaction time of 48 h at 30°C, variant PE-H Y250S produced 5.4 (± 0.6) mg/L MHET under the same conditions. This amount is considerably lower than reported for the *I. sakaiensis* PETase with more than 150 mg/L after 96 h reaction time at 30°C (Austin et al., 2018). However, it should be mentioned that activities are difficult to compare because different studies use PET substrates which differ among each other, e.g., by the degree of crystallinity. Obviously, a comprehensive comparative study of different PET degrading enzymes would be required. In case of PE-H, the marine origin of the producer *P. aestusnigri* suggests that natural substrates may be aliphatic polyesters produced by algae and plants, because marine bacteria of the *P. pertucinogena* lineage have been found associated with these organisms (Bollinger et al., 2020).

Rational Mutagenesis Resulted in PE-H Variant Y250S With Improved Activity

Wild type PE-H was unable to hydrolyze a PET film substrate obtained from a commercial PET bottle (PETb). This observation prompted us to identify differences in the amino acid sequences between PE-H and the *I. sakaiensis* PETase and analyze them by a site directed mutagenesis study. As the result, a single amino acid substitution (Y250S) was identified which led to a significant increase in enzymatic activity of PE-H toward different substrates, including PETb. In comparison to the results obtained with PETa, the best performing variant PE-H

Y250S showed a 45-fold reduced amount of MHET produced with PETb as the substrate. This observation can be explained by the molecular arrangement of the PET fibers in PETb which is known to comprise more crystalline regions and thus, is more recalcitrant to enzymatic degradation (Wei and Zimmermann, 2017). The highly ordered structure of crystalline PET hampers the enzymes access to single PET fibers, particularly at temperatures below the glass transition temperature of the polymer. Nevertheless, two single amino acid substitution variants, S256N and Y250S, produced detectable amounts of MHET from PETb while the wild type enzyme did not.

The Crystal Structure of PE-H Is the First Structure of Type IIa PET Hydrolytic Enzyme

In an attempt to rationalize the PE-H activity toward PET as a substrate and to explain the effect of the Y250S substitution, we report here the first crystal structure of a type IIa PET hydrolytic enzyme and its comparison with the crystal structure of the improved variant PE-H Y250S. Interestingly the comparison of both structures showed that the substitution Y250S replacing the aromatic residue tyrosine located next to the active site histidine by the small residue serine significantly improved the enzymatic activity toward different substrates. The relevance of this serine residue has also been observed with PETase variant S238F which showed an about 40% reduced enzymatic activity (Joo et al., 2018). Thus, a small, polar, and uncharged amino acid at the position next to the active histidine seems to be an important characteristic of PET hydrolytic enzymes of type IIb, whereas enzymes of type I and type IIa possess large aromatic residues at the corresponding position (see **Figure 1E** and **Supplementary Figure S1**). This finding is also supported by a very recent study which reported a significant increase in activity of the cutinase TfCut2 from *Thermobifida fusca* obtained by substitution of F209 (the corresponding position in PE-H is Y250) with serine and alanine (Furukawa et al., 2019). The authors tested additional substitutions at this position introducing amino acids with chemically different side-chains and concluded that the increase in activity correlated with the size of the respective side-chain. The structural analysis of PE-H and the variant Y250S showed a rearrangement of the loop connecting $\alpha 2$ - $\beta 3$, creating space which results in a better accessible active site. The role of the active site cleft size was also found to be important for PETase, which was reported to be three times wider at its widest point compared to *T. fusca* cutinase TfCut2 (Austin et al., 2018) and also wider compared to *Fusarium solani pisi* cutinase (Liu B. et al., 2018). Hence, the authors proposed that the wider active side cleft enables PETase to accommodate larger substrates like PET. The enhanced activity of PETase at lower temperatures compared to cutinases was attributed to enhanced flexibility within the active center whereby the active site proximal disulfide bridge diminishes loss of stability that is to be expected as tradeoff for enhanced flexibility (Fecker et al., 2018). This disulfide bridge is a common feature of all type II PET hydrolytic enzymes and is in consequence also found in PE-H. The reshaping of the active site cleft of PE-H may therefore be the main reason for

the enhanced catalytic activity observed in this study, enabling the enzyme to accommodate larger substrates as seen with PET from a commercial single use PET bottle. In PE-H, besides the steric effects of a larger amino acid, a polar contact between Y250 and E102 was observed which may contribute to narrowing the active site. However, most cutinases carry a phenylalanine at the corresponding position (Joo et al., 2018) which does not allow for a polar contact. This observation therefore does not explain the differences between PET hydrolytic enzymes of type I and II regarding PET hydrolysis. To reveal further differences between PET hydrolytic enzymes of types I, IIa, and IIb, the structures of one enzyme of each type (namely PE-H, Cut190, and PETase) were superimposed and three loop regions located close to the active site were identified as differing. Some amino acids of the corresponding regions in PETase were already reported to be involved in substrate interaction, for example Y87 (F98 in PE-H) and N246 (Y258 in PE-H) which were assigned to substrate binding subsites I and IIc (Joo et al., 2018), respectively.

The PET Binding Mode of PE-H

To gain insight into protein substrate interaction of PE-H with PET, molecular docking with substrates MHET, BHET, and a previously reported PET tetramer (Joo et al., 2018) was conducted. Interestingly, wild type PE-H was not found to viably bind the tested substrates in the active site, but substrate molecules accumulated in an adjacent groove. For variant Y250S, viable binding modes for MHET and BHET, but not the PET tetramer were found. However, biochemical data revealed catalytic activity of PE-H and variant Y250S and PET film as a substrate. This observation might be connected to the flexibility of the active site of PE-H, suggesting that PE-H can rearrange its active site cleft to accommodate respective substrates. In line with that, flexibility of the active site was shown for PETase and reported to be crucial for the enzyme activity at room temperature (Fecker et al., 2018). Furthermore, MHET was accommodated in a catalytically viable position in PE-H Y250S; thus, the observed absence of MHET hydrolysis cannot be attributed to low affinity or preferred binding in a detrimental position for hydrolysis. Molecular reasons for that substrate preference might be addressed in further studies.

The two distinct binding poses observed for variant PE-H Y250S hint at a mechanism in which one polymer unit binds to the groove adjacent to the catalytic site, a second unit bridges the distance to the catalytic site, and a third unit is cleaved from the polymer chain. This mechanism with the adjacent groove acting as an anchor point for the polymer could increase the processivity of PE-H, similar to the adjacent substrate binding site in Hyal lyases (Rigden and Jedrzejewski, 2003; Stern and Jedrzejewski, 2008). A similar PET binding mechanism that involves a binding groove that stabilizes different units of a polymeric substrate was proposed for PETase binding elements of 2-HE(MHET)₄ in subsites I, IIa, IIb, and IIc, facilitating the binding of the PET polymer (Joo et al., 2018). The presence of an adjacent substrate binding site may also contribute to the significant decrease in esterase activity of PE-H variants G254S, Y258N, and N259Q and the variant with the combined mutations. All three substitutions are located at the adjacent groove (**Figure 7F**)

and alter their shape and molecular recognition properties, presumably hampering substrate binding that way.

As we did not obtain valid docking poses for 2-HE(MHET)₄, we cannot comment on the *gauche*-to-*trans* ratio of the substrate's OC-CO torsion angle when bound to the catalytic site, which has been discussed recently (Joo et al., 2018; Seo et al., 2019; Wei et al., 2019b). Our lowest-energy pose of 2-HE(MHET)₄ (Figure 7B), which is located in the adjacent groove, shows all-*gauche* torsion angles. This result is in line with low *trans*-to-*gauche* ratios of (9 – 14): (91 – 86) experimentally determined for amorphous PET (Schmidt-Rohr et al., 1998; Wei et al., 2019b). We note, though, that even an increase in the *trans* content by a factor of ~3 as discussed (Joo et al., 2018; Seo et al., 2019; Wei et al., 2019b) relates to changes in the conformational free energy of the substrate on the order of the thermal energy and, thus, may be compensated by favorable interactions with the protein.

CONCLUSION

Polyester hydrolases are of considerable interest for a variety of biotechnological applications (Nikolaivits et al., 2018), for example the removal of cyclic PET oligomers from polyester fibers in the textile industry (Riegels et al., 1997). As far as biocatalytic degradation of PET in an industrial context is concerned, elevated temperatures close to the glass transition temperature of PET are desirable (Wei and Zimmermann, 2017). Hence, protein engineering of PE-H would be required to design a PE-H variant for efficient PET hydrolysis at elevated temperatures as has been demonstrated for PETase (Son et al., 2019). However, additional applications appear feasible for PE-H as it has been demonstrated that the PE-H homologous enzyme PpelaLip originating from the closely related genus *Pseudomonas pelagia* can be used for the biodegradation of different synthetic polyesters and may thus be applicable for waste water treatment (Haernvall et al., 2017). In this case, the activity of the respective biocatalyst at low temperatures is an advantage allowing for the hydrolysis of synthetic polymers at 15°C (Haernvall et al., 2018).

We have described here the identification, biochemical and structural characterization of the polyester hydrolase PE-H from the marine mesophilic bacterium *P. aestusnigri*. The crystal structure of PE-H represents the first structure of a type IIa PET hydrolytic enzyme thus closing the gap between PET hydrolytic enzymes of type I and IIb. We furthermore succeeded to significantly increase the enzymatic activity of PE-H toward different substrates by introducing a single amino acid substitution, namely Y250S. This substitution resulted in a rearrangement of the active site conformation, favored by prevention of a polar contact of Y250 located next to the catalytic active histidine, and a loop region of the active site cleft. Furthermore, a PET polymer binding mechanism was proposed based on molecular docking computations. Our results thus provide important information regarding structural features required for efficient polyester degradation and indicate that marine bacteria such as *P. aestusnigri* may prove as a prolific source for such enzymes.

DATA AVAILABILITY STATEMENT

Structures were deposited in the protein data bank (<https://www.rcsb.org>) under the accession codes 6SBN (WT PE-H) and 6SCD (PE-H Y250S).

AUTHOR CONTRIBUTIONS

K-EJ conceived the research concept. AB, ST, MF, and SS designed the experiments. AB, ST, and EK-G performed the experimental work. SK, AH, and SS performed the crystallization trials and structure solution. CG and HG conducted the molecular docking computations, discussed the results, and wrote the corresponding parts of the manuscript. AB, ST, and AH analyzed the data and wrote the draft manuscript. K-EJ and MF revised the manuscript. All authors read and approved the final manuscript.

FUNDING

The authors received funding from the European Union's Horizon 2020 Research and Innovation Program (Blue Growth: Unlocking the potential of Seas and Oceans) through the Project "INMARE" under grant agreement no. 634486. ST is financially supported by the Ministry of Culture and Science of the German State of North Rhine-Westphalia within in the framework of the NRW Strategieprojekt BioSC (No. 313/323-400-00213). MF acknowledges grant BIO2017-85522-R, from the Ministry of Science, Innovation and Universities, with the cofunds of the ERDF and the Agencia Estatal de Investigación (AEI). The Center for Structural Studies is funded by the Deutsche Forschungsgemeinschaft (DFG Grant number 417919780). The funding bodies had no role in the design of the study and collection, analysis, and interpretation of data or in writing the manuscript.

ACKNOWLEDGMENTS

The authors gratefully acknowledge the funding by the organizations mentioned in the Funding section. The authors thank the beamline scientists of the ID29 at ESRF (Grenoble, France) and at P13 at DESY (Hamburg, Germany) and Maha Raauf for excellent experimental support with PE-H mutagenesis. Computational support by the "Zentrum für Informations und Medientechnologie" at the Heinrich-Heine-Universität Düsseldorf and the computing time provided by the John von Neumann Institute for Computing (NIC) to HG on the supercomputer JUWELS at Jülich Supercomputing Centre (JSC) (user ID: HKF7) are gratefully acknowledged.

SUPPLEMENTARY MATERIAL

The Supplementary Material for this article can be found online at: <https://www.frontiersin.org/articles/10.3389/fmicb.2020.00114/full#supplementary-material>

REFERENCES

- Adrados, A., de Marco, I., Caballero, B. M., López, A., Laresgoiti, M. F., and Torres, A. (2012). Pyrolysis of plastic packaging waste: a comparison of plastic residuals from material recovery facilities with simulated plastic waste. *Waste Manag.* 32, 826–832. doi: 10.1016/j.wasman.2011.06.016
- Almagro Armenteros, J. J., Tsirigos, K. D., Sønderby, C. K., Petersen, T. N., Winther, O., Brunak, S., et al. (2019). SignalP 5.0 improves signal peptide predictions using deep neural networks. *Nat. Biotechnol.* 37, 420–423. doi: 10.1038/s41587-019-0036-z
- Altschul, S. F., Gish, W., Miller, W., Myers, E. W., and Lipman, D. J. (1990). Basic local alignment search tool. *J. Mol. Biol.* 215, 403–410. doi: 10.1016/S0022-2836(05)80360-2
- Austin, H. P., Allen, M. D., Donohoe, B. S., Rorrer, N. A., Kearns, F. L., Silveira, R. L., et al. (2018). Characterization and engineering of a plastic-degrading aromatic polyesterase. *Proc. Natl. Acad. Sci. U.S.A.* 115, E4350–E4357. doi: 10.1073/pnas.1718804115
- Barth, M., Oeser, T., Wei, R., Then, J., Schmidt, J., and Zimmermann, W. (2015). Effect of hydrolysis products on the enzymatic degradation of polyethylene terephthalate nanoparticles by a polyester hydrolase from *Thermobifida fusca*. *Biochem. Eng. J.* 93, 222–228. doi: 10.1016/j.bej.2014.10.012
- Blakesley, R. W., and Boezi, J. A. (1977). A new staining technique for proteins in polyacrylamide gels using coomassie brilliant blue G250. *Anal. Biochem.* 82, 580–582. doi: 10.1016/0003-2697(77)90197-X
- Bollinger, A., Thies, S., Katzke, N., and Jaeger, K.-E. (2020). The biotechnological potential of marine bacteria in the novel lineage of *Pseudomonas pertucinogena*. *Microb. Biotechnol.* 13, 19–31. doi: 10.1111/1751-7915.13288
- Chen, C.-C., Han, X., Ko, T.-P., Liu, W., and Guo, R.-T. (2018). Structural studies reveal the molecular mechanism of PETase. *FEBS J.* 285, 3717–3723. doi: 10.1111/febs.14612
- Chen, S., Su, L., Billig, S., Zimmermann, W., Chen, J., and Wu, J. (2010). Biochemical characterization of the cutinases from *Thermobifida fusca*. *J. Mol. Catal. B Enzym.* 63, 121–127. doi: 10.1016/j.molcatb.2010.01.001
- Collaborative Computational Project. (1994). The CCP4 suite: programs for protein crystallography. *Acta Crystallogr. Sect. D* 50, 760–763. doi: 10.1107/S0907444994003112
- Danso, D., Schmeisser, C., Chow, J., Zimmermann, W., Wei, R., and Leggewie, C. (2018). New insights into the function and global distribution of polyethylene terephthalate (PET)-degrading bacteria and enzymes in marine and terrestrial metagenomes. *Appl. Environ. Microbiol.* 84:e02773-17. doi: 10.1128/AEM.02773-17
- Diedrich, D., Hamacher, A., Gertzen, C. G. W., Alves Avelar, L. A., Reiss, G. J., Kurz, T., et al. (2016). Rational design and diversity-oriented synthesis of peptoid-based selective HDAC6 inhibitors. *Chem. Commun.* 52, 3219–3222. doi: 10.1039/c5cc10301k
- Dittrich, J., Schmidt, D., Pfeiffer, C., and Gohlke, H. (2019). Converging a knowledge-based scoring function: DrugScore²⁰¹⁸. *J. Chem. Inf. Model.* 59, 509–521. doi: 10.1021/acs.jcim.8b00582
- Edelheit, O., Hanukoglu, A., and Hanukoglu, I. (2009). Simple and efficient site-directed mutagenesis using two single-primer reactions in parallel to generate mutants for protein structure-function studies. *BMC Biotechnol.* 9:61. doi: 10.1186/1472-6750-9-61
- Emsley, P., Lohkamp, B., Scott, W. G., and Cowtan, K. (2010). Features and development of Coot. *Acta Crystallogr. Sect. D* 66, 486–501. doi: 10.1107/S0907444910007493
- Fecker, T., Galaz-Davison, P., Engelberger, F., Narui, Y., Sotomayor, M., Parra, L. P., et al. (2018). Active site flexibility as a hallmark for efficient PET degradation by *I. sakaiensis* PETase. *Biophys. J.* 114, 1302–1312. doi: 10.1016/j.bpj.2018.02.005
- Furukawa, M., Kawakami, N., Tomizawa, A., and Miyamoto, K. (2019). Efficient degradation of poly(ethylene terephthalate) with *Thermobifida fusca* cutinase exhibiting improved catalytic activity generated using mutagenesis and additive-based approaches. *Sci. Rep.* 9:16038. doi: 10.1038/s41598-019-52379-z
- Gasteiger, E., Hoogland, C., Gattiker, A., Duvaud, S., Wilkins, M. R., Appel, R. D., et al. (2005). “Protein identification and analysis tools on the ExPASy server,” in *The Proteomics Protocols Handbook*, ed. J. M. Walker, (Totowa, NJ: Humana Press), 571–607. doi: 10.1385/1-59259-890-0:571
- Gomila, M., Mulet, M., Lalucat, J., and García-Valdés, E. (2017). Draft genome sequence of the marine bacterium *Pseudomonas aestusnigri* VGX014T. *Genome Announc.* 5:e00765-17. doi: 10.1128/genomeA.00765-17
- Goodsell, D. S., Morris, G. M., and Olson, A. J. (1996). Automated docking of flexible ligands: applications of AutoDock. *J. Mol. Recognit* 9, 1–5. doi: 10.1002/(sici)1099-1352(199601)9:1<1::aid-jmr241<3.0.co;2-6
- Green, M. R., and Sambrook, J. (2012). *Molecular Cloning: A Laboratory Manual*, 4th Edn. Cold Spring Harbor, NY: Cold Spring Harbor Laboratory Press.
- Haernvall, K., Zitzenbacher, S., Biundo, A., Yamamoto, M., Schick, M. B., Ribitsch, D., et al. (2018). Enzymes as enhancers for the biodegradation of synthetic polymers in wastewater. *ChemBioChem* 19, 317–325. doi: 10.1002/cbic.201700364
- Haernvall, K., Zitzenbacher, S., Wallig, K., Yamamoto, M., Schick, M. B., Ribitsch, D., et al. (2017). Hydrolysis of ionic phthalic acid based polyesters by wastewater microorganisms and their enzymes. *Environ. Sci. Technol.* 51, 4596–4605. doi: 10.1021/acs.est.7b00062
- Hajighasemi, M., Tchigvintsev, A., Nocek, B. P., Flick, R., Popovic, A., Hai, T., et al. (2018). Screening and characterization of novel polyesterases from environmental metagenomes with high hydrolytic activity against synthetic polyesters. *Environ. Sci. Technol.* 52, 12388–12401. doi: 10.1021/acs.est.8b04252
- Han, X., Liu, W., Huang, J.-W., Ma, J., Zheng, Y., Ko, T.-P., et al. (2017). Structural insight into catalytic mechanism of PET hydrolase. *Nat. Commun.* 8:2106. doi: 10.1038/s41467-017-02255-z
- Hanahan, D. (1983). Studies on transformation of *Escherichia coli* with plasmids. *J. Mol. Biol.* 166, 557–580.
- Herrero Acero, E., Ribitsch, D., Steinkellner, G., Gruber, K., Greimel, K., Eiteljoerg, I., et al. (2011). Enzymatic surface hydrolysis of PET: effect of structural diversity on kinetic properties of cutinases from *Thermobifida*. *Macromolecules* 44, 4632–4640. doi: 10.1021/ma200949p
- Joo, S., Cho, I. J., Seo, H., Son, H. F., Sagong, H.-Y., Shin, T. J., et al. (2018). Structural insight into molecular mechanism of poly(ethylene terephthalate) degradation. *Nat. Commun.* 9:382. doi: 10.1038/s41467-018-02881-1
- Kabsch, W. (2010). XDS. *Acta Crystallogr. Sect. D* 66, 125–132. doi: 10.1107/S0907444909047337
- Kawai, F., Oda, M., Tamashiro, T., Waku, T., Tanaka, N., Yamamoto, M., et al. (2014). A novel Ca²⁺-activated, thermostabilized polyesterase capable of hydrolyzing polyethylene terephthalate from *Saccharomonospora viridis* AHK190. *Appl. Microbiol. Biotechnol.* 98, 10053–10064. doi: 10.1007/s00253-014-5860-y
- Krieger, V., Hamacher, A., Gertzen, C. G. W., Senger, J., Zwinderman, M. R. H., Marek, M., et al. (2017). Design, multicomponent synthesis, and anticancer activity of a focused histone deacetylase (HDAC) inhibitor library with peptoid-based cap groups. *J. Med. Chem.* 60, 5493–5506. doi: 10.1021/acs.jmedchem.7b00197
- Laemmli, U. (1970). Cleavage of structural proteins during the assembly of the head of bacteriophage T4. *Nature* 227, 680–685. doi: 10.1038/227680a0
- Lebreton, L., Slat, B., Ferrari, F., Sainte-Rose, B., Aitken, J., Marthouse, R., et al. (2018). Evidence that the Great Pacific Garbage Patch is rapidly accumulating plastic. *Sci. Rep.* 8:4666. doi: 10.1038/s41598-018-22939-w
- Liu, B., He, L., Wang, L., Li, T., Li, C., Liu, H., et al. (2018). Protein crystallography and site-direct mutagenesis analysis of the poly(ethylene terephthalate) hydrolase PETase from *Ideonella sakaiensis*. *Chembiochem* 19, 1471–1475. doi: 10.1002/cbic.201800097
- Liu, C., Shi, C., Zhu, S., Wei, R., and Yin, C.-C. (2018). Structural and functional characterization of polyethylene terephthalate hydrolase from *Ideonella sakaiensis*. *Biochem. Biophys. Res. Commun.* 508, 289–294. doi: 10.1016/j.bbrc.2018.11.148
- Miyakawa, T., Mizushima, H., Ohtsuka, J., Oda, M., Kawai, F., and Tanokura, M. (2015). Structural basis for the Ca²⁺-enhanced thermostability and activity of PET-degrading cutinase-like enzyme from *Saccharomonospora viridis* AHK190. *Appl. Microbiol. Biotechnol.* 99, 4297–4307. doi: 10.1007/s00253-014-6272-8
- Moharir, R. V., and Kumar, S. (2019). Challenges associated with plastic waste disposal and allied microbial routes for its effective degradation: a comprehensive review. *J. Clean. Prod.* 208, 65–76. doi: 10.1016/j.jclepro.2018.10.059
- Molitor, R., Bollinger, A., Kubicki, S., Loeschcke, A., Jaeger, K., and Thies, S. (2020). Agar plate-based screening methods for the identification of polyester

- hydrolysis by *Pseudomonas* species. *Microb. Biotechnol.* 13, 274–284. doi: 10.1111/1751-7915.13418
- Nikolaivits, E., Kanelli, M., Dimarogona, M., and Topakas, E. (2018). A middle-aged enzyme still in its prime: recent advances in the field of cutinases. *Catalysts* 8:612. doi: 10.3390/CATAL8120612
- Nolasco-Soria, H., Moyano-López, F., Vega-Villasante, F., del Monte-Martínez, A., Espinosa-Chaurand, D., Gisbert, E., et al. (2018). “Lipase and phospholipase activity methods for marine organisms,” in *Lipases and Phospholipases. Methods in Molecular Biology (Methods and Protocols)*, ed. G. Sandoval, (New York, NY: Humana Press), 139–167. doi: 10.1007/978-1-4939-8672-9_7
- Numoto, N., Kamiya, N., Bekker, G.-J., Yamagami, Y., Inaba, S., Ishii, K., et al. (2018). Structural dynamics of the PET-degrading cutinase-like enzyme from *Saccharomonospora viridis* AHK190 in substrate-bound states elucidates the Ca²⁺-driven catalytic cycle. *Biochemistry* 57, 5289–5300. doi: 10.1021/acs.biochem.8b00624
- Palm, G. J., Reisky, L., Böttcher, D., Müller, H., Michels, E. A. P., Walczak, M. C., et al. (2019). Structure of the plastic-degrading *Ideonella sakaiensis* MHETase bound to a substrate. *Nat. Commun.* 10:1717. doi: 10.1038/s41467-019-09326-3
- Peix, A., Ramírez-Bahena, M. H., and Velázquez, E. (2018). The current status on the taxonomy of *Pseudomonas* revisited: an update. *Infect. Genet. Evol.* 57, 106–116. doi: 10.1016/j.meegid.2017.10.026
- PlasticsEurope. (2018). *Plastics – the Facts*. Brussels: PlasticsEurope. Available at: https://www.plasticseurope.org/application/files/6315/4510/9658/Plastics_the_facts_2018_AF_web.pdf
- Popovic, A., Hai, T., Tchigvintsev, A., Hajighasemi, M., Nocek, B., Khusnutdinova, A. N., et al. (2017). Activity screening of environmental metagenomic libraries reveals novel carboxylesterase families. *Sci. Rep.* 7:44103. doi: 10.1038/srep44103
- Ribitsch, D., Acero, E. H., Greimel, K., Eiteljoerg, I., Trotscha, E., Freddi, G., et al. (2012). Characterization of a new cutinase from *Thermobifida alba* for PET-surface hydrolysis. *Biocatal. Biotransformation* 30, 2–9. doi: 10.1019/10242422.2012.644435
- Ribitsch, D., Hromic, A., Zitzenbacher, S., Zartl, B., Gamerith, C., Pellis, A., et al. (2017). Small cause, large effect: structural characterization of cutinases from *Thermobifida cellulosilytica*. *Biotechnol. Bioeng.* 114, 2481–2488. doi: 10.1002/bit.26372
- Riegels, M., Koch, R., Pedersen, L., and Lund, H. (1997). Enzymatic Hydrolysis of Cyclic oligomers. Patent No. WO 97/27237. Geneva: World Intellectual Property Organization.
- Rigden, D. J., and Jedrzejewski, M. J. (2003). Structures of *Streptococcus pneumoniae* hyaluronate lyase in complex with chondroitin and chondroitin sulfate disaccharides. Insights into specificity and mechanism of action. *J. Biol. Chem.* 278, 50596–50606. doi: 10.1074/jbc.M307596200
- Rochman, C. M. (2018). Microplastics research—from sink to source. *Science* 360, 28–29. doi: 10.1126/science.aar7734
- Roth, C., Wei, R., Oeser, T., Then, J., Föllner, C., Zimmermann, W., et al. (2014). Structural and functional studies on a thermostable polyethylene terephthalate degrading hydrolase from *Thermobifida fusca*. *Appl. Microbiol. Biotechnol.* 98, 7815–7823. doi: 10.1007/s00253-014-5672-0
- Schmidt-Rohr, K., Hu, W., and Zumbulyadis, N. (1998). Elucidation of the chain conformation in a glassy polyester, PET, by two-dimensional NMR. *Science* 280, 714–717. doi: 10.1126/science.280.5364.714
- Sehnal, D., Svobodová Vařeková, R., Berka, K., Pravda, L., Navrátilová, V., Banáš, P., et al. (2013). MOLE 2.0: advanced approach for analysis of biomacromolecular channels. *J. Cheminform.* 5:39. doi: 10.1186/1758-2946-5-39
- Seo, H., Cho, I. J., Joo, S., Son, H. F., Sagong, H., Choi, S. Y., et al. (2019). Reply to “Conformational fitting of a flexible oligomeric substrate does not explain the enzymatic PET degradation.”. *Nat. Commun.* 10:5582. doi: 10.1038/s41467-019-13493-8
- Sievers, F., Wilm, A., Dineen, D., Gibson, T. J., Karplus, K., Li, W., et al. (2011). Fast, scalable generation of high-quality protein multiple sequence alignments using Clustal Omega. *Mol. Syst. Biol.* 7:539. doi: 10.1038/msb.2011.75
- Son, H. F., Cho, I. J., Joo, S., Seo, H., Sagong, H.-Y., Choi, S. Y., et al. (2019). Rational protein engineering of thermo-stable PETase from *Ideonella sakaiensis* for highly efficient PET degradation. *ACS Catal.* 9, 3519–3526. doi: 10.1021/acscatal.9b00568
- Sotriffer, C. A., Gohlke, H., and Klebe, G. (2002). Docking into knowledge-based potential fields: a comparative evaluation of DrugScore. *J. Med. Chem.* 45, 1967–1970. doi: 10.1021/jm025507u
- Stern, R., and Jedrzejewski, M. J. (2008). Carbohydrate polymers at the center of life's origins: the importance of molecular processivity. *Chem. Rev.* 108, 5061–5085. doi: 10.1021/cr078240l
- Studier, F. W. (2005). Protein production by auto-induction in high density shaking cultures. *Protein Expr. Purif.* 41, 207–234. doi: 10.1016/j.pep.2005.01.016
- Studier, F. W., and Moffatt, B. A. (1986). Use of bacteriophage T7 RNA polymerase to direct selective high-level expression of cloned genes. *J. Mol. Biol.* 189, 113–130. doi: 10.1016/0022-2836(86)90385-2
- Sulaiman, S., Yamato, S., Kanaya, E., Kim, J., Koga, Y., Takano, K., et al. (2012). Isolation of a novel cutinase homolog with polyethylene terephthalate-degrading activity from leaf-branch compost by using a metagenomic approach. *Appl. Environ. Microbiol.* 78, 1556–1562. doi: 10.1128/AEM.06725-11
- Sulaiman, S., You, D.-J., Kanaya, E., Koga, Y., and Kanaya, S. (2014). Crystal structure and thermodynamic and kinetic stability of a metagenome-derived LC-cutinase. *Biochemistry* 53, 1858–1869. doi: 10.1021/bi401561p
- Taniguchi, I., Yoshida, S., Hiraga, K., Miyamoto, K., Kimura, Y., and Oda, K. (2019). Biodegradation of PET: current status and application aspects. *ACS Catal.* 9, 4089–4105. doi: 10.1021/acscatal.8b05171
- Wei, R., Breite, D., Song, C., Gräning, D., Ploss, T., Hille, P., et al. (2019a). Biocatalytic degradation efficiency of postconsumer polyethylene terephthalate packaging determined by their polymer microstructures. *Adv. Sci.* 6:1900491. doi: 10.1002/advs.201900491
- Wei, R., Oeser, T., Schmidt, J., Meier, R., Barth, M., Then, J., et al. (2016). Engineered bacterial polyester hydrolases efficiently degrade polyethylene terephthalate due to relieved product inhibition. *Biotechnol. Bioeng.* 113, 1658–1665. doi: 10.1002/bit.25941
- Wei, R., Song, C., Gräning, D., Schneider, T., Bielytskiy, P., Böttcher, D., et al. (2019b). Conformational fitting of a flexible oligomeric substrate does not explain the enzymatic PET degradation. *Nat. Commun.* 10:5581. doi: 10.1038/s41467-019-13492-9
- Wei, R., and Zimmermann, W. (2017). Microbial enzymes for the recycling of recalcitrant petroleum-based plastics: how far are we? *Microb. Biotechnol.* 10, 1308–1322. doi: 10.1111/1751-7915.12710
- Wheeler, D. L., Church, D. M., Federhen, S., Lash, A. E., Madden, T. L., Pontius, J. U., et al. (2003). Database resources of the National Center for Biotechnology. *Nucleic Acids Res.* 31, 28–33. doi: 10.1093/nar/gkv1290
- Woodcock, D. M., Crowther, P. J., Doherty, J., Jefferson, S., DeCruz, E., Noyer-Weidner, M., et al. (1989). Quantitative evaluation of *Escherichia coli* host strains for tolerance to cytosine methylation in plasmid and phage recombinants. *Nucleic Acids Res.* 17, 3469–3478. doi: 10.1093/nar/17.9.3469
- Yoshida, S., Hiraga, K., Takehana, T., Taniguchi, I., Yamaji, H., Maeda, Y., et al. (2016). A bacterium that degrades and assimilates poly(ethylene terephthalate). *Science* 351, 1196–1199. doi: 10.1126/science.aad6359

Conflict of Interest: HG and K-EJ are employed by Forschungszentrum Jülich GmbH.

The remaining authors declare that the research was conducted in the absence of any commercial or financial relationships that could be construed as a potential conflict of interest.

Copyright © 2020 Bollinger, Thies, Knieps-Grünhagen, Gertzen, Kobus, Höppner, Ferrer, Gohlke, Smits and Jaeger. This is an open-access article distributed under the terms of the Creative Commons Attribution License (CC BY). The use, distribution or reproduction in other forums is permitted, provided the original author(s) and the copyright owner(s) are credited and that the original publication in this journal is cited, in accordance with accepted academic practice. No use, distribution or reproduction is permitted which does not comply with these terms.



Biotransformation of Phthalate Plasticizers and Bisphenol A by Marine-Derived, Freshwater, and Terrestrial Fungi

Lena Carstens^{1,2}, Andrew R. Cowan¹, Bettina Seiwert³ and Dietmar Schlosser^{1*}

¹ Department of Environmental Microbiology, Helmholtz Centre for Environmental Research - UFZ, Leipzig, Germany,

² Institute for Environmental Microbiology and Biotechnology, University of Duisburg-Essen, Essen, Germany, ³ Department of Analytical Chemistry, Helmholtz-Centre for Environmental Research - UFZ, Leipzig, Germany

OPEN ACCESS

Edited by:

Ren Wei,
University of Greifswald, Germany

Reviewed by:

Hongzhi Tang,
Shanghai Jiao Tong University, China
Jeongdae Im,
Kansas State University, United States

*Correspondence:

Dietmar Schlosser
dietmar.schlosser@ufz.de

Specialty section:

This article was submitted to
Microbiotechnology,
a section of the journal
Frontiers in Microbiology

Received: 10 December 2019

Accepted: 13 February 2020

Published: 28 February 2020

Citation:

Carstens L, Cowan AR, Seiwert B
and Schlosser D (2020)
Biotransformation of Phthalate
Plasticizers and Bisphenol A by
Marine-Derived, Freshwater,
and Terrestrial Fungi.
Front. Microbiol. 11:317.
doi: 10.3389/fmicb.2020.00317

Phthalate esters (PEs, Phthalates) are environmentally ubiquitous as a result of their extensive use as plasticizers and additives in diverse consumer products. Considerable concern relates to their reported xenoestrogenicity and consequently, microbial-based attenuation of environmental PE concentrations is of interest to combat harmful downstream effects. Fungal PE catabolism has received less attention than that by bacteria, and particularly fungi dwelling within aquatic environments remain largely overlooked in this respect. We have compared the biocatalytic and biosorptive removal rates of di-*n*-butyl phthalate (DBP) and diethyl phthalate (DEP), chosen to represent two environmentally prominent PEs of differing structure and hydrophobicity, by marine-, freshwater-, and terrestrial-derived fungal strains. Bisphenol A, both an extensively used plastic additive and prominent environmental xenoestrogen, was included as a reference compound due to its well-documented fungal degradation. Partial pathways of DBP metabolism by the ecophysiologically diverse asco- and basidiomycete strains tested were proposed with the help of UPLC-QTOF-MS analysis. Species specific biochemical reaction steps contributing to DBP metabolism were also observed. The involved reactions include initial cytochrome P450-dependent monohydroxylations of DBP with subsequent further oxidation of related metabolites, de-esterification via either hydrolytic cleavage or cytochrome P450-dependent oxidative O-dealkylation, transesterification, and demethylation steps - finally yielding phthalic acid as a central intermediate in all pathways. Due to the involvement of ecophysiologically and phylogenetically diverse filamentous and yeast-like fungi native to marine, freshwater, and terrestrial habitats the results of this study outline an environmentally ubiquitous pathway for the biocatalytic breakdown of plastic additives. Beyond previous research into fungal PE metabolism which emphasizes hydrolytic de-esterification as the primary catabolic step, a prominent role of cytochrome P450 monooxygenase-catalyzed reactions is established.

Keywords: biosorption, biotransformation, cytochrome P450, endocrine disrupting chemicals, fungi, micropollutant, phthalate esters, plastic additives

INTRODUCTION

Environmental plastic pollution poses a global threat to ecosystems and human health. Beyond the plastic polymers themselves, environmental and human health risks are related to the release of various additives incorporated to improve certain properties of the plastic (Hermabessiere et al., 2017; Hahladakis et al., 2018). Phthalate esters (PEs, phthalates) represent a prominent group of persistent organic micropollutants. Structurally, PEs are dialkyl or alkyl aryl esters of benzenedicarboxylic (phthalic) acid, differing by their side chain moiety length which commands their hydrophobicity (Gao and Wen, 2016; Ren et al., 2018). The worldwide and environmental ubiquity of these compounds arises from their extensive use as plastic additives (plasticizers) to provide flexibility in the manufacturing of plastic products such as polyvinyl chloride, and as a common additive in various consumer products (i.e. cosmetics, paints, lubricants, adhesives, insecticides, packaging) (Gao and Wen, 2016). Loss can occur at any stage of product lifecycle, with chemical leaching particularly relevant to plasticizers as the absence of covalent binding to the plastic resin leaves their migration unhindered (Cartwright et al., 2000; Gao and Wen, 2016; Hahladakis et al., 2018). Consequently, PE levels are highest in urbanized areas and those directly within the vicinity of production (Cartwright et al., 2000; Liang et al., 2008; Sun et al., 2013). Careless disposal coupled with atmospheric deposition and rainfall transfer has led to widespread environmental contamination. PEs have been recorded in atmospheric samples from remote regions of the Atlantic and Arctic Oceans, and are also found in human breast milk, blood, and urine (Net et al., 2015). A study published in the International Journal of Hygiene and Environmental Health detected such compounds in urine samples of a remote Bolivian forager-horticulturist group, suggesting widespread exposure even out with industrialized populations (Sobolewski et al., 2017).

Structural parallels between PEs and the hormone estrogen have led to investigations into their xenoestrogenicity and potential activity as endocrine disrupting chemicals (EDCs). EDCs interfere with the normal homeostatic balance of a spectrum of biological processes, particularly those linked with development and reproduction (Diamanti-Kandarakis et al., 2009). Significant crossover of several PEs and the natural estrogen 17 β -estradiol (E2) was profiled in regards to downstream gene expression using high-throughput screening via DNA microarray analysis (Parveen et al., 2008). A number of *in vivo* and epidemiological studies have highlighted trends between PE exposure in human populations and negative manifestations witnessed in male and female reproductive development (Colon et al., 2000; Diamanti-Kandarakis et al., 2009; Jeng, 2014). Similar adverse effects have been reported in terrestrial and aquatic wildlife populations, including annelids and molluscs which are both phyla of ecological importance (Oehlmann et al., 2009).

Bacteria are capable of degrading PEs under aerobic and anaerobic conditions, with many utilizing them as sole sources of carbon and energy for growth. Partial degradation yielding

breakdown products such as phthalic acid (PA) or benzoate (BA), and the failure to grow on such PE-derived metabolites has also been reported for certain bacterial species (Liang et al., 2008; Gao and Wen, 2016; Ren et al., 2018). Comparatively, fungal PE degradation has received less attention. This statement is particularly applicable to filamentous fungi dwelling within aquatic environments and also yeasts, with previous fungal based studies predominantly focusing on terrestrial ligninolytic and non-ligninolytic species (Liang et al., 2008; Luo et al., 2012; Gao and Wen, 2016; Pezzella et al., 2017). A few studies describe fungal growth on di-2-ethylhexyl phthalate (DEHP) and dimethyl phthalate esters (DMPEs) when present as the sole carbon and energy source (Luo et al., 2011; Pradeep and Benjamin, 2012). Nevertheless, the majority of the corresponding reports point to a predominance of cometabolic PE biotransformation in fungi (Gartshore et al., 2003; Lee et al., 2007; Hwang et al., 2012; Luo et al., 2012; Ahuactzin-Perez et al., 2016; Ahuactzin-Perez et al., 2018).

Generally, microbial metabolism of PEs involves the primary biotransformation of the phthalic diester (parent compound) via a monoester form into PA, followed by complete mineralization of PA into CO₂ and H₂O (Staples et al., 1997; Liang et al., 2008; Ren et al., 2018). De-esterification of PEs (i.e. the enzymatic removal of alkyl chains from the PA moiety leading to the formation of carboxylic groups) can proceed via either hydrolytic cleavage or oxidative O-dealkylation. The successive enzymatic hydrolysis of phthalate diesters to the corresponding monoesters and then to PA is the most common PE transformation pathway in bacteria under both aerobic and anaerobic conditions, having also been reported for fungi (Lee et al., 2007; Liang et al., 2008; Ahuactzin-Perez et al., 2016, 2018; Ren et al., 2018). The alternative breakdown pathway involving alkyl chain removal via O-dealkylation is known to be catalyzed by cytochrome P450 monooxygenase systems in mammals, however it is not well understood in fungi and prokaryotes (Lee et al., 2007; Liang et al., 2008; Girvan and Munro, 2016; Cantú Reinhard and De Visser, 2017). Additionally, phthalates with longer side chains than diethyl phthalate (DEP) may first undergo alkyl chain shortening via β -oxidation, a process initiated by cytochrome P450 mediated hydroxylation, prior to de-esterification occurring (Amir et al., 2005; Liang et al., 2008). Lastly, transesterification involving the introduction of shorter alkyl chains in exchange for longer ones may alternatively take place, followed by de-esterification to yield PA as a central intermediate (Jackson et al., 1996; Cartwright et al., 2000; Lee et al., 2007; Liang et al., 2008).

To our knowledge, previous research aiming at fungal PE metabolism has either solely emphasized hydrolytic de-esterification as the primary step (Kim et al., 2003, 2005; Kim and Lee, 2005; Ahn et al., 2006; Luo et al., 2011, 2012; Hwang et al., 2012; Ahuactzin-Perez et al., 2016, 2018), or did not further elucidate the mechanisms of the suggested primary de-esterification step(s) (i.e. hydrolysis or oxidative O-dealkylation) (Lee et al., 2007). Furthermore, extracellular fungal oxidoreductases such as laccase and lignin-modifying peroxidases are not known to act on PEs directly, and extracellular unspecific peroxygenases (UPOs) of fungi have been reported to oxidize only a few PEs albeit slowly

(Hwang et al., 2012; Macellaro et al., 2014; Karich et al., 2017; Pezzella et al., 2017). Thus, hydrolytic enzymes (e.g. cutinases, esterases, lipases) and intracellular oxidative cytochrome P450s can be considered as primary candidates for initiating the biocatalytic breakdown of PEs in fungi (Kim et al., 2005; Ghaly et al., 2010; Okamoto et al., 2011; Ahuactzin-Perez et al., 2016; Cantú Reinhard and De Visser, 2017; Ren et al., 2018), with major evidence for the latter remaining to be established. Aside from enzymatic removal, biosorption via physio-chemical processes such as adsorption, absorption, and ion interactions may also contribute and must be accounted for when investigating PE fate within the environment (Liang et al., 2008; Gadd, 2009; Net et al., 2015). Fungal biosorption of PEs and other hydrophobic environmental pollutants is a well-known phenomenon (Lee et al., 2007; Hofmann and Schlosser, 2016).

In this study we aim to broaden the scope of fungal biocatalytic and biosorptive removal of PEs from the environment through a comparative assessment of marine-, freshwater-, and terrestrial-derived asco- and basidiomycetes, i.e. members of the two major fungal groups harboring most of the known fungal pollutant degraders (Harms et al., 2011). Di-*n*-butyl phthalate (DBP) and DEP were chosen as target compounds as they represent environmentally prominent PE pollutants with differing structures and hydrophobicities (Net et al., 2015; Hermabessiere et al., 2017; Hahladakis et al., 2018; Salaudeen et al., 2018). Owing to its recalcitrant nature and recognition as a priority regulated pollutant by the European Union (Directive 2011/65/EU revision 2015/863; EU, 2015) and the U.S. Environmental Protection Agency (EPA) (Gao and Wen, 2016), additional focus was placed upon investigating removal of this compound. Previously reported fungal biotransformation metabolites of DBP have been attributed to de-esterification, hydrolysis, and transesterification reactions, with little known about possible oxidative breakdown mechanisms (Kim and Lee, 2005; Lee et al., 2007; Luo et al., 2012). Nevertheless, the longer alkyl chains of DBP compared to DEP could potentially make the compound susceptible to oxidative fungal biotransformation reactions such as β -oxidation (Amir et al., 2005; Liang et al., 2008). We have therefore chosen to employ DBP as a model compound to investigate the potential role of cytochrome P450 monooxygenase reactions in fungal PE biotransformation, via the application of the cytochrome P450 inhibitor piperonyl butoxide (PB) in conjunction with mass spectrometry based structural elucidation of biotransformation products. This inhibitor was chosen due to its prior use in assessing the role of cytochrome P450s in fungal biotransformation of EDCs (Subramanian and Yadav, 2009), pharmaceutical residues (Marco-Urrea et al., 2009), pesticides and other xenobiotic compounds (Syed and Yadav, 2012; Coelho-Moreira et al., 2018). Bisphenol A (BPA), another extensively used plastic additive and prominent environmental micropollutant established as an EDC (Hermabessiere et al., 2017; Hahladakis et al., 2018), was included as a reference compound due to its well documented degradation by both, extracellular (laccase, peroxidases) and intracellular (cytochrome P450 monooxygenases) fungal enzymes (Cajthaml, 2015; Hofmann and Schlosser, 2016; Im and Löffler, 2016). Owing to the reported environmental co-occurrence of BPA

and PEs (Tran et al., 2015; Notardonato et al., 2019) fungal biotransformation and biosorption capacities were assessed upon employing BPA, DBP, and DEP in mixture, hereby verifying the reported fungal peculiarity to attack multiple pollutants simultaneously (Harms et al., 2011). Extracellular laccase and peroxidase activities were concomitantly monitored in these experiments due to a possible role of such enzymes in BPA oxidation. Pathways for the fungal and bacterial metabolism of BPA are well established (Wang et al., 2014; Cajthaml, 2015; Im and Löffler, 2016), and hence were not the focus of the present study.

MATERIALS AND METHODS

Chemicals

Unless stated otherwise all chemicals used were of analytical grade, or in the case of chromatographic solvents, gradient grade or ULC/MS grade (mass spectrometry). Bisphenol A (BPA, purity 95%) was provided by Fluka (Sigma-Aldrich, St. Louis, MO, United States; now belonging to Merck Group, Darmstadt, Germany). Dibutyl phthalate (DBP, purity > 99%), diethyl phthalate (DEP, purity 99.5%), and piperonyl butoxide (PB) of technical grade (purity 90%) were purchased from Sigma-Aldrich. 2,2'-Azinobis-(3-ethylbenzothiazoline-6-sulfonic acid) (ABTS, purity > 98%) was obtained from AppliChem (Darmstadt, Germany). All other chemicals were purchased from Merck, Sigma-Aldrich and Th. Geyer GmbH (Renningen, Germany).

Source, Identification and Maintenance of Fungal Strains

The fungal strains employed within the present study are compiled in **Table 1**. They were chosen as representatives of different ecophysiological groups and were derived from various, and in cases, rarely investigated habitats exhibiting diverse environmental conditions. The strains 1-DS-2013-S2 and 1-DS-2013-S4 were isolated from sand containing algal debris from the alluvial zone and algae growing on breakwater groins, respectively. Corresponding samples used for fungal isolation were acquired from a beach in the region of Wustrow (Mecklenburg-Western Pomerania, Germany) on the Baltic Sea (coordinates: 54°21'32.246"N, 12°23'39.725"E) in 2013. Pure fungal cultures were obtained using a previously described procedure (Junghanns et al., 2008a), and sent to the Belgian Coordinated Collections of Microorganisms/Mycothèque de l'Université catholique de Louvain (BCCM/MUCL, Louvain-la-Neuve, Belgium) for identification. According to DNA sequencing and morphological examination, strain 1-DS-2013-S2 is a member of the Helotiales (Leotiomyces) and considered to be of the genus *Ascocoryne*. *Ascocoryne* sp. 1-DS-2013-S2 is related to other Helotiales members originating from aquatic habitats (freshwater and marine sediments). Strain 1-DS-2013-S4 was identified as *Paradendryphiella arenariae* of the *Pleosporaceae*, a species well known from decaying marine and estuarine plants, and beach sands (Overy et al., 2014).

TABLE 1 | Overview of fungal strains employed in the present study.

Fungal strain	Phylogeny (phylum, class, order)	Habitat/ characteristics	References
<i>Acephala</i> sp. strain JU-A-2 (DSM 27592)	Ascomycota, Leotiomycetes, Helotiales	Peatland isolate	Singh et al., 2014
<i>Ascochyta</i> sp. strain 1-DS-2013-S2	Ascomycota, Leotiomycetes, Helotiales	Marine isolate	This study
<i>Clavariopsis aquatica</i> De Wild. strain WD(A)-00-01	Ascomycota, Sordariomycetes, Microascales	Aquatic hyphomycete, freshwater isolate	Junghanns et al., 2008a
<i>Paradendryphiella arenariae</i> (Nicot) Woudenberg and Crous strain 1-DS-2013-S4	Ascomycota, Dothideomycetes, Pleosporales	Marine isolate	This study
<i>Phoma</i> sp. strain UHH 5-1-03 (DSM 22425)	Ascomycota, Dothideomycetes, Pleosporales	Freshwater isolate	Junghanns et al., 2008a
<i>Stachybotrys chlorohalonata</i> Andersen and Trane strain A-2008-2 (DSM 27588)	Ascomycota, Sordariomycetes, Hypocreales	Constructed wetland isolate	Singh et al., 2014
<i>Stropharia rugosoannulata</i> Farlow ex Murrill DSM 11372	Basidiomycota, Agaricomycetes, Agaricales	Litter inhabiting, causes white-rot decay of lignocellulose	Singh et al., 2014
<i>Trichosporon porosum</i> (Stautz) Middelhoven, Scorzett and Fell strain JU-K-2 (DSM 27593)	Basidiomycota, Tremellomycetes, Trichosporonales	Peatland isolate	Singh et al., 2014

Strains without a DSM accession number, which denotes deposition at the German Collection of Microorganisms and Cell Cultures (DSMZ; Braunschweig, Germany), are available from the strain collection of the Department of Environmental Microbiology at the Helmholtz Centre for Environmental Research - UFZ (Leipzig, Germany). The provided phylogenetic information was derived from the NCBI taxonomy database (<https://www.ncbi.nlm.nih.gov/Taxonomy/Browser/wwwtax.cgi>).

The aquatic hyphomycete *Clavariopsis aquatica* strain WD(A)-01 represents an exclusively aquatic species frequently observed in rivers and streams (Junghanns et al., 2008a; Krauss et al., 2011). *Phoma* sp. strain UHH 5-1-03 (DSM 22425) has an ascomycete affiliation and originates from the Saale river, Germany (Junghanns et al., 2008a). *Stachybotrys chlorohalonata* strain A-2008-2 (DSM 27588) and *Acephala* sp. strain JU-A-2 (DSM 27592) were previously isolated from a constructed wetland and peatland, respectively (Singh et al., 2014), and represent fungal taxa known from several terrestrial habitats. The anamorphic yeast *Trichosporon porosum*, with the herein applied strain JU-K-2 (DSM 27593) likewise being derived from peatland (Singh et al., 2014), is also typical for terrestrial environments and related to the loubieri/laibachii group of species that assimilate

hemicelluloses and phenolic compounds (Middelhoven et al., 2001). *Stropharia rugosoannulata* is a well-characterized terrestrial litter-inhabiting basidiomycete species causing white-rot decay of lignocellulosic materials (Schlosser and Hofer, 2002; Singh et al., 2014). The phylogenetic relationships among the fungal strains employed in this study are compiled in **Figure 1**.

Fungal strains were maintained on agar plates containing 2% malt extract (w/v) solidified with 1.5% agar (pH 5.7). For the marine-derived fungal isolates, further 2% malt extract agar plates were supplemented with an artificial seawater component, which was composed of 23.93 g/L NaCl, 10.83 g/L MgCl₂ × 6 H₂O, 4.01 g/L Na₂SO₄, 1.52 g/L CaCl₂ × 2 H₂O, 677 mg/L KCl, 196 mg/L NaHCO₃, 98 mg/L KBr, 26 mg/L H₃BO₃, 24 mg/L SrCl₂ × 6 H₂O, and 3 mg/L NaF (Kester et al., 1967). These plates were employed in order to mimic conditions of the marine environment (indicated in the text where applicable). All plates were incubated at 20°C in the dark.

Assessment of Fungal Micropollutant Removal Rates

Pre-cultures were established for subsequent batch tests with active and NaN₃-inactivated fungal cultures in 100-mL Erlenmeyer flasks containing 30 mL of a 2% (w/v) malt extract medium (pH 5.7) (Hofmann and Schlosser, 2016). Deviating from this, 30 mL of a defined nitrogen-limited medium containing 56 mM glucose and 1.2 mM diammonium tartrate as carbon and nitrogen sources (Schlosser and Hofer, 2002; Krueger et al., 2015b) was also used for fungal pre-cultivation where indicated in the text. Further pre-cultivation media used for marine-derived fungal strains in a series of experiments (see below) additionally contained the aforementioned artificial seawater component according to (Kester et al., 1967). For certain experiments, pre-cultivation media was additionally supplemented with 50 μM CuSO₄ and 1 mM vanillic acid to stimulate laccase production (Junghanns et al., 2008b; Hofmann and Schlosser, 2016) (indicated where applicable below). Each flask was inoculated with 0.5 mL of a mycelial suspension, which was prepared from corresponding fungal agar plate cultures (Junghanns et al., 2008b; Hofmann and Schlosser, 2016). Thereafter, the flasks were incubated on a rotary shaker (New BrunswickTM Innova 44; Eppendorf, Hamburg, Germany) at 20°C and 120 rpm in the dark. After 6 days of incubation, half of the growing fungal cultures were inactivated with 1 g/L NaN₃. Following a further day of incubation, fungal biomass was separated from pre-culture media for transfer to pollutant removal flasks by centrifugation in 50-mL conical tubes at 7197 × g and 20°C for 10 min (Eppendorf centrifuge 5430R, rotor FA-35-6-30, Eppendorf, Hamburg, Germany). After discarding supernatant, the biomass pellet was washed with 30 mL of a synthetic mineral salts medium devoid of a source of carbon and energy (pH 6.8; Stanier et al., 1966) and separated in a second centrifugation step. The resulting supernatant was discarded again and the biomass pellet was transferred into new 100-mL Erlenmeyer flasks containing 30 mL of the mineral salts medium mentioned before, which had been supplemented with

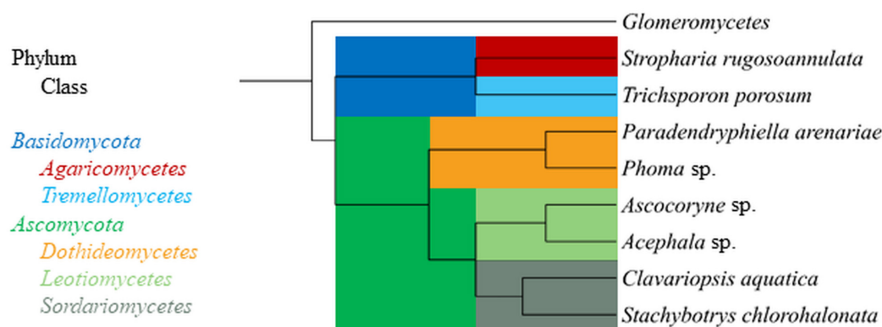


FIGURE 1 | Phylogenetic tree displaying relationship of fungal strains used in this study based on NCBI taxonomy data (<https://www.ncbi.nlm.nih.gov/taxonomy>), generated in phyloT (<https://phyloT.biobyte.de/>) and visualized with iTOL (<http://itol.embl.de/>). The class Glomeromycetes (Tedersoo et al., 2018) is shown as an outgroup.

the cytochrome P450 inhibitor PB and/or micropollutant(s) prior to fungal biomass addition.

One series of experiments addressed the contribution of fungal biotransformation and biosorption processes to overall DBP removal, and the influence of the cytochrome P450 inhibitor PB on DBP removal in a resting cell approach employing the aforementioned mineral salts medium, similarly as applied before (Hofmann and Schlosser, 2016). DBP was added to mineral medium from a stock solution prepared in methanol containing 10% (w/v) Tween 80 (included to improve compound aqueous solubility), to yield a final concentration of 62.5 μM (procedure modified from Hofmann and Schlosser, 2016). Further DBP- and mineral medium-containing flasks were additionally supplemented with PB, which was added from a stock solution in methanol with 10% Tween 80 yielding a final concentration of 1 mM. Thereafter, active fungal biomass was added as described before. Control experiments intended to assess the biosorption share of overall DBP removal were established by adding previously NaN_3 -inactivated fungal biomass (see before) to flasks with DBP-containing mineral media, which in addition had been amended with NaN_3 at 1 g/L. Fungal biomass was omitted in further negative controls, which were amended with PB and/or DBP only. For comparability, final methanol and Tween 80 concentrations in these experiments were always adjusted to 1% (v/v) and 0.1% (w/v), respectively.

Additional experiments aiming at the verification of fungal micropollutant biotransformation and biosorption capacities under more complex conditions intended to match real environmental situations more closely were also carried out. Two types of fungal pre-culture media were applied, i.e. the defined nitrogen-limited medium and the complex 2% malt extract medium described before (Schlosser and Hofer, 2002; Krueger et al., 2015b; Hofmann and Schlosser, 2016). Both media were additionally supplemented with 50 μM CuSO_4 and 1 mM vanillic acid to stimulate laccase production (Junghanns et al., 2008b; Hofmann and Schlosser, 2016), due to the potential involvement of this enzyme in BPA biotransformation (Cajthaml, 2015; Im and Löffler, 2016). For marine-derived strains, the artificial seawater component (Kester et al., 1967) was included in the respective media used for agar plate-based inoculum

production, liquid pre-cultivation, and subsequent pollutant removal experiments (see above). The micropollutants BPA, DBP and DEP were applied in mixture and added from a combined stock solution (prepared in methanol containing 10% Tween 80 in addition). Final individual micropollutant concentrations were 62.5 μM , corresponding to final sum methanol and Tween 80 concentrations of 0.5 and 0.05%, respectively. Control experiments employing NaN_3 -inactivated fungal biomass, and control experiments omitting fungal biomass were carried out as described above.

Fungal cultures were always incubated at 20°C and 120 rpm in the dark, and sampled for ultra performance liquid chromatography (UPLC) analysis of micropollutant concentrations, extracellular laccase and peroxidase activity measurements (only for experiments employing pollutant mixtures), and fungal dry biomass determination (see below) at the time points indicated in the text. Triplicate experiments were always performed.

Respective micropollutant removal rates were determined for each fungal strain. Pseudo-first-order kinetics were assumed for the removal of micropollutants from solution (Hofmann and Schlosser, 2016) following Equation 1.

$$v_t = c_t * k' \quad (1)$$

where the removal rate v_t ($\mu\text{M}/\text{h}$) at a given time point t in is directly proportional to the micropollutant concentration c_t (μM) at time point t , and k' (1/h) represents the corresponding apparent first-order decay constant. Data of pollutant concentrations versus time (means from triplicate experiments) were fitted using non-linear regression (Equation 2) without error weighting, using OriginPro software (version 2018 95G b9.5.1.195; OriginLab Corp., Northampton, MA, United States).

$$c_t = c_a + c_s * e^{-k't} \quad (2)$$

In the exponential fit function (Equation 2), c_a (μM) represents a bottom asymptote micropollutant concentration approached at infinite time where micropollutant removal was incomplete, c_s corresponds to the removal rate-governing micropollutant concentration at $t = 0$ (μM) (with the sum of

c_a and c_s yielding the initial micropollutant concentration), and t is the time of incubation in presence of micropollutant (h). Where micropollutant removal was achieved within the duration of the experiment, c_a was set to 0 μM . The initial (maximal) removal rates at $t = 0$ were obtained by multiplying respective c_s and k' values. Obtained volume-based initial removal rates were normalized using the initial fungal dry biomass concentrations (g/L) of active and inactive fungal cultures, thereby obtaining specific initial rate values (nmol/h/g). A positive difference in specific initial removal rates between active and inactive cultures was taken to indicate the specific rate of fungal biotransformation.

Initial biomass-specific pollutant removal rates represent maximal rates operative at maximal pollutant concentrations (i.e. at the time point of pollutant addition). Removal rates for a given pollutant are expected to decline as pollutant concentrations decrease, due to species specific first-order decay constants and sorption characteristics, and in the case of active fungal cultures possibly also a decrease in physiological activity resulting from nutrient depletion (Martin et al., 2007, 2009; Hofmann and Schlosser, 2016). Hence, initial pollutant removal rates derived from exponential regression of data are not linearly correlated with the amounts of pollutants removed during longer time periods. A sufficient exponential regression fit (coefficient of determination (COD) value < 0.9) could not be obtained in every situation. In addition, initial removal rates calculated from formally successful exponential regressions were sometimes artificially high due to a steep curve cut by a bottom asymptote. Data flawed by such complications was not further considered. To ensure comparability of pollutant removal rates for each fungal strain tested, and to account for the aforementioned difficulties, removal rates based on reduction of micropollutant concentration over selected time periods (based on triplicates) were manually calculated according to Equation 3.

$$v_{0-t} = (c_0 - c_t)/(t - 0) \quad (3)$$

where v_{0-t} represents the average removal rate over a given time period, c_0 (μM) corresponds to the micropollutant concentration at $t = 0$, and c_t the micropollutant concentration at the time point of consideration as indicated in the text. Overall rates were obtained for micropollutant removal over the full experiment duration. The obtained volume-based removal rates were biomass-normalized as described for the initial (maximal) removal rates before, thereby obtaining specific rates (nmol/h/g). A positive difference in specific removal rates between active and inactive cultures was taken to indicate the specific rate of fungal biotransformation.

Formation of DBP Biotransformation Products

In order to investigate the formation of biotransformation products from DBP and to assess the influence of the cytochrome P450 inhibitor PB on these processes, fungi were pre-cultivated on liquid 2% malt extract medium for a total of 7 days as described before (with inactivation of half of the fungal cultures by addition of 1 g/L NaN_3 on culture day 6). Thereafter, fungal

biomass was transferred to new flasks containing PB- and/or DBP-amended mineral medium as already explained above. PB and/or DBP was added from methanolic stock solutions to yield final concentrations of 1 mM and 250 μM , respectively. Tween 80 was omitted in these experiments, in order to avoid interferences in the subsequent mass spectrometry-based analyses (see below). Control experiments employing NaN_3 -inactivated fungal biomass were carried out as above. Fungal cultures were incubated at 20°C and 120 rpm in the dark as described before and sampled for analysis of biotransformation metabolites at the time points indicated in the text. Triplicate experiments were always performed. Ultra performance liquid chromatography-quadrupole time-of-flight mass spectrometry (UPLC-QTOF-MS) analysis of DBP biotransformation products was performed as described in the **Supplementary Material**.

Analysis of Micropollutant Concentrations Using Ultra Performance Liquid Chromatography (UPLC)

Aqueous samples (0.5 mL) taken from cell-free supernatants of fungal cultures at the time points indicated in the text were placed in 1.5-mL Eppendorf tubes, supplemented with 0.5 mL methanol, thoroughly mixed and stored at -20°C until further use (Hofmann and Schlosser, 2016). Prior to UPLC analysis, samples were thawed and subjected to centrifugation at $20817 \times g$ and 4°C for 10 min (Eppendorf centrifuge 5430R, rotor type FA-45-30-11; Eppendorf, Hamburg, Germany) to ensure biomass free supernatant. UPLC analysis was carried out using an AquityTM UPLC system (Waters, Eschborn, Germany) equipped with an AquityTM UPLC BEH C18 column (1.7 μM particle size, 2.1×50 mm; Waters) as described before (Hofmann and Schlosser, 2016), with the following modifications. Eluent A consisted of 10% (v/v) methanol in deionized water (Q-Gard 2, Millipore, Schwalbach, Germany) and eluent B of methanol, both acidified to pH 3.0 with 0.1% (v/v) formic acid. The following elution profile was applied for DBP analysis in experiments employing DBP as a single pollutant: isocratic elution at 30% B for 0.14 min, linear increase to 35% B until 5 min, further linear increase to 99.9% B until 5.5 min, isocratic elution at 99.9% B until 8.0 min, linear decrease to 30% B until 8.2 min, and isocratic elution at 30% B until 8.5 min (0.5 mL/min flow rate). For analysis of pollutant mixtures consisting of BPA, DBP and DEP, the elution profile was modified as follows: isocratic elution at 30% B for 0.14 min, linear increase to 30% B until 5 min, further linear increase to 35% B until 5.5 min, again linear increase to 99.9% B until 7.0 min, isocratic elution at 99.9% B until 7.2 min, linear decrease to 30% B until 7.5 min (0.5 mL/min flow rate). The detection wavelength was set to 278 nm. The methods were calibrated using external standards.

Determination of Extracellular Laccase and Peroxidase Activities in Supernatants of Fungal Cultures

Laccase activity was routinely determined following the oxidation of 2 mM ABTS in McIlvaine buffer (pH 4.0) at 420 nm, as previously described (Junghanns et al., 2008b; Hofmann and

Schlosser, 2016). Peroxidase activity was determined following the oxidation of 2 mM ABTS in presence of 100 μ M H₂O₂ and 1 mM ethylenediaminetetraacetate (EDTA) disodium salt in 50 mM sodium malonate buffer (pH 4.5) (peroxidase procedure modified from Schlosser et al., 2000). Peroxidase activities were corrected for laccase activities through omitting H₂O₂. Enzyme activities are expressed in international units (U), where 1 U is defined as the amount of enzyme capable of oxidizing 1 μ mol ABTS per minute. All enzymatic assays were performed using a GENios Plus microplate reader (Tecan, Männedorf, Switzerland).

Fungal Dry Biomass Determination

Fungal dry biomasses of the active and NaN₃-inactivated fungal cultures were determined at the time point of micropollutant addition, using a gravimetric procedure previously described (Hofmann and Schlosser, 2016).

RESULTS

Micropollutant Removal by Fungal Cultures

Fungal DBP Removal and Influence of PB

The removal of DBP was followed by UPLC analysis of fungal culture supernatants. DBP was removed to varying degrees depending on the respective fungal strain and cultivation condition (Figure 2 and Table 2). In active fungal cultures (i.e. those omitting PB and NaN₃), the DBP concentration had decreased to approximately 31 μ M and values below the quantification limit within 3.5 h of incubation, corresponding to relative removals (i.e. in relation to the actual quantified initial concentration) of approximately 36–100% (Figure 2). With the exception of *S. chlorohalonata* (approximately 44% of the initial concentration remaining), DBP was completely removed by active fungal cultures within 14 days (336 h; Figure 2). In PB-inhibited cultures, DBP concentrations were reduced to values ranging from 51 to 9 μ M after 3.5 h, corresponding to a relative reduction of approximately 21–81% already within this time period. Similarly within 3.5 h of incubation, 22–94% of DBP was absent from the sampled supernatant of NaN₃-inactivated fungal cultures, suggesting a considerable influence of biosorption on the reduction of DBP concentration. In fungal biomass-free negative controls, the initially applied DBP concentration remained constant over the whole duration of the experiment (data not shown).

A comparison of fungal biomass-normalized DBP removal rates obtained from active, PB-inhibited, and NaN₃-inactivated cultures of the investigated fungal strains revealed strain-specific contributions of biotransformation and biosorption to total DBP removal (i.e. the sum of biosorption and biotransformation) (Table 2). DBP removal attributed to biosorption was most prominent in the marine isolate *Ascocoryne* sp., and least pronounced in the yeast *T. porosum* (Table 2). After 48 h of incubation, DBP was completely removed in NaN₃-inactivated cultures of *Acephala* sp. (Figure 2). For all other NaN₃-inactivated fungal cultures, the DBP concentrations tended to level off over the duration of the

experiment, suggesting that sorption equilibria were reached. DBP biotransformation can be deduced from the observed biomass-normalized initial DBP removal rates of fungal strains according to the following rank order: *C. aquatica* > *Acephala* sp. > *Phoma* sp. > *S. rugosoannulata* > *T. porosum*. Though suggested by the respective time courses of DBP concentrations in active and NaN₃-inactivated fungal cultures as shown in Figure 2, biotransformation remained ambiguous upon considering the corresponding biomass-normalized DBP removal rates for *Ascocoryne* sp., *P. arenariae*, and *S. chlorohalonata*; also due to considerably high errors associated with the respective data (Table 2).

Compared to active fungal cultures, biomass-normalized DBP removal rates were reduced in the presence of the cytochrome P450 inhibitor PB by more than 50% within the first 24 h of incubation in *Ascocoryne* sp., *C. aquatica*, and *S. rugosoannulata* (Table 2). A similarly strong inhibition of DBP removal caused by PB was evident for *S. chlorohalonata* (Figure 2), even though initial DBP removal rates could not reliably be determined for active cultures of this fungus (Table 2). A comparatively weaker effect of PB on DBP removal could be inferred for *Phoma* sp. (Figure 2 and Table 2). These results clearly indicate the involvement of cytochrome P450 monooxygenases in the first biocatalytic step of DBP removal in these fungi. The influence of PB on DBP removal remained inconclusive for *Acephala* sp., *P. arenariae*, and *T. porosum*, where corresponding results may partly have been biased by the quite rapid initial DBP removal especially observed with *Acephala* sp. and *P. arenariae* (Figure 2 and Table 2).

Fungal Removal of Micropollutants Applied in Mixture

In order to verify the micropollutant biotransformation and biosorption capacities of the marine- and freshwater-derived fungal strains under more complex conditions intended to match real environmental situations more closely, pollutant mixtures composed of BPA, DBP, and DEP were applied to the fungal cultures (Figure 3 and Tables 3–6). An artificial seawater component was additionally included in media used for the marine-derived fungus (Kester et al., 1967).

After fungal pre-cultivation on a previously described defined nitrogen-limited medium (Schlosser and Hofer, 2002; Krueger et al., 2015b), concomitant biotransformation of DBP and DEP by the Baltic Sea isolate *Ascocoryne* sp. was clearly evident whereas biotransformation of BPA was not apparent (Figure 3 and Table 3). Similarly, the obligate freshwater inhabitant (aquatic hyphomycete) *C. aquatica* removed substantial amounts of DBP and DEP, but not of BPA when present in mixture (Figure 3 and Table 5). Biotransformation of all applied micropollutants was indicated for the marine isolate *P. arenariae*, as well as for the freshwater-derived ascomycete *Phoma* sp. (Figure 3 and Tables 4, 6). The efficiency of biotransformation (in terms of biomass-normalized removal rates) followed the rank order *Phoma* sp. > *P. arenariae* for BPA, *Ascocoryne* sp. > *Phoma* sp. > *C. aquatica* > *P. arenariae* for DBP, and *C. aquatica* > *P. arenariae* > *Ascocoryne* sp. > *Phoma* sp. for DEP (Tables 3–6). The biotransformation rate of DBP was higher than that of DEP in *Ascocoryne* sp. (Figure 3 and Table 3), whereas

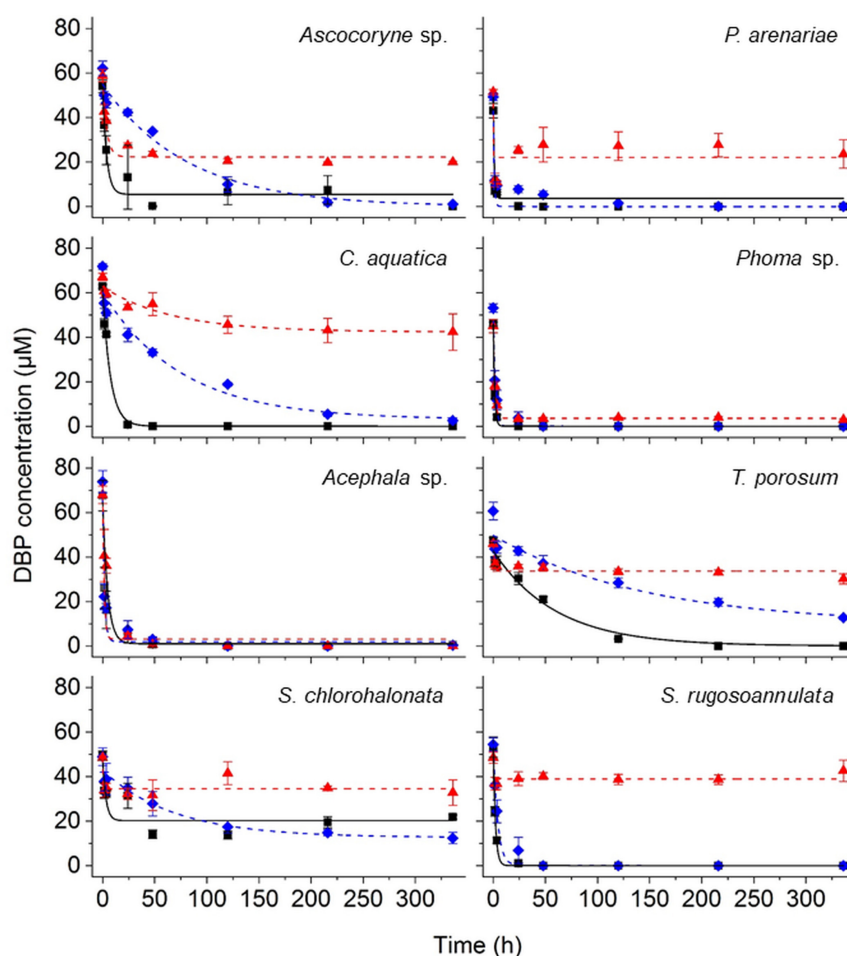


FIGURE 2 | Time courses of DBP concentrations in active (black squares), PB-inhibited (blue diamonds), and Na₃N-inactivated cultures (red triangles) of the marine-derived strains *Ascocoryne* sp. and *P. arenariae*, the freshwater-derived strains *C. aquatica* and *Phoma* sp., the peatland isolates *Acephala* sp. and *T. porosum*, the constructed wetland isolate *S. chlorohalonata*, and the litter-inhabiting basidiomycete *S. rugosoannulata*. The corresponding lines (solid black, dotted blue, and dotted red lines for active, PB-inhibited, and Na₃N-inactivated cultures, respectively) arise from data fitting of measured DBP concentrations as described in the materials and methods section. Symbols represent means \pm standard deviations from triplicate cultures.

the opposite was observed for the other tested fungi (Figure 3 and Tables 4–6). Biomass-normalized removal rates accounting for biosorption were generally highest for DBP (the most hydrophobic compound among the tested micropollutants), followed by those observed for BPA and DEP (Tables 3–6). For all three micropollutants the determined biosorption rates were highest in *Ascocoryne* sp., followed by *Phoma* sp., *C. aquatica*, and *P. arenariae* (Tables 3–6); similar to the results obtained from application of DBP only (Table 2).

Extracellular laccase and peroxidase activities were monitored since these enzymes are well known to oxidize BPA efficiently (Cajthaml, 2015). Laccase activities steadily increased in *Phoma* sp., with a maximum of 98.7 ± 13.2 U/L (mean \pm standard deviation for triplicate cultures) after 144 h of incubation and subsequently declined to 80.5 ± 11.3 U/L at the end of the experiment (312 h of incubation). No meaningful laccase activities were detected for any other fungal strain and for Na₃N-inactivated cultures of *Phoma* sp. (all activities measured below 1

U/L). Likewise, peroxidase activities were only detected for active *Phoma* sp. cultures. A maximal peroxidase activity was quickly established, with 38.8 ± 19.7 U/L already measurable following 48 h of incubation. This slowly declined to 34.2 ± 26.4 U/L at around 144 h of incubation, followed by a steeper decline to ~ 6 U/L at the end of incubation. No evidence for peroxidase activity was obtained from the other fungal strains and for Na₃N-inactivated cultures of *Phoma* sp.

Fungal pre-cultivation on 2% malt extract medium (Hofmann and Schlosser, 2016) in place of the defined nitrogen-limited medium reported above yielded considerably higher fungal dry biomasses for all of the tested fungi except *C. aquatica* (data not shown). Nevertheless, the biomass-normalized micropollutant removal rates and laccase activities obtained were qualitatively comparable to those observed upon fungal pre-cultivation on defined nitrogen-limited medium (data not shown), hereby confirming that the applied cultivation media had no decisive influence on the respective

TABLE 2 | DBP removal rates and influence of PB on DPB removal observed with fungal cultures.

Fungus and mode of rate calculation	Removal rate (nmol/h/g)				PB inhibition (%)
	Active	NaN ₃ -inactivated	Biotransformation	PB-inhibited	
<i>Ascocoryne</i> sp.					
Initial rate	5442 ± 1773	7649 ± 2266	0	295 ± 62	95 ± 37
24 h rate	738 ± 224	1071 ± 132	0	359 ± 52	51 ± 17
Overall rate	70 ± 9	95 ± 17	0	79 ± 9	0
<i>P. arenariae</i>					
Initial rate	5095 ± 852	FNS	NA	5486 ± 1670	0
24 h rate	205 ± 21	179 ± 15	26 ± 26	198 ± 17	3 ± 0
Overall rate	15 ± 2	14 ± 3	1 ± 3	17 ± 1	0
<i>C. aquatica</i>					
Initial rate	3050 ± 445	171 ± 76	2879 ± 451	280 ± 106	91 ± 37
24 h rate	954 ± 48	317 ± 20	637 ± 52	472 ± 42	51 ± 5
Overall rate	69 ± 4	41 ± 11	28 ± 12	76 ± 4	0
<i>Phoma</i> sp.					
Initial rate	3090 ± 354	2389 ± 239	701 ± 427	2470 ± 406	20 ± 4
24 h rate	170 ± 19	156 ± 20	14 ± 28	183 ± 21	0
Overall rate	12 ± 1	11 ± 1	1 ± 2	14 ± 2	0
<i>Acephala</i> sp.					
Initial rate	4091 ± 678	1790 ± 387	2301 ± 781	5708 ± 1273	0
24 h Rate	290 ± 12	356 ± 18	0	314 ± 10	0
Overall rate	23 ± 2	27 ± 2	0	25 ± 2	0
<i>T. porosum</i>					
Initial rate	86 ± 14	FNS	NA	FNS	NA
24 h rate	86 ± 10	62 ± 6	24 ± 11	90 ± 11	0
Overall rate	17 ± 1	7 ± 1	10 ± 1	17 ± 1	0
<i>S. chlorohalonata</i>					
Initial rate	FNS	FNS	NA	61 ± 23	NA
24 h rate	105 ± 23	131 ± 17	0	81 ± 9	22 ± 5
Overall rate	11 ± 1	9 ± 3	2 ± 3	15 ± 1	0
<i>S. rugosoannulata</i>					
Initial rate	7341 ± 585	FNS	NA	3624 ± 616	51 ± 10
24 h rate	626 ± 67	199 ± 18	427 ± 70	572 ± 94	9 ± 2
Overall rate	46 ± 5	9 ± 3	37 ± 6	47 ± 4	0

Fungal strains were first sorted according to their origin (marine-derived, freshwater, peatland, constructed wetland, soil litter) and then in alphabetical order, in line with Figure 2. Removal rates of DBP observed with active, PB-inhibited and NaN₃-inactivated fungal cultures (controls) were always based on corresponding fungal dry biomasses at the time point of DPB addition. The fungal dry biomasses were 2.31 ± 0.26 and 1.22 ± 0.05 (*Ascocoryne* sp.), 8.73 ± 0.68 and 6.09 ± 0.15 (*P. arenariae*), 2.71 ± 0.13 and 1.79 ± 0.12 (*C. aquatica*), 11.24 ± 1.26 and 11.17 ± 0.88 (*Phoma* sp.), 8.81 ± 0.23 and 7.44 ± 0.14 (*Acephala* sp.), 8.32 ± 0.38 and 6.77 ± 1.94 (*T. porosum*), 7.22 ± 0.56 and 5.19 ± 0.94 (*S. chlorohalonata*), and 3.47 ± 0.23 and 1.97 ± 0.30 g/L (*S. rugosoannulata*) (first value always for both fully active and PB-inhibited cultures, second value always for NaN₃-inactivated cultures; values always means ± standard deviations from triplicate cultures). Initial (maximal) removal rates were calculated from exponential fits of DBP concentrations over time. Fits yielding COD values < 0.9 were considered as insufficient and initial rates were omitted in such cases (FNS, fit not sufficient). Alternatively, removal rates were also calculated based upon the reduction of DBP concentrations over time periods of 24 (24 h rate) and 336 h (end of the incubation period; overall rate). Removal rates attributed to biotransformation were expressed as the difference between the removal rates obtained from active (representing biotransformation + biosorption) and NaN₃-inactivated fungal cultures (representing biosorption only). PB inhibition is the relative inhibition (%) of DBP removal in PB amended compared to fully active fungal cultures. Data represent means ± standard deviations (standard errors in case of initial rates and the thereof derived parameters) from triplicate cultures (calculated according to Gaussian error propagation rules). NA, not applicable.

fundamental capacities of the tested fungi for pollutant biotransformation and biosorption. Peroxidase activities were not recorded in any of the tested fungi following this alternate pre-cultivation.

Formation of DBP Biotransformation Products in Fungal Cultures

UPLC-QTOF-MS was applied to analyze DBP biotransformation products in fungal cultures substantiating biochemical DBP

alteration as a cause for its removal, whilst concomitantly investigating effects of the cytochrome P450 inhibitor PB on metabolite formation, and allowing partial pathways for DBP metabolization by ecophysiologicaly diverse fungi to be established. The Baltic Sea-derived *Ascocoryne* sp., the freshwater isolate *Phoma* sp., the environmentally ubiquitous mold *S. chlorohalonata* (all ascomycetes), the terrestrial litter-decaying basidiomycete *S. rugosoannulata*, and the soil-dwelling basidiomyceteous yeast *T. porosum* were chosen for this purpose.

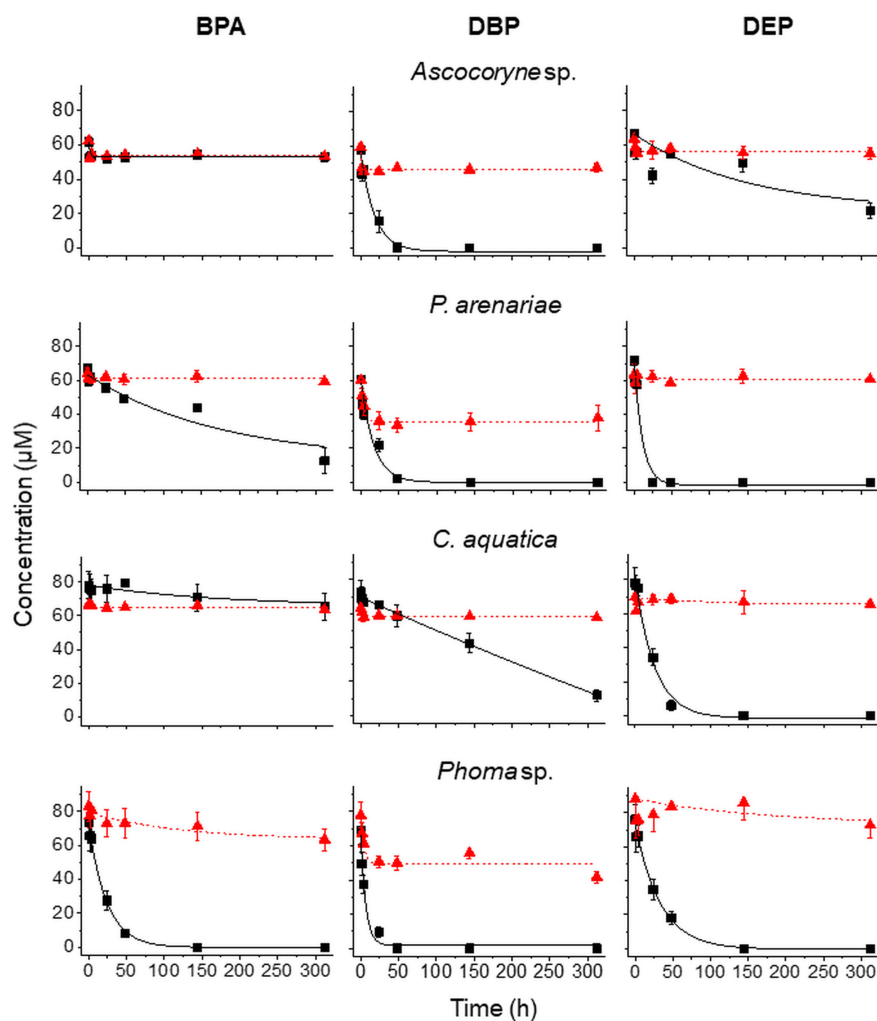


FIGURE 3 | Time courses of BPA (left), DBP (middle), and DEP concentrations (right) upon compound application in mixture to active (black squares) and NaN_3 -inactivated cultures (red triangles) of *Ascocoryne* sp., *P. arenariae*, *C. aquatica*, and *Phoma* sp. (from top to bottom), which were pre-grown on defined nitrogen-limited media as described in the materials and methods section. The corresponding lines (solid black and dotted red lines for active and NaN_3 -inactivated cultures, respectively) arise from data fitting of measured compound concentrations as described in the materials and methods section. Symbols represent means \pm standard deviations from triplicate cultures.

Tentative structures and mass spectral characteristics of DBP metabolites detected in fungal cultures with UPLC-QTOF-MS (operated in positive centroid mode) which were absent from the corresponding control cultures are listed in **Supplementary Table S1**. The accompanying number of the transformation products (TPs), as shown in **Supplementary Table S1**, indicates the respective mass of the corresponding molecular ion (always down rounded). No further DBP biotransformation products were detected using UPLC-QTOF-MS in negative electrospray ionization mode (data not shown). Low concentrations of the biotransformation metabolites did not allow for their isolation from the biological matrix in amounts sufficient for confirmation by nuclear magnetic resonance spectroscopy. Overall, the detected DBP biotransformation products comprise; (i) a range of compounds lacking additional oxygen atoms (compared to parent DBP) such as monobutyl phthalate (MBP),

PA, and TPs 217 and 203; (ii) several compounds indicating the introduction of one oxygen atom (TPs 317, 315, 275, 261, 259, and 247); and (iii) a group of products containing two additional oxygen atoms in their structure (TPs 333, 331, 305, and 291; **Supplementary Table S1**).

Table 7 depicts the appearance of (i) DBP biotransformation products without additional oxygen atoms in active and PB-inhibited fungal cultures, as observed at different time points of fungal cultivation. The compounds MBP, PA, and the methylated PA derivatives, TP 217 and 203, were detected in all investigated fungal cultures. The concentrations of these DBP metabolites could not be determined since reference standards for compound quantification were not available. Therefore, peak areas of DBP biotransformation products in UPLC-QTOF-MS total ion current chromatograms were set in relation to the parent DBP peak area recorded at the time point of DBP addition (start of

the experiment), respectively, and expressed as relative intensities (%). However, due to the potentially varying UPLC-QTOF-MS signal intensities of the different compounds the values thus obtained do not reflect real compound concentrations. Nevertheless, they enable direct comparisons of the respective DBP metabolite amounts within one fungus and in between different fungal species. Furthermore, these relative intensities may reasonably be expected to provide an impression about the order of magnitude of the respective quantities of the various DBP biotransformation products. The formation of MBP was clearly inhibited in the presence of PB in all fungal strains except *Ascocoryne* sp. (Table 7), suggesting a cytochrome P450 monooxygenase-dependent oxidative O-dealkylation as the major cause of the primary removal of one butyl chain from DBP in *Phoma* sp., *S. chlorohalonata*, *S. rugosoannulata*, and *T. porosum*. By contrast, the formation of MBP in *Ascocoryne* sp. in the presence of PB points to a prominent hydrolytic de-esterification, albeit without ruling out some

possibly accompanying oxidative dealkylation of DBP to MBP. Additionally, the formation of PA and its potential precursor TP 217 was not inhibited by PB in *Ascocoryne* sp. and *Phoma* sp. (not shown for TP 217 formation by *Ascocoryne* sp. in Table 7, due to a generally low amount of TP 217 in this fungus). In contrast, for the other metabolites and all other tested fungi (regardless of the respective DBP metabolite produced) such an inhibition was always observed (Table 7). The direct precursors of the DBP breakdown products TP 217, TP 203, and PA could not be confirmed based on the obtained data, due to numerous possibilities for the respective reactions leading to their formation (Figure 4). Nevertheless, a positive influence of cytochrome P450-dependent reaction steps to yield the central DBP intermediate PA and its potential precursors TP 217 and 203 can be inferred for *S. chlorohalonata*, *S. rugosoannulata*, and *T. porosum*, whereas in *Ascocoryne* sp. and *Phoma* sp. transesterification and hydrolytic de-esterification reactions control the formation of TP 217 and PA, respectively.

Time courses for the appearance of: (ii) DBP breakdown products with one additional oxygen atom (TPs 317, 315, 275, 261, 259, and 247), and (iii) two additional oxygen atoms in their structures (TPs 333 and 331; not shown for TP 305 and 291 which occurred only in small amounts) for active and PB-inhibited fungal cultures are shown in Table 8. Among these DBP biotransformation products, more than one isomer was detected for the TPs 317 (2 isomers), 275 (3), 261 (2), 333 (4), 331 (2), 305 (2), and 291 (4) (indicated by corresponding retention times in Supplementary Table S1, respectively). The occurrence of biotransformation

TABLE 3 | Removal rates of BPA, DBP, and DEP applied in mixture to *Ascocoryne* sp. cultures.

Pollutant/description	Removal rate (nmol/h/g)		
	Initial rate	24 h Rate	Overall rate
BPA			
Active cultures	FNR	679 ± 228	47 ± 12
NaN ₃ -inactivated cultures	FNR	917 ± 252	71 ± 21
Biotransformation	NA	0	0
DBP			
Active cultures	4367 ± 1101	2828 ± 478	299 ± 16
NaN ₃ -inactivated cultures	FNR	1452 ± 202	94 ± 25
Biotransformation	NA	1376 ± 519	205 ± 30
DEP			
Active cultures	FNS	1638 ± 358	232 ± 28
NaN ₃ -inactivated cultures	FNS	690 ± 512	67 ± 28
Biotransformation	NA	948 ± 629	165 ± 40

Removal rates of BPA, DBP, and DEP observed with active and NaN₃-inactivated *Ascocoryne* sp. cultures (controls) were always based on corresponding fungal dry biomasses at the time point of addition of pollutant mixtures. The fungal dry biomasses were 0.69 ± 0.02 and 0.46 ± 0.05 g/L for active and NaN₃-inactivated cultures, respectively (values always means ± standard deviations from triplicate cultures). Initial (maximal) removal rates were calculated from exponential fits of micropollutant concentrations over time. Fits yielding COD values < 0.9 were considered as insufficient and initial rates were omitted in such cases (FNS, fit not sufficient). Also, formally successful fits yielding unrealistic removal rates due to initial sharp decreases in micropollutant concentrations and resulting steep curve cuts by the related bottom asymptotes were not considered (FNR, fit not realistic). Alternatively, removal rates were also calculated based upon the reduction of micropollutant concentrations over time periods of 24 (24 h rate) and 312 h (end of the incubation period; overall rate). Removal rates attributed to biotransformation were expressed as the difference between removal rates obtained from active (representing biotransformation + biosorption) and NaN₃-inactivated fungal cultures (representing biosorption only). Data represent means ± standard deviations (standard errors in case of initial rates and the thereof derived share of biotransformation) from triplicate cultures (calculated according to Gaussian error propagation rules). NA, not applicable.

TABLE 4 | Removal rates of BPA, DBP, and DEP applied in mixture to *P. arenariae* cultures.

Pollutant, cultivation variant and share of biotransformation	Removal rate (nmol/h/g)		
	Initial rate	24 h Rate	Overall rate
BPA			
Active cultures	FNS	168 ± 48	62 ± 10
NaN ₃ -inactivated cultures	FNS	37 ± 52	6 ± 4
Biotransformation	NA	131 ± 71	56 ± 11
DBP			
Active cultures	1145 ± 260	572 ± 64	69 ± 4
NaN ₃ -inactivated cultures	2279 ± 474	401 ± 98	29 ± 10
Biotransformation	0	171 ± 117	40 ± 11
DEP			
Active cultures	2198 ± 650	1059 ± 70	82 ± 5
NaN ₃ -inactivated cultures	FNS	21 ± 121	4 ± 9
Biotransformation	NA	1038 ± 140	78 ± 10

Removal rates of BPA, DBP, and DEP observed with active and NaN₃-inactivated *P. arenariae* cultures (controls) were always based on corresponding fungal dry biomasses at the time point of addition of pollutant mixtures. The fungal dry biomasses were 3.13 ± 0.17 and 2.78 ± 0.13 g/L for active and NaN₃-inactivated cultures, respectively (values always means ± standard deviations from triplicate cultures). For further explanations please refer to Table 3.

TABLE 5 | Removal rates of BPA, DBP, and DEP applied in mixture to *C. aquatica* cultures.

Pollutant, cultivation variant and share of biotransformation	Removal rate (nmol/h/g)		
	Initial rate	24 h Rate	Overall rate
BPA			
Active cultures	FNS	114 ± 579	49 ± 45
NaN ₃ -inactivated cultures	FNS	213 ± 214	22 ± 14
Biotransformation	NA	0	27 ± 47
DBP			
Active cultures	223 ± 569	377 ± 359	241 ± 36
NaN ₃ -inactivated cultures	FNS	441 ± 123	43 ± 13
Biotransformation	NA	0	198 ± 39
DEP			
Active cultures	3610 ± 640	2274 ± 549	311 ± 43
NaN ₃ -inactivated cultures	FNS	146 ± 372	32 ± 20
Biotransformation	NA	2128 ± 663	279 ± 47

Removal rates of BPA, DBP, and DEP observed with active and NaN₃-inactivated *C. aquatica* cultures (controls) were always based on corresponding fungal dry biomasses at the time point of addition of pollutant mixtures. The fungal dry biomasses were 0.90 ± 0.07 and 0.47 ± 0.05 g/L for active and NaN₃-inactivated cultures, respectively (values always means ± standard deviations from triplicate cultures). For further explanations please refer to **Table 3**.

TABLE 6 | Removal rates of BPA, DBP, and DEP applied in mixture to *Phoma* sp. cultures.

Pollutant, cultivation variant and share of biotransformation	Removal rate (nmol/h/g)		
	Initial rate	24 h Rate	Overall rate
BPA			
Active cultures	1448 ± 89	1019 ± 226	125 ± 15
NaN ₃ -inactivated cultures	31 ± 40	342	44 ± 24
Biotransformation	1147 ± 97	722 ± 410	81 ± 29
DBP			
Active cultures	4547 ± 1032	1310 ± 148	117 ± 13
NaN ₃ -inactivated cultures	FNS	799 ± 257	82 ± 20
Biotransformation	NA	511 ± 315	35 ± 24
DEP			
Active cultures	1053 ± 116	915 ± 231	129 ± 15
NaN ₃ -inactivated cultures	FNS	276 ± 418	35 ± 29
Biotransformation	NA	639 ± 478	94 ± 33

Removal rates of BPA, DBP, and DEP observed with active and NaN₃-inactivated *Phoma* sp. cultures (controls) were always based on corresponding fungal dry biomasses at the time point of addition of pollutant mixtures. The fungal dry biomasses were 2.10 ± 0.03 and 1.58 ± 0.12 g/L for active and NaN₃-inactivated cultures, respectively (values always means ± standard deviations from triplicate cultures). For further explanations please refer to **Table 3**.

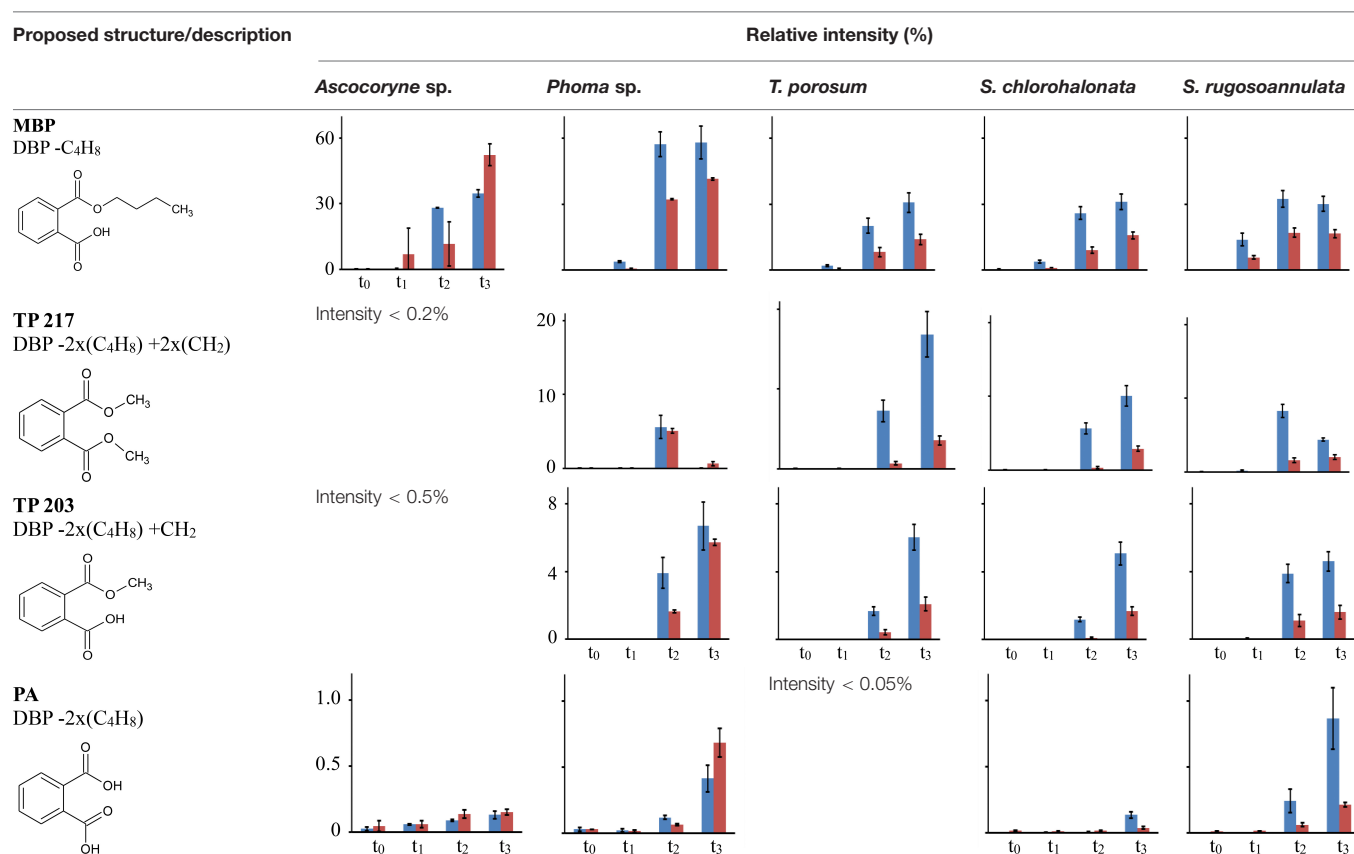
products in the form of different isomers most likely reflects structural alterations at different carbon atom positions in the respective metabolite molecule. Related possible (albeit thus far

hypothetical) structures are exemplified for TPs 331, 317, and 261 in **Supplementary Table S1**. Fungus-specific differences with regard to the preferential formation of certain isomers over others were noticed. However, we here abstain from presenting related data as it is impossible to assign corresponding chemical structures to the different isomers unambiguously. All of the DBP metabolites listed in **Table 8** could be detected in *Ascocoryne* sp., *Phoma* sp., *S. chlorohalonata*, and *S. rugosoannulata*, whereas in *T. porosum* only the TPs 275 and 331 were found. TP formation was strongly inhibited in presence of PB as would be expected for the involvement of cytochrome P450 monooxygenase systems, which also applies to TPs 305 and 291 not shown in **Table 8**. Beyond primary monohydroxylation of DBP as indicated by the formation of TP 317, the deduced structures of other DBP biotransformation products depicted in **Table 8** suggest further oxidation steps such as subsequent hydroxylation to dihydroxy compounds (TP 333), the formation of carbonyl or carboxyl groups (TPs 259, 315, 331), and alkyl chain shortening likely via β -oxidation (TP 305). De-esterification (TP 261) and transesterification (TPs 247, 275, 291) of oxidized DBP metabolites, and further hydroxylation following transesterification (TP 247) is also supported by the proposed structures.

In summary, the detection of DBP metabolites presented in **Tables 7, 8**, and in the **Supplementary Table S1** clearly confirms biotransformation of DBP by *Ascocoryne* sp., *Phoma* sp., *S. chlorohalonata*, *S. rugosoannulata*, and *T. porosum*. A corresponding compilation of major biochemical steps proposed for the metabolization of DBP by these fungi based upon a combined consideration of the respective metabolite structure proposals, relative intensities of metabolite peak areas, and time courses of both DBP removal and metabolite formation in conjunction with corresponding PB effects (**Figure 2**, **Tables 2, 7, 8**, and **Supplementary Table S1**), is presented in **Figure 4**. Potentially, the addition of methanol to fungal cultures (applied to improve DBP solubility) may have resulted in overestimations of methylated DBP derivatives presumably formed by transesterification. Fungal, as well as bacterial, cutinases, esterases, and lipases are well known to utilize short-chain alcohols such as methanol as substrates in transesterification reactions (Kim et al., 2005; Okamoto et al., 2011; Lotti et al., 2015). However, such possible experimental artifacts would not have impaired the identification of most of the major reaction steps indicated by blue solid arrows in **Figure 4**.

DISCUSSION

In this study the ability of ecophysiologically diverse asco- and basidiomycete fungi to biotransform the PE representatives DBP and DEP, and the plastic precursor chemical BPA was demonstrated. UPLC-QTOF-MS analysis of DBP metabolites in fungal cultures confirmed DBP biotransformation and enabled us to establish the major biochemical reaction steps contributing to DBP metabolization in the Baltic Sea isolate *Ascocoryne* sp., the freshwater-derived strain *Phoma* sp., the environmentally ubiquitous mold *S. chlorohalonata* (all belonging to the

TABLE 7 | Fungal DBP transformation products without additional oxygen atoms in their structures.

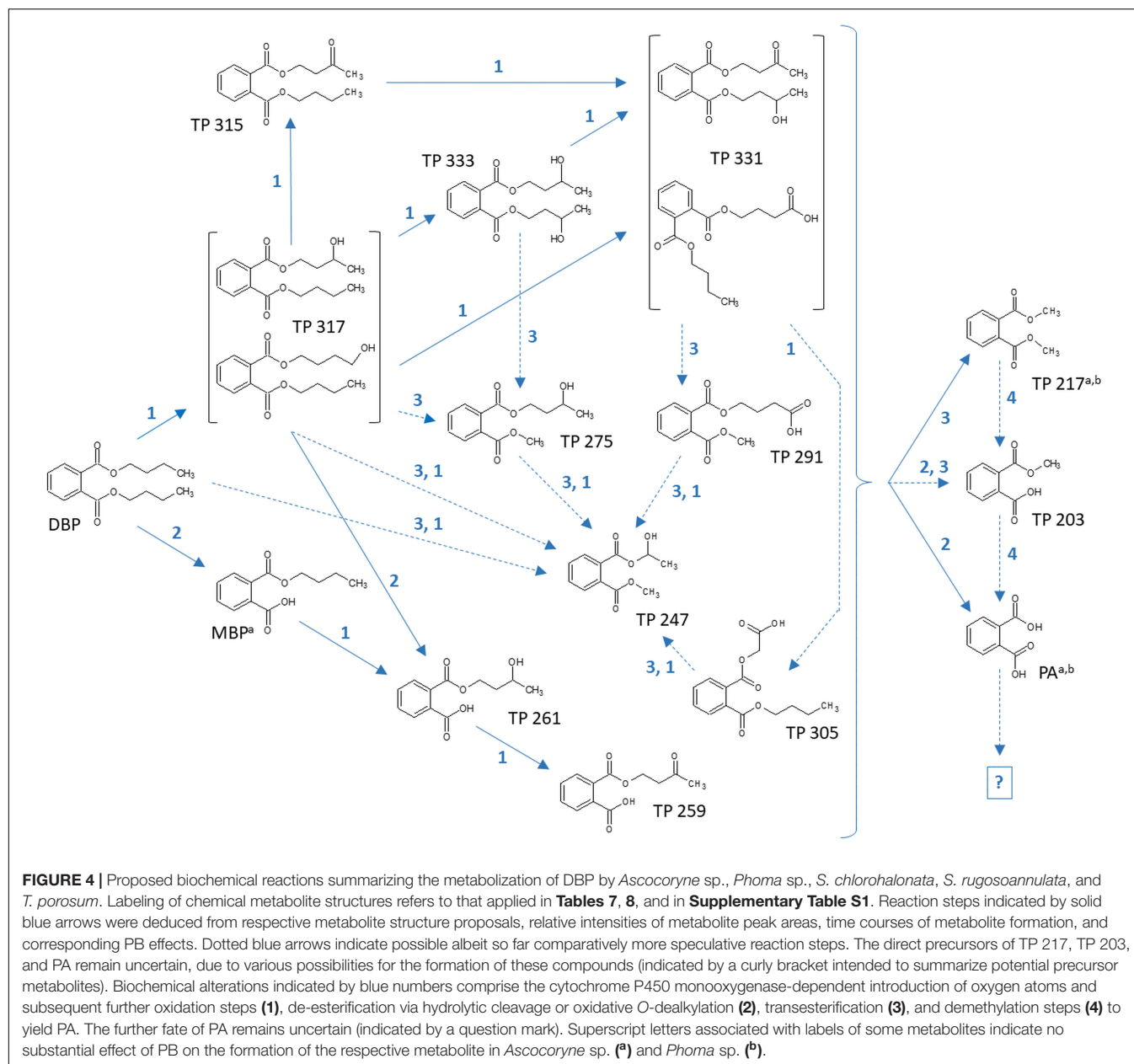
DBP transformation products were sorted in descending order according to their molecular masses. Labeling of the proposed chemical structures and respective chemical alterations (compared to parent DBP) indicated beneath correspond to those applied in the **Supplementary Table S1**. Relative intensities (%) were expressed as peak areas of DBP biotransformation products in UPLC-QTOF-MS total ion current chromatograms relative to the parent DBP peak area recorded at the time point of DBP addition (start of the experiment), respectively. Blue and red bars indicate relative transformation product intensities in active and PB-inhibited fungal cultures, respectively (means \pm standard deviations from triplicate cultures are always shown). For fungi displaying DBP metabolites with relative intensities below one tenth of the maximum value recorded for the metabolite of concern in any fungus, bar graphs were omitted (corresponding intensity ranges are given instead). Fungal cultures were sampled for UPLC-QTOF-MS analysis at the beginning of experiments (time point of DBP addition; t_0), after 1.5 (*Ascooryne* sp., *Phoma* sp.) and 3.5 h (all other fungi), respectively (t_1), after 48 h (all tested fungi; t_2), and at the respective termination of experiment (192 h for *Ascooryne* sp. and *Phoma* sp.; 216 h for all other tested fungi) (t_3).

Ascomycota), the litter decaying basidiomycete *S. rugosoannulata* and the basidiomycetous yeast *T. porosum* (**Figure 4**).

In *Ascooryne* sp., concomitant initial hydrolytic de-esterification and cytochrome P450-catalyzed monohydroxylation of DBP at similar rates is suggested. These initial steps are supported by comparatively high relative intensities of the corresponding transformation products (MBP and TP 317, respectively), the missing influence of PB on MBP formation, and its clearly suppressive effect on the formation of TP 317 (**Figure 4** and **Tables 7, 8**). *Ascooryne* sp. biotransformed DBP to a greater degree than DEP (**Figure 3** and **Table 3**), despite DBP having a lower aqueous solubility ($\log K_{ow} = 4.27$ vs. $\log K_{ow} = 2.54$; Cousins and Mackay, 2000; Net et al., 2015) and hence presumably lower bioavailability compared to DEP. This suggests that neither potential bioavailability limitations caused by compound solubility, nor the greater carbon chain lengths of the alkyl esters had a negative influence on the efficiency of the initial PE biotransformation step(s) in this fungus. Similarly, a slightly more efficient hydrolysis of DBP than of DEP was

reported for a bacterial PE-hydrolyzing enzyme isolated from culture broth of *Nocardia erythropolis* (Kurane et al., 1984). Hydrolysis of structurally related PEs, including DBP and DEP, at similar rates has also been reported for other bacteria and isolated esterase preparations (both bacterial and eukaryotic, i.e. from bovine pancreas), whereas PEs with branched and hence more bulky alkyl substituents were comparatively hydrolyzed slower (Saito et al., 2010; Huang et al., 2019). Furthermore, extracellular esterases have been implicated in initial PE hydrolysis in fungi (Lee et al., 2007; Hwang et al., 2012; Ahuactzin-Perez et al., 2016). A substantial role of hydrolytic PE de-esterification in *Ascooryne* sp. as stipulated above is in line with the aforementioned observations. In this context, an initial attack on PEs by extracellular enzymes could potentially help to avoid or diminish bioavailability limitations related to compound uptake by fungal cells for intracellular biotransformation steps.

By contrast, a more efficient DEP biotransformation compared to that of DBP, as observed with all other fungi investigated in this respect (**Figure 3** and **Tables 4–6**), may



indicate a possible influence of PE bioavailability on the biotransformation efficiency, as would be expected from the need for compound uptake prior to initial intracellular biotransformation steps. An initial attack on PEs catalyzed by intracellular cytochrome P450s, as implicated in *Phoma* sp. and supported by inhibitory effects of PB on fungal DBP removal (**Figure 2** and **Table 2**), is in accordance with such possible bioavailability effects. The DBP transformation product profile observed with *Phoma* sp. (**Tables 7, 8**) suggests initial DBP biotransformation dominated by de-esterification via cytochrome P450-catalyzed oxidative O-dealkylation, albeit obviously accompanied by DBP monohydroxylation and further oxidation steps to remarkable extents. Cytochrome P450 monooxygenase reactions are previously implicated in

the metabolization of the anti-inflammatory pharmaceutical diclofenac by *Phoma* sp. (Hofmann and Schlosser, 2016).

DBP de-esterification to MBP, and subsequent de- and/or transesterification steps controlled by cytochrome P450-dependent initial oxidative dealkylation form the major DBP metabolization pathway in *T. porosum*, whereas DBP hydroxylation and further oxidation of corresponding metabolites seems negligible (**Tables 7, 8**). This yeast species was described to be inactive on the comparatively more hydrophobic and hence less water soluble PE dioctyl phthalate (DOP; log K_{ow} = 7.32; Cousins and Mackay, 2000; Net et al., 2015; Sabev et al., 2006) possibly due to a lower bioavailability and/or mechanistic biochemical constraints of the degradability of DOP compared to DBP. Limited growth of *Trichosporon* DMI-5-1, a

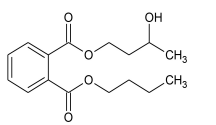
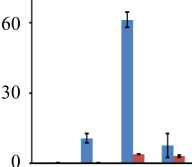
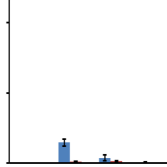
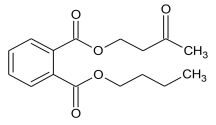
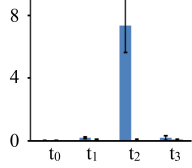
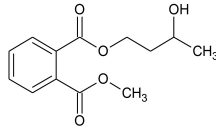
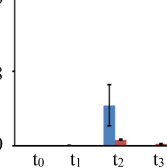
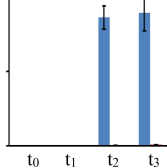
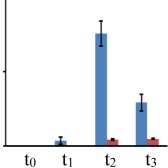
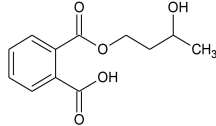
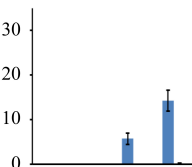
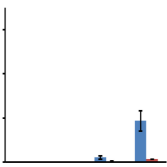
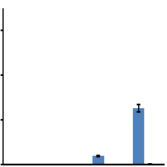
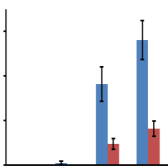
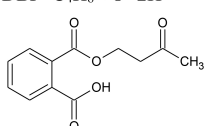
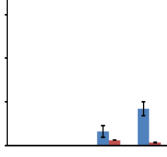
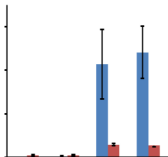
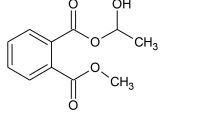
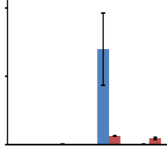
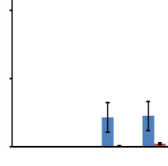
yeast isolate obtained from costal sediment, on different DMPEs was reported previously (Luo et al., 2011). Initial hydrolysis of DMPEs by *Trichosporon* DMI-5-1 led to the accumulation of aromatic products (monoesters, terephthalic acid), without their further breakdown.

Prominent initial bioconversion of DBP to MBP via oxidative O-dealkylation, and subsequent production of TP 217, TP 203, and PA, governed by cytochrome P450-dependent reactions is also suggested for both *S. chlorohalonata* and *S. rugosoannulata* (Tables 7, 8), although these fungi are phylogenetically distant. Contrary to *T. porosum*, cytochrome P450-dependent

hydroxylation reactions can be deduced to appreciable extents for *S. chlorohalonata* and *S. rugosoannulata*.

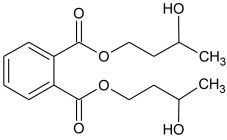
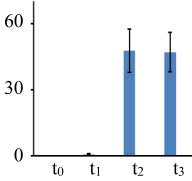
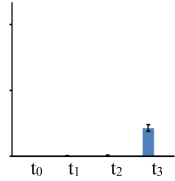
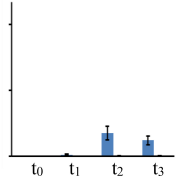
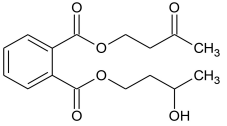
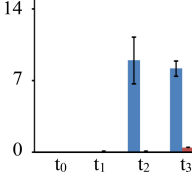
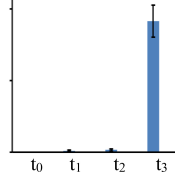
The present study establishes a prominent role of cytochrome P450 monooxygenase-catalyzed reactions during DBP metabolism in the majority of the investigated fungi, with corresponding results remaining inconclusive only for the peatland isolate *Acephala* sp. and the Baltic Sea isolate *P. arenariae* (see sub-section Fungal DBP Removal and Influence of PB). DBP hydroxylation and oxidative O-dealkylation processes, as stipulated for the investigated fungi above and compiled in Figure 4, represent typical reactions of cytochrome

TABLE 8 | Fungal DBP biotransformation products containing one or two additional oxygen atoms in their structures.

Proposed structure/description	Relative intensity (%)				
	<i>Ascoconyria</i> sp.	<i>Phoma</i> sp.	<i>T. porosum</i>	<i>S. chlorohalonata</i>	<i>S. rugosoannulata</i>
TP 317 DBP +O 			ND	Intensity < 0.005%	Intensity < 0.1%
TP 315 DBP +O -2H 		Intensity < 0.005%	ND	Intensity < 0.005%	Intensity < 0.05%
TP 275 DBP -C4H8 +CH2 +O 	Intensity < 0.5%		Intensity < 0.05%		
TP 261 DBP -C4H8 +O 			ND		
TP 259 DBP -C4H8 +O -2H 	Intensity < 0.1%		ND	Intensity < 0.5%	
TP 247 DBP -2x(C4H8) +C2H4 +O 	Intensity < 0.01%		ND	Intensity < 0.05%	

(Continued)

TABLE 8 | Continued

Proposed structure/description	Relative intensity (%)				
	<i>Ascocoryne</i> sp.	<i>Phoma</i> sp.	<i>T. porosum</i>	<i>S. chlorohalonata</i>	<i>S. rugosoannulata</i>
TP 333 DBP +2O 			ND	Intensity < 2%	
TP 331 DBP +2O -2H 			Intensity < 0.02%	Intensity < 0.05%	Intensity < 0.5%

DBP biotransformation products were grouped according to the number of additional oxygen atoms (i.e. one or two) in their structures and then sorted in descending order according to their molecular masses. Labeling of the proposed chemical structures and respective chemical alterations (compared to parent DBP) indicated beneath correspond to those applied in the **Supplementary Table S1**. Relative intensities (%) were expressed as peak areas of DBP biotransformation products in UPLC-QTOF-MS total ion current chromatograms relative to the parent DBP peak area recorded at the time point of DBP addition (start of the experiment), respectively. Blue and red bars indicate relative metabolite intensities in active and PB-inhibited fungal cultures, respectively (means \pm standard deviations from triplicate cultures are always shown). For DBP biotransformation products occurring in the form of different isomers (see **Supplementary Table S1**) only the isomer appearing with the highest relative intensity, respectively, is shown. For fungi displaying DBP metabolites with relative intensities below one tenth of the maximum value recorded for the metabolite of concern in any fungus, bar graphs were omitted (corresponding intensity ranges are given instead). TPs 305 and 291 (**Supplementary Table S1**) are not shown because of their generally low relative intensities (below 1.0 and 0.5% in any fungus, respectively). Fungal cultures were sampled for UPLC-QTOF-MS analysis at the beginning of experiments (time point of DBP addition; t_0), after 1.5 (*Ascocoryne* sp., *Phoma* sp.) and 3.5 h (all other fungi), respectively (t_1), after 48 h (all tested fungi; t_2), and at the respective termination of experiment (192 h for *Ascocoryne* sp. and *Phoma* sp.; 216 h for all other tested fungi) (t_3).

P450s also relevant to mammal PE metabolism (Choi et al., 2012, 2013; Girvan and Munro, 2016; Cantú Reinhard and De Visser, 2017). Cytochrome P450-catalyzed oxidations are commonly substrate-specific, as well as regio-, and frequently stereoselective, with different isoenzymes being responsible for the respective type of reaction, its selectivity, and hence also product variability (Choi et al., 2012; Syed and Yadav, 2012; Girvan and Munro, 2016; Cantú Reinhard and De Visser, 2017). The enormous catabolic versatility of certain fungal lineages is partly based on corresponding inventories of multiple cytochrome P450-encoding genes (Harms et al., 2011; Syed and Yadav, 2012; Syed et al., 2013). The occurrence of isomeric DBP biotransformation products observed within the present study (**Supplementary Table S1**) has also been reported for human di-2-ethylhexyl terephthalate metabolism (Silva et al., 2015), and may well reflect superimpositions of reactions of P450 isoenzymes with different selectivities. The influence of cytochrome P450-dependent reactions on the formation of the potential TP 203 precursor TP 217 observed with *S. chlorohalonata*, *S. rugosoannulata*, and *T. porosum* (**Table 7**) may be explained by the cytochrome P450-catalyzed formation of an upstream intermediate, since TP 217 most likely directly arises from a transesterification and not from a cytochrome P450 reaction. The same may apply to TP 203 and PA, where an influence of cytochrome P450-dependent steps on compound formation by the aforementioned fungi was also observed (**Table 7**). However, TP 203 and PA could also be produced from TPs 217 and 203, respectively, by cytochrome P450-dependent *O*-demethylation reactions

(Girvan and Munro, 2016). *O*-demethylation reactions are well-known from fungi, where cytochrome P450 lanosterol 14 α -demethylase is a prominent target for antifungal agents (Durairaj et al., 2016; Wang et al., 2019), and also from bacteria (Mallinson et al., 2018). The successive demethylation of TP 217 (dimethyl phthalate ester) via TP 203 (monomethyl phthalate ester) to PA was proposed for complex microbial communities of soil (Cartwright et al., 2000).

Different from *S. chlorohalonata*, *S. rugosoannulata*, and *T. porosum*, cytochrome P450-dependent reactions did not control the production of TP 217 and PA by *Ascocoryne* sp. and *Phoma* sp. (**Figure 4** and **Table 7**). In these fungi, transesterification and hydrolytic de-esterification reactions apparently govern the formation of TP 217 and PA, respectively. Hereby, PA could be produced from DBP in two successive hydrolytic steps, with MBP being formed as an intermediate. PA production by DEHP hydrolysis via the corresponding monoester has been proposed for the white-rot basidiomycete *Pleurotus ostreatus* (Ahuactzin-Perez et al., 2018). Rapid complete enzymatic hydrolysis of various PEs followed by spontaneous oxo-bridge formation to yield 1,3-isobenzofurandione (IBF) was reported for fungal cutinase, whereas application of fungal esterase to the same PEs yielded the corresponding monoesters in addition to IBF (Kim et al., 2003, 2005; Kim and Lee, 2005; Kim and Song, 2009). A bacterial esterase converting structurally diverse PEs into their corresponding monoesters, and a monoester hydrolase subsequently producing PA from such monoesters have also

been described (Huang et al., 2019). PA can additionally be formed by hydrolytic demethylation steps from products of transesterification reactions such as TPs 217 and 203 (**Figure 4**). Dimethyl phthalate (i.e. TP 217 in **Figure 4**) hydrolysis to monomethyl phthalate (TP 203) and its subsequent hydrolysis to PA is known from the aforementioned bacterial esterase and monoester hydrolase, respectively (Huang et al., 2019). Alternatively, a novel bacterial feruloyl esterase has been reported to convert DBP, DEP, and dimethyl phthalate (TP 217) directly into PA via hydrolysis steps (Wu et al., 2019).

The transesterification reactions proposed within the present study (**Figure 4**) corroborate previous research addressing microbial PE metabolism (Cartwright et al., 2000; Kim et al., 2005; Lee et al., 2007; Okamoto et al., 2011). Nevertheless, as an alternative to transesterifications catalyzed by hydrolytic enzymes, methylated products such as those indicated in **Figure 4** (TPs 291, 275, 247, 217, 203) could also be produced upon methylation of hydroxyl groups by fungal O-methyltransferases; a very common reaction in fungal metabolism of xenobiotics (Harms et al., 2011; Wang et al., 2014; Hofmann and Schlosser, 2016). Enzymatic transesterifications only proceed in the presence of alcohol, which is often used as a solvent for PEs in corresponding studies (Kim et al., 2003, 2005; Kim and Lee, 2005; Okamoto et al., 2011) and thus may bias corresponding results. The environmental relevance of such reactions remains to be established as environmental concentrations of alcohols is expectedly rather low (Okamoto et al., 2011).

It remains to be elucidated whether the central PE intermediate PA is further metabolized by the fungi investigated within the present study (**Figure 4**). At a first glance, the comparatively low relative intensities of this compound shown in **Table 7** do not indicate its accumulation. The breakdown of the aromatic PA core of DEHP to butanediol by *Fusarium culmorum*, and complete degradation of PA by the white-rot fungus *Pleurotus ostreatus* were previously suggested (Ahuactzin-Perez et al., 2016; Ahuactzin-Perez et al., 2018). By contrast, monoaromatic breakdown products of DMPEs were not further degraded by *Fusarium* sp. and yeast (Luo et al., 2011, 2012). The bacterial utilization of non-toxic fungal DBP breakdown products as sole carbon and energy sources has been demonstrated before (Ahuactzin-Perez et al., 2014).

The considerably higher biotransformation rate of BPA observed with *Phoma* sp. compared to *P. arenariae* in the present study (**Figure 3** and **Tables 4, 6**) could be attributed to BPA oxidation by extracellular laccases and/or peroxidases, for which activities were only recorded in *Phoma* sp., in addition to cell-bound enzymes (Cajthaml, 2015; Hofmann and Schlosser, 2016). The demonstrated concomitant biotransformation of more than one organic pollutant observed with several fungi (**Figure 3** and **Tables 3–6**) is a typical fungal characteristic (Harms et al., 2011). To the best of our knowledge, bioconversion of BPA as suggested for *P. arenariae* (**Figure 3** and **Table 4**) has not yet been reported. *Phoma* sp. was already previously shown to act on BPA as well as on other prominent micropollutants present in water (Hofmann and Schlosser, 2016). Moreover, *S. rugosoannulata* has been reported to metabolize BPA in addition to other

organic environmental pollutants before (Kabiersch et al., 2011; Pozdnyakova et al., 2018).

The observed degree of micropollutant biosorption onto fungal mycelia recorded within the present study (DBP > BPA > DEP; **Figure 3** and **Tables 3–6**) reflects the hydrophobicity of the tested compounds in terms of their respective octanol-water partition coefficients (log K_{ow} values of 4.27, 3.32, and 2.54 for DBP, BPA, and DEP, respectively; Cousins and Mackay, 2000; Margot et al., 2013; Net et al., 2015). Individual differences observed with regard to the biosorptive capacities of the tested fungi (**Figures 2, 3** and **Tables 2–6**) can be attributed to their individual cell surface properties, which may further change in response to growth conditions and proximity of hydrophobic environmental pollutants (Linder et al., 2005; Chau et al., 2009; Hanano et al., 2015). In addition to simple physical removal, biosorption has been implicated in aiding the efficiency and variety of micropollutants actively removed. Nguyen et al. (2014) reported increased biotransformation for a number of compounds via whole-cell treatment, compared to cell-free enzymatic processes. The authors argued that increased exposure to mycelium-associated/intracellular biocatalysts provided access to further catabolic processes in addition to those of extracellular secretions (compound specific). High biotransformation rates have been reported for compounds exhibiting strong sorption to fungal cell surfaces (Hofmann and Schlosser, 2016). One could argue that a local increase in compound concentration (i.e. association with mycelium) would establish a concentration gradient and thereby drive contaminant fluxes toward nearby biocatalysts (Johnsen et al., 2005; Semple et al., 2007). In the present study DBP showed strongest sorption, however it was not always the most efficiently biotransformed micropollutant (**Figure 3** and **Tables 3–6**). Aside from other contributory effects (e.g. enzyme specificities, redox potentials, compound toxicity), it may also be postulated that strong biosorption impedes enzyme access to such compounds. In line with this argument, application of differently hydrophobic PEs to the flagellated protist *Karenia brevis* (the cause of the Florida red tide) resulted in an increase in bioaccumulation and toxicity, and a decrease in PE biodegradation with increasing PE hydrophobicity (Sun et al., 2019).

The results of the present study imply an environmentally ubiquitous fungal potential for the biocatalytic breakdown of plastic additives, which comprises ecophysiological and phylogenetically diverse filamentous and yeast-like fungi dwelling in marine, freshwater and terrestrial habitats. Being part of the complex microbial communities of terrestrial as well as aquatic environments, such fungal activities may contribute to diminish concentrations and mitigate the adverse effects of PEs and other plastic additives following their release into the environment. The loss of plasticizers from polymers due to biocatalytic process proceeding on polymer surfaces (e.g. biodegradation by fungi-containing biofilms) may make plastics more brittle thus potentially contributing to polymer disaggregation and microplastics formation (Krueger et al., 2015a; Hahladakis et al., 2018). Potential adverse or positive environmental and human health impacts possibly resulting from such processes still need to be assessed

(Krueger et al., 2015a; Hahladakis et al., 2018; Jiang, 2018). Finally, fungi capable of attacking plastic additives and other micropollutants could be exploited in biotechnologies aimed at the reduction of environmental contamination from sources such as wastewater treatment plants (Pezzella et al., 2017; Hofmann et al., 2018).

DATA AVAILABILITY STATEMENT

The raw data supporting the conclusions of this article will be made available on request by the authors, without undue reservation, to any qualified researcher.

AUTHOR CONTRIBUTIONS

LC, AC, and DS conceived and designed the experiments. LC and AC performed the experiments. BS performed the UPLC-QTOF-MS analyses. LC, AC, BS, and DS analyzed the obtained data, interpreted the obtained results, and wrote the manuscript.

FUNDING

This work was co-funded by the Erasmus+ program of the European Union (scholarship of AC), the Heinrich Böll Stiftung

(scholarship of LC), and supported by the Helmholtz Association of German Research Centers within the frame of the integrated project 'Controlling Chemicals' Fate' of the Chemicals In The Environment (CITE) research program (conducted at the Helmholtz Centre for Environmental Research - UFZ). Further funding was provided by the European Commission as a part of the BIOCLEAN project (EC grant agreement no. 312100).

ACKNOWLEDGMENTS

We are grateful to Madlen Schröter, Stefanie Loth, and Petra Keil (all from UFZ) for excellent technical assistance. This publication included content from LC's master thesis (Carstens, 2018), available online (<https://stud.epsilon.slu.se/13656/>), and AC's master theses, available upon request. LC thanks Harald Cederlund from the Department of Molecular Sciences, SLU in Uppsala, Sweden for supervision of her master thesis.

SUPPLEMENTARY MATERIAL

The Supplementary Material for this article can be found online at: <https://www.frontiersin.org/articles/10.3389/fmicb.2020.00317/full#supplementary-material>

REFERENCES

- Ahn, J. Y., Kim, Y. H., Min, J., and Lee, J. (2006). Accelerated degradation of dipentyl phthalate by *Fusarium oxysporum* f. sp. *pisi* cutinase and toxicity evaluation of its degradation products using bioluminescent bacteria. *Curr. Microbiol.* 52, 340–344. doi: 10.1007/s00284-005-0124-9
- Ahuactzin-Perez, M., Tlecuitl-Beristain, S., Garcia-Davila, J., Gonzalez-Perez, M., Gutierrez-Ruiz, M. C., and Sanchez, C. (2016). Degradation of di(2-ethyl hexyl) phthalate by *Fusarium culmorum*: kinetics, enzymatic activities and biodegradation pathway based on quantum chemical modeling. *Sci. Total Environ.* 566–567, 1186–1193. doi: 10.1016/j.scitotenv.2016.05.169
- Ahuactzin-Perez, M., Tlecuitl-Beristain, S., Garcia-Davila, J., Santacruz-Juarez, E., Gonzalez-Perez, M., Gutierrez-Ruiz, M. C., et al. (2018). A novel biodegradation pathway of the endocrine-disruptor di(2-ethyl hexyl) phthalate by *Pleurotus ostreatus* based on quantum chemical investigation. *Ecotoxicol. Environ. Saf.* 147, 494–499. doi: 10.1016/j.ecoenv.2017.09.004
- Ahuactzin-Perez, M., Torres, J. L., Rodriguez-Pastrana, B. R., Soriano-Santos, J., Diaz-Godinez, G., Diaz, R., et al. (2014). Fungal biodegradation of dibutyl phthalate and toxicity of its breakdown products on the basis of fungal and bacterial growth. *World J. Microbiol. Biotechnol.* 30, 2811–2819. doi: 10.1007/s11274-014-1705-1
- Amir, S., Hafidi, M., Merlina, G., Hamdi, H., Jouraiphy, A., El Gharous, M., et al. (2005). Fate of phthalic acid esters during composting of both lagooning and activated sludges. *Process Biochem.* 40, 2183–2190. doi: 10.1016/j.procbio.2004.08.012
- Cajthaml, T. (2015). Biodegradation of endocrine-disrupting compounds by ligninolytic fungi: mechanisms involved in the degradation. *Environ. Microbiol.* 17, 4822–4834. doi: 10.1111/1462-2920.12460
- Cantú Reinhard, F. G., and De Visser, S. P. (2017). Biodegradation of cosmetics products: a computational study of cytochrome P450 metabolism of phthalates. *Inorganics* 5:77. doi: 10.3390/inorganics5040077
- Carstens, L. (2018). *Biodegradation of Organic Micropollutants Dibutyl Phthalate and Bisphenol A by Fungi*. Master's thesis, Swedish University of Agricultural Sciences, Uppsala.
- Cartwright, C. D., Owen, S. A., Thompson, I. P., and Burns, R. G. (2000). Biodegradation of diethyl phthalate in soil by a novel pathway. *FEMS Microbiol. Lett.* 186, 27–34. doi: 10.1111/j.1574-6968.2000.tb09077.x
- Chau, H. W., Si, B. C., Goh, Y. K., and Vujanovic, V. (2009). A novel method for identifying hydrophobicity on fungal surfaces. *Mycol. Res.* 113, 1046–1052. doi: 10.1016/j.mycres.2009.06.007
- Choi, K., Joo, H., Campbell, J. L. Jr., Andersen, M. E., and Clewell, H. J. III. (2013). *In vitro* intestinal and hepatic metabolism of Di(2-ethylhexyl) phthalate (DEHP) in human and rat. *Toxicol. In Vitro* 27, 1451–1457. doi: 10.1016/j.tiv.2013.03.012
- Choi, K., Joo, H., Campbell, J. L. Jr., Clewell, R. A., Andersen, M. E., and Clewell, H. J. III. (2012). *In vitro* metabolism of di(2-ethylhexyl) phthalate (DEHP) by various tissues and cytochrome P450s of human and rat. *Toxicol. In Vitro* 26, 315–322. doi: 10.1016/j.tiv.2011.12.002
- Coelho-Moreira, J. D. S., Brugnari, T., Sa-Nakanishi, A. B., Castoldi, R., De Souza, C. G. M., Bracht, A., et al. (2018). Evaluation of diuron tolerance and biotransformation by the white-rot fungus *Ganoderma lucidum*. *Fungal Biol.* 122, 471–478. doi: 10.1016/j.funbio.2017.10.008
- Colon, I., Caro, D., Bourdony, C. J., and Rosario, O. (2000). Identification of phthalate esters in the serum of young Puerto Rican girls with premature breast development. *Environ. Health Perspect.* 108, 895–900. doi: 10.1289/ehp.00108895
- Cousins, I., and Mackay, D. (2000). Correlating the physical-chemical properties of phthalate esters using the 'three solubility' approach. *Chemosphere* 41, 1389–1399. doi: 10.1016/s0045-6535(00)00005-9
- Diamanti-Kandarakis, E., Bourguignon, J. P., Giudice, L. C., Hauser, R., Prins, G. S., Soto, A. M., et al. (2009). Endocrine-disrupting chemicals: an Endocrine Society scientific statement. *Endocr. Rev.* 30, 293–342.
- Durairaj, P., Hur, J. S., and Yun, H. (2016). Versatile biocatalysis of fungal cytochrome P450 monooxygenases. *Microb. Cell Fact.* 15:125. doi: 10.1186/s12934-016-0523-6
- EU, (2015). Commission Delegated Directive (EU) 2015/863 of 31 March 2015 Amending Annex II to Directive 2011/65/EU of the European Parliament and of the Council as Regards the List of Restricted Substances. Available at: https://eur-lex.europa.eu/eli/dir_del/2015/863/oj (accessed January 30, 2020).

- Gadd, G. M. (2009). Biosorption: critical review of scientific rationale, environmental importance and significance for pollution treatment. *J. Chem. Technol. Biotechnol.* 84, 13–28. doi: 10.1002/jctb.1999
- Gao, D. W., and Wen, Z. D. (2016). Phthalate esters in the environment: a critical review of their occurrence, biodegradation, and removal during wastewater treatment processes. *Sci. Total Environ.* 541, 986–1001. doi: 10.1016/j.scitotenv.2015.09.148
- Gartshore, J., Cooper, D. G., and Nicell, J. A. (2003). Biodegradation of plasticizers by *Rhodotorula rubra*. *Environ. Toxicol. Chem.* 22, 1244–1251. doi: 10.1002/etc.5620220609
- Ghaly, A. E., Dave, D., Brooks, M. S., and Budge, S. (2010). Production of biodiesel by enzymatic transesterification: review. *Am. J. Biochem. Biotechnol.* 6, 54–76. doi: 10.3844/ajbbsp.2010.54.76
- Girvan, H. M., and Munro, A. W. (2016). Applications of microbial cytochrome P450 enzymes in biotechnology and synthetic biology. *Curr. Opin. Chem. Biol.* 31, 136–145. doi: 10.1016/j.cbpa.2016.02.018
- Hahladakis, J. N., Velis, C. A., Weber, R., Iacovidou, E., and Purnell, P. (2018). An overview of chemical additives present in plastics: migration, release, fate and environmental impact during their use, disposal and recycling. *J. Hazard. Mater.* 344, 179–199. doi: 10.1016/j.jhazmat.2017.10.014
- Hanano, A., Shaban, M., Almously, I., and Al-Ktaifani, M. (2015). *Saccharomyces cerevisiae* SHSY detoxifies petroleum *n*-alkanes by an induced CYP52A58 and an enhanced order in cell surface hydrophobicity. *Chemosphere* 135, 418–426. doi: 10.1016/j.chemosphere.2014.11.011
- Harms, H., Schlosser, D., and Wick, L. Y. (2011). Untapped potential: exploiting fungi in bioremediation of hazardous chemicals. *Nat. Rev. Microbiol.* 9, 177–192. doi: 10.1038/nrmicro2519
- Hermabessiere, L., Dehaut, A., Paul-Pont, I., Lacroix, C., Jezequel, R., Soudant, P., et al. (2017). Occurrence and effects of plastic additives on marine environments and organisms: a review. *Chemosphere* 182, 781–793. doi: 10.1016/j.chemosphere.2017.05.096
- Hofmann, U., Fenu, A., Beffa, T., Beimfohr, C., Weemaes, M., Yu, L., et al. (2018). Evaluation of the applicability of the aquatic ascomycete *Phoma* sp. UHH 5-1-03 for the removal of pharmaceutically active compounds from municipal wastewaters using membrane bioreactors. *Eng. Life Sci.* 18, 510–519. doi: 10.1002/elsc.201800070
- Hofmann, U., and Schlosser, D. (2016). Biochemical and physicochemical processes contributing to the removal of endocrine-disrupting chemicals and pharmaceuticals by the aquatic ascomycete *Phoma* sp. UHH 5-1-03. *Appl. Microbiol. Biotechnol.* 100, 2381–2399. doi: 10.1007/s00253-015-7113-0
- Huang, H., Zhang, X. Y., Chen, T. L., Zhao, Y. L., Xu, D. S., and Bai, Y. P. (2019). Biodegradation of structurally diverse phthalate esters by a newly identified esterase with catalytic activity toward Di(2-ethylhexyl) phthalate. *J. Agric. Food Chem.* 67, 8548–8558. doi: 10.1021/acs.jafc.9b02655
- Hwang, S. S., Kim, H. Y., Ka, J. O., and Song, H. G. (2012). Changes in the activities of enzymes involved in the degradation of butylbenzyl phthalate by *Pleurotus ostreatus*. *Microbiol. Biotechnol.* 22, 239–243. doi: 10.4014/jmb.1107.07050
- Im, J., and Löffler, F. E. (2016). Fate of bisphenol A in terrestrial and aquatic environments. *Environ. Sci. Technol.* 50, 8403–8416. doi: 10.1021/acs.est.6b00877
- Jackson, M. A., Labeda, D. P., and Becker, L. A. (1996). Isolation for bacteria and fungi for the hydrolysis of phthalate and terephthalate esters. *J. Ind. Microbiol.* 16, 301–304. doi: 10.1007/s11356-011-0525-1
- Jeng, H. A. (2014). Exposure to endocrine disrupting chemicals and male reproductive health. *Front. Public Health* 2:55. doi: 10.3389/fpubh.2014.00055
- Jiang, J.-Q. (2018). Occurrence of microplastics and its pollution in the environment: a review. *Sustain. Prod. Consum.* 13, 16–23. doi: 10.1016/j.spc.2017.11.003
- Johnsen, A. R., Wick, L. Y., and Harms, H. (2005). Principles of microbial PAH-degradation in soil. *Environ. Pollut.* 133, 71–84. doi: 10.1016/j.envpol.2004.04.015
- Junghanns, C., Krauss, G., and Schlosser, D. (2008a). Potential of aquatic fungi derived from diverse freshwater environments to decolourise synthetic azo and anthraquinone dyes. *Bioresour. Technol.* 99, 1225–1235. doi: 10.1016/j.biortech.2007.02.015
- Junghanns, C., Parra, R., Keshavarz, T., and Schlosser, D. (2008b). Towards higher laccase activities produced by aquatic ascomycetous fungi through combination of elicitors and an alternative substrate. *Eng. Life Sci.* 8, 277–285. doi: 10.1002/elsc.200800042
- Kabiersch, G., Rajasarkka, J., Ullrich, R., Tuomela, M., Hofrichter, M., Virta, M., et al. (2011). Fate of bisphenol A during treatment with the litter-decomposing fungi *Stropharia rugosoannulata* and *Stropharia coronilla*. *Chemosphere* 83, 226–232. doi: 10.1016/j.chemosphere.2010.12.094
- Karich, A., Ullrich, R., Scheibner, K., and Hofrichter, M. (2017). Fungal unspecific peroxygenases oxidize the majority of organic EPA priority pollutants. *Front. Microbiol.* 8:1463. doi: 10.3389/fmicb.2017.01463
- Kester, D. R., Duedall, I. W., Connors, D. N., and Pytkowicz, R. M. (1967). Preparation of artificial seawater. *Limnol. Oceanogr.* 12, 176–179.
- Kim, Y. H., and Lee, J. (2005). Enzymatic degradation of dibutyl phthalate and toxicity of its degradation products. *Biotechnol. Lett.* 27, 635–639. doi: 10.1007/s10529-005-3631-7
- Kim, Y. H., Lee, J., and Moon, S. H. (2003). Degradation of an endocrine disrupting chemical, DEHP [di-(2-ethylhexyl)-phthalate], by *Fusarium oxysporum* f. sp. *pisi* cutinase. *Appl. Microbiol. Biotechnol.* 63, 75–80. doi: 10.1007/s00253-003-1332-5
- Kim, Y. H., Min, J., Bae, K. D., Gu, M. B., and Lee, J. (2005). Biodegradation of dipropyl phthalate and toxicity of its degradation products: a comparison of *Fusarium oxysporum* f. sp. *pisi* cutinase and *Candida cylindracea* esterase. *Arch. Microbiol.* 184, 25–31. doi: 10.1007/s00203-005-0026-z
- Kim, Y. M., and Song, H. G. (2009). Effect of fungal pellet morphology on enzyme activities involved in phthalate degradation. *J. Microbiol.* 47, 420–424. doi: 10.1007/s12275-009-0051-8
- Krauss, G. J., Sole, M., Krauss, G., Schlosser, D., Wesenberg, D., and Barlocher, F. (2011). Fungi in freshwaters: ecology, physiology and biochemical potential. *FEMS Microbiol. Rev.* 35, 620–651. doi: 10.1111/j.1574-6976.2011.00266.x
- Krueger, M. C., Harms, H., and Schlosser, D. (2015a). Prospects for microbiological solutions to environmental pollution with plastics. *Appl. Microbiol. Biotechnol.* 99, 8857–8874. doi: 10.1007/s00253-015-6879-4
- Krueger, M. C., Hofmann, U., Moeder, M., and Schlosser, D. (2015b). Potential of wood-rotting fungi to attack polystyrene sulfonate and its depolymerisation by gloeophyllum trabeum via hydroquinone-driven fenton chemistry. *PLoS One* 10:e0131773. doi: 10.1371/journal.pone.0131773
- Kurane, R., Suzuki, T., and Fukuoka, S. (1984). Purification and some properties of a phthalate ester hydrolyzing enzyme from *Nocardia erythropolis*. *Appl. Microbiol. Biotechnol.* 20, 378–383.
- Lee, S. M., Lee, J. W., Koo, B. W., Kim, M. K., Choi, D. H., and Choi, I. G. (2007). Dibutyl phthalate biodegradation by the white rot fungus, *Polyporus brumalis*. *Biotechnol. Bioeng.* 97, 1516–1522. doi: 10.1002/bit.21333
- Liang, D. W., Zhang, T., Fang, H. H., and He, J. (2008). Phthalates biodegradation in the environment. *Appl. Microbiol. Biotechnol.* 80, 183–198.
- Linder, M. B., Szilvay, G. R., Nakari-Setälä, T., and Penttilä, M. E. (2005). Hydrophobins: the protein-amphiphiles of filamentous fungi. *FEMS Microbiol. Rev.* 29, 877–896. doi: 10.1016/j.femsrev.2005.01.004
- Lotti, M., Pleiss, J., Valero, F., and Ferrer, P. (2015). Effects of methanol on lipases: molecular, kinetic and process issues in the production of biodiesel. *Biotechnol. J.* 10, 22–30. doi: 10.1002/biot.201400158
- Luo, Z.-H., Pang, K.-L., Wu, Y.-R., Gu, J.-D., Chow, R. K. K., and Vrijmoed, L. L. P. (2012). “Degradation of phthalate esters by *Fusarium* sp. DMT-5-3 and *Trichosporon* sp. DMI-5-1 isolated from mangrove sediments,” in *Biology of Marine Fungi*, ed. C. Raghukumar, (Heidelberg: Springer), 299–328. doi: 10.1007/978-3-642-23342-5_15
- Luo, Z. H., Wu, Y. R., Pang, K. L., Gu, J. D., and Vrijmoed, L. L. (2011). Comparison of initial hydrolysis of the three dimethyl phthalate esters (DMPEs) by a basidiomycetous yeast, *Trichosporon* DMI-5-1, from coastal sediment. *Environ. Sci. Pollut. Res. Int.* 18, 1653–1660. doi: 10.1007/s11356-011-0525-1
- Macellaro, G., Pezzella, C., Cicatiello, P., Sannia, G., and Piscitelli, A. (2014). Fungal laccases degradation of endocrine disrupting compounds. *Biomed. Res. Int.* 2014:614038. doi: 10.1155/2014/614038
- Mallinson, S. J. B., Machovina, M. M., Silveira, R. L., Garcia-Borras, M., Gallup, N., Johnson, C. W., et al. (2018). A promiscuous cytochrome P450 aromatic

- O-demethylase for lignin bioconversion. *Nat. Commun.* 9:2487. doi: 10.1038/s41467-018-04878-2
- Marco-Urrea, E., Perez-Trujillo, M., Vicent, T., and Caminal, G. (2009). Ability of white-rot fungi to remove selected pharmaceuticals and identification of degradation products of ibuprofen by *Trametes versicolor*. *Chemosphere* 74, 765–772. doi: 10.1016/j.chemosphere.2008.10.040
- Margot, J., Kienle, C., Magnet, A., Weil, M., Rossi, L., De Alencastro, L. F., et al. (2013). Treatment of micropollutants in municipal wastewater: ozone or powdered activated carbon? *Sci. Total Environ.* 46, 480–498. doi: 10.1016/j.scitotenv.2013.05.034
- Martin, C., Corvini, P. F. X., Vinken, R., Junghanns, C., Krauss, G., and Schlosser, D. (2009). Quantification of the influence of extracellular laccase and intracellular reactions on the isomer-specific biotransformation of the xenoestrogen technical nonylphenol by the aquatic hyphomycete *Clavariopsis aquatica*. *Appl. Environ. Microbiol.* 75, 4398–4409. doi: 10.1128/AEM.00139-09
- Martin, C., Moeder, M., Daniel, X., Krauss, G., and Schlosser, D. (2007). Biotransformation of the polycyclic musks HHCb and AHTN and metabolite formation by fungi occurring in freshwater environments. *Environ. Sci. Technol.* 41, 5395–5402. doi: 10.1021/es0711462
- Middelhoven, W. J., Scorzett, G., and Fell, J. W. (2001). *Trichosporon porosum* comb. nov., an anamorphic basidiomycetous yeast inhabiting soil, related to the loubieri/laibachii group of species that assimilate hemicelluloses and phenolic compounds. *FEMS Yeast Res.* 1, 15–22. doi: 10.1016/s1567-1356(00)00002-7
- Net, S., Sempere, R., Delmont, A., Paluselli, A., and Ouddane, B. (2015). Occurrence, fate, behavior and ecotoxicological state of phthalates in different environmental matrices. *Environ. Sci. Technol.* 49, 4019–4035. doi: 10.1021/es505233b
- Nguyen, L. N., Hai, F. I., Yang, S. F., Kang, J. G., Leusch, F. D. L., Roddick, F., et al. (2014). Removal of pharmaceuticals, steroid hormones, phytoestrogens, UV-filters, industrial chemicals and pesticides by *Trametes versicolor*: role of biosorption and biodegradation. *Int. Biodeter. Biodegr.* 88, 169–175. doi: 10.1016/j.ibiod.2013.12.017
- Notardonato, I., Protano, C., Vitali, M., Bhattacharya, B., and Avino, P. (2019). A method validation for simultaneous determination of phthalates and bisphenol A released from plastic water containers. *Appl. Sci.* 9:2945. doi: 10.3390/app9142945
- Oehlmann, J., Schulte-Oehlmann, U., Kloas, W., Jagnytsch, O., Lutz, I., Kusk, K. O., et al. (2009). A critical analysis of the biological impacts of plasticizers on wildlife. *Philos. Trans. R. Soc. Lond. B Biol. Sci.* 364, 2047–2062. doi: 10.1098/rstb.2008.0242
- Okamoto, Y., Toda, C., Ueda, K., Hashizume, K., and Kojima, N. (2011). Transesterification in the microbial degradation of phthalate esters. *J. Health Sci.* 57, 293–299. doi: 10.1248/jhs.57.293
- Overy, D. P., Bayman, P., Kerr, R. G., and Bills, G. F. (2014). An assessment of natural product discovery from marine (sensu strictu) and marine-derived fungi. *Mycology* 5, 145–167. doi: 10.1080/21501203.2014.931308
- Parveen, M., Inoue, A., Ise, R., Tanji, M., and Kiyama, R. (2008). Evaluation of estrogenic activity of phthalate esters by gene expression profiling using a focused microarray (EstrArray (R)). *Environ. Toxicol. Chem.* 27, 1416–1425. doi: 10.1897/07-399
- Pezzella, C., Macellaro, G., Sannia, G., Raganati, F., Olivieri, G., Marzocchella, A., et al. (2017). Exploitation of *Trametes versicolor* for bioremediation of endocrine disrupting chemicals in bioreactors. *PLoS One* 12:e0178758. doi: 10.1371/journal.pone.0178758
- Pozdnyakova, N., Schlosser, D., Dubrovskaya, E., Balandina, S., Sigida, E., Grinev, V., et al. (2018). The degradative activity and adaptation potential of the litter-decomposing fungus *Stropharia rugosoannulata*. *World J. Microbiol. Biotechnol.* 34:133. doi: 10.1007/s11274-018-2516-6
- Pradeep, S., and Benjamin, S. (2012). Mycelial fungi completely remediate di(2-ethylhexyl)phthalate, the hazardous plasticizer in PVC blood storage bag. *J. Hazard. Mater.* 235–236, 69–77. doi: 10.1016/j.jhazmat.2012.06.064
- Ren, L., Lin, Z., Liu, H., and Hu, H. (2018). Bacteria-mediated phthalic acid esters degradation and related molecular mechanisms. *Appl. Microbiol. Biotechnol.* 102, 1085–1096. doi: 10.1007/s00253-017-8687-5
- Sabev, H. A., Handley, P. S., and Robson, G. D. (2006). Fungal colonization of soil-buried plasticized polyvinyl chloride (pPVC) and the impact of incorporated biocides. *Microbiology* 152, 1731–1739. doi: 10.1099/mic.0.28569-0
- Saito, T., Hong, P., Tanabe, R., Nagai, K., and Kato, K. (2010). Enzymatic hydrolysis of structurally diverse phthalic acid esters by porcine and bovine pancreatic cholesterol esterases. *Chemosphere* 81, 1544–1548. doi: 10.1016/j.chemosphere.2010.08.020
- Salaudeen, T., Okoh, O., Agunbiade, F., and Okoh, A. (2018). Fate and impact of phthalates in activated sludge treated municipal wastewater on the water bodies in the Eastern Cape, South Africa. *Chemosphere* 203, 336–344. doi: 10.1016/j.chemosphere.2018.03.176
- Schlosser, D., Grey, R., Höfer, C., and Fahr, K. (2000). “Degradation of chlorophenols by basidiomycetes,” in *Bioremediation of Contaminated Soils*, eds D. L. Wise, D. J. Trantolo, E. J. Cichon, H. I. Inyang, and U. Stottmeister, (New York, NY: Marcel Dekker), 393–408.
- Schlosser, D., and Hofer, C. (2002). Laccase-catalyzed oxidation of Mn^{2+} in the presence of natural Mn^{3+} chelators as a novel source of extracellular H_2O_2 production and its impact on manganese peroxidase. *Appl. Environ. Microbiol.* 68, 3514–3521. doi: 10.1128/aem.68.7.3514-3521.2002
- Sample, K. T., Doick, K. J., Wick, L. Y., and Harms, H. (2007). Microbial interactions with organic contaminants in soil: definitions, processes and measurement. *Environ. Pollut.* 150, 166–176. doi: 10.1016/j.envpol.2007.07.023
- Silva, M. J., Samandar, E., Calafat, A. M., and Ye, X. (2015). Identification of di-2-ethylhexyl terephthalate (DEHTP) metabolites using human liver microsomes for biomonitoring applications. *Toxicol. In Vitro* 29, 716–721. doi: 10.1016/j.tiv.2015.02.002
- Singh, S., Harms, H., and Schlosser, D. (2014). Screening of ecologically diverse fungi for their potential to pretreat lignocellulosic bioenergy feedstock. *Appl. Microbiol. Biotechnol.* 98, 3355–3370. doi: 10.1007/s00253-014-5563-4
- Sobolewski, M., Weiss, B., Martin, M., Gurven, M., and Barrett, E. (2017). Toxicanthropology: phthalate exposure in relation to market access in a remote forager-horticulturalist population. *Int. J. Hyg. Environ. Health* 220, 799–809. doi: 10.1016/j.ijheh.2017.03.009
- Stanier, R. Y., Palleroni, N. J., and Doudoroff, M. (1966). The aerobic pseudomonads: a taxonomic study. *J. Gen. Microbiol.* 43, 159–271. doi: 10.1099/00221287-43-2-159
- Staples, C. A., Peterson, D. R., Parkerton, T. F., and Adams, W. J. (1997). The environmental fate of phthalate esters: a literature review. *Chemosphere* 35, 667–749. doi: 10.1016/s0045-6535(97)00195-1
- Subramanian, V., and Yadav, J. S. (2009). Role of P450 monooxygenases in the degradation of the endocrine-disrupting chemical nonylphenol by the white rot fungus *Phanerochaete chrysosporium*. *Appl. Environ. Microbiol.* 75, 5570–5580. doi: 10.1128/aem.02942-08
- Sun, C., Zhang, G., Zheng, H., Liu, N., Shi, M., Luo, X., et al. (2019). Fate of four phthalate esters with presence of *Karenia brevis*: uptake and biodegradation. *Aquat. Toxicol.* 206, 81–90. doi: 10.1016/j.aquatox.2018.11.010
- Sun, J., Huang, J., Zhang, A., Liu, W., and Cheng, W. (2013). Occurrence of phthalate esters in sediments in Qiantang River, China and inference with urbanization and river flow regime. *J. Hazard. Mater.* 24, 142–149. doi: 10.1016/j.jhazmat.2012.12.057
- Syed, K., Nelson, D. R., Riley, R., and Yadav, J. S. (2013). Genomewide annotation and comparative genomics of cytochrome P450 monooxygenases (P450s) in the polypore species *Bjerkandera adusta*, *Ganoderma* sp. and *Phlebia brevispora*. *Mycologia* 105, 1445–1455. doi: 10.3852/13-002
- Syed, K., and Yadav, J. S. (2012). P450 monooxygenases (P450ome) of the model white rot fungus *Phanerochaete chrysosporium*. *Crit. Rev. Microbiol.* 38, 339–363. doi: 10.3109/1040841X.2012.682050
- Tedersoo, L., Sanchez-Ramirez, S., Koljalg, U., Bahram, M., Doring, M., Schigel, D., et al. (2018). High-level classification of the Fungi and a tool for evolutionary ecological analyses. *Fungal Divers.* 90, 135–159. doi: 10.1007/s13225-018-0401-0
- Tran, B. C., Teil, M. J., Blanchard, M., Alliot, F., and Chevreuil, M. (2015). BPA and phthalate fate in a sewage network and an elementary river of France. Influence of hydroclimatic conditions. *Chemosphere* 119, 43–51. doi: 10.1016/j.chemosphere.2014.04.036

- Wang, J., Yamada, Y., Notake, A., Todoroki, Y., Tokumoto, T., Dong, J., et al. (2014). Metabolism of bisphenol A by hyper lignin-degrading fungus *Phanerochaete sordida* YK-624 under non-ligninolytic condition. *Chemosphere* 109, 128–133. doi: 10.1016/j.chemosphere.2014.01.029
- Wang, S. Q., Wang, Y. F., and Xu, Z. (2019). Tetrazole hybrids and their antifungal activities. *Eur. J. Med. Chem.* 170, 225–234. doi: 10.1016/j.ejmech.2019.03.023
- Wu, S., Nan, F., Jiang, J., Qiu, J., Zhang, Y., Qiao, B., et al. (2019). Molecular cloning, expression and characterization of a novel feruloyl esterase from a soil metagenomic library with phthalate-degrading activity. *Biotechnol. Lett.* 41, 995–1006. doi: 10.1007/s10529-019-02693-3

Conflict of Interest: The authors declare that the research was conducted in the absence of any commercial or financial relationships that could be construed as a potential conflict of interest.

Copyright © 2020 Carstens, Cowan, Seiwert and Schlosser. This is an open-access article distributed under the terms of the Creative Commons Attribution License (CC BY). The use, distribution or reproduction in other forums is permitted, provided the original author(s) and the copyright owner(s) are credited and that the original publication in this journal is cited, in accordance with accepted academic practice. No use, distribution or reproduction is permitted which does not comply with these terms.



Unraveling 1,4-Butanediol Metabolism in *Pseudomonas putida* KT2440

Wing-Jin Li¹, Tanja Narancic^{2,3}, Shane T. Kenny⁴, Paul-Joachim Niehoff¹, Kevin O'Connor^{2,3}, Lars M. Blank¹ and Nick Wierckx^{1,5*}

¹ Institute of Applied Microbiology-iAMB, Aachen Biology and Biotechnology-ABBt, RWTH Aachen University, Aachen, Germany, ² UCD Earth Institute and School of Biomolecular and Biomedical Science, University College Dublin, Dublin, Ireland, ³ BEACON – SFI Bioeconomy Research Centre, University College Dublin, Dublin, Ireland, ⁴ Bioplastech Ltd., NovaUCD, Belfield Innovation Park, University College Dublin, Dublin, Ireland, ⁵ Institute of Bio- and Geosciences IBG-1: Biotechnology, Forschungszentrum Jülich, Jülich, Germany

OPEN ACCESS

Edited by:

Lei Chen,
Tianjin University, China

Reviewed by:

Shanshan Liu,
The First Affiliated Hospital of Bengbu
Medical College, China
Matilde Fernandez,
University of Granada, Spain

*Correspondence:

Nick Wierckx
n.wierckx@fz-juelich.de

Specialty section:

This article was submitted to
Microbiotechnology,
a section of the journal
Frontiers in Microbiology

Received: 16 December 2019

Accepted: 20 February 2020

Published: 17 March 2020

Citation:

Li W-J, Narancic T, Kenny ST,
Niehoff P-J, O'Connor K, Blank LM
and Wierckx N (2020) Unraveling
1,4-Butanediol Metabolism
in *Pseudomonas putida* KT2440.
Front. Microbiol. 11:382.
doi: 10.3389/fmicb.2020.00382

Plastics, in all forms, are a ubiquitous cornerstone of modern civilization. Although humanity undoubtedly benefits from the versatility and durability of plastics, they also cause a tremendous burden for the environment. Bio-upcycling is a promising approach to reduce this burden, especially for polymers that are currently not amenable to mechanical recycling. Wildtype *P. putida* KT2440 is able to grow on 1,4-butanediol as sole carbon source, but only very slowly. Adaptive laboratory evolution (ALE) led to the isolation of several strains with significantly enhanced growth rate and yield. Genome re-sequencing and proteomic analysis were applied to characterize the genomic and metabolic basis of efficient 1,4-butanediol metabolism. Initially, 1,4-butanediol is oxidized to 4-hydroxybutyrate, in which the highly expressed dehydrogenase enzymes encoded within the PP_2674-2680 *ped* gene cluster play an essential role. The resulting 4-hydroxybutyrate can be metabolized through three possible pathways: (i) oxidation to succinate, (ii) CoA activation and subsequent oxidation to succinyl-CoA, and (iii) beta oxidation to glycolyl-CoA and acetyl-CoA. The evolved strains were both mutated in a transcriptional regulator (PP_2046) of an operon encoding both beta-oxidation related genes and an alcohol dehydrogenase. When either the regulator or the alcohol dehydrogenase is deleted, no 1,4-butanediol uptake or growth could be detected. Using a reverse engineering approach, PP_2046 was replaced by a synthetic promoter (14g) to overexpress the downstream operon (PP_2047-2051), thereby enhancing growth on 1,4-butanediol. This work provides a deeper understanding of microbial 1,4-butanediol metabolism in *P. putida*, which is also expandable to other aliphatic alpha-omega diols. It enables the more efficient metabolism of these diols, thereby enabling biotechnological valorization of plastic monomers in a bio-upcycling approach.

Keywords: laboratory evolution, *Pseudomonas putida*, proteomics, genomics, plastic upcycling

INTRODUCTION

Plastics, in all forms, are an ubiquitous cornerstone of modern civilization. They contribute greatly to a more efficient society, i.e., through the reduction of packaging weight, the increase in shelf life of foods, and the insulation of homes and refrigerators. Although humanity undoubtedly benefits from the versatility and durability of plastics, these characteristics also make them a tremendous

burden for the environment. To reduce this impact, strategies beyond incineration, landfill and inefficient recycling are needed.

One of these approaches involves bio-upcycling, the microbial degradation of plastics and its conversion into value-added material (Wierckx et al., 2015; Narancic and O'Connor, 2017). Proofs of principle for the microbial conversion of selected plastics are already available. For instance, polyethyleneterephthalate (PET) was pyrolyzed and subsequently converted to polyhydroxyalkanoates (PHA) (Kenny et al., 2008; Kenny et al., 2012). A similar processes enabled conversion of polystyrene and polyethylene to PHA (Ward et al., 2006; Guzik et al., 2014). Polyurethanes (PU) are hardly amenable to mechanical recycling due to their molecular diversity and the fact that many PU are thermosets which can't be molten and re-molded. PU are produced by reacting aliphatic or aromatic diisocyanates with polyols and α,ω -diols as chain extenders. Depending on the monomer composition and chain lengths, polymer properties are diverse, which is key for PU's versatility. Applications can be found in paints and coatings, in building insulation and as sealants, as well as in flexible foams and absorbents for many end-user products like pillows and mattresses. In the context of a bio-upcycling strategy, bacteria and fungi have been found to degrade PU, including several *Pseudomonads* which grow on PU at high rates (Howard, 2002). A range of PU-degrading ester- and urethane hydrolases have been identified (Hung et al., 2016; Schmidt et al., 2017; Danso et al., 2019; Magnin et al., 2019a,b). Besides this, chemical recycling of PU is also possible with more mature technologies (Zia et al., 2007; Behrendt and Naber, 2009). In addition to the diamines, which are relatively valuable and can be extracted (Bednarz et al., 2017), typical PU monomers like adipic acid, 1,4-butanediol, and ethylene glycol are released during the process of depolymerization. Degradation pathways for ethylene glycol (Franden et al., 2018; Li et al., 2019) and adipic acid (Parke et al., 2001) are known. Yet, surprisingly little is known about the microbial catabolism of 1,4-butanediol.

1,4-butanediol is one of the major chain extenders used in the production of polyurethanes. It is also a common co-monomer in many polyesters such as polybutylene terephthalate and polybutylene adipate terephthalate. As commodity chemical, 1,4-butanediol is used to manufacture 2.5 million tons of plastics and polyesters (Yim et al., 2011). Additionally, it is used as a platform chemical to produce tetrahydrofuran and γ -butyrolactone, with a total market size valued at USD 6.19 billion in 2015 and is still growing (Grand View Research, 2017). So far, research was mainly focused on the sustainable production of 1,4-butanediol (Burgard et al., 2016). Its *de novo* microbial production was achieved in *E. coli* by identifying and implementing artificial routes for 1,4-butanediol biosynthesis (Yim et al., 2011). The verified and tested pathway starts with the TCA cycle intermediate succinyl-CoA. The heterologous CoA-dependent succinate semialdehyde dehydrogenase (SucD) from *Clostridium kluyveri* and either a native or heterologous 4-hydroxybutyrate dehydrogenase from *C. kluyveri*, *Porphyromonas gingivalis* or *Ralstonia eutropha* catalyze the reaction from succinyl-CoA to 4-hydroxybutyrate. After CoA activation, 4-hydroxybutyryl-CoA will be further reduced by alcohol and aldehyde dehydrogenases

to the final product 1,4-butanediol. In addition to this commonly used pathway, alternative potential routes via α -ketoglutarate, glutamate or acetyl-CoA were described (Yim et al., 2011). Conversion of xylose to 1,4-butanediol has also been described (Liu and Lu, 2015).

Butanol is a substrate with structural similarities to 1,4-butanediol. Usually, butanol concentrations above 1–2% (135–270 mM) are toxic or at least growth-inhibiting for most of microbes, including *Pseudomonas putida* BIRD-1, DOT-T1E, and KT2440 (Cuenca et al., 2016). Nevertheless, *Pseudomonas* exhibits promising traits on tolerating, assimilating or at least surviving butanol (Rühl et al., 2009). To cope with butanol, classic solvent defense mechanisms like efflux pumps, membrane modifications or rebalancing of the redox state are activated (Ramos et al., 2002; Basler et al., 2018). Further, *P. putida* KT2440 is capable of rapid butanol oxidation to butyrate via a variety of alcohol- and aldehyde dehydrogenases (Simon et al., 2015; Vallon et al., 2015; Cuenca et al., 2016). Prominent among these are PedE, PedH, and PedI alcohol and aldehyde dehydrogenases, encoded in the so-called ped cluster. These have a highly relaxed substrate specificity and are capable of oxidizing, among others, ethanol, phenylethanol, butanol, and butanal (butyraldehyde) (Wehrmann et al., 2017). The resulting butyrate is CoA-activated by acyl-CoA synthetases like AcsA1 (PP_4487), and subsequently undergoes β -oxidation.

Non-pathogenic *Pseudomonads* have an established track record in bioremediation and biodegradation processes (Samanta et al., 2002; Spini et al., 2018; Tahseen et al., 2019), and different strains of this genus are also suitable candidates to perform bio-upcycling (Kenny et al., 2008; Wierckx et al., 2015; Wilkes and Aristilde, 2017). One of the widely used biotechnological hosts is *P. putida* KT2440, which possesses extensive metabolic abilities (Nelson et al., 2002; Nikel et al., 2014; Nikel and de Lorenzo, 2018). Being a soil bacterium and therefore exposed to different environmental surroundings, it is equipped with tolerances and metabolic capabilities toward a broad spectrum of substances. The 6.18 Mb genome of *P. putida* KT2440 harbors a broad spectrum of oxygenases, oxidoreductases as well as hydrolases, transferases, and dehydrogenases (Belda et al., 2016). This wide range of enzymes enables *P. putida* KT2440 to modify an abundance of alcohols and aldehydes (Wierckx et al., 2011).

In this work, *P. putida* KT2440 strains with an enhanced growth rate on 1,4-butanediol are obtained by adaptive laboratory evolution (ALE), and analyzed by proteomics and genome resequencing in order to determine possible degradation routes. The improved growth phenotype was subsequently reverse-engineered into the wildtype, thereby generating a deeper understanding of 1,4-butanediol metabolism and broadening the applicability of *P. putida* for plastic upcycling.

MATERIALS AND METHODS

Chemicals, Media, and Cultivation Conditions

The chemicals used in this work were obtained from Carl Roth (Karlsruhe, Germany), Sigma-Aldrich (St. Louis, MO,

United States), or Merck (Darmstadt, Germany) unless stated otherwise. Glycerol was kindly provided by Bioeton (Kyritz, Germany).

All strains used in this work are listed in **Table 1**. Cultivations were performed in LB – complex medium (10 g L⁻¹ tryptone, 5 g L⁻¹ yeast extract and 5 g L⁻¹ sodium chloride) or, for quantitative microbiology experiments, in mineral salt medium (MSM) (Hartmans et al., 1989), solidified when needed with 1.5% agar (w/v), containing different amount of C source. Precultures were supplied with 20 mM glucose, whereas 20 mM 1,4-butanediol were used for studies with 1,4-butanediol.

For plasmid maintenance, *E. coli* strains and *P. putida* KT2440 strains were cultivated in media supplemented with 50 mg L⁻¹ kanamycin, which was sterilized by using a 0.2 µm syringe filter (Carl Roth GmbH + Co. KG, Karlsruhe, Germany).

Liquid cultivations were incubated at 30°C for *Pseudomonas* and 37°C for *E. coli*, 200 rpm shaking speed with an amplitude of 50 mm in a Multitron shaker (INFORS, Bottmingen, Switzerland) using 100 mL non-baffled Erlenmeyer flasks with metal caps, containing 10 mL culture volume for a pre-culture and 500 mL non-baffled Erlenmeyer flasks with metal caps, containing 50 mL culture volume for a main culture.

For online growth detection, 96-well plates with 200 µL or 24-well plates with 4–3 mL culture volume were inoculated with a pre-culture containing 4–3 mL MSM with 20 mM glucose in 24-well System Duetz plates (Enzyscreen, Heemstede, The Netherlands), cultivated in a Multitron shaker (INFORS, Bottmingen, Switzerland) with a 300 rpm shaking speed with an amplitude of 50 mm. Inoculated Growth Profiler® plates were incubated at 30°C, 225 rpm shaking speed with an amplitude of 50 mm in the Growth Profiler® 960 (Enzyscreen, Heemstede, The Netherlands).

Adaptive laboratory evolution (ALE) was performed as follows: a pre-culture of *P. putida* KT2440, cultivated in MSM with 20 mM glucose, was used to inoculate 250 mL clear glass Boston bottles with Mininert valves (Thermo Fisher Scientific, Waltham, MA, United States) containing 20 mM 1,4-butanediol for the adaptation on 1,4-butanediol (final OD₆₀₀ of 0.01). Serial transfers were reinoculated several times after the cultures reached an OD₆₀₀ of at least 0.5, with a starting OD₆₀₀ of 0.1. After growth was detected (usually overnight), single colonies were isolated from ALE cultures by streaking samples on LB agar plates. After ALE on 1,4-butanediol, two strains (B10.1 and B10.2) out of 72 strains were selected according to their growth behavior in MSM with 20 mM 1,4-butanediol determined using the Growth Profiler® 960 (Enzyscreen, Heemstede, The Netherlands).

Growth experiments for PHA accumulation were carried out in 250 mL Erlenmeyer flasks containing 50 mL of nitrogen limited MSM medium supplemented with 80 mM 1,4 butanediol. Nitrogen limited MSM medium contains 9 g/L Na₂HPO₄·12H₂O, 1.5 g/L KH₂PO₄, 0.25 g/L NH₄Cl, trace elements. An overnight culture was prepared by inoculating 2 mL of medium with a single colony from a plate and incubating overnight at 30°C and shaking at 200 rpm. Five hundred micro liter of the 2 mL MSM overnight culture was used as an inoculum for the 50 mL cultures which were incubated under the same

conditions for 48 h. Octanoic acid (20 mM) was added to some flasks after 24 h.

Molecular Work

DNA Procedures

The construction of plasmids was performed either by standard restriction-ligation or Gibson assembly (Gibson et al., 2009) using the NEBuilder HiFi DNA Assembly (New England Biolabs, Ipswich, MA, United States). DNA modifying enzymes were purchased from New England Biolabs, for dephosphorylation Fast AP Thermo Sensitive Alkaline Phosphatase (Thermo Fisher Scientific, Langenselbold, Germany) was used. Primers were purchased as unmodified DNA oligonucleotides from Eurofins Genomics (Ebersberg, Germany) and are listed in **Supplementary Table S1**. Clonal DNA sequences were amplified using the Q5 High-Fidelity Polymerase (New England Biolabs, Ipswich, MA, United States). DNA- ligations were performed by using T4 ligase from Fermentas (Thermo Fisher Scientific, Langenselbold, Germany) according to the protocol. Arbitrary-primed PCR was performed as described by Martínez-García et al. (2014). For the transformation of DNA assemblies and purified plasmids (**Supplementary Table S2**) into competent *E. coli* a heat shock protocol was performed (Hanahan, 1983). For *P. putida* transformations either conjugational transfer or electroporation were performed as described by Wynands et al. (2018). Knockout strains were obtained using the pEMG system described by Martínez-García and de Lorenzo (2011) with a modified protocol described by Wynands et al. (2018). Plasmid inserts and gene deletions were confirmed by Sanger sequencing performed by Eurofins Genomics (Ebersberg, Germany).

In order to perform PCR directly from bacteria the alkaline polyethylene glycol-based method was used (Chomczynski and Rymaszewski, 2006). Therefore, cell material was picked and dissolved in 50 µL of the reagent, containing 60 g PEG 200 with 0.93 mL 2 M KOH and 39 mL water, with a pH of 13.4. After incubation for 3–15 min, 2 µL of the sample was used as template in a 25 µL PCR reaction.

Analytical Methods

Growth Monitoring Methods

Bacterial growth was monitored as optical density at a wavelength of $\lambda = 600$ nm (OD₆₀₀) with an Ultrospec 10 Cell Density Meter (GE Healthcare, Little Chalfont, Buckinghamshire, United Kingdom). Growth rates (μ) are determined by fitting an exponential curve to a plot of OD₆₀₀ over time of a culture in the exponential phase. The online analysis of growth using the Growth Profiler® was analyzed using the Growth Profiler® Control software V2_0_0. Cell densities are expressed as G-value, which is derived from imaging analysis of microtiter plates with transparent bottoms.

PHA Analysis

Cells were harvested by centrifugation at 3320 × g for 10 min and then lyophilized and weighed for determination of cell dry weight. PHA content was determined by subjecting lyophilized cells to acidic methanolysis (Brandl et al., 1988; Lageveen et al., 1988). Five to ten milligram of dried cells were resuspended

TABLE 1 | *Pseudomonas putida* strains used in this work with listed genotype and references.

No.	Strain	Genotype	References
1	KT2440 wildtype	Cured, restriction-deficient derivative of <i>P. putida</i> mt-2	Bagdasarian et al., 1981
2	B10.1	KT2440 ALE in BDO, single strain A6	This work
3	B10.2	KT2440 ALE in BDO, single strain C2	This work
4	KT2440 ΔPP_2046	ΔPP_2046 in KT2440	This work
	B10.1 ΔPP_2046	ΔPP_2046 in B10.1	This work
	B10.2 ΔPP_2046	ΔPP_2046 in B10.2	This work
5	KT2440 ΔPP_2046:14g	ΔPP_2046:14g in KT2440	This work
	B10.1 ΔPP_2046:14g	ΔPP_2046:14g in B10.1	This work
	B10.2 ΔPP_2046:14g	ΔPP_2046:14g in B10.2	This work
6	KT2440 Δped	ΔpedE-I in KT2440	Li et al., 2019
7	KT2440 ΔpedE	ΔpedE in KT2440	This work
	KT2440 ΔpedH	ΔpedH in KT2440	This work
8	KT2440 ΔpedI	ΔpedI in KT2440	This work
9	KT2440 ΔPP_2047-2051	knockout PP_2047-51 in KT2440	This work
	B10.A ΔPP_2047-2051	knockout PP_2047-51 in B10.A	This work
	B10.B ΔPP_2047-2051	knockout PP_2047-51 in B10.B	This work
10	KT2440 ΔPP_2049	ΔPP_2049 in KT2440	This work
	B10.1 ΔPP_2049	ΔPP_2049 in B10.1	This work
	B10.2 ΔPP_2049	ΔPP_2049 in B10.2	This work
11	KT2440 ΔPP_2051	ΔPP_2051 in KT2440	This work
	B10.1 ΔPP_2051	ΔPP_2051 in B10.1	This work
	B10.2 ΔPP_2051	ΔPP_2051 in B10.2	This work
	KT2440 ΔPP_0411-13	ΔPP_0411-13	This work
	B10.1 ΔPP_0411-13	ΔPP_0411-13	This work
	B10.2 ΔPP_0411-13	ΔPP_0411-13	This work

in 2 mL of acidified methanol (15% H₂SO₄, v/v) and 2 mL of chloroform containing 6 mg/l benzoate methyl ester as an internal standard. The solution was placed in 15 mL Pyrex test tubes, sealed and incubated at 100°C for 3 h. The tubes were then placed on ice for 1 min. One milliliter of water was added to each tube and the solution mixed by vigorous vortexing. The phases were allowed to separate, and the organic phase was removed and passed through a filter before further analysis.

The 3-hydroxyalkanoic acid methyl esters were analyzed by gas chromatography (GC) using an Agilent 6890N chromatograph equipped with a HP Innnowax column (30 m × 0.25 mm × 0.5 μm) and a flame ionization detector (FID). An oven ramp cycle was employed as follows, 120°C for 5 min, increasing by 3°C/min to 180°C, 180°C for 10 min. A 20:1 split was used with helium as the carrier gas and an inlet temperature of 250°C. Commercially available 3-hydroxyalkanoic acids (Bioplastech Ltd., Dublin, Ireland) were methylated as described above for PHA samples and used as standards to identify PHA monomers.

Extracellular Metabolites

For measuring extracellular metabolites, samples taken from liquid cultivation were centrifuged for 3 min at 17,000 × g to obtain supernatant for High-Performance Liquid Chromatography (HPLC) analysis using a Beckman System Gold 126 Solvent Module equipped with a Smartline 2300 refractive index detector (Knauer, Berlin, Germany). Analytes were eluted using a 300 × 8 mm organic acid resin

column together with a 40 × 8 mm organic acid resin precolumn (both from CS Chromatographie, Langerwehe, Germany) with 5 mM H₂SO₄ as mobile phase at a flow rate of 0.7 mL min⁻¹ at 70°C (Li et al., 2019).

Genome Sequencing

Genomic DNA for resequencing was isolated through a High Pure PCR Template Preparation Kit (ROCHE life science, Basel, Switzerland). Sequencing and SNP/InDel (single nucleotide polymorphism/insertion and deletion polymorphism) calling was done by GATC (Konstanz, Germany) using Illumina technology as paired-end reads of 125 base pairs. To map the reference sequence against the database, BWA with default parameters was used (Li and Durbin, 2009). SNPs and InDels, analyzed by GATK's UnifiedGenotyper (McKenna et al., 2010; DePristo et al., 2011), were listed and visualized with the Integrative Genomics Viewer (IGV) (Thorvaldsdóttir et al., 2013).

The sequences have been deposited in the NCBI Sequence Read Archive (SRA) with the accession number SRP148839 for ethylene glycol ALE strains (including our laboratory wildtype SRX4119395 used in this study) and SRP148839 for the 1,4-butanediol ALE strains.

Proteomics

The evolved strains B10.1 and B10.2 were cultivated along with the wild type *P. putida* KT2440 in 50 mL MSM medium supplemented with 20 mM 1,4-butanediol or 13 mM glucose (both equivalent to 80 mM C). The cultures were harvested

by centrifugation and prepared for proteomic analysis as previously described (Narancic et al., 2016). Samples were sent to T. Narancic at University of Dublin to perform the following protocol. For total protein concentrations, peptide fragments obtained by trypsin digestion were analyzed on the Q-Exactive Hybrid Quadrupole Orbitrap Mass Spectrometer (MS; Thermo Fisher Scientific) connected to a Dionex Ultimate 3000 (RSLCnano; Thermo Fisher Scientific) chromatography system (Buffer A: 97% water, 2.5% acetonitrile, 0.5% acetic acid; buffer B: 97% acetonitrile, 2.5% water, 0.5% acetic acid; all solvents were LC-MS grade). The mass spectrometer was operated in positive ion mode with a capillary temperature of 320°C and a potential of 2300 V applied to the frit. All data were acquired with the MS operating in automatic data-dependent switching mode. A high-resolution (70,000) MS scan (300–1600 m/z) was performed using the Q Exactive to select the 12 most intense ions prior to MS/MS analysis using HCD. The identification and quantification were performed using the Andromeda peptide identification algorithm integrated into MaxQuant (Cox and Mann, 2008; Cox et al., 2011). *P. putida* KT2440 protein sequence database downloaded from UniProt¹ in April 2016 was used as a reference (The UniProt Consortium, 2019). Label-free quantification (LFQ) was used to compare the expression level of proteins across samples and growth conditions (Wang et al., 2003). Proteins with a twofold change or higher and a significant change in *t*-test (FDR 0.01) were automatically accepted, while spectra with no specific change were manually checked for quality.

Each sample had three biological replicates, and each biological replicate was then prepared for the proteomic analysis as a technical replicate. Statistical analysis was performed using Perseus and built-in Welch's *t*-test with FDR set at 0.01 (Tyanova et al., 2016). The proteins with at least twofold change were functionally annotated using David bioinformatics (Huang et al., 2009a,b) and clustered into orthologous groups using EggNOG (Huerta-Cepas et al., 2016).

Detection of Dehydrogenase Activity

To perform the enzyme assay, cells from a pre-culture were used to inoculate the main culture containing 20 mM glucose and 5 mM 1,4-butanediol. After 16 h of cultivation, crude extract was isolated using BugBuster (Merck, Darmstadt, Germany) and was desalted using PD-desalting columns (GE Healthcare, Buckinghamshire, United Kingdom) and eluted in 100 mM glycinglycin buffer. Protein concentrations were estimated by standard Bradford test at 595 nm. For the dehydrogenase assay, a modified protocol from Kagi and Vallee (1960) was followed, in which 5 mM 4-hydroxybutyrate or 4% ethanol as control were used as substrate. The formation of NADH was measured at 340 nm in a 96-well-plate at 30°C in a well plate reader from Synergy Mx from Biotek (Bad Friedrichshall, Germany). To obtain a homogeneous mixture, after the addition of NAD⁺ or 4-hydroxybutyrate, the well-plate was shaken for 3 s at highest speed available.

Statistics

Statistical probability values were, if not stated otherwise, calculated using a paired Student's *t*-distribution test with homogeneity of variance ($n = 3$, significance level of 0.05). In case of duplicates, errors are expressed as deviation from the mean ($n = 2$).

RESULTS

Isolation of Strain With Enhanced Growth on 1,4-Butanediol by ALE

To study the growth of *P. putida* KT2440 and possible intermediate production when metabolizing 1,4-butanediol, growth experiments in shake flasks were performed. The wildtype showed poor growth ($\mu_{\max} = 0.082 \pm 0.004 \text{ h}^{-1}$) on MSM with 20 mM 1,4-butanediol, requiring more than 50 h to consume all substrate ($t = 49$; $1.3 \pm 0.1 \text{ mM}$), while secreting high levels of the oxidation product 4-hydroxybutyrate ($t = 49 \text{ h}$; $16.8 \pm 0.3 \text{ mM}$) (Figure 1). This slow growth implies that in principle the metabolic routes are present in *P. putida* KT2440, but they are not operating optimally under the chosen conditions.

To enhance its ability to grow on 1,4-butanediol, wildtype *P. putida* KT2440 was subjected to ALE. This method is known to enable the selection of mutated strains with enhanced properties toward specific environments, likely affecting transcriptional regulatory systems (Dragosits and Mattanovich, 2013; Lennen et al., 2019; Li et al., 2019). Cultures of *P. putida* KT2440 were serially re-inoculated to fresh media containing 20 mM 1,4-butanediol ten times, as soon as growth was observed in form of optical densities above 0.8 (Figure 1). All three parallel evolution lines grew with the same trend. While the first three batches reached an OD₆₀₀ between 0.8 and 2 after 3–4 days, later batches reached an OD₆₀₀ between 2.5 and 3.5 after 2 days or less. The ALE was stopped after approximately 47 generations, when growth on 1,4-butanediol reached an OD₆₀₀ of 2.5 overnight. Single colonies were isolated by streaking the three ALE cultures on LB plates. From each of the three evolution lines, 24 single colonies were tested for growth on 1,4-butanediol in a 96-well plate using a Growth Profiler® (Figure 1). Overall, the growth of these single clones was relatively similar, indicating a rather homogeneous evolved population. The two strains with the highest growth rates were selected, from different evolutionary lines, according to their growth in MSM with 20 mM 1,4-butanediol. These isolated clonal strains are named B10.1 and B10.2 (Figure 1).

The two evolved strains grew faster on 1,4-butanediol than the wildtype, even after several generations in complex medium or MSM containing glucose, indicating that the observed phenotype was evolutionary fixed in the genome. The single evolved isolates B10.1 and B10.2 reach growth rates of $0.33 \pm 0.054 \text{ h}^{-1}$ and $0.31 \pm 0.001 \text{ h}^{-1}$, respectively. In contrast to the wildtype they completely consume all carbon source, reaching maximum biomass concentrations of $1.05 \pm 0.0 \text{ g}_{\text{cdw}} \text{ L}^{-1}$ and $0.96 \pm 0.02 \text{ g}_{\text{cdw}} \text{ L}^{-1}$ after 33 h. This translates to an average biomass yield of $0.56 \pm 0.025 \text{ g/g}$ for the evolved strains. This relatively high yield

¹ www.uniprot.org

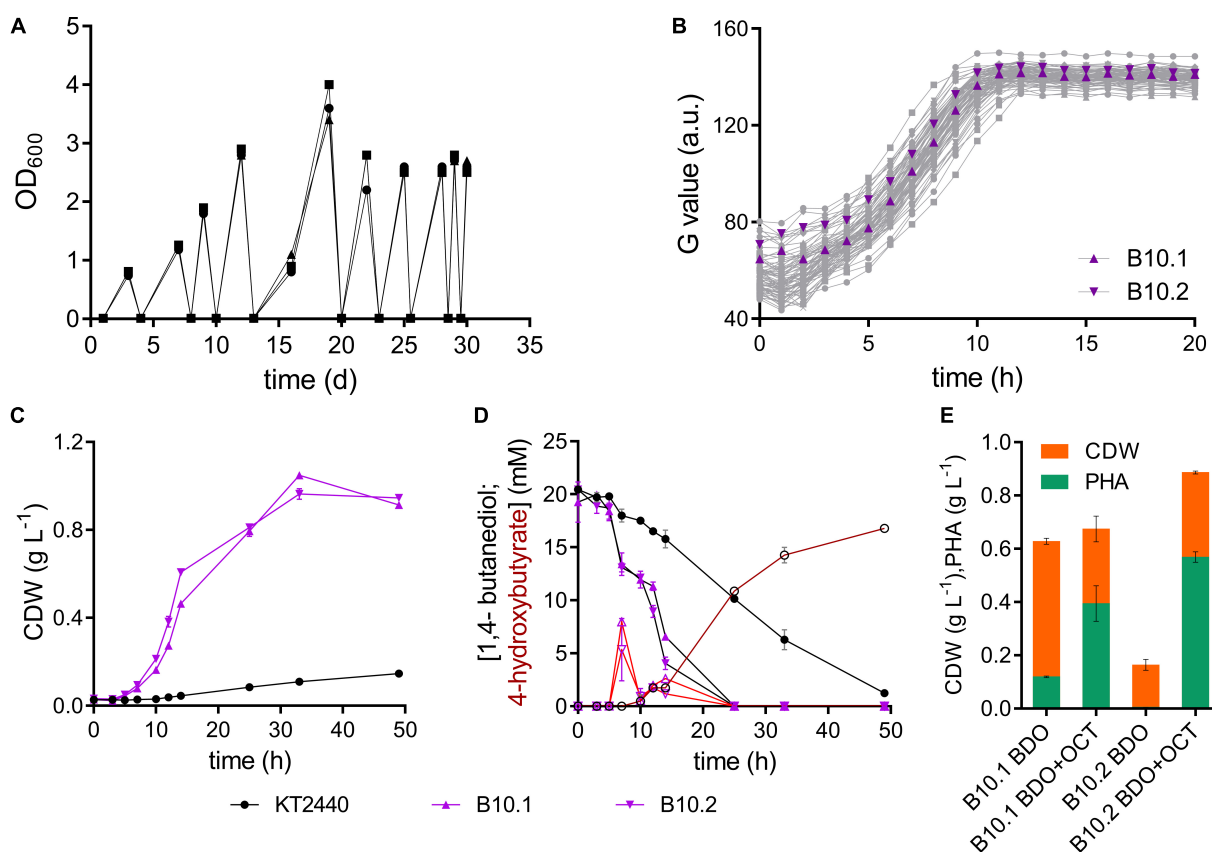


FIGURE 1 | Adaptive laboratory evolution of *P. putida* KT2440 on 1,4-butanediol. **(A)** Three parallel sequential batch cultivations on MSM with 20 mM 1,4-butanediol. **(B)** Growth of single strains isolated from each ALE batch on MSM with 20 mM 1,4-butanediol. The strains B10.1 (purple triangle) and B10.2 (purple inverted triangle) were selected for further investigation. Growth was detected via a Growth Profiler® using a 96-well plate. **(C)** Biomass growth and **(D)** 1,4-butanediol (closed symbols, black lines) and 4-hydroxybutyrate (open symbols, red lines) measured in cultures of the wildtype and evolved strains B10.1 and B10.2 in MSM with 20 mM 1,4-butanediol. **(E)** Growth and PHA formation of strains B10.1 and B10.2 cultivated for 48 h in nitrogen-limited MSM medium with 80 mM 1,4-butanediol (BDO), supplemented with or without 20 mM octanoic acid (OCT) after 24 h. Cultures took place in 250 mL Erlenmeyer shake flasks with a culture volume of 50 mL. Error bars indicate the deviation of the mean ($n = 2$).

is likely caused by the high degree of reduction of butanediol, providing considerable reducing equivalents especially in the initial oxidation reactions (Li et al., 2019). In contrast to the wildtype, the evolved strains only transiently accumulate low concentrations of 4-hydroxybutyrate, which are rapidly metabolized within 4 h (Figure 1). All 1,4-butanediol and derivatives that could be detected by HPLC were consumed within 25 h, although biomass still increased significantly beyond this point. Other intermediates not detected by HPLC, possibly the lactone of 4-hydroxybutyrate, could likely accumulate transiently in the cultures of the evolved strains. However, the high biomass yield suggests that all carbon source was consumed at the end of the culture.

In order to assess the applicability of these evolved strains in a bio-upcycling approach, they were cultured in a nitrogen-limited MSM medium with 80 mM 1,4-butanediol. Further cultures were supplemented with 20 mM octanoic acid after 24 h. These conditions enable the production of polyhydroxyalkanoate (PHA) from a (co)-feed of 1,4-butanediol. Without octanoic acid co-feed, strain B10.1 strains reached a final biomass concentration of $0.63 \pm 0.11 \text{ g L}^{-1}$, of which 19% ($0.12 \pm 0.003 \text{ g}$

L^{-1}) is PHA. Surprisingly, strain B10.2 reached a much lower biomass density, with only 3% PHA. With an octanoic acid co-feed, strain B10.2 reached the highest biomass concentrations of $0.89 \pm 0.005 \text{ g L}^{-1}$, of which 64% ($0.57 \pm 0.02 \text{ g L}^{-1}$) is PHA (Figure 1). This proves that 1,4-butanediol can be used as a (co)-substrate for the production of a value-added biopolymer, thereby in principle enabling the upcycling of e.g., hydrolyzed PU or polyester waste.

Evolution successfully yielded strains with a 4- or 3.7-fold improved growth rate on 1,4-butanediol compared to the wildtype. The fact that the wildtype accumulates much more 4-hydroxybutyrate than the evolved strains indicates that this is likely the main metabolic bottleneck which was affected by ALE.

Systems Analysis of 1,4-Butanediol Degradation in *P. putida* KT2440

To investigate the molecular basis of their enhanced growth on 1,4-butanediol, the genomes of the evolved strains B10.1 and B10.2 were resequenced (NCBI SRA accession number SRP148839). The sequences were compared to our laboratory

wildtype (SRX4119395) and a reference database genome of *P. putida* KT2440 (Belda et al., 2016, AE015451.2). A comparison of the latter two was previously described in the context of ethylene glycol metabolism in *P. putida* (Li et al., 2019). Therefore, we focus here only on differences between our laboratory wildtype and the B10 strains. In the evolved strains B10.1 and B10.2, seven and eight mutations, respectively, were identified in addition to the mutations already present in the laboratory wildtype. Most of these mutations were either silent or intergenic. In addition to these, in the genome of B10.1, an in-frame deletion of 69 bp was found in PP_2139, encoding DNA topoisomerase I. Since this enzyme is related to DNA replication and repair (Wang, 2002), this alteration is unlikely to affect 1,4-butanediol metabolism specifically. However, this mutation might still be favorable in a general sense by affecting growth rate through DNA replication. Furthermore, a missense mutation was identified B10.2 that affects PP_2889, encoding the transmembrane anti-sigma factor PrtR (Calero et al., 2018; **Supplementary Table S3**). An amino exchange (A240G, GCG/GGG) in this regulator, involved in temperature-related protease production (Burger et al., 2000), might enhance tolerance toward 1,4-butanediol and its oxidation products. Both of these mutations are likely related to general ALE effects selecting for faster growth or higher tolerance to chemical stressors, rather than affecting the operation of the metabolic network.

The PP_2046 gene, encoding for a LysR-type transcriptional regulator, stood out for being mutated in both evolved strains, with each carrying a different mutation. In B10.1, a nonsense mutation caused the loss of the start codon (ATG/ATA), while in B10.2 a missense mutation caused an amino acid exchange (E34G, GAG/GGG) in the helix-turn-helix DNA binding domain of the regulator (**Supplementary Figure S1** and **Supplementary Table S3**). The mutations in this regulator likely affect the expression of the adjacent operon PP_2047-51 which encodes an iron-containing alcohol dehydrogenase, as well as enzymes involved in β -oxidation (Li et al., 2019).

In addition to the analysis of the changes on the genome level, proteomic analysis of the evolved strains and the wildtype during growth on glucose and 1,4-butanediol was conducted. This was done to identify relevant enzymes that are either constitutively expressed or natively induced by 1,4-butanediol. Three biological samples from each strain and culture condition, either grown on glucose or 1,4-butanediol in MSM, were harvested at mid-log phase (**Supplementary Figure S2**). The samples were normalized using total protein concentration to give the same starting protein concentration for all replicates.

In total, 2122 proteins were identified across all samples and growth conditions, representing 40% of the *P. putida* KT2440 proteome. The identified proteins exhibited a wide range of annotated biophysical (molecular mass, isoelectric point), biochemical (functional annotations) and structural (domains) properties, suggesting that the analysis was not biased in favor of, or against, any protein class.

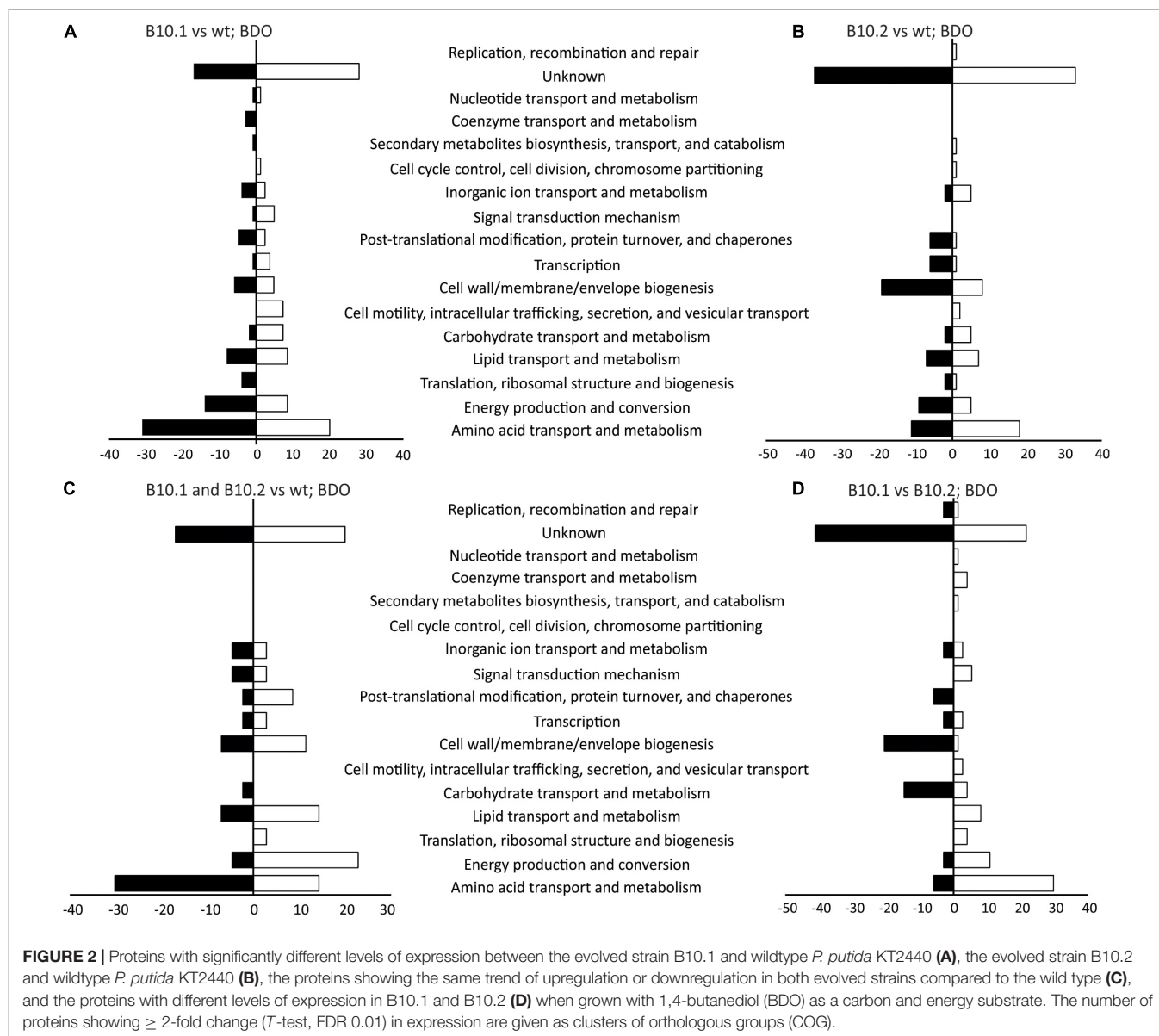
When cultivated on 1,4-butanediol the evolved strain B10.1 expressed 19 proteins which were not present in the wildtype,

while 313 proteins were up- or downregulated at least two-fold compared to the wildtype. When evolved strain B10.2 was compared to the wildtype, 138 proteins showed at least two-fold difference in expression. The two evolved strains differed in their expression of 126 proteins. A large fraction of the differentially expressed proteins have no known function (**Figure 2** and **Supplementary Data File S2**). The second-largest group can be categorized in amino acid metabolism and transport according to the clusters of orthologous groups (COG) classification (Tatusov et al., 1997). The likely reason for this large number of proteins with different expression levels is a large difference in growth rate of the B10 strains and the wildtype on 1,4-butanediol and the turnover of proteins during growth.

The top three highest expressed proteins during growth on glucose as well as 1,4-butanediol were PedE (ethanol dehydrogenase – PP_2674), PedI (aldehyde dehydrogenase – PP_2680) and Tu-B (PP_0452), an elongation factor which is involved in the regulation of protein synthesis by mediating aminoacyl tRNA into a free site of ribosomes (Noel and Whitford, 2016). The latter Tu-B is a general growth-associated protein (Klumpp et al., 2009). The former two proteins are encoded within the ped cluster (PP_2663-80) (Li et al., 2019). To focus on 1,4-butanediol metabolism, specific proteins with activities in putative catabolic pathways (**Figure 3**) and associated transport steps were further investigated.

Genome sequencing uncovered mutations in PP_2046. The corresponding protein was not detected in the proteome analysis, indicating no or a low basal expression below the detection limit of the applied method, which is not uncommon for transcriptional regulators. Proteins encoded by the downstream β -oxidation-related operon were strongly upregulated in the wildtype grown on 1,4-butanediol vs. glucose, including a 3-hydroxyacyl-CoA dehydrogenase (PP_2047, 22-fold), an acyl-CoA dehydrogenase (PP_2048, 16-fold), an iron-containing alcohol dehydrogenase (PP_2049, 52-fold), and an acetyl-CoA acetyltransferase (PP_2051, 25-fold). The hypothetical protein PP_2050 was not detected. On top of this strong induction by 1,4-butanediol in the wildtype, the genes in this operon were even further induced by 2.4- to 3-fold in the evolved strains compared to the wildtype (**Figure 3** and **Supplementary Data File S2**).

Theoretically, 1,4-butanediol can be metabolized through three possible pathways, all branching off at the point of 4-hydroxybutyrate. This 4-hydroxybutyrate was rapidly formed in cultivations of wildtype *P. putida* KT2440 on 1,4-butanediol, and also accumulates transiently with the B10 strains (**Figure 1**). This shows that oxidation of 1,4-butanediol to 4-hydroxybutyrate via alcohol and aldehyde oxidases already occurs at a high rate in the wildtype. The high expression levels of PedE, PedH and PedI suggest that these enzymes are major players in these oxidation steps. Although the encoding genes were not affected by the ALE, and they are only marginally upregulated when the strains were grown with 1,4-butanediol in comparison with growth on glucose, they are constitutively expressed on a very high level. This indicates a considerable metabolic investment of *P. putida* to be prepared for alcohol and aldehyde oxidation. This rapid oxidation is especially important for tolerance against the



highly toxic aldehydes (Franden et al., 2018). Apparently, *P. putida* encounters such aldehydes often enough in its native environment to warrant this high constitutive expression. Besides these two enzymes, a number of other oxidoreductases are strongly induced upon growth on 1,4-butanediol vs. glucose. These include the GMC family oxidoreductase PP_0056 (BetA-I, along with its associated transporter PP_0057), the iron-containing alcohol dehydrogenase PP_2049, the 3-hydroxybutyrate dehydrogenase PP_3073 (HbdH), the isoquinoline oxidoreductase PP_3621-3 (IorAB-adhB), and the aldehyde dehydrogenase PP_5258 (amaB).

The resulting 4-hydroxybutyrate can theoretically be further oxidized by the same enzymes. However, the presence of a negatively charged carboxylate moiety likely affects substrate binding and it is more plausible that one or several other oxidoreductases with annotated activities on molecules with

a carboxylate group similar to 4-hydroxybutyrate perform these oxidations. Several of such enzymes were upregulated during growth on 1,4-butanediol vs. glucose, including a 3-hydroxyisobutyrate dehydrogenase (PP_4666, MmsB) and a methylmalonate semialdehyde dehydrogenase (PP_4667 MmsA-II) (Steele et al., 1992; Zhou et al., 2013) for the alcohol oxidation step. The resulting succinate semialdehyde can be oxidized by the annotated succinate semialdehyde dehydrogenases PP_0213 (GabD-I) and PP_3151 (SadI), but also possibly by the methylmalonate-semialdehyde dehydrogenase PP_4667 (MmsA-II). The resulting oxidation product succinate can be further metabolized in the TCA cycle. The low growth rate of the wildtype indicates that, although multiple putative proteins for both activities are expressed at a high level, these latter two oxidations only occur at a low rate at best, with a likely bottleneck in the oxidation of 4-hydroxybutyrate.

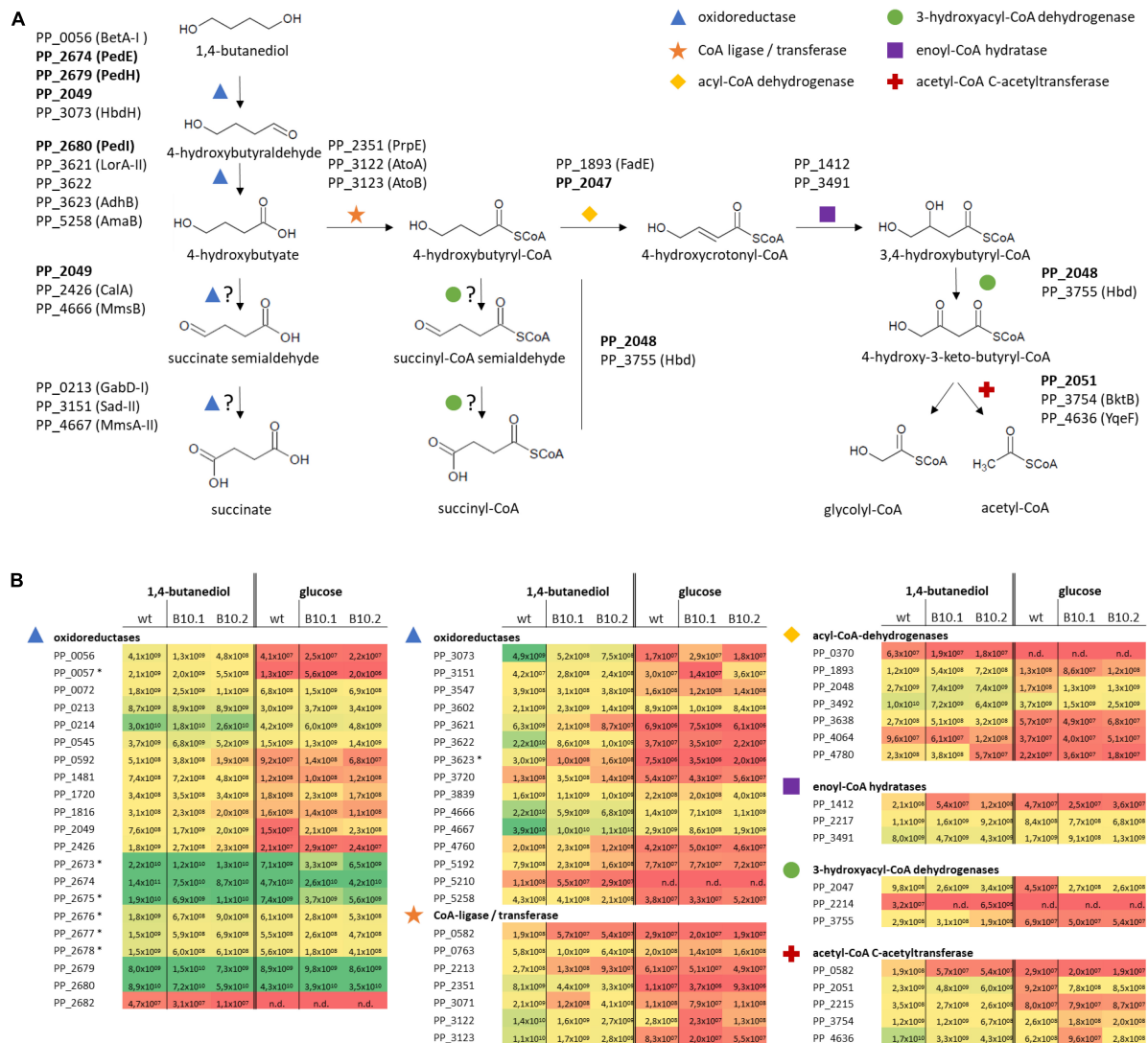


FIGURE 3 | Hypothetical pathways for 1,4-butanediol metabolism **(A)** and expression levels (Label Free Quantification, LFQ; Tyanova et al., 2016) representing the sum of the ion signal recorded in the mass spectrometer for all peptides derived from each protein of the corresponding proteins **(B)**. Colors correspond to LFQ levels, red for low, yellow for average, and green for high values. Proteins which are strongly upregulated in response to growth on MSM with 1,4-butanediol compared to growth with glucose, or which have high expression level in all tested conditions, are indicated in **(A)**, with proteins further investigated in this work in bold. Protein expression levels **(B)** of selected proteins for *P. putida* KT2440 and the evolved strains B10.1 and B10.2 growing in MSM with glucose or 1,4-butanediol are listed as oxidoreductases (blue triangle), CoA-ligases (orange star), acyl-CoA dehydrogenases (yellow diamond), 3-hydroxyacyl-CoA dehydrogenase (green circle), enoyl-CoA hydratases (purple rectangle), and acetyl-CoA C-acetyltransferase (red cross). n/d, not detected. In case of operons, associated transporters or accessory proteins are included, marked with *.

As an alternative hypothesis to this direct oxidation route, 4-hydroxybutyrate can also be CoA-activated via CoA ligases or transferases. After CoA activation, 4-hydroxybutyryl-CoA can undergo β -oxidation, possibly through enzymes encoded by the PP_2047-51 operon downstream of PP_2046, which would result in glycolyl-CoA and acetyl-CoA (Figure 4). Other β -oxidation related proteins were also identified by the proteome analysis. Glycolyl-CoA may be converted into glycolate and subsequently metabolized through native pathways of *P. putida* (Li et al., 2019). Theoretically, 4-hydroxybutyryl-CoA could also be further oxidized by acyl-CoA dehydrogenases

to generate succinyl-CoA, provided that these have a side activity on the 4-hydroxy group instead of their usual 3-hydroxylated substrates.

Also of note was the relatively strong differential expression of genes related to the metabolism and transport of amines. The PP_0411-4 operon was highly expressed in the wildtype, but not in the evolved strains, during growth on 1,4-butanediol (Supplementary Data File S2). This operon encodes a polyamine ABC transporter for spermidine and putrescine, which are structurally and chemically similar to 1,4-butanediol. In spite of this large differential expression, no genomic mutations were

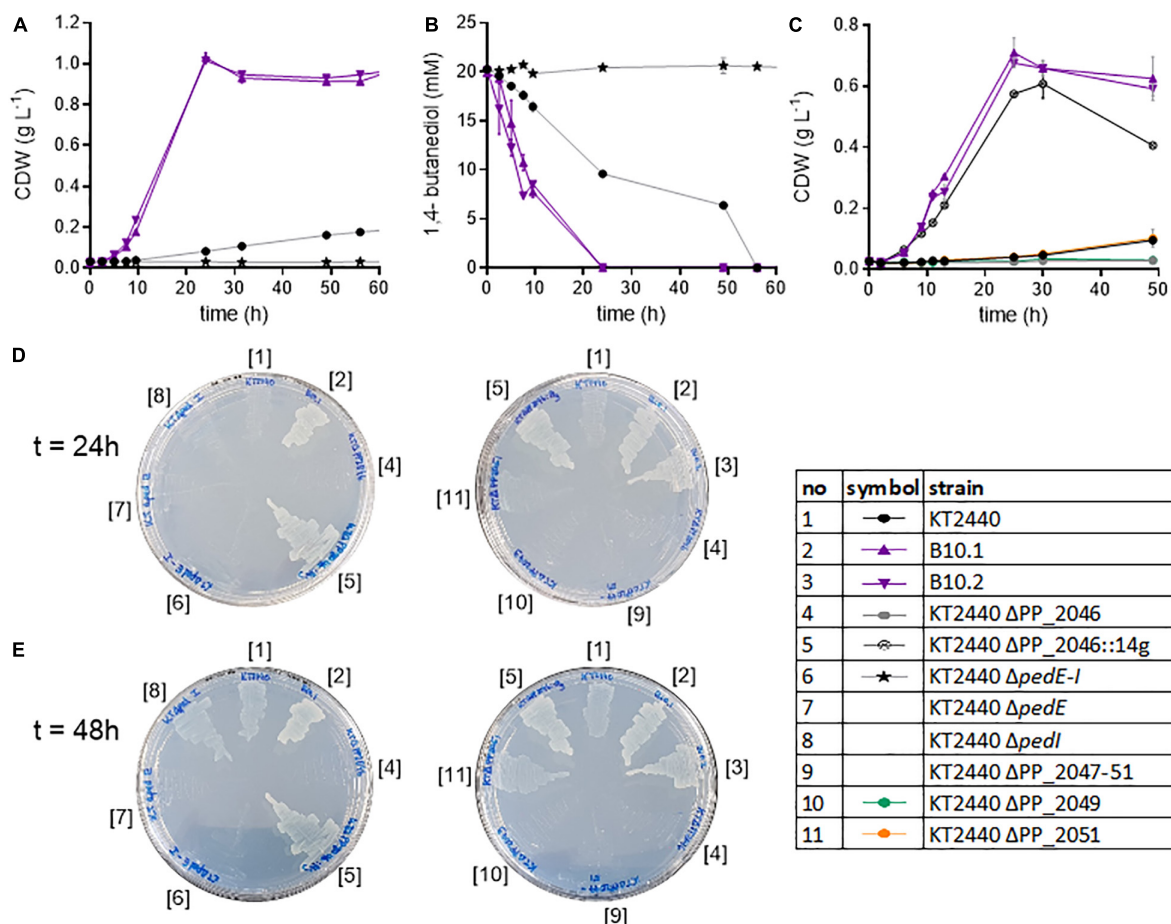


FIGURE 4 | Analysis of knockout strains of *P. putida* KT2440. Biomass growth (A) and 1,4-butanediol concentrations (B) of the wildtype, evolved strains and the Δ pedE-I knockout cultivated in shake flasks in MSM with 20 mM 1,4-butanediol. Growth of selected strains on 20 mM 4-hydroxybutyrate (C). Growth of selected strains on MSM agar plates with 20 mM 1,4-butanediol after 24 h (D) and 48 h (E). Strain numbers next to the plates correspond to full strain names listed in Table 1. The contrast of the images was increased by 20% to improve visibility. Error bars indicate the deviation of the mean ($n = 2$).

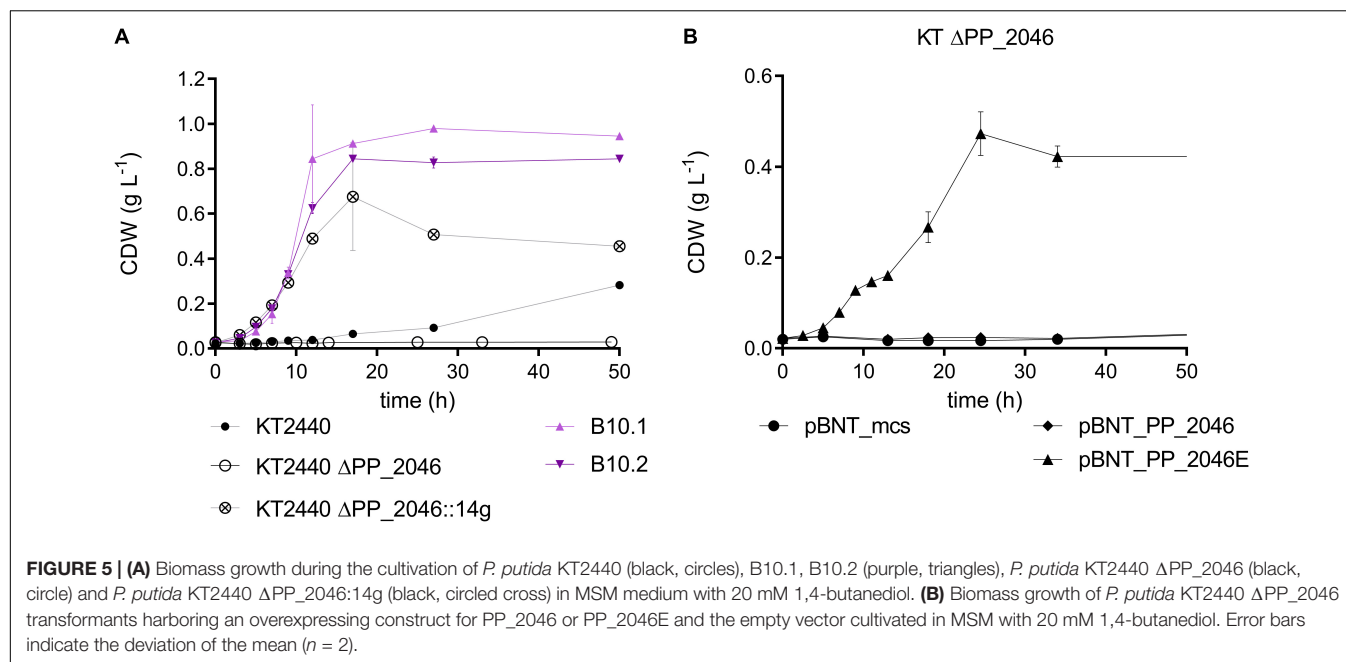
found in the evolved strains surrounding the operon, and the knockout of PP_0411-14 in *P. putida* KT2440 did not influence growth on 1,4-butanediol (data not shown). In contrast, operons encoding metabolic pathways for 4-aminobutanoate (PP_2013-15), ethanolamine (PP_0542-44), and ornithine (PP_0999-1001) were strongly upregulated on 1,4-butanediol vs. glucose (Supplementary Data File S2). The metabolism of some of these amines shares metabolic intermediates with the putative 1,4-butanediol pathways (Bandounas et al., 2011). Possibly, the high accumulation of 4-hydroxybutyrate in the wildtype induced the expression of these genes, leading to a misregulation during growth on 1,4-butanediol. Alternatively, one of the aldehyde intermediates may undergo amination, or the diamine transporter may facilitate uptake of 1,4-butanediol or its oxidation products.

Pathway Validation

The abovementioned genomic and proteomic analyses indicate several possible genes and enzymes that are either natively

expressed at a high level, upregulated in the presence of 1,4-butanediol, or activated by ALE. To test the relevance of these genes for 1,4-butanediol metabolism, several knockout strains were generated. The dehydrogenases encoded in the ped cluster (PP_2673-80) were constitutively expressed at a high level (Figure 3). To test the importance of these dehydrogenases to the degradation of 1,4-butanediol, the entire cluster (Δ pedE-I), as well as individual genes *pedE* and *pedI*, were knocked out in *P. putida* KT2440. When *P. putida* KT2440 Δ pedE-I was cultivated in MSM with 1,4-butanediol no growth could be observed, nor was the substrate taken up or converted to 4-hydroxybutyrate (Figure 4). Therefore, this cluster appears to be essential for the uptake and metabolism of 1,4-butanediol. The fact that no oxidation products were observed strongly suggests that these enzymes catalyze the initial oxidation steps.

The single knockouts of *pedE* and *pedI* were streaked on MSM plates containing 20 mM 1,4-butanediol as sole carbon source. Of these knockouts, *P. putida* KT2440 Δ pedE did not grow, while the Δ pedI strain displayed growth similar to the wildtype after 48 h (Figure 4). Thus, the PQQ-dependent alcohol dehydrogenase

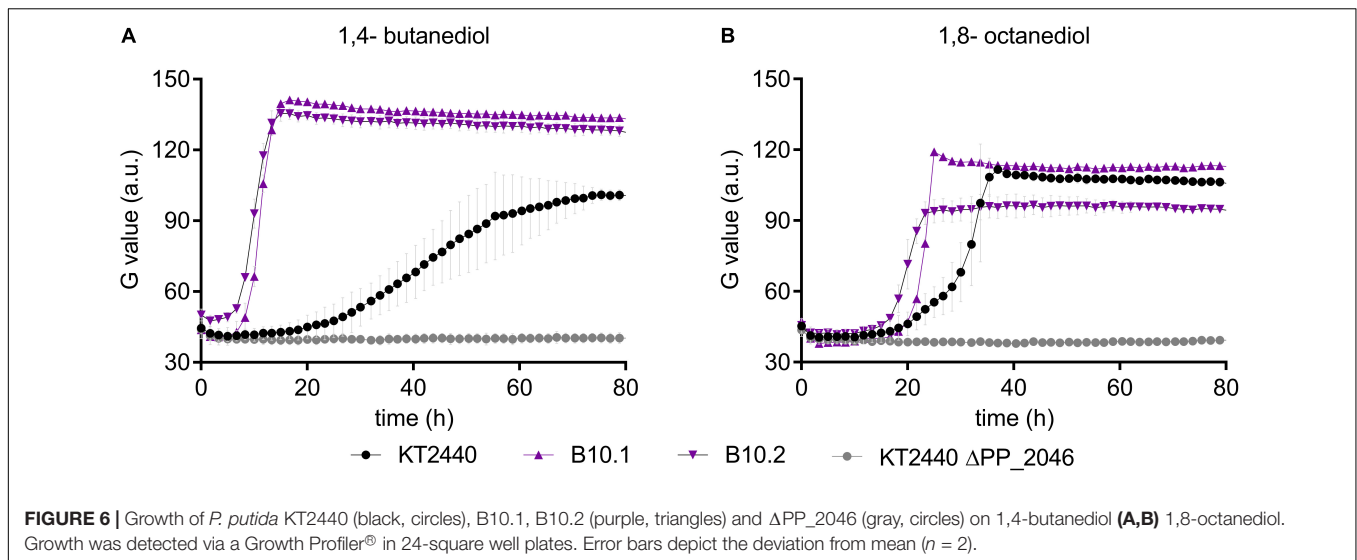


PedE is likely responsible for the oxidation of 1,4-butanediol, while, surprisingly, the aldehyde dehydrogenase PedI does not seem to play an essential role in the further oxidation steps, likely because of the high redundancy of aldehyde dehydrogenases in *P. putida*. PedE, a homolog to ExaA from *P. aeruginosa*, is an extensively investigated pyrroloquinoline quinone alcohol dehydrogenase with a broad substrate activity, including 1-butanol and 1,4-butanediol (Takeda et al., 2013). Furthermore, Wehrmann et al. (2017) showed activities of PedE toward structural similar alcohols and aldehydes of 1,4-butanediol, like 1-butanol and butyraldehyde. Additionally, the first steps of 1-butanol assimilation in *P. putida* BIRD-1 also involve homologs of the *ped* cluster (Simon et al., 2015; Vallon et al., 2015; Cuenca et al., 2016). The other dehydrogenases encoded within the *ped* cluster, PedH and also PedI, seem to be of minor relevance. PedE and PedH are both ethanol dehydrogenases but are inversely regulated by lanthanides. In the absence of those rare earth elements, *pedE* expression is induced and *pedH* is repressed (Wehrmann et al., 2017). Both PedE and PedH are highly expressed, but considering the absence of lanthanides, it is likely that PedH is not active.

The mutations found in PP_2046 and the upregulation of the adjacent operon PP_2047-51 strongly indicates an important role of the encoded enzymes. This operon contains an iron-containing alcohol dehydrogenase encoded by PP_2049 in addition to β -oxidation related genes. In literature, this dehydrogenase is placed in a context of β -oxidation, likely due to its association with the other genes in the PP_2047-51 operon (Poblete-Castro et al., 2012). However, PP_2049 is classified as an iron-containing alcohol dehydrogenase, which belongs to type III non-homologous NAD(P)⁺-dependent alcohol dehydrogenases (Mitchell et al., 2019). This family is known to have activity toward methanol, ethanol, propanol, and butanol (Hui et al.,

1987; Gaona-López et al., 2016). It is highly likely that PP_2049 oxidizes one or more of the alcohol groups of 1,4-butanediol. Thus, neither direct oxidation to succinate nor β -oxidation can be ruled out by the observed mutation in PP_2046 and the upregulation of the associated operon. In order to determine the relevance of the operon and to distinguish between the effect of the alcohol dehydrogenase and the β -oxidation related genes, the operon and individual genes PP_2046, PP_2049, and PP_2051 were knocked out in wildtype *P. putida* KT2440 and in the evolved strains B10.1 and B10.2. Care was taken to avoid polar effects in the in-operon knockouts by leaving start and stop codons of overlapping genes intact using the pEMG system (Martínez-García and de Lorenzo, 2011). Deletion strains were tested for their ability to grow on MSM with 1,4-butanediol or 4-hydroxybutyrate as sole carbon source (Figure 4).

Both the wildtype and the evolved strains were unable to grow on 1,4-butanediol or 4-hydroxybutyrate when the regulator PP_2046, or the alcohol dehydrogenase PP_2049 were deleted (Figures 4, 5). The knockout of the whole operon also abolished growth. In contrast, deletion of PP_2051 did not affect growth on 1,4-butanediol (Supplementary Figure S3). This strongly suggests that PP_2049 is the main enzyme involved in the oxidation of 4-hydroxybutyrate. Both individual knockout strains of PP_2049 and *pedE* were unable to grow on 1,4-butanediol, making it unlikely that they oxidize the same substrate. More likely, the PP_2049 dehydrogenase is essential for the oxidation of 4-hydroxybutyrate, while PedE oxidizes 1,4-butanediol. Attempts to obtain direct biochemical evidence for the oxidation hypothesis with dehydrogenase assays on whole cell extracts of *P. putida* KT2440 wildtype, B10.1, and Δ PP_2046 with 4-hydroxybutyrate as a substrate were unsuccessful (Supplementary Figure S4) although this might be caused by instability of the PP_2049 enzyme and should



be investigated further. The lack of phenotype of the PP_2051 mutant suggests that β -oxidation is not involved, however, this is no clear proof since several other acetyl-CoA C-acetyltransferases are also expressed on a similar level (Figure 3).

The deletion of PP_2046 apparently causes a downregulation of the operon, while the mutations in PP_2046 in the evolved strains cause an overexpression of the adjacent operon. This is evident in the proteome data and also described in Li et al. (2019) for the E34G mutation in the context of ethylene glycol metabolism. In fact, the strains evolved on ethylene glycol also grow efficiently on 1,4-butanediol (Supplementary Figure S5). Expression *in trans* of the mutated regulator from B10.2 containing this mutation (denoted as PP_2046E) in *P. putida* KT2440 Δ PP_2046 enhanced growth of the wildtype on 1,4-butanediol, while expression of the native version could not restore growth (Figure 5). The regulator PP_2046 groups in the LysR-type family, which mainly contains transcriptional activators, repressors, and even dual function activators/repressors with a helix-turn-helix (HTH) DNA-binding domain at the N-terminus (Pérez-Rueda and Collado-Vides, 2000; Maddocks and Oyston, 2008). Both mutations found in the B10.1 and B10.2 evolved strains are located in the first third of the gene, in the HTH domain. While the B10.1 version of PP_2046 lost its native start codon, alternatives start codons are present (Supplementary Figure S1). The fact that only the mutated version of PP_2046 can enable growth on 1,4-butanediol, while its deletion abolishes growth, strongly suggests that this gene encodes an activator of the downstream operon, with an unknown inducer outside of the 1,4-butanediol context. It seems that a modification of the HTH domain is key to creating a constitutive activator.

In order to test whether overexpression of the PP_2047-51 operon alone was sufficient to enable faster growth on 1,4-butanediol, PP_2046 was replaced by the strong constitutive promoter P_{14g} , facing the operon, resulting in the strain *P. putida* KT2440 Δ PP_2046:14g. Indeed, the growth on 1,4-butanediol was enhanced by 3.43-fold compared to the wildtype (Figure 5).

This further indicates that the PP_2047-51 operon is the main determinant enabling fast growth on 1,4-butanediol. However, growth of this strain was somewhat slower than that of the evolved strains (Δ PP_2046:14g: $0.249 \pm 0.004 \text{ h}^{-1}$), indicating that other factors, possibly also regulated by PP_2046, are at play.

In this context, it should be noted that no gene encoding a CoA-ligase or transferase is present within the operon, which would be required for 1,4-butanediol degradation through β -oxidation. However, several of such enzymes were upregulated in the presence of 1,4-butanediol (Figure 3). To test whether the upregulation of this operon in the evolved strains enables enhanced β -oxidation, growth of the wildtype, the evolved strains, and Δ PP_2046 were analyzed on longer-chain α,ω -diols. The Δ PP_2046 strain did not grow on any of the tested diols. In contrast, both the evolved strain and the wildtype grew on 1,4-butanediol and 1,8-octanediol, with the evolved strains growing at a significantly higher rate (Figure 6). Surprisingly, none of the strains grew on 1,6-hexanediol or 1,7-heptanediol. A similar trend of faster growth by the evolved strains was also observed on butanol (Supplementary Figure S6). Since these substrates can only be metabolized through β -oxidation, these results strongly suggest that the upregulation of the PP_2047-51 operon enables higher activity of this pathway, and they prove that PP_2046 is an essential regulator for the metabolism of these short- to medium-chain alcohols.

CONCLUSION

Adaptive laboratory evolution was successfully used to enhance growth of *P. putida* KT2440 on 1,4-butanediol. Putative degradation pathways of this important plastic monomer were contextualized with leads from genome resequencing and proteome analysis, which were verified by knockout and overexpression analyses and physiological data. The alcohol dehydrogenases PedE and PP_2049 were found to be essential for growth on 1,4-butanediol, with the latter also being required for

growth on 4-hydroxybutyrate. Mutations in the transcriptional regulator PP_2046 were the main cause of enhanced growth in the ALE strains. The evolved phenotype could be reproduced through reverse engineering, either by overexpression of the PP_2047-51 operon by promoter exchange, or through *in trans* expression of the mutated regulator. In all, the knockout analysis favors the hypothesis of direct oxidation of 1,4-butanediol, via 4-hydroxybutyrate, to succinate. However, the alternative β -oxidation hypothesis can't be ruled out, and possibly both pathways operate simultaneously.

DATA AVAILABILITY STATEMENT

The sequences have been deposited in the NCBI Sequence Read Archive (SRA) with the accession number SRP148839 for ethylene glycol ALE strains (including our laboratory wildtype SRX4119395 used in this study) and SRP148839 for the 1,4-butanediol ALE strains. Raw data for all figures shown is available from the author upon reasonable request.

AUTHOR CONTRIBUTIONS

NW and LB conceived the study with the help of KO'C and TN. NW supervised the study with support of LB and KO'C. NW and W-JL designed the experiments. W-JL performed the experiments with the help of P-JN. TN performed the proteome analysis. W-JL and NW prepared the figures and wrote the manuscript with the help of all authors. All authors have read and approved the final version of this

manuscript, analyzed, and interpreted the data. SK oversaw PHA production experiments.

FUNDING

The RWTH and UCD researchers acknowledge funding from the European Union's Horizon 2020 Research and Innovation Programme under Grant Agreement No. 633962 for the project P4SB and No. 863922 for the project MIX-UP. NW was supported by the German Research Foundation through the Emmy Noether project WI 4255/1-1. The laboratory of LB was partially funded by the Deutsche Forschungsgemeinschaft (DFG, German Research Foundation) under Germany's excellence strategy within the clusters of excellence 236 "TMFB – Tailor-Made Fuels from Biomass" and 2186 "FSC – The Fuel Science Center." TN and KO'C acknowledge the funding from Science Foundation Ireland Research Centre Grant No. SFI/16/RC/3889.

ACKNOWLEDGMENTS

We gratefully acknowledge Janosch Klebensberger (University of Stuttgart), Gregg Beckham (NREL), Jörg Pietruszka (HHU Düsseldorf), as well as all P4SB partners, for helpful discussion.

SUPPLEMENTARY MATERIAL

The Supplementary Material for this article can be found online at: <https://www.frontiersin.org/articles/10.3389/fmicb.2020.00382/full#supplementary-material>

REFERENCES

- Bagdasarian, M., Lurz, R., Rückert, B., Franklin, F. C. H., Bagdasarian, M. M., Frey, J., et al. (1981). Specific-purpose plasmid cloning vectors II. Broad host range, high copy number, RSF 1010-derived vectors and a host-vector system for gene cloning in *Pseudomonas*. *Gene* 16, 237–247. doi: 10.1016/0378-1119(81)90080-9
- Bandounas, L., Ballerstedt, H., de Winde, J. H., and Ruijsenaars, H. J. (2011). Redundancy in putrescine catabolism in solvent tolerant *Pseudomonas putida* S12. *J. Biotechnol.* 154, 1–10. doi: 10.1016/j.jbiotec.2011.04.005
- Basler, G., Thompson, M., Tullman-Ercek, D., and Keasling, J. (2018). A *Pseudomonas putida* efflux pump acts on short-chain alcohols. *Biotechnol. Biofuels* 11:136. doi: 10.1186/s13068-018-1133-9
- Bednarz, A., Spieß, A. C., and Pfennig, A. (2017). Reactive and physical extraction of bio-based diamines from fermentation media. *J. Chem. Technol. Biotechnol.* 92, 1817–1824. doi: 10.1002/jctb.5183
- Behrendt, G., and Naber, B. (2009). The chemical recycling of polyurethanes. *J. Univ. Chem. Technol. Metall.* 44, 3–23.
- Belda, E., van Heck, R. G. A., José Lopez-Sanchez, M., Cruveiller, S., Barbe, V., Fraser, C., et al. (2016). The revisited genome of *Pseudomonas putida* KT2440 enlightens its value as a robust metabolic chassis. *Environ. Microbiol.* 18, 3403–3424. doi: 10.1111/1462-2920.12320
- Brandl, H., Gross, R. A., Lenz, R. W., and Fuller, R. C. (1988). *Pseudomonas oleovorans* as a source of poly(beta-hydroxyalkanoates) for potential applications as biodegradable polyesters. *Appl. Environ. Microbiol.* 54, 1977–1982. doi: 10.1128/aem.54.8.1977-1982.1988
- Burgard, A., Burk, M. J., Osterhout, R., van Dien, S., and Yim, H. (2016). Development of a commercial scale process for production of 1,4-butanediol from sugar. *Curr. Opin. Biotechnol.* 42, 118–125. doi: 10.1016/j.copbio.2016.04.016
- Burger, M., Woods, R. G., McCarthy, C., and Beacham, I. R. (2000). Temperature regulation of protease in *Pseudomonas fluorescens* LS107d2 by an ECF sigma factor and a transmembrane activator. *Microbiology* 146(Pt. 12), 3149–3155. doi: 10.1099/00221287-146-12-3149
- Calero, P., Jensen, S. I., Bojanović, K., Lennen, R. M., Koza, A., and Nielsen, A. T. (2018). Genome-wide identification of tolerance mechanisms toward p-coumaric acid in *Pseudomonas putida*. *Biotechnol. Bioeng.* 115, 762–774. doi: 10.1002/bit.26495
- Chomczynski, P., and Rymaszewski, M. (2006). Alkaline polyethylene glycol-based method for direct PCR from bacteria, eukaryotic tissue samples, and whole blood. *Biotechniques* 40, 454, 456, 458. doi: 10.2144/000112149
- Cox, J., and Mann, M. (2008). MaxQuant enables high peptide identification rates, individualized p.p.b.-range mass accuracies and proteome-wide protein quantification. *Nat. Biotechnol.* 26, 1367–1372. doi: 10.1038/nbt.1511
- Cox, J., Neuhauser, N., Michalski, A., Scheltema, R. A., Olsen, J. V., and Mann, M. (2011). Andromeda: a peptide search engine integrated into the MaxQuant environment. *J. Proteome Res.* 10, 1794–1805. doi: 10.1021/Pr101065j
- Cuenca, M. D. S., Roca, A., Molina-Santiago, C., Duque, E., Armengaud, J., Gómez-García, M. R., et al. (2016). Understanding butanol tolerance and assimilation in *Pseudomonas putida* BIRD-1: an integrated omics approach. *Microbiol. Biotechnol.* 9, 100–115. doi: 10.1111/1751-7915.12328
- Danso, D., Chow, J., and Streit, W. R. (2019). Plastics: environmental and Biotechnological Perspectives on Microbial Degradation. *Appl. Environ. Microbiol.* 85:e01095-19. doi: 10.1128/AEM.01095-19
- DePristo, M. A., Banks, E., Poplin, R., Garimella, K. V., Maguire, J. R., Hartl, C., et al. (2011). A framework for variation discovery and genotyping using

- next-generation DNA sequencing data. *Nat. Genet.* 43, 491–498. doi: 10.1038/ng.806
- Dragosits, M., and Mattanovich, D. (2013). Adaptive laboratory evolution – principles and applications for biotechnology. *Microb. Cell Fact.* 12:64. doi: 10.1186/1475-2859-12-64
- Franden, M. A., Jayakody, L. N., Li, W.-J., Wagner, N. J., Cleveland, N. S., Michener, W. E., et al. (2018). Engineering *Pseudomonas putida* KT2440 for efficient ethylene glycol utilization. *Metab. Eng.* 48, 197–207. doi: 10.1016/j.ymben.2018.06.003
- Gaona-López, C., Julián-Sánchez, A., and Riveros-Rosas, H. (2016). Diversity and Evolutionary Analysis of Iron-Containing (Type-III) Alcohol Dehydrogenases in Eukaryotes. *PLoS One* 11:e0166851. doi: 10.1371/journal.pone.0166851
- Gibson, D. G., Young, L., Chuang, R.-Y., Venter, J. C., Hutchison, C. A., and Smith, H. O. (2009). Enzymatic assembly of DNA molecules up to several hundred kilobases. *Nat. Methods* 6, 343–345. doi: 10.1038/nmeth.1318
- Grand View Research (2017). *1,4- Butanediol (BDO) Market Report 1,4- Butanediol (BDO) Market Analysis By Application (Tetrahydrofuran (THF), Polybutylene Terephthalate (PBT), Gamma-Butyrolactone (GBL), Polyurethane (PU)), By Region (North America, Europe, Asia Pacific, CSA, MEA), And Segment Forecasts, 2018 - 2025*. San Francisco, CA: Grand View Research, Inc.
- Guzik, M. W., Kenny, S. T., Duane, G. F., Casey, E., Woods, T., Babu, R. P., et al. (2014). Conversion of post consumer polyethylene to the biodegradable polymer polyhydroxyalkanoate. *Appl. Microbiol. Biotechnol.* 98, 4223–4232. doi: 10.1007/s00253-013-5489-2
- Hanahan, D. (1983). Studies on transformation of *Escherichia coli* with plasmids. *J. Mol. Biol.* 166, 557–580. doi: 10.1016/S0022-2836(83)80284-8
- Hartmans, S., Smiths, J. P., van der Werf, M. J., Volkerling, F., and de Bont, J. A. M. (1989). Metabolism of styrene oxide and 2-phenylethanol in the styrene-degrading *Xanthobacter* strain 124X. *Appl. Environ. Microbiol.* 55, 2850–2855. doi: 10.1128/aem.55.11.2850-2855.1989
- Hiu, S. F., Zhu, C. X., Yan, R. T., and Chen, J. S. (1987). Butanol-ethanol dehydrogenase and butanol-ethanol-isopropanol dehydrogenase: different alcohol dehydrogenases in two strains of *Clostridium beijerinckii* (*Clostridium butylicum*). *Appl. Environ. Microbiol.* 53, 697–703. doi: 10.1128/aem.53.4.697-703.1987
- Howard, G. T. (2002). Biodegradation of polyurethane: a review. *Int. Biodeterior. Biodegradation* 49, 245–252. doi: 10.1016/S0964-8305(02)00051-3
- Huang, D. W., Sherman, B. T., and Lempicki, R. A. (2009a). Bioinformatics enrichment tools: paths toward the comprehensive functional analysis of large gene lists. *Nucleic Acids Res.* 37, 1–13. doi: 10.1093/nar/gkn923
- Huang, D. W., Sherman, B. T., and Lempicki, R. A. (2009b). Systematic and integrative analysis of large gene lists using DAVID bioinformatics resources. *Nat. Protoc.* 4, 44–57. doi: 10.1038/nprot.2008.211
- Huerta-Cepas, J., Szklarczyk, D., Forslund, K., Cook, H., Heller, D., Walter, M. C., et al. (2016). eggNOG 4.5: a hierarchical orthology framework with improved functional annotations for eukaryotic, prokaryotic and viral sequences. *Nucleic Acids Res.* 44, D286–D293. doi: 10.1093/nar/gkv1248
- Hung, C.-S., Zingarelli, S., Nadeau, L. J., Biffinger, J. C., Drake, C. A., Crouch, A. L., et al. (2016). Carbon catabolite repression and impranil polyurethane degradation in *Pseudomonas protegens* Strain Pf-5. *Appl. Environ. Microbiol.* 82, 6080–6090. doi: 10.1128/AEM.01448-16
- Kagi, J. H., and Vallee, B. H. (1960). The role of zinc in alcohol dehydrogenase. V. The effect of metal-binding agents on the structure of the yeast alcohol dehydrogenase molecule. *J. Biol. Chem.* 235, 3188–3192.
- Kenny, S. T., Runic, J. N., Kaminsky, W., Woods, T., Babu, R. P., Keely, C. M., et al. (2008). Up-Cycling of PET (Polyethylene Terephthalate) to the biodegradable plastic PHA (Polyhydroxyalkanoate). *Environ. Sci. Technol.* 42, 7696–7701. doi: 10.1021/es801010e
- Kenny, S. T., Runic, J. N., Kaminsky, W., Woods, T., Babu, R. P., and O'Connor, K. E. (2012). Development of a bioprocess to convert PET derived terephthalic acid and biodiesel derived glycerol to medium chain length polyhydroxyalkanoate. *Appl. Microbiol. Biotechnol.* 95, 623–633. doi: 10.1007/s00253-012-4058-4
- Klumpp, S., Zhang, Z., and Hwa, T. (2009). Growth rate-dependent global effects on gene expression in bacteria. *Cell* 139, 1366–1375. doi: 10.1016/j.cell.2009.12.001
- Lageveen, R. G., Huisman, G. W., Preusting, H., Ketelaar, P., Eggink, G., and Witholt, B. (1988). Formation of polyesters by *Pseudomonas oleovorans*: effect of substrates on formation and composition of poly-(R)-3-hydroxyalkanoates and poly-(R)-3-hydroxyalkenoates. *Appl. Environ. Microbiol.* 54, 2924–2932. doi: 10.1128/aem.54.12.2924-2932.1988
- Lennen, R. M., Jensen, K., Mohammed, E. T., Malla, S., Börner, R. A., Chekina, K., et al. (2019). Adaptive laboratory evolution reveals general and specific chemical tolerance mechanisms and enhances biochemical production. *bioRxiv* [Preprint]. doi: 10.1101/634105
- Li, H., and Durbin, R. (2009). Fast and accurate short read alignment with Burrows-Wheeler transform. *Bioinformatics* 25, 1754–1760. doi: 10.1093/bioinformatics/btp324
- Li, W.-J., Jayakody, L. N., Franden, M. A., Wehrmann, M., Daun, T., Hauer, B., et al. (2019). Laboratory evolution reveals the metabolic and regulatory basis of ethylene glycol metabolism by *Pseudomonas putida* KT2440. *Environ. Microbiol.* 21, 3669–3682. doi: 10.1111/1462-2920.14703
- Liu, H., and Lu, T. (2015). Autonomous production of 1,4-butanediol via a de novo biosynthesis pathway in engineered *Escherichia coli*. *Metab. Eng.* 29, 135–141. doi: 10.1016/j.ymben.2015.03.009
- Maddocks, S. E., and Oyston, P. C. F. (2008). Structure and function of the LysR-type transcriptional regulator (LTTR) family proteins. *Microbiology* 154, 3609–3623. doi: 10.1099/mic.0.2008/022772-0
- Magnin, A., Hoornaert, L., Pollet, E., Laurichesse, S., Phalip, V., and Avérous, L. (2019a). Isolation and characterization of different promising fungi for biological waste management of polyurethanes. *Microbiol. Biotechnol.* 12, 544–555. doi: 10.1111/1751-7915.13346
- Magnin, A., Pollet, E., Perrin, R., Ullmann, C., Persillon, C., Phalip, V., et al. (2019b). Enzymatic recycling of thermoplastic polyurethanes: synergistic effect of an esterase and an amidase and recovery of building blocks. *Waste Manag.* 85, 141–150. doi: 10.1016/j.wasman.2018.12.024
- Martínez-García, E., Aparicio, T., Lorenzo, V., de, and Nikel, P. I. (2014). New transposon tools tailored for metabolic engineering of gram-negative microbial cell factories. *Front. Bioeng. Biotechnol.* 2:46. doi: 10.3389/fbioe.2014.00046
- Martínez-García, E., and de Lorenzo, V. (2011). Engineering multiple genomic deletions in Gram-negative bacteria: analysis of the multi-resistant antibiotic profile of *Pseudomonas putida* KT2440. *Environ. Microbiol.* 13, 2702–2716. doi: 10.1111/j.1462-2920.2011.02538.x
- McKenna, A., Hanna, M., Banks, E., Sivachenko, A., Cibulskis, K., Kernysky, A., et al. (2010). The genome analysis toolkit: a MapReduce framework for analyzing next-generation DNA sequencing data. *Genome Res.* 20, 1297–1303. doi: 10.1101/gr.107524.110
- Mitchell, A. L., Attwood, T. K., Babbitt, P. C., Blum, M., Bork, P., Bridge, A., et al. (2019). InterPro in 2019: improving coverage, classification and access to protein sequence annotations. *Nucleic Acids Res.* 47, D351–D360. doi: 10.1093/nar/gky1100
- Narancic, T., and O'Connor, K. E. (2017). Microbial biotechnology addressing the plastic waste disaster. *Microbiol. Biotechnol.* 10, 1232–1235. doi: 10.1111/1751-7915.12775
- Narancic, T., Scollica, E., Kenny, S. T., Gibbons, H., Carr, E., Brennan, L., et al. (2016). Understanding the physiological roles of polyhydroxybutyrate (PHB) in *Rhodospirillum rubrum* S1 under aerobic chemoheterotrophic conditions. *Appl. Microbiol. Biotechnol.* 100, 8901–8912. doi: 10.1007/s00253-016-7711-5
- Nelson, K. E., Weinle, C., Paulsen, I. T., Dodson, R. J., Hilbert, H., Martins, et al. (2002). Complete genome sequence and comparative analysis of the metabolically versatile *Pseudomonas putida* KT2440. *Environ. Microbiol.* 4, 799–808.
- Nikel, P. I., and de Lorenzo, V. (2018). *Pseudomonas putida* as a functional chassis for industrial biocatalysis: from native biochemistry to trans-metabolism. *Metab. Eng.* 50, 142–155. doi: 10.1016/j.ymben.2018.05.005
- Nikel, P. I., Martínez-García, E., and de Lorenzo, V. (2014). Biotechnological domestication of *Pseudomonads* using synthetic biology. *Nat. Rev. Microbiol.* 12, 368–379. doi: 10.1038/nrmicro3253
- Noel, J. K., and Whitford, P. C. (2016). How EF-Tu can contribute to efficient proofreading of aa-tRNA by the ribosome. *Nat. Commun.* 7:13314. doi: 10.1038/ncomms13314
- Parke, D., García, M. A., and Ornston, L. N. (2001). Cloning and Genetic Characterization of dca Genes Required for -Oxidation of Straight-Chain

- Dicarboxylic Acids in *Acinetobacter* sp. Strain ADP1. *Appl. Environ. Microbiol.* 67, 4817–4827. doi: 10.1128/AEM.67.10.4817-4827.2001
- Pérez-Rueda, E., and Collado-Vides, J. (2000). The repertoire of DNA-binding transcriptional regulators in *Escherichia coli* K-12. *Nucleic Acids Res.* 28, 1838–1847. doi: 10.1093/nar/28.8.1838
- Poblete-Castro, I., Escapa, I. F., Jäger, C., Puchalka, J., Lam, C. M. C., Schomburg, D., et al. (2012). The metabolic response of *P. putida* KT2442 producing high levels of polyhydroxyalkanoate under single- and multiple-nutrient-limited growth: highlights from a multi-level omics approach. *Microb. Cell Fact.* 11:34. doi: 10.1186/1475-2859-11-34
- Ramos, J. L., Duque, E., Gallegos, M.-T., Godoy, P., Ramos-Gonzalez, M. I., Rojas, A., et al. (2002). Mechanisms of solvent tolerance in gram-negative bacteria. *Annu. Rev. Microbiol.* 56, 743–768. doi: 10.1146/annurev.micro.56.012302.161038
- Rühl, J., Schmid, A., and Blank, L. M. (2009). Selected *Pseudomonas putida* strains able to grow in the presence of high butanol concentrations. *Appl. Environ. Microbiol.* 75, 4653–4656. doi: 10.1128/AEM.00225-09
- Samanta, S. K., Singh, O. V., and Jain, R. K. (2002). Polycyclic aromatic hydrocarbons: environmental pollution and bioremediation. *Trends Biotechnol.* 20, 243–248. doi: 10.1016/S0167-7799(02)01943-1
- Schmidt, J., Wei, R., Oeser, T., Dedavid, E., Silva, L. A., Breite, D., et al. (2017). Degradation of Polyester Polyurethane by Bacterial Polyester Hydrolases. *Polymers* 9:65. doi: 10.3390/polym9020065
- Simon, O., Klebensberger, J., Mükschel, B., Klaiber, I., Graf, N., Altenbuchner, J., et al. (2015). Analysis of the molecular response of *Pseudomonas putida* KT2440 to the next-generation biofuel n-butanol. *J. Proteom.* 122, 11–25. doi: 10.1016/j.jprot.2015.03.022
- Spini, G., Spina, F., Poli, A., Blieux, A.-L., Regnier, T., Gramellini, C., et al. (2018). Molecular and Microbiological Insights on the Enrichment Procedures for the Isolation of Petroleum Degrading Bacteria and Fungi. *Front. Microbiol.* 9:2543. doi: 10.3389/fmicb.2018.02543
- Steele, M. I., Lorenz, D., Hatter, K., Park, A., and Sokatch, J. R. (1992). Characterization of the *mmsAB* operon of *Pseudomonas aeruginosa* PAO encoding methylmalonate-semialdehyde dehydrogenase and 3-hydroxyisobutyrate dehydrogenase. *J. Biol. Chem.* 267, 13585–13592.
- Tahseen, R., Arslan, M., Iqbal, S., Khalid, Z. M., and Afzal, M. (2019). Enhanced degradation of hydrocarbons by gamma ray induced mutant strain of *Pseudomonas putida*. *Biotechnol. Lett.* 41, 391–399. doi: 10.1007/s10529-019-02644-y
- Takeda, K., Matsumura, H., Ishida, T., Samejima, M., Igarashi, K., Nakamura, N., et al. (2013). The two-step electrochemical oxidation of alcohols using a novel recombinant PQQ alcohol dehydrogenase as a catalyst for a bioanode. *Bioelectrochemistry* 94, 75–78. doi: 10.1016/j.bioelechem.2013.08.001
- Tatusov, R. L., Koonin, E. V., and Lipman, D. J. (1997). A genomic perspective on protein families. *Science* 278, 631–637. doi: 10.1126/science.278.5338.631
- The UniProt Consortium (2019). UniProt: a worldwide hub of protein knowledge. *Nucleic Acids Res.* 47, D506–D515. doi: 10.1093/nar/gky1049
- Thorvaldsdóttir, H., Robinson, J. T., and Mesirov, J. P. (2013). Integrative Genomics Viewer (IGV): high-performance genomics data visualization and exploration. *Brief. Bioinform.* 14, 178–192. doi: 10.1093/bib/bbs017
- Tyanova, S., Temu, T., Sinitcyn, P., Carlson, A., Hein, M. Y., Geiger, T., et al. (2016). The perseus computational platform for comprehensive analysis of (prote)omics data. *Nat. Methods* 13, 731–740. doi: 10.1038/nmeth.3901
- Vallon, T., Simon, O., Rendgen-Heugle, B., Frana, S., Mükschel, B., Broicher, A., et al. (2015). Applying systems biology tools to study n-butanol degradation in *Pseudomonas putida* KT2440. *Eng. Life Sci.* 15, 760–771.
- Wang, J. C. (2002). Cellular roles of DNA topoisomerases: a molecular perspective. *Nat. Rev. Mol. Cell Biol.* 3, 430–440. doi: 10.1038/nrm831
- Wang, W., Zhou, H., Lin, H., Roy, S., Shaler, T. A., Hill, L. R., et al. (2003). Quantification of Proteins and Metabolites by Mass Spectrometry without Isotopic Labeling or Spiked Standards. *Anal. Chem.* 75, 4818–4826. doi: 10.1021/AC026468x
- Ward, P. G., Goff, M., Donner, M., Kaminsky, W., and O'Connor, K. E. (2006). A two step chemo-biotechnological conversion of polystyrene to a biodegradable thermoplastic. *Environ. Sci. Technol.* 40, 2433–2437. doi: 10.1021/es0517668
- Wehrmann, M., Billard, P., Martin-Meriadec, A., Zegeye, A., and Klebensberger, J. (2017). Functional Role of Lanthanides in Enzymatic Activity and Transcriptional Regulation of Pyrroloquinoline Quinone-Dependent Alcohol Dehydrogenases in *Pseudomonas putida* KT2440. *mBio* 8:e00570-17. doi: 10.1128/mBio.00570-17
- Wierckx, N., Koopman, F., Ruijsenaars, H. J., and de Winde, J. H. (2011). Microbial degradation of furanic compounds: biochemistry, genetics, and impact. *Appl. Microbiol. Biotechnol.* 92, 1095–1105. doi: 10.1007/s00253-011-3632-5
- Wierckx, N., Prieto, M. A., Pomposiello, P., Lorenzo, V., de, O., Connor, K., et al. (2015). Plastic waste as a novel substrate for industrial biotechnology. *Microbiol. Biotechnol.* 8, 900–903. doi: 10.1111/1751-7915.12312
- Wilkes, R. A., and Aristilde, L. (2017). Degradation and metabolism of synthetic plastics and associated products by *Pseudomonas* sp. *capabilities and challenges*. *J. Appl. Microbiol.* 123, 582–593. doi: 10.1111/jam.13472
- Wynands, B., Lenzen, C., Otto, M., Koch, F., Blank, L. M., and Wierckx, N. (2018). Metabolic engineering of *Pseudomonas taiwanensis* VLB120 with minimal genomic modifications for high-yield phenol production. *Metab. Eng.* 47, 121–133. doi: 10.1016/j.ymben.2018.03.011
- Yim, H., Haselbeck, R., Niu, W., Pujol-Baxley, C., Burgard, A., Boldt, J., et al. (2011). Metabolic engineering of *Escherichia coli* for direct production of 1,4-butanediol. *Nat. Chem. Biol.* 7, 445–452. doi: 10.1038/nchembio.580
- Zhou, S., Mohan Raj, S., Ashok, S., Edwardraja, S., Lee, S.-G., and Park, S. (2013). Cloning, expression and characterization of 3-hydroxyisobutyrate dehydrogenase from *Pseudomonas denitrificans* ATCC 13867. *PLoS One* 8:e62666. doi: 10.1371/journal.pone.0062666
- Zia, K. M., Bhatti, H. N., and Ahmad Bhatti, I. (2007). Methods for polyurethane and polyurethane composites, recycling and recovery: a review. *React. Funct. Polym.* 67, 675–692. doi: 10.1016/j.reactfunctpolym.2007.05.004

Conflict of Interest: SK was employed by the company Bioplastech Ltd. KO'C was employed by university college Dublin. He has a shareholding in the company Bioplastech Ltd.

The remaining authors declare that the research was conducted in the absence of any commercial or financial relationships that could be construed as a potential conflict of interest.

Copyright © 2020 Li, Narancic, Kenny, Niehoff, O'Connor, Blank and Wierckx. This is an open-access article distributed under the terms of the Creative Commons Attribution License (CC BY). The use, distribution or reproduction in other forums is permitted, provided the original author(s) and the copyright owner(s) are credited and that the original publication in this journal is cited, in accordance with accepted academic practice. No use, distribution or reproduction is permitted which does not comply with these terms.



Toward Biorecycling: Isolation of a Soil Bacterium That Grows on a Polyurethane Oligomer and Monomer

María José Cárdenas Espinosa¹, Andrea Colina Blanco¹, Tabea Schmidgall¹, Anna Katharina Atanasoff-Kardjalieff¹, Uwe Kappelmeyer¹, Dirk Tischler², Dietmar H. Pieper³, Hermann J. Heipieper^{1*} and Christian Eberlein¹

¹ Department of Environmental Biotechnology, Helmholtz Centre for Environmental Research – UFZ, Leipzig, Germany,

² Interdisciplinary Ecological Center, TU Bergakademie Freiberg, Freiberg, Germany, ³ Microbial Interactions and Processes Research Group, Helmholtz Centre for Infection Research – HZI, Braunschweig, Germany

OPEN ACCESS

Edited by:

Ren Wei,
University of Greifswald, Germany

Reviewed by:

Welliang Dong,
Nanjing Tech University, China
Ping Xu,
Shanghai Jiao Tong University, China

*Correspondence:

Hermann J. Heipieper
hermann.heipieper@ufz.de

Specialty section:

This article was submitted to
Microbiotechnology,
a section of the journal
Frontiers in Microbiology

Received: 13 December 2019

Accepted: 26 February 2020

Published: 27 March 2020

Citation:

Cárdenas Espinosa MJ,
Colina Blanco A, Schmidgall T,
Atanasoff-Kardjalieff AK,
Kappelmeyer U, Tischler D,
Pieper DH, Heipieper HJ and
Eberlein C (2020) Toward
Biorecycling: Isolation of a Soil
Bacterium That Grows on
a Polyurethane Oligomer
and Monomer.
Front. Microbiol. 11:404.
doi: 10.3389/fmicb.2020.00404

The fate of plastic waste and a sustainable use of synthetic polymers is one of the major challenges of the twenty first century. Waste valorization strategies can contribute to the solution of this problem. Besides chemical recycling, biological degradation could be a promising tool. Among the high diversity of synthetic polymers, polyurethanes are widely used as foams and insulation materials. In order to examine bacterial biodegradability of polyurethanes, a soil bacterium was isolated from a site rich in brittle plastic waste. The strain, identified as *Pseudomonas* sp. by 16S rRNA gene sequencing and membrane fatty acid profile, was able to grow on a PU-diol solution, a polyurethane oligomer, as the sole source of carbon and energy. In addition, the strain was able to use 2,4-diaminotoluene, a common precursor and putative degradation intermediate of polyurethanes, respectively, as sole source of energy, carbon, and nitrogen. Whole genome sequencing of the strain revealed the presence of numerous catabolic genes for aromatic compounds. Growth on potential intermediates of 2,4-diaminotoluene degradation, other aromatic growth substrates and a comparison with a protein data base of oxygenases present in the genome, led to the proposal of a degradation pathway.

Keywords: plastic, biorecycling, *Pseudomonas*, polyurethane, diaminotoluene, aromatics degradation, aromatic diamines

INTRODUCTION

Plastics are heavily used in our modern society and the global production rates increase since decades. With about 3.5 million tons polyurethanes were the fifth most demanded synthetic polymers in Europe in 2015 (Plasticseurope, 2016). The uses of polyurethanes are manifold with the major field of application being insulation materials. Common precursors used to synthesize polyurethanes are polyisocyanates and polyols together with additives such as catalysts, cross linkers and chain extenders, among others. Despite forming urethane bonds with the polyisocyanates, polyols additionally can contain ether or ester bonds, resulting

in polyether or polyester polyurethanes, respectively. On the other hand, the polyisocyanate compounds can have an aliphatic, polycyclic or aromatic nature. Two of the most widely used diisocyanates for PU synthesis are 4,4'-methylene diphenyl diisocyanate (MDI) and toluene-2,4-diisocyanate (TDI) and their precursors 4,4'-diaminodiphenylmethane (MDA) and 2,4-diaminotoluene (2,4-TDA), respectively. Next to an alcohol and carbon dioxide, primary amines are also formed after chemical hydrolysis of the urethane bond (Marchant et al., 1987).

Post-consumer plastics are already a major challenge for the environment and will be an even bigger one in the future. The biodegradation is often hampered by the durability, crystallinity and macroscopic structure of the polymers. For polyurethanes, the diverse chemical composition increases the obstacles for both, biological and chemical recycling. Reports on the degradation of polyurethanes mostly focus on polyester-based ones, fungal as well bacterial and enzymatic hydrolysis were reported (Wang et al., 1997; Russell et al., 2011; Krasowska et al., 2012; Shah et al., 2013; Magnin et al., 2019). The biodegradation of polyether-based PU is far less documented and was usually achieved by fungal activity (Matsumiya et al., 2010; Álvarez-Barragán et al., 2016).

The biodegradation of synthetic polymers in general is a two-step process. It involves the attack by extracellular enzymes overcoming the macromolecular structure of the polymers and providing monomers and oligomers for the second step, which is the mineralization of the latter inside the cell. The two steps can be carried out by a single species, or more likely by at least two. Regularly, aromatic monomers are released by the activity of extracellular enzymes. During microbial degradation of aromatic compounds typically mono- and dioxygenases are involved in ring hydroxylation and cleavage. The hydroxylation of the aromatic ring results in catecholic compounds (with at least two adjacent hydroxyl groups) reducing the aromatic character of the compound and facilitating the oxygenolytic cleavage of the ring. The latter can be intradiolic (*ortho*-cleavage) or extradiolic (*meta*-cleavage).

Studies that identified the products of PU hydrolysis found the diamines TDA and MDA (Matsumiya et al., 2010; Cregut et al., 2013; Magnin et al., 2019). Both amines have been proposed in the European Chemicals Agency to be identified as "Substances of Very High Concern," specifically in the category of "Carcinogenic, Mutagenic or toxic to Reproduction" (European Chemicals Agency, 2019). The carcinogenicity of TDA compounds was demonstrated with experimental studies in animals (Baua, 2008). To understand the fate of the diamines released from PU degradation and in order to investigate the monomer and oligomer metabolism in plastics degradation in general, we screened for bacteria capable to degrade both, 2,4-TDA and PU oligomer (Polyurethane diol solution, Sigma-Aldrich). From a site rich in brittle plastic waste, a *Pseudomonas* species was isolated on 2,4-TDA and positively tested for growth on the PU oligomer as the sole source of carbon and energy. Genome sequencing and the screening for potential carbon substrates led to a hypothetical degradation pathway of 2,4-TDA in the isolated *Pseudomonas* strain.

MATERIALS AND METHODS

Growth Conditions

The bacteria were grown in mineral media, as reported before (Hartmans et al., 1989), containing the following compounds (per liter demineralized water): 7 g $\text{Na}_2\text{HPO}_4 \times 2 \text{H}_2\text{O}$; 2.8 g KH_2PO_4 ; 0.5 g NaCl; 0.1 g NH_4Cl ; 0.1 g $\text{MgSO}_4 \times 7 \text{H}_2\text{O}$; 10 mg FeSO_4 ; 5 mg MnSO_4 ; 6.4 mg ZnCl_2 ; 1 mg $\text{CaCl}_2 \times 6 \text{H}_2\text{O}$; 0.6 mg BaCl_2 ; 0.36 mg $\text{CoSO}_4 \times 7 \text{H}_2\text{O}$; 0.36 mg $\text{CuSO}_4 \times 5 \text{H}_2\text{O}$; 6.5 mg H_3BO_3 ; 10 mg EDTA; 146 μl HCl (37%). The nitrogen-deficient mineral media did not contain NH_4Cl . As sole source of carbon and energy either 4 g/l disodium succinate (Sigma-Aldrich), 2 mM 2,4-TDA (Sigma-Aldrich) or 3 g/l PU oligomer (Sigma-Aldrich, dihydroxy-functional oligomer, aliphatic urethane of proprietary composition) was added. For growth on solid media 3.5% of agar was added. Cells were cultivated in 50 ml shaking cultures at 30°C at 150 rpm. All chemicals used were reagent grade and obtained from commercial sources. Optical density was measured at a wavelength of 560 nm (Perkin Elmer, Lambda 2S). Toluene, benzene, aniline, 2,4-dihydroxytoluene (4-methylresorcinol), methylsuccinate, sodium benzoate, 2-aminobenzoate (anthranilate), phenol, *o*-xylene, catechol, 4-methylcatechol and benzene-1,2,4-triol (hydroxyhydroquinone) were tested if they serve as sole source of carbon and energy for the isolated bacteria in 100, 200, and 300 mg/l concentrations and OD at 560 nm was measured to evaluate growth.

Bacterial Strain Isolation and Identification

For the isolation of bacteria from soil, three samples from a site rich in brittle plastic waste (Paunsdorf, Leipzig, Germany) were used. 1 g of each sample was dissolved in 9 mL of NaCl 0.9% m/V, diluted 1:10 and stored at 4°C. Afterward, dilution series of 10^{-1} , 10^{-2} , and 10^{-3} were prepared. 150 μL of the diluted soil solutions were added to agar plates containing mineral medium and different concentrations of 2,4-TDA (2, 5, and 10 mM) as sole carbon and energy source. The plates were stored at 30°C. After 5 days of incubation bacteria were transferred to fresh plates, agar plates without carbon source were used as control. The complete 16S rRNA gene sequence was obtained from the TDA1 genome and used for an alignment with other known *Pseudomonas* species by making use of the RDP data base (Wang et al., 1997).

Toxicity Test for 2,4-TDA

In order to test the toxic effect of 2,4-TDA on the isolated strain during growth with the readily metabolizable carbon source disodium succinate (4 g/L), 2,4-TDA was added at different concentrations to exponentially growing cultures as described earlier (Heipieper et al., 1995). The control was a culture growing with succinate as the carbon source without the addition of 2,4-TDA.

Membrane Lipid Fatty Acid Composition

The membrane fatty acid profile for selected strains was obtained. For the phospholipid fatty acids (PLFA) extraction, bacterial cells were harvested from an overnight culture and then centrifuged

for 7 min at 13000 rpm. The pellet was washed with 1.5 mL of 10 mM KNO₃, centrifuged and PLFA extraction was done as reported before (Bligh and Dyer, 1959), methylation was achieved by addition of 0.6 mL of 20% boron trifluoride in methanol (Morrison and Smith, 1964). The identification and quantification of the fatty acid methyl esters (FAME) was done using gas chromatography with flame ionization detector (GC-FID, Agilent Technologies, 6890N Network GC System, 7683B Series Injector). A CP-Sil 88 column (Varian CP7488) was used as stationary phase and helium as carrier gas. The temperature ramp programmed was: 2 min 40°C isotherm, a gradient increase to 220°C (8°C × min⁻¹) and 10 min 220°C isotherm.

Genome Sequencing of Selected Strain

Genomic DNA was extracted (DNeasy® Blood & Tissue Kit, QIAGEN) according to the manufacturer's protocol for Gram-negative strains. The quantity of extracted DNA was checked by nanodrop followed by the library preparation with the Nextera XT DNA library kit (Illumina, San Diego, CA, United States). The library was checked with an Agilent technology Bioanalyzer 2100. Paired-end libraries were sequenced using Illumina v3 chemistry on a Illumina MiSeq sequencer with a 250-bp paired-end protocol according to the manufacturer's instructions. The sequencing reads were demultiplexed by MiSeq reporter software (Illumina). The draft genome sequences were assembled using the Velvet assembly program (Zerbino and Birney, 2008). The RAST queue (Aziz et al., 2008) was used to annotate by using *P. putida* KT2440 as reference strain. For the annotation of dioxygenases the AROMADEG data base was used in addition (Duarte et al., 2014). To reveal similarities to known enzymes (mono- and dioxygenases, enzymes involved in aromatics degradation) amino acid sequences of genes present in the genome of TDA1 were compared to UniprotKB database or by using the basic local alignment search tool (BLAST) data base in NCBI as reported before (Altschul et al., 1997). The suggestion of genes possibly involved in the degradation was based on significant amino acid sequence similarities, i.e., a high coverage (at least 80%) and similarity (at least 30%) as well as a low *E* value (1×10^{-8} or lower) given by BLAST when compared to the sequences to known and described enzymes. Dioxygenases or enzymes with an aromatic substrate were analyzed mainly by deploying the AROMADEG data base.

HPLC Measurements

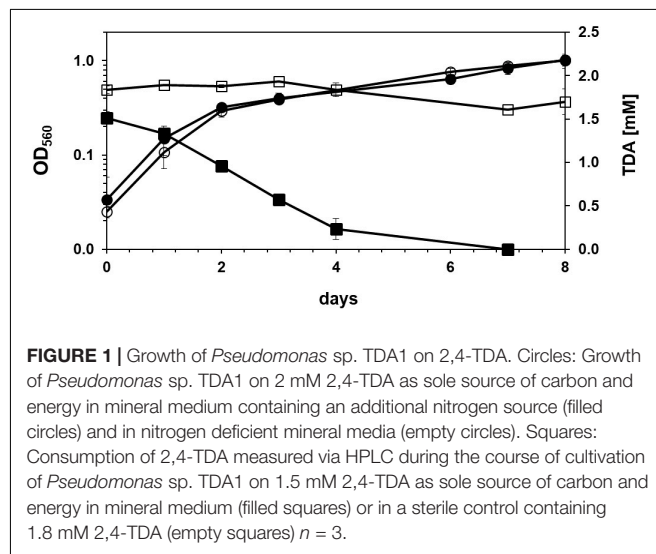
2,4-TDA degradation was monitored by measuring the decrease in concentration. The experiment was performed in triplicates. 50 mL of 2 mM 2,4-TDA media were inoculated with the isolated bacterial strain. 1 mL of the culture was collected and mixed with an equal amount of methanol. A calibration curve for the concentrations between 0.1 mM and 3 mM of 2,4-TDA was prepared. All the samples were centrifuged (7 min, 13000 rpm) at room temperature and filtered through a 0.45 µm polyethersulfone membrane syringe filter (Whatman™-GE Healthcare). 75 µl of the sample was analyzed by high performance liquid chromatography (HPLC; LC- 20AB,

Shimadzu). All the samples and standards were measured using a C18 column (LiChroCART® 125-4, RP-18e, 5 µm, Merck KGaA). Isocratic elution of 2,4-TDA was conducted with 39.5% methanol, 59.5% distilled water and 1.0% triethylamine at a flow rate of 0.65 ml min⁻¹ (Freedman et al., 1996). The temperature of the column was kept constant at 25°C. Detection was done with a photodiode array detector, using a deuterium lamp as light source, at 278 nm (SPD-M20A, Shimadzu).

RESULTS

The screening performed with soil samples taken from a site rich in brittle plastic waste led to the isolation of two bacterial strains that grew on agar plates containing mineral medium with 2,4-TDA as sole carbon and energy source and showed growth in liquid media containing 2 mM 2,4-TDA. Any isolated bacteria that did grow on agar plates without any carbon source were discarded to exclude autotrophic growth on 2,4-TDA agar plates. One strain, named TDA1, was chosen for further investigations. **Figure 1** shows the growth of the TDA1 isolate on 2 mM 2,4-TDA as sole carbon and energy source. The growth rate was 0.04 h⁻¹ corresponding to a generation time of 14 h⁻¹ during exponential growth phase. The degradation of 2,4-TDA was quantified using HPLC. The 2,4-TDA was consumed by the bacterial strain whereas the sterile control only shows a minor decrease in 2,4-TDA concentrations (**Figure 1**). 2,4-TDA at a concentration of 2 mM was shown to be the optimal concentration, because lower and higher concentrations yielded lower optical densities (data not shown). This was also verified in toxicity tests where 2,4-TDA was added to cells growing exponentially with succinate as carbon and energy source (**Figure 2**). The growth rate with succinate in the presence of 2 mM 2,4-TDA was reduced by 55% compared to the untreated control whereas higher concentrations caused significantly higher growth inhibition.

Remarkably, strain TDA1 was also able to grow in a nitrogen-deficient mineral media containing only 2,4-TDA



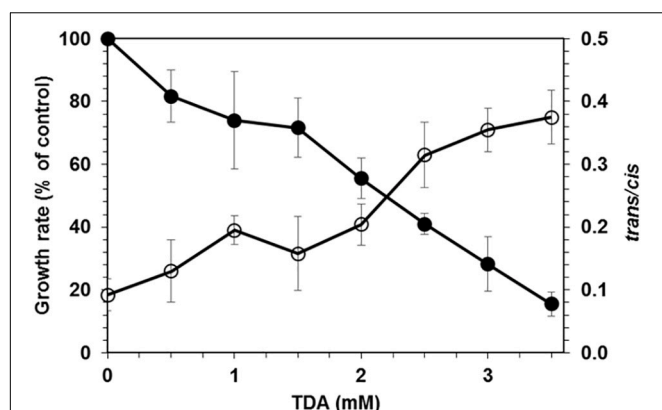


FIGURE 2 | Effect of 2,4-TDA on *P. putida* KT2440. Filled circles: Effect of 2,4-TDA on growth of *P. putida* KT2440. The growth rate after the addition of 2,4-TDA to exponentially growing cells is given relative to a control without 2,4-TDA. Empty circles: Effect of different 2,4-TDA concentrations on the *trans/cis* ratio of unsaturated fatty acids of *P. putida* KT2440.

as sole carbon and nitrogen source. Optical densities were similar to those obtained with ammonium chloride as nitrogen source (Figure 1). Next to 2,4-TDA also other (aromatic) compounds were tested if they serve as sole source of carbon and energy for the isolated strain. Toluene, benzene, aniline, 2,4-dihydroxytoluene and methylsuccinate did not support growth of the TDA1 strain, whereas benzoate, 2-aminobenzoate (anthranilate), phenol, *o*-xylene, catechol, 4-methylcatechol and benzene-1,2,4-triol served as a growth substrate (Table 1). In addition, the strain grew on an aliphatic oligomeric PU substrate of proprietary composition (PU diol solution, Sigma-Aldrich). Optical densities of about 0.8 were obtained with a concentration of 3 g/l (about 9 mM) of the oligomeric PU as sole carbon and energy source (data not shown).

The whole genome sequence has been deposited at DDBJ/ENA/GenBank under the accession WOVH00000000. The version described in this paper is version WOVH01000000. The

TABLE 1 | Growth spectrum for *Pseudomonas* sp. TDA1.

Carbon source	Growth
Toluene	–
Benzene	–
Aniline	–
2,4-Dihydroxytoluene (4-Methylresorcinol)	–
Methylsuccinate	–
Sodium benzoate	+
2-Aminobenzoate (Anthranilate)	+
Phenol	+
<i>o</i> -Xylene	+
Catechol	+
4-Methylcatechol	+
Benzene-1,2,4-triol (Hydroxyhydroquinone)	+

Aromatic substrates that were tested as sole source of carbon and energy for strain TDA1. Plus, growth. Minus, no growth.

gene locus tag is GNP06_XXXXX, the corresponding five-digit number is given in the text for each gene mentioned. Using the complete 16S rRNA gene sequence (gene 02555), the strain was identified as *Pseudomonas* sp. strain that shows high similarity with *P. oryzihabitans* and various *P. putida* strains. The strain TDA1 will be referred to as *Pseudomonas* sp. TDA1 in this paper. In addition, the phospholipid fatty acid profile of the strain TDA1 showed the presence of the following fatty acids: C14:0, C16:0, C16:1*trans*, C16:1*cis*, 17*cyclo*, C18:0, C18:1*trans*, C18:1*cis*, and 19*cyclo* (data not shown) comprising more than 95% of the total fatty acids of the strain. The fatty acid composition and pattern of TDA1 was the same as the one of strain *P. putida* KT2440 which was used as a control and benchmark. In addition, the gene for the *cis-trans* isomerase of unsaturated fatty acids (CTI), an important marker gene for the genus *Pseudomonas* (Palleroni, 2015; Eberlein et al., 2018), is present in the TDA1 genome (gene 13840) revealing more than 90% amino acid sequence identity with several *Pseudomonas* CTIs already present in the protein BLAST database (for example: Accession numbers Q8RJN7, A0A059V043, and F8FYU0). Also, the CTI phenotype, regularly given as solvent stress-depending increase in the *trans/cis* ratio of unsaturated fatty acids, was detected in the presence of 2,4-TDA in *P. putida* KT2440 (Figure 2).

Among pathways for degradation of central catecholic intermediates, genes encoding enzymes of the catechol branch of the 3-oxoadipate pathway (catechol 1,2-dioxygenase, muconate cycloisomerase and muconolactone isomerase, genes 25335, 25340, 25345) as well as those encoding the protocatechuate branch (α - and β -subunit of protocatechuate 3,4-dioxygenase, 3-carboxymuconate cycloisomerase and 4-carboxymuconolactone decarboxylase; genes 17435, 17430, 07520, and 07510) and the respective 3-oxoadipate enol-lactone hydrolases (genes 20490 and 07515, respectively) were identified. In addition, genes encoding enzymes for the formation of homogentisate (4-hydroxyphenylpyruvate dioxygenases, genes 05520 and 05730) and a homogentisate 1,2-dioxygenase pathway (genes 17645, 17650, and 17655) as well as a homoprotocatechuate pathway including a LigB type 3,4-dihydroxyphenylacetate 2,3-dioxygenase (gene 05110) were observed. Genes encoding enzymes of the corresponding *meta*-cleavage pathway for homoprotocatechuate were found: 5-carboxymethyl-2-hydroxymuconate semialdehyde dehydrogenase (gene 05115), 5-carboxymethyl-2-hydroxymuconate isomerase (gene 05105), 5-carboxymethyl-2-oxo-hex-3-ene-1,7-dioate decarboxylase (genes 05120 or 05125), and 2-oxo-hepta-3-ene-1,7-dioic acid hydratase (gene 05095). An additional dioxygenase was identified (gene 06545) which according to AROMADEG (Duarte et al., 2014) belongs to a family of extradiol dioxygenases of the vicinal oxygen chelate superfamily of extradiol dioxygenases comprising, among others, enzymes using miscellaneous substrates such as 2,3-dihydroxybenzoate and clustered with proteobacterial extradiol dioxygenases of unknown function (comprising among others YP_046462, an extradiol dioxygenase of *Acinetobacter baylyi* ADP1).

Genes coding for archetype catechol 2,3-dioxygenases such as *xylE*, *catE*, or *nahA*, extradiol dioxygenases belonging to family I.2 of the vicinal oxygen chelate superfamily, showing a

preference for monocyclic substrates and specifically cluster in XXII according to the revised phylogeny of AROMADEG (Eltis and Bolin, 1996; Vaillancourt et al., 2004; Pérez-Pantoja et al., 2009), are not present in the genome of TDA1. Neither ring cleaving dioxygenases involved in aminoaromatic degradation like 5-aminosalicylate 1,2 dioxygenase (Stolz and Knackmuss, 1993), 2-aminophenol 1,6-dioxygenase (Takenaka et al., 1997; Wu et al., 2005) nor hydroxybenzoquinol 1,2-dioxygenase (Travkin et al., 1997; Kitagawa et al., 2004; Wang et al., 2007; Pérez-Pantoja et al., 2009) are encoded in the TDA1 genome.

At least seven genes encoding putative α -subunits of Rieske non-heme iron dioxygenases are present in the genome of TDA1. They were analyzed using AROMADEG (Duarte et al., 2014): it was shown, that genes 26235, 17905, and 06615 are distantly related to enzymes of the phthalate family of Rieske dioxygenases. Gene 26235 probably encodes a vanillate O-demethylase with 76.2% amino acid sequence similarity to P12609 from *Pseudomonas* strain ATCC 19151. The product of gene 06615 shows significant amino acid sequence similarity of 47% with toluene 4-sulfonate monooxygenase TsaM1 (accession P94679) from *Comamonas testosteroni* T-2 (Locher et al., 1991a,b). Among enzymes of documented function, also the product of gene 17905 shows similarity to toluene 4-sulfonate monooxygenase TsaM1, however, only to a low extent of 33%. The gene product of 06600 clearly is a member of the phthalate family of Rieske oxygenases. According to AROMADEG, it belongs to a cluster comprising putative phthalate 4,5-dioxygenase from *Ralstonia eutropha* JMP134 (accession YP298987). Gene 19420 encodes a protein with 73.8% similarity with CntA carnitine monooxygenase (accession D0C9N6) of *Acinetobacter baumannii* ATCC 19606 and thus may be responsible for carnitine transformation to form trimethylamine and malic semialdehyde. The protein encoded by gene 25270 belongs to cluster I of the benzoate family of Rieske dioxygenases (enzymes involved in indole acetic acid degradation and related enzymes). Gene 08315 encodes a benzoate 1,2-dioxygenase (cluster XI, benzoate and 2-chlorobenzoate dioxygenases of the benzoate family of Rieske dioxygenases) with 97.1% identity with BenA of *P. putida* GJ31 (accession AAX47023).

Neither gene clusters encoding proteins involved in the side-chain oxidation of methyl-substituted aromatics, namely the two-component xylene/*p*-cymene monooxygenase, which consist of a hydroxylase related to AlkB alkane hydroxylase and a reductase (Worsey and Williams, 1975; Eaton, 1996) were observed in the genome, nor are multicomponent soluble diiron benzene/toluene or phenol/methylphenol monooxygenases encoded. However, five genes coding for flavin depending monooxygenases were detected (genes 05080, 17225, 06905, 06505, 06585). Gene products of 05080 and 06585 show high amino acid sequence similarity to 4-hydroxyphenylacetate 3-hydroxylase from *Acinetobacter baumannii* (accession Q6Q272) of 72.1% and 72.6%, respectively (Thotsaporn et al., 2004). The product of gene 17225 exhibits high sequence identity to documented 4-hydroxybenzoate 3-monooxygenases such as the enzymes P00438 from *P. fluorescens* (74.9%) or

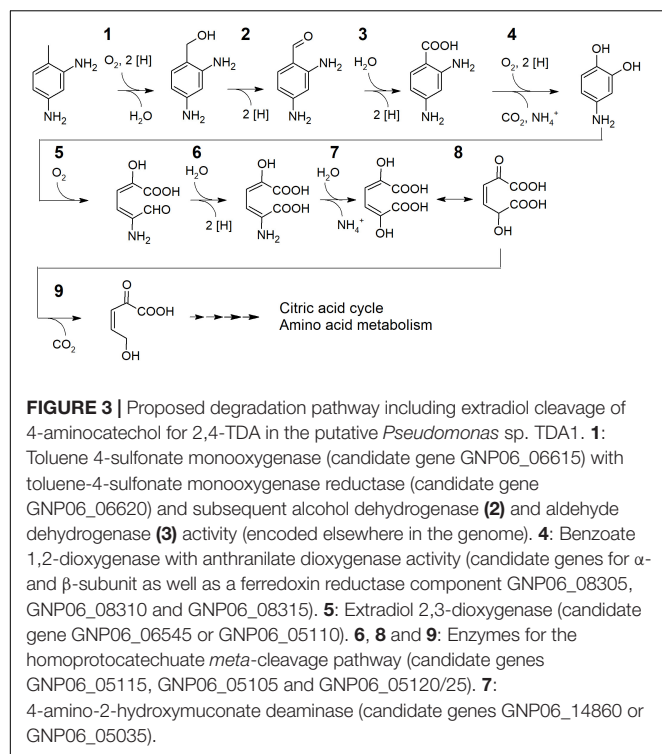
P20586 from *P. aeruginosa* (74.6%). In contrast to that, the function of flavin monooxygenases 06505 and 06905 remains unknown.

The release of nitrogen from aromatic amines can occur before ring cleavage in form of ammonia (Aoki et al., 1983; Chang et al., 2003; Takenaka et al., 2003), but also after ring opening (Takenaka et al., 2000). The latter is done by 2-aminomuconate deaminase during 2-aminophenol degradation by *Pseudomonas* sp. AP-3. This enzyme belongs to the YjgF/YER057c/UK114 family (also known as the Rid family). Five members of this family were observed to be encoded in the genome of the strain TDA1 (genes 01225, 03255, 14860, 17920, 05035). For two of these gene products significant similarities to 2-aminomuconate deaminase of *Pseudomonas* sp. AP-3 (accession Q9KWS2) could be documented: 36% for the gene product of 14860 and 32% for the gene product of 05035.

DISCUSSION

A bacterial strain capable of degrading both, an oligomeric PU and a PU building block was obtained from soil samples. According to our knowledge, this is the first report on the isolation of a bacterial pure culture for the polyurethane precursor 2,4-TDA. A powerful metabolic potential of the strain is given because of the ability to use both as sole source of carbon and energy, a monomer and an oligomer of PU. 2,4-TDA was used not only as the carbon and but also as a nitrogen source. That concentrations higher than 2 mM 2,4-TDA did not increase the optical densities further, might be due to toxic effect. Also for *P. putida* KT2440 it was shown, that concentrations above 2 mM 2,4-TDA diminished growth. The isolate was identified as *Pseudomonas* sp. strain by 16S rRNA gene sequence analysis and by comparing the fatty acid profile to the one of *P. putida* KT2440. The isolation of a *Pseudomonas* strain from the same oligomeric PU material was reported before (Mukherjee et al., 2011). Moreover, microbial attack on polyurethanes by species of the genus *Pseudomonas* was documented earlier (Howard and Blake, 1998; Howard, 2002; Gautam et al., 2007; Peng et al., 2014; Hung et al., 2016). The fact that PU polymers or components do not only meet the carbon but also the nitrogen demand was confirmed in this study. Earlier reports also had shown that polyisocyanates may serve as nitrogen source (Darby and Kaplan, 1968; Crabbe et al., 1994; Nakajima-Kambe et al., 1995; Kloss et al., 2009).

Considering the genomic potential and the substrate spectrum a degradation pathway for 2,4-TDA with candidate genes encoding the enzymes involved can be suggested (Figure 3). Although also a monooxygenation of an aromatic ring lacking hydroxyl groups has been reported in the case of styrene (Beltrametti et al., 1997), an initiation of the degradation of not yet activated aromatics by flavin monooxygenases is rather unlikely (Van Berkel et al., 2006). In contrast to that, hydroxylation of substituents at the aromatic ring, like the methyl group of toluene, is common (Assinder and Williams,



1990). However, strain TDA1 does not grow on toluene (Table 1) and the only putative methyl group oxidizing enzymes encoded are those with similarity to toluene 4-sulfonate monooxygenase TsaM1 (accession P94679) from *Comamonas testosteroni* T-2 (Locher et al., 1991a,b). Therefore, it can be assumed that the methyl group is hydroxylated to a primary alcohol (candidate gene 06615) with the help of an electron transferring unit. For the latter, a gene encoding for a protein sharing 48.1% sequence similarity with toluene-4-sulfonate monooxygenase reductase subunit TsaB1 (accession P94680) in *Comamonas testosteroni* is located adjacent to 06615. Obviously, the methyl oxidizing enzyme present needs a substituent in *para* position on the aromatic ring to function as the strain cannot grow on toluene. The following steps yielding 2,4-diaminobenzoate (4-aminoanthranilate) would be catalyzed by an alcohol dehydrogenase and subsequently by an aldehyde dehydrogenase encoded elsewhere in the genome. Strain TDA1 uses anthranilate as the sole source of carbon and energy which typically is catalyzed by an anthranilate 1,2-dioxygenase (Cain, 1968; Eby et al., 2001; Schühle et al., 2001; Chang et al., 2003; Liu et al., 2010; Costaglioli et al., 2012; Kim et al., 2015). No such enzyme is encoded in the genome of TDA1. However, some benzoate dioxygenases are reported to transform anthranilate to catechol (Yamaguchi and Fujisawa, 1980; Haddad et al., 2001) and a gene cluster encoding a benzoate 1,2-dioxygenase α - and β -subunit as well as a ferredoxin reductase component (genes 08305, 08310, 08315) is conserved in the genome. It is therefore conceivable that 2,4-diaminobenzoate is transformed by benzoate 1,2-dioxygenase yielding 4-aminocatechol as central intermediate.

Studies showed that aromatic compounds with electron-donating substituents, such as amino groups, are preferably degraded via the *meta*-cleavage pathway (Ribbons, 1965; Seidman et al., 1969; Bugg and Ramaswamy, 2008; Shukla et al., 2016). It can therefore be speculated that the putative intermediate 4-aminocatechol is transformed by an extradiol dioxygenase; and a respective extradiol dioxygenase of the vicinal chelate superfamily is actually encoded in the genome (candidate gene 06545). A second extradiol dioxygenase, a homoprotocatechuate 2,3-dioxygenase of the LigB superfamily (Roper and Cooper, 1990), is encoded by gene 05110 located within a gene cluster encoding enzymes for the further metabolism of the homoprotocatechuate ring-cleavage product via the *meta*-cleavage pathway. Several publications state that homoprotocatechuate 2,3-dioxygenase is promiscuous and may accept 4-nitrocatechol as a substrate (Groce et al., 2004; Henderson et al., 2012; Kovaleva and Lipscomb, 2012; Mbughuni et al., 2012). If the 06545 extradiol dioxygenase or a promiscuous homoprotocatechuate dioxygenase is involved in 2,4-TDA degradation by strain TDA1 remains to be elucidated. Further degradation of the putative ring-cleavage product 4-amino-2-hydroxymuconate semialdehyde may then be performed by homoprotocatechuate *meta*-cleavage pathway enzymes with 5-carboxymethyl-2-hydroxymuconic semialdehyde dehydrogenase encoded by gene 05115 forming 4-amino-2-hydroxymuconate. As the next step, the formed 4-amino-2-hydroxymuconate could be deaminated by an aminomuconate deaminase (candidate genes 14860 or 05035) similar to the deamination after ring cleavage in the degradation pathway of aminophenol in *Pseudomonas* sp. AP-3 (Takenaka et al., 2000) or in nitrobenzene degradation in *Pseudomonas pseudoalcaligenes* JS4 (He and Spain, 1997). For the latter, the enzyme 2-aminomuconate deaminase does not depend on cofactors and deamination of its substrate even happens spontaneously in acidic environments (Ichiyama et al., 1965). In the metabolism of 4-amino-3-hydroxybenzoic acid in *Bordetella* sp. 10d the amino group is cleaved off already from the muconic semialdehyde intermediate by a 2-amino-5-carboxymuconicsemialdehyde deaminase (Orii et al., 2006). The resulting intermediate 2,5-dihydroxy-muconate probably undergoes tautomerization (gene 05105) and could be further subjected to a decarboxylation step (gene 05120 or 05125). Following the *meta*-cleavage pathway, a hydroxylation would take place after the decarboxylation and the corresponding hydratase is also present in the genome of TDA1 (gene 05095). However, how exactly the degradation pathway is continued to lead to central metabolites of the citric acid cycle or amino acid metabolism needs to be elucidated in further studies.

To sum up, a preliminary degradation pathway of 2,4-TDA is proposed. In the peripheral pathway 4-aminocatechol is formed after oxidation of the methyl group of diaminotoluene and subsequent dioxygenation with concomitant decarboxylation and deamination. Ring cleavage of 4-aminocatechol in TDA1 would be possible in an extradiol manner (candidate gene 06545) and further employment of the homoprotocatechuate

meta-pathway (genes 05115, 05105, 05120/25) with the second deamination potentially taking place after the formation of 5-amino 2-hydroxymuconate (candidate genes 14860 or 05035).

The majority of the enzymes involved in the proposed pathway must be promiscuous regarding their substrate specificity, i.e., they need to accept especially amino substituted analogs. Due to the low steric hindrance of an additional amino group substrate promiscuity might be favored. Enzymes involved in aromatics degradation exhibiting significant activity with substituted substrate analogs were reported before (Pascal and Huang, 1986; Smith et al., 1990; He and Spain, 1997; Eby et al., 2001; Chang et al., 2003; Guzik et al., 2011). However, the proposed degradation pathway of 2,4-TDA in the putative *Pseudomonas* strain TDA1 needs further confirmation via proteomic, transcriptomic analysis or *in vitro* assays with potential intermediates of the proposed pathway. Identifying the key enzymes for the degradation of both, 2,4-TDA as putative degradation product as well as precursor of PUs (Matsumiya et al., 2010; Magnin et al., 2019) and for the oligomeric PU could help to equip well known and biotechnological used lab strains like *P. putida* KT2440 for monomer degradation in two-step biorecycling processes.

REFERENCES

- Altschul, S. F., Madden, T. L., Schaffer, A. A., Zhang, J. H., Zhang, Z., Miller, W., et al. (1997). Gapped BLAST and PSI-BLAST: a new generation of protein database search programs. *Nucleic Acids Res.* 25, 3389–3402.
- Álvarez-Barragán, J., Domínguez-Malfavon, L., Vargas-Suárez, M., González-Hernández, R., Aguilar-Osorio, G., and Loza-Tavera, H. (2016). Biodegradative activities of selected environmental fungi on a polyester polyurethane varnish and polyether polyurethane foams. *Appl. Environ. Microbiol.* 82, 5225–5235. doi: 10.1128/AEM.01344-16
- Aoki, K., Shinke, R., and Nishira, H. (1983). Microbial-metabolism of aromatic-amines.3. Metabolism of Aniline by *Rhodococcus-Erythropolis* an-13. *Agric. Biol. Chem.* 47, 1611–1616.
- Assinder, S. J., and Williams, P. A. (1990). The tol plasmids - determinants of the catabolism of toluene and the xylenes. *Adv. Microb. Physiol.* 31, 1–69.
- Aziz, R. K., Bartels, D., Best, A. A., Dejongh, M., Disz, T., Edwards, R. A., et al. (2008). The RAST server: rapid annotations using subsystems technology. *Bmc Genomics* 9:75. doi: 10.1186/1471-2164-9-75
- Baua, T. (2008). 4-Diamine: Summary Risk Assessment Report. Available at: <https://echa.europa.eu/documents/10162/a306907a-8401-4a75-8a84-88b9f225d5cf> (accessed October 2019).
- Beltrametti, F., Marconi, A. M., Bestetti, G., Colombo, C., Galli, E., Ruzzi, M., et al. (1997). Sequencing and functional analysis of styrene catabolism genes from *Pseudomonas fluorescens* ST. *Appl. Environ. Microbiol.* 63, 2232–2239.
- Bligh, E. G., and Dyer, W. J. (1959). A rapid method of total lipid extraction and purification. *Can. J. Biochem. Physiol.* 37, 911–917.
- Bugg, T. D., and Ramaswamy, S. (2008). Non-heme iron-dependent dioxygenases: unravelling catalytic mechanisms for complex enzymatic oxidations. *Curr. Opin. Chem. Biol.* 12, 134–140. doi: 10.1016/j.cbpa.2007.12.007
- Cain, R. B. (1968). Anthranilic acid metabolism by microorganisms. formation of 5-hydroxyanthranilate as an intermediate in anthranilate metabolism by *Nocardia Opaca*. *Antonie Van Leeuwenhoek* 34, 417–432.
- Chang, H. K., Mohseni, P., and Zylstra, G. J. (2003). Characterization and regulation of the genes for a novel anthranilate 1,2-dioxygenase from *Burkholderia cepacia* DBO1. *J. Bacteriol.* 185, 5871–5881.
- Costaglioli, P., Barthe, C., Claverol, S., Brozel, V. S., Perrot, M., Crouzet, M., et al. (2012). Evidence for the involvement of the anthranilate degradation pathway in *Pseudomonas aeruginosa* biofilm formation. *Microbiol. Open* 1, 326–339. doi: 10.1002/mbo3.33

DATA AVAILABILITY STATEMENT

The whole genome sequence has been deposited at DDBJ/ENA/GenBank under the accession WOVH00000000. The version described in this article is version WOVH01000000.

AUTHOR CONTRIBUTIONS

MC, CE, UK, and HH conceived and designed the experiments. MC, AC, TS, and AA-K performed the experiments. DT performed the genome sequencing and annotation. DP, UK, CE, and HH analyzed the data. HH and CE contributed reagents, materials, and analysis tools. MC, CE, DP, and HH wrote the manuscript.

FUNDING

The Financial support by the European Union's Horizon 2020 Research and Innovation Program under grant agreement no. 633962 for the project P4SB is greatly appreciated.

- Crabbe, J. R., Campbell, J. R., Thompson, L., Walz, S. L., and Schultz, W. W. (1994). Biodegradation of a Colloidal Ester-Based Polyurethane by Soil Fungi. *Int. Biodeter. Biodegr.* 33, 103–113.
- Cregut, M., Bedas, M., Durand, M. J., and Thouand, G. (2013). New insights into polyurethane biodegradation and realistic prospects for the development of a sustainable waste recycling process. *Biotechnol. Adv.* 31, 1634–1647. doi: 10.1016/j.biotechadv.2013.08.011
- Darby, R. T., and Kaplan, A. M. (1968). Fungal susceptibility of polyurethanes. *Appl. Microbiol.* 16, 900–910.
- Duarte, M., Jauregui, R., Vilchez-Vargas, R., Junca, H., and Pieper, D. H. (2014). AromaDeg, a novel database for phylogenomics of aerobic bacterial degradation of aromatics. *Database* 2014:bau118. doi: 10.1093/database/bau118
- Eaton, R. W. (1996). p-Cumate catabolic pathway in *Pseudomonas putida* Fl: cloning and characterization of DNA carrying the cmt operon. *J. Bacteriol.* 178, 1351–1362. doi: 10.1128/jb.178.5.1351-1362.1996
- Eberlein, C., Baumgarten, T., Starke, S., and Heipieper, H. J. (2018). Immediate response mechanisms of Gram-negative solvent-tolerant bacteria to cope with environmental stress: cis-trans isomerization of unsaturated fatty acids and outer membrane vesicle secretion. *Appl. Microbiol. Biotechnol.* 102, 2583–2593. doi: 10.1007/s00253-018-8832-9
- Eby, D. M., Beharry, Z. M., Coulter, E. D., Kurtz, D. M. Jr., and Neidle, E. L. (2001). Characterization and evolution of anthranilate 1,2-dioxygenase from *Acinetobacter* sp. strain ADP1. *J. Bacteriol.* 183, 109–118.
- Eltis, L. D., and Bolin, J. T. (1996). Evolutionary relationships among extradiol dioxygenases. *J. Bacteriol.* 178, 5930–5937.
- European Chemicals Agency (2019). *European Chemicals Agency*. Available at: <https://echa.europa.eu/home> (accessed October 2019).
- Vaillancourt, F. H., Bolin, J. T., Eltis, L. D. (2004). "Ring-cleavage dioxygenases," in *Pseudomonas*, ed. J. Ramos (New York, NY: Kluwer Academic/Plenum Publishers), 359–395.
- Freedman, D. L., Shanley, R. S., and Scholze, R. J. (1996). Aerobic biodegradation of 2,4-dinitrotoluene, aminonitrotoluene isomers, and 2,4-diaminotoluene. *J. Hazard Mater.* 49, 1–14.
- Gautam, R., Bassi, A. S., Yanful, E. K., and Cullen, E. (2007). Biodegradation of automotive waste polyester polyurethane foam using *Pseudomonas chlororaphis* ATCC55729. *Int. Biodeter. Biodegr.* 60, 245–249.

- Groce, S. L., Miller-Rodeberg, M. A., and Lipscomb, J. D. (2004). Single-turnover kinetics of homoprotocatechuate 2,3-dioxygenase. *Biochemistry* 43, 15141–15153.
- Guzik, U., Greń, I., Hupert-Kocurek, K., and Wojcieszynska, D. (2011). Catechol 1,2-dioxygenase from the new aromatic compounds – Degrading *Pseudomonas putida* strain N6. *Int. Biodeterioration Biodegrad.* 65, 504–512. doi: 10.1016/j.ibiod.2011.02.001
- Haddad, S., Eby, D. M., and Neidle, E. L. (2001). Cloning and expression of the benzoate dioxygenase genes from *Rhodococcus* sp. strain 19070. *Appl. Environ. Microbiol.* 67, 2507–2514.
- Hartmans, S., Smits, J. P., Van Der Werf, M.J., Volkerling, F., and De Bont, J. A. M. (1989). Metabolism of styrene oxide and 2-phenylethanol in the styrene-degrading *Xanthobacter* strain 124X. *Appl. Environ. Microbiol.* 55, 2850–2855.
- He, Z. G., and Spain, J. C. (1997). Studies of the catabolic pathway of degradation of nitrobenzene by *Pseudomonas pseudoalcaligenes* JS45: removal of the amino group from 2-aminomuconic semialdehyde. *Appl. Environ. Microbiol.* 63, 4839–4843.
- Heipieper, H. J., Löffeld, B., Keweloh, H., and De Bont, J. A. M. (1995). The *cis/trans* isomerisation of unsaturated fatty acids in *Pseudomonas putida* S12: an indicator for environmental stress due to organic compounds. *Chemosphere* 30, 1041–1051.
- Henderson, K. L., Le, V. H., Lewis, E. A., and Emerson, J. P. (2012). Exploring substrate binding in homoprotocatechuate 2,3-dioxygenase using isothermal titration calorimetry. *J. Biol. Inorg. Chem.* 17, 991–994. doi: 10.1007/s00775-012-0929-5
- Howard, G. T. (2002). Biodegradation of polyurethane: a review. *Int. Biodeter. Biodegr.* 49, 245–252.
- Howard, G. T., and Blake, R. C. (1998). Growth of *Pseudomonas fluorescens* on a polyester-polyurethane and the purification and characterization of a polyurethanase-protease enzyme. *Int. Biodeter. Biodegr.* 42, 213–220.
- Hung, C. S., Zingarelli, S., Nadeau, L. J., Biffinger, J. C., Drake, C. A., Crouch, A. L., et al. (2016). Carbon catabolite repression and imranil polyurethane degradation in *Pseudomonas protegens* Strain Pf-5. *Appl. Environ. Microbiol.* 82, 6080–6090.
- Ichiyama, A., Nakamura, S., Kawai, H., Honjo, T., Nishizuka, Y., Hayaishi, O., et al. (1965). Studies on the metabolism of the benzene ring of tryptophan in mammalian tissues. ii. enzymic formation of alpha-aminomuconic acid from 3-hydroxyanthranilic acid. *J. Biol. Chem.* 240, 740–749.
- Kim, D., Yoo, M., Kim, E., and Hong, S. G. (2015). Anthranilate degradation by a cold-adapted *Pseudomonas* sp. *J. Basic Microbiol.* 55, 354–362. doi: 10.1002/jobm.201300079
- Kitagawa, W., Kimura, N., and Kamagata, Y. (2004). A novel p-nitrophenol degradation gene cluster from a gram-positive bacterium. *Rhodococcus opacus* SAO101. *J. Bacteriol.* 186, 4894–4902.
- Kloss, J. R., Pedrozo, T. H., Follmann, H. D., Peralta-Zamora, P., Dionísio, J. A., Akcelrud, L., et al. (2009). Application of the principal component analysis method in the biodegradation polyurethanes evaluation. *Mater. Sci. Eng. C* 29, 470–473.
- Kovaleva, E. G., and Lipscomb, J. D. (2012). Structural basis for the role of tyrosine 257 of homoprotocatechuate 2,3-dioxygenase in substrate and oxygen activation. *Biochemistry* 51, 8755–8763. doi: 10.1021/bi301115c
- Krasowska, K., Janik, H., Grady, A., and Rutkowska, M. (2012). Degradation of polyurethanes in compost under natural conditions. *J. Appl. Polym. Sci.* 125, 4252–4260.
- Liu, X., Dong, Y., Li, X., Ren, Y., Li, Y., Wang, W., et al. (2010). Characterization of the anthranilate degradation pathway in *Geobacillus thermodenitrificans* NG80-2. *Microbiology* 156, 589–595. doi: 10.1099/mic.0.031880-0
- Locher, H. H., Leisinger, T., and Cook, A. M. (1991a). 4-Toluene sulfonate methylmonooxygenase from *Comamonas testosteroni* T-2: purification and some properties of the oxygenase component. *J. Bacteriol.* 173, 3741–3748.
- Locher, H. H., Malli, C., Hooper, S. W., Vorherr, T., Leisinger, T., and Cook, A. M. (1991b). Degradation of p-toluic acid (p-toluenecarboxylic acid) and p-toluenesulphonic acid via oxygenation of the methyl sidechain is initiated by the same set of enzymes in *Comamonas testostemni* T-2. *J. Gen. Microbio.* 137, 221–2208.
- Magnin, A., Pollet, E., Perrin, R., Ullmann, C., Persillon, C., Phalip, V., et al. (2019). Enzymatic recycling of thermoplastic polyurethanes: synergistic effect of an esterase and an amidase and recovery of building blocks. *Waste Manag.* 85, 141–150. doi: 10.1016/j.wasman.2018.12.024
- Marchant, R. E., Zhao, Q., Anderson, J. M., and Hiltner, A. (1987). Degradation of a Poly(Ether Urethane Urea) Elastomer - Infrared and Xps Studies. *Polymer* 28, 2032–2039.
- Matsumiya, Y., Murata, N., Tanabe, E., Kubota, K., and Kubo, M. (2010). Isolation and characterization of an ether-type polyurethane-degrading micro-organism and analysis of degradation mechanism by *Alternaria* sp. *J. Appl. Microbiol.* 108, 1946–1953. doi: 10.1111/j.1365-2672.2009.04600.x
- Mbughuni, M. M., Meier, K. K., Munck, E., and Lipscomb, J. D. (2012). Substrate-mediated oxygen activation by homoprotocatechuate 2,3-Dioxygenase: intermediates formed by a tyrosine 257 variant. *Biochemistry* 51, 8743–8754. doi: 10.1021/bi301114x
- Morrison, W. R., and Smith, L. M. (1964). Preparation of fatty acid methyl esters and dimethylacetals from lipids with boron fluoride-methanol. *J. Lipid Res.* 5, 600–608.
- Mukherjee, K., Tribedi, P., Chowdhury, A., Ray, T., Joardar, A., Giri, S., et al. (2011). Isolation of a *Pseudomonas aeruginosa* strain from soil that can degrade polyurethane diol. *Biodegradation* 22, 377–388. doi: 10.1007/s10532-010-9409-1
- Nakajima-Kambe, T., Onuma, F., Kimpara, N., and Nakahara, T. (1995). Isolation and characterization of a bacterium which utilizes polyester polyurethane as a sole carbon and nitrogen source. *FEMS Microbiol. Lett.* 129, 39–42.
- Orii, C., Takenaka, S., Murakami, S., and Aoki, K. (2006). Metabolism of 4-amino-3-hydroxybenzoic acid by *Bordetella* sp. strain 10d: a different modified meta-cleavage pathway for 2-aminophenols. *Biosci. Biotechnol. Biochem.* 70, 2653–2661.
- Palleroni, N. J. (2015). “Pseudomonas,” in *Bergey's Manual of Systematics of Archaea and Bacteria*, eds W. B. Whitman, F. Rainey, P. Kämpfer, M. Trujillo, J. Chun, P. De Vos, B. Hedlund, and S. Dedys (Hoboken, NJ: John Wiley & Sons, Inc), 1–105.
- Pascal, R. A. Jr., and Huang, D. S. (1986). Reactions of 3-ethylcatechol and 3-(methylthio)catechol with catechol dioxygenases. *Arch. Biochem. Biophys.* 248, 130–137. doi: 10.1016/0003-9861(86)90409-1
- Peng, Y. H., Shih, Y. H., Lai, Y. C., Liu, Y. Z., Liu, Y. T., and Lin, N. C. (2014). Degradation of polyurethane by bacterium isolated from soil and assessment of polyurethanolytic activity of a *Pseudomonas putida* strain. *Environ. Sci. Pollut. Res. Int.* 21, 9529–9537. doi: 10.1007/s11356-014-2647-8
- Pérez-Pantoja, D., Donoso, R., Junca, H., González, B., and Pieper, D. H. (2009). “Phylogenomics of aerobic bacterial degradation of aromatics,” in *Handbook of Hydrocarbon and Lipid Microbiology*, ed. K. N. Timmis (Berlin: Springer), 1355–1397.
- Plasticseurope (2016). “Plastics – the facts 2016,” in *An Analysis of European Plastics Production, Demand and Waste Data*, Brussels.
- Ribbons, D. W. (1965). Microbiological degradation of aromatic compounds. *Annu. Rep. Prog. Chem.* 62:445.
- Roper, D. I., and Cooper, R. A. (1990). Subcloning and nucleotide sequence of the 3,4-dihydroxyphenylacetate (homoprotocatechuate) 2,3-dioxygenase gene from *Escherichia coli* C. *FEBS Lett.* 275, 53–57.
- Russell, J. R., Huang, J., Anand, P., Kucera, K., Sandoval, A. G., Dantzler, K. W., et al. (2011). Biodegradation of polyester polyurethane by endophytic fungi. *Appl. Environ. Microbiol.* 77, 6076–6084. doi: 10.1128/AEM.00521-11
- Schühle, K., Jahn, M., Ghisla, S., and Fuchs, G. (2001). Two similar gene clusters coding for enzymes of a new type of aerobic 2-aminobenzoate (anthranilate) metabolism in the bacterium *Azoarcus evansii*. *J. Bacteriol.* 183, 5268–5278.
- Seidman, M. M., Toms, A., and Wood, J. M. (1969). Influence of side-chain substituents on position of cleavage of benzene ring by *Pseudomonas fluorescens*. *J. Bacteriol.* 97, 1192–1197.
- Shah, Z., Krumholz, L., Aktas, D. F., Hasan, F., Khattak, M., and Shah, A. A. (2013). Degradation of polyester polyurethane by a newly isolated soil bacterium. *Bacillus subtilis* strain MZA-75. *Biodegr* 24, 865–877. doi: 10.1007/s10532-013-9634-5
- Shukla, A., Singh, B., Singh Cameotra, S., and Kahlon, S. R. (2016). *Pseudomonas Oxxygenases: Nature and Function*. Switzerland. Berlin: Springer.

- Smith, M. R., Ratledge, C., and Crook, S. (1990). Properties of cyanogen bromide-activated, Agarose-immobilized catechol 1,2-dioxygenase from freeze-dried extracts of *Nocardia* Sp. NCIB 10503. *Enzyme Microbial. Technol.* 12, 945–949. doi: 10.1016/0141-0229(90)90114-6
- Stolz, A., and Knackmuss, H. J. (1993). Bacterial Metabolism of 5-aminosalicylic acid - enzymatic conversion to L-Malate. Pyruvate and Ammonia. *J. Gen. Microbiol.* 139, 1019–1025.
- Takenaka, S., Murakami, S., Kim, Y. J., and Aoki, K. (2000). Complete nucleotide sequence and functional analysis of the genes for 2-aminophenol metabolism from *Pseudomonas* sp. AP-3. *Arch. Microbiol.* 174, 265–272.
- Takenaka, S., Murakami, S., Shinke, R., Hatakeyama, K., Yukawa, H., and Aoki, K. (1997). Novel genes encoding 2-aminophenol 1,6-dioxygenase from *Pseudomonas* species AP-3 growing on 2-aminophenol and catalytic properties of the purified enzyme. *J. Biol. Chem.* 272, 14727–14732.
- Takenaka, S., Okugawa, S., Kadowaki, M., Murakami, S., and Aoki, K. (2003). The metabolic pathway of 4-aminophenol in *Burkholderia* sp strain AK-5 differs from that of aniline and aniline with C-4 substituents. *Appl. Environ. Microbiol.* 69, 5410–5413.
- Thotsaporn, K., Sucharitakul, J., Wongratana, J., Suadee, C., and Chaiyen, P. (2004). Cloning and expression of p-hydroxyphenylacetate 3-hydroxylase from *Acinetobacter baumannii*: evidence of the divergence of enzymes in the class of two-protein component aromatic hydroxylases. *Biochim. Biophys. Acta* 1680, 60–66.
- Travkin, V. M., Jadan, A. P., Briganti, F., Scozzafava, A., and Golovleva, L. A. (1997). Characterization of an intradiol dioxygenase involved in the biodegradation of the chlorophenoxy herbicides 2,4-D and 2,4,5-T. *Febs Lett.* 407, 69–72.
- Van Berkel, W. J., Kamerbeek, N. M., and Fraaije, M. W. (2006). Flavoprotein monooxygenases, a diverse class of oxidative biocatalysts. *J. Biotechnol.* 124, 670–689.
- Wang, G. B., Labow, R. S., and Santerre, J. P. (1997). Biodegradation of a poly(ester)urea-urethane by cholesterol esterase: Isolation and identification of principal biodegradation products. *J. Biomed. Mater. Res.* 36, 407–417.
- Wang, Q., Garrity, G. M., Tiedje, J. M., and Cole, J. R. (2007). Naive Bayesian classifier for rapid assignment of rRNA sequences into the new bacterial taxonomy. *Appl. Environ. Microbiol.* 73, 5261–5267.
- Worsey, M. J., and Williams, P. A. (1975). Metabolism of toluene and xylenes by *Pseudomonas putida* (arvilla) mt-2: evidence for a new function of the TOL plasmid. *J. Bacteriol.* 124, 7–13. doi: 10.1128/JB.124.1.7-13.1975
- Wu, J. F., Sun, C. W., Jiang, C. Y., Liu, Z. P., and Liu, S. J. (2005). A novel 2-aminophenol 1,6-dioxygenase involved in the degradation of p-chloronitrobenzene by *Comamonas* strain CNB-1: purification, properties, genetic cloning and expression in *Escherichia coli*. *Arch. Microbiol.* 183, 1–8.
- Yamaguchi, M., and Fujisawa, H. (1980). Purification and characterization of an oxygenase component in benzoate 1,2-dioxygenase system from *Pseudomonas arvilla* C-1. *J. Biol. Chem.* 255, 5058–5063.
- Zerbino, D. R., and Birney, E. (2008). Velvet: algorithms for de novo short read assembly using de Bruijn graphs. *Genome Res.* 18, 821–829. doi: 10.1101/gr.074492.107

Conflict of Interest: The authors declare that the research was conducted in the absence of any commercial or financial relationships that could be construed as a potential conflict of interest.

Copyright © 2020 Cárdenas Espinosa, Colina Blanco, Schmidgall, Atanasoff-Kardjaleff, Kappelmeyer, Tischler, Pieper, Heipieper and Eberlein. This is an open-access article distributed under the terms of the Creative Commons Attribution License (CC BY). The use, distribution or reproduction in other forums is permitted, provided the original author(s) and the copyright owner(s) are credited and that the original publication in this journal is cited, in accordance with accepted academic practice. No use, distribution or reproduction is permitted which does not comply with these terms.



Microbial Degradation and Valorization of Plastic Wastes

Jiakang Ru¹, Yixin Huo^{1,2} and Yu Yang^{1*}

¹ Department of Biology, School of Life Science, Beijing Institute of Technology, Beijing, China, ² Key Laboratory of Molecular Medicine and Biotherapy, Beijing Institute of Technology, Beijing, China

OPEN ACCESS

Edited by:

Ren Wei,
University of Greifswald, Germany

Reviewed by:

Jose Ignacio Jimenez,
University of Surrey, United Kingdom
Kaili Nie,
Beijing University of Chemical
Technology, China
Nick Wierckx,
Forschungszentrum Jülich GmbH,
Germany

*Correspondence:

Yu Yang
yooyoung@bit.edu.cn

Specialty section:

This article was submitted to
Microbiotechnology,
a section of the journal
Frontiers in Microbiology

Received: 25 October 2019

Accepted: 02 March 2020

Published: 21 April 2020

Citation:

Ru J, Huo Y and Yang Y (2020)
Microbial Degradation
and Valorization of Plastic Wastes.
Front. Microbiol. 11:442.
doi: 10.3389/fmicb.2020.00442

A growing accumulation of plastic wastes has become a severe environmental and social issue. It is urgent to develop innovative approaches for the disposal of plastic wastes. In recent years, reports on biodegradation of synthetic plastics by microorganisms or enzymes have sprung up, and these offer a possibility to develop biological treatment technology for plastic wastes. In this review, we have comprehensively summarized the microorganisms and enzymes that are able to degrade a variety of generally used synthetic plastics, such as polyethylene (PE), polystyrene (PS), polypropylene (PP), polyvinyl chloride (PVC), polyurethane (PUR), and polyethylene terephthalate (PET). In addition, we have highlighted the microbial metabolic pathways for plastic depolymerization products and the current attempts toward utilization of such products as feedstocks for microbial production of chemicals with high value. Taken together, these findings will contribute to building a conception of bio-upcycling plastic wastes by connecting the biodegradation of plastic wastes to the biosynthesis of valuable chemicals in microorganisms. Last, but not least, we have discussed the challenges toward microbial degradation and valorization of plastic wastes.

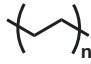


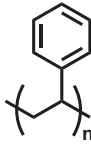

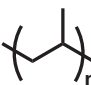

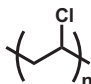

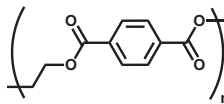

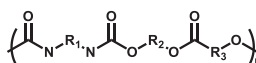

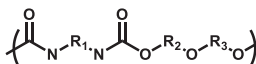
Keywords: plastic wastes, biodegradation, valorization, depolymerase, protein engineering, synthetic biology

INTRODUCTION

Synthetic plastics, including polyethylene (PE), polystyrene (PS), polypropylene (PP), polyvinyl chloride (PVC), polyurethane (PUR), and polyethylene terephthalate (PET) (**Table 1**), have become fundamental to almost every aspect of our lives. According to the latest statistics of Plastics-Europe, the global yield of plastics reached 348 million tons in 2018 (Plastics Europe, 2018). China and the European Union account for 29.4 and 18.5%, ranking first and second in the world, of all the world's plastic use, respectively (China Plastics Industry, 2017; Plastics Europe, 2018). Concomitant with the growing consumption of plastics, the generation of plastic wastes increases rapidly around the world. It is predicted that up to 26 billion tons of plastic wastes will be produced by 2050, and more than half will be thrown away into landfills and finally enter ecospheres, such as oceans and lakes, leading to serious environmental pollution (Jambeck et al., 2015; Lönnstedt and Eklöv, 2016; Geyer et al., 2017). As a result, plastic wastes have become a malevolent symbol of our wasteful society.

The current methods for disposing of plastic wastes mainly include landfilling, incineration, and mechanical and chemical recycling (Peng et al., 2018). In most countries, especially the developing countries, landfilling is the major method for plastic wastes disposal due to its operability and low

TABLE 1 | Types and properties of generally used synthetic plastics.

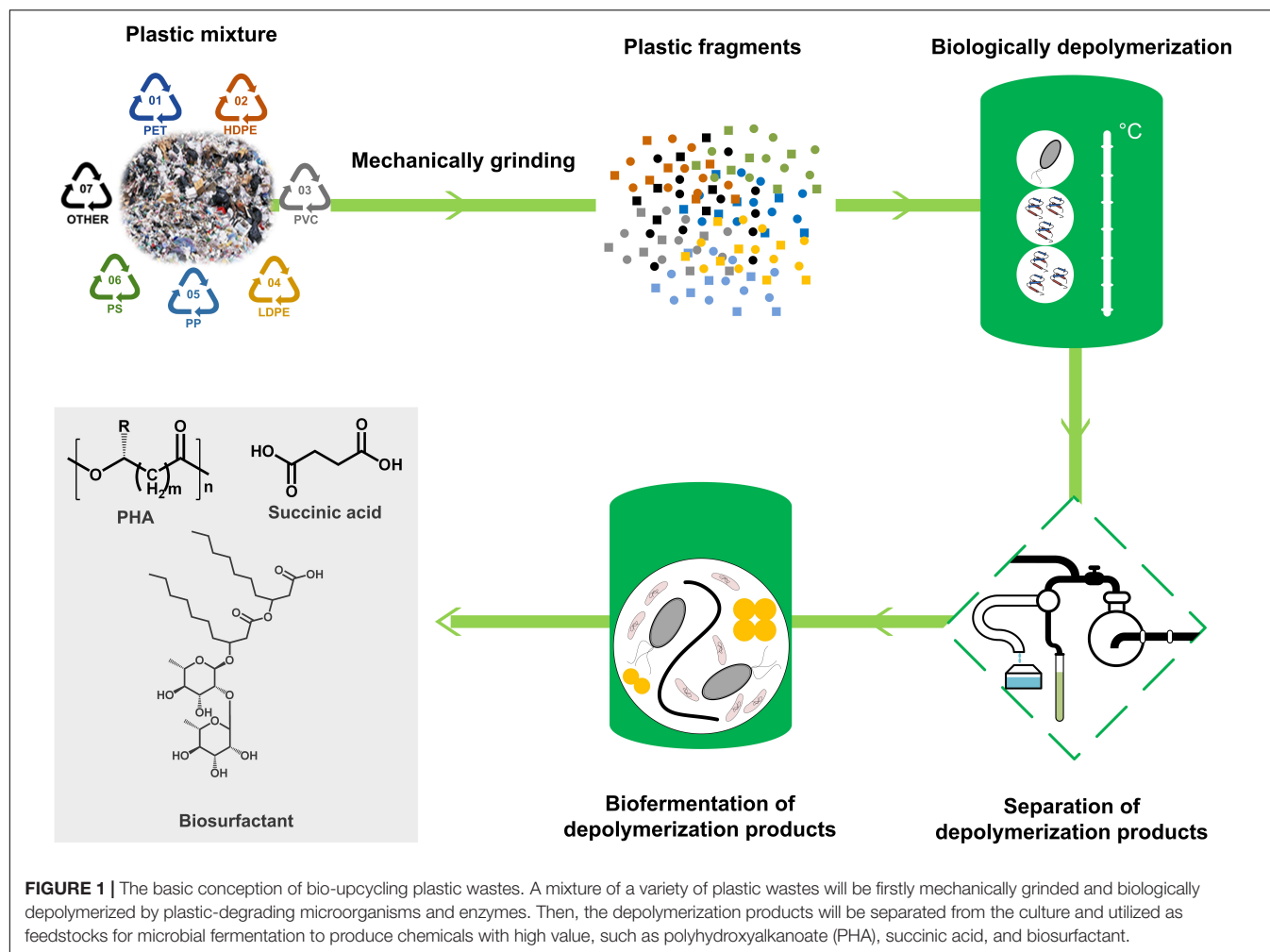
Plastics	Abbreviation	Structure formula	T _m (°C) ^a	T _g (°C) ^b	X _C (%) ^c	Recycling codes
High-density polyethylene	HDPE		200–300	–120	80–90	
Low-density polyethylene	LDPE		160–260	–120	45–65	
Polystyrene	PS		240	63–112	–	
Polypropylene	PP		130	–10–18	60–70	
Polyvinyl chloride	PVC		100–260	60–70	–	
Polyethylene terephthalate	PET		260	80	40–60	
Polyester polyurethane	Polyester PUR		8–20 (soft)	–75 to –50 (soft) 185–205 (hard)	40–50	
Polyether polyurethane	Polyether PUR		–95 (soft) 100 (hard)	–10 to 45 (soft) 190–240 (hard)		

^aT_m, melting temperature. ^bT_g, glass transition temperature. ^cX_C, crystallinity.

cost. However, the accumulated plastic wastes have occupied a great amount of land. Incineration of plastic wastes can reduce the demand of landfills and recover heat energy, but we also need to reduce the environmental effects of secondary pollutants generated from the incinerating process, such as dioxins, carbon monoxide, nitrogen oxides, and so on. Although mechanical recycling has become the primary recycling method and is applied for reusing thermoplastic wastes, the properties of most recycled materials are significantly compromised after a number of processing cycles, and the resulting commercial values are thus limited. As an alternative, chemical recycling can recover the monomers and other chemicals from plastic wastes, but its success relies on the affordability of processes and the efficiency of catalysts (Rahimi and García, 2017). Nowadays, it is reported that only 9 and 12% of global plastic wastes is recycled and incinerated, while up to 79% is discarded into landfills or the natural environment, indicating that there is a great need for exploring innovative recycling methods to dispose of plastic wastes (Garcia and Robertson, 2017; Geyer et al., 2017).

In recent years, a number of studies have reported that several microorganisms and enzymes are capable of degrading synthetic plastics. Although numerous reviews and viewpoints on the topic of biodegradation of plastic have been published,

they have mainly focused on the biodegradation of a single kind of plastic, such as PE (Restrepo-Flórez et al., 2014), PS (Ho et al., 2018), PP (Arutchelvi et al., 2008), PUR (Cregut et al., 2013; Peng et al., 2018; Magnin et al., 2019c), and PET (Wei and Zimmermann, 2017a; Kawai et al., 2019; Taniguchi et al., 2019). A comprehensive review into biodegradation of all main kinds of plastic is necessary (Wei and Zimmermann, 2017b). Moreover, a review focusing on not only the biodegradation but also the biological upcycling of plastic wastes is even more attractive (Wierckx et al., 2015; Salvador et al., 2019; Blank et al., 2020). In this review, we have summarized the microorganisms and enzymes that have been proven to be capable of degrading plastics, such as PE, PS, PP, PVC, PUR, and PET, as well as the microbial metabolic pathways of the plastic depolymerization products and the current attempts toward utilization of these products as feedstocks for microbial valorization. Based on the above understandings, we have attempted to develop a biologically upcycling conception for plastic wastes through building a metabolic link between biodegradation of plastic wastes and biosynthesis of valuable chemicals in microorganisms (Figure 1). Finally, we have discussed the existing knowledge gaps and challenges facing microbial degradation and valorization of plastic wastes.



MICROBIAL DEGRADATION OF SYNTHETIC PLASTICS

A number of microorganisms capable of degrading polyolefins (PE, PS, and PP), PVC, PUR, and PET have been isolated from the open environment, such as the soil of a plastic-dumping site, waste of mulch films, marine water, soil contaminated by crude oil, sewage sludge, landfills, and the guts of plastic-eating worms (Tables 2–7). The screening of plastic-degrading microorganisms is crucial for identifying the depolymerases and other key enzymes involved in plastic degradation.

PE

As early as the 1970s, Albertsson carried out an experiment on microbial degradation of ^{14}C -labeled PE (average weight molecular weight of 300,000 Da) by using three different soil microbiotas as inocula (Albertsson, 1978). In terms of the release of $^{14}\text{CO}_2$, the microbial degradation rate of PE was calculated to be in the range of 0.36–0.39% after 2 years (Albertsson, 1978). When the ^{14}C -labeled PE was extracted with cyclohexane to get rid of its low molecular weight components (average weight molecular weight of 1,000 Da), the microbial degradation rate

dropped to 0.16% (Albertsson, 1980). Therefore, it was concluded that the release of $^{14}\text{CO}_2$ was mainly derived from the microbial degradation of the low molecular weight PE fraction, which was similar to the microbial degradation of straight-chain *n*-alkanes (Albertsson, 1980). After that, Kawai et al. claimed that the upper limit of molecular weight for PE degradation by microorganisms was about 2,000 Da based on the results of a numerical simulation (Kawai et al., 1999, 2002, 2004; Watanabe et al., 2003, 2004).

Although the high molecular weight was considered as a key factor impeding the microbial degradation of PE, the physicochemical pretreatments, including UV irradiation (Albertsson et al., 1987; Albertsson and Karlsson, 1988, 1990), chemical oxidizing agents (Brown et al., 1974), and thermo-oxidation (Lee et al., 1991), could facilitate the microbial degradation of long-chain PE since these pretreatments led to the depolymerization of long-chain PE as well as the formation of low molecular weight products (Albertsson et al., 1995, 1998; Erlandsson et al., 1998; Hakkarainen and Albertsson, 2004). Consequently, it was assumed that the environmental degradation of long-chain PE could be achieved by the synergistic actions of photo- or thermo-oxidation and the biological activity of microorganisms (Hakkarainen and Albertsson, 2004).

TABLE 2 | Bacteria, fungi, and enzymes associated with polyethylene (PE) biodegradation.

Strain/Enzyme	Isolated source	Tested PE	Incubation time, d	Weight loss, %	Molecular weight	Degradation products	References
<i>Rhodococcus ruber</i> C208	Soil of disposal site	LDPE film	30	4	–	–	Orr et al., 2004
<i>Bacillus sphaericus</i> Alt; <i>Bacillus cereus</i> BF20	Marine water	LDPE film	180	2.5–10	–	–	Sudhakar et al., 2008
<i>Arthrobacter</i> sp. GMB5; <i>Pseudomonas</i> sp. GMB7	Plastic waste dumpsites	HDPE film	30	12–15	–	–	Balasubramanian et al., 2010
<i>Pseudomonas</i> sp. E4	Soil	LMWPE	80	–	–	–	Yoon et al., 2012
<i>Pseudomonas</i> sp. AKS2	Waste dumping soil	LDPE film	45	5	–	–	Tribedi and Sil, 2013
<i>Bacillus subtilis</i> H1584	Marine water	LDPE film	30	1.75	–	–	Harshvardhan and Jha, 2013
<i>Enterobacter asburiae</i> YT1; <i>Bacillus</i> sp. YP1	Gut of waxworm	LDPE film	60	6–11	Decreased	Detected	Yang et al., 2014
<i>Serratia marcescens</i>	Ground soil	LLDPE film	70	36	–	–	Azeko et al., 2015
<i>Achromobacter xylooxidans</i>	Soil	HDPE film	150	9.38	–	–	Kowalczyk et al., 2016
<i>Zalerion maritimum</i>	Marine environment	PE pellets	28	–	–	–	Paço et al., 2017
<i>Phormidium lucidum</i> ; <i>Oscillatoria subbrevis</i>	Domestic sewage water	LDPE film	42	–	–	–	Sarmah and Rout, 2018
<i>Alcanivorax borkumensis</i>	Mediterranean Sea	LDPE film	7	3.5	–	–	Delacuvellerie et al., 2019
manganese peroxidase	<i>Phanerochaete chrysosporium</i>	PE film	12	–	Decreased	–	Iiyoshi et al., 1998
soybean peroxidase	Soybean	HDPE film	2 h	–	–	–	Zhao et al., 2004
laccase	<i>Rhodococcus ruber</i> C208	LDPE film	30	2.5	Decreased	–	Santo et al., 2013
<i>alkB</i> gene	<i>Pseudomonas</i> sp. E4	LMWPE sheet	80	19.3	–	–	Yoon et al., 2012
<i>alkB1</i> , <i>alkB2</i> gene	<i>Pseudomonas aeruginosa</i> E7	LMWPE film	50	19.6–27.6	–	–	Jeon and Kim, 2016a

TABLE 3 | Bacteria, fungi, and enzymes associated with polystyrene (PS) biodegradation.

Strain/Enzyme	Isolated source	Tested PS	Incubation time, d	Weight loss, %	Molecular weight	Degradation products	References
<i>Xanthomonas</i> sp.; <i>Sphingobacterium</i> sp.; <i>Bacillus</i> sp. STR-YO	Field soil	PS film	8	40–56	–	–	Eisaku et al., 2003
<i>Rhodococcus ruber</i> C208	Soil of disposal site	PS film	56	0.8	–	–	Mor and Sivan, 2008
<i>Microbacterium</i> sp. NA23; <i>Paenibacillus urinalis</i> NA26; <i>Bacillus</i> sp. NB6; <i>Pseudomonas aeruginosa</i> NB26	Soil buried expanded PS film	PS film	56	–	–	Detected	Atiq et al., 2010
<i>Rhizopus oryzae</i> NA1; <i>Aspergillus terreus</i> NA2; <i>Phanerochaete chrysosporium</i> NA3	Soil buried expanded PS film	PS film	56	–	Increased	Detected	Atiq, 2011
<i>Exiguobacterium</i> sp. YT2	Mealworm's gut	PS film	60	7.5%	Decreased	Detected	Yang et al., 2015c
hydroquinone peroxidase	<i>Azotobacter beijerinckii</i> HM121	PS film	20 min	–	Decreased	Detected	Nakamiya et al., 1997

Nevertheless, it was intriguing to figure out whether the long-chain PE (molecular weight > 2,000 Da) could be degraded by microorganisms from nature. A number of strains capable of degrading un-pretreated PE have been isolated from a variety of environments, including mulch films, marine water, soil contaminated by crude oil, sewage sludge, and landfills (Table 2; Orr et al., 2004; Sivan et al., 2006; Sudhakar et al., 2008; Balasubramanian et al., 2010; Yoon et al., 2012; Tribedi and Sil, 2013; Harshvardhan and Jha, 2013; Yang et al., 2014; Azeko et al., 2015; Kowalczyk et al., 2016; Paço et al., 2017; Sarmah and Rout, 2018; Delacuvellerie et al., 2019). Some of these strains showed the ability to utilize un-pretreated PE as a carbon source

based on the characterizations of biofilm formation on PE films, weight loss of PE materials, surface deterioration, and changes in the mechanical and thermal properties of PE (Table 2). For example, it was reported that the weight loss of un-pretreated PE degraded by a strain *Serratia marcescens* reached 36% in an incubation period of 70 days (Azeko et al., 2015). Moreover, two cyanobacteria, *Phormidium lucidum* and *Oscillatoria subbrevis*, exhibited the capability of degrading 30% of the initial weight of tested PE over a 42-day period (Sarmah and Rout, 2018). However, these promising reports of PE degradation based on weight loss are less convincing since there is no additional evidence to support that the weight loss is caused by the

TABLE 4 | Bacteria, fungi, and enzymes associated with polypropylene (PP) biodegradation.

Strain/Enzyme	Isolated source	Tested PP	Incubation time, d	Weight loss, %	Molecular weight	Degradation products	References
<i>Pseudomonas stutzeri</i> ; <i>Bacillus subtilis</i> ; <i>Bacillus flexus</i>	Plastic-dumping site	PP film	365	–	–	Detected	Arkatkar et al., 2010
<i>Phanerochaete chrysosporium</i> ; <i>Engyodontium album</i>	Plastic-dumping site	PP film	365	4–5	–	Detected	Jeyakumar et al., 2013
<i>Stenotrophomonas panacihumi</i>	Soil of waste storage yard	PP film	90	–	Increased	–	Jeon and Kim, 2016b
<i>Aneurinibacillus aneurinilyticus</i> ; <i>Brevibacillus agri</i> ; <i>Brevibacillus</i> sp.; <i>Brevibacillus brevis</i>	Landfills and sewage	PP film and pellets	140	22.8–27.0	–	Detected	Skariyachan et al., 2018
<i>Bacillus</i> sp. strain 27; <i>Rhodococcus</i> sp. strain 36	Mangrove environments	PP microplastic	40	4–6.4	–	–	Auta et al., 2018

TABLE 5 | Bacteria, fungi, and enzymes associated with polyvinyl chloride (PVC) biodegradation.

Strain/Enzyme	Isolated source	Tested PVC	Incubation time, d	Weight loss, %	Molecular weight	Degradation products	References
<i>Alternaria</i> sp. TOF-46	Japanese bathrooms	Plasticized PVC rim	180	–	–	–	Moriyama et al., 1993
<i>Polyporus versicolor</i> ; <i>Pleurotus sajor caju</i>	Lignocellulosic waste	PVC film	30	–	–	Detected	Kirbas et al., 1999
<i>Aureobasidium pullulans</i>	Leaf/wood surfaces	Plasticized PVC	7	–	–	–	Webb et al., 1999
<i>Aspergillus niger</i>	PVC wires	Plasticized PVC film	365	–	–	–	Gumargalieva et al., 1999
<i>Aureobasidium pullulans</i>	Atmosphere	Plasticized PVC film	42	3.7	–	–	Webb et al., 2000
<i>Penicillium janthinellum</i>	PVC buried in soil	Plasticized PVC sheet	300	–	–	–	Sabev et al., 2006
<i>Mycobacterium</i> sp. NK0301	Garden soil	Plasticized PVC film	3	–	–	Detected	Nakamiya et al., 2005
<i>Chryseomicrobium imtechense</i> ; <i>Lysinibacillus fusiformis</i> ; <i>Acinetobacter calcoaceticus</i> ; <i>Stenotrophomonas pavanii</i>	Landfill leachate	Plasticized PVC curtain	34	–	–	–	Latorre et al., 2012
<i>Phanerochaete chrysosporium</i> ; <i>Lentinus tigrinus</i> ; <i>Aspergillus niger</i> ; <i>Aspergillus sydowii</i>	PVC film buried in soil	PVC film	300	–	Decreased	Detected	Ali et al., 2014
<i>Acanthopleurobacter pedis</i> ; <i>Bacillus cereus</i> ; <i>Pseudomonas otitidis</i> ; <i>Bacillus aerius</i>	Plastic disposal sites	PVC film	90	–	Decreased	Detected	Anwar et al., 2016
<i>Bacillus</i> sp. AIW2	Marine	Un-plasticized PVC film	90	0.26	–	Detected	Kumari et al., 2019
<i>Phanerochaete chrysosporium</i>	Plastic disposal site	PVC film	28	31	–	Detected	Khatoun et al., 2019
<i>Pseudomonas citronellolis</i>	Soil	Plasticized PVC film	45	13	Decreased	–	Giacomucci et al., 2019

degradation of the long-chain PE other than the low molecular weight components in PE.

Notably, a few studies reported that the waxworms, possessing an inherent ability to feed on and digest beeswax, could chew, and eat PE films (Yang et al., 2014; Bombelli et al., 2017; Chalup et al., 2018; Kundungal et al., 2019). The biodegradation of PE has been detected through contact with the homogenate of the waxworm *Galleria mellonella* (Bombelli et al., 2017) or after passage through the gut of the lesser waxworm *Achroia grisella* (Kundungal et al., 2019), according to the changes in chemical compositions characterized by the analyses of Fourier transform infrared spectroscopy (FTIR) and nuclear magnetic resonance (NMR). However, further investigations are necessitated in order to determine whether the depolymerization of PE has occurred in the waxworm gut.

As intestinal microbial symbionts have been recognized as indispensable for the digestion of insects (Engel and Moran, 2013),

we have hypothesized that the microbial symbionts in the waxworm gut also play an important part in the degradation of PE (Yang et al., 2014). Two bacterial strains, *Enterobacter asburiae* YT1 and *Bacillus* sp. YP1, were isolated from the gut of waxworm *Plodia interpunctella*, and their PE-degrading capability was documented within a limited incubation period of 60 days based on the characterizations of biofilm formation, changes in the PE physical properties (tensile strength and surface topography), chemical structure (hydrophobicity and appearance of carbonyl groups), molecular weight (accompanied by the formation of daughter products), and weight loss (Table 2). These findings indicated that the bacteria from waxworms could be a promising source for the further screening PE-degrading microbes (Yang et al., 2014; Yang et al., 2015a).

Although a diverse range of PE-degrading microbes has been reported, only four microbial enzymes have been shown to be responsible for PE degradation (Table 2). Iiyoshi et al. (1998)

TABLE 6 | Bacteria, fungi, and enzymes associated with polyurethane (PUR) biodegradation.

Strain/Enzyme	Isolated source	Tested PUR	Incubation time, d	Weight loss, %	Molecular weight	Degradation products	References
<i>Chaetomium globosum</i>	Soil	Polyester/polyether PUR film	21	–	–	–	Darby and Kaplan, 1968
<i>Curvularia senegalensis</i>	Soil	Impranil DLN	7	–	–	–	Crabbe et al., 1994
<i>Geomyces pannorum</i>	Acidic soil	Impranil DLN	150	–	–	–	Cosgrove et al., 2007
<i>Alternaria</i> sp. PURDK2	Environment	Polyether PUR film	70	27.5	–	Detected	Matsumiya et al., 2010
<i>Pestalotiopsis microspora</i>	Plant stems	Impranil DLN,	14	–	–	–	Russell et al., 2011
<i>Aspergillus flavus</i>	Plastic disposal sites	Polyester PUR film	30	60.6	–	–	Mathur and Prasad, 2012
<i>Cladosporium tenuissimum</i>	Garden soil	Impranil DLN; polyether varnish	14	65	–	Detected	Álvarez-Barragán et al., 2016
<i>Aspergillus tubingensis</i>	Waste disposal site	Polyester PUR beads	20	–	–	–	Khan et al., 2017
<i>Aspergillus</i> sp. S45	Waste-dumping site	Polyester PUR film	28	15–20	–	Detected	Osman et al., 2017
<i>Penicillium</i> sp.	PUR wastes	Impranil DLN; polyester/polyether PUR film	60	8.9	Decreased	–	Magnin et al., 2019a
<i>Corynebacterium</i> sp., B12; <i>Pseudomonas aeruginosa</i>	Soil	Polyester PUR foam	84	1.2–17.7	–	–	Kay et al., 1991
<i>Comamonas acidovorans</i>	Soil	Polyester PUR film	7	–	–	Detected	Nakajima-Kambe et al., 1995
<i>Bacillus</i> sp.	Soil	Impranil DLN	4	–	–	–	li et al., 1998
<i>Pseudomonas fluorescens</i>	Soil	Impranil DLN	ND	–	–	–	Howard and Blake, 1998
<i>Pseudomonas chlororaphis</i>	Soil	Impranil DLN	ND	–	–	–	Howard et al., 1999
<i>Bacillus subtilis</i>	Soil	Impranil DLN	ND	–	–	–	Rowe and Howard, 2002
<i>Acinetobacter gomeri</i>	Soil	Impranil DLN	ND	–	–	–	Howard and Burks, 2012
<i>Alicyclophilus</i> sp. BQ1	Decomposed soft foam	Polyester PUR film	100	–	–	Detected	Oceguera-Cervantes et al., 2007
<i>Bacillus pumilus</i>	PUR-contaminated water	Impranil DLN	3	–	–	–	Nair and Kumar, 2007
<i>Pseudomonas chlororaphis</i>	Soil	Ester PUR foam	12	–	–	–	Gautam et al., 2007
<i>Bacillus</i> sp. AF8; <i>Pseudomonas</i> sp. AF9; <i>Micrococcus</i> sp. 10; <i>Arthrobacter</i> sp. AF11; <i>Corynebacterium</i> sp. AF12	Soil	Polyester PUR film	28	–	–	–	Shah et al., 2008
<i>Bacillus subtilis</i> ; <i>Pseudomonas aeruginosa</i>	Soil	Polyester PUR pellets	20	–	–	Detected	Shah et al., 2016
<i>Pseudomonas putida</i>	Soil	Impranil DLN	8	–	–	–	Peng et al., 2014
<i>Bacillus safensis</i>	Cedar wood	Impranil DLN;	7	–	–	–	Nakkabi et al., 2015a,b
<i>Aspergillus niger</i> ; <i>Cladosporium herbarum</i>	Natural humid conditions	Polyether PUR foam	70	–	–	–	Filip, 1979
<i>Staphylococcus epidermidis</i>	An intravenous catheter	Polyether PUR film	30	–	–	–	Jansen et al., 1991
<i>Alternaria tenuissima</i>	Infected leaves	Polyether PUR film	60	–	–	–	Oprea et al., 2018
<i>Pseudomonas denitrificans</i> , <i>Pseudomonas fluorescens</i> , <i>Bacillus subtilis</i> , <i>Yarrowia lipolytica</i>	Soil	Polyether PUR film	150	2.8–10.5	–	–	Stepien et al., 2017
esterase	<i>Curvularia senegalensis</i>	Impranil DLN	21	–	–	–	Crabbe et al., 1994
pudA	<i>Comamonas acidovorans</i>	Polyester PUR film	2	–	–	–	Akutsu et al., 1998
lipase	<i>Bacillus subtilis</i>	Impranil DLN	1	–	–	–	Rowe and Howard, 2002
pulA	<i>Pseudomonas fluorescens</i>	Impranil DLN	ND	–	–	–	Ruiz and Howard, 1999
pueA	<i>Pseudomonas chlororaphis</i>	Impranil DLN	6 h	–	–	–	Stern and Howard, 2000
pueB	<i>Pseudomonas chlororaphis</i>	Impranil DLN	20 h	–	–	–	Howard et al., 2001b
LC cutinase; TfCut2; Tcur1278; Tcur0390	Compost metagenomic library; <i>Thermobifida fusca</i>	Impranil DLN; polyester PUR cubes	100 h	0.3–3.2	decreased	–	Schmidt et al., 2017
Esterase E3576	Protéus (France)	Polyester/polyether PUR film	51	33	–	Detected	Magnin et al., 2019b

TABLE 7 | Enzymes associated with polyethylene terephthalate (PET) biodegradation.

Enzyme	Isolated source	Tested PET	Crystallinity, %	Reaction temperature, °C	Incubation time, d	Weight loss, %	References
TfH	<i>Thermobifida fusca</i>	PET bottle and pellets	9	55	21	54.2	Müller et al., 2005
HiC; PmC; PsC	<i>Humicola insolens</i> ; <i>Pseudomonas mendocina</i> ; <i>Fusarium solani</i>	Low-crystallinity PET film	7	70	6	97%	Ronkvist et al., 2009
LC-cutinase	Compost metagenomic library	Low-crystallinity PET film	8.4	50	7	50	Sulaiman et al., 2012
Cut190	<i>Saccharomonospora viridis</i>	Low-crystallinity PET film	8.4	63	3	27	Kawai et al., 2014
IsPETase	<i>Ideonella sakaiensis</i>	Low-crystallinity PET film	1.9	30	0.75	–	Yoshida et al., 2016
IsPETase	<i>Ideonella sakaiensis</i>	Low-crystallinity PET film	–	30	1	1	Wei et al., 2019b
TfCut2	<i>Thermobifida fusca</i>	Low-crystallinity PET chip	7	70	5	97	Wei et al., 2019a

found that manganese peroxidase (MnP), from lignin-degrading fungi *Phanerochaete chrysosporium*, could decrease the tensile strength and average molecular weight of PE film. Zhao et al. (2004) also found that the combination of soybean peroxidase (SBP) and hydrogen peroxide could oxidize the surface of PE film and diminish the surface hydrophobicity. Santo et al. (2013) showed that the extracellular laccase secreted by the PE-degrading bacterium, *Rhodococcus ruber* C208, could oxidize the PE films to generate carbonyl groups and decrease the molecular weight. While these past studies have identified the above peroxidase and laccase to be capable of catalyzing the degradation of PE, their catalytic mechanisms in the process of microbial degradation of PE remained unclear. In addition, three alkane hydroxylase genes, *alkB*, *alkB1*, and *alkB2*, were cloned in *Escherichia coli* and the resulting recombinant strains were found to be able to degrade low molecular-weight PE (Table 2; Yoon et al., 2012; Jeon and Kim, 2015, 2016a). These results indicated that the *alkB*, *alkB1*, or *alkB2* played a key role in the degradation of low molecular-weight PE. Additionally, a recent study based on quantum mechanics calculations also suggested that the enzymatic cleavage of carbon–carbon bonds of polyolefins (PE and PS) by oxidases or oxygenases was possible (Xu et al., 2019). However, future efforts are required to characterize the biochemical functions of the oxidases or oxygenases, such as the enzymes encoded by the genes *alkB*, *alkB1*, or *alkB2*, within the biodegradation of PE.

PS

Guillet et al. (1974) first used two types of ^{14}C -PS (α - and β - ^{14}C) as substrates to assess microbial degradation of PS in both soil and activated sewage sludge, and they showed that less than 0.01% could be degraded to $^{14}\text{CO}_2$ in the course of 8 weeks. Afterward, ^{14}C -labeled PS was also used as a substrate to determine the degradation of PS by soil microbiota, 17 lignin-degrading fungi, and five mixed floras (Sielicki et al., 1978; Kaplan et al., 1979). According to the release of $^{14}\text{CO}_2$, the degradation rate was only 1.5–3.0% during 16 weeks, up to 0.24% within 5 weeks, and 0.04–0.57% within 11 weeks (Sielicki et al., 1978; Kaplan et al., 1979).

Besides the mixed flora, researchers have also tried to isolate PS-degrading microbes from different environment samples (Table 3). Eisaku et al. (2003) reported that three soil

microorganisms, *Xanthomonas* sp., *Sphingobacterium* sp., and *Bacillus* sp. STR-YO, could degrade PS. Mor and Sivan (2008) found that an actinomycete, *Rhodococcus ruber* C208, was able to utilize PS as its sole carbon source to grow, and this led to a weight loss of 0.8% within 8 weeks. In addition, three fungi and three bacteria were isolated from the soil-buried expanded PS films, and they could adhere and grow on PS (Table 3; Atiq et al., 2010; Atiq, 2011). However, the reported biodegradation rates of PS by these strains was quite low, and there was no evidence of changes in either the physical or chemical properties of its long-chain PS molecules after microbial degradation.

Extraordinarily, mealworms (larvae of *Tenebrio molitor*) were reported to be able to eat and rapidly degrade up to 50% of ingested Styrofoam (trade name of PS foam) during 24 h, and this was supported by the change in chemical composition, reduction in molecular weight, and the isotopic trace after passage through the intestinal tract (Yang et al., 2015b). With the same protocols, the PS-degrading capability was also documented in a broader range of mealworms from 12 different locations worldwide, indicating that PS degradation in mealworms is ubiquitous (Yang et al., 2018). This discovery also inspired researchers to explore more insect species, such as dark mealworms (*Tenebrio obscurus*) (Peng et al., 2019) and superworms (*Zophobas atratus*) (Yang et al., 2020), that also could eat and degrade PS.

We wondered whether the microbial symbionts associated with mealworms and superworms contributed to the degradation of PS. While the gut microbial symbionts were suppressed with antibiotics, the PS-degrading capacity of mealworms or superworms was impaired. This result indicated that gut microbial symbionts played an important role in the biodegradation of ingested Styrofoam (Yang et al., 2015c, Yang et al., 2020). Furthermore, one strain of *Exiguobacterium* sp. YT2, isolated from the gut of *Tenebrio molitor*, was proven to be capable of degrading 7.5% weight of PS *in vitro* within 60 days, while the decrease in molecular weight of the residual PS pieces and the release of water-soluble daughter products were also detected (Yang et al., 2015c; Table 3). At the time of writing, more bacteria have been isolated from the gut of plastic-eating mealworms or superworms, and their potential for PS degradation is still under assessment (Xia et al., 2019).

With respect to the PS-degrading enzymes, only hydroquinone peroxidase, secreted by a lignin-degrading

bacterium *Azotobacter beijerinckii* HM121, was able to depolymerize PS into low molecular products in the presence of non-aqueous medium of dichloromethane (Nakamiya et al., 1997).

PP

In 1993, microbial degradation of PP was firstly assessed by cultures enriched from sandy soils containing PE wastes (Cacciari et al., 1993). After an incubation period of 175 days, the amount of degradation products, which were extracted with methylene chloride, accounted for 40% of the initial weight of tested PP. However, 90% of the extracted products were identified as aromatic esters, which were derived from the plasticizers, a chemical added especially into plastic to adjust the flexibility, workability, or stretchability. Meanwhile, only 10% of the extracted products were identified as hydrocarbons ($C_{10}H_{22}$ to $C_{31}H_{64}$) that may be derived from the degradation of PP itself. This result indicated that the plasticizers, other than the PP itself, were prone to be degraded by the sandy soil microorganisms (Cacciari et al., 1993).

From that time on, several microorganisms from different environmental samples have been tested for their potential to degrade PP (Table 4). For example, when PP films were incubated with soil microbiota from a plastic-dumping site, 0.4% weight loss and 33% increase in the crystallinity of residual PP were observed after 12 months, implying that the amorphous parts of PP could be degraded by soil microbiota (Arkatkar et al., 2009). Additionally, it was found that three bacteria and two fungal strains (Table 4), isolated from the soil of a plastic-dumping site, could utilize PP as their carbon source for growth and degrade 0.05–5% of PP after incubation for 12 months (Arkatkar et al., 2010; Jeyakumar et al., 2013). Mixed consortia of four bacterial isolates, from waste management landfills and sewage treatment plants, could also degrade the PP strips and pellets with a weight loss of 44.2–56.3% after 140 days (Skariyachan et al., 2018). Moreover, two marine bacteria of *Bacillus* sp. strain 27 and *Rhodococcus* sp. strain 36, isolated from mangrove environments, were also able to grow in aqueous synthetic media containing PP microplastics and caused a weight loss of 4.0–6.4% after 40 days (Auta et al., 2018). However, it is hard to determine whether the weight loss caused by the reported microbes above was attributed to the depolymerization of the long-chain PP or the degradation of the low molecular weight components, as the analyses of changes in molecular weight were absent.

A mesophilic strain, *Stenotrophomonas panacihumi* PA3-2, isolated from the soil of an open storage yard for municipal solid waste, was reported to be able to degrade two kinds of low molecular weight PP (Mn: 2,800, 3,600 Da) and one high molecular weight PP (Mn: 44,000 Da) with a biodegradability of 12.7–20.3% in terms of CO_2 release and an increase in the molecular weight after 90 days (Jeon and Kim, 2016b). The results indicated that this strain could only degrade the low molecular weight fractions rather than the long-chain PP.

Until now, there are no enzymes reported to be capable of degrading PP, and little knowledge is available for the mechanism of microbial degradation of PP (Arutchelvi et al., 2008). However, similar to PE, it was found that the physicochemical

pretreatments, including γ -irradiation (Alariqi et al., 2006), UV irradiation (Jeyakumar et al., 2013), thermo-oxidation (Jeyakumar et al., 2013), and blend with degradable additives, could facilitate the microbial degradation of PP (Jeyakumar et al., 2013; Jain et al., 2018).

PVC

Among all main kinds of synthetic plastics, PVC possesses the highest proportion of plasticizer (up to 50%). As plasticizers can be utilized by many fungi or bacteria as sources of nutrient carbons, plasticized PVC is usually susceptible to fungal or bacterial attack (Berk, 1950; Berk et al., 1957; Bessems, 1988; Kurane, 1988; Gumargalieva et al., 1999; Webb et al., 1999). For instance, a number of plasticized PVC bathroom items, such as bathtub lids, bath mats, and shower curtains, were found to be damaged by a variety of fungi (Table 5; Moriyama et al., 1993). Several fungal isolates (Table 5) from various environmental samples, such as atmosphere (Webb et al., 2000), plasticized PVC sheets buried in the grassland soil (Sabev et al., 2006; Ali et al., 2014), and plastic wastes disposal sites (Khatoon et al., 2019), also exhibited the ability to deteriorate the plasticized PVC. In addition, a number of bacterial strains (Table 5), isolated from garden soil, landfill leachate, waste disposal sites, and marine environments, have also been reported to be able to degrade the plasticized PVC (Nakamiya et al., 2005; Latorre et al., 2012; Anwar et al., 2016; Kumari et al., 2019; Giacomucci et al., 2019). However, these abovementioned plasticized PVC-degrading microorganisms just metabolized a component of the plasticizer [such as bis (2-ethylhexyl) phthalate, DEHP] rather than the backbone of PVC. Microorganisms capable of degrading both PVC and plasticizers have not been discovered so far. Thus, the key enzymes involved in the microbial degradation of PVC are still unknown.

In future screening experiments, it is important to characterize the ability of strains to depolymerize the long-chain molecules of PVC by using virgin plastic in which low molecular weight components (monomers, oligomers, and plasticizers) were extracted by use of a suitable solvent or determining the decrease in the average molecular weight and the broadening of the molecular weight distribution of the residues after degradation.

PUR

PUR is the universal nomenclature for the plastic derived from the condensation of polyisocyanates and polyols with the linkages of intramolecular urethane bonds (Table 1). Depending on the chemical structures of the polyols used, PUR synthesized from polyester polyol is designated as polyester PUR, while that synthesized from polyether polyol is termed as polyether PUR.

In 1968, the initial research into microbial degradation of PUR was made by Darby and Kaplan. They found that seven fungi can grow on the surface of solid polyester PUR (Table 6; Darby and Kaplan, 1968). Since then, a number of fungi have been proven to be able to degrade polyester PUR (Table 6; Crabbe et al., 1994; Cosgrove et al., 2007; Russell et al., 2011; Mathur and Prasad, 2012; Álvarez-Barragán et al., 2016; Khan et al., 2017; Osman et al., 2017; Magnin et al., 2019a). In addition to fungi, many bacteria also have been demonstrated to be capable

of degrading polyester PUR (Table 6; Kay et al., 1991, 1993; Nakajima-Kambe et al., 1995, 1997; Howard and Blake, 1998; Ii et al., 1998; Howard et al., 1999, 2001a,b; Rowe and Howard, 2002; Oceguera-Cervantes et al., 2007; Gautam et al., 2007; Nair and Kumar, 2007; Shah et al., 2008, 2013a,b, 2016; Howard and Burks, 2012; Peng et al., 2014; Nakkabi et al., 2015a,b; Pérez-Lara et al., 2016).

With regard to polyether PUR (Table 6), it was much less susceptible to microbial degradation in comparison to the polyester PUR (Darby and Kaplan, 1968). Notwithstanding, in 1979, Filip observed growth of *Aspergillus niger* and *Cladosporium herbarum* in shake cultures with polyether PUR resilient foam as the sole nutrient source (Filip, 1979). Afterward, Jansen et al. isolated a strain of *Staphylococcus epidermidis* KH11 from an infected catheter and demonstrated its capacity to utilize polyether PUR in the absence of any organic nutrients (Jansen et al., 1991). In 2010, a fungus, *Alternaria* sp. PURDK2, was reported to be able to degrade 27.5% of the weight of tested polyether PUR foam in the Luria-Bertani (LB) glucose agar after 70 days. Furthermore, this fungus was also capable of degrading two small molecule analogs of PUR, ethylphenylcarbamate (EPC) and diphenylmethane-4,4'-dibutylurea (D-MDI), into aniline and ethanol, indicating that the fungus could secrete urethane-bond-degrading enzymes (Matsumiya et al., 2010). In 2016, eight fungal strains (Table 6) were showed be able to grow in mineral medium with a polyether PUR varnish as the sole carbon source and degrade 65% of solid polyether PUR foams in 50% potato dextrose broth (PDB) over 21 days (Álvarez-Barragán et al., 2016). Stepien et al. found that three bacteria and one yeast (Table 6) could degrade commercial polyether PUR films (Tecoflex®) and cause a weight loss of 2.8–10.5% within 5 months (Stepien et al., 2017). Oprea et al. assessed the biodegradability of pyridine-based polyether PUR elastomers by a fungus *Alternaria tenuissima*, and found that the fungus could decrease the mechanical properties and deteriorate the surface morphology after 60 days (Oprea et al., 2018).

The genes and enzymes contributing to microbial degradation of polyester PUR have been widely investigated (Table 6). In 1994, Crabbe et al. purified an esterase from a polyester PUR-degrading fungus, *Curvularia senegalensis*, and showed that this esterase can cleavage the ester bonds in the soft segments of polyester PUR (Crabbe et al., 1994). While Akutsu et al. purified a cell surface-bond polyester PUR-degrading esterase from the polyester PUR-degrading bacterium *Comamonas acidovorans* TB-35, Nomura et al. cloned a gene *pudA* encoding polyester PUR-degrading esterase in this strain (Akutsu et al., 1998; Nomura et al., 1998). Howard et al. purified a protease from *Pseudomonas fluorescens* (Vega et al., 1999), an esterase from *Comamonas acidovorans* (Allen et al., 1999), three esterases from *Pseudomonas chlororaphis* (Howard et al., 1999; Ruiz et al., 1999), and a lipase from *Bacillus subtilis* (Rowe and Howard, 2002). All the purified serine hydrolases above have the same hydrolytic capacity to emulsify polyester PUR. In addition, they also cloned a gene named *pulA* from *Pseudomonas fluorescens* (Ruiz and Howard, 1999) and two genes, *pueA* and *pueB*, from *Pseudomonas chlororaphis* (Stern and Howard, 2000; Howard et al., 2001b). These genes encoded three different

esterases involved in the microbial degradation of emulsified polyester PUR by *Pseudomonas fluorescens* and *Pseudomonas chlororaphis*. In 2017, Schmidt et al. found that four polyester hydrolases, LC cutinase, TfCut2, Tcur1278, and Tcur0390, were able to degrade emulsified polyester PUR (Schmidt et al., 2017). Among these three cutinase, LC cutinase caused weight losses of up to 4.9 and 4.1% of two commercial polyester PUR elastomers of Elastollan B85A-10 and C85A-10, respectively, within a reaction time of 200 h at 70°C. Recently, an esterase (E3576), screened from 50 commercially available hydrolases, was shown to be able to hydrolyze a waterborne polyester PUR dispersion and degrade a solid polycaprolactone polyol-based polyester PUR with weight loss of 33% after 51 days (Magnin et al., 2019b). However, this esterase (E3576) cannot degrade poly(hexamethylene adipate) diol-based polyester PUR films, indicating that the chemical structures of the polyol segments significantly affect the biodegradability of polyester PUR (Kim and Kim, 1998; Magnin et al., 2019b).

Although the above reported lipases or esterases were able to rapidly degrade the emulsified polyester PUR (Impranil DLN) by cleaving the ester bonds in the polyester polyols segments, they exhibited a weak capability of degrading the solid polyester PUR substrates, such as PUR film, foam, and elastomer (Schmidt et al., 2017). The degradation products were not identified, and the biochemical mechanism was still unclear. Moreover, no specific depolymerases have been reported to be able to degrade the polyether PUR and cleave the urethane bones in both polyester and polyether PUR.

PET

The purpose of initial efforts to find out the hydrolases capable of hydrolyzing PET was to modify the surface wettability of PET fabrics (Hsieh and Cram, 1998; Yoon et al., 2002; Gübitz and Paulo, 2003; Alisch et al., 2004; Fischer-Colbrie et al., 2004; O'Neill and Cavaco-Paulo, 2004; Zhang et al., 2004; Silva et al., 2005; Vertommen et al., 2005). In the process of enzymatic surface modification, ester linkages on the surface of PET were hydrolyzed to produce polar hydroxyl and carboxylic groups, but the inner bulk of PET was not degraded. In a recent review focusing on enzymatic degradation of PET, Kawai et al. defined those hydrolases with moderate surface-hydrolyzing capability as *PET surface-modifying enzymes* (Kawai et al., 2019). By contrast, the hydrolases with significant capability of hydrolyzing the inner bulk of PET (causing at least 10% weight loss) were termed as *PET hydrolases* (Kawai et al., 2019). Hereinafter, only the reported *PET hydrolases* were reviewed (Table 7).

In 2005, Müller et al. (2005) reported that a cutinase-like hydrolase TfH, from an actinomycete *Thermobifida fusca*, can effectively degrade up to 50% of the initial weight of low-crystallinity PET (IcPET, 9%) at 55°C for 3 weeks. This is the first report on the enzymatic degradation of the inner bulk of PET films that opens the door for enzymatic PET recycling in the future (Müller, 2006). Thereafter, Ronkvist et al. compared the PET-hydrolyzing activities of three cutinases from different microorganisms, *Humicola insolens* (HiC, now named *Thermomyces insolens*), *Pseudomonas mendocina* (PmC),

and *Fusarium solani* (FsC), using lcPET films (7%) and high-crystallinity biaxially oriented PET films (hcPET, 35%) as substrates (Ronkvist et al., 2009). Results showed that HiC caused a 97% weight loss of lcPET film (7%) at 70°C within 96 h, while PmC or FsC only led to a weight loss up to 5%. Thus, HiC can be designated as *PET hydrolase*, while PmC and FsC should be ascribed to *PET surface-modifying enzymes*. However, the three cutinases could hardly hydrolyze the hcPET films (35%). After that, Sulaiman et al. (2012) found that a LC-cutinase, encoded by one gene from the metagenomic library of leaf-branch compost, can efficiently hydrolyze low-crystallinity PET package film (lcPET-P, 8.4%) at 50°C and generate up to 50% weight loss over 7 days. In addition, Kawai et al. found that a cutinase Cut190, from *Saccharomonospora viridis* AHK190, can hydrolyze the lcPET (7%) and lcPET-P (8.4%) at 63°C, resulting in a weight loss of 13.5 and 27.0% for lcPET and lcPET-P, respectively, over 3 days (Kawai et al., 2014). It was recently shown that the recombinant *Thermobifida fusca* cutinase TfCut2 expressed by *B. subtilis* could degrade the lcPET films (7%) with a weight loss up to 97.0% and two low-crystallinity PET samples from postconsumer packages (AP-PET, 5%; CP-PET, 6%) with maximum weight losses of 50.5 and 56.6%, respectively, within 120 h at 70°C (Wei et al., 2019a).

Remarkably, Yoshida et al. found a bacterium, *Ideonella sakaiensis* 201-F6, capable of degrading lcPET films (1.9%) at an ambient temperature, and they identified a PET-hydrolyzing enzyme, termed as *IsPETase*, from this bacterium (Yoshida et al., 2016). The *IsPETase* was heat-labile (20~45°C) and exhibited greater PET degradation activity than the above reported *PET hydrolases* at a mesophilic temperature of 30°C (Yoshida et al., 2016; Taniguchi et al., 2019). Nevertheless, the degradation rate of lcPET film (7%) by *IsPETase* at 30°C over a 24 h-incubation period was only 1% (weight loss), which was markedly lower than that caused by the above reported *PET hydrolases* at a thermophilic temperature (50~70°C) (Wei et al., 2019a,b). Moreover, the hydrolytic activity of *IsPETase* against lcPET films (1.9%) was obviously higher than that for hcPET films (30~40%) (Yang et al., 2016; Yoshida et al., 2016).

Overall, the above reported *PET hydrolases* are prone to degrade the lcPET (<10%) but not the hcPET (Vertommen et al., 2005; Ronkvist et al., 2009; Yang et al., 2016; Yoshida et al., 2016; Wei et al., 2019a). The effect of different crystallinity on the enzymatic degradation could be explained by the changes in the macromolecular aggregate structures of the polymer. Polymer molecules generally pack together in a non-uniform way with a mixture of ordered regions (crystalline-like) and disordered domains (amorphous). As the polymer chains in the amorphous domains are less densely packed than those in the crystalline domains, the lcPET, comprising a high proportion of amorphous domains, is more susceptible to enzymatic degradation. However, the high-crystallinity PET (30~40%) represents the most abundant types of postconsumer plastic, and methods for lowering the crystallinity of PET to enhance the enzymatic degradation are highly sought.

Additionally, the enzymatic hydrolytic reactions of PET are inclined to take place under the temperature close to the glass transition temperature of PET (T_g , 65~75°C). Under

such a thermophilic temperature, the polymer chains in the amorphous PET domains can gain enough mobility to access the active sites of *PET hydrolases* (Ronkvist et al., 2009; Wei and Zimmermann, 2017a; Kawai et al., 2019). As a result, it suggests that efficient enzymatic degradation of PET requires thermostable PET depolymerases. Approaches of glycosylation (Shirke et al., 2018) and rational protein engineering, such as the optimization of surface salt bridge (Shirke et al., 2016), mutation of Ca^{2+} and Mg^{2+} binding sites (Then et al., 2015), introduction of disulfide bridge (Then et al., 2016), stabilization of a $\beta 6$ - $\beta 7$ connecting loop, and extension of subsite IIc (Son et al., 2019), have been applied to improve the thermostability of these *PET hydrolases*. Notwithstanding, there is room for increasing the half-life of PET hydrolases above 65°C.

MICROBIAL VALORIZATION OF PLASTIC WASTES

The initial step of the microbial degradation process is to secrete depolymerases to break down the long-chain polymers into low molecular weight oligomers or monomers, which can be further assimilated into microbial cells or metabolized into CO_2 . According to the principle of circular economy, these depolymerization products could be exploited for the biosynthesis of high-value chemicals through specific metabolic pathways, which could be considered as a way of valorizing plastic wastes (Wierckx et al., 2015).

From TPA, EG, and 6-Hydroxyhexanoate to Succinic Acids and Polyhydroxyalkanoate (PHA)

Enzymatic hydrolysis of PET could release constituent monomers ethylene glycol (EG), terephthalic acid (TPA), mono(ethylene terephthalate) (MHET), and bis(2-hydroxyethyl)TPA (BHET) by cleaving the ester bond (Ronkvist et al., 2009; Yoshida et al., 2016). Among these products, MHET could be further degraded into TPA and EG by the action of MHETase (**Figure 2**; Yoshida et al., 2016; Palm et al., 2019). In addition, the ester linkages in polycaprolactone polyol-based PUR (PCL-based PUR) could be hydrolyzed by an esterase (E3576) to generate 6-hydroxyhexanoate (Magnin et al., 2019b). These products could be further metabolized by specific microorganisms through different metabolic pathways (**Figure 2**; Brzostowicz et al., 2003; Yoshida et al., 2016).

In bacterial species, a TPA transporter is implicated in the transport of TPA into the cell (Hosaka et al., 2013). Once inside the cell, the TPA can be transformed into 1,6-dihydroxycyclohexa-2,4-diene-dicarboxylate (DCD) by the activity of the TPA dioxygenase (TPADO). DCD is further oxidized by the 1,2-dihydroxy-3,5-cyclohexadiene-1,4-dicarboxylate dehydrogenase (TphB) to form protocatechuate (PCA) (**Figure 2**; Wang et al., 1995; Choi et al., 2005; Sasoh et al., 2006). The PCA could be degraded by the *ortho*-, *meta*-, and *para*-cleavage pathways under the catalysis of 3,4-dioxygenase (PCDO), 4,5-dioxygenase, and 2,3-dioxygenase, respectively

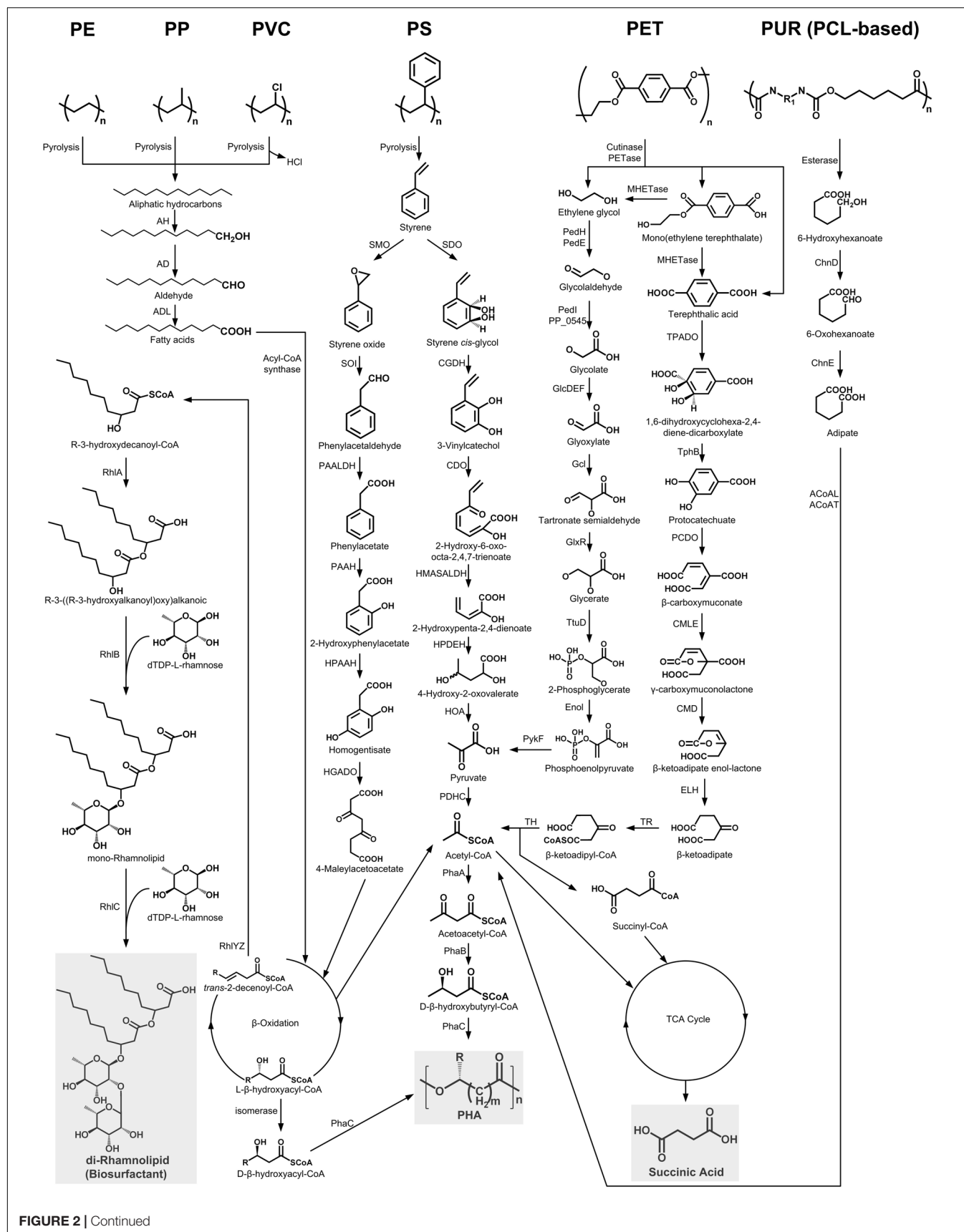


FIGURE 2 | Continued

FIGURE 2 | Continued

The metabolic pathways of depolymerization products of six kinds of plastics. Plastics: PE, polyethylene; PS, polystyrene; PP, polypropylene; PVC, polyvinyl chloride; PUR, polyurethane; PCL, polycaprolactone diol; PET polyethylene terephthalate. Enzymes: AH, alkane hydroxylase; AD, alcohol dehydrogenase; ALD, aldehyde dehydrogenase; RhlYZ, R-specific enoyl-CoA hydratase; RhlA, HAA synthetase; RhlB, rhamnosyltransferase 1; RhlC, rhamnosyltransferase 2; SMO, styrene monooxygenase; SOI, styrene oxide isomerase; PAALDH, phenacetaldehyde dehydrogenase; PAAH, phenylacetate hydroxylase; HPAAH, 2-hydroxyphenylacetate hydroxylase; HGADO, homogentisate 1,2-dioxygenase; SDO, styrene dioxygenase; CGDH, *cis*-glycol dehydrogenase; CDO, catechol 2,3-dioxygenase; HMASALDH, 2-hydroxymuconic acid semialdehyde hydrolase; HPDEH, 2-hydroxypenta-2,4-dienoate hydratase; HOA, 4-hydroxy-2-oxovalerate aldolase; PDHC, pyruvate dehydrogenase complex; PhaA, β -ketothiolase; PhaB, acetoacetyl-CoA reductase; PhaC, PHA synthase; PedH, quinoprotein alcohol dehydrogenase; PedE, quinoprotein alcohol dehydrogenase; PedI, aldehyde dehydrogenase family protein; PP_0545, aldehyde dehydrogenase family protein; GlcDEF, glycolate oxidase; Gcl, glyoxylate carboligase; GlxR, tartronate semialdehyde reductase; TtuD, hydroxypyruvate reductase; PykF, pyruvate kinase; TPADO, TPA dioxygenase; TphB, 1,2-dihydroxy-3,5-cyclohexadiene-1,4-dicarboxylate dehydrogenase; PCDO, protocatechuate 3,4-dioxygenase; CMLE, β -carboxy-*cis*,*cis*-muconate lactonizing enzyme; CMD, β -carboxymuconolactone decarboxylase; ELH, enollactone hydrolase; TR, β -ketoadipate:succinyl-CoA transferase; TH, β -ketoadipyl-CoA thiolase; ChnD, 6-hydroxycaproate dehydrogenase; ChnE, 6-oxohexanoic dehydrogenase; ACoAL, adipate-CoA ligase; ACoAT, acetyl-CoA C-acyltransferase.

(Harwood and Parales, 1996). Of these, the *ortho*-cleavage pathway has been thoroughly studied. The resulting metabolite, β -carboxymuconate (CM), will eventually be converted into acetyl-CoA and succinyl-CoA, which can enter the tricarboxylic acid (TCA) cycle to generate succinic acid (Figure 2).

In 2008, Kenny et al. first isolated three microorganisms, *Pseudomonas putida* GO16, *Pseudomonas putida* GO19, and *Pseudomonas frederiksbergensis* GO23, which could utilize TPA for not only growth but also accumulation of medium chain length PHA (mclPHA). Subsequently, they used the TPA fraction from PET pyrolysis as the feedstock for microbial production of mclPHA by these *Pseudomonas* species. The maximal production rate of PHA reached approximately $8.4 \text{ mg} \cdot \text{l}^{-1} \cdot \text{h}^{-1}$ (Kenny et al., 2008). When TPA and glycerol waste from biodiesel manufacture were co-supplied to *Pseudomonas putida* GO16 in a fed-batch bioreactor, the production rate of PHA reached approximately $108.8 \text{ mg} \cdot \text{l}^{-1} \cdot \text{h}^{-1}$ (Kenny et al., 2012).

EG could be metabolized by many kinds of microorganisms through two different pathways (Figure 2). In the pathway of acetogens, EG is degraded to ethanol and acetaldehyde, which is eventually transformed to acetate via acetyl-CoA (Trifunović et al., 2016). In contrast, through the pathway of *Pseudomonas aeruginosa*, EG is initially oxidized into glycolate by a series of dehydrogenases, and the generated glycolate will be further transformed into glyoxylate by the glycolate oxidase (GlcDEF). Glyoxylate could be converted into glycerate, which finally forms pyruvate (Figure 2; Child and Willetts, 1978; Kataoka et al., 2001).

P. putida KT2440 could accumulate mclPHA under nitrogen-limiting conditions but could not efficiently utilize EG as its sole carbon source. Through adaptive laboratory evolution, one mutant of *P. putida* KT2440 that could utilize EG as its sole carbon source was isolated. Comparative genomic analyses between the wild strain and the mutant revealed that a transcriptional regulator, GclR, played a central role in repressing the glyoxylate carboligase pathway (Li et al., 2019). With this knowledge, Franden et al. (2018) demonstrated that the overexpression of a combination of the glyoxylate carboligase (Gcl) operon with the glycolate oxidase (GlcDEF) operon endowed *P. putida* KT2440 with the ability to utilize EG as a sole carbon source for growth and accumulate in nitrogen-limiting M9 medium.

As for 6-hydroxyhexanoate, the hydrolysis product of PCL-based PUR, it is first converted to 6-oxohexanoic by the 6-hydroxyhexanoate dehydrogenase (ChnD). 6-oxohexanoic is

eventually transformed into adipate by the action of the 6-oxohexanoic dehydrogenase (ChnE). After ligation with CoA, the adipate will be further converted to 3-oxoadipyl-CoA, which finally forms succinyl-CoA and acetyl-CoA that enter the TCA cycle with the production of succinic acid (Figure 2; Brzostowicz et al., 2003).

From Aromatic Hydrocarbons to Succinic Acids and PHA

Styrene, the aromatic monomer of PS, could be generated from the PS pyrolysis in the absence of air (Kaminsky and Kim, 1999) and is directly utilized as a carbon source by many microorganisms via two different catabolic pathways (Figure 2; O'Leary et al., 2002).

The first one is the direct aromatic ring cleavage pathway (Figure 2). In this pathway, the aromatic ring of styrene is firstly hydroxylated to styrene *cis*-glycol by styrene dioxygenase (SDO). Styrene *cis*-glycol is then further oxidized by a *cis*-glycol dehydrogenase (CGDH) to form 3-vinylcatechol. This product is degraded into pyruvate, which is further converted to acetyl-CoA by the pyruvate dehydrogenase complex (PDHC). Acetyl-CoA will finally enter the TCA cycle to generate succinic acid or be transformed into acetoacetyl-CoA, which could form β -D-Hydroxybutyryl-CoA or could be converted to PHA by an acetoacetyl-CoA reductase (PhaB) or a PHA synthase (PhaC), respectively (Anderson and Dawes, 1990). The other styrene metabolism pathway involves vinyl side-chain oxidation (Figure 2). Styrene is first converted into phenylacetic acid (PAA) by several enzymes, such as styrene monooxygenase (SMO), styrene oxide isomerase (SOI), and phenylacetaldehyde dehydrogenase (PAALDH). PAA is further hydroxylated and passed through the β -oxidation process to yield acetyl-CoA, which will then enter the TCA cycle or be converted into PHA (O'Leary et al., 2005; Oelschlägel et al., 2018).

In 2005, Ward et al. first found that *Pseudomonas putida* CA-3 could convert the metabolite of styrene, PAA, into polyhydroxyalkanoate (PHA) when a limiting concentration of nitrogen was added to the growth medium. Their finding built the metabolic link between styrene degradation and PHA accumulation in *P. putida* CA-3 and found a trail for the microbial valorization of PS waste into valuable chemicals (Ward et al., 2005; Nikodinovic-Runic et al., 2011).

Afterward, Ward et al. (2006) used the styrene oil, the pyrolysis products of PS waste at 520°C in a fluidized bed reactor, as the

sole source of carbon and energy to support the growth and PHA accumulation of *P. putida* CA-3 in the shake flask experiments. In a run, the transformation rate from PS waste to PHA was 10%. In order to improve the conversion rate, Goff et al. performed a batch fermentation of *P. putida* CA-3 grown on styrene oil in a stirred tank reactor with an optimized nitrogen feeding strategy (Goff et al., 2007).

From Aliphatic Hydrocarbons to Fatty Acids, PHA, and Biosurfactants

Although PE, PP, and PVC, with similar carbon–carbon backbone chains, have been shown to be degraded by a number of microorganisms, the key depolymerases involved in the degradation process and the resulting depolymerization products remain unknown. However, pyrolysis in the absence of air could be an alternative method that can effectively depolymerize those plastic wastes into low molecular weight aliphatic hydrocarbons (Aguado et al., 2002).

It has been reported that the pyrolytic hydrocarbons of PE can be degraded via a terminal oxidation process similar to the microbial degradation pathway of *n*-alkane (Figure 2; Yoon et al., 2012; Jeon and Kim, 2015, 2016a). This process starts by the oxidation of a terminal methyl group by an alkane hydroxylase (AH) to generate a primary alcohol, which is further oxidized by an alcohol dehydrogenase (AD) to the corresponding aldehyde and finally converted into fatty acids by an aldehyde dehydrogenase (ADL) (Rojo, 2009). Fatty acids are then conjugated to CoA by an acyl-CoA synthase and further processed by β -oxidation to produce acetyl-CoA, L- β -hydroxyacyl-CoA, and *trans*-2-decenoyl-CoA (Figure 2).

Acetyl-CoA can enter the TCA cycle to generate succinic acid or acetoacetyl-CoA, which can be finally converted to PHA under the appropriate condition (Anderson and Dawes, 1990). The L- β -hydroxyacyl-CoA is isomerized into D- β -hydroxyacyl-CoA, which can finally be converted into PHA through a PHA synthase (PhaC) (Sabirova et al., 2006). In addition, the *trans*-2-decenoyl-CoA is hydrated by the R-specific enoyl-CoA hydratase (RhlYZ) to form R-3-hydroxydecanoyl-CoA, which then acts as the direct lipid precursor used by the R-3-((R-3-hydroxyalkanoyl)oxy) alkanolic acids (HAA) synthase (RhlA) for the synthesis of HAAs. HAA, combined with dTDP-L-rhamnosides, can be converted into rhamnolipid biosurfactants by the rhamnosyltransferase 1 (RhlB) and the rhamnosyltransferase 2 (RhlC) (Abdel-Mawgoud et al., 2014).

Guzik et al. (2014) first used the pyrolytic hydrocarbons of PE as the starting material for microbial fermentation to produce PHA. *Pseudomonas aeruginosa* PAO-1, tested from 23 bacterial strains capable of degrading hydrocarbons or producing PHA, was reported to be able to accumulate PHA with almost 25% of cell dry weight when supplied with PE pyrolytic hydrocarbons and biosurfactants. Another bacterial strain, *Ralstonia eutropha* H16 (previously known as *Cuprivadus necator* or *Wausternia eutropha*), also exhibited PHA accumulation when supplied with non-oxygenated PE pyrolytic hydrocarbons as a carbon source in a nitrogen-rich tryptone soya broth (TSB) growth medium (Johnston et al., 2017). In contrast to PE pyrolysis in the absence of air, pyrolysis in the presence of air would not only cleave the long chains of PE but also introduce the carbonyl and hydroxyl groups into the backbone of pyrolytic hydrocarbons, which could improve the bioavailability of pyrolytic hydrocarbons as a carbon source for

TABLE 8 | Strains for the valorization of depolymerization products of plastics.

Plastics	Depolymerization methods	Depolymerization products	Strains	Metabolites	Yields	References
PET	Pyrolysis at 450°C	TPA	<i>Pseudomonas putida</i> GO16, <i>Pseudomonas putida</i> GO19, <i>Pseudomonas frederiksbergensis</i> GO23	PHA	8.4 mg · l ⁻¹ · h ⁻¹	Kenny et al., 2008
PET	Pyrolysis	TPA	<i>Pseudomonas putida</i> GO16	PHA	108.8 mg · l ⁻¹ · h ⁻¹	Kenny et al., 2012
PET	–	EG	<i>Pseudomonas putida</i> KT2440	PHA	0.06 g PHA per g EG	Franden et al., 2018
PS	–	Styrene	<i>Pseudomonas putida</i> CA-3	PHA	0.11 g PHA per g carbon	Ward et al., 2005
PS	–	Styrene	<i>Pseudomonas putida</i> CA-3	PHA	3.36 g · l ⁻¹	Nikodinovic-Runic et al., 2011
PS	Pyrolysis at 520°C	Styrene	<i>Pseudomonas putida</i> CA-3	PHA	62.5 mg PHA per g styrene	Ward et al., 2006
PS	Pyrolysis	Styrene	<i>Pseudomonas putida</i> CA-3	PHA	0.28 g PHA per g styrene	Goff et al., 2007
PE	Pyrolysis	Paraffins from C8 to C32	<i>Pseudomonas aeruginosa</i> PAO-1	PHA	25% of the cell dry weight	Guzik et al., 2014
PE	Pyrolysis	Hydrocarbons	<i>Ralstonia eutropha</i> H16	PHA	0.46 g · l ⁻¹	Johnston et al., 2017
PE	Pyrolysis in air	Oxidized hydrocarbons	<i>Ralstonia eutropha</i> H16	PHA	1.24 g · l ⁻¹	Radecka et al., 2016
PP	Pyrolysis at 540°C	Branched chain fatty alcohols and alkenes	<i>Yarrowia lipolytica</i> 78-003	Fatty acids	492 mg · l ⁻¹ over 312 h	Mihreteab et al., 2019
PP	Thermal oxidation at 80–100°C in the oxygen–ozone mixture	Oxidized PP fragments	<i>Ralstonia eutropha</i> H16	PHA	1.36 g · l ⁻¹	Johnston et al., 2019
–	–	n-hexadecane	<i>Renibacterium salmoninarum</i> 27BN	Rhamnolipid	0.92 g · l ⁻¹	Christova et al., 2004
–	–	n-hexadecane	<i>Dietzia maris</i> As-13-3	Di-rhamnolipid	120 mg · l ⁻¹	Wang et al., 2014

microbial fermentation to produce PHA by the strain *Ralstonia eutropha* H16 (Radecka et al., 2016).

In addition, PP could also be depolymerized into branched chain fatty alcohols and alkenes by pyrolysis. In 2019, Mihreteab et al. reported that strain *Yarrowia lipolytica* 78-003 was able to convert such depolymerization products to value-added fatty acids when mixed with biosurfactants and trace nutrients. During a period of 312 h, *Y. lipolytica* 78-003 assimilated more than 80% of the substrate and produced up to 492 mg L⁻¹ lipids mainly composed of C₁₆-C₁₈ unsaturated fatty acids (Mihreteab et al., 2019). Johnston et al. (2019) found that *R. eutropha* H16 could utilize oxidized PP fragments as an additional carbon source to produce PHA in TSB medium.

As for PVC, although the pyrolysis at 300°C in the N₂ flow has been showed to be able to depolymerize PVC into hydrocarbons along with the dechlorination in the form of HCl (Yuan et al., 2014), there are no reports about microbial strains that can utilize PVC pyrolysis products as carbon source so far. However, as these products are of similar chemical compositions to those of PE and PP, it is justifiable to believe that the strains of *P. aeruginosa*, *R. eutropha* H16, and *Yarrowia lipolytica* 78-003, which are able to assimilate the pyrolysis hydrocarbons of PE and PP, could also utilize PVC pyrolysis products to produce valuable chemicals.

Microbial growth on hydrocarbons is often associated with the production of biosurfactant, which can emulsify the hydrophobic hydrocarbons in aqueous media to increase the bioavailability of hydrocarbons to the cells. For instance, the strain *Renibacterium salmoninarum* 27BN was found to be able to produce rhamnolipids when grown on *n*-hexadecane (Christova et al., 2004). An oil-degrading bacterium *Dietzia maris* As-13-3, isolated from deep sea hydrothermal field, could also produce di-rhamnolipid as a biosurfactant, while tetradecane, *n*-hexadecane, and pristane were utilized as sole carbon sources (Wang et al., 2014). These results imply that pyrolysis hydrocarbons of PE, PP, and PVC could also be utilized as feedstocks to produce biosurfactants by these known hydrocarbon-degrading and biosurfactant-producing microorganisms.

CONCLUDING REMARKS AND FUTURE PROSPECTS

As described above, a number of plastic-degrading microorganisms and enzymes have been sourced from the environment. However, an understanding of depolymerases

contributing to the breakdown of plastics remains scarce. Therefore, future efforts should be devoted to identifying more depolymerases from the plastic-degrading microorganisms. In addition, enhancing the efficiency of enzymatic degradation is a big challenge. On the one hand, the macromolecular aggregate structures of plastics, such as the crystalline structures and cross-linking networks, impede the enzymatic degradation. The development of physical pretreatments, such as mechanical grinding and γ -irradiations, may help disorder these macromolecular aggregate structures and improve enzymatic degradation (Alariqi et al., 2006). On the other hand, approaches of rational protein engineering and direction evolution are necessary to improve the activity and stability of depolymerases, which will benefit the enhancement of enzymatic degradation efficiency.

While the long-chain polymer molecules could have been effectively depolymerized into small subunits (monomers or oligomers) by depolymerases, these small depolymerization products would be incorporated into cells as the feedstocks for metabolism (Table 8). Based on the advances in the understanding of the depolymerases and the microbial metabolic pathways of depolymerization products, it is fascinating to apply synthetic biology to build microbial cell factories that could depolymerize plastic wastes and utilize the small depolymerization products to produce chemicals with high value (Wierckx et al., 2015; Salvador et al., 2019; Blank et al., 2020). If this is manageable, it would not only contribute to the disposal of plastic wastes but also establish an improved cyclic utilization of plastics.

AUTHOR CONTRIBUTIONS

YY generated the idea and designed the project. YH contributed to the analysis and discussion. JR and YY prepared the figures and tables. YY and JR wrote the manuscript.

FUNDING

This work was supported by grants from National Natural Science Foundation of China (Nos. 31961133015 and 51603004), the Young Elite Scientist Sponsorship Program of the China Association of Science and Technology (No. 2017QNRC001), and the Beijing Institute of Technology Research Fund Program for Young Scholars (No. 3160011181804).

REFERENCES

- Abdel-Mawgoud, A. M., Lépine, F., and Déziel, E. (2014). A stereospecific pathway diverts β -oxidation intermediates to the biosynthesis of rhamnolipid biosurfactants. *Chem. Biol.* 21, 156–164. doi: 10.1016/j.chembiol.2013.11.010
- Aguado, R., Olazar, M., San José, M. J., Gaisán, B., and Bilbao, J. (2002). Wax formation in the pyrolysis of polyolefins in a conical spouted bed reactor. *Energ. Fuel* 16, 1429–1437. doi: 10.1021/ef020043w
- Akutsu, Y., Nakajima-Kambe, T., Nomura, N., and Nakahara, T. (1998). Purification and properties of a polyester polyurethane-degrading enzyme from *Comamonas acidovorans* TB-35. *Appl. Environ. Microbiol.* 64, 62–67. doi: 10.1128/aem.64.1.62-67.1998
- Alariqi, S. A., Kumar, A. P., Rao, B. S. M., and Singh, R. P. (2006). Biodegradation of γ -sterilised biomedical polyolefins under composting and fungal culture environments. *Polym. Degrad. Stab.* 91, 1105–1116. doi: 10.1016/j.polymdegradstab.2005.07.004
- Albertsson, A. C. (1978). Biodegradation of synthetic polymers. II. A limited microbial conversion of 14C in polyethylene to 14CO₂ by some soil fungi. *J. Appl. Polym. Sci.* 22, 3419–3433. doi: 10.1002/app.1978.070221207
- Albertsson, A. C. (1980). Microbial and oxidative effects in degradation of polyethylene. *J. Appl. Polym. Sci.* 25, 1655–1671. doi: 10.1002/app.1980.070250813

- Albertsson, A. C., Andersson, S. O., and Karlsson, S. (1987). The mechanism of biodegradation of polyethylene. *Polym. Degrad. Stab.* 18, 73–87. doi: 10.1016/0141-3910(87)90084-x
- Albertsson, A. C., Barenstedt, C., Karlsson, S., and Lindberg, T. (1995). Degradation product pattern and morphology changes as means to differentiate abiotically and biotically aged degradable polyethylene. *Polymer* 36, 3075–3083. doi: 10.1016/0032-3861(95)97868-g
- Albertsson, A. C., Erlandsson, B., Hakkarainen, M., and Karlsson, S. (1998). Molecular weight changes and polymeric matrix changes correlated with the formation of degradation products in Biodegraded Polyethylene. *J. Environ. Polym. Degrad.* 6, 187–195.
- Albertsson, A. C., and Karlsson, S. (1988). The three stages in degradation of polymers—polyethylene as a model substance. *J. Appl. Polym. Sci.* 35, 1289–1302. doi: 10.1002/app.1988.070350515
- Albertsson, A. C., and Karlsson, S. (1990). The influence of biotic and abiotic environments on the degradation of polyethylene. *Prog. Polym. Sci.* 15, 177–192. doi: 10.1016/0079-6700(90)90027-x
- Ali, M. I., Ahmed, S., Robson, G., Javed, I., Ali, N., Atiq, N., et al. (2014). Isolation and molecular characterization of polyvinyl chloride (PVC) plastic degrading fungal isolates. *J. Basic Microbiol.* 54, 18–27. doi: 10.1002/jobm.201200496
- Alisch, M., Feuerhack, A., Müller, H., Mensak, B., Andreus, J., and Zimmermann, W. (2004). Biocatalytic modification of polyethylene terephthalate fibres by esterases from actinomycete isolates. *Biocatal. Biotrans.* 22, 347–351. doi: 10.1080/10242420400025877
- Allen, A. B., Hilliard, N. P., and Howard, G. T. (1999). Purification and characterization of a soluble polyurethane degrading enzyme from *Comamonas acidovorans*. *Int. Biodeter. Biodegr.* 43, 37–41.
- Álvarez-Barragán, J., Domínguez-Malfavón, L., Vargas-Suárez, M., Gonzalez-Hernandez, R., Aguilar-Osorio, G., and Loza-Tavera, H. (2016). Biodegradative activities of selected environmental fungi on a polyester polyurethane varnish and polyether polyurethane foams. *Appl. Environ. Microbiol.* 82, 5225–5235. doi: 10.1128/AEM.01344-16
- Anderson, A. J., and Dawes, E. A. (1990). Occurrence, metabolism, metabolic role, and industrial uses of bacterial polyhydroxyalkanoates. *Microbiol. Mol. Biol. Res.* 54, 450–472. doi: 10.1128/mmbr.54.4.450-472.1990
- Anwar, M. S., Kapri, A., Chaudhry, V., Mishra, A., Ansari, M. W., Souche, Y., et al. (2016). Response of indigenously developed bacterial consortia in progressive degradation of polyvinyl chloride. *Protoplasma* 253, 1023–1032. doi: 10.1007/s00709-015-0855-9
- Arkatkar, A., Arutchelvi, J., Bhaduri, S., Uppara, P. V., and Doble, M. (2009). Degradation of untreated and thermally pretreated polypropylene by soil consortia. *Int. Biodeter. Biodegr.* 63, 106–111. doi: 10.1016/j.ibiod.2008.06.005
- Arkatkar, A., Juwarkar, A. A., Bhaduri, S., Uppara, P. V., and Doble, M. (2010). Growth of *Pseudomonas* and *Bacillus* biofilms on pretreated polypropylene surface. *Int. Biodeter. Biodegr.* 64, 530–536. doi: 10.1016/j.ibiod.2010.06.002
- Arutchelvi, J., Sudhakar, M., Arkatkar, A., Doble, M., Bhaduri, S., and Uppara, P. V. (2008). Biodegradation of polyethylene and polypropylene. *Indian J. Biotechnol.* 7, 9–22.
- Atiq, N. (2011). *Biodegradability of Synthetic Plastics Polystyrene and Styrofoam by Fungal Isolates*. Islamabad: Quaid-i-Azam University Press.
- Atiq, N., Garba, A., Ali, M. I., Andleeb, S., Khan, N. A., and Robson, G. D. (2010). Isolation and identification of polystyrene biodegrading bacteria from soil. *Afr. J. Microbiol. Res.* 4, 1537–1541.
- Auta, H. S., Emenike, C. U., Jayanthi, B., and Fauziah, S. H. (2018). Growth kinetics and biodeterioration of polypropylene microplastics by *Bacillus* sp. and *Rhodococcus* sp. isolated from mangrove sediment. *Mar. Pollut. Bull.* 127, 15–21. doi: 10.1016/j.marpolbul.2017.11.036
- Azeko, S. T., Etuk-Udo, G. A., Odusanya, O. S., Malatesta, K., Anuku, N., and Soboyejo, W. O. (2015). Biodegradation of linear low density polyethylene by *Serratia marcescens* subsp. *marcescens* and its cell free extracts. *Waste Biomass Valor.* 6, 1047–1057. doi: 10.1007/s12649-015-9421-0
- Balasubramanian, V., Natarajan, K., Hemambika, B., Ramesh, N., Sumathi, C. S., Kottaimuthu, R., et al. (2010). High-density polyethylene (HDPE)-degrading potential bacteria from marine ecosystem of Gulf of Mannar, India. *Lett. Appl. Microbiol.* 51, 205–211. doi: 10.1111/j.1472-765X.2010.02883.x
- Berk, S. (1950). Effect of fungus growth on the tensile strength of polyvinyl chloride films plasticized with three plasticizers. *ASTM Bull.* 168, 53–55.
- Berk, S., Ebert, H., and Teitell, L. (1957). Utilization of plasticizers and related organic compounds by fungi. *Ind. Eng. Chem.* 49, 1115–1124. doi: 10.3390/ijerph16132441
- Bessemers, E. (1988). The biodeterioration of plasticized PVC and its prevention. *J. Vinyl Technol.* 10, 3–6. doi: 10.1002/vnl.730100103
- Blank, L. M., Narancic, T., Mampel, J., Tiso, T., and O'Connor, K. (2020). Biotechnological upcycling of plastic waste and other non-conventional feedstocks in a circular economy. *Curr. Opin. Biotechnol.* 62, 212–219. doi: 10.1016/j.copbio.2019.11.011
- Bombelli, P., Howe, C. J., and Bertocchini, F. (2017). Polyethylene bio-degradation by caterpillars of the wax moth *Galleria mellonella*. *Curr. Biol.* 27, R292–R293. doi: 10.1016/j.cub.2017.02.060
- Brown, B. S., Mills, J., and Hulse, J. M. (1974). Chemical and biological degradation of waste plastics. *Nature* 250, 161–163. doi: 10.1038/250161a0
- Brzostowicz, P. C., Walters, D. M., Thomas, S. M., Nagarajan, V., and Rouviere, P. E. (2003). mRNA differential display in a microbial enrichment culture: simultaneous identification of three cyclohexanone monooxygenases from three species. *Appl. Environ. Microbiol.* 69, 334–342. doi: 10.1128/aem.69.1.334-342.2003
- Cacciari, I., Quatrini, P., Zirletta, G., Mincione, E., Vinciguerra, V., Lupattelli, P., et al. (1993). Isotactic polypropylene biodegradation by a microbial community: physicochemical characterization of metabolites produced. *Appl. Environ. Microbiol.* 59, 3695–3700. doi: 10.1128/aem.59.11.3695-3700.1993
- Chalup, A., Ayup, M. M., Monmany Garzia, A. C., Malizia, A., Martin, E., De Cristóbal, R., et al. (2018). First report of the lesser wax moth *Achroia grisella* F. (Lepidoptera: Pyralidae) consuming polyethylene (silo-bag) in northwestern Argentina. *J. Apic. Res.* 57, 569–571. doi: 10.1080/00218839.2018.1484614
- Child, J., and Willetts, A. (1978). Microbial metabolism of aliphatic glycols bacterial metabolism of ethylene glycol. *Biochim. Biophys. Acta* 538, 316–327. doi: 10.1016/0304-4165(78)90359-8
- China Plastics Industry (2017). Data from: In 2017, the Total Output of China's Plastic Products was 751.155 Million Tons, an Increase of 3.4% Year-on-Year (EB/OL). Available online at: <http://www.iplast.cn/shownews.asp?id=6625> (accessed October 2, 2019).
- Choi, K. Y., Kim, D., Sul, W. J., Chae, J. C., Zylstra, G. J., Kim, Y. M., et al. (2005). Molecular and biochemical analysis of phthalate and terephthalate degradation by *Rhodococcus* sp. strain DK17. *FEMS Microbiol. Lett.* 252, 207–213. doi: 10.1016/j.femsle.2005.08.045
- Christova, N., Tuleva, B., Lalchev, Z., Jordanova, A., and Jordanov, B. (2004). Rhamnolipid biosurfactants produced by *Renibacterium salmoninarum* 27BN during growth on n-hexadecane. *Z. Naturforsch. C* 59, 70–74. doi: 10.1515/znc-2004-1-215
- Cosgrove, L., McGeechan, P. L., Robson, G. D., and Handley, P. S. (2007). Fungal communities associated with degradation of polyester polyurethane in soil. *Appl. Environ. Microbiol.* 73, 5817–5824. doi: 10.1128/aem.01083-07
- Crabbe, J. R., Campbell, J. R., Thompson, L., Walz, S. L., and Schultz, W. W. (1994). Biodegradation of a colloidal ester-based polyurethane by soil fungi. *Int. Biodeter. Biodegr.* 33, 103–113. doi: 10.1016/0964-8305(94)90030-2
- Cregut, M., Bedas, M., Durand, M. J., and Thouand, G. (2013). New insights into polyurethane biodegradation and realistic prospects for the development of a sustainable waste recycling process. *Biotechnol. Adv.* 31, 1634–1647. doi: 10.1016/j.biotechadv.2013.08.011
- Darby, R. T., and Kaplan, A. M. (1968). Fungal susceptibility of polyurethanes. *Appl. Microbiol.* 16, 900–905. doi: 10.1128/aem.16.6.900-905.1968
- Delacuvellerie, A., Cyriaque, V., Gobert, S., Benali, S., and Wattiez, R. (2019). The platisphere in marine ecosystem hosts potential specific microbial degraders including *Alcanivorax borkumensis* as a key player for the low-density polyethylene degradation. *J. Hazard. Mater.* 380:120899. doi: 10.1016/j.jhazmat.2019.120899
- Eisaku, O., Linn, K., Takeshi, E., Taneaki, O., and Yoshinobu, I. (2003). Isolation and characterization of polystyrene degrading microorganisms for zero emission treatment of expanded polystyrene. *Environ. Eng. Res.* 40, 373–379.
- Engel, P., and Moran, N. A. (2013). The gut microbiota of insects—diversity in structure and function. *FEMS Microbiol. Rev.* 37, 699–735. doi: 10.1111/1574-6976.12025
- Erlandsson, B., Karlsson, S., and Albertsson, A. C. (1998). Correlation between molar mass changes and CO₂ evolution from biodegraded ¹⁴C-labeled

- ethylene-vinyl alcohol copolymer and ethylene polymers. *Acta Polym.* 49, 363–370. doi: 10.1002/(sici)1521-4044(199807)49:7<363::aid-apol363>3.0.co;2-u
- Filip, Z. (1979). Polyurethane as the sole nutrient source for *Aspergillus niger*, and *Cladosporium herbarum*. *Appl. Microbiol. Biotechnol.* 7, 277–280. doi: 10.1007/bf00498022
- Fischer-Colbrie, G., Heumann, S., Liebminger, S., Almansa, E., Cavaco-Paulo, A., and Guebitz, G. M. (2004). New enzymes with potential for PET surface modification. *Biocatal. Biotrans.* 22, 341–346. doi: 10.1080/10242420400024565
- Fransen, M. A., Jayakody, L. N., Li, W. J., Wagner, N. J., Cleveland, N. S., Michener, W. E., et al. (2018). Engineering *Pseudomonas putida* KT2440 for efficient ethylene glycol utilization. *Metab. Eng.* 48, 197–207. doi: 10.1016/j.ymben.2018.06.003
- Garcia, J. M., and Robertson, M. L. (2017). The future of plastics recycling. *Science* 358, 870–872.
- Gautam, R., Bassia, S., Yanful, E. K., and Cullen, E. (2007). Biodegradation of automotive waste polyester polyurethane foam using *Pseudomonas chlororaphis* ATCC55729. *Int. Biodeterior. Biodegrad.* 60, 245–249. doi: 10.1016/j.ibiod.2007.03.009
- Geyer, R., Jambeck, J., and Law, K. L. (2017). Production, use, and fate of all plastics ever made. *Sci. Adv.* 3:e1700782. doi: 10.1126/sciadv.1700782
- Giacomucci, L., Raddadi, N., Soccio, M., Lotti, N., and Fava, F. (2019). Polyvinyl chloride biodegradation by *Pseudomonas citronellolis* and *Bacillus flexus*. *New Biotechnol.* 52, 35–41. doi: 10.1016/j.nbt.2019.04.005
- Goff, M., Ward, P. G., and O'Connor, K. E. (2007). Improvement of the conversion of polystyrene to polyhydroxyalkanoate through the manipulation of the microbial aspect of the process: a nitrogen feeding strategy for bacterial cells in a stirred tank reactor. *J. Biotechnol.* 132, 283–286. doi: 10.1016/j.jbiotec.2007.03.016
- Gübitz, G. M., and Paulo, A. C. (2003). New substrates for reliable enzymes: enzymatic modification of polymers. *Curr. Opin. Biotechnol.* 14, 577–582. doi: 10.1016/j.copbio.2003.09.010
- Guillet, J. E., Regulski, T. W., and McAneney, T. B. (1974). Biodegradability of photodegraded polymers. II. Tracer studies of biooxidation of Ecolyte PS polystyrene. *Environ. Sci. Technol.* 8, 923–925. doi: 10.1016/j.chemosphere.2008.07.035
- Gumargalieva, K. Z., Zaikov, G. E., Semenov, S. A., and Zhdanova, O. A. (1999). The influence of biodegradation on the loss of a plasticiser from poly (vinyl chloride). *Polym. Degrad. Stab.* 63, 111–112. doi: 10.1016/s0141-3910(98)00071-8
- Guzik, M. W., Kenny, S. T., Duane, G. F., Casey, E., Woods, T., Babu, R. P., et al. (2014). Conversion of post consumer polyethylene to the biodegradable polymer polyhydroxyalkanoate. *Appl. Microbiol. Biotechnol.* 98, 4223–4232. doi: 10.1007/s00253-013-5489-2
- Hakkarainen, M., and Albertsson, A. C. (2004). “Environmental degradation of polyethylene,” in *Long Term Properties of Polyolefins*, ed. A. C. Albertsson (Berlin: Springer), 177–200. doi: 10.1007/b13523
- Harshvardhan, K., and Jha, B. (2013). Biodegradation of low-density polyethylene by marine bacteria from pelagic waters, Arabian Sea, India. *Mar. Pollut. Bull.* 77, 100–106. doi: 10.1016/j.marpolbul.2013.10.025
- Harwood, C. S., and Parales, R. E. (1996). The β -ketoadipate pathway and the biology of self-identity. *Annu. Rev. Microbiol.* 50, 553–590. doi: 10.1146/annurev.micro.50.1.553
- Ho, B. T., Roberts, T. K., and Lucas, S. (2018). An overview on biodegradation of polystyrene and modified polystyrene: the microbial approach. *Crit. Rev. Biotechnol.* 38, 308–320. doi: 10.1080/07388551.2017.1355293
- Hosaka, M., Kamimura, N., Toribami, S., Mori, K., Kasai, D., Fukuda, M., et al. (2013). Novel tripartite aromatic acid transporter essential for terephthalate uptake in *Comamonas* sp. strain E6. *Appl. Environ. Microbiol.* 79, 6148–6155. doi: 10.1128/AEM.01600-13
- Howard, G. T., and Blake, R. C. (1998). Growth of *Pseudomonas fluorescens* on a polyester-polyurethane and the purification and characterization of a polyurethanase-protease enzyme. *Int. Biodeterior. Biodegrad.* 42, 213–220. doi: 10.1016/s0964-8305(98)00051-1
- Howard, G. T., and Burks, T. (2012). Growth of *Acinetobacter gerveri* P7 on polyurethane and the purification and characterization of a polyurethanase enzyme. *Biodegradation* 23, 561–573. doi: 10.1007/s10532-011-9533-6
- Howard, G. T., Ruiz, C., and Hilliard, N. P. (1999). Growth of *Pseudomonas chlororaphis* on a polyester-polyurethane and the purification and characterization of a polyurethanase-esterase enzyme. *Int. Biodeterior. Biodegrad.* 43, 7–12. doi: 10.1016/s0964-8305(98)00057-2
- Howard, G. T., Vicknair, J., and Mackie, R. I. (2001a). Sensitive plate assay for screening and detection of bacterial polyurethanase activity. *Lett. Appl. Microbiol.* 32, 211–214. doi: 10.1046/j.1472-765x.2001.00887.x
- Howard, G. T., Crother, B., and Vicknair, J. (2001b). Cloning, nucleotide sequencing and characterization of a polyurethanase gene (pueB) from *Pseudomonas chlororaphis*. *Int. Biodeterior. Biodegrad.* 47, 141–149. doi: 10.1016/s0964-8305(01)00042-7
- Hsieh, Y. L., and Cram, L. A. (1998). Enzymatic hydrolysis to improve wetting and absorbency of polyester fabrics. *Text. Res. J.* 68, 311–319. doi: 10.1177/004051759806800501
- Ii, R. C. B., Norton, W. N., and Howard, G. T. (1998). Adherence and growth of a *Bacillus* species on an insoluble polyester polyurethane. *Int. Biodeterior. Biodegrad.* 42, 63–73. doi: 10.1016/s0964-8305(98)00048-1
- Iiyoshi, Y., Tsutsumi, Y., and Nishida, T. (1998). Polyethylene degradation by lignin-degrading fungi and manganese peroxidase. *J. Wood Sci.* 44, 222–229. doi: 10.1007/bf00521967
- Jain, K., Bhunia, H., and Sudhakara Reddy, M. (2018). Degradation of polypropylene-poly-L-lactide blend by bacteria isolated from compost. *Bioremediat. J.* 22, 73–90. doi: 10.1080/10889868.2018.1516620
- Jambeck, J. R., Geyer, R., Wilcox, C., Siegler, T. R., Perryman, M., Andrady, A., et al. (2015). Marine pollution. Plastic waste inputs from land into the ocean. *Science* 347, 768–771. doi: 10.1126/science.1260352
- Jansen, B., Schumacher-Perdreau, F., Peters, G., and Pulverer, G. (1991). Evidence for degradation of synthetic polyurethanes by *Staphylococcus epidermidis*. *Zentralbl. Bakteriol.* 276, 36–45. doi: 10.1016/s0934-8840(11)80216-1
- Jeon, H. J., and Kim, M. N. (2015). Functional analysis of alkane hydroxylase system derived from *Pseudomonas aeruginosa* E7 for low molecular weight polyethylene biodegradation. *Int. Biodeter. Biodegr.* 103, 141–146. doi: 10.1016/j.ibiod.2015.04.024
- Jeon, H. J., and Kim, M. N. (2016a). Comparison of the functional characterization between alkane monooxygenases for low-molecular-weight polyethylene biodegradation. *Int. Biodeter. Biodegr.* 114, 202–208. doi: 10.1016/j.ibiod.2016.06.012
- Jeon, H. J., and Kim, M. N. (2016b). Isolation of mesophilic bacterium for biodegradation of polypropylene. *Int. Biodeter. Biodegr.* 115, 244–249. doi: 10.1016/j.ibiod.2016.08.025
- Jeyakumar, D., Chirsteen, J., and Doble, M. (2013). Synergistic effects of pretreatment and blending on fungi mediated biodegradation of polypropylenes. *Bioresour. Technol.* 148, 78–85. doi: 10.1016/j.biortech.2013.08.074
- Johnston, B., Jiang, G., Hill, D., Adamus, G., Kwiecień, I., Zięba, M., et al. (2017). The molecular level characterization of biodegradable polymers originated from polyethylene using non-oxygenated polyethylene wax as a carbon source for polyhydroxyalkanoate production. *Bioengineering* 4:73. doi: 10.3390/bioengineering4030073
- Johnston, B., Radecka, I., Chiellini, E., Barsi, D., Ilieva, V. I., Sikorska, W., et al. (2019). Mass spectrometry reveals molecular structure of polyhydroxyalkanoates attained by bioconversion of oxidized polypropylene waste fragments. *Polymers* 11:1580. doi: 10.3390/polym11101580
- Kaminsky, W., and Kim, J. S. (1999). Pyrolysis of mixed plastics into aromatics. *J. Anal. Appl. Pyrol.* 51, 127–134. doi: 10.1016/s0165-2370(99)00012-1
- Kaplan, D. L., Hartenstein, R., and Sutter, J. (1979). Biodegradation of polystyrene, poly(methyl methacrylate), and phenol formaldehyde. *Appl. Environ. Microbiol.* 38, 551–553. doi: 10.1128/aem.38.3.551-553.1979
- Kataoka, M., Sasaki, M., Hidalgo, A.-R. G. D., Nakano, M., and Shimizu, S. (2001). Glycolic acid production using ethylene glycol-oxidizing microorganisms. *Biosci. Biotechnol. Biochem.* 65, 2265–2270. doi: 10.1271/bbb.65.2265
- Kawai, F., Kawabata, T., and Oda, M. (2019). Current knowledge on enzymatic PET degradation and its possible application to waste stream management and other fields. *Appl. Microbiol. Biotechnol.* 103, 4253–4268. doi: 10.1007/s00253-019-09717-y
- Kawai, F., Oda, M., Tamashiro, T., Waku, T., Tanaka, N., Yamamoto, M., et al. (2014). A novel Ca^{2+} -activated, thermostabilized polyesterase capable of hydrolyzing polyethylene terephthalate from *Saccharomonospora viridis* AHK190. *Appl. Microbiol. Biotechnol.* 98, 10053–10064. doi: 10.1007/s00253-014-5860-y

- Kawai, F., Shibata, M., Yokoyama, S., Maeda, S., Tada, K., and Hayashi, S. (1999). Biodegradability of scott-gealed photodegradable polyethylene and polyethylene wax by microorganisms. *Macromol. Symp.* 144, 73–84. doi: 10.1002/masy.19991440108
- Kawai, F., Watanabe, M., Shibata, M., Yokoyama, S., and Sudate, Y. (2002). Experimental analysis and numerical simulation for biodegradability of polyethylene. *Polym. Degrad. Stab.* 76, 129–135. doi: 10.1016/s0141-3910(02)00006-x
- Kawai, F., Watanabe, M., Shibata, M., Yokoyama, S., Sudate, Y., and Hayashi, S. (2004). Comparative study on biodegradability of polyethylene wax by bacteria and fungi. *Polym. Degrad. Stab.* 86, 105–114. doi: 10.1016/j.polymdegradstab.2004.03.015
- Kay, M. J., McCabe, R. W., and Morton, L. H. G. (1993). Chemical and physical changes occurring in polyester polyurethane during biodegradation. *Int. Biodeter. Biodegr.* 31, 209–225. doi: 10.1016/0964-8305(93)90006-n
- Kay, M. J., Morton, L. H. G., and Prince, E. L. (1991). Bacterial degradation of polyester polyurethane. *Int. Biodeter. Biodegr.* 27, 205–222. doi: 10.1016/0265-3036(91)90012-g
- Kenny, S. T., Runic, J. N., Kaminsky, W., Woods, T., Babu, R. P., Keely, C. M., et al. (2008). Up-cycling of pet (polyethylene terephthalate) to the biodegradable plastic pha (polyhydroxyalkanoate). *Environ. Sci. Technol.* 42, 7696–7701. doi: 10.1021/es801010e
- Kenny, S. T., Runic, J. N., Kaminsky, W., Woods, T., Babu, R. P., and O'Connor, K. E. (2012). Development of a bioprocess to convert PET derived terephthalic acid and biodiesel derived glycerol to medium chain length polyhydroxyalkanoate. *Appl. Microbiol. Biotechnol.* 95, 623–633. doi: 10.1007/s00253-012-4058-4
- Khan, S., Nadir, S., Shah, Z. U., Shah, A. A., Karunarathna, S. C., Xu, J., et al. (2017). Biodegradation of polyester polyurethane by *Aspergillus tubingensis*. *Environ. Pollut.* 225, 469–480. doi: 10.1016/j.envpol.2017.03.012
- Khatoun, N., Jamal, A., and Ali, M. I. (2019). Lignin peroxidase isoenzyme: a novel approach to biodegrade the toxic synthetic polymer waste. *Environ. Technol.* 40, 1366–1375. doi: 10.1080/09593330.2017.1422550
- Kim, Y. D., and Kim, S. C. (1998). Effect of chemical structure on the biodegradation of polyurethanes under composting conditions. *Polym. Degrad. Stab.* 62, 343–352. doi: 10.1016/s0141-3910(98)00017-2
- Klrbas, N., Keskin, N., and Güner, A. (1999). Biodegradation of polyvinylchloride (PVC) by white rot fungi. *B. Environ. Contam. Tox.* 63, 335–342. doi: 10.1007/s001289900985
- Kowalczyk, A., Chyc, M., Ryszka, P., and Latowski, D. (2016). *Achromobacter xylosoxidans* as a new microorganism strain colonizing high-density polyethylene as a key step to its biodegradation. *Environ. Sci. Pollut. Res. Int.* 23, 11349–11356. doi: 10.1007/s11356-016-6563-y
- Kumari, A., Chaudhary, D. R., and Jha, B. (2019). Destabilization of polyethylene and polyvinylchloride structure by marine bacterial strain. *Environ. Sci. Pollut. Res. Int.* 26, 1507–1516. doi: 10.1007/s11356-018-3465-1
- Kundungal, H., Gangarapu, M., Sarangapani, S., Patchaiyappan, A., and Devipriya, S. P. (2019). Efficient biodegradation of polyethylene (HDPE) waste by the plastic-eating lesser waxworm (*Achroia grisella*). *Environ. Sci. Pollut. Res. Int.* 26, 18509–18519. doi: 10.1007/s11356-019-05038-9
- Kurane, R. (1988). Biodegradation of phthalate ester in Japan. *Biosci. Ind.* 46, 3173–3177.
- Latorre, I., Hwang, S., and Montalvo-Rodriguez, R. (2012). Isolation and molecular identification of landfill bacteria capable of growing on di-(2-ethylhexyl) phthalate and deteriorating PVC materials. *J. Environ. Health Sci. Part A* 47, 2254–2262. doi: 10.1080/10934529.2012.707549
- Lee, B., Pometto, A. L., Fratzke, A., and Bailey, T. B. (1991). Biodegradation of degradable plastic polyethylene by *Phanerochaete* and *Streptomyces* species. *Appl. Environ. Microbiol.* 57, 678–685. doi: 10.1128/aem.57.3.678-685.1991
- Li, W. J., Jayakody, L. N., Franden, M. A., Wehrmann, M., Daun, T., Hauer, B., et al. (2019). Laboratory evolution reveals the metabolic and regulatory basis of ethylene glycol metabolism by *Pseudomonas putida* KT2440. *Environ. Microbiol.* 21, 3669–3682. doi: 10.1111/1462-2920.14703
- Lönnstedt, O. M., and Eklöv, P. (2016). Environmentally relevant concentrations of microplastic particles influence larval fish ecology. *Science* 352, 1213–1216. doi: 10.1126/science.aad8828
- Magnin, A., Hoornaert, L., Pollet, E., Laurichesse, S., Phalip, V., and Avérous, L. (2019a). Isolation and characterization of different promising fungi for biological waste management of polyurethanes. *Microb. Biotechnol.* 12, 544–555. doi: 10.1111/1751-7915.13346
- Magnin, A., Pollet, E., Phalip, V., and Avérous, L. (2019c). Evaluation of biological degradation of polyurethanes. *Biotechnol. Adv.* 39:107457. doi: 10.1016/j.biotechadv.2019.107457
- Magnin, A., Pollet, E., Perrin, R., Ullmann, C., Persillon, C., Phalip, V., et al. (2019b). Enzymatic recycling of thermoplastic polyurethanes: synergistic effect of an esterase and an amidase and recovery of building blocks. *Waste Manag.* 85, 141–150. doi: 10.1016/j.wasman.2018.12.024
- Mathur, G., and Prasad, R. (2012). Degradation of polyurethane by *Aspergillus flavus* (ITCC 6051) isolated from soil. *Appl. Biochem. Biotechnol.* 167, 1595–1602. doi: 10.1007/s12010-012-9572-4
- Matsumiya, Y., Murata, N., Tanabe, E., Kubota, K., and Kubo, M. (2010). Isolation and characterization of an ether-type polyurethane-degrading microorganism and analysis of degradation mechanism by *Alternaria* sp. *J. Appl. Microbiol.* 108, 1946–1953.
- Mihreteab, M., Stubblefield, B. A., and Gilbert, E. S. (2019). Microbial bioconversion of thermally depolymerized polypropylene by *Yarrowia lipolytica* for fatty acid production. *Appl. Microbiol. Biotechnol.* 103, 7729–7740. doi: 10.1007/s00253-019-09999-2
- Mor, R., and Sivan, A. (2008). Biofilm formation and partial biodegradation of polystyrene by the actinomycete *Rhodococcus ruber*. *Biodegradation* 19, 851–858. doi: 10.1007/s10532-008-9188-0
- Moriyama, Y., Kimura, N., Inoue, R., and Kawaguchi, A. (1993). Examination of fungal deterioration on plasticized polyvinyl chloride by cryo-scanning electron microscopy. *Int. Biodeter. Biodegr.* 31, 231–239. doi: 10.1016/0964-8305(93)90008-p
- Müller, R. J. (2006). Biological degradation of synthetic polyesters—Enzymes as potential catalysts for polyester recycling. *Process Biochem.* 41, 2124–2128. doi: 10.1016/j.procbio.2006.05.018
- Müller, R. J., Schrader, H., Profe, J., Dresler, K., and Deckwer, W. D. (2005). Enzymatic degradation of poly (ethylene terephthalate): rapid hydrolyse using a hydrolase from *T. fusca*. *Macromol. Rapid Commun.* 26, 1400–1405. doi: 10.1002/marc.200500410
- Nair, S., and Kumar, P. (2007). Molecular characterization of a lipase-producing *Bacillus pumilus* strain (NMSN-1d) utilizing colloidal water-dispersible polyurethane. *World J. Microbiol. Biotechnol.* 23, 1441–1449. doi: 10.1007/s11274-007-9388-5
- Nakajima-Kambe, T., Onuma, F., Akutsu, Y., and Nakahara, T. (1997). Determination of the polyester polyurethane breakdown products and distribution of the polyurethane degrading enzyme of *Comamonas acidovorans*, strain TB-35. *J. Food Sci. Technol.* 83, 456–460. doi: 10.1016/s0922-338x(97)83000-0
- Nakajima-Kambe, T., Onuma, F., Kimpara, N., and Nakahara, T. (1995). Isolation and characterization of a bacterium which utilizes polyester polyurethane as a sole carbon and nitrogen source. *FEMS Microbiol. Lett.* 129, 39–42. doi: 10.1111/j.1574-6968.1995.tb07554.x
- Nakamiya, K., Hashimoto, S., Ito, H., Edmonds, J. S., Yasuhara, A., and Morita, M. (2005). Microbial treatment of bis (2-ethylhexyl) phthalate in polyvinyl chloride with isolated bacteria. *J. Biosci. Bioeng.* 99, 115–119. doi: 10.1263/jbb.99.115
- Nakamiya, K., Ooi, T., and Kinoshita, S. (1997). Non-heme hydroquinone peroxidase from *Azotobacter beijerinckii* HM121. *J. Ferment. Bioeng.* 84, 14–21. doi: 10.1016/s0922-338x(97)82780-8
- Nakkabi, A., Sadiki, M., Fahim, M., Ittobane, N., Saad, I. K., Barkai, H., et al. (2015a). Biodegradation of poly(ester urethane)s by *Bacillus subtilis*. *Int. J. Environ. Res.* 9, 157–162.
- Nakkabi, A., Sadiki, M., Ibnssouda, S., and Fahim, M. (2015b). Biological degradation of polyurethane by a newly isolated wood bacterium. *Int. J. Recent Adv. Multidiscip. Res.* 2, 222–225.
- Nikodinovic-Runic, J., Casey, E., Duane, G. F., Mitic, D., Hume, A. R., Kenny, S. T., et al. (2011). Process analysis of the conversion of styrene to biomass and medium chain length polyhydroxyalkanoate in a two-phase bioreactor. *Biotechnol. Bioeng.* 108, 2447–2455. doi: 10.1002/bit.23187
- Nomura, N., Shigeno-Akutsu, Y., Nakajima-Kambe, T., and Nakahara, T. (1998). Cloning and sequence analysis of a polyurethane esterase of *Comamonas acidovorans* TB-35. *J. Ferment. Bioeng.* 86, 339–345. doi: 10.1016/s0922-338x(99)89001-1

- Oceguera-Cervantes, A., Carrillo-García, A., López, N., Bolaños-Núñez, S., Cruz-Gómez, M. J., Wachter, C., et al. (2007). Characterization of the polyurethanolytic activity of two *Alicyclophilus* sp. strains able to degrade polyurethane and n-methylpyrrolidone. *Appl. Environ. Microbiol.* 73, 6214–6223. doi: 10.1128/aem.01230-07
- Oelschlägel, M., Zimmerling, J., and Tischler, D. (2018). A review: The styrene metabolizing cascade of side-chain oxygenation as biotechnological basis to gain various valuable compounds. *Front. Microbiol.* 9:490. doi: 10.3389/fmicb.2018.00490
- O'Leary, N. D., O'Connor, K. E., Goff, M., and Dobson, A. D. (2002). Biochemistry, genetics and physiology of microbial styrene degradation. *FEMS Microbiol. Rev.* 26, 403–417. doi: 10.1111/j.1574-6976.2002.tb00622.x
- O'Leary, N. D., O'Connor, K. E., Ward, P., Goff, M., and Dobson, A. D. (2005). Genetic characterization of accumulation of polyhydroxyalkanoate from styrene in *Pseudomonas putida* CA-3. *Appl. Environ. Microbiol.* 71, 4380–4387. doi: 10.1128/aem.71.8.4380-4387.2005
- O'Neill, A., and Cavaco-Paulo, A. (2004). Monitoring biotransformations in polyesters. *Biocatal. Biotrans.* 22, 353–356. doi: 10.1080/10242420400025760
- Oprea, S., Potolinca, V. O., Gradinariu, P., and Oprea, V. (2018). Biodegradation of pyridine-based polyether polyurethanes by the *Alternaria tenuissima* fungus. *J. Appl. Polym. Sci.* 135:46096. doi: 10.1002/app.46096
- Orr, I. G., Hadar, Y., and Sivan, A. (2004). Colonization, biofilm formation and biodegradation of polyethylene by a strain of *Rhodococcus ruber*. *Appl. Microbiol. Biotechnol.* 65, 97–104.
- Osman, M., Satti, S. M., Luqman, A., Hasan, F., Shah, Z., and Shah, Z. Z. (2017). Degradation of polyester polyurethane by *Aspergillus* sp. strain S45 isolated from soil. *J. Polym. Environ.* 26, 301–310. doi: 10.1007/s10924-017-0954-0
- Paço, A., Duarte, K., da Costa, J. P., Santos, P. S., Pereira, R., Pereira, M. E., et al. (2017). Biodegradation of polyethylene microplastics by the marine fungus *Zalerion maritimum*. *Sci. Total Environ.* 586, 10–15. doi: 10.1016/j.scitotenv.2017.02.017
- Palm, G. J., Reisky, L., Böttcher, D., Müller, H., Michels, E. A., Walczak, M. C., et al. (2019). Structure of the plastic-degrading *Ideonella sakaiensis* MHETase bound to a substrate. *Nat. Commun.* 10:1717. doi: 10.1038/s41467-019-09326-3
- Peng, B. Y., Su, Y., Chen, Z., Chen, J., Zhou, X., Benbow, M. E., et al. (2019). Biodegradation of Polystyrene by Dark (*Tenebrio obscurus*) and Yellow (*Tenebrio molitor*) Mealworms (Coleoptera: Tenebrionidae). *Environ. Sci. Technol.* 53, 5256–5265. doi: 10.1021/acs.est.8b06963
- Peng, R. T., Xia, M. L., Ru, J. K., Huo, Y. X., and Yang, Y. (2018). Microbial degradation of polyurethane plastics. *Chin. J. Biotechnol.* 34, 1398–1409.
- Peng, Y. H., Shih, Y. H., Lai, Y. C., Liu, Y. Z., Liu, Y. T., and Lin, N. C. (2014). Degradation of polyurethane by bacterium isolated from soil and assessment of polyurethanolytic activity of a *Pseudomonas putida* strain. *Environ. Sci. Pollut. Res. Int.* 21, 9529–9537. doi: 10.1007/s11356-014-2647-8
- Pérez-Lara, L. F., Vargas-Suárez, M., López-Castillo, N. N., Cruz-Gómez, M. J., and Loza-Tavera, H. (2016). Preliminary study on the biodegradation of adipate/phthalate polyester polyurethanes of commercial type by *Alicyclophilus* sp. BQ8. *J. Appl. Polym. Sci.* 133:42992.
- Plastics Europe (2018). *Data From: Plastics - The Facts 2018: An Analysis of European Plastics Production, Demand and Waste Data (EB/OL)*. Available online at: <http://www.plasticseurope.org> (accessed October 2, 2019).
- Radecka, I., Irerere, V., Jiang, G., Hill, D., Williams, C., Adamus, G., et al. (2016). Oxidized polyethylene wax as a potential carbon source for PHA production. *Materials* 9:367. doi: 10.3390/ma9050367
- Rahimi, A., and García, J. M. (2017). Chemical recycling of waste plastics for new materials production. *Nat. Rev. Chem.* 1:0046.
- Restrepo-Flórez, J. M., Bassi, A., and Thompson, M. R. (2014). Microbial degradation and deterioration of polyethylene—A review. *Int. Biodeter. Biodegr.* 88, 83–90. doi: 10.1016/j.ibiod.2013.12.014
- Rojo, F. (2009). Degradation of alkanes by bacteria. *Environ. Microbiol.* 11, 2477–2490. doi: 10.1111/j.1462-2920.2009.01948.x
- Ronkvist, Å. M., Xie, W., Lu, W., and Gross, R. A. (2009). Cutinase-catalyzed hydrolysis of poly(ethylene terephthalate). *Macromolecules* 42, 5128–5138. doi: 10.1021/ma9005318
- Rowe, L., and Howard, G. T. (2002). Growth of *Bacillus subtilis* on polyurethane and the purification and characterization of a polyurethanase-lipase enzyme. *Int. Biodeter. Biodegr.* 50, 33–40. doi: 10.1016/s0964-8305(02)00047-1
- Ruiz, C., and Howard, G. T. (1999). Nucleotide sequencing of a polyurethanase gene (pulA) from *Pseudomonas fluorescens*. *Int. Biodeter. Biodegr.* 44, 127–131. doi: 10.1016/s0964-8305(99)00074-8
- Ruiz, C., Main, T., Hilliard, N. P., and Howard, G. T. (1999). Purification and characterization of two polyurethanase enzymes from *Pseudomonas chlororaphis*. *Int. Biodeter. Biodegr.* 43, 43–47. doi: 10.1016/s0964-8305(98)00067-5
- Russell, J. R., Huang, J., Anand, P., Kucera, K., Sandoval, A. G., Dantzer, K. W., et al. (2011). Biodegradation of polyester polyurethane by endophytic fungi. *Appl. Environ. Microbiol.* 77, 6076–6084. doi: 10.1128/AEM.00521-11
- Sabev, H. A., Handley, P. S., and Robson, G. D. (2006). Fungal colonization of soil-buried plasticized polyvinyl chloride (PVC) and the impact of incorporated biocides. *Microbiology* 152, 1731–1739. doi: 10.1099/mic.0.28569-0
- Sabirova, J. S., Ferrer, M., Lünsdorf, H., Wray, V., Kalscheuer, R., Steinbüchel, A., et al. (2006). Mutation in a “tesB-like” hydroxyacyl-coenzyme A-specific thioesterase gene causes hyperproduction of extracellular polyhydroxyalkanoates by *Alcanivorax borkumensis* SK2. *J. Bacteriol.* 188, 8452–8459. doi: 10.1128/jb.01321-06
- Salvador, M., Abdulmutalib, U., Gonzalez, J., Kim, J., Smith, A. A., Faulon, J. L., et al. (2019). Microbial genes for a circular and sustainable bio-PET economy. *Genes* 10:373. doi: 10.3390/genes10050373
- Santo, M., Weitsman, R., and Sivan, A. (2013). The role of the copper-binding enzyme-laccase—in the biodegradation of polyethylene by the actinomycete *Rhodococcus ruber*. *Int. Biodeter. Biodegr.* 84, 204–210. doi: 10.1016/j.ibiod.2012.03.001
- Sarmah, P., and Rout, J. (2018). Efficient biodegradation of low-density polyethylene by cyanobacteria isolated from submerged polyethylene surface in domestic sewage water. *Environ. Sci. Pollut. Res. Int.* 25, 33508–33520. doi: 10.1007/s11356-018-3079-7
- Sasoh, M., Masai, E., Ishibashi, S., Hara, H., Kamimura, N., Miyauchi, K., et al. (2006). Characterization of the terephthalate degradation genes of *Comamonas* sp. strain E6. *Appl. Environ. Microbiol.* 72, 1825–1832. doi: 10.1128/aem.72.3.1825-1832.2006
- Schmidt, J., Wei, R., Oeser, T., Dedavid, E., Silva, L. A., Breite, D., et al. (2017). Degradation of polyester polyurethane by bacterial polyester hydrolases. *Polymers* 9:65. doi: 10.3390/polym9020065
- Shah, A. A., Hasan, F., Akhter, J. I., Hameed, A., and Ahmed, S. (2008). Degradation of polyurethane by novel bacterial consortium isolated from soil. *Ann. Microbiol.* 58, 381–386. doi: 10.1007/bf03175532
- Shah, Z., Gulzar, M., Hasan, F., and Shah, A. A. (2016). Degradation of polyester polyurethane by an indigenously developed consortium of *Pseudomonas* and *Bacillus* species isolated from soil. *Polym. Degrad. Stab.* 134, 349–356. doi: 10.1016/j.polymdegradstab.2016.11.003
- Shah, Z., Krumholz, L., Aktas, D. F., Hasan, F., Khattak, M., and Shah, A. A. (2013a). Degradation of polyester polyurethane by a newly isolated soil bacterium, *Bacillus subtilis* strain MZA-75. *Biodegradation* 24, 865–877. doi: 10.1007/s10532-013-9634-5
- Shah, Z., Hasan, F., Krumholz, L., Aktas, D. F., and Shah, A. A. (2013b). Degradation of polyester polyurethane by newly isolated *Pseudomonas aeruginosa*, strain MZA-85 and analysis of degradation products by GC-MS. *Int. Biodeter. Biodegr.* 77, 114–122. doi: 10.1016/j.ibiod.2012.11.009
- Shirke, A. N., Basore, D., Butterfoss, G. L., Bonneau, R., Bystroff, C., and Gross, R. A. (2016). Toward rational thermostabilization of *Aspergillus oryzae* cutinase: insights into catalytic and structural stability. *Proteins* 84, 60–72. doi: 10.1002/prot.24955
- Shirke, A. N., White, C., Englaender, J. A., Zwarycz, A., Butterfoss, G. L., Linhardt, R. J., et al. (2018). Stabilizing leaf and branch compost cutinase (LCC) with glycosylation: mechanism and effect on PET hydrolysis. *Biochemistry* 57, 1190–1200. doi: 10.1021/acs.biochem.7b01189
- Sielicki, M., Focht, D. D., and Martin, J. P. (1978). Microbial degradation of (14C) polystyrene and 1,3-diphenylbutane. *Can. J. Microbiol.* 24, 798–803. doi: 10.1139/m78-134

- Silva, C. M., Carneiro, F., O'Neill, A., Fonseca, L. P., Cabral, J. S., Guebitz, G., et al. (2005). Cutinase—a new tool for biomodification of synthetic fibers. *J. Polym. Sci. Pol. Chem.* 43, 2448–2450. doi: 10.1002/pola.20684
- Sivan, A., Szanto, M., and Pavlov, V. (2006). Biofilm development of the polyethylene-degrading bacterium *Rhodococcus ruber*. *Appl. Microbiol. Biotechnol.* 72, 346–352. doi: 10.1007/s00253-005-0259-4
- Skariyachan, S., Patil, A. A., Shankar, A., Manjunath, M., Bachappanavar, N., and Kiran, S. (2018). Enhanced polymer degradation of polyethylene and polypropylene by novel thermophilic consortia of *Brevibacillus* sps. and *Aneurinibacillus* sp. screened from waste management landfills and sewage treatment plants. *Polym. Degrad. Stab.* 149, 52–68. doi: 10.1016/j.polymdegradstab.2018.01.018
- Son, H. F., Cho, I. J., Joo, S., Seo, H., Sagong, H. Y., Choi, S. Y., et al. (2019). Rational protein engineering of thermo-stable PETase from *Ideonella sakaiensis* for highly efficient PET degradation. *ACS Catal.* 9, 3519–3526. doi: 10.1021/acscatal.9b00568
- Stepien, A. E., Zebrowski, J., Piszczczyk, Ł., Boyko, V. V., Riabov, S. V., Dmitrieva, T., et al. (2017). Assessment of the impact of bacteria *Pseudomonas denitrificans*, *Pseudomonas fluorescens*, *Bacillus subtilis* and yeast *Yarrowia lipolytica* on commercial poly (ether urethanes). *Polym. Test.* 63, 484–493. doi: 10.1016/j.polymertesting.2017.08.038
- Stern, R. V., and Howard, G. T. (2000). The polyester polyurethanase gene (pueA) from *Pseudomonas chlororaphis* encodes a lipase. *FEMS Microbiol. Lett.* 185, 163–168. doi: 10.1111/j.1574-6968.2000.tb09056.x
- Sudhakar, M., Doble, M., Murthy, P. S., and Venkatesan, R. (2008). Marine microbe-mediated biodegradation of low- and high-density polyethylenes. *Int. Biodeter. Biodegr.* 61, 203–213. doi: 10.1016/j.ibiod.2007.07.011
- Sulaiman, S., Yamato, S., Kanaya, E., Kim, J. J., Koga, Y., Takano, K., et al. (2012). Isolation of a novel cutinase homolog with polyethylene terephthalate-degrading activity from leaf-branch compost by using a metagenomic approach. *Appl. Environ. Microbiol.* 78, 1556–1562. doi: 10.1128/AEM.06725-11
- Taniguchi, I., Yoshida, S., Hiraga, K., Miyamoto, K., Kimura, Y., and Oda, K. (2019). Biodegradation of PET: current status and application aspects. *ACS Catal.* 9, 4089–4105. doi: 10.1021/acscatal.8b05171
- Then, J., Wei, R., Oeser, T., Barth, M., Belisário-Ferrari, M. R., Schmidt, J., et al. (2015). Ca^{2+} and Mg^{2+} binding site engineering increases the degradation of polyethylene terephthalate films by polyester hydrolases from *Thermobifida fusca*. *Biotechnol. J.* 10, 592–598. doi: 10.1002/biot.201400620
- Then, J., Wei, R., Oeser, T., Gerdt, A., Schmidt, J., Barth, M., et al. (2016). A disulfide bridge in the calcium binding site of a polyester hydrolase increases its thermal stability and activity against polyethylene terephthalate. *FEBS Open Bio* 6, 425–432. doi: 10.1002/2211-5463.12053
- Tribedi, P., and Sil, A. K. (2013). Low-density polyethylene degradation by *Pseudomonas* sp. AKS2 biofilm. *Environ. Sci. Pollut. Res. Int.* 20, 4146–4153. doi: 10.1007/s11356-012-1378-y
- Trifunović, D., Schuchmann, K., and Müller, V. (2016). Ethylene glycol metabolism in the acetogen *Acetobacterium woodii*. *J. Bacteriol.* 198, 1058–1065. doi: 10.1128/JB.00942-15
- Vega, R. E., Main, T., and Howard, G. T. (1999). Cloning and expression in *Escherichia coli* of a polyurethane-degrading enzyme from *Pseudomonas fluorescens*. *Int. Biodeter. Biodegr.* 43, 49–55. doi: 10.1016/s0964-8305(98)00068-7
- Vertommen, M. A., Nierstrasz, V. A., Van Der Veer, M., and Warmoeskerken, M. M. (2005). Enzymatic surface modification of poly(ethylene terephthalate). *J. Biotechnol.* 120, 376–386. doi: 10.1016/j.jbiotec.2005.06.015
- Wang, W., Cai, B., and Shao, Z. (2014). Oil degradation and biosurfactant production by the deep sea bacterium *Dietzia maris* As-13-3. *Front. Microbiol.* 5:711. doi: 10.3389/fmicb.2014.00711
- Wang, Y. Z., Zhou, Y., and Zylstra, G. J. (1995). Molecular analysis of isophthalate and terephthalate degradation by *Comamonas testosteroni* YZW-D. *Environ. Health Perspect.* 103, 9–12. doi: 10.1289/ehp.95103s49
- Ward, P. G., de Roo, G., and O'Connor, K. E. (2005). Accumulation of polyhydroxyalkanoate from styrene and phenylacetic acid by *Pseudomonas putida* CA-3. *Appl. Environ. Microbiol.* 71, 2046–2052. doi: 10.1128/aem.71.4.2046-2052.2005
- Ward, P. G., Goff, M., Donner, M., Kaminsky, W., and O'Connor, K. E. (2006). A twostep chemo-biotechnological conversion of polystyrene to a biodegradable thermoplastic. *Environ. Sci. Technol.* 40, 2433–2437. doi: 10.1021/es0517668
- Watanabe, M., Kawai, F., Shibata, M., Yokoyama, S., and Sudate, Y. (2003). Computational method for analysis of polyethylene biodegradation. *J. Comput. Appl. Math.* 161, 133–144. doi: 10.1016/s0377-0427(03)00551-x
- Watanabe, M., Kawai, F., Shibata, M., Yokoyama, S., Sudate, Y., and Hayashi, S. (2004). Analytical and computational techniques for exogenous depolymerization of xenobiotic polymers. *Math. Biosci.* 192, 19–37. doi: 10.1016/j.mbs.2004.06.006
- Webb, J. S., Nixon, M., Eastwood, I. M., Greenhalgh, M., Robson, G. D., and Handley, P. S. (2000). Fungal colonization and biodeterioration of plasticized polyvinyl chloride. *Appl. Environ. Microbiol.* 66, 3194–3200. doi: 10.1128/aem.66.8.3194-3200.2000
- Webb, J. S., Van der Mei, H. C., Nixon, M., Eastwood, I. M., Greenhalgh, M., Read, S. J., et al. (1999). Plasticizers increase adhesion of the detritogenic fungus *Aureobasidium pullulans* to polyvinyl chloride. *Appl. Environ. Microbiol.* 65, 3575–3581. doi: 10.1128/aem.65.8.3575-3581.1999
- Wei, R., Breite, D., Song, C., Gräning, D., Ploss, T., Hille, P., et al. (2019a). Biocatalytic degradation efficiency of postconsumer polyethylene terephthalate packaging determined by their polymer microstructures. *Adv. Sci.* 6:1900491. doi: 10.1002/advs.201900491
- Wei, R., Song, C., Gräning, D., Schneider, T., Bielytskyi, P., Böttcher, D., et al. (2019b). Conformational fitting of a flexible oligomeric substrate does not explain the enzymatic PET degradation. *Nat. Commun.* 10:5582.
- Wei, R., and Zimmermann, W. (2017a). Biocatalysis as a green route for recycling the recalcitrant plastic polyethylene terephthalate. *Microb. Biotechnol.* 10, 1302–1307. doi: 10.1111/1751-7915.12714
- Wei, R., and Zimmermann, W. (2017b). Microbial enzymes for the recycling of recalcitrant petroleum-based plastics: how far are we? *Microb. Biotechnol.* 10, 1308–1322. doi: 10.1111/1751-7915.12710
- Wierckx, N., Prieto, M. A., Pomposiello, P., de Lorenzo, V., O'Connor, K., and Blank, L. M. (2015). Plastic waste as a novel substrate for industrial biotechnology. *Microb. Biotechnol.* 8, 900–903. doi: 10.1111/1751-7915.12312
- Xia, M., Wang, J., Huo, Y. X., and Yang, Y. (2019). *Mixta tenebrionis* sp. nov., isolated from the gut of the plastic-eating mealworm *Tenebrio molitor* L. *Int. J. Syst. Evol. Microbiol.* 70, 790–796. doi: 10.1099/ijsem.0.003826
- Xu, J., Cui, Z., Nie, K., Cao, H., Jiang, M., Xu, H., et al. (2019). A quantum mechanism study of the cc bond cleavage to predict the bio-catalytic polyethylene degradation. *Front. Microbiol.* 10:489.
- Yang, J., Yang, Y., Wu, W. M., Zhao, J., and Jiang, L. (2014). Evidence of polyethylene biodegradation by bacterial strains from the guts of plastic-eating waxworms. *Environ. Sci. Technol.* 48, 13776–13784. doi: 10.1021/es504038a
- Yang, S. S., Wu, W. M., Brandon, A. M., Fan, H. Q., Receveur, J. P., Li, Y., et al. (2018). Ubiquity of polystyrene digestion and biodegradation within yellow mealworms, larvae of *Tenebrio molitor* Linnaeus (Coleoptera: Tenebrionidae). *Chemosphere* 212, 262–271. doi: 10.1016/j.chemosphere.2018.08.078
- Yang, Y., Chen, J., Wu, W. M., Zhao, J., and Yang, J. (2015a). Complete genome sequence of *Bacillus* sp. YP1, a polyethylene-degrading bacterium from waxworm's gut. *J. Biotechnol.* 200, 77–78. doi: 10.1016/j.jbiotec.2015.02.034
- Yang, Y., Yang, J., Wu, W. M., Zhao, J., Song, Y., Gao, L., et al. (2015b). Biodegradation and mineralization of polystyrene by plastic-eating mealworms. 1. chemical and physical characterization and isotopic tests. *Environ. Sci. Technol.* 49, 12080–12086. doi: 10.1021/acs.est.5b02661
- Yang, Y., Yang, J., Wu, W. M., Zhao, J., Song, Y., Gao, L., et al. (2015c). Biodegradation and mineralization of polystyrene by plastic-eating mealworms. 2. role of gut microorganisms. *Environ. Sci. Technol.* 49, 12087–12093. doi: 10.1021/acs.est.5b02663
- Yang, Y., Wang, J., and Xia, M. (2020). Biodegradation and mineralization of polystyrene by plastic-eating superworms *Zophobas atratus*. *Sci. Total Environ.* 708:135233. doi: 10.1016/j.scitotenv.2019.135233
- Yang, Y., Yang, J., and Jiang, L. (2016). Comment on “A bacterium that degrades and assimilates poly (ethylene terephthalate)”. *Science* 353:759. doi: 10.1126/science.aaf8305
- Yoon, M. G., Jeon, H. J., and Kim, M. N. (2012). Biodegradation of polyethylene by a soil bacterium and *AlkB* cloned recombinant cell. *J. Bioremediat. Biodegrad.* 3:145.

- Yoon, M.-Y., Kellis, J., and Poulou, A. J. (2002). Enzymatic modification of polyester. *AATCC Rev.* 2, 33–36.
- Yoshida, S., Hiraga, K., Takehana, T., Taniguchi, I., Yamaji, H., Maeda, Y., et al. (2016). A bacterium that degrades and assimilates poly(ethylene terephthalate). *Science* 351, 1196–1199. doi: 10.1126/science.aad6359
- Yuan, G., Chen, D., Yin, L., Wang, Z., Zhao, L., and Wang, J. Y. (2014). High efficiency chlorine removal from polyvinyl chloride (PVC) pyrolysis with a gas-liquid fluidized bed reactor. *Waste Manag.* 34, 1045–1050. doi: 10.1016/j.wasman.2013.08.021
- Zhang, J., Wang, X., Gong, J., and Gu, Z. (2004). A study on the biodegradability of polyethylene terephthalate fiber and diethylene glycol terephthalate. *J. Appl. Polym. Sci.* 93, 1089–1096. doi: 10.1002/app.20556
- Zhao, J., Guo, Z., Ma, X., Liang, G., and Wang, J. (2004). Novel surface modification of high-density polyethylene films by using enzymatic catalysis. *J. Appl. Polym. Sci.* 91, 3673–3678. doi: 10.1002/app.13619
- Conflict of Interest:** The authors declare that the research was conducted in the absence of any commercial or financial relationships that could be construed as a potential conflict of interest.
- Copyright © 2020 Ru, Huo and Yang. This is an open-access article distributed under the terms of the Creative Commons Attribution License (CC BY). The use, distribution or reproduction in other forums is permitted, provided the original author(s) and the copyright owner(s) are credited and that the original publication in this journal is cited, in accordance with accepted academic practice. No use, distribution or reproduction is permitted which does not comply with these terms.



High Throughput Screening for New Fungal Polyester Hydrolyzing Enzymes

Simone Weinberger^{1,2†}, Reinhard Beyer³, Christoph Schüller³, Joseph Strauss³, Alessandro Pellis^{1†}, Doris Ribitsch^{1,2*} and Georg M. Guebitz^{1,2}

¹ Department of Agrobiotechnology, Institute of Environmental Biotechnology, University of Natural Resources and Life Sciences, Vienna, Austria, ² Austrian Center of Industrial Biotechnology (ACIB), Tulln an der Donau, Austria, ³ Department of Applied Genetics and Cell Biology, University of Natural Resources and Life Sciences, Vienna, Austria

OPEN ACCESS

Edited by:

Ren Wei,
University of Greifswald, Germany

Reviewed by:

Fusako Kawai,
Okayama University Japan, Japan
Natalia N. Pozdnyakova,
Institute of Biochemistry
and Physiology of Plants
and Microorganisms (RAS), Russia

*Correspondence:

Doris Ribitsch
doris.ribitsch@boku.ac.at;
doris.ribitsch@acib.at

†ORCID:

Simone Weinberger
orcid.org/0000-0002-2347-6162
Alessandro Pellis
orcid.org/0000-0003-3711-3087

Specialty section:

This article was submitted to
Microbiotechnology,
a section of the journal
Frontiers in Microbiology

Received: 20 December 2019

Accepted: 16 March 2020

Published: 24 April 2020

Citation:

Weinberger S, Beyer R,
Schüller C, Strauss J, Pellis A,
Ribitsch D and Guebitz GM (2020)
High Throughput Screening for New
Fungal Polyester Hydrolyzing
Enzymes. *Front. Microbiol.* 11:554.
doi: 10.3389/fmicb.2020.00554

There is a strong need for novel and more efficient polyester hydrolyzing enzymes in order to enable the development of more environmentally friendly plastics recycling processes allowing the closure of the carbon cycle. In this work, a high throughput system on microplate scale was used to screen a high number of fungi for their ability to produce polyester-hydrolyzing enzymes. For induction of responsible enzymes, the fungi were cultivated in presence of aliphatic and aromatic polyesters [poly(1,4-butylene adipate co terephthalate) (PBAT), poly(lactic acid) (PLA) and poly(1,4-butylene succinate) (PBS)], and the esterase activity in the culture supernatants was compared to the culture supernatants of fungi grown without polymers. The results indicate that the esterase activity of the culture supernatants was induced in about 10% of the tested fungi when grown with polyesters in the medium, as indicated by increased activity (to >50 mU/mL) toward the small model substrate *para*-nitrophenylbutyrate (pNPB). Incubation of these 50 active culture supernatants with different polyesters (PBAT, PLA, PBS) led to hydrolysis of at least one of the polymers according to liquid chromatography-based quantification of the hydrolysis products terephthalic acid, lactic acid and succinic acid, respectively. Interestingly, the specificities for the investigated polyesters varied among the supernatants of the different fungi.

Keywords: screening, fungi induction, polyester hydrolyzing enzymes, plastic degradation, environmentally friendly

INTRODUCTION

Polymers and especially polyesters are components of materials with industrially interesting properties such as chemical resistance, low production costs and simple processability. Therefore, the use of plastics in food packaging, clothing, electronics, construction, and various other industrial fields resulted in a worldwide plastic production of 348 million tons in 2017 (Association of Plastics Manufacturers in Europe and European Association of Plastics Recycling and Recovery Organisations [EPRO], 2018). However, the release of petrol-based synthetic polymers into the

environment poses a major threat to natural environment since they are barely biodegradable and accumulate in the ecosystems. Increased awareness of this problem led to intensive research for environmentally friendly alternatives in the last decades. One approach are biodegradable polymers, such as poly(lactic acid) (PLA) (Karamanlioglu et al., 2017), poly(butylene succinate) (PBS) (Pellis et al., 2016b) and poly(butylene adipate-co-terephthalate) (PBAT) (Perz et al., 2016c; Sisti et al., 2016).

Poly(butylene adipate-co-terephthalate) is a co-polyester consisting of the aliphatic monomers adipic acid and 1,4-butanediol and the aromatic monomer terephthalic acid (Vroman and Tighzert, 2009). Due to its special barrier properties it is widely used for food packaging or organic waste bags. Its biodegradability by microorganisms and enzymes is well known, therefore it is widely used as raw material for compostable plastics (Perz et al., 2016b). PBAT is manufactured in industrial scale by several companies and can be used in combination with other polymers such as PLA to manufacture blended materials. To obtain PLA, mainly starches and sugars are fermented to lactic acid, which is further processed to the polymer (Weng et al., 2013). Due to its high transparency and elastic modulus, PLA is used for disposable products and packing materials (Auras et al., 2004). The biodegradation of PLA under soil conditions is a slow process taking at least several months and depends on various factors like crystallinity and molecular weight (Shogren et al., 2003; Rudnik and Briassoulis, 2011a,b). Like PLA, PBS is another promising aliphatic biopolymer. The building blocks can be obtained *via* fermentative pathways from glucose or sucrose feedstock.

Organisms degrade polyesters by extracellular hydrolases which reduce the molar mass of the polymer to convert it to water-soluble intermediates and therefore to an accessible carbon source. Bacteria are well known producers of polyester degrading enzymes, especially of lipases and cutinases (Ronkvist et al., 2009; Ribitsch et al., 2011; Perz et al., 2016a,c). Furthermore, one of the most active enzyme on polyesters is from fungal origin, namely the cutinase from *Humicola insolens* (Weinberger et al., 2017a,b). Apart from the essential function in organisms, esterases and lipases are among the most widely used biocatalysts in the chemical industry (Wohlgemuth, 2010) and can potentially enable the recovery of the polymer building blocks. These building blocks can be used as carbon source for the fermentative production of products such as ethanol or lactic acid (Pellis et al., 2016b; Vecchiato et al., 2018). However, enzymatic hydrolysis of these polyesters is rather slow and hence more efficient enzymes would be required in order to implement an enzymatic recycling industry. In order to exploit nature for such polyester active enzymes, there is a strong demand for more efficient screening procedures which is addressed in this paper.

MATERIALS AND METHODS

Chemicals and Reagents

Poly(1,4-butylene succinate) (PBS) powders were supplied by Goodfellow (London, United Kingdom), PBAT powders were provided by BASF (Ludwigshafen am Rhein, Deutschland). PLA

powders and all other chemicals and solvents were purchased from Sigma-Aldrich at reagent grade, and used without further purification if not otherwise specified. Molecular weights [kDa] are listed in ESI **Supplementary Table S2**.

Cultivation of Fungi

Fungi were cultivated in a modified Moser (1963) medium containing (per liter) 10 g casein peptone, 1 g yeast extract, 2.5 g K_2HPO_4 , 0.25 g inositol, 375 mg $CaCl_2$, 50 mg $FeCl_3$, 750 mg $MgSO_4$, 50 mg $MnSO_4$, 5 mg $ZnSO_4$, 50 g glucose, 6 g soy peptone, 0.2 g KCl, 1.44 g Na_2HPO_4 , 0.24 g KH_2PO_4 and 10 g NaCl. When indicated, YES medium was also used which contains (per liter) 20 g yeast extract, 50 g sucrose, 500 mg $MgSO_4 \cdot 7H_2O$, 10 mg $ZnSO_4 \cdot 7H_2O$ and 5 mg $CuSO_4 \cdot 5H_2O$.

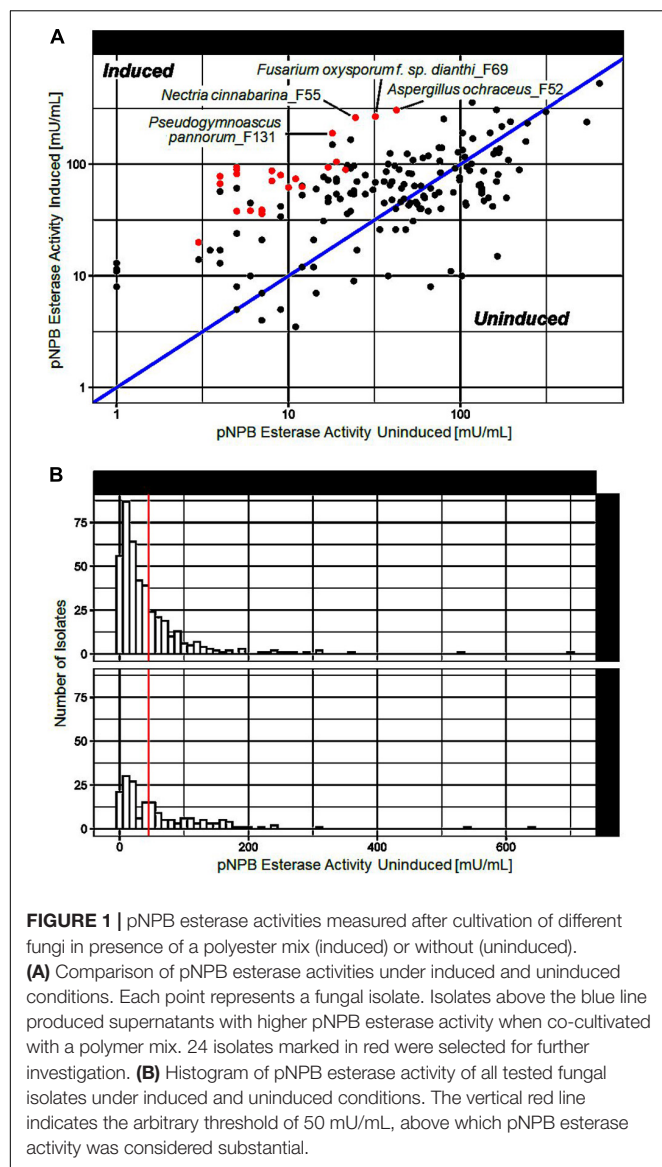
Fungal cultures were prepared from $-80^\circ C$ stocks stored as a mixture of spores and mycelium in glycerol. All isolates were isolated from environmental samples collected mainly from Central Europe and were of diverse origins ranging from soil, air and water samples to plant material or contaminated foodstuffs. Agar plates containing 33 g/L malt extract were inoculated using a sterile toothpick. Plates were then sealed and incubated in the dark at $24^\circ C$ for up to 14 days or until sufficient growth and sporulation occurred. Spores were harvested by adding 10 mL sterile PBSA (Phosphate NaCl buffer) supplemented with 0.01% Tween 80 to each plate by gently scraping. The spore solution was then aspirated and stored at $4^\circ C$ until further use.

A panel of 673 fungal isolates was screened for esterase activity. All pipetting steps were performed with a HAMILTON® liquid handling robot (Microlab STAR) to ensure reproducibility of the technical protocol. A standardized 24-well plate format fermentation enabled us to screen fungal isolates under induced (cultivation with polymer mix) and uninduced (without polymer mix) conditions. Each fermentation was set up with 1.6 mL of the modified Moser medium supplemented with 200 μL of a mixture containing PBS, PBAT, and PLA in equal amounts (10 g/L of each polymer) suspended in 0.1 M KH_2PO_4 buffer (pH 7), and 200 μL spore solution. For uninduced samples 200 μL 0.1 M KH_2PO_4 buffer was added instead of polymer mix. Samples were incubated for 24 days at $24^\circ C$ with gentle shaking. A control was added to each batch by adding 200 μL sterile PBSA instead of the spore solution. Each fermentation was run in 12 replicates and supernatants were subsequently pooled.

Upon harvest, the mycelium was manually removed using a sterile toothpick, the supernatant was then aspirated, transferred into a fresh vial and centrifuged at 3200 g for 20 min to remove residual mycelium. Subsequently, the supernatant was filtrated using a 0.2 μm polystyrene filter to obtain sterile filtrate and stored at $-20^\circ C$ until further use.

Esterase Activity

For activity measurements of induced and uninduced supernatants, *para*-nitrophenyl butyrate (pNPB) was used as substrate. The final assay mixture consisted of 200 μL of the substrate solution (86 μL of pNPB and 1000 μL of 2-methyl-2-butanol, added to 25 mL 0.1 M KH_2PO_4 buffer pH 7) and 50 μL of sample. The increase of the absorbance at 405 nm due to the hydrolytic release of *p*-nitrophenol at 405 nm [$\epsilon_{405\text{ nm}} = 9.72$



(mM cm)⁻¹] was measured over 10 min in cycles of 18 s at 30°C with a Synergy H1 microplate reader (BioTek Instruments, VT, United States) using 96-well micro-titer plates (Greiner 96 Well Flat Bottom Transparent Polystyrene). A negative control was included on each plate using 50 μ L 0.1 M KH₂PO₄ buffer instead of supernatant. The activity was calculated in units (U), where 1 unit is defined as the amount of extract required to hydrolyze 1 μ mol of substrate per minute under the given assay conditions.

Polymer Hydrolysis

Polymer powders (5.0 mg) were incubated with 1 mL of the culture supernatants showing a pNPB hydrolytic activity >50 mU/mL. Incubations were conducted for 21 days in an orbital shaker set at 100 rpm and 65°C since good enzyme stability and activity over time for the hydrolysis of various polyesters had been previously reported for these conditions (Pellis et al., 2016a; Gamerith et al., 2017b;

Weinberger et al., 2017b). Blank reactions were carried out in YES medium. All reactions were performed in duplicates.

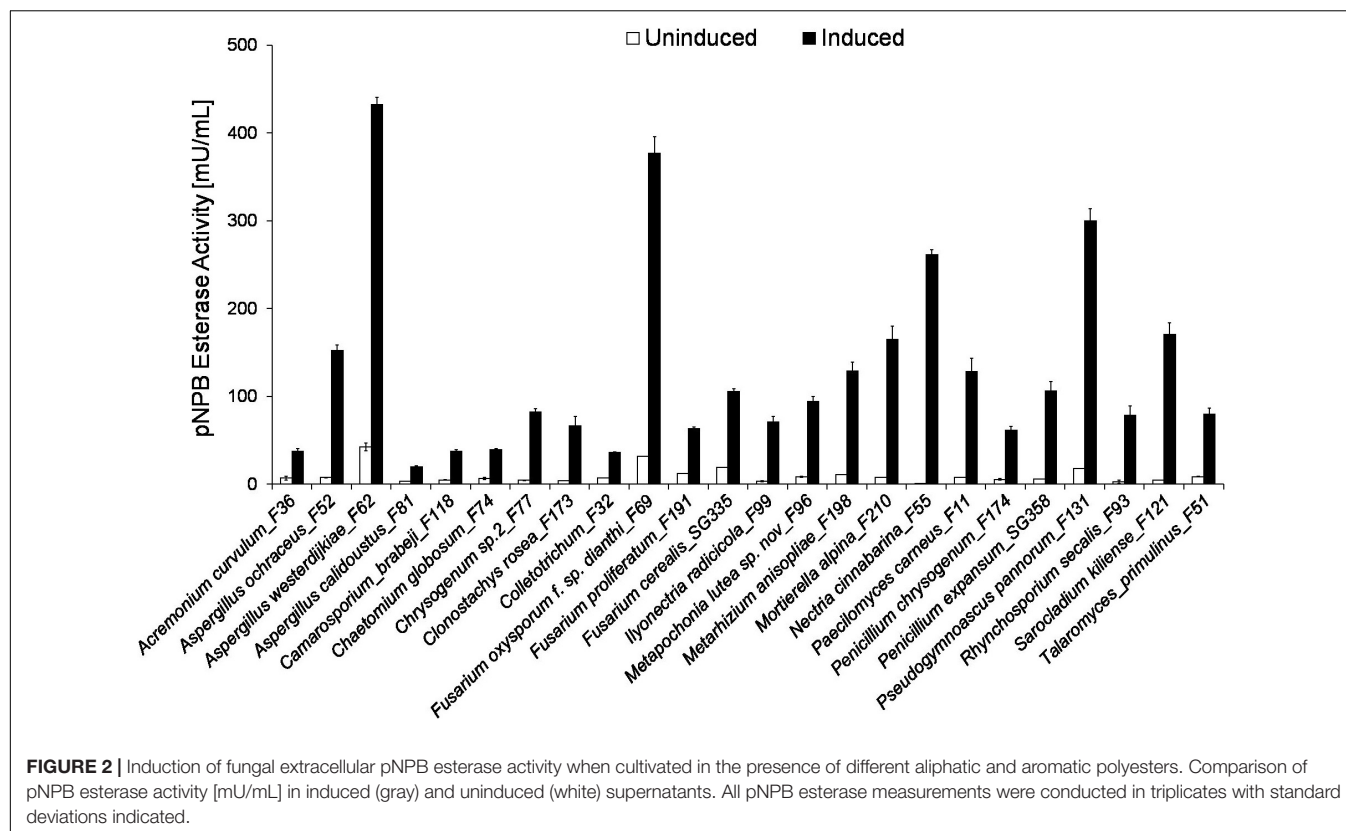
High-Performance Liquid Chromatography (HPLC)

After incubation, supernatants incubated with PBAT were diluted with ice-cold methanol (1:1 v/v) to precipitate the enzymes. The samples were centrifuged at 12,700 rpm (Centrifuge 5427 R, Eppendorf, Germany) for 15 min at 4°C, followed by a filtration through 0.45 μ m nylon syringe filters into high performance liquid chromatography (HPLC) vials. For analysis of the samples, a HPLC-DAD system consisting of a 1260 Infinity (Agilent Technologies, Palo Alto, CA, United States) coupled with a reversed phase column C18 (Poroshell 120 EC-C18 2.7 μ m 3.0 \times 150 mm) was used. The PBAT hydrolysis products were separated using a non-linear gradient as previously described (Quartinello et al., 2017) and detected with a photodiode array detector (Agilent Technologies, 1290 Infinity II, Vienna, Austria) at the wavelength of 245 nm. For the quantification of the released products bis(4-hydroxybutyl) terephthalate (BTaB), mono(4-hydroxybutyl) terephthalate (BTa) and terephthalic acid (Ta) (BASF, Ludwigshafen am Rhein, Deutschland), was used. For the quantification of the degradation products, external calibration curves in the range 0.005–1 mM (see ESI, **Supplementary Figure S1**) were used. Blanks were subtracted from the results.

Hydrolysis samples with PLA and PBS were precipitated following the Carrez method (Perz et al., 2016b) and filtered through 0.20 μ m Nylon filters (GVS, Indianapolis, United States). The analytes were separated by HPLC using refractive index detection (1100 series, Agilent Technologies, Palo Alto, CA, United States) equipped with an ICsep—ION—300 column (Transgenomic Organic, San Jose, CA, United States) of 300 mm by 7.8 mm and 7 μ m particle diameter. Column temperature was maintained at 45°C. Samples (40 μ L) were injected and separated by isocratic elution for 40 min at 0.325 mL min⁻¹ in 0.005 M H₂SO₄ as the mobile phase. Lactic acid and succinic acid were used for the calibration. For the quantification of the degradation products, external calibration curves in the range 0.01–20 mM (see ESI, **Supplementary Figure S2**) were used. Blanks were subtracted from the results.

RESULTS AND DISCUSSION

Screening of a culture collection of environmental fungal isolates collected mainly in Central Europe was performed in a partially automated setup to increase reproducibility and speed of the technical protocols applied (see ESI, **Supplementary Figure S3**). Inoculation of fungi was performed on a Hamilton liquid handling robot (Hamilton Microlab STAR) while screening was conducted in a 2-stage process. First, fungi were challenged with a polymer mix containing PBS, PLA, and PBAT and supernatants were tested for esterase activity. Fungal isolates which showed an activity above a soft threshold of 50 mU/mL were selected for a further second round of screening. During this second screening, fungal isolates were additionally cultivated without polymer mix to identify polymer-inducible esterase activity.



INDUCIBILITY

To investigate the induction of secreted polyester hydrolyzing enzymes, 673 different fungi were cultivated in the presence of a polymer mix of different aliphatic and aromatic polyesters, namely, PBS, PLA, and PBAT. After 3 weeks incubation esterase activity of the supernatants from polymer induced and control incubations were measured as described earlier. Out of the 673 fungi investigated, 66 strains showed elevated activity when cultivated in the presence of polyesters (**Figure 1**). Several isolates generated supernatants with substantial esterase activity (>50 mU/mL) under induced conditions and are highlighted in **Figure 1A**. **Figure 1B** shows the distribution of esterase activities measured during our screen.

The 24 strains exhibiting strongest induction are shown in **Figure 2**. These included three representatives of *Aspergillus* sp. and *Fusarium* sp., respectively, as well as *Penicillium* species, which are mold fungi and typical soil organisms. Representatives of all three genera were previously reported to produce extracellular esterases (Gautam et al., 2007; Mathur and Prasad, 2012; Hu et al., 2016; Álvarez-Barragán et al., 2016; Carniel et al., 2017; Khan et al., 2017; Osman et al., 2018). The highest induction from 1 to 261 mU/mL was found for *Nectria cinnabarina*_F55. Furthermore, *Sarocladium kiliense*_F121, *Rhynchosporium secalis*_F93, *Ilyonectria radicola*_F99 and *Mortierella alpina*_F210 showed strong induction of extracellular esterase activity (see ESI, **Supplementary Table S1**).

As fungal plant pathogens, *N. cinnabarina*_F55 are well known to produce extracellular enzymes capable of degrading cell wall components such as cutin, since they are essential during the invasion of the host. This is in good agreement with our previous results indicating that cutinases hydrolyze very efficiently synthetic polyesters (Pellis et al., 2016a; Weinberger et al., 2017b; Vecchiato et al., 2018). Enzyme production by *N. cinnabarina*_F55 was studied in the presence of natural substrates or plant cells (Purdy and Kolattukudy, 1973; Eddine et al., 2001; Hawthorne et al., 2001). Eddine et al. (2001) reported an extracellular lipase from *Nectria haematococca* (anamorph *Fusarium solani* f. sp. *pisi*) which showed an esterase activity of 12 U/mL for *p*-nitrophenyl palmitate, but was not tested on polymeric substrates. However, native and engineered esterases/cutinases from *F. solani* f. sp. *pisi* have previously been reported to hydrolyze polyesters including PET [poly(ethylene terephthalate)] (Araújo et al., 2007). Bridge et al. (1989) reported already in 1989 the production of esterases by different *Sarocladium* species (anamorph *Acremonium* sp.). Furthermore, *Acremonium* sp. was identified as producer of enzymes capable of degrading cellulose and chitin (Baldrian et al., 2011). *R. secalis*_F93 and *I. radicola*_F99 are pathogens of barely and other plants such as *Stellera chamaejasme* L, so research is focused on defending mechanisms of the host and not on the enzymes of the fungi (Daassi et al., 2016; Marzin et al., 2016; Penselin et al., 2016; Looseley et al., 2018). Overall, there is not much information available regarding the hydrolytic enzymes derived from these organisms.

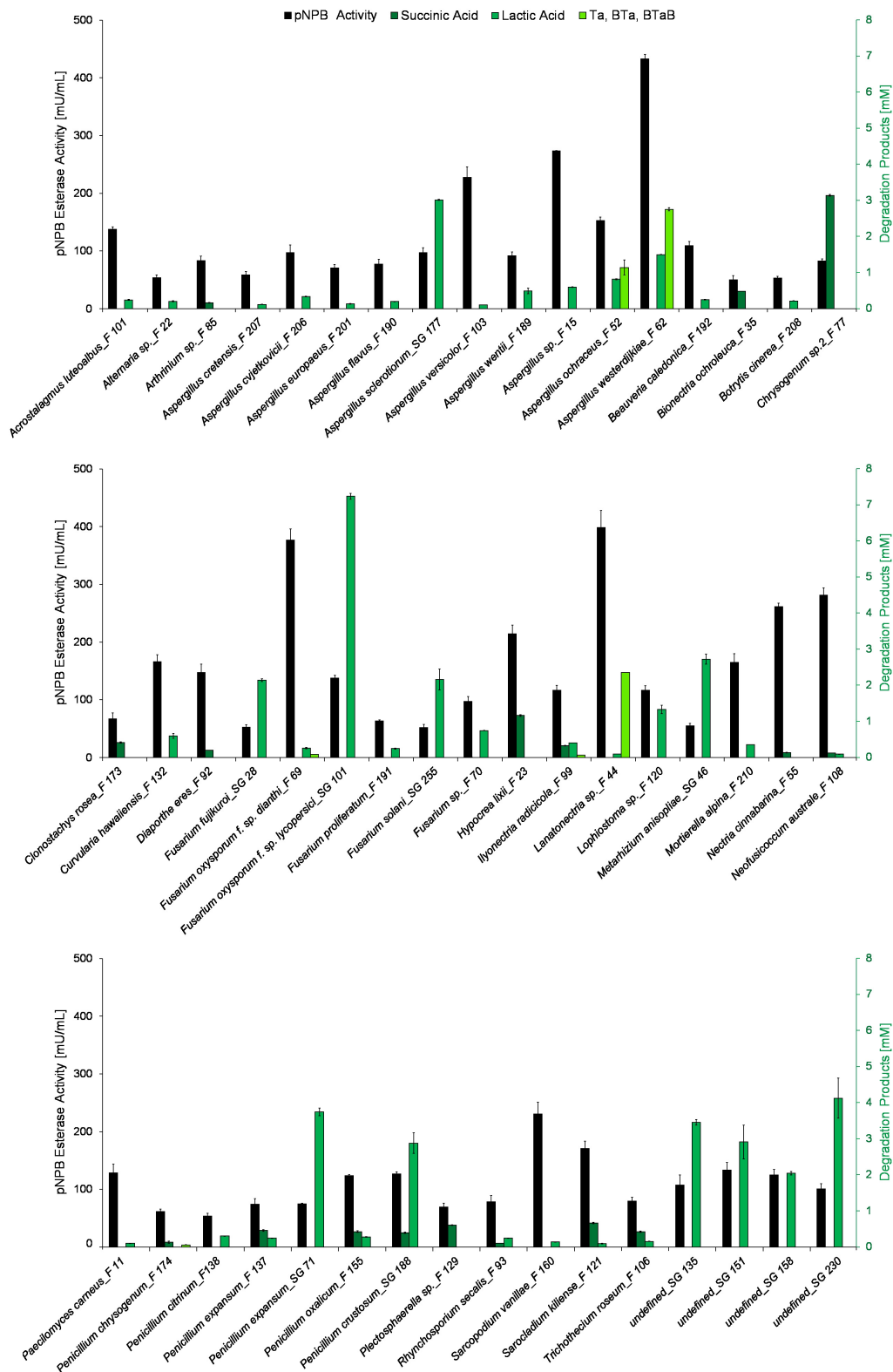


FIGURE 3 | Hydrolysis of different polyesters by supernatants of fungi cultivated in the presence of aliphatic and aromatic polyesters for enzyme induction. pNPB esterase activities [mU/mL] (gray) of fungal culture supernatants were compared with esterase activities on polymers which are shown as the amount of hydrolysis products after 3 weeks of incubation. Monomers from PBS (succinic acid) are shown in dark green, PLA products (lactic acid) are shown in green while hydrolysis products from PBAT (TA, BTA, BTAB) are shown in light green. All experiments were performed in duplicates as indicated by \pm standard deviation.

A lipase was reported from *Mortierella echinosphaera*. Esterase activity was found on p-nitrophenyl esters of different chain length (C2–C16), and potential for catalysis of polymerization reactions (Kotogán et al., 2018). Addition of lipids to the cultivation medium of *Mortierella* sp. resulted in induction of activities (Gaspar et al., 1999; Kotogán et al., 2014).

Hydrolysis of Polyesters by Fungal Supernatants

Those fungal supernatants showing pNPB hydrolytic activity of above 50 mU/mL were subsequently incubated with PLA, PBS, and PBAT, respectively. The quantification of the resulting hydrolysis products is shown in **Figure 3**. Although the pNPB esterase activity is relatively low when compared to commercial esterases such as Lipase B from *Candida antarctica* and a cutinase from *H. insolens*, several species of *Aspergillus*, *Fusarium*, and *Penicillium* were found to efficiently hydrolyze the tested polyesters (Carniel et al., 2017). Forty one of the 50 polymer-active strains degraded PLA, but to a different extent. The highest amount of lactic acid (7 mM) was produced by *Fusarium oxysporum* f. sp. *lycopersici*_SG 101. Amongst the tested polymers, the *F. oxysporum* f. sp. *lycopersici*_SG 101 supernatant showed a high activity on PLA. Interestingly, this supernatant had a relatively low activity of 138 mU/mL on pNPB, compared to *Aspergillus westerdijkiae*_F 62 (433 mU/mL), *Lanatonectria* sp._F 44 (398 mU/mL) and *Sarcopodium vanillae*_F 160 (230 mU/mL). This demonstrates that activity on the small substrate pNPB is suitable for high throughput pre-screening. However, this activity cannot be used to predict hydrolysis activity on distinct polyesters (Gamerith et al., 2017a; Weinberger et al., 2017b). Various *Fusarium* sp. are known to produce cutinases (Zhao et al., 2005; Mao et al., 2015), lipases (Shimada et al., 1993; Dell et al., 2016; Facchini et al., 2018), and other esterases (Luo et al., 2015; Ahuactzin-Pérez et al., 2016). Although both PBS and PLA are linear polyesters, only 17 of the fungi were able to degrade PBS. Seven of those strains were active only on PBS. The most active strain, a *Chrysogenum* sp._2_F 77, produced 3 mM succinic acid. The difference between PLA and PBS is most probably caused by the different crystallinities of these two aliphatic polymers. Since PBS is characterized by higher crystallinity, the tightly packed chains of this polymer avert enzymatic attack (Cho et al., 2001; Gigli et al., 2013). *Chrysogenum* sp. are known to produce acetyl xylan esterases able to cleave acetyl substituents from acetylated xylan, an important step for the degradation of lignocellulose. Yang et al. (2017) reported the activity of an acetyl xylan esterase from *Chrysogenum* P33 with an activity on p-nitrophenyl acetate of 35 mU/mg purified enzyme.

It is not surprising that PBAT was the most difficult polymer to hydrolyze for the fungal esterases due to its partially aromatic nature. *A. westerdijkiae*_F 62 was most efficient in the hydrolysis of PBAT as judged by the formation of 2.8 mM hydrolysis products. In relation to the different activities on pNPB (short model substrate), the data show the different substrate specificities of the esterases secreted by the

different fungi on PBAT, PBS, and PLA. The identification of such specificities can potentially enable the implementation of enzymes in processes related to substrate and product niches e.g., the selection of appropriate strains could be exploited for polymer degradation.

CONCLUSION

Our library screening procedure resulted in the identification of several fungal strains capable of producing enzymes with hydrolytic activity on aromatic and aliphatic polyesters. This function-based search method is the first step for the identification of fungi capable to become a novel source of enzymes active on polymers. In this work we demonstrated that the incubation of fungi with the target polymers can induce the production and secretion of enzymes hydrolyzing these polymers.

A further investigation of the supernatants resulting in identification and recombinant expression of the enzymes is currently ongoing and represents the next step toward a deeper understanding of the different tools that fungi could provide for an enhanced polymer degradation that would allow the closure of the carbon cycle.

DATA AVAILABILITY STATEMENT

All datasets generated for this study are included in the article/**Supplementary Material**.

AUTHOR CONTRIBUTIONS

GG, CS, DR, SW, and RB conceived and designed the experiments. SW and RB performed the experiments and analyzed the data. AP analyzed the used polyesters. SW, GG, DR, CS, JS, and AP wrote the manuscript.

FUNDING

This work was performed with financial funding from the NÖ Forschungs- und Bildungs ges.m.b.H. (NFB) and the provincial government of Lower Austria through the Science Calls (SC17-004). The Austrian Center of Industrial Biotechnology (ACIB) is gratefully acknowledged. AP thanks the FWF Erwin Schrödinger fellowship (Grant Agreement: J4014-N34) for financial support.

SUPPLEMENTARY MATERIAL

The Supplementary Material for this article can be found online at: <https://www.frontiersin.org/articles/10.3389/fmicb.2020.00554/full#supplementary-material>

REFERENCES

- Ahuactzin-Pérez, M., Tlecuitl-Beristain, S., García-Dávila, J., González-Pérez, M., Gutiérrez-Ruiz, M. C., and Sánchez, C. (2016). Degradation of di(2-ethyl hexyl) phthalate by *Fusarium culmorum*: kinetics, enzymatic activities and biodegradation pathway based on quantum chemical modeling pathway based on quantum chemical modeling. *Sci. Total Environ.* 56, 1186–1193. doi: 10.1016/j.scitotenv.2016.05.169
- Álvarez-Barragán, J., Domínguez-Malfavón, L., Vargas-Suárez, M., González-Hernández, R., Aguilar-Osorio, G., and Loza-Tavera, H. (2016). Biodegradative activities of selected environmental fungi on a polyester polyurethane varnish and polyether polyurethane foams. *Appl. Environ. Microbiol.* 82, 5225–5235. doi: 10.1128/AEM.01344-16
- Araújo, R., Silva, C., O'Neill, A., Micaelo, N., Guebitz, G., Soares, C. M., et al. (2007). Tailoring cutinase activity towards polyethylene terephthalate and polyamide 6,6 fibers. *J. Biotechnol.* 128, 849–857. doi: 10.1016/j.jbiotec.2006.12.028
- Association of Plastics Manufacturers in Europe, and European Association of Plastics Recycling and Recovery Organisations [EPRO], (2018). *Plastics – the Facts 2018*. Available at: https://www.plasticseurope.org/application/files/6315/4510/9658/Plastics_the_facts_2018_AF_web.pdf (accessed 10.22.19).
- Auras, R., Harte, B., and Selke, S. (2004). An overview of polylactides as packaging materials. *Macromol. Biosci.* 4, 835–864. doi: 10.1002/mabi.200400043
- Baldrian, P., Voříšková, J., Dobíášová, P., Merhautová, V., Lisá, L., and Valášková, V. (2011). Production of extracellular enzymes and degradation of biopolymers by saprotrophic microfungi from the upper layers of forest soil. *Plant Soil* 338, 111–125. doi: 10.1007/s11104-010-0324-3
- Bridge, P. D., Hawksworth, D. L., Kavishe, D. F., and Farnell, P. A. (1989). A revision of the species concept in *Sarocladium*, the causal agent of sheath-rot in rice and bamboo blight, based on biochemical and morphometric analyses. *Plant Pathol.* 38, 239–245. doi: 10.1111/j.1365-3059.1989.tb02139.x
- Carniel, A., Valoni, É., Nicomedes, J., Gomes, A., and Castro, A. M. D. (2017). Lipase from *Candida antarctica* (CALB) and cutinase from *Hemicola insolens* act synergistically for PET hydrolysis to terephthalic acid. *Process. Biochem.* 59, 84–90. doi: 10.1016/j.procbio.2016.07.023
- Cho, K., Lee, J., and Kwon, K. (2001). Hydrolytic degradation behavior of poly(butylene succinate)s with different crystalline morphologies. *J. Appl. Polym. Sci.* 79, 1025–1033. doi: 10.1002/1097-4628(20010207)79:6<1025::aid-app50>3.0.co;2-7
- Daassi, D., Zouari-Mechichi, H., Belbahri, L., Barriuso, J., Martínez, M. J., Nasri, M., et al. (2016). Phylogenetic and metabolic diversity of Tunisian forest wood-degrading fungi: a wealth of novelties and opportunities for biotechnology. *3 Biotech.* 6:46. doi: 10.1007/s13205-015-0356-8
- Dell, F., Facchini, A., Vici, A. C., Pereira, M. G., Atílio, J., Polizeli, M. D. L. T. M., et al. (2016). Enhanced lipase production of *Fusarium verticillioides* by using response surface methodology and wastewater pretreatment application. *J. Biochem. Technol.* 6, 996–1002.
- Eddine, A. N., Hannemann, F., and Schäfer, W. (2001). Cloning and expression analysis of NhL1, a gene encoding an extracellular lipase from the fungal pea pathogen *Nectria haematococca* MP VI (*Fusarium solani* f. sp. pisi) that is expressed in planta. *Mol. Gen. Genet.* 265, 215–224. doi: 10.1007/s004380000410
- Facchini, D. F., Pereira, G. M., Vici, C. A., Filice, M., Pessela, C. B., Guisan, M. J., et al. (2018). Immobilization effects on the catalytic properties of two *Fusarium verticillioides* lipases: stability, hydrolysis, transesterification and enantioselectivity improvement. *Catal* 8:84. doi: 10.3390/catal8020084
- Gamerith, C., Vastano, M., Ghorbanpour, S. M., Zitzenbacher, S., Ribitsch, D., Zumstein, M. T., et al. (2017a). Enzymatic degradation of aromatic and aliphatic polyesters by *P. pastoris* Expressed Cutinase 1 from *Thermobifida cellulolytica*. *Front. Microbiol.* 8:938. doi: 10.3389/fmicb.2017.00938
- Gamerith, C., Zartl, B., Pellis, A., Guillamot, F., Marty, A., Acero, E. H., et al. (2017b). Enzymatic recovery of polyester building blocks from polymer blends. *Process Biochem.* 59, 58–64. doi: 10.1016/j.procbio.2017.01.004
- Gaspar, M. L., Cunningham, M., Pollero, R., and Cabello, M. (1999). Mycological society of America occurrence and properties of an extracellular vinacea lipase in *Mortierella*. *Mycologia* 91, 108–113. doi: 10.1080/00275514.1999.12060997
- Gautam, R., Bassi, A. S., and Yanful, E. K. (2007). *Candida rugosa* lipase-catalyzed polyurethane degradation in aqueous medium. *Biotechnol. Lett.* 29, 1081–1086. doi: 10.1007/s10529-007-9354-1
- Gigli, M., Negroni, A., Zanolli, G., Lotti, N., Fava, F., and Munari, A. (2013). Environmentally friendly PBS-based copolymers containing PEG-like subunit: effect of block length on solid-state properties and enzymatic degradation. *React. Funct. Polym.* 73, 764–771. doi: 10.1016/j.reactfunctpolym.2013.03.007
- Hawthorne, B. T., Rees-George, J., and Crowhurst, R. N. (2001). Induction of cutinolytic esterase activity during saprophytic growth of cucurbit pathogens, *Fusarium solani* f. sp. cucurbitae races one and two (*Nectria haematococca* MPI and MPV, respectively). *FEMS Microbiol. Lett.* 194, 135–141. doi: 10.1111/j.1574-6968.2001.tb09458.x
- Hu, X., Gao, Z., Wang, Z., Su, T., Yang, L., and Li, P. (2016). Enzymatic degradation of poly(butylene succinate) by cutinase cloned from *Fusarium solani*. *Polym. Degrad. Stab.* 134, 211–219. doi: 10.1016/j.polymdegradstab.2016.10.012
- Karamanlioglu, M., Preziosi, R., and Robson, G. D. (2017). Abiotic and biotic environmental degradation of the bioplastic polymer poly(lactic acid): a review. *Polym. Degrad. Stab.* 137, 122–130. doi: 10.1016/j.polymdegradstab.2017.01.009
- Khan, S., Nadir, S., Shah, Z. U., Shah, A. A., Karunarathna, S. C., Xu, J., et al. (2017). Biodegradation of polyester polyurethane by *Aspergillus tubingensis*. *Environ. Pollut.* 225, 469–480. doi: 10.1016/j.envpol.2017.03.012
- Kotogán, A., Németh, B., Vágvolgyi, C., Papp, T., and Takó, M. (2014). Screening for extracellular lipase enzymes with transesterification capacity in *Mucoromycotina* strains. *Food Technol. Biotechnol.* 52, 73–82.
- Kotogán, A., Zambrano, C., Kecskeméti, A., Varga, M., Szekeres, A., Papp, T., et al. (2018). An organic solvent-tolerant lipase with both hydrolytic and synthetic activities from the oleaginous fungus *Mortierella echinosphaera*. *Int. J. Mol. Sci.* 19, 1–16. doi: 10.3390/ijms19041129
- Looseley, M. E., Griffe, L. L., Büttner, B., Wright, K. M., Middlefell-Williams, J., Bull, H., et al. (2018). Resistance to *Rhynchosporium commune* in a collection of European spring barley germplasm. *Theor. Appl. Genet.* 131, 2513–2528. doi: 10.1007/s00122-018-3168-5
- Luo, Z.-H., Ding, J.-F., Xu, W., Zheng, T.-L., and Zhong, T.-H. (2015). Purification and characterization of an intracellular esterase from a marine *Fusarium* fungal species showing phthalate diesterase activity. *Int. Biodeterior. Biodegradation* 97, 7–12. doi: 10.1016/j.ibiod.2014.10.006
- Mao, H., Liu, H., Gao, Z., Su, T., and Wang, Z. (2015). Biodegradation of poly(butylene succinate) by *Fusarium* sp. FS1301 and purification and characterization of poly(butylene succinate) depolymerase. *Polym. Degrad. Stab.* 114, 1–7. doi: 10.1016/j.polymdegradstab.2015.01.025
- Marzin, S., Hanemann, A., Sharma, S., Hensel, G., Kumlehn, J., Schweizer, G., et al. (2016). Are PECTIN ESTERASE INHIBITOR genes involved in mediating resistance to *Rhynchosporium commune* in Barley? *PLoS One* 11:e0150485. doi: 10.1371/journal.pone.0150485
- Mathur, G., and Prasad, R. (2012). Degradation of Polyurethane by *Aspergillus flavus* (ITCC 6051) isolated from soil. *Appl. Biochem. Biotechnol.* 167, 1595–1602. doi: 10.1007/s12010-012-9572-4
- Moser, M. (1963). Förderung der mykorrhizabildung in der forstlichen Praxis. *Mitt. Forst. Bundes-Versuchsanstalt* 60, 639–720.
- Osman, M., Satti, S. M., Luqman, A., Hasan, F., Shah, Z., and Shah, A. A. (2018). Degradation of polyester polyurethane by *Aspergillus* sp. strain s45 Isolated from Soil. *J. Polym. Environ.* 26, 301–310. doi: 10.1007/s10924-017-0954-0
- Pellis, A., Gamerith, C., Ghazaryan, G., Ortner, A., Herrero Acero, E., and Guebitz, G. M. (2016a). Ultrasound-enhanced enzymatic hydrolysis of poly(ethylene terephthalate). *Bioresour. Technol.* 218, 1298–1302. doi: 10.1016/j.biortech.2016.07.106
- Pellis, A., Herrero Acero, E., Ferrario, V., Ribitsch, D., Guebitz, G. M., and Gardossi, L. (2016b). The closure of the cycle: enzymatic synthesis and functionalization of bio-based polyesters. *Trends Biotechnol.* 34, 316–328. doi: 10.1016/j.tibtech.2015.12.009
- Penselin, D., Münsterkötter, M., Kirsten, S., Felder, M., Taudien, S., Platzer, M., et al. (2016). Comparative genomics to explore phylogenetic relationship, cryptic sexual potential and host specificity of *Rhynchosporium* species on grasses. *BMC Genomics* 17:953. doi: 10.1186/s12864-016-3299-5
- Perz, V., Baumschlager, A., Bleymaier, K., Zitzenbacher, S., Hromic, A., Steinkellner, G., et al. (2016a). Hydrolysis of synthetic polyesters by *Clostridium botulinum* esterases. *Biotechnol. Bioeng.* 113, 1024–1034. doi: 10.1002/bit.25874

- Perz, V., Bleymaier, K., Sinkel, C., Kueper, U., Bonnekesel, M., Ribitsch, D., et al. (2016c). Substrate specificities of cutinases on aliphatic-aromatic polyesters and on their model substrates. *N. Biotechnol.* 33, 295–304. doi: 10.1016/j.nbt.2015.11.004
- Perz, V., Hromic, A., Baumschlager, A., Steinkellner, G., Pavkov-Keller, T., Gruber, K., et al. (2016b). An esterase from anaerobic clostridium hathewayi can hydrolyze aliphatic-aromatic polyesters. *Environ. Sci. Technol.* 50, 2899–2907. doi: 10.1021/acs.est.5b04346
- Purdy, R. E., and Kolattukudy, P. E. (1973). Depolymerization of a hydroxy fatty acid biopolymer, cutin, by an extracellular enzyme from *Fusarium solani* f. pisi: isolation and some properties of the enzyme. *Arch. Biochem. Biophys.* 159, 61–69. doi: 10.1016/0003-9861(73)90429-3
- Quartinello, F., Vajnhandl, S., Volmajer Valh, J., Farmer, T. J., Vončina, B., Lobnik, A., et al. (2017). Synergistic chemo-enzymatic hydrolysis of poly(ethylene terephthalate) from textile waste. *Microb. Biotechnol.* 10, 1376–1383. doi: 10.1111/1751-7915.12734
- Ribitsch, D., Heumann, S., Trotscha, E., Herrero Acero, E., Greimel, K., Leber, R., et al. (2011). Hydrolysis of polyethyleneterephthalate by p-nitrobenzylesterase from *Bacillus subtilis*. *Biotechnol. Prog.* 27, 951–960. doi: 10.1002/btpr.610
- Ronkvist, Å.M., Xie, W., Lu, W., and Gross, R. A. (2009). Cutinase-catalyzed hydrolysis of poly(ethylene terephthalate). *Macromolecules* 42, 5128–5138. doi: 10.1021/ma9005318
- Rudnik, E., and Briassoulis, D. (2011a). Comparative biodegradation in soil behaviour of two biodegradable polymers based on renewable resources. *J. Polym. Environ.* 19, 18–39. doi: 10.1007/s10924-010-0243-7
- Rudnik, E., and Briassoulis, D. (2011b). Degradation behaviour of poly(lactic acid) films and fibres in soil under Mediterranean field conditions and laboratory simulations testing. *Ind. Crops Prod.* 33, 648–658. doi: 10.1016/J.INDCROP.2010.12.031
- Shimada, Y., Koga, C., Sugihara, A., Nagao, T., Takada, N., Tsunasaawa, S., et al. (1993). Purification and characterization of a novel solvent-tolerant lipase from *Fusarium heterosporum*. *J. Ferment. Bioeng.* 75, 349–352. doi: 10.1016/0922-338X(93)90132-R
- Shogren, R. L., Doane, W. M., Garlotta, D., Lawton, J. W., and Willett, J. L. (2003). Biodegradation of starch/polylactic acid/poly(hydroxyester-ether) composite bars in soil. *Polym. Degrad. Stab.* 79, 405–411. doi: 10.1016/S0141-3910(02)00356-7
- Sisti, L., Totaro, G., and Marchese, P. (2016). *PBS Makes its Entrance Into the Family of Biobased Plastics*. Hoboken, NJ: John Wiley & Sons.
- Vecchiato, S., Skopek, L., Jankova, S., Pellis, A., Ipsmiller, W., Aldrian, A., et al. (2018). Enzymatic recycling of high-value phosphor flame-retardant pigment and glucose from rayon fibers. *ACS Sustain. Chem. Eng.* 6, 2386–2394. doi: 10.1021/acssuschemeng.7b03840
- Vroman, I., and Tighzert, L. (2009). Biodegradable polymers. *Materials* 2, 307–344. doi: 10.3390/ma2020307
- Weinberger, S., Canadell, J., Quartinello, F., Yeniad, B., Arias, A., Pellis, A., et al. (2017a). Enzymatic degradation of poly(ethylene 2,5-furanoate) powders and amorphous films. *Catalysts* 7:318. doi: 10.3390/catal7110318
- Weinberger, S., Haernvall, K., Scaini, D., Ghazaryan, G., Zumstein, M. T., Sander, M., et al. (2017b). Enzymatic surface hydrolysis of poly(ethylene furanoate) thin films of various crystallinities. *Green Chem.* 19, 5381–5384. doi: 10.1039/c7gc02905e
- Weng, Y.-X., Jin, Y.-J., Meng, Q.-Y., Wang, L., Zhang, M., and Wang, Y.-Z. (2013). Biodegradation behavior of poly(butylene adipate-co-terephthalate) (PBAT), poly(lactic acid) (PLA), and their blend under soil conditions. *Polym. Test.* 32, 918–926. doi: 10.1016/J.POLYMTESTING.2013.05.001
- Wohlgemuth, R. (2010). *Large-Scale Applications of Hydrolases in Biocatalytic Asymmetric Synthesis*. Hoboken, NJ: Wiley Online Books.
- Yang, Y., Zhu, N., Yang, J., Lin, Y., Liu, J., Wang, R., et al. (2017). A novel bifunctional acetyl xylan esterase/arabinofuranosidase from *Penicillium chrysogenum* P33 enhances enzymatic hydrolysis of lignocellulose. *Microb. Cell Fact.* 16, 1–12. doi: 10.1186/s12934-017-0777-7
- Zhao, J.-H., Wang, X.-Q., Zeng, J., Yang, G., Shi, F.-H., and Yan, Q. (2005). Biodegradation of poly(butylene succinate-co-butylene adipate) by *Aspergillus versicolor*. *Polym. Degrad. Stab.* 90, 173–179. doi: 10.1016/J.POLYMDEGRADSTAB.2005.03.006

Conflict of Interest: The authors declare that the research was conducted in the absence of any commercial or financial relationships that could be construed as a potential conflict of interest.

Copyright © 2020 Weinberger, Beyer, Schüller, Strauss, Pellis, Ribitsch and Guebitz. This is an open-access article distributed under the terms of the Creative Commons Attribution License (CC BY). The use, distribution or reproduction in other forums is permitted, provided the original author(s) and the copyright owner(s) are credited and that the original publication in this journal is cited, in accordance with accepted academic practice. No use, distribution or reproduction is permitted which does not comply with these terms.



UV Pretreatment Impairs the Enzymatic Degradation of Polyethylene Terephthalate

Patricia Falkenstein¹, Daniel Gräsing¹, Pavlo Bielytskyi¹, Wolfgang Zimmermann², Jörg Matysik¹, Ren Wei^{2*†} and Chen Song^{1*}

OPEN ACCESS

Edited by:

Matthias E. Kaestner,
Helmholtz Centre for Environmental
Research (UFZ), Germany

Reviewed by:

Maurizio Petruccioli,
University of Tuscia, Italy
Ramón Alberto Batista-García,
Universidad Autónoma del Estado
de Morelos, Mexico
Fusako Kawai,
Okayama University Japan, Japan

*Correspondence:

Ren Wei
ren.wei@uni-greifswald.de
Chen Song
chen.song@uni-leipzig.de

†Present address:

Ren Wei
Institut für Biochemie, Universität
Greifswald, Greifswald, Germany

Specialty section:

This article was submitted to
Microbiotechnology,
a section of the journal
Frontiers in Microbiology

Received: 16 December 2019

Accepted: 25 March 2020

Published: 28 April 2020

Citation:

Falkenstein P, Gräsing D,
Bielytskyi P, Zimmermann W,
Matysik J, Wei R and Song C (2020)
UV Pretreatment Impairs
the Enzymatic Degradation
of Polyethylene Terephthalate.
Front. Microbiol. 11:689.
doi: 10.3389/fmicb.2020.00689

¹ Institut für Analytische Chemie, Universität Leipzig, Leipzig, Germany, ² Institut für Biochemie, Universität Leipzig, Leipzig, Germany

The biocatalytic degradation of polyethylene terephthalate (PET) emerged recently as a promising alternative plastic recycling method. However, limited activity of previously known enzymes against post-consumer PET materials still prevents the application on an industrial scale. In this study, the influence of ultraviolet (UV) irradiation as a potential pretreatment method for the enzymatic degradation of PET was investigated. Attenuated total reflection Fourier transform infrared (ATR-FTIR) and ¹H solution nuclear magnetic resonance (NMR) analysis indicated a shortening of the polymer chains of UV-treated PET due to intra-chain scissions. The degradation of UV-treated PET films by a polyester hydrolase resulted in significantly lower weight losses compared to the untreated sample. We also examined site-specific and segmental chain dynamics over a time scale of sub-microseconds to seconds using centerband-only detection of exchange, rotating-frame spin-lattice relaxation ($T_{1\rho}$), and dipolar chemical shift correlation experiments which revealed an overall increase in the chain rigidity of the UV-treated sample. The observed dynamic changes are most likely associated with the increased crystallinity of the surface, where a decreased accessibility for the enzyme-catalyzed hydrolysis was found. Moreover, our NMR study provided further knowledge on how polymer chain conformation and dynamics of PET can mechanistically influence the enzymatic degradation.

Keywords: solid-state NMR, chain dynamics, surface crystallinity, polyester hydrolases, plastic recycling

INTRODUCTION

Polyethylene terephthalate (PET) is one of the most widely used plastic type, especially as packaging material for the food industry and as synthetic fibers for the textile industry (World Economic Forum, 2016; Geyer et al., 2017; PlasticsEurope, 2019). Due to its low weight, high strength, optical transparency and low CO₂ permeability, PET is particularly suitable for the production of beverage bottles (Webb et al., 2013). In general, due to their versatile applicability and low manufacturing costs, plastics have become an indispensable part of our daily lives (Andrady and Neal, 2009), leading to a continuous increase in production which in 2018 amounted to 359 million

metric tons worldwide (PlasticsEurope, 2019). However, without appropriate treatment, plastic waste can persist in nature for centuries (World Economic Forum, 2016) and accumulate as hazardous pollution causing a serious environmental crisis (Rochman et al., 2013). Hence, reduction of plastic consumption as well as recycling of in-use polymer materials have been proposed to be proper approaches to solve the plastics pollution within the framework of a sustainable circular economy (Hopewell et al., 2009).

For chemical recycling of PET, polymer chains are broken down into their monomers which can be used to produce virgin plastics or synthetic chemicals (Geyer et al., 2016). However, high temperatures and pressures as well as toxic chemicals are usually required for chemical PET recycling, making this process cost- and energy-intensive (World Economic Forum, 2016). Alternatively, biocatalytic degradation of PET which was shown to function under mild conditions in the absence of harmful chemicals, emerged as an option (Wei and Zimmermann, 2017; Kawai et al., 2019; Salvador et al., 2019; Bollinger et al., 2020). Compared to the mesophilic PET hydrolases, e.g., the PETase from *Ideonella sakaiensis* (Yoshida et al., 2016; Han et al., 2017; Austin et al., 2018), thermophilic microbial enzymes are advantageous to the hydrolysis of the ester bonds in PET due to the fact that polymer chains are more easily accessible near its glass transition temperature (T_g) between 75 and 79°C (Ronkvist et al., 2009; Wei and Zimmermann, 2017; Wei et al., 2019a,b). However, long-term incubation in the T_g range is mandatory for PET degradation using the most active PET hydrolase identified so far (Wei and Zimmermann, 2017). Consequently, increased crystallinity of the polymers as a result of physical aging at this condition has been shown to hamper the enzymatic PET degradation (Wei et al., 2019a). Very recently, distinct conformations of PET segments derived by computational modeling and NMR experiments have provoked scientific discussions about the exact molecular mechanism of enzymatic PET degradation (Austin et al., 2018; Joo et al., 2018; Wei et al., 2019b). This knowledge would facilitate further exploration and engineering of enzyme variants toward enhanced PET hydrolytic activity, as well as of feasible pretreatment approaches to lower the degradation obstacle in terms of the polymer substrate.

UV light, an electromagnetic radiation in the 100-to-380-nm wavelength range, can induce photodegradation of recalcitrant polyolefins by generating free radicals (Ammala et al., 2011) and consequently facilitate the subsequent microbial degradation (Albertsson et al., 1987). PET can also absorb UV light as evidenced by photodegradation by sunlight under natural conditions leading to discoloration and brittleness on a macroscopic level (Day and Wiles, 1972b). These surface effects are likely to be associated with the cleavage of polymer chains resulting in a decrease of molecular weight and an increase of the amount of carboxylic acid end groups, accompanied by the evolution of volatile products like CO and CO₂ (Day and Wiles, 1972a,b,c; Blais et al., 1973). Moreover, PET structural and morphological changes caused by UV irradiation have been reported previously (Fechine et al., 2002). Enzymatic PET degradation is dependent on the mobility of the amorphous

regions as well as on the degree of crystallinity (Vertommen et al., 2005; Ronkvist et al., 2009; Wei et al., 2019a). Therefore, it is worthwhile to determine whether UV pretreatment has an effect on the dynamics of the shortened polymer chains and could possibly accelerate the biocatalytic degradation of PET.

In this study, we identified changes in enzymatic degradability and chain dynamics of PET caused by UV irradiation. The UV-induced PET chain scissions were quantified by both ATR-FTIR and ¹H NMR spectroscopic techniques. The biodegradability of PET before and after UV treatment was assessed using the thermophilic polyester hydrolase LC-cutinase (LCC) originated from a plant-containing compost (Sulaiman et al., 2012). To examine the UV-induced changes in crystallinity and chain dynamics over a time scale of sub-microseconds to seconds, four different types of solid-state NMR experiments, centerband-only detection of exchange (CODEX), $T_{1\rho}$, dipolar chemical shift correlation (DIPSHIFT), and cross polarization (CP) were conducted at both 30 and 70°C. The data contribute to an extended understanding of the exact enzymatic degradation mechanism at a molecular level.

MATERIALS AND METHODS

PET Samples

For the enzymatic degradation and solution NMR experiments, amorphous PET films with a thickness of 250 μm (Goodfellow, Ltd., Bad Nauheim, Germany, product number ES301445) were used. The PET film was cryogenically ground to powder with a particle size (ϕ) ranging from 0.25 to 0.5 mm for solid-state NMR measurements. UV irradiation of the PET samples was carried out over 14 days using a 1-kW xenon arc lamp (Müller GmbH Elektronik-Optik, Moosinning, Germany) which generated an emission spectrum similar to sunlight with a cut-off in the UV region at ca. 250 nm. Due to the heating effect, the IR radiation was filtered out by using a water filter. A water bath was used for further cooling the samples during irradiation (Figure 1A). The sample temperature monitored with an IR thermometer was kept below 45°C throughout the irradiation process.

ATR-FTIR Measurements

ATR-FTIR spectra were recorded with a Bruker Vector 22 FTIR spectrometer assembled with ATR accessory using a wavenumber range of 500–4000 cm⁻¹ with a resolution of 4 cm⁻¹.

¹H Solution NMR Measurements

¹H NMR experiments were performed with a Bruker DRX-600 NB spectrometer equipped with a 5-mm TXI probe (Rheinstetten, Germany) at a read-out temperature of 27°C. The optimized ¹H 90° pulse length was 9.0 μs. The data were recorded with 1 or 2 k scans and a recycle delay of 10 s. An exponential line broadening of 0.2 Hz was applied prior to data processing. The baseline was corrected manually afterward. Processed data were further analyzed using MestReNova 12.0.0 (Mestrelab Research S.L., Santiago de Compostela, Spain). Both untreated and UV-treated PET samples were dissolved

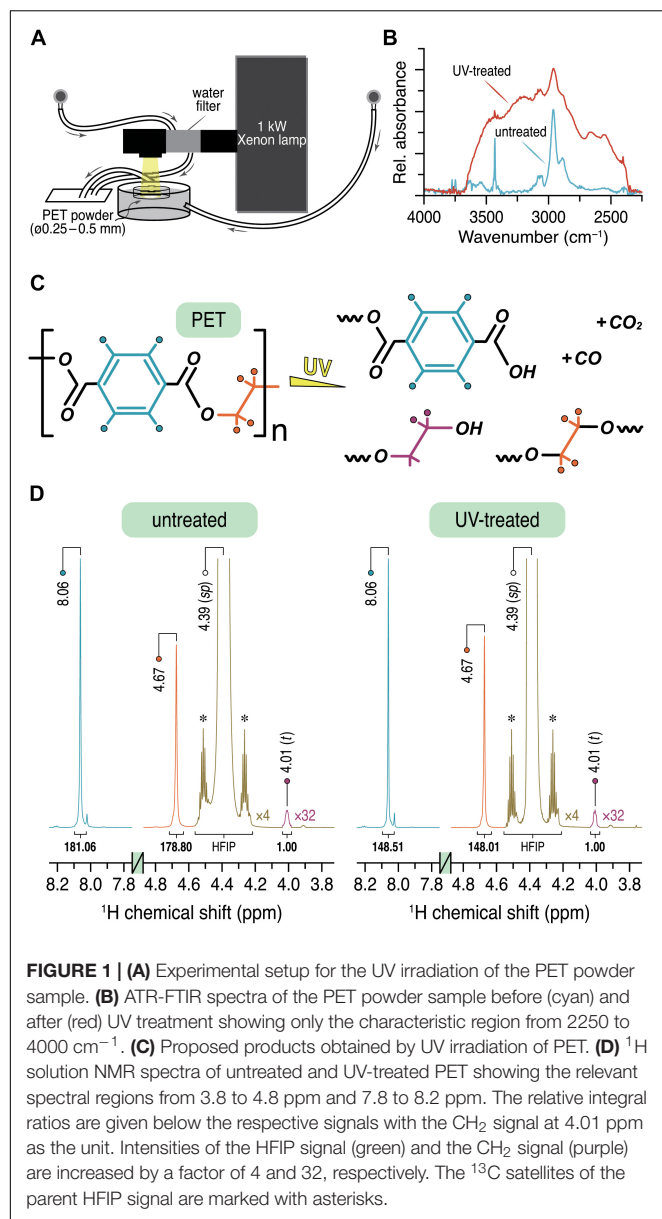


FIGURE 1 | (A) Experimental setup for the UV irradiation of the PET powder sample. (B) ATR-FTIR spectra of the PET powder sample before (cyan) and after (red) UV treatment showing only the characteristic region from 2250 to 4000 cm⁻¹. (C) Proposed products obtained by UV irradiation of PET. (D) ¹H solution NMR spectra of untreated and UV-treated PET showing the relevant spectral regions from 3.8 to 4.8 ppm and 7.8 to 8.2 ppm. The relative integral ratios are given below the respective signals with the CH₂ signal at 4.01 ppm as the unit. Intensities of the HFIP signal (green) and the CH₂ signal (purple) are increased by a factor of 4 and 32, respectively. The ¹³C satellites of the parent HFIP signal are marked with asterisks.

in hexafluoroisopropanol (HFIP, ≥ 99%, Carl Roth GmbH + Co. KG, Karlsruhe, Germany) and stored at room temperature for 5 days before measurement. The filtered PET solutions with a final concentration of approximately 14.3 μg/μL were pipetted into a 5-mm NMR tube and mixed at a ratio of 1:16 with chloroform-*d* (CDCl₃, 99.8% D, ARMAR AG, Döttingen, Switzerland) containing 0.03% (v/v) tetramethylsilane (TMS) as an internal standard (δ^H , 0.00 ppm).

Enzymatic Degradation Tests

Untreated and UV-treated PET films were cut into chips of 3 cm × 0.5 cm with an average weight of 44.7 and 44.3 mg, respectively. One PET chip was placed in a 2-mL reaction vial containing 1.8 mL of K₂HPO₄/Cl (1M, pH = 8.0) and 100 μg purified LC-cutinase, corresponding to a concentration

of 2 μM or 1.2 nmol/cm² of PET film surface area. LC-cutinase was expressed in *E. coli* BL21(DE3) and purified by immobilized metal ion chromatography similarly as previously reported (Schmidt et al., 2016). Degradation was performed by shaking the reaction vials on a thermoshaker TS1 (Biometra, Göttingen, Germany) at 70°C and 1000 rpm for 24 h. The reaction was stopped by cooling the samples in an ice bath, followed by withdrawing and washing the PET films sequentially with 0.1% SDS, ultrapure water and 70% ethanol. The PET films were dried at 50°C for > 24 h before they were subjected to gravimetric determination of the weight loss.

Solid-State NMR Measurements

Solid-state NMR experiments were performed with a Bruker AVANCE III 400 WB spectrometer (Rheinstetten, Germany) equipped with a 4-mm double resonance magic-angle spinning (MAS) probe. For all measurements approximately 80 mg of PET powder was packed into a 4-mm zirconia rotor. Prior to NMR acquisition, *in situ* incubation of the PET sample was performed for at least 12 h to avoid spectral changes during the experiments caused by physical aging (Hutchinson, 1995). All experiments were carried out at an ambient temperature of 30°C as well as at 70°C slightly below the *T_g* of PET.

¹H to ¹³C magnetization transfer was achieved by using linear 70–100% ¹H-ramped CP (Schaefer and Stejskal, 1976; Metz et al., 1994) with a contact time of 2 ms and a ¹³C r.f. lock field of 67 kHz, fulfilling the Hartmann–Hahn condition. Heteronuclear decoupling during acquisition was achieved with swept-frequency two-pulse phase modulation (Thakur et al., 2006; Vinod Chandran et al., 2008) at ¹H r.f. field of 100 kHz. Optimized ¹H and ¹³C 90° pulse lengths were 2.5 and 3.0 μs, respectively. ¹³C CP/MAS spectra were collected at a spinning frequency of 12.5 kHz with 2 k scans and a recycle delay of 2.5 s. Overall, 1604 data points were recorded. For the data processing, an exponential window function and zero filling to 8192 data points was applied prior to Fourier transformation.

DIPSHIFT (Hong et al., 1997) data were collected with a recycle delay of 4 s. The ¹H–¹H homonuclear dipolar decoupling during the *t*₁ evolution period was accomplished by using the phase modulated Lee–Goldburg (PMLG5) (Vinogradov et al., 2001) scheme. Each PMLG5 block consisted of 10 pulses with the following phases: 339.22, 297.65, 256.08, 214.51, 172.94, 352.94, 34.51, 76.08, 117.65, and 159.22° (m5m shape in Top-Spin 3.2 library). The optimized PMLG5 pulse was 2.08 μs with 80 kHz r.f. amplitude. For different experiments the number of scans per increment was varied between 768 and 1168. An exponential window function was applied and the data was zero-filled to 8192 points prior to Fourier transformation. The rigid-limit values for CH and CH₂ groups were determined experimentally by measuring DIPSHIFT curves for crystalline *bis*(2-hydroxyethyl) terephthalate (BHET) and fitting them in a site-specific manner. All DIPSHIFT curves were fitted with SIMPSON simulations (Bak et al., 2000) taking into account the PMLG scaling factor of 0.5 which was determined by observing the *J*-splitting of the CH and CH₂ groups of adamantane under PMLG5-decoupling using the same conditions.

CODEX (deAzevedo et al., 1999) data were recorded with a recycle delay of 2.5 s. At 30°C, 2k scans were accumulated, while at 70°C the number of scans was around 4 k (in multiples of 128). An exponential window function was applied and the data points were zero-filled to 8192 prior to Fourier transformation. A t_z filter time of 1.28 ms and mixing times (t_m) between 0.02 and 1.2 s were employed. The sum of the preparation and refocusing time was $10 t_r$ ($N = 10$). An extended phase cycle (Reichert et al., 2001) was used for proper cancelation of unwanted transverse components during t_m and t_z under fast MAS.

$T_{1\rho}(^1\text{H})$ relaxation times were measured with 392 and 784 scans for the untreated and UV-treated samples, respectively. A 66 kHz ^1H spin-lock field and a recycle delay of 4 s were used. The length of the spin-lock pulse was incremented in 13 steps varying between 0.01 and 50 ms. An exponential window function was applied in the ^{13}C dimension for processing while the data points were zero-filled up to 16 and 2048 data points in the ^1H and ^{13}C dimension, respectively. $T_{1\rho}(^1\text{H})$ relaxation times were obtained by least-squares fitting of the normalized peak intensities to a single exponential:

$$\frac{M(\tau)}{M(0)} = e^{-\frac{\tau}{T_{1\rho}}} \quad (1)$$

Here, $M(0)$ and $M(\tau)$ represent the initial intensity and the intensity at the applied spin-lock time τ , respectively.

For $T_{1\rho}(^1\text{H})$ and CODEX analysis OriginPro 8G (OriginLab Corporation, Northampton, MA) was used. Spectral fitting was done with MestReNova 12.0.0 (Mestrelab Research S.L., Santiago de Compostela, Spain). ^{13}C chemical shifts were externally referenced to the COO^- signal of solid tyrosine hydrochloride at 172.1 ppm.

RESULTS

ATR-FTIR and ^1H Solution NMR Analysis of PET Chain Scission Caused by UV Irradiation

To determine the chain scissions of PET by UV light (Figure 1A), surface sensitive ATR-FTIR measurements (Day and Wiles, 1972b,c; Blais et al., 1973; Fehine et al., 2004) were performed. The untreated PET sample (Figure 1B, cyan) showed the characteristic absorption bands, as expected. The band at 3060 cm^{-1} can be assigned to the aromatic C–H stretching and the corresponding aliphatic C–H stretching modes are represented by the bands at around 2960 and 2880 cm^{-1} (see also Holland and Hay, 2002). The first overtone of the fundamental C=O absorption at 1710 cm^{-1} (Supplementary Figure 1) appeared at $\sim 3430\text{ cm}^{-1}$ (Day and Wiles, 1972b). The same bands can be identified in the spectrum of the PET sample exposed to UV light for 14 days (Figure 1B, red). However, clear differences in the range between 2250 and 3700 cm^{-1} were observed. The broad absorption bands centered at around 3500 and 3250 cm^{-1} can be attributed to O–H stretching vibrations from the –COOH and –OH functional groups, respectively (Day and Wiles, 1972b). The shoulders at 2660 and

2550 cm^{-1} most likely originate from overtones and combination bands, characteristic for dimeric carboxylic acids (Schrader and Meier, 1974; Günzler and Gremlich, 2003). These distinctive absorption bands can therefore be ascribed to an increased carboxyl end group content in the UV-treated PET sample relative to the untreated one. It is also clear that the formation of additional carboxyl end groups was caused by the breakage of the ester C–O bonds in the main chain (Figure 1C), while the concentration of carboxyl end groups is too low and therefore not detectable in the corresponding ATR-FTIR spectrum of the untreated sample.

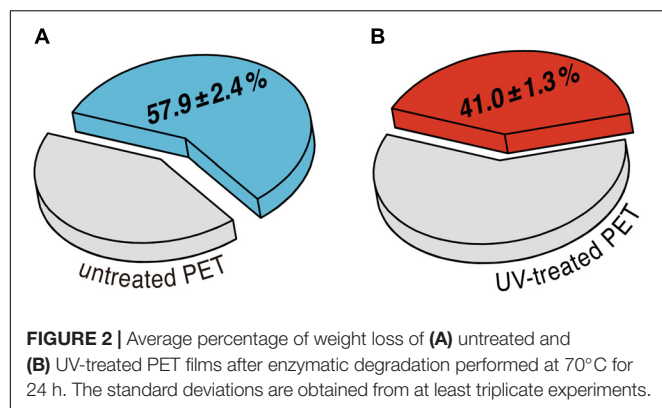
To quantify the intra-chain scissions of the UV-treated PET, the degree of polymerization (DP) was determined by ^1H NMR spectroscopy similarly as described before (Wei et al., 2019a). Both ^1H NMR spectra display two sharp singlets with almost identical integrals ($<\pm 1\%$) at 8.06 and 4.67 ppm (Figure 1D) which can be readily assigned to the four protons of the terephthalate ring and the oxyethylene units in the main chain, respectively (Kenwright et al., 1999; de Ilarduya and Muñoz-Guerra, 2014). A much weaker signal with δ^{H} of 4.01 ppm (2H , t , $^3J \approx 4.5\text{ Hz}$) corresponds to the methylene protons in α -position to the hydroxyl end group of the PET chain (Figure 1C). The DP value was determined according to the relative integral ratios of these three signals. Assuming that each PET chain possesses a single hydroxyl end group, a DP of 181.7 ± 1.6 was obtained for the untreated sample, while the UV-treated sample showed a DP value of 149.7 ± 0.4 with a reduction of 17.6%. Considering the molecular weight of 192.17 g/mol of a single PET repeating unit, the two DP values for the untreated and the UV-treated samples corresponded to an average molecular weight of about 35000 and 29000 g/mol, respectively.

Enzymatic Degradation of UV-Treated PET Films

To assess the effect of UV pretreatment on the enzymatic degradation of PET, we performed hydrolytic degradation of the untreated and the UV-treated PET films at 70°C for 24 h using purified recombinant LC-cutinase. The weight loss of the PET films after enzymatic hydrolysis was determined gravimetrically to evaluate the degradation performance. According to a previous study, weight loss of amorphous PET films could be quantitatively correlated with the release of degradation monomers including terephthalic acid, ethylene glycol (EG), mono(2-hydroxyethyl) terephthalate (MHET) and BHET (Barth et al., 2015). As shown in Figure 2, an absolute weight loss of $26.1 \pm 0.5\text{ mg}$ ($57.9 \pm 2.4\%$) and $18.2 \pm 0.9\text{ mg}$ ($41.0 \pm 1.3\%$) was determined for the control sample and the UV-treated PET sample, respectively, as a result of 24 h enzymatic hydrolysis.

^{13}C CP/MAS Experiments to Determine the Degree of Crystallinity in PET Before and After UV Irradiation

^{13}C CP/MAS spectra were recorded to determine the *trans/gauche* (*t/g*) ratio of the PET samples before and after UV irradiation. Amorphous PET exists as a mixture of *t* and *g*



conformers, whereby the *g* content usually significantly exceeds the *t* content. On the contrary, crystalline PET consists of 100% *t* conformation. The average OC–CO torsion angle of *t* and *g* states is about 180 and $\pm 60^\circ$, respectively (Schmidt-Rohr et al., 1998). A quantification for the *t/g* ratio was done by deconvolution of the ethylene carbon signals (Figure 3A), composed of both *t* and *g* conformations, corresponding to the crystalline and the amorphous phase of PET, respectively (Gabrielse et al., 1994; Choudhury et al., 2012). For the untreated PET sample, a *t/g* ratio of 0.19 ± 0.03 was calculated from the spectra at 30°C and a value of 0.23 ± 0.06 was determined at 70°C. After UV treatment the *t/g* ratio of the PET sample was increased at both 30 and 70°C with the values of 0.49 ± 0.08 and 0.67 ± 0.16 , respectively. The conformational changes of the PET chains associated with the UV treatment were also evident from the splitting of the carbonyl signals after UV irradiation (data not shown).

Site-Specific and Segmental PET Chain Dynamics

To analyze dynamical changes of untreated and UV-treated PET over a time scale of sub-microseconds to seconds, three different solid-state NMR experiments were conducted.

The DIPSHIFT experiment is used to quantify localized dynamics of proteins or polymers on the sub-microseconds time scale (Huster et al., 2001; deAzevedo et al., 2008; Ivanir-Dabora et al., 2015). Here, the order parameters *S* (ranging from 0 to 1 representing isotropic motion and a rigid limit, respectively) were determined at both 30 and 70°C for the PET samples before and after UV irradiation. The ^1H – ^{13}C dephasing curves extracted from the DIPSHIFT experiments including the calculated order parameters are shown in Figure 3B. The rigid limit with the order parameter *S* = 1 is represented here by BHET.

For the untreated PET sample an order parameter of *S* = 0.89 and 0.75 was obtained for the aromatic C–H group at 30 and 70°C, respectively. In the UV-treated PET sample, however, the phenylene unit revealed larger order parameters at both temperatures (*S* = 0.93 and 0.87 at 30 and 70°C, respectively). It is clear that more pronounced chain motions are detected for both samples at the higher temperature. Furthermore, after UV irradiation, the phenylene unit shows reduced mobility on the

sub-microseconds time scale at both temperatures with larger order parameters (*S* = 0.93 vs. 0.89 at 30°C, and *S* = 0.87 vs. 0.75 at 70°C). For the ethylene unit, the order parameters *S* for both *t* and *g* conformations were calculated. After UV treatment an order parameter of *S* = 0.98 was found for the *g* conformation, slightly larger than that of the untreated sample at 30°C (*S* = 0.95). At 70°C, *S* = 0.91 and 0.96 were observed before and after UV irradiation, respectively. For the *t* conformation of the ethylene unit *S* = 0.85 and 0.87 were determined for the untreated and UV-treated PET at 30°C, respectively. The order parameter obtained at 70°C for the untreated PET sample was *S* = 0.85 and 0.86 for UV-illuminated PET. The overall increased order parameters clearly indicate that the ethylene unit of PET is getting less mobile after UV degradation.

In addition, we also employed the CODEX experiment for characterization of slower segmental reorientations of the phenylene unit over a time scale of milliseconds to seconds (deAzevedo et al., 1999) which was reported to undergo ring-flip motions in PET about its 1,4-axis (Wilhelm and Spiess, 1996; Choudhury et al., 2012). By plotting the normalized exchange intensity which is the ratio of pure-exchange CODEX intensity to the reference intensity, against the different mixing times (*t_m*), the correlation time of the reorientation can be obtained (deAzevedo et al., 1999). In the case of PET, the curve was characterized by the following equation representing a stretched exponential (Choudhury et al., 2012):

$$\Delta S/S_0 = E_\infty(1 - e^{-(t_m/\tau_c)^\beta}) \quad (2)$$

Here, *E_∞* is the final exchange intensity and β is the stretch exponent. Moreover, τ_c represents the center of the correlation time distribution of the motion. Furthermore, the number *M* of equivalent orientational sites accessed by a specific carbon in the motional process as well as the fraction *f_m* of mobile segments can be calculated by means of *E_∞* (deAzevedo et al., 1999):

$$E_\infty = \frac{f_m(M-1)}{M} \quad (3)$$

The normalized pure-exchange CODEX intensities of the protonated aromatic carbons of the untreated and the UV-treated samples are plotted in Figure 4. At 70°C, a final exchange intensity of *E_∞* = 0.770 ± 0.040 and 0.412 ± 0.004 was determined for the untreated and the UV-treated sample, respectively. At 30°C, *E_∞* = 0.276 ± 0.016 was obtained for untreated PET and *E_∞* = 0.274 ± 0.015 for the UV-treated PET sample. The fraction of mobile segments is *f_m* = 54.9 ± 3.0 and 55.2 ± 3.2% for the UV-treated and the untreated PET sample at 30°C, respectively. The results are therefore similar at a temperature of 30°C. However, at 70°C the mobile fractions are increased, with *f_m* = 82.5 ± 0.9% for the UV-treated sample and *f_m* = 96.3 ± 5.0 or 102.7 ± 5.3%, depending on the chosen value for *M*, for the untreated PET sample. The number of equivalent orientational sites (*M*) accessed by one protonated aromatic carbon is *M* = 2 for the UV-treated sample at both temperatures and for the untreated PET sample at 30°C, indicating the 180° phenylene ring flip. For the untreated sample at 70°C the value of *M* is assumed to be 4 or 5, suggesting more complex motions

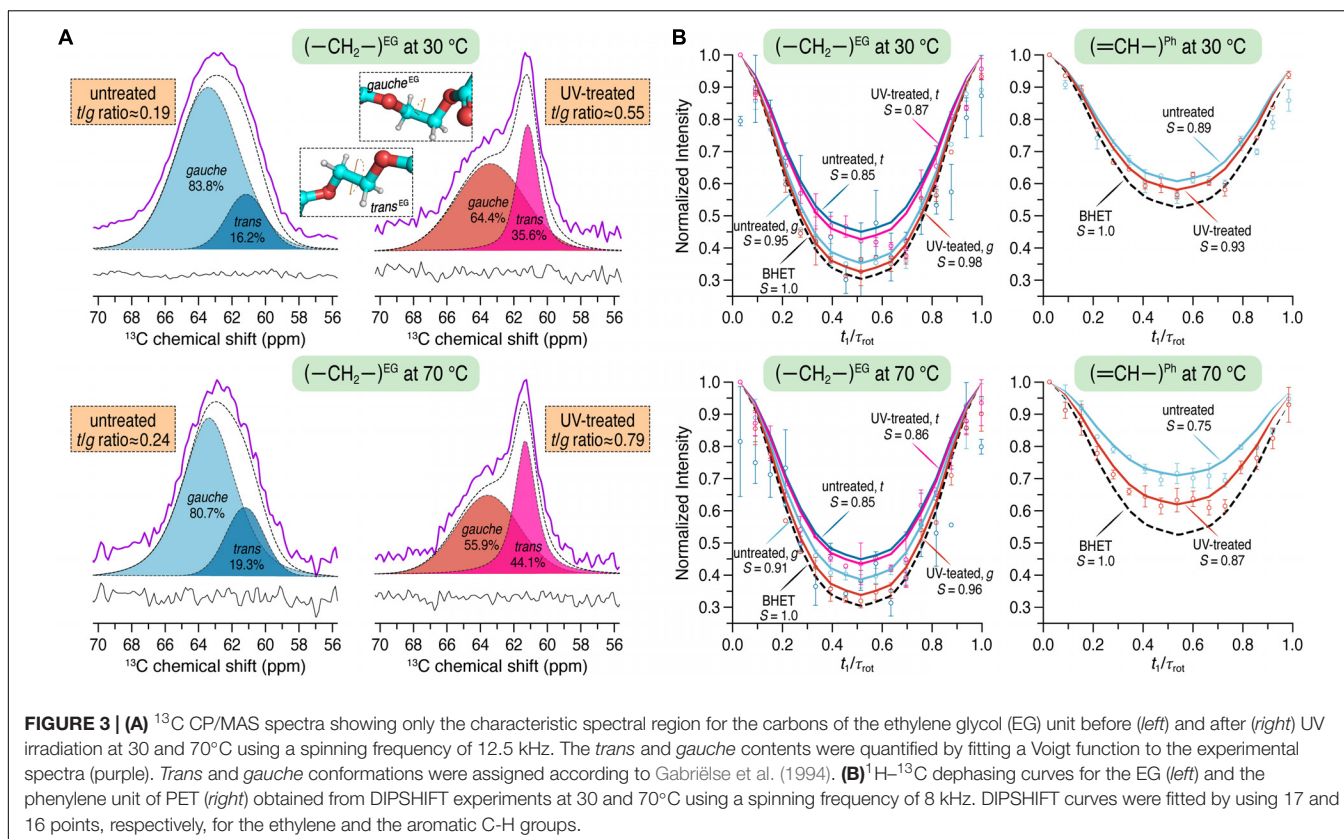


FIGURE 3 | (A) ^{13}C CP/MAS spectra showing only the characteristic spectral region for the carbons of the ethylene glycol (EG) unit before (left) and after (right) UV irradiation at 30 and 70 °C using a spinning frequency of 12.5 kHz. The *trans* and *gauche* contents were quantified by fitting a Voigt function to the experimental spectra (purple). *Trans* and *gauche* conformations were assigned according to Gabriëse et al. (1994). **(B)** ^1H - ^{13}C dephasing curves for the EG (left) and the phenylene unit of PET (right) obtained from DIPSHIFT experiments at 30 and 70 °C using a spinning frequency of 8 kHz. DIPSHIFT curves were fitted by using 17 and 16 points, respectively, for the ethylene and the aromatic C-H groups.

of the phenylene ring. Since the correlation time values are quite sensitive to curve shapes and single data points, their errors are large and these values are therefore not taken into account for evaluating dynamical changes of the PET samples (Choudhury et al., 2012). Results of the fitting of experimental data to a stretched exponential (Eq. 2) and data analysis using Eq. 3 are shown in **Supplementary Table 1**.

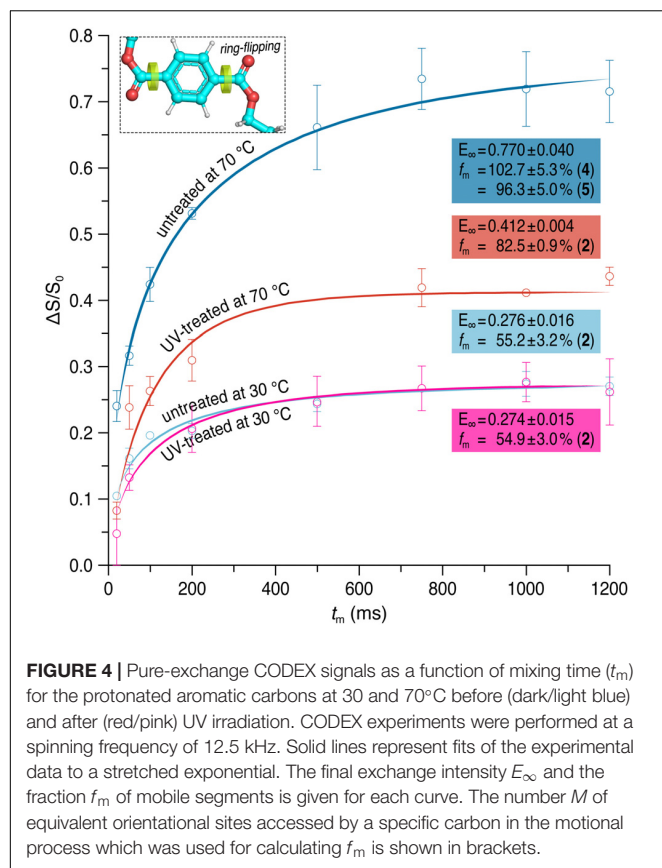
Furthermore, $T_{1\rho}(^1\text{H})$ relaxation times were measured for both PET samples which provide segmental information on dynamics over a time scale of microseconds to milliseconds (Schmidt-Rohr and Spiess, 1994). Since $T_{1\rho}(^1\text{H})$ experiments are susceptible to ^1H spin diffusion which results in the averaging of relaxation times, more global information about the PET chain motions can thus be obtained (VanderHart and Garroway, 1979; Gabriëse et al., 1994). To determine $T_{1\rho}(^1\text{H})$ times the normalized peak intensities were plotted against the spin-lock time τ and fitted to a single exponential for untreated and UV-treated PET. The values are summarized in **Figure 5**.

At 70 °C, $T_{1\rho}(^1\text{H})$ relaxation times determined for both untreated and UV-treated samples were shorter than those at 30 °C, indicating shorter average motional correlation times and thus faster motions, for example $T_{1\rho}(^1\text{H})_{70^\circ\text{C}} = 5.2 \pm 0.1$ ms vs. $T_{1\rho}(^1\text{H})_{30^\circ\text{C}} = 6.6 \pm 0.1$ ms for the protonated aromatic carbons in the untreated PET sample. After UV irradiation, the $T_{1\rho}(^1\text{H})$ values were larger at both temperatures, for example the $T_{1\rho}(^1\text{H})$ value was 12.2 ± 0.3 and 6.6 ± 0.1 ms for the protonated aromatic carbons in the UV-treated and the untreated sample at 30 °C, respectively. The ethylene and carbonyl peaks were

deconvoluted into amorphous and crystalline components for the UV-treated sample. For carbons in *t* conformation, the $T_{1\rho}(^1\text{H})$ times were significantly larger than those in *g* conformation (e.g., $T_{1\rho}(^1\text{H})_t = 20.3 \pm 0.8$ and $T_{1\rho}(^1\text{H})_g = 8.2 \pm 0.3$ for the ethylene carbons in the UV-treated sample at 30 °C), indicating that crystalline regions of PET with relatively high *t* content are more rigid than amorphous regions with chains in *g* conformation. The values for the ethylene carbons in *t* and *g* conformations at 30 °C are very similar to those determined by Choudhury et al. (2012) for semicrystalline PET.

DISCUSSION

The enzymatic degradation of post-consumer PET has emerged as an eco-friendly method for future applications in plastic recycling processes (Wei and Zimmermann, 2017). UV irradiation is a major abiotic factor responsible for the environmental plastic degradation (Gewert et al., 2015), and is thus considered as a potential pretreatment to mitigate the hurdles for biodegradation caused by polymer microstructures. Photodegradation-based pretreatment has proven to be beneficial for subsequent biodegradation of selected polyolefins (Koutny et al., 2006a,b; Restrepo-Flórez et al., 2014), however, so far rarely investigated for PET. Chain scission has been verified with PET samples exposed to sunlight for up to 42 days already in the 1970s (Day and Wiles, 1972b) providing a fundamental background for further studies. The PET samples in this study



were exposed to a UV light source which shows an emission spectrum similar to sunlight, thus making it possible to mimic natural illumination conditions. We used ATR-FTIR and ^1H solution NMR spectroscopy to analyze the PET samples after UV exposure. Both spectroscopic methods revealed an increased amount of end groups and a decreased average molecular mass from 35000 to 29000 g/mol (Figure 1D) thereby suggesting the PET sample has been partially photodegraded by the UV light.

However, the UV-treated PET samples showed an increased resistance against enzymatic degradation yielding lower weight losses of the material compared to an untreated control (Figure 2). To clarify this seeming contradiction, solid-state NMR spectroscopy is the method of choice as it provides detailed information at the atomic level. Therefore, we performed a series of solid-state NMR experiments with both the UV-treated and control PET samples. The ^{13}C CP/MAS experiment was used to determine the t/g ratio of the PET samples (Figure 3A), where a higher t content is detected for the UV-treated PET, indicative of an increased crystallinity as a result of UV exposure. These results are consistent with a previous study which reported a 100% increase of crystallinity of a semicrystalline PET sample after exposure to sunlight for 670 days determined by density measurement and differential scanning calorimetry (Aljoumaa and Abboudi, 2016). UV degradation is known to be a surface sensitive process (Day and Wiles, 1972b; Blais et al., 1973), and accordingly, the resulting increased crystallinity is considered to

affect only the surface of the sample. DIPSHIFT, $T_{1\rho}(^1\text{H})$ and CODEX experiments provide information about the dynamics of polymer chains in the untreated and the UV-irradiated PET on different time scales. Higher order parameters S (Figure 3B) were observed for the EG and the phenylene C–H groups after UV photodegradation, indicating that both regions became less mobile. Moreover, CODEX experiments revealed that the number of equivalent orientational sites M accessed by one carbon is highest for the untreated sample measured at 70°C (Figure 4), suggesting more complicated chain motions in untreated PET at this temperature. For the UV-treated sample only two-site jumps were observed at both temperatures which can be attributed to the already known 180° phenylene ring flip about the 1,4-axis indicating a partially restricted rotation at 70°C in comparison with that of the untreated sample. The t and g conformations were indistinguishable in the CODEX spectra, the lower mobility can thus be ascribed to the higher crystalline content in PET after UV irradiation, representing a more ordered system with for example a more hindered ring-flipping motion of the phenylene unit. In agreement with CODEX and DIPSHIFT data, the $T_{1\rho}(^1\text{H})$ relaxation times became larger after UV irradiation (Figure 5) which clearly indicates a reduction in segmental dynamics over a time scale of microseconds to milliseconds. The overall slower chain motions of the UV-treated PET sample can be ascribed to the change of microstructure in the surface layer. UV light can result in spontaneous chain scission in PET by oxidation and consequently shorten the polymer chains (Day and Wiles, 1972c). The shorter PET polymer chains are more prone to have fold among themselves and thus to be rearranged into inter-crystalline domains (Launay et al., 1994; Badia et al., 2012). Due to the increase in local temperature of the surface layer exposed to UV light, physical aging of short PET chains with a trend to more ordered structure thus occurred more easily. Increased crystallinity in the surface layer and consequently decreased polymer chain dynamics hampers the efficiency of biocatalytic degradation which is well-known as a surface erosion process (Ronkvist et al., 2009).

Recent studies on the mechanism of biocatalytic degradation by computational simulation and solid-state NMR indicated that the flexibility of both the polymer chain and the substrate binding cleft on the surface of the enzyme is crucial to ensure a high degradation performance against PET (Austin et al., 2018; Wei et al., 2019b). Here, for the PET sample treated with UV irradiation, an overall increased chain rigidity including the partially prohibited ring-flip motions of the phenylene units was observed. This would hamper the hydrophobic interactions between the aromatic phenylene units and the neighboring amino acids in the active site required for the binding of PET substrate (Austin et al., 2018; Wei et al., 2019b) and consequently diminish the efficiency of the enzymatic hydrolysis.

Besides the $-\text{COOH}$ and $-\text{OH}$ groups, the broadened $\text{C}=\text{O}$ band at $1800\text{--}1750\text{ cm}^{-1}$ in the ATR-FTIR spectrum of UV-treated PET (Supplementary Figure 1) gives an indication for vinyl ester end groups (Hesse et al., 2005). Additionally, the formation of aldehyde end groups is also conceivable (see also

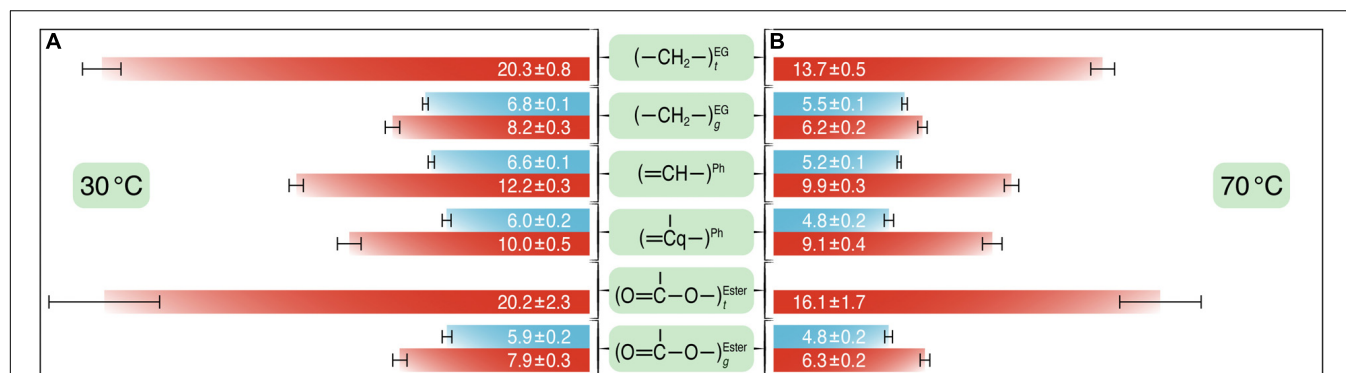


FIGURE 5 | The $T_{1\rho}(^1\text{H})$ relaxation times (in milliseconds) for the different carbons of PET before (blue) and after (red) UV irradiation at 30°C (A) and at 70°C (B). $T_{1\rho}(^1\text{H})$ experiments were performed at a spinning speed of 8 kHz with varying spin-lock pulse lengths between 0.01 and 50 ms. $T_{1\rho}(^1\text{H})$ values and corresponding error bars were obtained from the fits of the normalized peak intensities against the spin-lock time to a single exponential curve.

Gewert et al., 2015). The increased complexity of the PET surface upon UV irradiation supports the original proposal of a radical-based mechanism in photo-oxidative degradation (Day and Wiles, 1972a; Gotoh et al., 2011; Gewert et al., 2015). Since the biocatalytic degradation of low-crystalline PET has been shown to follow a processive exo-mechanism (Wei et al., 2019a), the formation of these alternative end groups as a result of UV treatment would impair the recognition of the polymer chain ends by the polyester hydrolase and consequently reduce the efficiency of a biocatalytic PET degradation.

In addition to the use of purified enzymes, the biodegradation of PET has also been shown with natural and engineered microbes in pure cultures at ambient temperatures (Yoshida et al., 2016; Moog et al., 2019). Using these whole-cell based systems, the degradation performance of PET was shown to rely on the activity and amount of the PET hydrolase expressed and secreted. A colonization of the PET polymer by the microbes has been considered as a requirement for an efficient degradation by their secreted enzymes. Nevertheless, only colonization of *Ideonella sakaiensis* on amorphous PET materials has been evidenced so far in correlation with a notable polymer degradation (Yoshida et al., 2016). More recently, another study speculated that microbial biofilm formation might be more pronounced on PET materials exposed to UV radiation for 30 min (Vague et al., 2019). However, the biodegradation of PET could not be unambiguously verified by either demonstrating the release of degradation products or by a significant weight loss. Therefore, the question whether UV treatment will influence a microbial colonization of PET at ambient temperatures remains still unsolved. Our recent study has indicated that thermophilic conditions at $\geq 70^\circ\text{C}$ are preferred for an efficient PET biodegradation (Wei et al., 2019b). A whole-cell based system with simultaneous microbial growth, enzyme expression and biocatalytic PET degradation at elevated temperature is a target of the ongoing research.

The UV fraction of natural sunlight has been shown to have similar aging effects on PET materials as the artificial light source used in this study (Aljoumaa and Abboudi, 2016). Concerning

marine litter, the PET debris is largely coming from PET beverage bottles with a higher crystallinity than the amorphous PET used in this study. A further exposure to sunlight can be expected to render them even less biodegradable serving as a vehicle for microbial attachment rather than a substrate for the accumulation of specific consortia able to degrade and assimilate the plastic (Oberbeckmann et al., 2014, 2016).

In summary, we investigated the chain conformational and dynamic changes as well as biodegradability of amorphous PET after UV pretreatment. Analysis by various spectroscopic techniques and enzymatic degradation studies revealed the formation of a surface layer with increased crystallinity as a result of UV treatment which consequently decreased polymer chain dynamics causing significantly retarded enzymatic hydrolysis. Our findings suggest that the exposure to UV light is not a feasible pretreatment approach to enhance the following biocatalytic degradation of PET, despite the occurrence of shorter polymer chains as a result of photodegradation. Further NMR studies are needed for in-depth understanding of how the polymer chain conformation and dynamics can influence the enzymatic biodegradation of PET at the molecular level.

DATA AVAILABILITY STATEMENT

All datasets generated for this study are included in the article/Supplementary Material.

AUTHOR CONTRIBUTIONS

JM and CS conceived the experiments. PF, DG, PB, JM, RW, and CS designed the experiments. PF performed NMR and ATR-FTIR experiments. RW performed enzymatic degradation of PET films. PF, RW, and CS analyzed the data. WZ and JM supervised the project. PF wrote the manuscript with extensive input from WZ, JM, RW, and CS. All the authors read and corrected the manuscript.

FUNDING

PF was supported by a scholarship of the Deutsche Bundesstiftung Umwelt (DBU, grant no. 20018/565).

ACKNOWLEDGMENTS

The authors thank Dr. J. Becker-Baldus (Goethe-Universität Frankfurt, Germany) for providing the CODEX pulse sequence, Dr. F. Link and Dr. M. Jabłońska (Universität Leipzig, Germany)

for the assistance in collecting the ATR-FTIR data and Prof. W. Gärtner (Universität Leipzig, Germany) for fruitful discussions. We acknowledge support from Universität Leipzig for Open Access Publishing.

SUPPLEMENTARY MATERIAL

The Supplementary Material for this article can be found online at: <https://www.frontiersin.org/articles/10.3389/fmicb.2020.00689/full#supplementary-material>

REFERENCES

- Albertsson, A.-C., Andersson, S. O., and Karlsson, S. (1987). The mechanism of biodegradation of polyethylene. *Polym. Degrad. Stab.* 18, 73–87. doi: 10.1016/0141-3910(87)90084-X
- Aljoumaa, K., and Abboudi, M. (2016). Physical ageing of polyethylene terephthalate under natural sunlight: correlation study between crystallinity and mechanical properties. *Appl. Phys. A* 122, 6. doi: 10.1007/s00339-015-9518-0
- Ammala, A., Bateman, S., Dean, K., Petinakis, E., Sangwan, P., Wong, S., et al. (2011). An overview of degradable and biodegradable polyolefins. *Prog. Polym. Sci.* 36, 1015–1049. doi: 10.1016/j.progpolymsci.2010.12.002
- Andrady, A. L., and Neal, M. A. (2009). Applications and societal benefits of plastics. *Philos. Trans. R. Soc. B* 364, 1977–1984. doi: 10.1098/rstb.2008.0304
- Austin, H. P., Allen, M. D., Donohoe, B. S., Rorrer, N. A., Kearns, F. L., Silveira, R. L., et al. (2018). Characterization and engineering of a plastic-degrading aromatic polyesterase. *Proc. Natl. Acad. Sci. U.S.A.* 115, E4350–E4357. doi: 10.1073/pnas.1718804115
- Badia, J. D., Strömberg, E., Karlsson, S., and Ribes-Greus, A. (2012). The role of crystalline, mobile amorphous and rigid amorphous fractions in the performance of recycled poly (ethylene terephthalate) (PET). *Polym. Degrad. Stab.* 97, 98–107. doi: 10.1016/j.polymdegradstab.2011.10.008
- Bak, M., Rasmussen, J. T., and Nielsen, N. C. (2000). SIMPSON: A general simulation program for solid-state NMR spectroscopy. *J. Magn. Reson.* 147, 296–330. doi: 10.1006/jmre.2000.2179
- Barth, M., Wei, R., Oeser, T., Then, J., Schmidt, J., Wohlgemuth, F., et al. (2015). Enzymatic hydrolysis of polyethylene terephthalate films in an ultrafiltration membrane reactor. *J. Membr. Sci.* 494, 182–187. doi: 10.1016/j.memsci.2015.07.030
- Blais, P., Day, M., and Wiles, D. M. (1973). Photochemical degradation of poly(ethylene terephthalate). IV. Surface changes. *J. Appl. Polym. Sci.* 17, 1895–1907. doi: 10.1002/app.1973.070170622
- Bollinger, A., Thies, S., Knieps-Grünhagen, E., Gertzen, C., Kobus, S., Höppner, A., et al. (2020). A novel polyester hydrolase from the marine bacterium *Pseudomonas aestusnigri* – Structural and functional insights. *Front. Microbiol.* 11:114. doi: 10.3389/fmicb.2020.00114
- Choudhury, R. P., Lee, J. S., Kriegl, R. M., Koros, W. J., and Beckham, H. W. (2012). Chain dynamics in antiplasticized and annealed poly(ethylene terephthalate) determined by solid-state NMR and correlated with enhanced barrier properties. *Macromolecules* 45, 879–887. doi: 10.1021/ma202012h
- Day, M., and Wiles, D. M. (1972a). Photochemical degradation of poly(ethylene terephthalate). III. Determination of decomposition products and reaction mechanism. *J. Appl. Polym. Sci.* 16, 203–215. doi: 10.1002/app.1972.070160118
- Day, M., and Wiles, D. M. (1972b). Photochemical degradation of poly(ethylene terephthalate). I. Irradiation experiments with the xenon and carbon arc. *J. Appl. Polym. Sci.* 16, 175–189. doi: 10.1002/app.1972.070160116
- Day, M., and Wiles, D. M. (1972c). Photochemical degradation of poly(ethylene terephthalate). II. Effect of wavelength and environment on the decomposition process. *J. Appl. Polym. Sci.* 16, 191–202. doi: 10.1002/app.1972.070160117
- de Ilarduya, A. M., and Muñoz-Guerra, S. (2014). Chemical structure and microstructure of poly(alkylene terephthalate)s, their copolyesters, and their blends as studied by NMR. *Macromol. Chem. Phys.* 215, 2138–2160. doi: 10.1002/macp.201400239
- deAzevedo, E. R., Hu, W.-G., Bonagamba, T. J., and Schmidt-Rohr, K. (1999). Centerband-only detection of exchange: Efficient analysis of dynamics in solids by NMR. *J. Am. Chem. Soc.* 121, 8411–8412. doi: 10.1021/ja992022v
- deAzevedo, E. R., Saalwächter, K., Pascui, O., de Souza, A. A., Bonagamba, T. J., and Reichert, D. (2008). Intermediate motions as studied by solid-state separated local field NMR experiments. *J. Chem. Phys.* 128, 104505. doi: 10.1063/1.2831798
- Fechine, G. J. M., Rabello, M. S., Souto Maior, R. M., and Catalani, L. H. (2004). Surface characterization of photodegraded poly(ethylene terephthalate). The effect of ultraviolet absorbers. *Polymer* 45, 2303–2308. doi: 10.1016/j.polymer.2004.02.003
- Fechine, G. J. M., Souto-Maior, R. M., and Rabello, M. S. (2002). Structural changes during photodegradation of poly(ethylene terephthalate). *J. Mater. Sci.* 37, 4979–4984. doi: 10.1023/A:1021067027612
- Gabriëse, W., Angad Gaur, H., Feyen, F. C., and Veeman, W. S. (1994). ¹³C solid-state NMR study of differently processed poly(ethylene terephthalate) yarns. *Macromolecules* 27, 5811–5820. doi: 10.1021/ma00098a040
- Gewert, B., Plassmann, M. M., and MacLeod, M. (2015). Pathways for degradation of plastic polymers floating in the marine environment. *Environ. Sci.: Process. Impacts* 17, 1513–1521. doi: 10.1039/c5em00207a
- Geyer, B., Lorenz, G., and Kandelbauer, A. (2016). Recycling of poly(ethylene terephthalate) – A review focusing on chemical methods. *Express Polym. Lett.* 10, 559–586. doi: 10.3144/expresspolymlett.2016.53
- Geyer, R., Jambeck, J. R., and Law, K. L. (2017). Production, use, and fate of all plastics ever made. *Sci. Adv.* 3, e1700782. doi: 10.1126/sciadv.1700782
- Gotoh, K., Yasukawa, A., and Kobayashi, Y. (2011). Wettability characteristics of poly(ethylene terephthalate) films treated by atmospheric pressure plasma and ultraviolet excimer light. *Polym. J.* 43, 545–551. doi: 10.1038/pj.2011.20
- Günzler, H., and Gremlich, H.-U. (2003). *IR-Spektroskopie*. Weinheim: Wiley-VCH.
- Han, X., Liu, W., Huang, J.-W., Ma, J., Zheng, Y., Ko, T.-P., et al. (2017). Structural insight into catalytic mechanism of PET hydrolase. *Nat. Commun.* 8, 2106. doi: 10.1038/s41467-017-02255-z
- Hesse, M., Meier, H., and Zeeh, B. (2005). *Spektroskopische Methoden in der organischen Chemie*, 7th Edn. Stuttgart: Thieme.
- Holland, B. J., and Hay, J. N. (2002). The thermal degradation of PET and analogous polyesters measured by thermal analysis—Fourier transform infrared spectroscopy. *Polymer* 43, 1835–1847. doi: 10.1016/S0032-3861(01)00775-3
- Hong, M., Gross, J. D., and Griffin, R. G. (1997). Site-resolved determination of peptide torsion angle Φ from the relative orientations of backbone N-H and C-H bonds by solid-state NMR. *J. Phys. Chem. B* 101, 5869–5874. doi: 10.1021/jp970887u
- Hopewell, J., Dvorak, R., and Kosior, E. (2009). Plastics recycling: Challenges and opportunities. *Philos. Trans. R. Soc. B* 364, 2115–2126. doi: 10.1098/rstb.2008.0311
- Huster, D., Xiao, L., and Hong, M. (2001). Solid-state NMR investigation of the dynamics of the soluble and membrane-bound colicin Ia channel-forming domain. *Biochemistry* 40, 7662–7674. doi: 10.1021/bi0027231
- Hutchinson, J. M. (1995). Physical aging of polymers. *Prog. Polym. Sci.* 20, 703–760. doi: 10.1016/0079-6700(94)00001-i
- Ivanir-Dabora, H., Nimerovsky, E., Madhu, P. K., and Goldbourt, A. (2015). Site-resolved backbone and side-chain intermediate dynamics in a

- carbohydrate-binding module protein studied by magic-angle spinning NMR spectroscopy. *Chem. Eur. J.* 21, 10778–10785. doi: 10.1002/chem.201500856
- Joo, S., Cho, I. J., Seo, H., Son, H. F., Sagong, H.-Y., Shin, T. J., et al. (2018). Structural insight into molecular mechanism of poly(ethylene terephthalate) degradation. *Nat. Commun.* 9, 382. doi: 10.1038/s41467-018-02881-1
- Kawai, F., Kawabata, T., and Oda, M. (2019). Current knowledge on enzymatic PET degradation and its possible application to waste stream management and other fields. *Appl. Microbiol. Biotechnol.* 103, 4253–4268. doi: 10.1007/s00253-019-09717-y
- Kenwright, A. M., Peace, S. K., Richards, R. W., Bunn, A., and MacDonald, W. A. (1999). End group modification in poly(ethylene terephthalate). *Polymer* 40, 2035–2040. doi: 10.1016/S0032-3861(98)00433-9
- Koutny, M., Lemaire, J., and Delort, A.-M. (2006a). Biodegradation of polyethylene films with prooxidant additives. *Chemosphere* 64, 1243–1252. doi: 10.1016/j.chemosphere.2005.12.060
- Koutny, M., Sancelme, M., Dabin, C., Pichon, N., Delort, A.-M., and Lemaire, J. (2006b). Acquired biodegradability of polyethylenes containing pro-oxidant additives. *Polym. Degrad. Stab.* 91, 1495–1503. doi: 10.1016/j.polymdegradstab.2005.10.007
- Launay, A., Thominet, F., and Verdu, J. (1994). Hydrolysis of poly(ethylene terephthalate): a kinetic study. *Polym. Degrad. Stab.* 46, 319–324. doi: 10.1016/0141-3910(94)90148-1
- Metz, G., Wu, X. L., and Smith, S. O. (1994). Ramped-amplitude cross polarization in magic-angle-spinning NMR. *J. Magn. Reson. Ser. A* 110, 219–227. doi: 10.1006/jmra.1994.1208
- Moog, D., Schmitt, J., Senger, J., Zarzycki, J., Rexer, K.-H., Linne, U., et al. (2019). Using a marine microalga as a chassis for polyethylene terephthalate (PET) degradation. *Microb. Cell Fact.* 18, 171. doi: 10.1186/s12934-019-1220-z
- Oberbeckmann, S., Loeder, M. G. J., Gerds, G., and Osborn, A. M. (2014). Spatial and seasonal variation in diversity and structure of microbial biofilms on marine plastics in Northern European waters. *FEMS Microbiol. Ecol.* 90, 478–492. doi: 10.1111/1574-6941.12409
- Oberbeckmann, S., Osborn, A. M., and Duhaime, M. B. (2016). Microbes on a bottle: Substrate, season and geography influence community composition of microbes colonizing marine plastic debris. *PLoS One* 11:e0159289. doi: 10.1371/journal.pone.0159289
- PlasticsEurope (2019). *Plastics - the Facts 2019*. Available online at: <https://www.plasticseurope.org/de/resources/publications/1804-plastics-facts-2019> (accessed October 14, 2019).
- Reichert, D., Bonagamba, T. J., and Schmidt-Rohr, K. (2001). Slow-down of ^{13}C spin diffusion in organic solids by fast MAS: A CODEX NMR study. *J. Magn. Reson.* 151, 129–135. doi: 10.1006/jmre.2001.2337
- Restrepo-Flórez, J.-M., Bassi, A., and Thompson, M. R. (2014). Microbial degradation and deterioration of polyethylene — A review. *Int. Biodeterior. Biodegrad.* 88, 83–90. doi: 10.1016/j.ibiod.2013.12.014
- Rochman, C. M., Browne, M. A., Halpern, B. S., Hentschel, B. T., Hoh, E., Karapanagioti, H. K., et al. (2013). Classify plastic waste as hazardous. *Nature* 494, 169–171. doi: 10.1038/494169a
- Ronkvist, Å. M., Xie, W., Lu, W., and Gross, R. A. (2009). Cutinase-catalyzed hydrolysis of poly(ethylene terephthalate). *Macromolecules* 42, 5128–5138. doi: 10.1021/ma9005318
- Salvador, M., Abdulmutalib, U., Gonzalez, J., Kim, J., Smith, A. A., Faulon, J.-L., et al. (2019). Microbial genes for a circular and sustainable bio-PET economy. *Genes* 10, 373. doi: 10.3390/genes10050373
- Schaefer, J., and Stejskal, E. O. (1976). Carbon-13 nuclear magnetic resonance of polymers spinning at the magic angle. *J. Am. Chem. Soc.* 98, 1031–1032. doi: 10.1021/ja00420a036
- Schmidt, J., Wei, R., Oeser, T., Belisário-Ferrari, M. R., Barth, M., Then, J., et al. (2016). Effect of Tris, MOPS, and phosphate buffers on the hydrolysis of polyethylene terephthalate films by polyester hydrolases. *FEBS Open Bio.* 6, 919–927. doi: 10.1002/2211-5463.12097
- Schmidt-Rohr, K., Hu, W., and Zumbulyadis, N. (1998). Elucidation of the chain conformation in a glassy polyester, PET, by two-dimensional NMR. *Science* 280, 714–717. doi: 10.1126/science.280.5364.714
- Schmidt-Rohr, K., and Spiess, H. W. (1994). *Multidimensional solid-state NMR and polymers*. London: Academic Press.
- Schrader, B., and Meier, W. (1974). *Raman/IR Atlas organischer Verbindungen*. Weinheim: Verlag Chemie.
- Sulaiman, S., Yamato, S., Kanaya, E., Kim, J.-J., Koga, Y., Takano, K., et al. (2012). Isolation of a novel cutinase homolog with polyethylene terephthalate-degrading activity from leaf-branch compost by using a metagenomic approach. *Appl. Environ. Microbiol.* 78, 1556–1562. doi: 10.1128/AEM.06725-11
- Thakur, R. S., Kurur, N. D., and Madhu, P. K. (2006). Swept-frequency two-pulse phase modulation for heteronuclear dipolar decoupling in solid-state NMR. *Chem. Phys. Lett.* 426, 459–463. doi: 10.1016/J.CPLETT.2006.06.007
- Vague, M., Chan, G., Roberts, C., Swartz, N. A., and Mellies, J. L. (2019). *Pseudomonas* isolates degrade and form biofilms on polyethylene terephthalate (PET) plastic. *bioRxiv* doi: 10.1101/647321
- VanderHart, D. L., and Garrowsay, A. N. (1979). ^{13}C NMR rotating frame relaxation in a solid with strongly coupled protons: Polyethylene. *J. Chem. Phys.* 71, 2773–2787. doi: 10.1063/1.438682
- Vertommen, M. A. M. E., Nierstrasz, V. A., van der Veer, M., and Warmoeskerken, M. C. G. (2005). Enzymatic surface modification of poly(ethylene terephthalate). *J. Biotechnol.* 120, 376–386. doi: 10.1016/j.jbiotec.2005.06.015
- Vinod Chandran, C., Madhu, P. K., Kurur, N. D., and Bräuniger, T. (2008). Swept-frequency two-pulse phase modulation (SW-TPPM) sequences with linear sweep profile for heteronuclear decoupling in solid-state NMR. *Magn. Reson. Chem.* 46, 943–947. doi: 10.1002/mrc.2285
- Vinogradov, E., Madhu, P. K., and Vega, S. (2001). Phase modulated Lee–Goldburg magic angle spinning proton nuclear magnetic resonance experiments in the solid state: A bimodal Floquet theoretical treatment. *J. Chem. Phys.* 115, 8983–9000. doi: 10.1063/1.1408287
- Webb, H. K., Arnott, J., Crawford, R. J., and Ivanova, E. P. (2013). Plastic degradation and its environmental implications with special reference to poly(ethylene terephthalate). *Polymers* 5, 1–18. doi: 10.3390/polym5010001
- Wei, R., Breite, D., Song, C., Gräising, D., Ploss, T., Hille, P., et al. (2019a). Biocatalytic degradation efficiency of postconsumer polyethylene terephthalate packaging determined by their polymer microstructures. *Adv. Sci.* 6, 1900491. doi: 10.1002/advs.201900491
- Wei, R., Song, C., Gräising, D., Schneider, T., Bielytskiy, P., Böttcher, D., et al. (2019b). Conformational fitting of a flexible oligomeric substrate does not explain the enzymatic PET degradation. *Nat. Commun.* 10, 5581. doi: 10.1038/s41467-019-13492-9
- Wei, R., and Zimmermann, W. (2017). Biocatalysis as a green route for recycling the recalcitrant plastic polyethylene terephthalate. *Microb. Biotechnol.* 10, 1302–1307. doi: 10.1111/1751-7915.12714
- Wilhelm, M., and Spiess, H. W. (1996). Detection of slow 180° phenylene flips in PET fibers via ^{13}C two-dimensional solid-state exchange NMR. *Macromolecules* 29, 1088–1090. doi: 10.1021/ma9516192
- World Economic Forum (2016). *The new plastics economy: Rethinking the future of plastics*. Available online at: <https://www.weforum.org/reports/the-new-plastics-economy-rethinking-the-future-of-plastics> (accessed January 19, 2016).
- Yoshida, S., Hiraga, K., Takehana, T., Taniguchi, I., Yamaji, H., Maeda, Y., et al. (2016). A bacterium that degrades and assimilates poly(ethylene terephthalate). *Science* 351, 1196–1199. doi: 10.1126/science.aad6359

Conflict of Interest: The authors declare that the research was conducted in the absence of any commercial or financial relationships that could be construed as a potential conflict of interest.

Copyright © 2020 Falkenstein, Gräising, Bielytskiy, Zimmermann, Matysik, Wei and Song. This is an open-access article distributed under the terms of the Creative Commons Attribution License (CC BY). The use, distribution or reproduction in other forums is permitted, provided the original author(s) and the copyright owner(s) are credited and that the original publication in this journal is cited, in accordance with accepted academic practice. No use, distribution or reproduction is permitted which does not comply with these terms.

Advantages of publishing in Frontiers



OPEN ACCESS

Articles are free to read
for greatest visibility
and readership



FAST PUBLICATION

Around 90 days
from submission
to decision



HIGH QUALITY PEER-REVIEW

Rigorous, collaborative,
and constructive
peer-review



TRANSPARENT PEER-REVIEW

Editors and reviewers
acknowledged by name
on published articles

Frontiers

Avenue du Tribunal-Fédéral 34
1005 Lausanne | Switzerland

Visit us: www.frontiersin.org

Contact us: frontiersin.org/about/contact



REPRODUCIBILITY OF RESEARCH

Support open data
and methods to enhance
research reproducibility



DIGITAL PUBLISHING

Articles designed
for optimal readership
across devices



FOLLOW US

@frontiersin



IMPACT METRICS

Advanced article metrics
track visibility across
digital media



EXTENSIVE PROMOTION

Marketing
and promotion
of impactful research



LOOP RESEARCH NETWORK

Our network
increases your
article's readership